Gonçalo Goulart da Silva Pinheiro

Differential
Setup of PI3K/AKT and JAK/STAT pathways in fibrotic vs regenerative healing in mammals

UAlg
UNIVERSIDADE DO ALGARVE

Faculdade de Medicina e Ciências Biomédicas

2024

Gonçalo Goulart da Silva Pinheiro

Differential Setup of PI3K/AKT and JAK/STAT pathways in fibrotic vs regenerative healing in mammals

PhD Program in Biomedical Sciences

This work was developed
under the supervision of:
Prof. Dr. Gustavo Tiscórnia
Profa. Dra. Inês Araújo

Faculdade de Medicina e Ciências Biomédicas

2024

This page was intentionally left blank

Differential
Setup of PI3K/AKT and JAK/STAT pathways in fibrotic vs regenerative healing in mammals

Declaração de autoria de trabalho

Declaro ser o autor deste trabalho, que é inédito e original. Autores e trabalhos consultados estão devidamente citados no texto e constam da listagem de referências incluída.

.

This work was performed at:

Molecular and Regenerative Medicine Lab

Neurogenesis Group

Center for Biomedical Research (CBMR)

Algarve Biomedical Center Research Institute (ABC-RI)

Center of Marine Sciences (CCMAR)

Faculdade de Medicina e Ciências Biomédicas da Universidade do Algarve

Campus de Gambelas, 8005-139 Faro, Portugal

This work was supported by National Portuguese funding through FCT – Fundação para a Ciência e a Tecnologia, scholarship SFRH/BD/130828/2017.

This page was intentionally left blank

Acknowledgements

The completion of this body of work owes itself to several helping hands, none necessarily less important than the others. So, in no particular order, I will start by thanking my supervisor, professor Gustavo Tiscórnia, PhD, for accepting me into his lab and having allowed me the chance to apply for a PhD with the University of Algarve, as well as creating, to the best of his abilities, the conditions required to see this work through, and having put up with my enormous stubbornness. I also thank my co-supervisor, professor Inês Araújo, PhD, for all her help with the burocratic aspects of this degree, and for contributing to the setup of the required conditions for me to perform this work.

Next, I want to extend a special thank you to four people who were of great importance and help throughout this journey. First, to Marta Vitorino, PhD, for her help and patience in too many ways to detail. She was indispensable in creating the ideal lab environment for me to perform this work, and was always available to help me to the best of her abilities.

Second, I want to thank Rui Machado, PhD, who made a valiant effort to accommodate all my requests pertaining to the analysis of the transcriptomic data, which he performed, sometimes at the expense of his personal time.

Third, to Gisela Serrão, MSc, who was invaluable in helping me set up my western blot protocol, and was always available to help me troubleshoot it, as well as to be a sympathetic issue to my complaints.

Last, but not least, I want to thank Maurícia Vinhas, MSc, who, even during complicated times, made what efforts were possible to free herself to help me operate the FACS machine, which was indispensable to the core results of this work.

I also want to extend my gratefulness to professor Ana Teresa Maia, PhD, who helped us with the experimental design of the transcriptomic experiment, professor Bibiana Ferreira, PhD, who shared lab equipment and reagents with me, and whom I consulted about my western blotting, professor Ashley Seifert, PhD, and Shishir Biswas, who very cordially allowed me to utilize the latter's re-analysis of their published data to perform my own re-interpretation, to Ana Mafalda Rocha, MSc, who sequence our transcriptomic samples, and to Vítor Fernandes, PhD, who helped me get started with my proliferative cell isolation experiments, and created the conditions I required to perform all the necessary animal experiments.

Finally, I want to thank all my friends (some which I have already mentioned) and family for their continued emotional support and shared good times, with a very special thank you to Daniela Baltazar, my (future) wife, who shared much of the stress and emotional burden of this long journey with me, and who, more than once, prevented me from quitting. I wouldn't be honest if I said I wouldn't have been able to do it without her, but she surely made it harder. (Pray for me, as I will surely pay for this jest!).

Resumo

A regeneração epimórfica em mamíferos é um fenómeno raro e pouco compreendido, mas há muito tempo que captura a imaginação humana, com a promessa de uma completa recuperação na sequência de um ferimento grave. Por esta razão, os cientistas estão há mais de um século a tentar compreender porque alguns animas têm um potencial desta característica tão superior aos humanos, para que talvez sejamos capazes de o recriar em nós.

Os vertebrados inferiores, como salamandras, sapos e peixes teleósteos, são capazes de regenerar vários tecidos e órgãos, incluindo o coração, mandíbula, apêndices, etc., recuperando completamente a funcionalidade. Compreender como um processo regenerativo é estabelecido em resposta a um ferimento, nestes organismos, tem-nos ajudado a compreender algumas limitações do nosso próprio sistema, mas uma compreensão completa requer o nosso entendimento de como este fenómeno ocorre em espécies mais próximas de nós, com as quais partilhamos, por exemplo, uma resposta imunitária adaptativa complexa.

Recentemente, algumas espécies de cervídeos e murídeos foram associados a uma impressionante capacidade de regenerar as suas hastes e tecidos associados, e os seus pavilhões auriculares e pele do dorso, respetivamente. Além disso, foi demonstrado que a regeneração nestes modelos tem uma forte relação com a resposta imunitária, e é dependente da sinalização MAPK/ERK, algo que também já foi demonstrado em processos regenerativos de vertebrados inferiores.

A sinalização MAPK/ERK é conhecida por controlar vários processos celulares, principalmente proliferação, portanto não é de espantar que esteja envolvida em eventos regenerativos. A sinalização MAPK/ERK também é conhecida por interagir com outras vias de sinalização intracelulares, principalmente com a sinalização PI3K/AKT, contribuindo para a integração de outros sinais, como disponibilidade nutricional e presença de fatores de stress, ajudando a célula a decidir o seu destino.

Apesar de ser indispensável para a regeneração, e ser capaz de induzir algumas características de regeneração num processo fibrótico, a sobre ativação da sinalização MAPK/ERK em mamíferos não é suficiente para o transformar completamente num evento regenerativo. Isto é indicativo de que provavelmente haverá outras vias de sinalização diferencialmente ativas entre os processos, e um melhor entendimento de como a proliferação é regulada nestes processos, em particular na regeneração em mamíferos, é necessário. Em particular, como é que células,

quando confrontadas com tal stress, tomam a decisão de proliferar, em vez de escolherem outro destino, como morte celular programada, e como é que o sistema imunitário influência este processo.

Com esse fim, de melhor entender essa regulação, neste trabalho procedemos ao isolamento de populações de células proliferativas que se formam durante o processo de resposta a uma perfuração circular do pavilhão auricular de duas espécies de mamífero, uma apresenta uma resposta regenerativa, e outra uma fibrótica, e analisámos os seus perfis transcricionais em vários pontos da sua resposta inicial a esse ferimento (hemóstase, inflamação e proliferação). Ao fazermos isso, observámos que, apesar de alguma, ainda que escassa, semelhança, estas duas populações proliferativas representam respostas amplamente distintas.

Em particular, o perfil transcricional de *A. cahirinus* mostrou uma forte associação com processos envolvidos no metabolismo energético e proliferação, enquanto o perfil transcricional das populações proliferativas de *M. musculus* associou-se mais significativamente com processos relacionados com dinâmicas citoplasmáticas, provavelmente associadas a migração, e diferenciação de vários tecidos.

Enquanto a regulação da proliferação de *M. musculus* se associou principalmente à via de sinalização de MAPK/ERK, o perfil transcritómico de *A. cahirinus* associou-se a mais vias de sinalização, nomeadamente à via PI3K/AKT, WNT e NF-KB, além de MAPK/ERK.
A comparação dos perfis transcricionais também sugeriu um envolvimento distinto de fatores de transcrição na regulação da proliferação. Também encontrámos uma associação do perfil transcricional de *A. cahirinus* com uma resposta apoptótica, associação essa que não foi observada em *M. musculus*.

Apesar de grupos distintos de vias de sinalização estarem associados com a resposta de cada uma das espécies estudadas, ambas as respostas são conhecidas por envolver igualmente algumas das mesmas vias de sinalização, mas com resultados distintos. Por causa disso, decidimos analisar como é que estas vias de sinalização estão montadas, e as dinâmicas da sua ativação em ambas as espécies.

Nós observámos que, aparentemente, a proporção de mediadores e as interações que estabelecem, em três vias de sinalização intracelulares, nomeadamente MAPK/ERK, PI3K/AKT e JAK/STAT, conhecidas por interagirem entre si na regulação de vários processos celulares, em particular na proliferação, não são idênticas entre as espécies.

Por exemplo, *M. musculus* aparenta ter uma preferência por ativar uma das isoformas de ERK1/2, enquanto o mesmo não se observa em *A. cahirinus*. Adicionalmente, as dinâmicas temporais de ativação sugerem que cada isoforma tem a sua própria dinâmica, com ERK2 aparentemente associado a uma resposta precoce, e ERK1 possivelmente envolvido no suporte da resposta proliferativa.

Quanto à via de sinalização PI3K/AKT, nós observámos uma abundância relativa consistentemente superior de AKT1 ativado em *M. musculus*, onde a sua ativação parece aumentar em particular nas primeiras 12h depois do ferimento. Além disso, a resposta desta via de sinalização aparenta ser bimodal, com um tipo de resposta precoce e outro mais tardio, possivelmente associado com uma indução de apoptose em *A. cahirinus* brevemente após lesão, algo que aparenta não acontecer em *M. musculus*. Esta indução talvez contribua para suster a proliferação, algo que tem sido associado com uma constante produção de fatores mitogénicos por parte de células pré-apoptóticas, que podem permanecer neste estado por largos períodos.

A via de sinalização JAK/STAT, por outro lado, exibe uma clara e sustentada proporção de JAK2 ativado mais elevada em *A. cahirinus*. No entanto, esta atividade superior não se traduziu em consideráveis diferenças nos níveis de ativação de STAT3, o que sugere que JAK2 poderá ter outros papéis no processo de resposta a ferimento nestas duas espécies. Isto poderá constituir um método que as células proliferativas, neste contexto, usam para integrar sinais do sistema imunitário na regulação da sua proliferação, visto que JAK2 pode transativar recetores que atuam acima da sinalização MAPK/ERK e PI3K/AKT, como os recetores ERBB.

No seu todo, o nosso trabalho sugere a existência de duas estratégias muito distintas de resposta a um ferimento, entre processos regenerativos e fibróticos em mamíferos, e sugere que isto não só se deve a uma resposta distinta aos mesmos estímulos, mas também que esta resposta distinta poderá dever-se a composições alternativas destas vias de sinalização intracelulares, que vão elas próprias gerar os resultados distintos destes dois tipos de resposta.

Mais exploração destas vias de sinalização, e da resposta dos seus participantes, aos estímulos presentes durante a resposta a ferimentos irão ajudar-nos a perceber o conjunto ideal de fatores a utilizar para transformar processos fibróticos em regenerativos em animais com potencial regenerativo inferior.

Palavras-Chave: *A. cahirinus*, Proliferação, JAK/STAT, PI3K/AKT, Transcritómica

This page was intentionally left blank

Abstract

Epimorphic regeneration in mammals is a rare and poorly understood phenomenon, but for long it has captured human imagination, with the promise of complete recovery from serious injury. For this reason, scientists have spent over a century attempting to understand why in some animal species this characteristic has a much higher potential than in Humans, so that we might recreate it in ourselves.

Lower vertebrates, like salamanders, anurans and teleost fish, are capable of regenerating several tissues and organs to full functionality, including heart, jaw, fins, limbs, etc. Understanding how regeneration is established in response to wounding, in these organisms, has helped us comprehend some limitations in our system, but full comprehension requires the understanding of how these phenomena occur in species closer to us, with which we share, for example, a complex adaptative immune response to injury.

Recently, a few species of cervids and murids have been shown to have the remarkable ability to regenerate antlers and associated tissues, and ear pinnas and dorsal skin, respectively. Furthermore, it was shown that regeneration in these models has a strong relationship with the immune response, and is dependent on MAPK/ERK signaling, something that had also been shown in the regenerative processes of lower vertebrates.

MAPK/ERK signaling is known for controlling several cellular processes, chiefly amongst them proliferation, so it is no wonder that it also does so during regeneration. MAPK/ERK is also known to interact with other intracellular pathways to perform this regulation, chiefly amongst them the PI3K/AKT pathway, which contributes to an integration of other cues, like nutrient availability and presence of stress factors, helping the cell decide its fate.

Despite the indispensability to regeneration, MAPK/ERK signaling overactivation in mammals is only capable of inducing some characteristics of regeneration in a fibrotic wound healing process, but not to fully transform it into a regenerative one. This indicates that other differentially regulated pathways are also likely involved, and a better understanding of how proliferation is regulated in the wound healing events of vertebrates, in particular in mammalian regeneration, is required. Particularly, how the cells, when faced with such stress, make the decision to proliferate, rather than another fate, like programmed cell death, and how the immune system exacts its influence over the process.

To that end, in this work we isolated proliferative cell populations formed during the wound healing response to full-thickness ear pinna punching of two mammalian species, one that mounts a regenerative response, and the other a fibrotic one, and analyzed their transcriptional profiles at several timepoints during the initial phases of wound healing (homeostasis, inflammation and proliferation). By doing this, we observed that despite some scarce similarities, the two proliferative populations mostly represented two wildly distinct responses to wounding.

In particular, the transcriptomic profile of *A. cahirinus* had a strong association with processes involved in energy metabolism and proliferation, while *M. musculus* proliferative cell population transcriptional profiles associated more significantly with processes associated with cytoplasmic dynamics, likely related with migration, and differentiation of several tissues.

While *M. musculus* proliferative regulation primarily associates with MAPK/ERK signaling, *A. cahirinus* transcriptomic profile associated with more signaling pathways, primarily PI3K/AKT, WNT and NF-KB, besides MAPK/ERK. Comparison of transcriptomic profiles also suggested differential involvement of transcription factors in the regulation of proliferation. We also found an association of the transcriptomic profile of *A. cahirinus* with an apoptotic response, and this was not observed for *M. musculus*.

Because, despite distinctive groups of signaling pathways being associated with the response of each species, both responses are known to equally involve some of the same pathways, but have distinct results, we decided to look at how these pathways are set up, and the dynamics of their activation in both species.

We found that it appears that the proportion of mediators and the interactions they establish, in three intracellular pathways, MAPK/ERK, PI3K/AKT and JAK/STAT, known for interacting in the regulation of several cellular processes, particularly proliferation, are not the same between species. For example, *M. musculus* appears to have a preference for activating a particular isoform of ERK, while the same preference is not found in *A. cahirinus*. Furthermore, the temporal dynamics of activation suggest that each isoform has its own dynamic activation, with ERK2 appearing to be an early responder, and ERK1 involved in sustaining proliferation.

As for the PI3K/AKT pathway, we found a consistently higher abundance of activated AKT1 in *M. musculus*, where its activation appears to be particularly increased in the first 12h. Furthermore, the response of this pathway also appears to be bimodal, with an early type of response and a later one, possibly associated with an early induction of apoptosis in *A. cahirinus*

that does not occur in *M. musculus*. This induction might contribute to sustain proliferation, which has been associated with a constant production of mitogens by proapoptotic cells, which can remain in this state for a long time.

In the JAK/STAT pathway, on the other hand, we saw a clear and sustained higher proportion of activated JAK2 in *A. cahirinus*. However, this higher activation did not translate to greatly differing activation levels of STAT3, which suggests to us that JAK2 might have other roles in the wound healing process of these two species. This might constitute a method for proliferative cells, in this context, to integrate immune signals in the regulation of their proliferation, seeing as JAK2 is known to transactivate receptors that operate upstream of the MAPK/ERK and PI3K/AKT pathways, like the ERBB receptors.

Overall, our work points to two very distinct strategies of response to wound healing between regenerative and fibrotic events in mammals, and suggest that this is due not just to a differential response to the same stimuli, but that this differential response actually comes from inherent differences to the setups of several intracellular pathways, which will themselves have different activities between these two types of response.

Further exploration of these pathways and the response of their effectors to the stimuli present in response to wounding will help us understand the set of ideal factors to be able to transform fibrotic processes into regenerative ones in organisms with lower regenerative potentials.

Keywords: *A. cahirinus*, Proliferation, JAK/STAT, PI3K/AKT, Transcriptomics

This page was intentionally left blank

Index

Index of Tables and Figures

1. Introduction

This page was intentionally left blank

Homeostasis in complex organisms like vertebrates is maintained, in part, by the capacity of the organism to replace aged or damaged cells, maintaining tissue and organ structure, functionality, integrity and health. This aspect of homeostasis (replacement of damage cells or tissues) can happen regularly, as a form of continuous or scheduled maintenance, or specifically in response to damage.

Regular renewal of tissues is called physiological regeneration[1]. This type of regeneration occurs in the absence of injury to the tissues and involves the slow and gradual substitution of a subset or all cells within that tissue, usually by cells of the same lineage, generated by resident tissue-specific stem/progenitor cells. Examples of these processes are found throughout all life forms, and in vertebrates they take the form of renewal of epidermis, digestive track lining replacement, replenishment of circulating cells, regrowth of endometrium during the oestrus cycle, and even some more curious examples like the seasonal regrowth of the antlers of cervids[2–4], among others.

Recreation of tissues lost due to injury or damage is called reparative regeneration[1]. Reparative regeneration can be subdivided into two distinct processes: *morphallaxis* and *epimorphosis*[1]. The primary distinction between these two processes is the requirement (epimorphosis), or not (morphallaxis), of cell proliferation. Morphallaxis is characterized by a reorganization and repatterning of neighboring cells of the damaged area, with the intent to occupy the space created by the missing tissue, substituting lost cells, and restoring shape and integrity to the tissue. A good example of morphallaxis is the regeneration of the body of *Hydra spp* upon injury.

Epimorphosis is characterized by proliferation of neighboring cell populations that will repopulate the damaged or missing tissue. This process usually involves progenitor cells of heterogeneous lineages, which will give rise to the types of cells present in the missing tissue. The production and organization of the correct types of cells can occur through the creation of an "informative center", a particular cluster of cells that confer positional and growth cues to a "proliferative region", a somewhat defined area of proliferative progenitor cells, or it can occur without one or the other, in a more "disorganized" fashion[5–8]. While classically the processes of *morphallaxis* and *epimorphosis* were viewed as independent strategies of repairing missing tissue, the current view is that, especially in more complex systems, one does not occur without the other[9].

When a regeneration event occurs in the 'organized' manner described, the organized tissue is referred to as the blastema[7,10]. In a blastema, the informative center is usually composed of a transient informative epithelial tissue and its underlying mesenchymal tissue, where stem/progenitor/dedifferentiated cells organize to proliferate, differentiate and regenerate the missing tissues. An example of this can be found in the regeneration of limb and tail of *A. mexicanum*, which are also characterized by, among other things, the deposition of pro-regenerative extracellular matrix and the existence of pro-regenerative nerve-derived signals[5]. On the other hand, examples of regenerative processes that do not require the formation of a blastema are the regeneration of the eye lens in newt[11], the regeneration of the ventricular apex of the zebrafish heart[12] and the regeneration of spiny mouse dorsal skin[5], among others. These are also examples of regenerative processes that involve both *epimorphosis* and *morphallaxis*.

As previously mentioned, all vertebrates perform regenerative processes, and these processes are vital for the maintenance of homeostasis. However, the vertebrate taxon has a great degree of variability of regenerative potential within it. For instances, the Amphibian class includes a larger number of taxa with very high regenerative potential, while the Mammalia class mostly contains species of much lower regenerative potential[1,10,13–15] (Figure 1.1).

One reason that might explain why the Mammalia class evolved towards a smaller regenerative potential is the cost/effectiveness ratio of a regenerative event[16]. As body size and life expectancy increase, nutritional requirements also increase, and the nutritional requirements for recreating larger organs make regeneration more energetically costly, and therefore less evolutionarily advantageous for larger animals. Either a large animal can function without the missing organ or tissue (and continues to forage for the necessary nutrients for survival) or it cannot, and redirecting energy destined for the pursuit of sustenance to the regrowth of missing tissue results in its demise. Possibly for this reason, animals who developed the capacity to quickly recover the integrity of their organism with minimal loss of energy (by scarring) acquired an evolutionary advantage over others, who responded to injuries with energetically costly regenerative events.

Furthermore, in almost all events of vertebrate regeneration, replacement of missing tissue or cells involves cell proliferation. Cell proliferation is a complex and sensitive process which requires several rearrangements of the genomic and cytoplasmic material of the cell. While this process is highly regulated, each replicative iteration exposes the cell to the risk of genomic alterations. One possible consequence of those alterations is oncogenic transformation, an event

with high risk to the organism. Perhaps because of this more complex organisms, with longer lifespans that could be subject to more instances of regeneration and that require the production of a larger number of cells to substitute the missing tissues, might have evolved limitations to repeated reentries into the cell cycle during the adult phases of their life cycles, thus leading to a decrease in regenerative potential.

Understanding how differences in proliferative potentials among vertebrate species are established might help us clarify the evolution of regeneration and, from a translational point of view, allow us to develop strategies to create a greater regenerative potential in Humans.

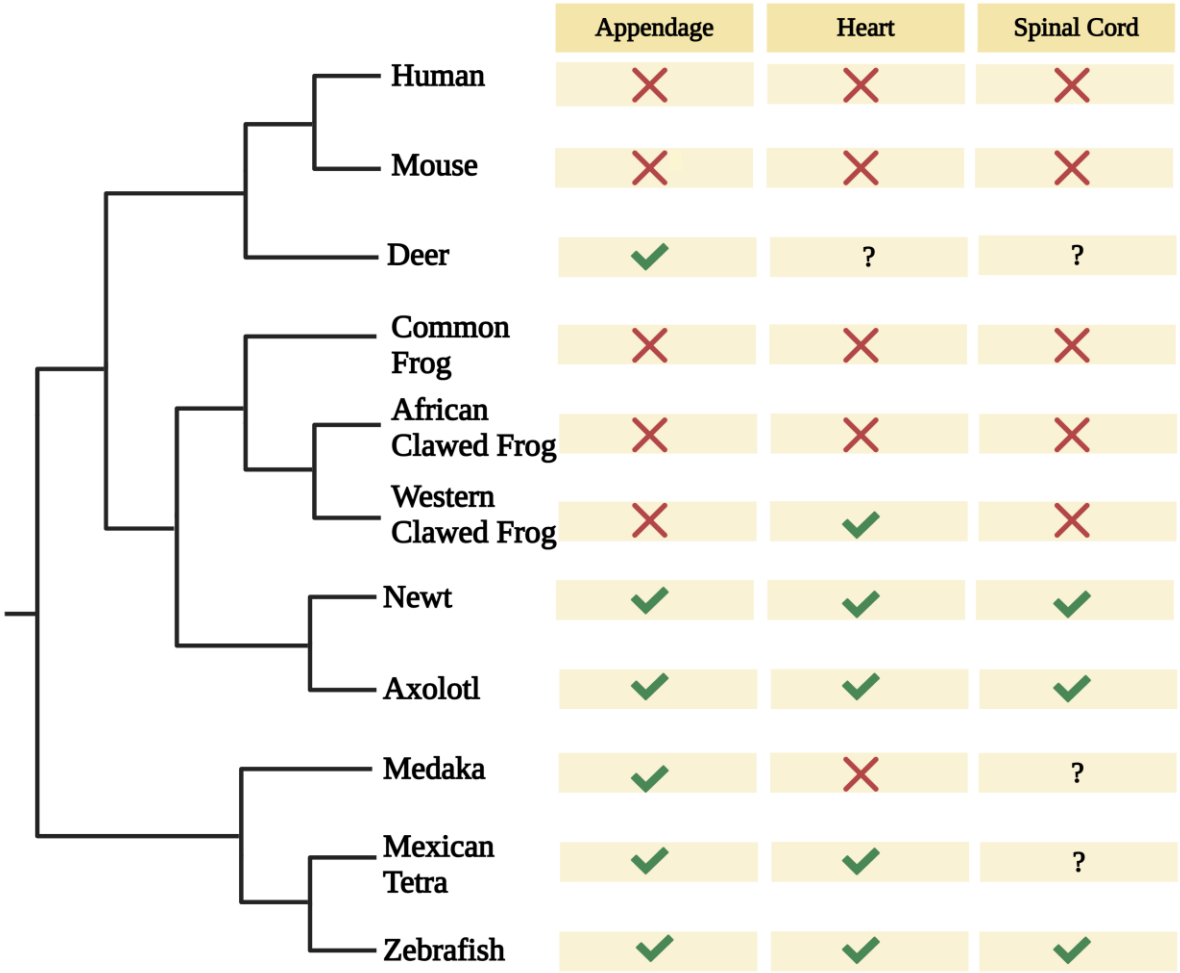

Figure 1.1 - Distribution of the regenerative potential across several models of vertebrates. This figure represents the phylogenetic relations of several regenerative vertebrate models, as well as their respective (known) regenerative potentials. Adapted from Khyeam, Lee and Huang, 2020[15] *and created with BioRender.com.*

This page was intentionally left blank

1.1. Wound Healing: Close or Recreate?

As pointed out before, the vertebrates vary greatly in their regenerative potential. Organisms like *Danio rerio, Oryzias latipes*, *Ambystoma mexicanum, Notophthalmus viridescens* and *Cynops phyrrogaster*, belonging to the Osteichthyes and Amphibian classes, are capable of regenerating a relatively larger range of tissues than other vertebrates, resulting in a near flawless reconstruction of adult organs like limbs, tails, fins, retinas, heart, brain, spinal cord, kidney, liver, among others[7,15,17–19].

In sharp contrast, in mammals, the majority of injuries result in an exacerbated inflammatory process that inhibits the proliferation of most cell types, leading to the formation of the fibrotic scar: a replacement tissue devoid of its original function and organization, composed of fewer cell types and with a simplified, more restrictive, extracellular matrix.

Why do we see these divergent responses in vertebrate groups? They share similar designs and developmental processes, and are injured by similar kinds of events, and yet, their wound healing response is quite different[20]. To understand why this occurs, we need to identify the key players in wound healing, and which might differ.

Wound healing is usually described as a set of four distinct, albeit overlapping, phases. These phases are Hemostasis, Inflammation, Proliferation and Remodeling. Each phase encompasses a complex system of cellular communications and interpretation of external cues, and alterations to the system can significantly impact the end result. In the next sections, we will briefly summarize each of these phases, and highlight what differences between reparative and regenerative events are known for each phase.

This page was intentionally left blank

1.1.1. Hemostasis

The wounding of an organism is regularly associated with a disruption of its external barrier. Given extensive vascular networks, wounds suffered by a vertebrate organism almost allways result in blood vessel damage and extrusion of blood. For this reason, evolution has selected for immediate and powerful reactions to quench blood loss. This is achieved, in vertebrates, by the quick formation of a thrombus, composed primarily of platelets (or cells with similar roles, like thrombocytes), red blood cells and extracellular matrix.

Platelets are anucleated circulating cells derived from polyploid megakaryocytes residing in the bone marrow. When circulating platelets attach, they become activated and start to aggregate, degranulate and coagulate. In healthy organisms this only occurs when there is blood vessel damage, and exposure of the subendothelial extracellular matrix (ECM).

The ECM present in the subendothelial space of blood vessels is rich in collagen I and III, von Willibrand factor, fibronectin and laminin. Its exposure reduces the inhibitory effect endothelial cells have on platelet coagulation[20–23], allowing platelets to adhere to the ECM through glycoprotein receptors like integrin α2β1 and GPVI, which strongly bind to collagen and von Willebrand factor [20–24].

Integrin αIIIbβ3 allows activated platelets to bind fibrinogen, which exists in circulation but is also released by activated platelets[25]. Through binding of fibrinogen, fibronectin and vWF, platelets form stable and resistant bridges between each other, forming a platelet plug. These attachments also create an "outside-in" set of signals that consolidates aggregation, making it irreversible[20–23,26,27]. This activation and aggregation of platelets constitutes what is called the Primary Hemostasis.

Platelet activation also results in their degranulation. Platelets contain three types of granules: α-granules, the dense granules and lysosomes. Their exocytosis releases several factors, like calcium, fibrinogen, von Willebrand factor, thromboxane A2, PF4, tissue factor (TF), and Factor V to the extracellular space, which also contributes to further activation of neighboring platelets[21–23,28–30]. Basic information regarding some of these factors can be found in Table 1.1.

Secondary hemostasis involves triggering of the coagulation cascade[32]. Mediated by Tissue Factor (TF, also called thromboplastin or CD142) coagulation results in the platelet plug being stabilized by an expanding fibrin mesh, which strengthens the barrier created and allows platelets to modify the size of the wound.

Table 1.1 - Contents of α-granules of platelets. Summarized in this table are the most relevant components of platelet α-granules secreted during platelet degranulation, and their functions in the hemostatic process.

Category	Proteins	Function
Adhesive Proteins	VWF, Fg, FN, VN, TSP1	Cell contact, hemostasis and clotting, ECM assembly
Membrane Glycoproteins	αIIβ3, αVβ3, GPIb, PECAM1, CD40L, TF, P-selectin	Platelet aggregation and adhesion, inflammation regulation, thrombin generation
Clotting Factors	FV/Va, FXI, Multimerin, Protein S, HMWK, Antithrombin III, TFPI	Regulation of thrombin production
Fibrinolytic Factors	Plasminogen, PAI-I, u-PA, TAFI	Production of plasmin and modelling of vasculature
Proteases and Inhibitors	TIMPs 1-4, MMP1/2/4/9, ADAMTS13, TACE, platelet inhibitor of FIX	Regulation of coagulation, angiogenesis and cellular behavior
Inflammatory mediators	RANTES, Il8, MIP1α, MCP3, Angiopoietin1, IGFBP3, Il6sR, PF4, βTG, HMGB1, FasL, TRAIL, SDF1α	Adhesive Proteins
Growth factors	PDGF, TGFβ1/2, EGF, IGF1, VEGFA/C, FGF2, HGF, BMP2/4/6	Chemotaxis, cell proliferation and differentiation

TF is primarily located extravascularly, being constitutively expressed in several cell types, like fibroblasts, pericytes, smooth muscle cells, epithelial cells, astrocytes, and cardiomyocytes[33]. In the presence of phosphatidylserine, membranous TF binds to small amounts of factor VIIa, released by activated platelets and in circulation, and forms the extrinsic tenase complex, which is activated by the extracellular presence of calcium, released by activated platelets[22].

Despite initially existing in low levels, extrinsic tenase is responsible for the initiation phase of coagulation, through activation of factor X and IX. Activated factor X (Xa) can further enhance factor VIIa availability by activating it, thus amplifying its own activation. This creates a positive feedback loop that quickly and greatly enhances the levels of FXa and FVa[22]. Together, these two factors constitute the "prothrombinase" complex, which is responsible for the cleavage of prothrombin into thrombin[29].

Thrombin is responsible for cleaving circulating fibrinogen into fibrin. This allows activated platelets to adhere to fibrin and create a large fibrin mesh. Thrombin further contributes to the formation of the fibrin mesh through factor XIII activation. FXIII is responsible for cross-

linking fibrin molecules, thus stabilizing the fibrin mesh. Another way thrombin contributes to the formation of the fibrin mesh is through inhibiting its degradation. Thrombin activates Thrombin Activatable Fibrinolysis Inhibitor (TAFI), protecting the clot from fibrinolysis. This fibrin mesh, together with the previously assembled provisional ECM, will be of great importance to the subsequent steps of wound healing, as we will see further on[20,21,29,30,44,45].

1.1.1.1. Hemostasis in Regeneration

While platelets are essential for hemostasis to occur competently, they do not seem indispensable for wound healing, as observed in experiments in mice with thrombocytopenia. These mice show an increase in macrophage and T cell invasion of the wound, but no changes in growth factor levels, rate of wound re-epithelialization, collagen synthesis or levels of angiogenesis when compared with healthy mice[36].

Despite not being indispensable for wound healing, platelets and platelet-derived products have been tested has enhancers of the reparative/regenerative capacity of several systems[21,37,38]. This has, in part, been associated with the angiogenic potential of platelets, since their α-granules are rich in growth factors (Table 1.1), and several of them potentiate angiogenesis. Furthermore, other factors contained in α-granules, like SDF-1α and PDGF, are involved in the recruitment and proliferation of some cell types[21,28,37–39]. Therefore, platelets might play a yet unidentified role in shaping the initial steps of wound healing, and the decision between reparative or regenerative wound healing.

Wound healing during the fetal phases of *in utero* development is considerably different from the process that occurs in adult individuals[40]. Fetal wound healing is usually scarless, faster, and almost always regenerative. For this reason, it has been the focus of many studies in the hope of replicating the fetal wound healing capacity in adults[40,41].

Despite the focus on studying fetal wound healing, very little attention has yet been given to the role platelets have in it. It is known that fetal platelets degranulate and aggregate less in response to injury, and also produce less PDGF, TGFβ1 and 2[42,43]. The transition from these characteristics of fetal platelets to the adult platelets occurs at the same time as the transition from scarless to scarring wound healing, and these factors have been associated with a more acute inflammatory response and pro-fibrotic healing[44,45], suggesting that these changes in platelet function might influence the outcome of the wound healing process[41].

It has also been shown that in neonates, fibrin network is composed by the 'fetal' version of fibrin, which produces a more porous, less three-dimensionally complex structure, composed of aligned fibers instead of highly crosslinked[46,47.] This fibrin network has also been demonstrated to have an increased rate of degradation, favoring fibrinolysis. Changes in platelet function and secretion might influence the onset of the subsequent phase, inflammation.

In lower vertebrate regenerative models, like *Ambystoma*, platelets are absent. In their stead, amphibians contain thrombocytes, a cell type that seems to participate in wound healing in the same fashion as platelets in mammals[48]. While the roles of thrombocytes have not been extensively dissected in wound healing and regenerative response, a clearer picture of differences between these cells and mammalian platelets, and of the role of these cells in amphibian regeneration, might yield important insights into therapeutic strategies.

This page was intentionally left blank

1.1.2. Inflammation

The immune response of vertebrates, when triggered by a lesion to tissues, begins with an immediate response of sensory neurons and tissue-resident immune cells. Antidromical transfer of action potentials among sensory neurons promotes the release of substance P and CGRP (Calcitonin Gene-Related Peptide), which will contribute to vasodilation, blood flow increase, vascular permeability, leukocyte recruitment and mast cell degranulation[49,50]. The release of histamine and serotonin will further increase the surrounding microvasculature permeability and the extrusion of other inflammatory cell chemoattractants from neighboring cells[51,52].

Mast cells are tissue-resident immune cells derived from the myeloid lineage and are known for their involvement in immune tolerance and allergies. When damaged, these cells quickly release inflammatory cytokines, vasodilatory and permeating agents, as well as other proteases that contribute to a strong recruitment of circulating immune cells to the wound.

At the same time, invasion of the wound by platelets, and their degranulation, contributes to the enrichment of the environment with more inflammatory modulators. Besides contributing to the formation of the thrombus, platelet granules are rich in growth factors (PDGF, TGFβ1, VEGFA, FGF2, etc.) and cytokines (RANTES, Il8, Il6sR, PF4, etc.)[53–60], as detailed in Table 1.1. Exocytosis of platelet granules releases these paracrine factors, and more, to the extracellular environment, leading to an accumulation of chemoattractants that will recruit cells like granulocytes, fibroblasts, B cells, T cells, among others[62,63].

The formation of the provisional matrix associated with the thrombus also contributes significantly to the recruitment of immune cells. Both components of the extracellular matrix, like collagens and glysoaminoglycans, and the fibrin network itself, can bind the growth factors and cytokines released by platelets, endothelial cells and tissue-resident immune cells, establishing a chemotactic gradient that contributes to further cell recruitment and migration[21].

Due to the fast response of platelets, mast cells, resident macrophages and the release of several damage markers from damaged cells in the tissue, the wounded region of the tissue quickly becomes enriched in Damage-associated molecular patterns (DAMPs), Pathogen-associated molecular patterns (PAMPs), hydrogen peroxide and chemokines, which start to recruit neutrophils and monocytes to the wound area[20,63,64].

1.1.2.1. Neutrophils

Neutrophils are granulocytes from the myeloid lineage, like mast cells, that are produced in the bone marrow and recruited to tissues exhibiting signals of infection or damage[20,63,64]. They are the most abundant leukocyte in adults and are a greatly important player in wound debridement and infection clearing, due to releasing toxic granules, producing an oxidative burst, and by its phagocytic capacity and the production of neutrophil extracellular traps (NETs). The role in tissue debridement that neutrophils perform is of great importance, as their removal tends to exacerbate the pathology of the tissue[65].

Neutrophils are the principal effector cells in the initiation of the inflammatory phase, recruited to the location of injury or infection by the factors released from platelet and mast cell degranulation, and N-formyl peptides released by bacteria and damaged cells[64,66,67]. Stimulation of pattern recognition receptors (PRR), like Toll-like receptors, C-type lectins, cytosolic NOD-like receptors and RIG-like receptors, informs neutrophils of the occurrence of an injury or infection. Once neutrophils in circulation arrive at the wounded region, they bind to the endothelium through adhesion receptors, like selectin/selectin ligands and integrins, and follow the leukocyte recruitment cascade, which is depicted in Figure 1.2: tethering, rolling, adhering, crawling and transmigrating to the inflamed tissue.

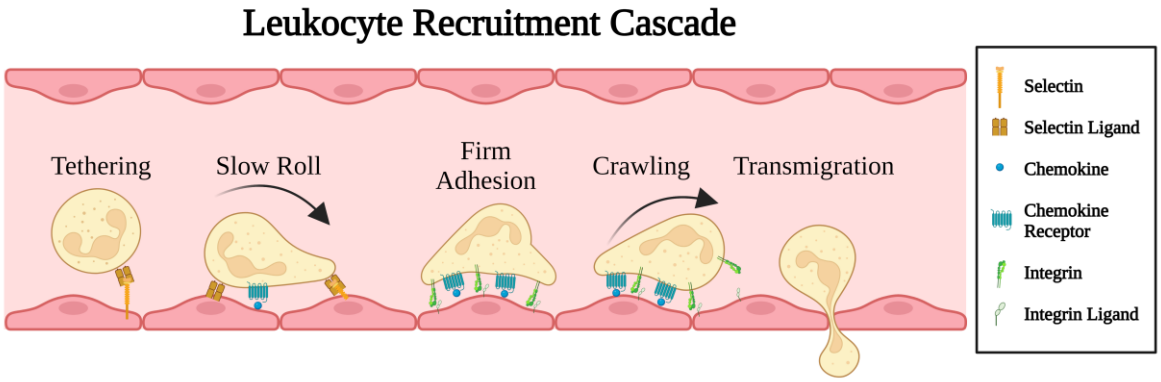

Figure 1.2 – Leukocyte recruitment cascade. Depicted are the five principal stages of the leukocyte recruitment cascade, as observable in neutrophils, as well as some of the principal types of receptors and ligands involved in the process. Adapted from Kolaczkowska and Kubes 2013[63] and created with BioRender.com.

Complete activation of neutrophils is a two-step process that is initiated with their priming by pro-inflammatory cytokines, like TNFα and Il-1β, or by activation of the cell surface receptors just mentioned. After this priming, exposure to PAMPs, growth factors or other chemoattractants completes the neutrophil activation[68].

On the day after injury, neutrophils can make up to 50% of the cells in the wound site[69,70]. This is considerably helped by the capacity that activated neutrophils have to expand their presence

on the tissue in time and number, by producing and releasing more neutrophil-recruiting chemoattractants[64]. They do so, for instance, by producing and releasing Il-17, which stimulates mesenchymal and myeloid cells to release several pro-inflammatory factors that recruit and activate neutrophils. Neutrophils also produce LTB4 and several cytokines, which also contribute to the recruitment of more neutrophils[71,72]. A summary of the chemokines, cytokines, growth factors, and other inflammatory mediators and chemoattractants released by neutrophils can be found in **Error! Reference source not found.**.

Table 1.2 - Cytokines, growth factos and other chemoattractants released by neutrophils. This table lists the known cytokines, chemokines, growth factos and other chemoattractants produced and released by Human neutrophils. Some diferences might exist in relation to other mammals. Adapted from Mantovani et al., 2011[72]

Neutrophil-secreted immunomodulatory factors (Human)								
CXC - Chemokines	CC- Chemokines	Pro-Inflammatory Cytokines	Anti-Inflammatory Cytokines	Immunoregulatory Cytokines	Colony-stimulating Factors	Angiogenic and Fibrinogenic Factors	TNF Superfamily Members	Other Cytokines
CXL1, CXL2, CXL3, CXL4, CXL5, CXL6, CXL8, CXL9, CXL10, CXL11	CCL2, CCL3, CCL4, CCL17, CCL18, CCL19, CCL20, CCL22	Il1 (α&β), Il6, Il7, Il9, Il16, Il17A, Il17F, Il18, MIF	Il1RA, Il4, Il10, TGFβ1, TGFβ2	IFNα, IFNγ, Il12, Il23	G-CSF, M-CSF, GM-CSF, Il3, SCF	HB-EGF, HGF, FGF2, TGFα, VEGF, Prokineticin2	APRIL, BAFF, CD30L, CD95L, LIGHT, LTβ, RANKL, TNF, TRAIL	Amphiregulin, BDNF, Midkine, NGF, NT4, Oncostatin M, PBEF

Mounting evidence suggests the existence of a few subtypes of neutrophils. In an experiment of inflammation response in tissue, a pro-inflammatory subtype, responsive to the pro-inflammatory chemokine CXCL2, that is characterized by the receptor phenotype $CD11b^{+}Gr\text{-}1^{+}CXCR4^{Low}$, and a pro-angiogenic subtype, responsive to VEGFA and characterized by high expression levels of MMP9 and CXCR4, were identified[63,73].

Other types of studies, in the area of auto-immune diseases and of cancer, for instances, have also suggested the existence of more than one subtype of neutrophil[74–76]. Particularly, the two subtypes suggested in cancer, N1 and N2, share some similarities with the two previously described. The N1 subtype has a direct antitumor effect, promoted by ROS production, and can activate $CD8^{+}$ T cells and dendritic cells (DCs), while N2 neutrophils have a more pro-angiogenic behavior, and facilitate cancer development through extracellular matrix remodeling, promotion of angiogenesis and immunomodulation[77].

Besides increasing their own recruitment, neutrophils also facilitate the recruitment of several other cell types. Proteins released from neutrophil granules, like azurocidin, LL37 and cathepsin G, promote and shape monocyte recruitment through activation of their formyl-peptide receptors, which allows monocytes to adhere to the endothelium and extravasate[78,79]. Neutrophils also condition endothelial cells to attract monocytes by shedding IL-6 and its soluble receptor (sIL-6R), which leads to a gp130-mediated endothelial activation, resulting in the expression of adhesion molecules, like VCAM1, and monocyte chemoattractants, like

CCL2[90]. Neutrophils are also capable of attracting monocytes through the release of 'find me' signals after becoming apoptotic. Monocytes will phagocyte these apoptotic neutrophils, contributing to the resolution of inflammation and promoting tissue repair[81].

It has also been shown that neutrophils, at least in humans, are a major source of cytokines crucial for the survival, maturation and differentiation of B cells, like BAFF19 and APRIL, as well as other B cell stimulating molecules, like TNFSF13B and CD40L, that promote IgM and IgG secretion[82].

The interaction of neutrophils with cells of the adaptative immune system is not limited to B-cells. In fact, interactions with T cells have been more thoroughly described and appear to be an important method of immune modulation during the inflammatory phase. The same neutrophils that were shown to be crucial to B-cell survival and maturation were also demonstrated to express T cell-supressive factors, like arginase 1 and iNOS.

It has also been shown that activated neutrophils can attract Th1 and Th17 cells by releasing CCL2, CXCL9, CXCL10 and CCL20, depending on the combination of released factors[83]. Neutrophils can also act as antigen-presenting cells (APCs), operating as alternative sources of primed $CD4^+$ and $CD8^+$ T cells, like Th1 and Th17 cells[94]. They also produce IFNγ, which promotes adaptative immunity through effects on MHC expression and T helper cell development[85–88]. A summary of the interactions of neutrophils with other cells of the immune system can be found in Figure 1.3.

Neutrophils also contribute to the recruitment of other inflammatory cells by reshaping the extracellular matrix (ECM). Release of granules containing proteases, like cathepsin G, elastase and protease 3, help shape the extracellular environment by breaking down the elastin, fibronectin, vimentin, laminin and Collagen IV matrices[89]. Besides degrading the ECM, enzymes like MMP9, which are produced by neutrophils, also degrade the intracellular matrix (ICM), including actin, tubulin, annexin 1 and HMGB1, promoting the removal of DAMP-containing ICM from damage cells[90].

Prolonged presence of neutrophils in the wound results in an accumulation of proteases and high protease activity. This ultimately leads to cleavage of growth factors and their receptors, excessive ECM degradation, impairment of vascular processes and blood flow, and increased tissue damage[91]. Therefore, timely resolution of inflammation is extremely important for the future health of the tissue.

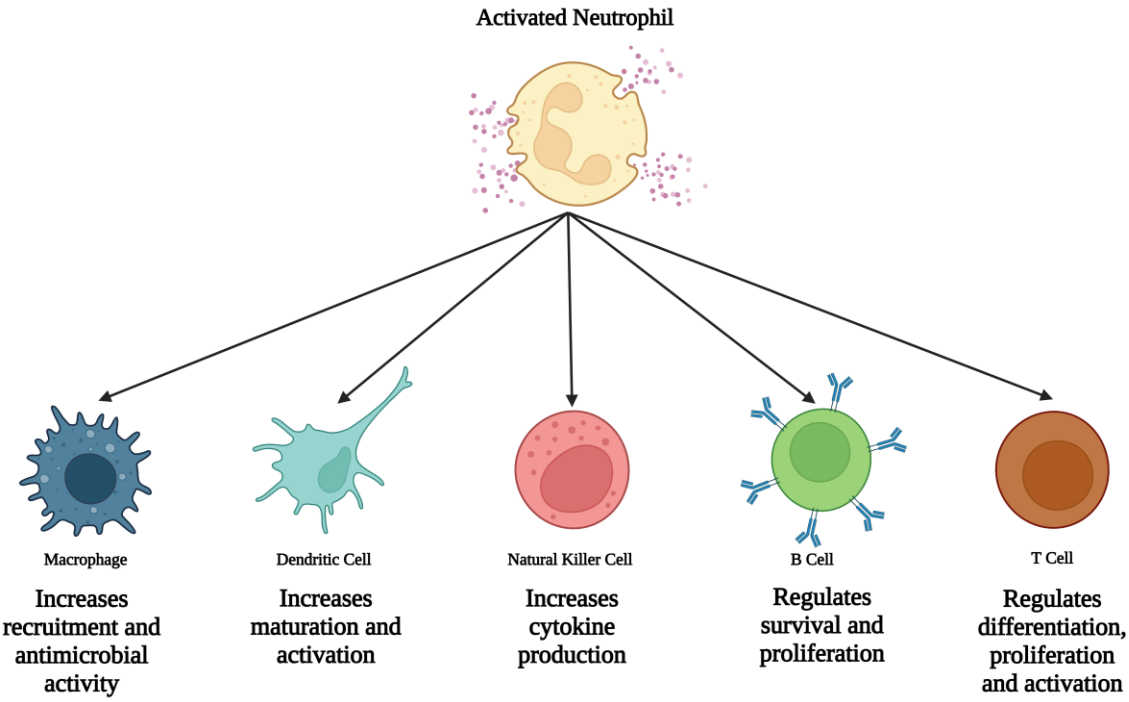

Figure 1.3 – Main neutrophil interactions with other immune cells. This image depicts the results of neutrophil interactions wih other cells of the immune system. This image was adapted from Mantovani et al., 2011[64] *and created with BioRender.com.*

Resolution of inflammation is a complex process that can be divided into two phases: Anti-inflammatory and pro-resolving[92]. The anti-inflammatory phase involves the release of anti-inflammatory mediators, like Il-10, and the inhibition of the NF-κB signaling pathway. The release of cytokine and chemokine receptor antagonists, like Il-1RA or soluble forms of the receptors, also helps to limit neutrophil recruitment.

During the late phases of inflammatory response, during the pro-resolving phase, neutrophils stop producing LTB4 and begin to produce LXA4, which inhibits neutrophil recruitment through the receptor LXA4R. Neutrophils also produce resolvins and protectin D1, which inhibit their transmigration and tissue infiltration by blocking LTB4 receptors[93–97].

They also influence the resolution of inflammation by blocking and scavenging pro-inflammatory chemokines and cytokines, like Il-1[98–100]. Lipid mediators such as LXA4, resolvin E1 and protectin D1 increase the expression of CCR5 in apoptotic neutrophils, which then act like decoys and scavengers for CCL3 and CCL5. The receptor Il-1R2 is also expressed at high levels in neutrophils, which is increased by anti-inflammatory signals like glucocorticoid hormones, and acts as a decoy receptor for Il-1, preventing Il-1R1 activation. Neutrophils that have been stimulated by anti-inflammatory cytokines like Il-10 are also a major source of Il-1Ra, a soluble form of Il-1 that binds and blocks Il-1R1, without activating it[101].

Besides inhibition of recruitment and alteration of neutrophil profiles, inflammation resolution requires their removal from the inflamed area[102]. Clearance of neutrophils occurs by apoptosis or necrosis, and engulfment by macrophages. Lack of engulfment by macrophages results in neutrophil lysis, and release of pro-inflammatory and cytotoxic molecules to the tissue, resulting in further damage.

1.1.2.2. Macrophages

Two to three days after injury, the chemokines and other pro-inflammatory factors released by mast cell and platelet degranulation, neutrophils, and in response to increased hypoxia-induced factors, like TGFβ, PDGF and CXCL12, as well as leftover pieces of the collagen, fibronectin and elastin extracellular matrix, will attract monocytes to the wound site[67]. Once inside the wound site, monocytes release cytokines and chemokines that will contribute to the recruitment of more neutrophils[67,70], whose degranulation will promote further recruitment of inflammatory monocytes. These will mature into macrophages, phagocyting pathogens, neutrophils and tissue debris[103,104]. This crosstalk between neutrophils and monocytes/macrophages is a key component of the wound repair, as they will cooperate all throughout the inflammatory phase of the wound healing event[105].

Macrophages can be subdivided into two subpopulations that have distinct characteristics and functions: The classically activated, or inflammatory, M1 macrophage and the alternatively activated, or anti-inflammatory, M2[106]. The phenotypes of these two subpopulations are plastic, being influenced by the environmental stimuli and responses of other macrophages, which have the capacity to condition and/or define their phenotypes, a process called 'macrophage polarization'[107–109].

The M1 phenotype is usually induced by cytokines like IFNγ and TNF-α, or through recognition of bacterial signals like LPS, and is characterized by a high production of pro-inflammatory cytokines, like TNF-α, Il-1 (α and β), Il-6, Il-12, Il-18, Il-23, Il-27 and COX-2, and the Th1 cell-attracting chemokines CXCL9, CXCL10 and CXCL11[110–113]. These macrophages are responsible for initiating the inflammatory response and participate in the removal of pathogens from the tissue, through production of nitric oxide, reactive nitrogen species (RNS) and activation of the NADPH oxidase system, which leads to the generation of ROS, and promote cytotoxic adaptative immunity by upregulating MHC class II molecules and the co-stimulatory molecules CD40, CD80, CD86. The activity of M1 macrophages can, therefore, impair wound healing and tissue regeneration, and this is balanced by the activity of M2 macrophages, which decreases the damaging effects of M1 activity[107,114].

The anti-inflammatory M2 phenotype is induced by Il-3, Il-4, Il-10, Il-22 and Il-33. Il-3 and Il-4 are recognized by Il-4Rα and Il-10 is recognized by Il-10R, which leads to STAT6 or STAT3 activation, respectively, promoting M2 polarization[112,115,116]. M2 macrophages have an anti-inflammatory cytokine profile, characterized by low production of Il-12 and high production of

Il-10 and TGFβ. They also express high levels of endocytic receptors, including the scavenger receptors CD163, Stabilin-1, CD206, CD301, Dectin-1 and CD209, and recruit Th2, regulatory T cells (Tregs), eosinophils and basophils through secretion of CCL17, CCL18, CCL22 and CCL24[113,117]. Unlike M1 macrophages, M2 macrophages do not produce Nitric Oxide (NO). They instead express high levels of Arginin-1, that plays a role in polyamine production, which are necessary for collagen synthesis, cell proliferation and tissue remodeling[118,119].

M2 macrophages can be further subdivided into four subsets[120–123]: M2a are polarized by Il-3 and Il-4 and present high levels of CD206, the Il-1 decoy receptor II (Il-RII) and the Il-1 receptor antagonist (Il-1RA). M2b are activated by immune complexes (ICs), Toll-like receptor agonists and Il-1R ligands, and produce both pro- and anti-inflammatory cytokines, like Il-10 and Il-1β, Il-6 and TNF-α. M2c are induced by glucocorticoids and Il-10, and exhibit strong anti-inflammatory activities against apoptotic cells, through the release of Il-10 and TGFβ. The final subset of M2 macrophages, M2d, are polarized by Toll-like receptor agonists through the adenosine receptor, which is followed by suppression of pro-inflammatory cytokine release and induction of the release of anti-inflammatory cytokines and VEGF, which confers these macrophages pro-angiogenic characteristics. The different subsets of macrophages, their polarizers and products are summarized in Figure 1.4.

The M2 subpopulations are essential players in the resolution of inflammation through phagocytosis of debris, damaged and dead cells, and apoptotic neutrophils[124–126]. This activity reduces the production of inflammatory cytokines, like TNF-α and Il-1β, 6 and 8, in M1 macrophages through a mechanism involving autocrine or paracrine stimulation with TGFβ, which also leads to a decrease in monocyte and macrophage recruitment. The phagocytosis of apoptotic cells also promotes the production of the anti-inflammatory cytokine Il-10, while inhibiting the pro-inflammatory cytokines Il-12, 23 and 27.

Indeed, the efferocytosis of neutrophils triggers an anti-inflammatory phenotype in macrophages, which transition from the M1 phenotype to the M2[102,125,125,128]. A delay in neutrophil efferocytosis, due to low influx of macrophages or other, leads to inefficient removal of DAMPs, extending the inflammatory phase and delaying the onset of the proliferative phase. This can result in the presence of macrophages and apoptotic cells even during the remodeling phase, with serious consequences to the pathology of the healing tissue[129,130].

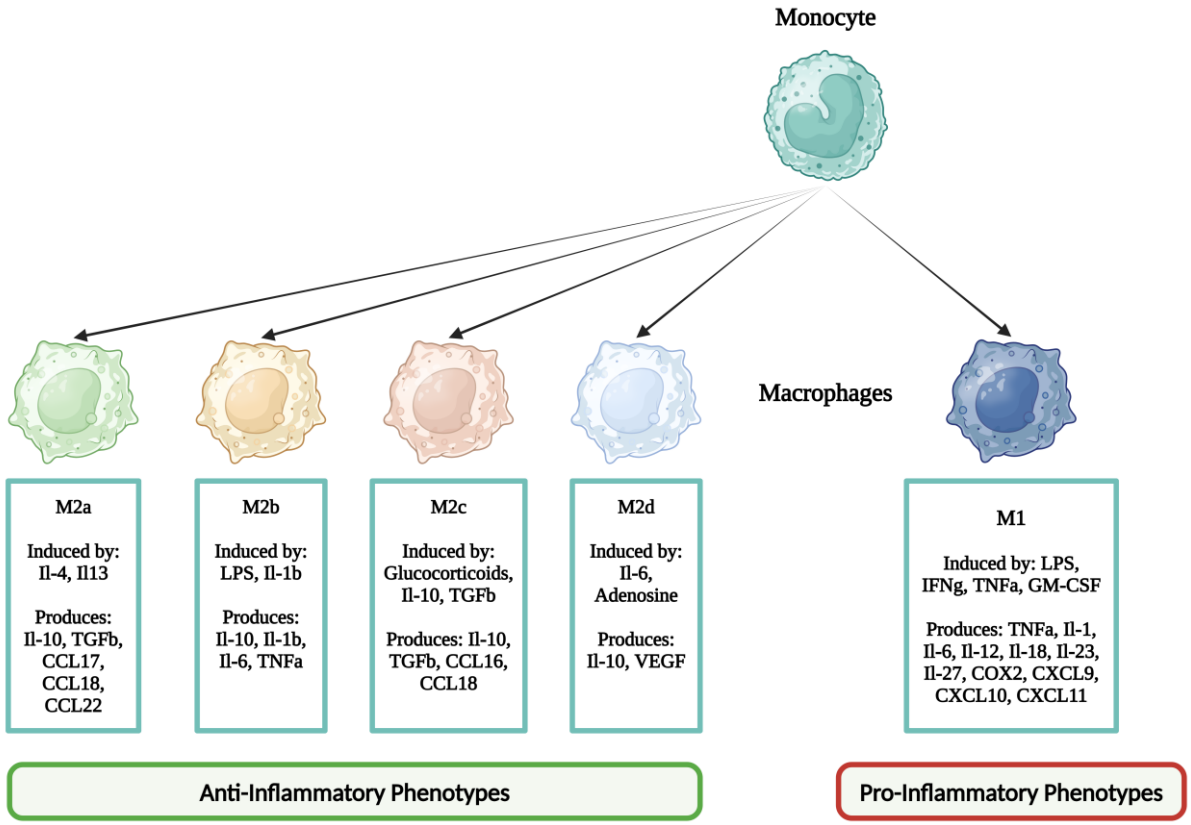

Figure 1.4 - Macrophages and their subsets. Depicted in this figure are the different types of macrophages, and in particular the M2 subclasses, as well as the mediators they produce, and which induce their differentiation. This image was adapted from Pérez and Rius-Pérez, 2022[1395] *and created with BioRender.com.*

Under homeostatic conditions, normal blood flow insures a correct oxygenation of the tissues. Upon injury, due to vasoconstriction and hemostasis, proper oxygenation of the tissue is compromised, creating a hypoxic environment. Macrophages adapt to this hypoxia by shifting their energetic metabolism towards glycolysis. Also, activation of Hypoxia-Inducible Factor (HIF) 1 and 2 leads to significant functional changes, like the production of CXCR4, CXCL12, angiogenic factor and VEGF[118,119].

M1 macrophages metabolism tends to shift towards the anaerobic glycolytic pathway, since these macrophages are usually associated with acute infections and are required to quickly mount a robust anti-microbial response in a hypoxic microenvironment. As such, IFN-γ and LPS stimulation induce a strong glucose uptake, while suppressing fatty acid metabolism[131–133].

M2 macrophages, in turn, do not tend to adapt to a hypoxic environment, since their functions associated with wound healing require a more sustained supply of energy, which is best provided by the oxidative metabolism of glucose and/or fatty acids. These macrophages tend

to have higher mitochondrial activity and oxidative phosphorylation. For this reason, they also tend to appear in the wounded tissue later.

Initially, macrophages found in the wound site are primarily M1 macrophages, since they have the capacity to operate in hypoxic conditions and are essential for the removal of microbial invaders[134]. They are also responsible for ECM reshaping, which results in the creation of DAMPs that exacerbate the pro-inflammatory state of the wound[135]. These DAMPs are recognized by Toll-like receptors on the membranes of other macrophages, activating classical inflammatory pathways[136].

Macrophage numbers usually peak around day 3 post injury, and this high number is maintained approximately until day 5, when their levels start to decrease, until they reach baseline levels by day 10[137]. Like neutrophils, macrophages also contribute to the increase in their number through recruitment of more monocytes to the wound site. This is achieved through the stimulation of a heightened production of Monocyte chemoattractant protein 1 (MCP1), which is mainly secreted by activated fibroblasts, endothelial cells, vascular smooth muscle cells, T cells and other monocytes[138,139]. MCP1 activates chemotaxis responses in monocytes, through the CCR2, which migrate towards the site of injury. MCP1, together with Il-8 or CXCL8, also induces a firm adhesion response in monocytes to vascular endothelium, helping them transmigrate from the blood vessels.

Mature macrophages produce several important growth factors and cytokines, like TNFα, IL-1, FGF, PDGF, etc., that will attract and stimulate fibroblasts, myofibroblasts and endothelial cells to invade, and proliferate in, the wound area. M2 macrophages that express the surface marker Tie2, in particular, also contribute to new vessel formation by branching endothelial vessels and connecting them to the systemic vasculature, in a process called ‘vascular mimicry’, as well as produce and release VEGF that stimulates blood vessel sprouting[140–144].

1.1.2.3. Adaptative Immunity

Another important partner of macrophages in wound healing and immune responses are the dendritic cells (DCs), which in the skin exist as Langerhans cells. These cells share several characteristics with macrophages, including their phagocytic activity, surface markers and response to the same growth factors, but their primary distinction is a weaker antigen-presenting capacity of the first. When DCs identify an antigen, they will present it to T cells in the wounded tissue, but also migrate to the draining lymph nodes, where they will continue to activate T cell responses[145].

In the murine species, two subtypes of resident DCs have been found, the $CD11b^+$ and the $CD103^+$[146–149]. The $CD103^+$ subtype is also Langerin positive, and they are responsible for cross-presenting antigens to induce $CD8^+$ T cell responses. They are also responsible for identifying dead cells, by detecting F-actin and other DAMPs through the CLEC9A receptor, and viral infections through the TLR3, which identifies dsRNA (typical of viral infections). The $CD11b^+$ subtype preferentially present antigens to $CD4^+$ T cells, but they can also present to Treg cells to dampen the immune response[150,151].

Langerhan cells are derived from early myeloid progenitors (EMPs) that migrate into the epidermis during embryonic develop and persist in the tissue into adulthood, if stimulated by signals from neighboring keratinocytes[152,153]. They are recognizable by their characteristic surface receptor CD207, or Langerin. When these cells recognize an antigen, they downregulate E-Cadherin, which maintains their contact with keratinocytes, and migrate from the epidermis to draining lymph nodes, to initiate the T cell-mediated adaptative immune response[154,155].

Macrophages and DCs are the primary activators and recruiters of adaptative immune cells. Early after wounding, tissue-resident macrophages and DCs respond to DAMPs and PAMPs by internalizing and digesting them. Fragments of these digested molecules are then used as antigens to activate the adaptative immune response, in the form of B and T cells. T cells are a particularly important type of cells in response to wounding and infection, with several subtypes playing different, but somewhat overlapping, parts. The role of T cells in wound healing has not been very extensively studied, but it is known that alterations in T cell functions have been associated with exacerbated skin fibrosis due to Th2 $CD4^+$ T cells production of Il-4, Il-5 and Il-13[156]. Because of this lack of bibliographic support on the roles of T cells during wound healing, we will detail their relevance in the context of infection and tumor response, and highlight where aspects of the response might be similar to wound healing.

T cells have been broadly grouped in $CD4^+$ and $CD8^+$ αβ T cells, γδ T cells and natural killer T (NKT) cells. αβ T cells are activated by antigen recognition through T cell receptors (TCRs), co-stimulation from MHC receptors in antigen-presenting cells (APC) and cytokines, that induce clonal expansion and differentiation. Activated αβ T cells are responsible for killing infected cells, producing cytokines, and regulating immune responses.

$CD8^+$ T cells, in particular, are critical in the fighting against intracellular pathogens and in the elimination of malignant cells in cancer[157]. Upon activation, $CD8^+$ T cells undergo a robust expansion, giving rise to effector and memory T cells. Effector cells, also known as $CD8^+$ Cytotoxic T lymphocytes (CTLs), directly induce target cell death by Fas/FasL signaling and release of the cytolytic mediator perforin, which creates pores in target cells, through which granule serine proteases (granzymes) can enter to induce apoptosis. Memory $CD8^+$ T cells are important to induce a rapid and strong reaction to antigen re-encounter.

Initial activation of $CD8^+$ T cells involves TCR signaling and co-stimulatory signals, coupled with cytokine signaling through Il-2, Il-12, Il-21, Il-27, type 1 IFN and IFNγ[158,159]. Il-2 and Il-12 induce effector T cell differentiation through induction of Blimp-1, T-bet and Id2 expression. IFNα and β initiate activation of $CD8^+$ T cell by stimulating clonal expansion and production of IFNγ, through STAT4 activity, which synergize to induce T-bet (encoded by Tbx21) expression, while Il-21 and 27 promote Blimp-1 expression, leading to a differentiation in effector T cells[160–163]. Differentiation into effector T cells is completed by cytokine signaling, through Il-7, Il-10, Il-15 and Il-21. Memory $CD8^+$ T cell differentiation is achieved through WNT signaling, with the TCF1 and FOXO1 transcription factor activity being indispensable.

Metabolically, naïve $Cd8^+$ T cells depend on glycolysis and mitochondrial oxidative phosphorylation for their cellular processes. Proliferative TEs have to ensure higher metabolic rates by upregulating the glycolytic and glutaminolytic pathways. This is induced by TCR signaling and co-stimulation, which activates the mTOR end of the PI3K/AKT pathway, leading to and upregulation of Myc, glucose transporter type 1 (GLUT1) and the glutamine transporter SLC32A1/2[164].

TM cells, on the other hand, skew their metabolic regulation towards fatty acid oxidation for energy production, and they do so in response to Il-15, which leads to an upregulation of the long-chain fatty acid transporter CPT1A. When re-stimulated with a given antigen, TM cells quickly switch their energy production to glycolysis[165–169].

The response of $CD8^+$ T cells to infection, following priming by DCs, can be divided into four stages, as depicted in Figure 1.5, with the first occurring immediately upon recognition of the pathogen and lasting 7 days, comprising the expansion phase where $CD8^+$ T cells proliferate[170,171]. At day 8, stage two, called peak of expansion, TEs and TM percursors reach their maximum number and stop proliferating. At stage three, the contraction phase, which lasts from day 9 after infection to day 15, the majority of T cells undergo apoptosis, but a few survive to stage four, the memory phase, and differentiate into memory T cells.

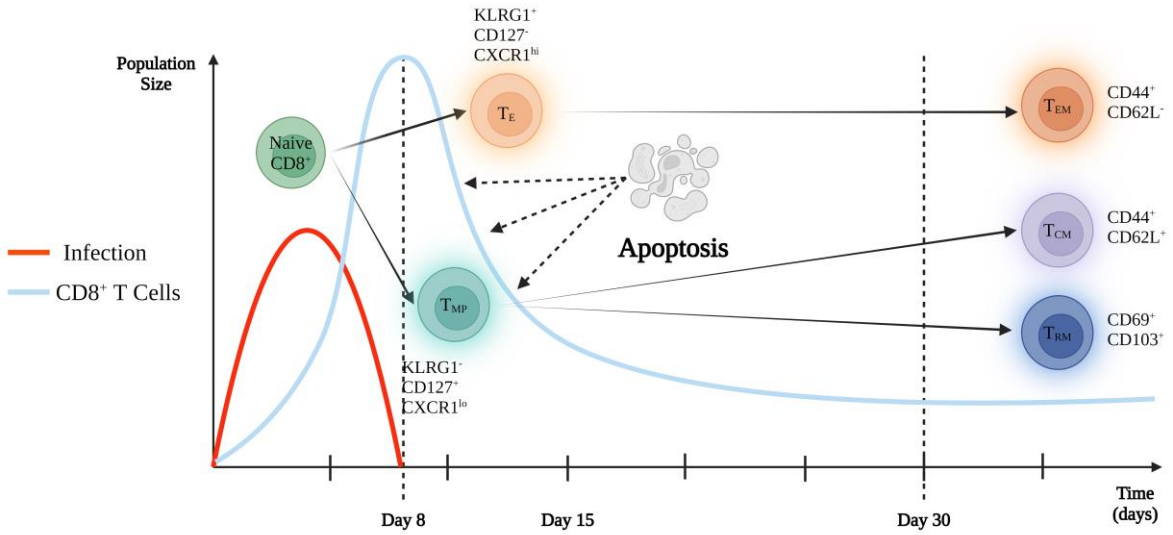

Figure 1.5 - Evolution of the $CD8^+$ T cell response to acute infection. This figure represents the dynamics of differentiation of $CD8^+$ T cells in response to acute infection, particularly by viruses, as well as their characteristic surface receptor and transcription factor expression, and their released factors that have been identified as relevant in the response to the acute infection and to cellular communication. T_E – Effector T Cell; T_{MP} – Memory Precursor T cell; T_{EM} – Effector memory T cell; T_{CM} – Central memory T cell; T_{RM} – Resident memory T cell. This image was adapted from Sun et al., 2023[1241] and created with BioRender.com.

$CD4^+$ T cells are perhaps the most important adaptative immune cell type in wound healing, seeing as deregulation of their activity often leads to pathological outcomes, both in wound healing and tumor response. For instances, $CD4^+$ T cell help is indispensable for the generation of memory $CD8^+$ T cells and their response to re-stimulation, which it does by secreting Il-2 and Il-21, as well as CD40L signaling[172,173,174–177].

$CD4^+$ T cells are activated by MHC class II receptors on APCs, costimulatory stimulation and cytokine signaling, and differentiate into a few subsets, such as Th1, Th2, Treg, follicular helper T (Tfh), Th17, Th9, Th22 and $CD4^+$ CTLs[178,179].

Th1 cells are the primary subset responsible for the response against intracellular bacteria and viruses, through the production of the pro-inflammatory cytokine IFNγ. They are characterized by their expression of the cytokines IFNγ, TNFα and β, and Il-2, the chemokine receptors CXCR3 and CCR5, and the transcription factors STAT4 and T-BET[178,180–182].

IFNγ and Il-12 are essential for Th1 differentiation. Through STAT1 signaling, and in parallel with TCR stimulation, IFNγ induces the expression of T-BET, which suppresses Th2/Th17 differentiation, and further increases the expression of IFNγ and promotes the expression of Il-12Rβ2, conferring the capacity to respond to Il-12. Il-12 signaling, through STAT4 activity, supports T-bet expression[183,184].

Th1 cells are important activators of pro-inflammatory macrophages, due to their secretion of Il-2, IFNγ and TNFα and β, besides their exhibition of CD40L[211]. Th1 cells also have a relevant anti-tumor activity, with higher numbers of Th1 cells correlating with better clinical outcomes for several tumor types[185–191]. Production of IFNγ and Il-12 by Th1 cells enhances survival, proliferation and cytolytic function of $CD8^+$ CTLs and NK cells, and IFNγ can further enhance MHC expression and lead to tumor-derived antigen presentation[191–193].

Th2 cells are responsible for acting against helminth infections and, more relevant to our area of interest, they facilitate tissue repair during wound healing but also contribute to chronic inflammation situations like asthma and allergies[194,195]. This subset of $CD4^+$ T cells are characterized by GATA3 expression and the production of Il-4, Il-5 and Il-13. Th2 cells also express Il-2 and Il-10, as well as the chemokine receptors CCR3 and CCR4, and the transcription factor STAT6.

Th2 cells are activated by Il-4 secreted by DCs and innate lymphoid cell group 2 (ILC2), which binds to Il-4R and leads to the expression of GATA3, through STAT6 activity[196–198]. Activated $CD4^+$ T cells produce Il-4, which further promotes Th2 differentiation. Il-4Ra and Il-4 expression are also maintained through Il-2 induced STAT5 activity.

In the context of tumors, Th2 cells have been shown to suppress tumor growth through activation of eosinophils and M2 macrophage recruitment[199–201]. Memory Th2 also produce Il-4, which enhances NK cytotoxic activities, resulting in a strong anti-tumor activity. Th2 cells can also induce terminal differentiation of cancer cells through secretion of Il-3, Il-5, Il-13 and GM-CSF[202,203]. However, Il-4 produced by Th2 can also lead to monocyte and macrophage signaling that promotes cancer metastasis, and attenuate Th1 anti-tumor responses[204,205]. This differential regulation of tumor development might be related with distinct Th2 states, with cells that express higher levels of Il-10 and TGFβ contributing to tumor progression, while cells with higher expression of Il-3, Il-5, Il-13 and GM-CSF having a more pro-inflammatory, anti-tumoral influence[206].

Probably the most important adaptative immune cells in wound healing, Tregs are the subset of $CD4^+$ T cells responsible for maintaining immune tolerance through suppression of pro-inflammatory immune response. Tregs are characterized by high expression of Il-2Rα (also known as CD25), Il-10, Il-35, TGFβ and the transcription factor FOXP3[208,209].

Treg differentiation is induced by TCR/CD28 stimulation, which induces FoxP3 expression through the activation of NFκB, AP-1 and NFAT. TGFβ also contributes to FoxP3 expression, by activating SMAD 2 and SMAD 3, and by inducing FoxO1 and FoxO3 as well, in the absence of PI3K/AKT signaling[210–217]. FoxP3 expression is also increased by STAT5-mediated Il-2 signaling[311].

Tregs can be subdivided into two subset that have different developmental origins: Thymic Tregs (tTregs or nTregs), also known as natural Tregs, and induced Tregs (iTregs) that differentiate from conventional $CD4^+$ T cells in the periphery, after antigen presentation and in the presence of TGFβ and Il-2[219,220].

Tregs contribute to immunosuppression by several mechanisms, including directly killing TEs, APCs and NK cells through the release of perforin and granzyme B, as well as inducing apoptosis by Fas/FasL signaling[221,222]. Tregs also secrete inhibitory cytokines, like Il-10, Il-33, Il-35, Il-37 and TGFβ, and express, in high levels, coinhibitory surface molecules like CTLA4, PD-1, LAG3, TIM3 and TIGIT[223–232].

Another way Treg cells contribute to immunosuppression is through suppression of $CD8^+$ T cell effector and proliferative programs through CTLA4 signaling, keeping them quiescent[233]. Tregs also contribute to their own recruitment, through the expression of several chemokine ligands and receptors[234,235].

1.1.2.3.1. JAK/STAT Pathway

Our understanding of how inflammatory processes are established is incomplete without our understanding of how paracrine or autocrine signals are perceived intracellularly by the cell, and how they influence cellular processes. External signals, released by other cells or foreign entities, are detected by cell surface receptors that translate the external cues into modifications to cytoplasmic proteins that propagate these alterations down a cascade of interactions, culminating in an effect on gene expression. These intracellular pathways control all aspects of cell dynamics, and response to inflammation and damage is no exception.

One of the primary intracellular pathways that are activated in response to inflammatory cues is the JAK/STAT signaling pathway. Besides being involved in immune responses, JAK activation is also involved in regulation of cell proliferation, differentiation and migration, as well as cell death (in particular, apoptosis), in the context of hematopoiesis, immune development, mammary gland development, adipogenesis and sexually dimorphic growth.

The JAK/STAT pathway responds to several external signals, including cytokines, like Interleukins (2 through 7), interferons and GM-CSF, and growth factors, like growth hormone (GH), epidermal growth factor (EGF) and platelet-derived growth factor (PDGF)[236–237]. Overall, the JAK/STAT pathway can respond to about 60 different factors, and these signals are recognized by several tyrosine kinase-associated receptors (RTKs), which recruit the tyrosine kinases JAKs.

In mammals there are four known JAKs, JAK1, 2 and 3, and TYK2[239]. These constitute a family of non-transmembrane tyrosine kinases that can phosphorylate both RTKs, as well as other RTK-associated proteins with specific Src-homology 2 (SH2) domains. JAK1, JAK2 and TYK2 are considered to be expressed ubiquitously, while JAK3 is primarily associated with hematopoietic cells[240,241].

JAK activation occurs once the ligand binds to the receptor, promoting their multimerization, which brings recruited JAKs close to each other. This approximation of JAK proteins allows them to auto or trans-phosphorylate each other, becoming active[242]. The activated JAKs will then phosphorylate the intracellular tails of the receptor, creating docking sites for latent, cytoplasmic STATs, as well as phosphorylate the STATs themselves and the tyrosine residues in several other downstream target proteins, activating them[243].

The STAT family is composed of seven members, STAT1, STAT2, STAT3, STAT4, STAT5A, STAT5B, and STAT6[244,245]. Each STAT is composed of a N-terminal conserved domain, which is important for STAT phosphorylation and dimer-dimer interactions, a DNA-binding domain, a SH3-like domain, a SH2 domain, which contributes to protein-protein interactions, and a C-terminal transcription domain, also known as transactivation domain (AD), which contains highly conserved tyrosine (Y) and serine (S) phosphorylation residues, required for STAT activation[246].

Classically, the JAK/STAT pathway is described as activated JAKs phosphorylating the conserved tyrosine residues in a STAT monomer, allowing it to bind the SH2 domain of another phosphorylated STAT monomer, producing a conformational change that allows the STAT dimer's translocation to the nucleus. 'Canonical' phosphorylations occur in Y701 in STAT1, Y690 in STAT2, Y705 in STAT3, Y693 in STAT4, Y694 in STAT5 and Y641 in STAT6[247].

Activated STATs form complexes with each other, usually dimers (than can be homo or heterodimers), through binding of SH2 domains. The dimers are then translocated to the nucleus, through a mechanism that is dependent on importin α5 and the Ran nuclear import pathway, where they will exert direct influence on the transcriptional activity of several target genes, including negative regulators of the JAK/STAT pathway[248–250]. A representation of the JAK/STAT pathway can be found in Figure 1.6 .

Besides forming dimers, STATS are also able, through their N-terminal domain interactions, to form tetramers[251–253]. These complexes are important for gene expression regulation, because they allow the combinatorial regulation of high-affinity and low-affinity binding sites, contributing to the complete transcriptional response by STAT1 to type II IFN signaling, by STAT3 to Il-6 signaling, and by STAT5 in NK cell homeostasis, Treg cell function and CTL proliferation[251,252,254,255].

While the response to multiple cytokine and growth factor signaling is more commonly performed through STAT homodimers, response to IFNs I and III is driven by STAT1 and 2 heterodimers that, together with IRF9, form the interferon-stimulated gene factor 3 (ISGF3) complex[256,257]. The constitutive NLS of IRF9 facilitates nuclear localization of the complex.

Although STAT activation is often preferentially induced by a dominant cytokine or growth factor, like STAT1 by IFNγ, which induces the expression of a similar group of genes, regardless of the circumstance (called the 'IFN signature'), many cytokines have been reported

to activate almost all STATs in particular circumstances or tissues, and all STATs have been identified as being activated by the most studied cytokines[233,258,259].

An example of this is the response to Il-12 signaling in T cells. When activated by Il-12, STAT4 activity drives IFNγ production and Th1 differentiation. IFNα and β can also activate STAT4 (besides ISGF3), through IFNαβR, but this does not lead to sufficient IFNγ production, nor Th1 differentiation. However, in the absence of STAT1, IFNα and β signaling is sufficient to increase IFNγ production, but STAT4 activation through IFNαβR cannot sustain IFNγ production like Il-12 signaling can[260–262].

In macrophages, JAK1 and STAT3 are activated by Il-6 or Il-10 signaling. Although Il-6R and Il-10R signal through, apparently, identical mediators, the results of both signals are clearly distinct. Il-10 signaling negatively regulates the inflammatory response of activated macrophages and dendritic cells, while Il-6 signaling tends to lead to a more intense inflammatory response[263–267]. Furthermore, Il-4 and Il-13 signaling, through STAT6, are distinct between T cells and macrophages, or other non-lymphocyte cells. In macrophages, the Arg1 gene is greatly induce, which is not observed in T cells, indicating that the regulatory network of genes downstream of this activation is not the same in both types of cells[268–275].

Despite the preference of IFNγ signaling for STAT1, studies show that it might also activate STAT3, at least in the absence of STAT1, leading to the expression of Cebpb, Socs3 and Gadd45. This is likely due to absence of occupancy of the receptor by the dominant STAT, allowing the binding and activation of another STAT[276,277]. Another example of this is the capacity of STAT5-activating cytokines to use STAT6 in STAT5's absence[278].

Besides activating STAT4, Il-12 can also activate STAT3, while Il-4 is capable of activating not just STAT6, but also STAT5. In some cases, although less common, cytokines can activate with comparable efficiency more than one STAT, like the case of Il-27 and its activation of both STAT1 and STAT3[279–281].

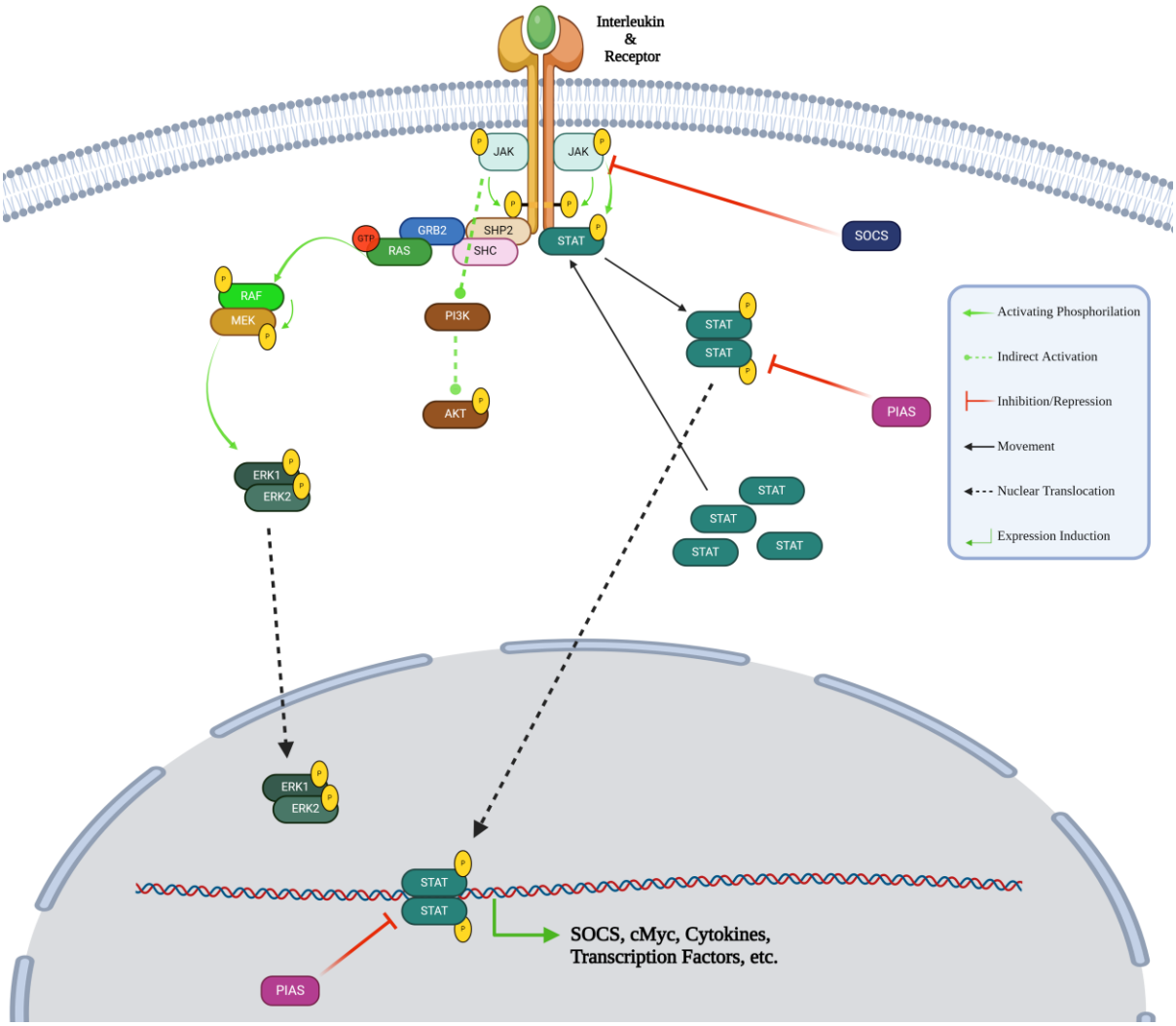

Figure 1.6 – 'Canonical' Interleukin signaling through the JAK/STAT pathway. Depicted in this picture are the main factors involved in Il-induced JAK/STAT signaling, as well as its interactions with other intracellular pathways, namely the MAPK/ERK and PI3K/AKT pathways. Image created with BioRender.com

These observations suggest that cytokines can activate several STATs in different proportions, and it is the stoichiometry of these differential activations that promote differential outcomes in the signaling of factors that, apparently, activate the same mediators in the pathway.

This hypothesis is further supported by observations like both Il-6 and Il-27 being capable of activating STAT3 and inducing a STAT3-driven transcriptional signature in Th cells. However, these signals lead to expression regulation of unique sets of target genes, which are determined, at least in part, by differential activity of STAT1[282]. A similar observation was also done for Il-21 signaling[283].

This happens because STATs are a limiting resource, and even slight changes in cellular concentrations of these factors have significant effects. For example, varying levels of STAT1 and STAT4 determine the response to cytokines in $CD8^+$ T cells and NK cells, and changes in

the availability of STAT5 or STAT4 affect T cell differentiation, with higher levels of STAT5 promoting Treg differentiation, while STAT 4 promotes Th2 differentiation[284–287].

Besides varying abundance of STATs, these observations can also be explained by the existence of synergetic and antagonistic actions of STAs. These interactions can occur by direct, physical contact, serine phosphorylations of the AD, cooperative DNA binding and synthesis of specific inhibitors[247].

For example, STAT1 and STAT3 are clear cases of both synergistic and antagonistic interactions. Il-2 and Il-12 signaling, as an example of synergy, leads to a greater IFNγ expression due to serine phosphorylation of both STAT1 and STAT3[288]. However, antagonism can occur in the responses to IFNs and STAT3-activating cytokines[289,290].

Besides STAT3, STAT1 can also establish antagonistic relationships with STAT4. For example, Il-12 and Il-18 antagonize IFNα signaling through inhibition of transcription of STAT1 and of type I IFN-signaling downstream targets[291]. Also, while both STAT1 and 4 are activated in NK and $CD8^+$ T cells in response to type I IFN-signaling, STAT1 antagonizes STAT4 trough impairment of IFNγ production[262].

Most of these antagonistic relationships are the result of three families of JAK/STAT pathway inhibitors: SOCS, PIAS and PTPs. SOCS are a family of STAT inhibitory proteins composed of 8 members, cytokine-inducible SH2-containing protein (CIS), SOCS1, SOCS2, SOCS3, SOCS4, SOCS5, SOCS6, and SOCS7[292].

CIS and SOCS1, 2 and 3, participate in a negative feedback loop of cytokine signaling through JAK/STAT pathway, while SOCS4, 5, 6 and 7 primarily regulate growth factor receptor signaling[293–296]. SOCS3, for instances, is preferentially induced by Il-6 signaling, while SOCS1 mostly participates in the regulation of IFN signaling, but also of Il-2, Il-4 and Il-12 family of cytokine signaling[247]. Despite some specificity towards the STAT that induces their expression, SOCS are also capable of regulating multiple STATs, just as a STAT is capable of inducing multiple SOCS[297].

SOCS negative regulatory roles are performed in three ways: SOCS binds a phosphating agent at the receptor, impeding the recruitment of the signal transducer to the receptor; SOCS binds JAKs directly, preventing other interactions with, for instances, STATs; or SOCS specifically inhibits the activity of the RTKs. SOCS can also induce ubiquitination via elongin BC and the E3 ligase Cullin5[247,298].

To give concrete examples, SOCS1 and 3 kinase inhibitory regions (KIR) are capable of inhibiting the kinase activity of JAK1, 2 and TYK2 by blocking access to both ATP and substrate. SOCS SH2 domains, which allow them to associate with RTKs, also impede JAK kinase activity, by accelerating proteasome-mediated degradation of the whole signal transduction complex. And SOCS3 kinase inhibitory region is capable of blocking JAK2's substrate-binding region, thus preventing its activity[299–303].

Besides inhibition of JAK activity, the JAK/STAT pathway is also regulated by inhibitors of STAT activity. PIAS (Protein Inhibitor of Activated STAT) are a group of proteins from the c-IAP family that regulate apoptosis, cell survival and tissue renewal in homeostatic conditions[304–306]. This group is composed of five proteins, PIAS1, PIAS3, PIAS4 (PIASγ), PIASxα and PIASxβ which, unlike SOCS proteins, are thought to be constitutively expressed[307,308].

PIAS, like SOCS on JAKs, inhibit STAT activity through three different mechanisms: First, PIAS association with STATs block their ability to interact with the DNA. Second, PIAS recruit inhibitory transcriptional cofactors to STAT-regulated genes. Third, PIAS mediates STAT SUMOylation, leading to their degradation[309–311].

PIAS have been shown to have some specificity for STATs. For instances, PIAS1 and 4 interact primarily with STAT1, while PIAS3 interacts with STAT3 and 5, and PIASx (α and β) with STAT4[311,312]. Besides their regulation of STATs, PIAS have also been associated with the regulation of other pathways, like the NF-κB[247].

The third group of JAK/STAT pathway inhibitors are the PTPs. PTPs are a large family of proteins, with 107 identified members, which are classified in four distinct classes, depending on their catalytic domains. Class I, which is the largest, containing 99 proteins, is composed of the classical phosphorylated tyrosine-specific PTPs and dual-specificity phosphatases (DSPs). Classical PTPs can be further subdivided into receptor PTPs (PTPR) and non-receptor PTPs (PTPN)[313–315]. The best characterized PTP, SHP1, and CD45 belong to this class. SHP1, which contains two SH2 domains, can bind to either phosphorylated JAKs or receptors, and facilitate their dephosphorylation.

Class II includes only low molecular weight phosphatases (LMWPTP), while Class III includes three Cdc25 phosphatases (A, B and C) and Class IV contains four tyrosine and serine/tyrosine phosphatases, called Eya1, Eya2, Eya3 and Eya4[313].

Despite the 'Classical' depiction of this pathway, under normal physiological conditions cells receive signals from multiple signaling pathways. As we have detailed, immune cell activation

tends to involve TLR signaling, co-stimulation and cytokine signaling. The activation of their respective receptors promotes synergetic intracellular pathway activity, like through JAK/STAT and NF-κB, as is the case in NK cells, where Il-18 signaling, through the NF-κB pathway, and Il-12 signaling, through STAT4 activation, lead to the maximal IFNγ expression[316].

Our understanding of this crosstalk between intracellular pathways is still limited, but the best characterized ones involve the MAPK/ERK pathway and the PI3K/AKT pathway, as represented in Figure 1.6. Phosphorylation of RTKs by JAKs creates docking sites for SH2-containing adapter proteins from other signaling pathways, like SHP2 and SHC, which recruit GRB2 and activate the RAS cascade. Another example of this is the phosphorylation of the insulin receptor substrate (IRS) and p85, which activate the PI3K/AKT pathway[246,317,318]. Proteomic analysis of Il-2-stimulated $CD8^+$ T cells identified 90% of the phospho-proteome as being JAK-dependent modifications, with the remaining 10% being mediated by the SRC family kinase activity, which includes PI3K and AKT[319].

RTK signaling can also promote JAK/STAT activity through 'non-canonical' pathways. For example, RTKs like EGFR and PDGFR are capable of activating STATs in a JAK-independent manner, probably through the SRC kinase. MAPK can also specifically phosphorylate a serine residue near the C-terminus of most STATs, enhancing their transcriptional activity. Besides MAPK/ERK and PI3K/AKT, multiple interactions with the TGFβ signaling pathway have also been reported[320].

1.1.2.3.2. NF-κB Pathway

Another intracellular pathway of great importance in the immune response to wound healing in vertebrates is the 'Nuclear factor of κ-light chain of enhancer-activated B cells' (NF-κB) pathway.

In fact, this highly conserved pathway is perhaps the most important in immune response and immune cell development, not just in vertebrates but also in more 'basal' organisms. But besides its importance to immunity, the NF-κB has also been associated with the regulation of cell proliferation, apoptosis and, through a combinatorial effect of the previous three, metastasis of cancer cells[321–327].

In the context of immune response, the NF-κB pathway is 'classically' seen as responsible for inducing the production of pro-inflammatory mediators, and activation and differentiation of immune cells[328]. Today we know that NF-κB's role in immune response can be both pro- and anti-inflammatory, depending on the context[329–331]. NF-κB's role in the apoptotic response to stimuli was also 'classically' seen as pro-cellular death, but more evidence showed that that response is more nuanced, further sustaining the dual role in inflammation regulation of NF-κB[332–336].

In mammals, the NF-κB superfamily consists of five distinct transcription factors: NF-κB1 (also known as p50), NF-κB2 (p52), RelA (p65), RelB and REL (c-Rel)[337]. These proteins are characterized by containing a Rel homology domain (RHD) and a conserved N-terminal domain, responsible for DNA binding, dimerization and nuclear localization. This superfamily is further subdivided into two groups based on the similarity of amino acid sequences of the RHD: The NF-κB family, containing NF-κB1 and NF-κB2, and the Rel family, containing Rel, RelA and RelB.

NF-κB1 and NF-κB2 are the result of post-translational processing of the precursor proteins p105 and p100, respectively, and contain ankyrin (ANK) repeat domains in their C-terminal regions, which contribute to the formation of dimers with other NF-κB family members. The Rel family of proteins, in turn, have no protein precursors, and have a conserved transactivation domain in their C-terminal region[338]. While p105 processing is viewed as predominantly constitutive, the processing of p100 is tightly regulated, and dependent on CD40, LTβR and B-cell-activating-factor receptor (BAFFR) signaling[339,340].

Almost all NF-κB transcription factors can form functional homo and heterodimers between them, with the exception of RelB, which is only capable of forming heterodimers[341]. The most common NF-κB dimer is the heterodimer composed of NF-κB1 and RelA. The inductive or

repressive function of each dimer is not dependent on the combination of transcription factors, but rather the region of DNA they bind and the type of interaction they establish with other transcription factors. However, homodimers of NF-κB1 have shown a propensity to exert a repressive effect on NF-κB target gene expression and inhibit inflammation[339,342–348].

The NF-κB pathway is represented in the literature as being divided into two sets of mediators, the 'canonical' and the 'non-canonical', with some shared, but mostly different, responsibilities[349–351]. The 'canonical' pathway is involved in cell survival and proliferation, epithelial-to-mesenchymal transformations (EMT), angiogenesis, inflammation, mainly through the production of pro-inflammatory cytokines, chemokines and other inflammatory mediators production, like GM-CSF signal transduction, myeloid progenitor cell differentiation, like the decision between M1 and M2 macrophage phenotypes, and cancer metastasis[352–359].

The 'non-canonical' pathway has been associated with primary and secondary lymphoid organogenesis, B cell development and function, and DC function and cell-mediated immunity[360–363]. Because of their different roles in the immune system and immune response, we will describe them separately.

In the canonical pathway, five families of pattern recognizing receptors (PRRs) operate upstream of the pathway, including TLRs, NOD-like receptors (NLRs), RIG-I-like receptors (RLRs), C-type lectin receptors (CLRs) and cytosolic DNA sensors[136,350,367–370]. These receptors respond to signals like TNF, Il-1 and other TLRs, as well as microbial products and other pro-inflammatory cytokines.

The first step in the intracellular signaling cascade of the NF-κB pathway is the activation of the TGFβ-activated kinase 1 (TAK1, or MAP3K7) which will activate the IκB kinases (IKKs) complex[328,339,341,371,372]. The previously mentioned receptors all share a conserved Toll/Il-1R domain called TIR, which allows their dimerization with other TIR-containing receptors. This dimerization recruits intracellular adapter proteins that contain TIR-domains, like MYD88, MAL/TIRAP, TRIF/TICAM1 and TRAM/TICAM2[373,374].

These adapters recruit and activate members of the IRAK family, like IRAK1, whose association with MYD88 induces IRAK1 hyperphosphorylation, leading to its dissociation from MYD88 and association with the downstream adaptor TRAF6, resulting in activation of TAK1[375]. TAK1 activation by TRAF6 depends on a non-classical polyubiquitinylation of TRAF6 through TRAF6-regulated IKK activator 1 (TRIKA1), which is a dimeric ubiquitin-conjugating enzyme complex that synthetizes polyubiquitin chains on IKKγ and TRAF6. Other

IKKs activators activated by TRAF6 include mitogen-activated protein kinase kinase kinase (MAP3Ks), MEKK1 and MEKK3[325,376–380].

The IKKs complex is a large kinase complex that includes two homologous catalytically active subunits, IKKα (or IKK1) and IKKβ (IKK2), and an auxiliary subunit called IKKγ (more commonly referred to as NF-κB essential modulator, or NEMO)[371,381–384]. In the canonical pathway, only the IKKβ catalytical subunit is present, with IKKα being relevant for the non-canonical pathway.

IKKs phosphorylates IκBs in two serine residues in IκBs N-terminal region, leading to their ubiquitination by the ubiquitin ligase, and degradation by the 26S proteasome. This releases NF-κB from IκBs inhibition, allowing its translocation to the nucleus, where it will perform its transcription factor role. The most common dimers involved in this activation process are the NF-κB1/RELA and the NF-κB1/c-REL heterodimers. A visual representation of the NF-κB pathway (both the canonical and non-canonical paths) can be found in Figure 1.7.

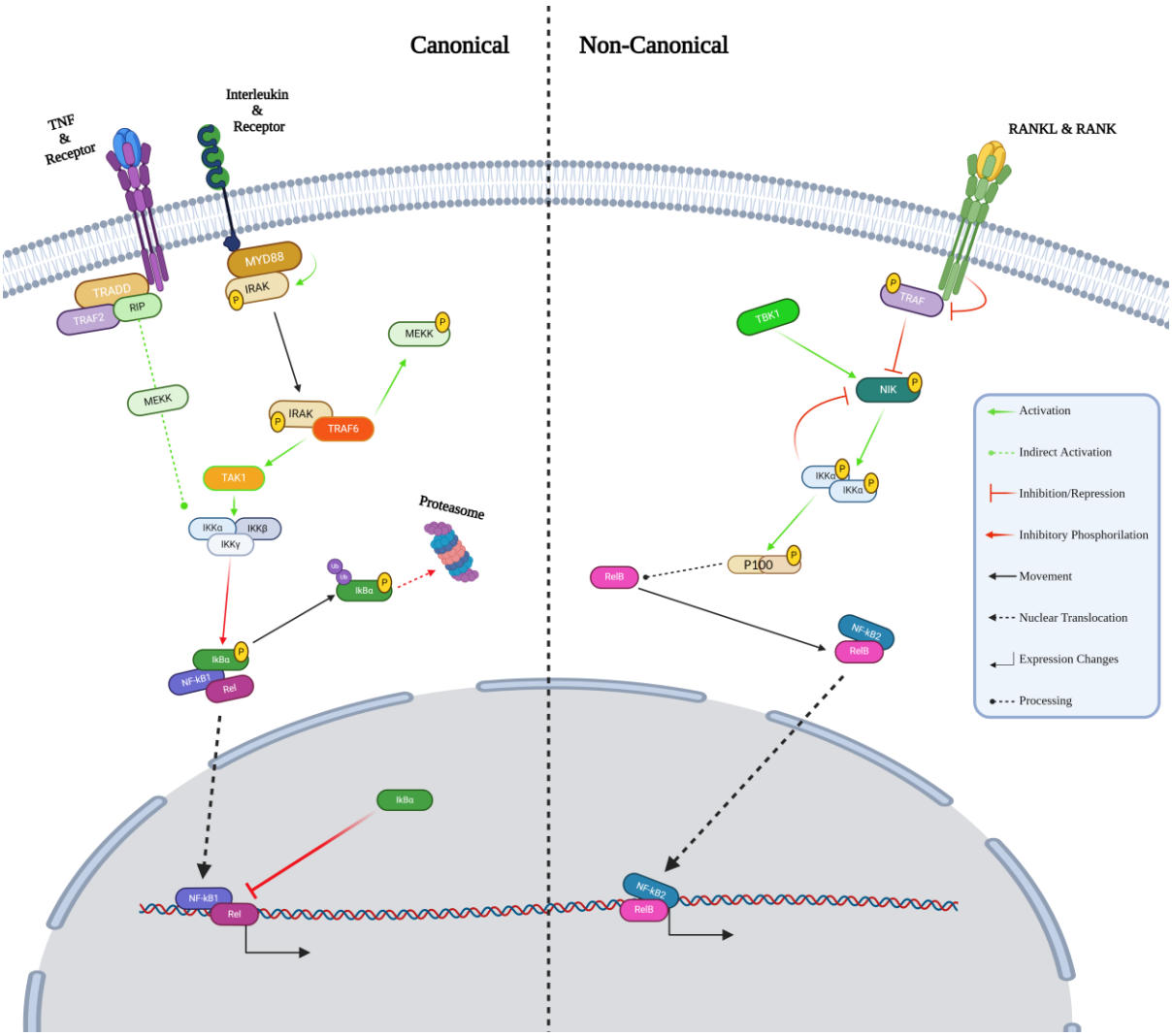

Figure 1.7 – The NF-κB signaling pathway. Schematic representation of both the 'canonical' and 'non-canonical' paths of the NF-κB pathway, with some of their regulators. Imaged adapted from Zhang et al., 2021[323] and created with BioRender.com

Inhibitors of nuclear factor κ B (IκBs) are a family of proteins responsible for the inhibition of NF-κB (as the name indicates), which are characterized by the presence of ANK repeats, that interact with the RHD domains of NF-κB proteins, preventing their entry in the nucleus. This family of proteins has eight members, which are IκBα, IκBβ, IκBε, IκBζ,IκBNS and Bcl-3, and p100 and p105, which are also able to inhibit NF-κB's activity by binding through their ANK repeats, which are still present prior to processing[340,341,350,385–388].

One of the most relevant targets of the canonical pathway is the Nfkbia gene (which encodes IκBα). IκBα's quick production, after having been previously degraded by the proteasome, allows it to quickly bind the NF-κB dimer still present in the nucleus. This dissociates the NF-κB dimer from the DNA and leads to its export from the nucleus to the cytoplasm, where it will remain latent[385,389–391].

This method of regulation of the pathway is likely responsible for the robust and transient activation of NF-κB, which is characteristic of the canonical pathway. In resting cells, NF-κB proteins are predominantly cytoplasmatic, due to their association with IκBs. IκBε works in a similar way to IκBα, but its delayed expression provides NF-κB activity a slower negative feedback regulation[389–393].

IκBβ binding to NF-κB has an opposite effect to that of its sisters. Upon binding to RELA or c-REL, hypophosphorylated IκBβ impairs the inhibitory effect of IκBα, allowing the inductive function of the NF-κB on gene expression[383,394].

The canonical pathway can also be activated by signaling through the TNFR superfamily, through a slightly different set of mediators[395,396]. Some members of this group contain a death domain (DD) in their cytoplasmic regions, which can recruit the TNF-receptor-associated death domain (TRADD) protein, which associates with TRAF2 and RIP. TRAF2 is then able to recruit the IKKs complex, where RIP activates its catalytic subunits via MEKK3[397]. Receptors of the TNF superfamily that do not have DDs are still able to activate the NF-κB pathway through their TRAF-interacting motifs, by directly recruiting TRAF proteins[395].

Another version of the NF-κB pathway, viewed as 'non-canonical', is activated by specific TNF family cytokines, specifically Lymphotoxin B (TNFSF3), CD40L, BAFF, RANKL and TNFSF13B, through the activation of receptors like receptor activator of NF-κB (RANK), TNFR2, fibroblast growth factor-inducible factor 14 (FN14), CD27, CD30 and OX40 (also known as CD134)[358,387,398–405]. Despite their association with the non-canonical pathway, these receptors also participate in the canonical NF-κB pathway, and can mediate the functional cooperation between both paths.

An important characteristic of these receptors are the cytoplasmic motifs that recruit TNFR-associated factor 2 (TRAF2), TRAF3 or both. However, some non-TNFR receptors have also been shown to participate in the activation of the non-canonical NF-κB pathway, namely macrophage colony-stimulating factor receptor (MCSFR), which mediates the differentiation and proliferation of macrophages[406].

Upon stimulation, these receptors lead to the degradation of TRAF3, which is a NF-κB inducing kinase (NIK, also known as MAP3K14) inhibitor, role it performs by binding to NIK's N-terminal region and causing its degradation through a ubiquitination-dependent method, that also requires the participation of TRAF2 and the ubiquitin E3 ligase cellular inhibitor of apoptosis (which exist in two forms, cIAP1 and cIAP2, that are commonly referred to as only cIAP)[407–409]. However, in some receptors, like LTβR, the recruitment of TRAF3 to the receptor seems to be sufficient to separate it from NIK, allowing non-canonical pathway activation[410,411].

In resting conditions, newly synthesized NIK is rapidly bound by TRAF3 and degraded, which keeps NIK levels very low[412–415]. NIK regulation also involves its phosphorylation by TBK1 on S862, which is located in NIK's degradation domain, contributing to its instability. IKKα also contributes to the regulation of NIK through negative feedback, since IKKα phosphorylates a residue in the C-terminus of NIK, which leads to its degradation. Due to this regulation, activation of the non-canonical pathway is usually slow and persistent[351,415].

TRAF3 degradation allows the accumulation of NIK, which will activate IKKα to phosphorylate p100 at specific C-terminal serine residues (S866 and 870), leading to its processing[416,417]. This NF-κB alternative pathway is characterized by this processing, which results in the activation of its primary targets, RELB and NF-κB2, that form heterodimers and translocate to the nucleus to regulate gene expression[387,416–418].

Unprocessed p100 functions as an IκB protein, since it can bind other NF-κB transcription factors, particularly RELB and RELA, retaining them in the cytoplasm[419–422]. When phosphorylated by IKKα, p100 will be ubiquitinated by the β-transducin repeats containing proteins (β-TrCP) E3 ligase, resulting in its processing to generate NF-κB2.

In the nucleus, RELB/NF-κB2 heterodimers are responsible for activating genes relevant for the differentiation and function of several immune cell types. Optimal gene regulation by these heterodimers also depends on other transcription factors, namely activator protein 1 (AP1), STATs and interferon regulatory factors (IRFs)[423–425].

The non-canonical path can also regulate the canonical path. For example, RELB was identified as regulating IκBα stability, limiting canonical pathway activation[426]. RELB might also

interfere with canonical NF-κB gene regulation through interaction with RELA[427,428]. IKKα can also interfere in the canonical pathway by regulating the stability and promoter recruitment of RELA and c-REL through phosphorylation of their C-terminals, which leads to their proteasomal degradation[429].

Canonical and non-canonical pathway regulation and interactions have been shown to be of great importance for a number of cellular processes related with immunity. For example, DCs sense infection and tissue damage through the canonical pathway, but they also activate the non-canonical pathway by the stimulation of receptors like CD40, LTβR and RANK[430,431]. In particular, DC induction of $CD8^+$ T cell responses, via antigen presenting pathway and cross-priming, is dependent on RELB activity, and high levels of RELB expression and nuclear presence are associated with DC maturation[432–434].

T cell maturation and function is also regulated by both paths of the NF-κB pathway. For instances, naïve T cell activation through TCR and co-stimulatory signals depends on the canonical path[322]. After activation, some TNFRs induced are capable of mediating the activation of the non-canonical path, which participates in the directing of T cell fate towards NK cells and γδT cells[435–438].

Interference with the NF-κB pathway has been shown to also influence the function and maturation of several $CD4^+$ T cell subpopulations. For example, Th1 differentiation is influenced by both paths of the NF-κB pathway since IFNγ production relies on RELA, and T-bet is regulated by RELB[439,440].

Importantly, besides their own intrinsic regulation, both paths of the NF-κB pathway interact and are regulated by other intracellular signaling cascades, in particular the PI3K/AKT pathway and the JAK/STAT pathway. For example, the stimulation of TCRs result in the formation of a very large multi-proteomic receptor complex, which leads to AKT activation. Furthermore, PDK1 was shown to have an important role in assembling this receptor complex, mediating recruitment of proteins important for the NF-κB pathway[441,442].

Another very unusual mechanism through which the PI3K/AKT pathway interacts with the NF-κB pathway involves the non-canonical path and its role in complement membrane attack complexes (MACS), which are structures that form in response to complement activation in host defenses against pathogens or immune reactions[443]. This constitutes a particular method of fast non-canonical pathway activation, which does not require TRAF3 degradation, but rather involves MAC-induced phosphorylation of AKT, and the formation of a signalosome complex that includes AKT and NIK, where activated AKT stabilizes NIK.

Besides the PI3K/AKT pathway, interactions with the JAK/STAT pathway have been shown to, for instances, regulate the nuclear presence of NF-κB transcription factors. The ubiquitin ligase complex of Elongin B, Elongin C, Cullin and SOCS1 promotes ubiquitination and degradation of nuclear RELA. PIAS1 has also been shown to move to promoter regions of NF-κB target genes after being phosphorylated by IKKα, inhibiting the DNA-binding of STAT1 and RELA-containing dimers[444–449].

In the opposite direction, IKKβ has been shown to inhibit the activation of STAT1 in macrophages, and NF-κB signaling synergy with Il-4 signaling promotes Th2 cell differentiation, through activation of STAT6[450–452].

This page was intentionally left blank

1.1.2.4. Inflammation in Regeneration

The immune response to injury is probably one of the best studied aspects of regeneration, since in the last decades several publications identified the importance of modulation of the inflammatory response to the outcome of the wound healing process[7,20,35,36,40,67,81,454–459]. The role of inflammation and immune response during wound healing and, more particularly, regeneration has been studied in several contexts, from fetal scarless wounding to mouse digit tip regeneration, and several common trends have emerged.

In fetal scarless wound healing the role of the immune system has been proposed to be minimal, seeing as it is still very insipient in its development[41]. In fact, the fetal wound healing process occurs with virtually no inflammatory response. It has been proposed that this is partially because of decreased fetal platelet aggregation and degranulation, as well as reduced production of TGFβ1 and 2[42,45,460].

Furthermore, fetal wound healing is characterized by lower numbers of mast cells, neutrophils and macrophages, with reduced phagocytic capacities, as well as reduced production of pro-inflammatory cytokines, like Il-6 and 8, that are also produced for a reduced amount of time[54,461–465]. Additionally, fetal DCs have a suppressed response to allogeneic antigens, inhibit Treg induction and T cell-derived TNFα production[466].

The notion that absence of inflammation is responsible for the regenerative capacity of fetal tissues finds support in the observation that a reduction in inflammation of postnatal wounds reduces scarring[460,467,468]. However, it has been proposed that, rather than an absolute absence of inflammatory response, fetal scarless wound healing is the result of different proportions and dynamics between pro and anti-inflammatory mediators[46,461].

For example, the ratio of TGFβ3 to TGFβ1 is higher in scarless fetal wound healing than in scarring and adult skin, and increased TGFβ3 in adult wounds reduces scar formation[41,468–470]. The temporal dynamics of these two isoforms also differ between scarless and scarring wounds, with TGFβ3 being present sooner than TGFβ1 in scarless wounds, while the opposite is true for scarring wounds[459,471–473].

It was also shown that fetal skin expresses higher levels of Il-10, and that this increased expression is necessary for scarless wound healing, through downregulation of Il-6 and 8 and, possibly, through a STAT3-mediated regulation of hyaluronan metabolism[474–476]. Differences pertaining to the modulation of the ECM have also been observed, like the ratio of MMPs to TIMPs being higher in scarless fetal wound healing than in adult scarring wound healing[477].

The greatest volume of evidence in favor of the idea that it is an appropriate balance between pro and anti-inflammatory mediators, rather than an absence of pro-inflammatory mediators, that yields a regenerative outcome to wound healing comes from studies of immune responses during the regenerative events of lower vertebrates[7,8,478,479].

Lower vertebrate's macrophages and neutrophils share common markers with their mammalian equivalents, as is the case of F4/80, and α-Naphthyl acetate esterase (NAE) and Myeloperoxidase activity, as well as a myriad of genes relevant for the development of several different lymphocyte populations, like CD2 and CD79a[480–488]. This contributes to similarities between macrophage and neutrophil functions across vertebrates, as well as large commonalities between the responses of these cells in distinct tissues, like limb, heart and eye lens[489–491].

Indeed, tail fin regeneration in *Danio* requires macrophages to promote an anti-inflammatory environment that is permissive to regeneration, but nevertheless involves the production of pro and anti-inflammatory signals, ECM remodeling, and clearance of debris and senescent cells, much like their mammalian counterparts, and macrophage depletion has been shown to impair limb regeneration[490]. This capacity of tail fin regeneration to occur despite pro-inflammatory signals and activity of macrophages has been associated with an early clearance of these pro-inflammatory mediators, and a conservation of anti-inflammatory mediators, likely the result of M2 macrophage activity[492,493].

The hypothesis that regenerative outcomes in lower vertebrates are the result of M2-mediated inflammatory processes, instead of M1-mediated, gained further support from studies performed in lizards, where the regenerating response of the tail was associated with the presence of M2-like macrophages, while the scarring response of the limb was associated with the presence of M1-like macrophages[494,495].

In another example of the requirement of inflammatory processes for regeneration to occur, in *C. pyrroghaster*'s lens regeneration the recruitment of myeloid cells is not just essential, but also sufficient to promote ectopic lens regeneration, when transplanted into an uninjured eye[496]. Myeloid cell indispensability to regeneration, in particular through macrophage activity, was further demonstrated by clodronate-loaded liposome (Clo-Lipo) treatment of *Ambystoma* regenerating limbs and hearts, and *Podarcis muralis* tail[489,497,498].

Clo-Lipo treatments targets ATP production in phagocytic cells, leading to their apoptosis, and this primarily targets macrophages, with little effect on neutrophils. This treatment severely impaired regeneration of limb and heart in *Ambystoma*, as well as blastema formation and tail

regrowth in *Podarcis*. The signals that regulate macrophage recruitment are not fully understood yet[479], however evidence suggests that in the regenerating limb blastema progenitors that express PRRX1 contribute to myeloid cell recruitment through production of Il-8[499,500].

Newts, salamanders and larval anurans regenerative events are associated with weak immune responses[501]. However, this is not due to absence of immune cells, as in the regenerating limb of *Ambystoma*, macrophages, neutrophils, T and B cells are recruited to the regenerating stump[497,499,502,503]. Immigration of leukocytes to the injury site in *Ambystoma* is comparable with mammalian wounds, and analysis of inflammation-related genes in larval *Xenopus* and *Ambystoma* show that there are similarities between the major cytokines, chemokines and growth factors present in the regenerative events of their limbs and mammalian acute wounds[497,504].

Therefore, the weaker immune response has been explained by the presence of a lower diversity of MHC receptors and a simple immunoglobulin repertoire, composed of weak IgM immunity, resulting in decrease T cell activation, cytokine secretion and, therefore, inflammation[7]. This weaker immune response in lower vertebrates has also been linked with slower and less robust adaptative humoral responses[505].

Nevertheless, evidence of a possible requirement of T cells in *Ambystoma* limb regeneration comes from the observation that regeneration is impaired in a dose-dependent manner by the immunosuppressant Cyclosporin A, which is rescuable by Il-2 treatment[506]. In *Xenopus*, the requirement of T cells has also been proposed, due to the observation that tail regeneration during the regenerative window of tadpoles involves a significant lymphocyte infiltration, which correlates with high expression of TNFα in the thymus. Non-regenerative phases of tadpole development also exhibit thymus activation, but the size is irreversibly decreased in relation to non-amputated siblings[507].

More recently it has also been shown that Tregs infiltrate the regenerating heart, spinal chord and retina of *D. rerio* and stimulate the proliferation of precursor cells, like cardiomyocytes, neural progenitor cells and Müller glia cells[508]. This function of Tregs appears to be a non-immunological role, and depends on the transcription factor FOXP3a, which induces the expression of pro-regenerative factors like Nrg1, NT3 and Igfs.

Skin-resident cells, like DCs, Langerhans cells and dendritic epidermal T cell-like cells (DETCs) have also been shown to exist in anurans, similarly to mammals[509]. While the

functional role of these cells has not been broadly explored in amphibians, it has been proposed that LCs contribute to scar formation[503,510].

Another important aspect of the immune response is the complement system, which promotes opsonization, chemotaxis and cell lysis. Analysis of *D. rerio* genome showed a high conservation of components of this system in comparison with mammals, but this system has not been fully analyzed in other lower vertebrates, like samalanders, despite expression of their constituents being observed during limb, heart and lens regeneration[511–515]. During limb regeneration in *Ambystoma* and *Notophtalmus*, C3 and C5 are up regulated, which also happens in *Notophtalmus* lens regeneration. As for heart regeneration, the C5aR1 has been observed overexpressed after 48 hours of cardial apical resection in *Danio* and *Ambystoma*, and inhibition of this receptor reduced cardiomyocyte proliferation, suggesting a requirement of the complement system for regeneration[512].

Overall, lower vertebrate wound healing is characterized by reduced hemostasis, shorter inflammatory stages, reduced infiltration, possibly due to lower circulating monocyte and neutrophil levels, as well as by a significant delay in ECM production and assembly[2]. Furthermore, studies of initial wound healing dynamics in *Ambystoma* have identified the presence of both pro and anti-inflammatory cytokines, namely Il-1β, Il-4, Il-5, Il-6, Il-10, Il-13, Il-17, Il-23, IFNγ and TNFα, occurring concurrently[497], while in mammals pro-inflammatory and anti-inflammatory cytokine production seem to overlap less, with the first being the prevalent group during the hemostasis and inflammation phases of wound healing, while the second group is prevalent during re-epithelialization and tissue remodeling[516].

While mammals have a relatively limited regenerative potential, some organisms and tissues present good opportunities to study the regulation of the immune system in regenerative events and its interaction with the regenerating tissue, albeit with some limitations[517,518].

For example, in 2021 Rabiller et al., showed that hematopoietic macrophage efferocytosis directs regeneration of the adipocyte tissue in the subcutaneous fat pad of *M. musculus*[516]. In contrast to medullar macrophages, that contribute to an inflammatory response and promote scar formation, these authors showed that most resident macrophages display an anti-inflammatory profile and are responsible for a regenerative response.

Related with these observations, in 2020 Wu and colleagues showed the importance of macrophage phenotypic switch for the decision between regenerative and fibrotic repair in mammalian pancreas[518]. The authors showed that, through Il-4Rα-mediated JAK/STAT6

signaling and PI3K/AKT signaling, acinar-to-ductal metaplasia after acute pancreatitis was possible.

The relevance of macrophage activity in wound healing of mammals was also shown in the context of heart and skeletal muscle wounding in mice. Early infiltration of M1 macrophages was associated with clearance of necrotic tissue, and disrupted M1 macrophage polarization perturbed heart healing and skeletal muscle regeneration[519–521].

Furthermore, M1 and M2 macrophages were proposed to have clear and distinct roles, with M1 recruiting and stimulating satellite cell proliferation, through production of Il-1β, Il-6, TNFα and G-CSF, and M2 mediating differentiation and growth through IGF1 and TGFβ[519,522,523]. Macrophage activity in mice and humans has also been shown to regulate hepatic and kidney regeneration in response to WNT signaling[524,525].

Besides the role of macrophages, both eosinophils and Tregs have also been shown as necessary for activation of satellite cells during skeletal muscle regeneration, and this has been linked with Il-4 production by eosinhophils, which activate fibro/adipocyte progenitors (FAPs), necessary for debris clearance, and with amphiregulin secretion by Tregs, which enhances satellite cell activation and differentiation[526,527].

Neutrophils have also been associated with regulation of immune responses in regenerative contexts in mice, by converting pro-inflammatory macrophages into anti-inflammatory through neutrophil efferocytosis and ROS release[124,528]. However, neonatal mice lacking both macrophage and functioning neutrophils are able to repair skin wounds without delay or scar formation. Dying cells and debris are instead removed by 'stand-in phagocytic fibroblasts'[529].

The complement system has also been shown to play a role in murine regeneration, particularly in skeletal muscle, through C3a-mediated CCL5 recruitment of monocytes and macrophages towards regenerating tissue, as well as in cardiac repair, with C5aR1 enhancing cardiomyocyte proliferation[512,530].

Despite relevant contributions of other immune cell types, the outcome of a wound healing event seems to be primarily influenced by the dynamics of macrophages, even in more complex regenerative contexts. For example, in the epimorphic regeneration of the murine digit tip, Clo-Lipo treatment was shown to prevent regeneration by reducing bone histolysis, re-epithelialization and blastema formation[531].

This was further confirmed in another mammalian epimorphic regeneration model, *A. cahirinus* ear pinna full thickness wounding, where Clo-Lipo treatment led to inhibition of blastema

formation and, consequently, regeneration[531,532]. In this set of experiments, Simkin et al. showed that both *A. cahirinus* and *M. musculus* contained relatively equal profiles of circulating leukocytes, with lympochytes being the most abundant and eosinophils being the smallest population.

However, they also showed that *M. musculus* has a greater level of phagocytic cells invading the wounded tissue 3 days after injury, point at which the numbers of phagocytic cells (measured by CD11b detection) were the highest in both species. Furthermore, they observed that while *Mus* immune response was characterized by an initial higher abundance of neutrophils, that decrease and are substituted by macrophages by day 7 post injury, in *Acomys* the recruitment of neutrophils to the injured tissue was slower and at lower levels than in *Mus*.

As for macrophages, it was observed that in both species they persisted in the wound for up to two weeks after injury. However, while M1 macrophage numbers increased in the distal region of the wound of *Mus*, the same did not occur in *Acomys*, where they stayed proximal to the wound. As for M2 macrophages, while in *Acomys* they appeared regionalized to a region directly beneath the epidermis and centrally in the blastema, distally from the wound, in *Mus* these cells were found distributed throughout the connective tissue distal to the injury. This led the authors to propose that the *Acomys* ear pinna blastema is relatively free of M1 macrophages.

This work was followed by another where the authors focused their inquiry on neutrophils[533]. In this work, which very interestingly compared wild and laboratory-adapted species of regenerative and reparative murids, Cyr et al. observed that lab-bred *A. cahirinus* had fewer circulating neutrophils than both wild and lab-bred *M. musculus*, and these lower percentages were accompanied by significantly higher percentages of lymphocytes and lower percentages of monocytes. This led the authors to propose that reduced levels of phagocytic cells in the immune responses of regenerative murid species might be compensated by increased levels of lymphocytes.

The authors also demonstrated that *A. cahirinus* neutrophils had higher phagocytic activity than their counterparts in *M. musculus*, and that the killing ability of the serum and whole blood of *A. cahirinus* was also higher. In fact, they propose that bacteria killing in *Mus* is primarily achieved by neutrophils, or a neutrophil/serum combination, while in *Acomys* this killing ability appeared to be driven exclusively by factors present in the serum.

Work from the same lab further expanded our knowledge of the immune regulation of regenerative wounds in *Acomys*, by focusing on the role of T cells[534]. First, the authors showed that both regenerative and fibrotic wound healing processes share an initial set of pro-

inflammatory factors, namely Il-6, TNFα, CCL3, CSF2 and CXCL1, but with lower levels in the regenerating tissues, particularly of Il-6, CCL2 and CXCL1. Interestingly, despite initial lower levels of Il-6 in *A. cahirinus*, these did not return to basal or lower after the inflammatory phase, unlike *Mus*.

Some local increases of certain factors were associated with regeneration, specifically Il-12 and Il-17, as well as a stronger influx of activated and regulatory T cells, expressing Cd8, Ctla4, Il2ra, Foxp3 and Tnfrsf4, in the dermis, during the inflammatory phase of wound healing. Conversely, local increase of CCL2 was found to be specific to fibrotic repair, as was the higher activation of STAT3 in response to the higher levels of Il-6 during the inflammatory phase and the accumulation of inactivated Th cells. Curiously, STAT3 activation increased afterwards, upon formal blastema formation and widespread throughout it, while it declined in the fibrotic repair of *Mus* and was only visible in distal epidermis.

In another study of *A. cahirinus* immune responses in regenerative tissues, this time focusing on skin of the dorsum[535], Brant et al. observed that normal skin of *Acomys* shows a higher number of mast cells, which are more prominent in the papillary dermis around hair follicles in both species, but become dispersed throughout the granulation tissue of *Acomys* upon injury, while they were nearly absent in *Mus* wounds.

Furthermore, the authors observed that *Acomys* wounds never contained F4/80$^+$ macrophages, while these were found in uninjured skin and in damaged connective tissue below the panniculus carnosus muscle. They also saw higher upregulation of iNos, associated with classical activation of macrophages (M1 polarization), and Dectin1 and Arg1, associated with alternative activation (M2), in *Mus*, while in *Acomys* the expression of these genes was not detected, which led them to propose that there are no mature macrophages in the wounds of *Acomys*.

They also measured cytokine levels in the dorsal wounds of *Mus* and *Acomys*, and found that 18 of the detectable cytokines in *Mus* were not detectable in *Acomys*. These included GM-CSF, G-CSF, CXCL10, CXCL11 and MIP1b, secreted primarily by macrophages, and CCL1, MCP5 and M-CSF, which are macrophage chemoattractants/inducers, and whose absence might help explain the lack of F4/80$^+$ macrophages in *Acomys* wounds. Of the detected cytokines in *Acomys*, C5/C5a, Il-16, MCP1, MIP1a, MIP2 and TNFα were found at lower levels than in *Mus*, while RANTES was the only cytokine found at higher levels in *Acomys* than in *Mus*.

In another work, the same lab focused on the regenerative properties of skeletal muscle in *A. cahirinus*, particularly the tibialis anterior (TA) muscle[536]. In this regenerative model, the

authors showed that NF-κB and TGFβ1 expression had the same temporal dynamics between *A. cahirinus* and *M. musculus*, but levels of it were higher in *Mus*, suggesting lower inflammation and fibrosis in *A. cahirinus* skeletal muscle regeneration.

Furthermore, NF-κB expression co-localized with F4/80 expression in *Mus*, and acid phosphatase activity (an indicator of muscle fibrosis) was clearly present in *Mus* but virtually absent in *Acomys*. This was correlated with the levels of CXCL12, a chemokine with an anti-inflammatory role, which showed an overexpression in *A. cahirinus* injured TA, while it was downregulated in *Mus*.

As in dorsal skin wounding, no $F4/80^+$ macrophages were detected in *Acomys* regenerating TA. Through CD86 labeling, the authors confirmed that this means an absence of M1 macrophages from healing tissues in *A. cahirinus*, but not in *M. musculus*, where they abound. Additionally, the authors detected similar levels of M2 macrophages in both species.

Overall, observations performed in *Acomys* suggest that its wound healing is characterized by a weaker inflammatory response, with fewer phagocytic myeloid cells invading the tissue, especially in earlier timepoints, and that these cells, particularly macrophages, might present a more immature phenotype, with a skew towards anti-inflammatory subtypes, thus generating a less inflammatory environment.

In another example of the rare epimorphic regenerative response of mammals (although debatable)[4,10], Sinha et al. compared the wound healing responses between the regenerative velvet of the antlers and the reparative dorsal skin of the reindeer *Rangifer tarandus*. The authors confirmed a remarkable capacity for regeneration of full-thickness injuries to the velvet, whereas identical injury to the back skin healed through scarring, due in part to distinct patterns of stromal immune signaling.

Velvet fibroblasts in the reindeer's antlers exhibited a transcriptomic profile indicative of an immunosuppressive secretome, while fibroblasts of the dorsal skin maintained a heightened inflammatory state. Velvet wounds had reduced myeloid recruitment and arrested neutrophil and macrophage maturation, as well as an accelerated clearance of infiltrated leukocytes, which was at least partially due to the particular activities of site-specific fibroblasts.

scRNA-seq identified similar immune cell populations in peripheral blood from systemic or antler-specific locations, likely also with comparable maturity. However, velvet was shown to harbor more resident immune cells than back skin, which nevertheless had an enrichment of $CSF1R^+$ macrophages. Furthermore, recruited cell populations to the wound site varied in magnitude, distribution and maturity state, between antler velvet and back skin.

At 3 days post injury, there was a higher amount of immune cells in the back skin than in the velvet wounds. This distinction was not evident at 7 days, while by 14 days after injury the levels differed again, with the immune infiltrate persisting in back skin but being predominantly resolved in the antler velvet.

More interesting than the levels of immune infiltrates was their significant heterogeneity and maturation state, with back skin being enriched with S100A8/A9^{+}CSF3R^{+} neutrophils at day 3, S100A8/A9^{+}CSF1R^{+} macrophages throughout the surveyed time and CD3E^{+} T cells at day 14 post injury. Additionally, macrophages with a phenotype similar to the 'initial/early' phenotype were found enriched in antler velvet regeneration at day 3, while Thbs1^{+} macrophages, associated with oxidative stress and antimicrobial activity, were dominant in back wounds.

The authors posited that fibroblast-derived signals might regulate the immune response in each tissue. To confirm this, they co-cultured primary dermal fibroblasts from back skin and velvet with circulating immune cells of the same reindeer. scRNA-seq of these immune cells made evident considerable differences in expression, with velvet-conditioned macrophages exhibiting a more immature phenotype, while back skin neutrophils appeared to be the most terminally differentiated.

Overall, their work suggested that pro-regenerative fibroblasts have a secretome enriched in keratinocyte-stimulating and immune-repellant factors, like BMP3, BMP4, NDP, INHbA, FGF10 and LAMC3, and SLIT 2 and 3, respectively. On the other hand, pro-inflammatory fibroblasts express a role of factors involved in innate and adaptive leukocyte recruitment, like CSF1, CCL2, CXCL12 and PTGS2, as well as members of the complement and coagulation cascades, namely C3, C4a and CFH, and PLAU, PLAT and PROS1, respectively, that contribute to the activation of immune and vascular responses.

Through a comprehensive overview of the bibliography, we realize that vertebrate regenerative models share several similarities in their immune response. As immune signaling has been shown to regulate proliferation in several cell types and contexts, it stands to reason that regulation of proliferation is achieved through similar mechanisms in vertebrates.

This page was intentionally left blank

1.1.3. Proliferation

Also known as the growth phase[20], the proliferative phase of the wound healing can be divided into four distinct, yet related, processes, namely re-epithelialization, fibroplasia, angiogenesis and peripheral nerve repair.

Re-epithelialization starts shortly after wounding, within the first 24 hours, with basal keratinocytes differentiating, loosening their adhesions to each other and to the basal lamina, and migrating between the fibrin clot and the rich collagen matrix of the dermis, forming a leading edge, also known as the migrating epithelial tongue, while keratinocytes that migrate behind them (suprabasal keratinocytes) proliferate to provide more cells to fill the wound[537]. As they proliferate, suprabasal keratinocytes closest to the leading-edge change shape and migrate over the basal keratinocytes, becoming the leading cells.

This behavior is stimulated in keratinocytes by cell-cell and cell-ECM interactions, growth factors and cytokines, released by several types of cells[538–540]. Paracrine interactions between keratinocytes, fibroblasts, neutrophils, monocyte/macrophages and endothelial cells activates MAPK/ERK signaling, which results in an increase in cytokines, growth factors and other biomolecules production, which will promote epithelial-mesenchymal interactions between keratinocytes and fibroblasts. These interactions stimulate fibroblasts to further release growth factors and support keratinocyte proliferation[541–544].

The role of growth factors responsible for this keratinocyte behavior include Epidermal growth factor (EGF), Heparin-binding Epidermal growth factor (HB-EGF), TGFα, Fibroblast growth factor 2 (FGF2) and Keratinocyte growth factor (KGF)[545,546]. These factors lead to the upregulation of K6, K16 and K17, which are important for keratinocyte migration, which is further stimulated by production of Il-1, Il-6 and TNFα in the wounded tissue, which stimulates fibroblasts to further produce keratinocyte-stimulating factors[539,543,547,548].

Keratinocyte migration through the fibrin plug is possible due to the production of MMPs by basal keratinocytes at the leading edge[549,550]. During their migration, keratinocytes actively interact with fibroblasts, endothelial cells and immune cells in the wound, with CCL2 produced by keratinocytes contributing to the activation of macrophages, neutrophils and T cells[138,551].

Fibroplasia is the term employed to reference the processes fibroblasts develop during wound healing, and includes keratinocyte stimulation, immune system recruitment and modulation, ECM production and reshaping, and wound contraction[552]. Fibroblasts are an heterogeneous,

incompletely defined group of cells, that are characterized by great plasticity and differential roles and behaviors, depending on their tissue of origin and their tissue of action[543,553,554].

Fibroblasts respond, through the MAPK/ERK and PI3K/AKT pathways, to several extracellular signals that include the previously mentioned Il-1 and TNFα, but also to TGFβ, Platelet-derived growth factor (PDGF), EGF and FGF2[555,556]. These factors are released, as mentioned, by keratinocytes, but also platelets, macrophages, endothelial cells and fibroblasts themselves, operating in an autocrine way. This results, among other things, in an alteration of the ECM surface receptors in fibroblasts, which initially express higher levels of integrins α3β1 and α5β1, but gradually transition to a higher abundance of integrin α2β1[557].

In interaction with ECM components like FN, fibrinogen and thrombin, these factors stimulate fibroblasts to proliferate and produce specific integrin receptors and ECM factors, like collagens, fibronectin, and others, but also modulators of ECM assembly, namely metalloproteinases (MMPs) and their inhibitors, like TIMPs[541,557,558]. Furthermore, keratinocyte signaling is capable of inducing an anti-fibrotic effect in fibroblasts, inducing an upregulation of urokinase-type plasminogen activator (uPA), MMP1 and MMP3 and a downregulation of pro-fibrotic factors like connective tissue growth factor (CTGF), ColI, ColIII, FN, plasminogen activator inhibitor 1 and TIMPs 2 and 3[559].

The first fibroblasts to invade the wound area are reticular fibroblasts, expressing proto-myofibroblast markers like β and γ actin. These fibroblasts begin to migrate into the wound at day 3, where they will deposit new ECM and reshape the fibrin clot and damaged ECM, creating a new connective tissue, called granulation tissue. This new ECM is an essential scaffold and an instructive map for the migration of inflammatory cells, endothelial cells, other fibroblasts and more[560–562].

Besides reticular fibroblasts, several studies suggest that fibrocytes also contribute to the fibroblast population during wound healing. Immature fibrocytes secrete MMP2, 7, 8 and 9, which promote their migration to the granulation tissue, as well as endothelial cells[563,564]. Fibrocytes seem to have a reduced capacity to synthesize collagen when compared with dermal fibroblasts. However, fibrocytes have been shown to be able to upregulate collagen production in dermal fibroblasts, as well as chemotaxis, proliferation and differentiation into myofibroblasts (MFs), likely through CTGF and TGFβ1 production and secretion.

Myofibroblasts are differentiated fibroblasts and fibrocytes that exhibit characteristic expression of cytoskeletal proteins, particularly α-smooth muscle actin (αSMA), but also H1-calponin and γSMA, as well as EDA-Fibronectin, and have an increased stress fiber and focal

adhesion assembly[562,565–567]. Fibrocytes and fibroblasts likely differentiate into αSMA-expressing myofibroblasts through TGFβ1 and PDGF stimulation[568–570].

TGFβ and PDGF signaling induces the expression of αSMA and muscle myosin, which form intracellular stress fibers that attach to the fibronexus, a cell-ECM structure that links actin filaments to extracellular collagen and fibronectin, through integrins at focal adhesion sites. The contraction of these stress fibers condenses the ECM, creating empty spaces that can accommodate more collagen deposition, resulting in the contraction of the wound. In fibrotic wound healing, this accumulation of collagen leads to an almost avascular and acellular tissue, where 80 to 90% of the ECM is composed of type I collagen[562,571–574]. TNFα has been shown to be able to suppress this process through reducing the stability of TGFβ mRNA[575].

Proto-myofibroblasts in the granulation tissue also increase collagen deposition, altering the tensile strength of the tissue[576]. Because fibroblasts can sense the rigidity of the tissue, and the direction of the mechanical load, and translate it to gene expression, this increased deposition of collagen further supports their differentiation into myofibroblasts. An example of the effects of this mechano-transduction is the activation of Slug-mediated TGFβ signaling by vimentin, an intermediate filament of the cytoskeleton, which triggers epithelial-to-mesenchymal transition (EMT), proliferation, differentiation and collagen deposition of fibroblasts, which in turn leads to keratinocyte differentiation, also contributing to re-epithelialization[577–583].

Besides accommodating more collagen and further contributing to a change in the tensile strength of the tissue, this condensation of the ECM also releases TGFβ from its extracellular latent complex by increasing its proximity and availability to cells[584,585]. This availability of TGFβ, helped by its production by activated fibroblasts, is also important to, in later stages of repair, revert the activation of keratinocytes, by inducing basal cell-specific markers such as K5 and K14, thus reducing their proliferation[539].

Myofibroblasts are eventually cleared from the wound tissue via apoptosis, when tissue integrity is sufficient[586]. Impaired clearance of myofibroblasts from the repaired tissue leads to pathological tissues, like fibrotic scar tissue or keloid formation[20,455,587].

As the tissue is reconstituted, another important process has to occur, in order to supply the growing tissue with the necessary nutrients, i.e. neovascularization[560]. Angiogenesis, the creation of new vessels, is thought to be a process developed in two phases: In the first, new blood vessels are created through proliferation of endothelial cells and pericytes, which will then be pruned and remodeled in the second phase. Blood vessel destruction, hemostasis, vessel

contraction and the accelerated cellular metabolism working to repair the injury leads to hypoxic conditions shortly after damage occurs[144,588–595].

In these conditions, vascular endothelial cells, fibroblasts, keratinocytes and macrophages are stimulated to produce hypoxia inducible factor 1 (HIF1), which in turn stimulates VEGF, FGF, PDGF, TGFβ, angiogenin, angiotropin and agiopoietin 1 (Ang1) production and secretion, triggering neovascularization. VEGF has been shown to bind specifically to fibrin, facilitating its localization and mitogenic activity, which is mediated by upregulation of several integrin receptors in endothelial cells (ECs), namely integrins αvβ3, α1β1 and α2β1, and increases the expression of BCL2[596–598].

Angiogenesis requires the activation of local microvascular ECs, present in the inner surface of blood vessels, which in a hypoxic environment respond to growth factors like VEGF and PDGF, becoming activated[599]. Pro-angiogenic hypoxic effects are mediated through HIF1, which further upregulates VEGF, and VEGF-mediated expression of endothelial nitric oxide synthase (eNOS) and heme oxygenase 1 (HO1)[600,601]. This establishes an essential VEGF gradient, correlated with a parallel hypoxic gradient, which stimulates activated ECs to migrate towards central hypoxic regions[602].

Activated ECs help to break down the ECM in the granulation tissue, which allows them to proliferate and migrate, and form new cell-cell junctions, thus contributing to the branching out and formation of new capillaries.

Capillary sprouting, which occurs in response to VEGF and PDGF, as mentioned, but also FGF, TGFβ and angiopoietins, is carried out by three different subsets of ECs: Highly migratory tip cells, whose function is to guide the sprout towards a VEGF gradient, highly proliferative stalk cells, that elongate the sprout, and quiescent phalanx cells, that will form the lining of the blood vessel[592,603–608].

ECM factors, like collagens, laminins, vitronectin, and especially fibronectin, also promote endothelial cell proliferation, survival and migration[609,610]. Tip cells migrate by extending their filopodia in search of the greatest concentration of VEGF, as well as evading negative cues, like thrombospondin 1 and 2, and decorin, while stalk cells trail them, maintaining the integrity of existing capillaries[611–617].

Eventually, immature EC structures anastomose with preexisting blood vessels, likely due to EC expression of surface receptors like P-selectin, E-selectin, ICAM1 and VCAM1, creating insipient endothelial tubules. These structures now have a lumen and generate a basal

membrane, and ECs release PDGF, that recruits PDGFRβ-expressing pericytes, which cover the new vessels, stabilizing them[618–623].

After new blood vessel formation, the second phase, pruning, starts with the contraction of selected blood vessels. ECs of the inner walls of blood vessels bind to each other on opposite sides in increasing numbers, until the lumen is occluded and blood flow ceases. Then, the ECs of the retracting branch disintegrate and die by apoptosis, leaving a remodeled vascular network behind[802]. Ultimately, fibroblast production and modeling of ECM gives these new blood vessels their required support, establishing them as fully functional[572,625].

Finally, peripheral nerve repair occurs in response to peripheral nerve transection, which causes retraction of the stumps. Poor vascularization of the space between stumps leads to a hypoxic environment, which triggers the release of VEGF by macrophages, promoting angiogenesis along the original basement membrane of the nerve, while the distal stump degenerates by Wallerian degeneration[455,626].

Schwann cells (SCs) detach from degenerating axons, that release their myelin, and dedifferentiate into a progenitor-like state[627–629]. Dedifferentiated SCs interact with fibroblasts at the injury site through EphrinB-EphB2 contacts, which promotes and orients SC migration and appears to contribute to myofibroblast differentiation. At the same time, dedifferentiated SCs produce monocyte chemoattractant protein 1 (MCP1), Il-1 (α and β) and pancreatitis-associated protein III (PAPIII), which recruits more macrophages to the damaged nerve region, to help clean myelin and axon debris[630–632].

These macrophages also promote vascularization of the space between the two stumps, by release of VEGF and HIF, thus preparing the site for axonal regrowth. At the same time, dedifferentiated SCs migrate along the new vasculature, forming Büngner bands and guiding regrowing axons. Upon reinnervation, SCs re-differentiate and remyelinate axons, contributing to the termination of the inflammatory response.

Underlying all the processes occurring during this phase is the proliferation of several cell types, including keratinocytes, ECs and fibroblasts, among others. Therefore, understanding how proliferation is regulated in these cells is paramount to understand how the proliferative phase is setup and regulated.

This page was intentionally left blank

1.1.3.1. Regulation of Proliferation

Proliferation in vertebrates is regulated by several intracellular pathways that are activated by external factors, like hormones, growth factors, cytokines, extracellular matrix components, etc. Growth factors, in particular, are a common strategy for cells to communicate with each other the need to proliferate.

In the context of wound healing, as we have seen, several cell types are required to proliferate for the wound to close and missing tissue to be reconstituted or, at least, replaced with a semi-functional one. Amongst these cell types, probably the highest portion belong to the highly heterogeneous group of fibroblasts, followed by keratinocytes and other epithelial cell types. In all these cells proliferation regulation has been associated, at least partially, by signaling involving RTKs.

The most widely studied family of RTKs is the ErbB family of receptors, and their downstream signaling, particularly in the context of cancer. In 1984 the oncogene v-ErbB was found to contain transformations of Egfr motifs[633], suggesting a role of EGFR in cell transformation. From then on, Egfr overexpression was found to be positively correlated with the progression of carcinomas, sarcomas, non-small cell lung cancer and malignant gliomas, and the levels of Egfr were shown to predict tumor grade, patient prognosis, and relapse rate[634–636].

This relevance in cancer has led to the great body of work produced about this pathway, resulting in a profound understanding of its regulation and complexity[812]. Besides being a highly significant player in cancer development, the EGFR signaling pathway is also of extreme importance during embryonic development[636,637]. This is clearly observable in mice mutant for any of the ERBB receptors, which exhibit severe malformations of several tissues, explaining why studies involving the regulation of proliferation in several contexts tend to focus on EGFR signaling.

The EGFR signaling pathway is composed of four receptor tyrosine kinases – EGFR (also known as ERBB1), ERBB2, ERBB3 and ERBB4[634,638]. These are known to form homodimers and heterodimers[639], and there is ample evidence that different dimers lead to different outputs of the pathway[640–643]. Eleven ligands are known to activate this pathway – Epidermal Growth Factor (EGF), transforming growth factor-α (TGFα), amphiregulin (AREG), epiregulin (EREG), betacellulin (BTC), heparin-binding Egf-like growth factor (HB-EGF), epigen (EPI) and Neuregulin 1-4 (NRG1-4).

These ligands show specificity for the receptors, with EGF, TGFα and AREG binding only to EGFR; BTC, HB-EGF, EPI and EREG bind to either EGFR and/or ERBB4; and the NRGs can bind ERBB3 and ERBB4, although NRG 3 and 4 can only bind to ERBB4[634,638]. There are no known ligands of ERBB2, and this is likely due to ERBB2's extracellular region being shorter than the rest of its siblings, with the ligand-binding domains missing.

Ligand binding to the ERBB receptor is the initial step of pathway activation, resulting in a conformational change of the receptor that exposes its extracellular dimerization domain, allowing contact with another ligand-bound ERBB receptor[644]. Dimerization of the extracellular region of the receptor leads to further conformational changes to the dimer pair, that result in dimerization of intracellular domains as well[645]. Because ligand binding causes these conformational changes, not only is the receptor autophosphorylated but, depending on the dimer, one receptor can also trans-autophosphorylate its pair[646]. In the case of ERBB2, which cannot bind ligands, this dimerization occurs because the native shape of the ERBB2 receptor resembles that of the active form of other ERBB receptors, leading to the suspicion that signaling through ERBB2 could be constitutive[644,647].

Besides autoactivation, ERBB receptors can also suffer transactivation, which constitutes an activation of the ERBB internal signaling pathway even in the absence of appropriate ligands for the ERBB receptors. This can happen, for instances, when JAK2 is activated by cytokine signaling, and activated JAK2 phosphorylates tyrosine residues in the intracellular domains of EGFR and ERBB2, resulting in receptor activation[648,649]. Another way this can happen is through the activity of downstream effectors of the pathway, likely constituting a way for the pathway to regulate its own level of activity[650,651].

The activating phosphorylations of the ERBB receptors occur primarily in tyrosine residues in their cytoplasmic tails, mainly Y703, Y920, Y992, Y1045, Y1068, Y1086, Y1148, and Y117, and lead to the recruitment of several proteins that contain SH2 and PTB domains, as well as proteins containing the domains SH3, 14-3-3, bromo and PH, to the intracellular tails of ERBB receptors[634,638].

Known to bind active ERBB receptors are the proteins SHC, GRB7, GRB2, CRK, NCK, PLCγ, SRC, PI3K, SHP1, SHP2 and CBL. The activation of these signal mediators results in the modulated activation of intracellular pathways, like ERK/MAPK, PI3K/AKT, and JAK/STAT.

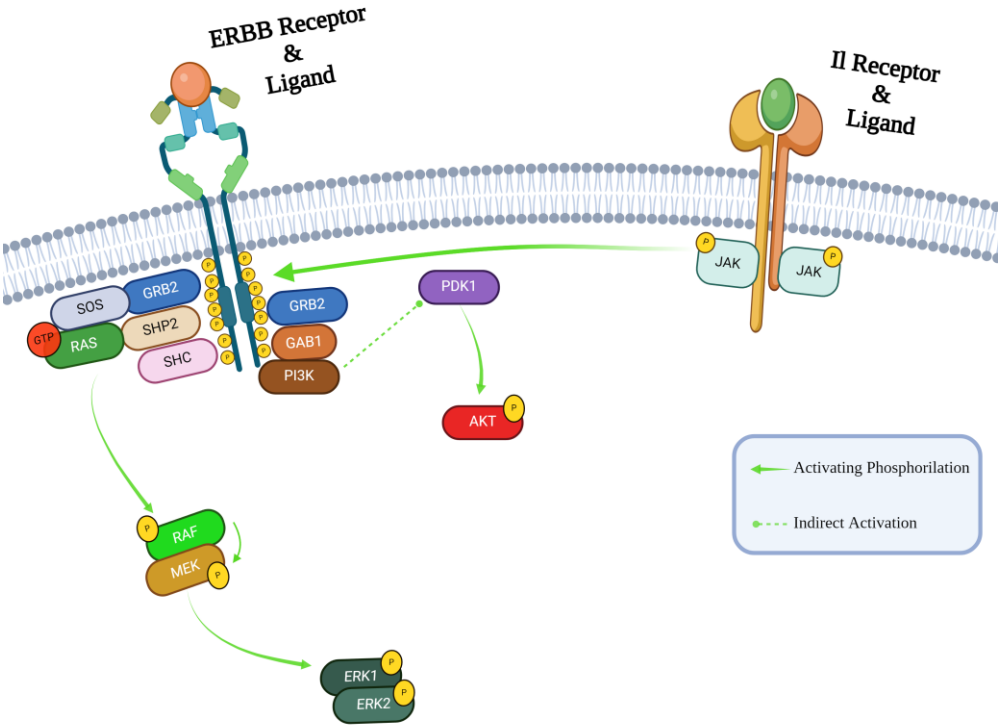

Figure 1.8 – The ERBB signaling pathway. This figure summarizes the the activation of the the PI3K/AKT and MAPK/ERK pathways by the ERBB family of receptors. Image adapted from Wee and Wang, 2017[634] *and created with BioRender.com.*

1.1.3.1.1. The ERK/MAPK Pathway

The MAPK pathway is a group of intracellular signaling paths that share the trait of being composed by MAP kinases. This pathway is involved in the regulation of cell motility, survival, apoptosis, response to stress, metabolism, differentiation and proliferation[830–832].

The MAPK pathway can be divided into two types of paths, with distinct subsets of mediators: Conventional and Atypical. The conventional paths are the ERK1/2 path, the JNK path, the p38 path and the ERK5 path[655,656]. The atypical paths are the ERK3/4 path, the ERK7 path and the NLK path[657]. These pathways are activated through different upstream signals, namely calcium activation, RTK-mediated Ras activation, Protein Kinase C (PKC) activation and G protein-coupled receptor (GPCR)[658]. A summary of the involvement of the different paths in cellular processes can be found in Table 1.3, and we will detail some of them beneath.

Table 1.3 - MAPK/ERK Pathway: Conventional and Atypical Path Mediators. This table summarizes the MAPK, MAPKK and MAPKKK factors associated with each of the known paths of the MAPK/ERK pathway, for both 'Canonical' and 'Atypical' paths. Depicted in this figure is also a list of the biological processes to which each path has been associated to. Question marks represent unknown elements of each path. Table adapted from Lavoie, Gagnon and Therrien, 2020[652]

MAPK/ERK Pathway							
	Conventional Paths				Atypical Paths		
	ERK1/2	JNK	p38	ERK5	ERK3/4	ERK7	NLK
Processes	Proliferation, Survival, Growth, Metabolism, Migration, Differentiation	Proliferation, Survival, Metabolism, Differentiation, Apoptosis, Inflammation	Proliferation, Growth, Metabolism, Differentiation, Apoptosis, Inflammation	Proliferation, Differentiation	Migration, Differentiation	Migration, Autophagy	Proliferation, Differentiation
Stimuli	Mitogens, Serum, Cytokines, GPCRs, Ca^{2+}	Serum, Cytokines, Stress	Serum, Cytokines, Stress	Mitogens, Serum, Stress	Serum, Stress	Mitogens, Stress	Serum, Cytokines, GPCRs, Ca^{2+}
MAPKKK	ARAF, BRAF, RAF1, KSR1,KSR2, TPL2, MOS	MEKK1-4, TOAK1/2, TAK1, DLK1, MLK2/3, ASK1/2, TLP2/COT	MEKK1-4, TOAK1/2, TAK1, DLK1, MLK2/3, ASK1/2, TLP2/COT	MEKK2/3	PAK	?	TAK1
MAPKK	MEK1, 2	MKK4, 7	MKK3, 4, 6	MEK5	?	?	HIPK2
MAPK	**ERK1, 2**	**JNK1, 2, 3**	**p38α, β, γ, δ**	**ERK5**	**ERK3, 4**	**ERK7**	**NLK**

In the conventional paths, three to five layers of protein kinases, known as MAP4K (MAPK Kinase, Kinase, Kinase), MAP3K, MAPKK and MAPK, as well as MAPK-activated protein kinases (MAPKAPK), establish hierarchical interactions with each other in order to propagate signalling.

The most comprehensively studied path in the MAPK/ERK pathway is the ERK1/2 path (commonly referred to by just ERK), due to its involvement in proliferation regulation in development, tissue homeostasis and cancer. The first step of activation of this pathway by RTKs is the recruitment of GRB2 and SHC to the cell membrane, which are capable of then recruiting guanine nucleotide exchange factors. A visual depiction of this pathway can be found in Figure 1.9.

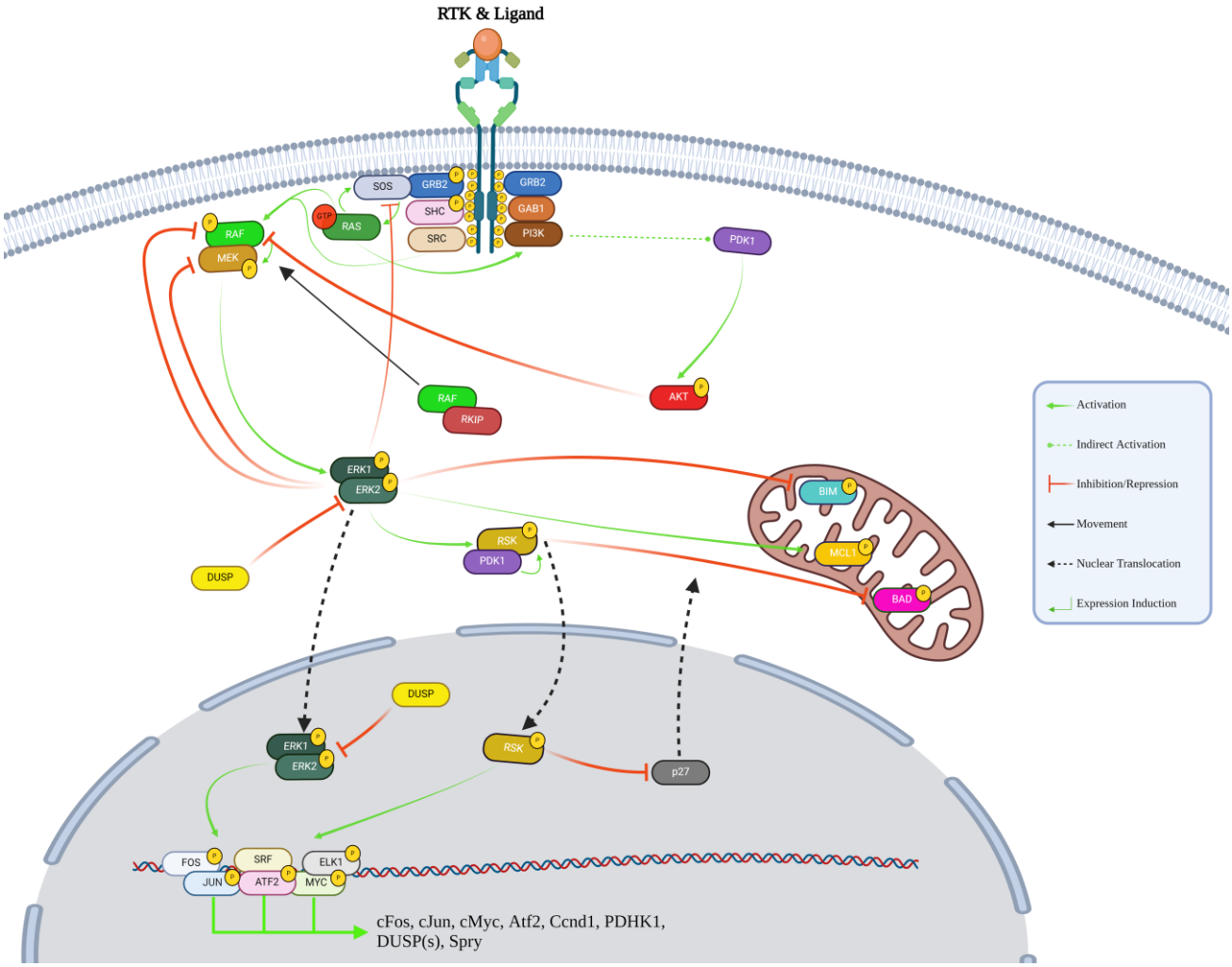

Figure 1.9 - The ERK1/2 path of the MAPK/ERK pathway. The figure depicts the ERK1/2 canonical path of the MAPK/ERK pathway and some of its intervenients, as well as some transcription factors it regulates and some of the genes whose expression they induce. Image created with BioRender.com.

Phosphorylated residues in the RTK, like Y1068 and Y1086 of the ERBB receptor, recruit GRB2, while phosphorylation of Y1148 and Y1173 recruits SHC[659,660]. SHC binding to the receptor leads to additional phosphorylations, like Y317 in SHC, which creates other binding sites for GRB2. Furthermore, SHC can also be phosphorylated by SRC at Y239/240, further increasing GRB2's affinity for it[634,661].

Activated GRB2 has the important role of recruiting SOS to the receptor, by binding to its proline-rich carboxy-terminal tail[662]. GRB2 can also recruit SOS to the receptor by binding phospholipase D, which produces phosphatidic acid, another important recruiter of SOS[663,664].

SOS is a guanine nucleotide exchange factor that can activate RAS, by inducing it to exchange GDP for GTP[665]. RAS is inactive in the GDP-bound conformation but becomes active in the GTP-bound conformation[666]. Increased recruitment of SOS to the receptor will increase the amount of available RAS-GTP in the membrane[667,668].

Not only is SOS capable of recruiting RAS to the receptor, but RAS can also recruit more SOS, greatly potentiating RAS activation[669]. Besides the SOS-mediated guanine exchange, RAS activation also requires SHP2 dephosphorylation of an SRC-mediated phosphorylation at RAS's Y32 residue, which impedes RAF binding to RAS[670,671].

RAS is a major signaling hub, responsible for the activation of important downstream effectors like RAF and PI3K[672,673]. Activated RAS interacts with RAF1, whose phosphorylation at S338 and Y341 permits the binding of MEK1/2[674–678]. RAF dimers, or RAF/MEK heterodimers, are recruited to the plasma membrane when sufficient RAS activation has occurred, where RAS dimers activate them[679]. A transient MEK-RAF-RAF-MEK tetramer is formed, which facilitates RAF activation via cis-autophosphorylation of the RAF activation loop[680,681].

RAS activation of RAF is not complete, however. RAS seems to mediate the phosphorylation at S338, which occurs through RAF autophosphorylation, while another activating phosphorylation at Y341 is promoted by SRC[676,682]. Additionally, regulation of RAF is also achieved by phosphorylations at S471, T491 and S494, that stimulate RAF activity, and by phosphorylation at S259 and S621, which are inhibitory because they allow RAF to be sequestered by 14-3-3 family proteins. Phosphorylation at S259 is particularly interesting because it is catalyzed by AKT, and constitutes a way by which the PI3K/AKT pathway might regulate ERK/MAPK activity[683].

Also interesting are the phosphorylations of S23, 49, 289, 296, 301 and 642, which are proposed to be catalyzed by ERK in a negative feedback, constituting a form of pathway autoregulation[684]. Besides being phosphorylated by AKT, RAS itself can activate PI3K, making itself a hub of signal integration between the ERK/MAPK and the PI3K/AKT pathways[672].

RAF refers to three closely related proteins of the same family, RAF1, ARAF and BRAF, which have some differences in activity, tissue distribution and regulation[685]. For example, ARAF has the weakest kinase activity of the three, while BRAF has the strongest. RAF's consensus molecular structure contains three conserved regions of significant importance for RAF

activity. Conserved region 1 (CR1) binds RAS, CR2 has many regulatory serine and threonine residues, and CR3, in the C-terminal region, is the functional catalytic region, which confers activated RAF its serine/threonine protein kinase activity[686,687]. RAF activation, as mentioned, requires its localization to the membrane through RAS interaction, dimerization and several post-translational modifications, but also dissociation from the RAF kinase inhibitor (RKIP) and binding to the RAS kinase inhibitor[688–690].

RAF has as primary substrates MEK1/2, which are threonine/tyrosine dual specificity kinases[691,692]. Upon activation, RAF's CR3 domain can interact with MEK1 and MEK2 (generally referred to as MEK1/2 due to their similarity). MEK1/2 binding to RAF allows RAF to activate them by phosphorylating residues S217 and S221 in their activation segments[693].

MEK1/2 are a rare dual-specificity kinase, capable of phosphorylating tyrosine and threonine residues[694]. MEK1/2 can form heterodimers or homodimers, and the composition of these dimers slightly alters their signaling niches[695,696]. Activated MEK1/2 can directly interact with ERK1/2, phosphorylating them in TEY motifs in their activation loops, first at T202 and then Y204, activating them[697]. Besides activating them, MEK1/2 binding of ERK1/2 also anchors them in the cytoplasm, because MEK's NES localizes them to the cytoplasm[698].

MEK1/2 heterodimers are regulated, in part, by a negative feedback of ERK1/2 activity, which phosphorylates MEK1 on Y292[699]. This results in the dephosphorylation of the serine residues in MEK1's activation loop, inhibiting it. An analogous regulatory loop is not present in MEK2, which could constitute a method for the pathway itself to adjust its signaling niche, by changing the stoichiometry between activated homodimers and heterodimers.

ERK 1 and 2 are a pair of proline-directed serine/threonine kinases that seem to be activated as a dimer in most contexts. ERK1/2 can phosphorylate, and therefore regulate, over six hundred substrates, including transcription factors, cytoskeletal elements, apoptotic regulators, kinases and phosphatases, RNA processing machinery, among others, making it the primary regulator of proliferation in the cell[700,701]. ERK can form both homo and heterodimers, just like MEK, and these can be phosphorylated or unphosphorylated, but the dimerization equilibrium favors dual phosphorylated dimers[702]. Unlike MEK, ERK does not need to be a dimer to be phosphorylated, despite subsequent dimerization[703].

ERK substrates are both cytoplasmic and nuclear, and are further expanded by the indirect activity of ERK through the RSK and MSK kinases[704]. Cytoplasmic function of ERK is possible due to its retention in the cytoplasm, both through MEK1/2 binding, as mentioned, but also through PEA15, MKP3 and β-Arrestin[686,705,706]. Curiously, a vast number of ERK1/2

cytoplasmic targets are players in its own pathway, like SOS, RAF and MEK, constituting targets of ERK/MAPK negative feedback autoregulation.

An important ERK1/2 cytoplasmic substrate, not belonging to the upstream pathway, is RSK, which exists in three isoforms (RSK1, 2 and 3). RSK is phosphorylated by ERK1/2 on its T573 and Y359/S363 residues, which results in a partial activation of RSK[707–709]. This phosphorylation induces a conformational change that allows RSK to autophosphorylate its S380 residue, creating a docking site for PDK1[710]. PDK1 phosphorylates RSK on S221, fully activating it, leading to its translocation to the nucleus[711].

In the nucleus, RSK activates transcription factors like cFOS, NUR77 and SRF, which are particularly important for cell proliferation, and will also help regulate NF-κB activity[712–717]. SRF, in association with three ternary complex factors (TCFs - ELK 1, 3 and 4), contributes to the induction of expression of the immediate early genes (IEG) cFos, cJun, cMyc and Atf2, which are the primary regulators of cell cycle progression. RSK is, therefore, responsible not only for IEG expression, but also for their activation.

Besides regulating the expression and activity of the IEGs, RSK might algo contribute to proliferation regulation by phosphorylating the cell cycle inhibitor p27 on Y198, resulting in its nuclear exclusion[718,719]. Another way RSK regulates proliferation is by phosphorylating MAD1, a cMyc expression suppressor, contributing to its accelerated degradation and an increase of cMyc expression[720]. Together, all these roles make RSK a very important cog on the machinery of proliferation regulation.

Besides leading to the nuclear translocation and activation of RSK, ERK1/2 activation also contributes to their own nuclear translocation. While cytoplasmic ERK1/2 is primarily found in dimeric form, nuclear ERK tends to be monomeric[721,722]. The most recent model to explain nuclear translocation of ERK involves phosphorylation on the SPS motif of ERK's NTS, facilitating Importin-7 binding. Importin-7 then escorts ERK through the nuclear pore, and upon nuclear entry the RAN GTPase dissociates ERK from Importin-7[723,724]. While ERK phosphorylation is necessary and sufficient for initial rapid translocation to the nucleus, sustained nuclear signaling requires transcriptional induction of nuclear anchoring proteins[698,725].

Nuclear ERK1/2 phosphorylates several transcription factors, like the IEGs FOS, JUN, ELK1, MYC and ATF2, stabilizing them and inhibiting their degradation[726]. FOS, for instances, is phosphorylated by ERK1/2 at S374 and by RSK at S362, and JUN is phosphorylated by ERK1/2 at S63 and S73[727,728]. This stabilization allows FOS and JUN to form AP-1 complexes

and augment their availability in the nucleus. AP-1 is responsible for the induction of important cell cycle regulators like Ccnd1, the gene of Cyclin D1. ERK1/2 also phosphorylate MYC, inhibiting its degradation[729,730]. Sustained ERK activity also facilitates inhibition of anti-proliferative expression regulators TOB and FOXO4a, further contributing for cell cycle progression[731,732].

Has we have mentioned, ERK1/2 directly regulate hundreds of factors, several of which constitute ways for ERK to regulate its own activity (Figure 1.9). Besides the negative regulation of MEK1 that we previously identified, ERK can also phosphorylate both RAF1 and BRAF, interfering in their ability to be recruited to RAF[684,733]. ERK can also mediate inhibitory phosphorylations of SOS, either directly or through the activation of RSK2[734,735].

ERK has been shown to phosphorylate RTKs, as well as an important scaffold protein, KSR. KSR binds RAF, MEK1/2 and ERK1/2, enhancing MAPK/ERK signaling, as well as controlling specificity, subcellular localization and duration of interactions[736,737]. For instances, KSR forms inactive complexes with MEK, but helps enhance its translocation to the membrane, upon RAF activation, and stability of RAF-MEK binding[738]. Therefore, an inhibitory KSR phosphorylation by ERK that decreases its ability to bind to RAF and MEK results in a negative feedback loop on ERK activation. In turn, an example of ERK positively regulating its pathway activity is the phosphorylation of RKIP, relieving RAF and MEK from its inhibitory effect[690,739].

Besides direct interactions with several different mediators, the MAPK/ERK pathway also influences its own regulation through genomic processes, in particular through the induction of the expression of dual-specificity phosphatases (Dusps) and the tumor suppressor sprout (Spry)[740].

DUSP proteins can bind both phosphorylated and unphosphorylated ERK1/2 and inactivate it or keep it inactive. DUSPs 6, 7 and 9 are cytoplasmic variants that have specificity for each ERK, while variants 1, 2, 4 and 5 are nuclear and can bind both ERK proteins, as well as JNK and p38[741,742]. DUSP2, 4, 5 and 6 also have an important function in keeping ERK1/2 in specific locations in the cell, with variants 2, 4 and 5 sequestering ERK in the nucleus, while DUSP6 keeps them in the cytoplasm[705,743,744]. Not only does ERK regulate Dusp expression, but it also regulates their activity. For example, ERK can phosphorylate DUSP1 and 4, increasing their stability and enhancing their phosphatase activity[745,746].

Moving on to SPRY proteins, four isoforms have been identified in mammals, with SPRY2 exhibiting the most significant inhibition of MAPK signaling, at the level of RAF activation[747].

SPRY1 and SPRY2 have been suggested to regulate ERK pathway activity at the level of RAS and the RTKs[748]. As for SPRY4, it was shown that it can inhibit RAF activation by RAS-independent paths, but not RAS-mediated activation[749]. SPRY regulation of MAPK/ERK pathway constitutes a rapid negative feedback loop, with their activity, similarly to DUSPs, also being regulated by post-translational modifications mediated by ERK activity[742,750,751].

As we have discussed, the ERK1/2 typical ERK/MAPK pathway activation culminates in the expression of genes necessary for proliferation induction, but not only. For example, MAPK/ERK signaling also regulates apoptosis[752]. While MAPK/ERK regulation can both promote, and inhibit, apoptosis, hyperactivity of ERK signaling as mostly been associated with the inhibition of apoptosis[753].

ERK regulation of apoptosis seems to occur primarily through the intrinsic pathway (or mitochondrial pathway) by, for instances, phosphorylating BIM, a pro-apoptotic protein, thus inhibiting its activity, and MCL1, an anti-apoptotic protein, stabilizing it[754,755] (Figure 1.9)

The intrinsic pathway is controlled by the B cell lymphoma 2 (BCL2) family of proteins, which is composed of the anti-apoptotic factors BCL2, BCL-xL, MCL1, BCL-W and A1, that bind the BH3 domains of pro-apoptotic factors BAX and BAK, sequestering them[756].

Upon cellular insults, like DNA damage, osmotic stress, or absence of growth factors, BH3-only proteins (BOP), like BIM, BAD, BMF, BID and PUMA, associated with BH3 domains of BCL2 family members, resulting in the release of BAK and BAX[757]. BAK and BAX can then oligomerize, forming pores in the outer mitochondrial membrane. This leads to the uncoupling of the electron transport chain, and release of apoptogenic factors like cytochrome C. Released cytochrome C in the cytoplasm stimulates the apoptosome complex, which creates a succession of caspase activations, starting with the cleavage of caspase 9, then 3 and 7, committing the cell to apoptosis.

BIM is the most potent pro-apoptotic BOP, likely because it can associate with all the anti-apoptotic proteins, while other BOPs seem more selective[758]. Upon serum stimulation, BIMEL, one of the splicing variants of BIM, is phosphorylated by ERK on at least four residues[759]. These ERK-mediated phosphorylations regulate BIM by two means: They increase BIMEL turnover by signaling it to proteasomal degradation, and they provoke a dissociation of BIMEL from anti-apoptotic factors like BCL-xL and MCL1[759,760].

ERK activity also inhibits the pro-apoptotic functions of other BOPs. For example, ERK phosphorylates BIK, stimulating its degradation, and BMF, blocking its activity[761,762]. ERK also regulates BOPs activation through indirect mechanisms, like activating RSK. RSK in turn

inhibits BAD by phosphorylating two of its serine residues, creating a binding site for 14-3-3 family proteins that will translocate BAD from the mitochondrial membrane to the cytoplasm, while also blocking its interaction with anti-apoptotic factors BCL-xL and BCL2[763,764]. ERK can also regulate apoptosis further downstream of its activation cascade, by phosphorylating caspase 9 and preventing its cleavage[765]. Finally, ERK activity can also promote anti-apoptotic factors like MCL1, whose phosphorylation by ERK increases its stability, slowing down its turnover and promoting cell survival[755].

Another way the ERK pathway regulates apoptosis is by expression regulation, through the repression of Bcl2l11 (BIM) gene. ERK exerts this influence by phosphorylating the transcription activator FOXO3a, which promotes its nuclear exclusion and proteasomal degradation[932]. ERK also regulates the expression of Bcl2, Bcl2l1 (enconding BCL-xL) and Mcl1 in various cellular contexts[763,766].

ERK is not only capable of regulating several substrates and processes on its own, but also in cooperation with other pathways, and the regulation of apoptosis is a good example of this. For example, both MAPK/ERK and PI3K/AKT signaling stimulate cap-dependent translation of the apoptosis inhibitor BIRC5 (also known as Survivin)[767].

Proliferation is a process that requires a high level of energy production. For this reason, and since the MAPK/ERK is an important regulator of proliferation, it is no wonder that it is also involved in the metabolic regulation of energy production. Fast proliferating cells, particularly cancer cells, in which this phenomenon has been extensively demonstrated, favor glycolysis as a source of energy, in detriment of oxidative phosphorylation (OxPhos), a phenomenon called Warburg effect[768].

While relevant ERK targets in glycolysis regulation have not been formally identified, suspects of this role include MYC and the transcription factor hypoxia-inducible factor 1α (HIF1α), which are both directly phosphorylated by ERK, resulting in their nuclear accumulation and transcriptional activity[769–773]

Independently or collectively, MYC and HIFα modulate the expression of several genes involved in aerobic respiration and glucose metabolism. They also prevent pyruvate from entering the tricarboxylic acid (TCA) cycle, by cooperatively enhancing the expression of pyruvate dehydrogenase kinase 1 (PDHK1) that blocks the conversion of pyruvate to acetyl-CoA, through suppression of the activity of pyruvate dehydrogenase[771,774–778].

The switch to aerobic glycolysis by rapidly proliferating cells in mammals requires the expression of the embryonic pyruvate kinase M2 (PKM2)[779]. Activated ERK2 phosphorylates

PKM2 and promotes its conversion to a transcription co-activator, resulting in MYC expression[780]. ERK also regulates another important glycolysis enzyme, the 6-phosphofructo-2-kinase/fructose 2,6-biphosphatase 2 (PFKFB2), through RSK, which phosphorylates PFKFB2, stimulating its activity and increasing glycolytic flux[781].

One final cellular process whose regulation involves MAPK/ERK activity is migration. Activation of ERK signaling is capable of initiating a migratory response to mechano-transduction cues or cell stimulation by soluble factors[782].

Cell migration is a three-step process that involves protrusion of the cell leading edge (lamellipodium), attachment of the lamellipodium to the substrate (through focal adhesions) and contraction of the trailing edge, at the same time as rear-end focal adhesions are dissolved[783]. This process is primarily regulated by the cyclic activation of RHO family GTPases (RHO, RAC1 and CDC42), that regulate the formation of actin and actomyosin filaments, as well as focal adhesion dynamics[784].

ERK regulation of migration occurs through phosphorylation of important components of, for instances, lamellipodia formation, with ERK activity influencing the rate and polarity of actin polymerization. To do this, ERK phosphorylates WASF2 and ABI1, two components of the WAVE2 regulatory complex (WRC) that is a key effector of RAC1 for migration regulation[785,786]. These phosphorylations increase the interaction of WRC with actin and the actin nucleator complex ARP2-ARP3, which stimulates polarized actin filamentation at the leading edge and, therefore, forward motion[787,788]. ERK, through RSK, also leads to filamin A phosphorylation, which increases stability in the cell cortex by both crosslinking actin filaments, and binding to integrins[789].

Focal adhesions are composed of transmembrane integrins that are attached to the extracellular matrix, talin, vinculin and zyxin connected to the actin cytoskeleton, as well as a series of signaling and scaffolding proteins like focal adhesion kinase 1 (FAK1) and paxillin. ERK activity on focal adhesions mostly promotes their turnover[790,791].

ERK is recruited to nascent focal adhesions by SRC-phosphorylated paxillin[792–796]. This allows ERK to phosphorylate paxillin and FAK, which seem to serve two distinct purposes. Paxillin phosphorylation by ERK increases FAK recruitment and local stimulation of RAC1 activity, which promotes actin filament extension and focal adhesion turnover at the leading edge. On the other hand, ERK phosphorylation of FAK at S910 promotes FAK dephosphorylation and inhibition by the phosphatase PTP-PEST[797]. This dual role of ERK has been suggested to maintain dynamic adhesions that allow rapid cell migration.

ERK activity also has a widespread effect on actin cytoskeleton dynamics and regulation, through the phosphorylation of several RHO family guanine nucleotide exchange factors and GTPase-activating proteins, but also through the transcriptional regulation of cytoskeletal factors[798]. For example, ERK appears to both positively and negatively control the function of nuclear MRTF, which is recruited to promoters containing SRF, and activates a transcriptional program that is mostly involved in actin cytoskeleton homeostasis, involving hundreds of genes that control the structure and dynamics of the actin cytoskeleton, like actin itself, vinculin, zyxin and integrin[799,800].

As we've just detailed, the MAPK/ERK pathway is indispensable to the correct regulation of several cellular functions, particularly proliferation, operating as an integrator of several cell-state cues, but also information from other pathways.

1.1.3.1.2. The PI3K/AKT pathway

Another pathway with various responsibilities in cellular dynamics is the PI3K/AKT pathway, which is involved in metabolic regulation, cell growth, cell survival, differentiation, and proliferation[801,802]. The role of this pathway in proliferation is particularly evident in tumorigenic events, with several cancer types being associated with hyperactivity of PI3K/AKT due to mutations to one or more of its constituents[803,804].

The canonical path of the PI3K/AKT pathway is activated by stimulation of RTKs or GPCRs, which recruit one or more isoforms of the class I PI3K family to the plasma membrane[805]. Class I can be subdivided in subclass IA (PI3Kα, β, and δ), which are activated by receptor tyrosine kinases, and subclass IB (PI3Kγ), which is activated by G protein-coupled receptors, depending on the type of catalytic isoform they contain[804,806]. Subunits α and β are ubiquitously expressed, while δ and γ are primarily expressed in lymphocytes[807–810]. Class I PI3K are obligatory dimers composed by a regulatory subunit, p85, which binds to the receptor, and a catalytic subunit, p110, which mediates the generation of PIP_3[811], which is the most important role of class I PI3Ks. These phosphorylate $PI4,5P_2$, thereby producing PIP_3, which can also be generated by class II PI3Ks activity on PI4P[805].

The recruitment of class I PI3K, upon activation, to RTKs, like the ERBB receptors, varies depending on the receptor. For example, ERBB3 and ERBB4 bind PI3K directly, while ERBB1 and ERBB2 do not[812–814]. This occurs because p85 is capable of recognizing a motif of the ERBB proteins that is only present in ERBB3 and ERBB4[814]. Interactions with ERBB1 and 2 have to be mediated by GAB1, which binds to ERBB receptors through GRB2[815–818]. Binding of GAB1 by GRB2 induces the phosphorylation of GAB1 on Y446, 472 and 589, which become binding sites for PI3K's p85 subunit[818]. Since PI3K's activity leads to further GAB1 recruitment, this constitutes a feedback loop of signal amplification. Besides GAB1, RAS and CBL are also capable of mediating the recruitment of PI3K to the receptor[812,819,820].

Regardless of the isoform of PI3K recruited and the method of recruitment, their output is identical: Re-localization of inactive AKT to membrane sites of PIP_3 accumulation. PIP_3 is an important secondary messenger, and the principal mediator of PI3K activity, by recruiting PH (pleckstrin homology) domain-containing proteins, like AKT, RHO, RAC, RAS, RAF and GAB1/2, to the membrane[803,821,822]. PI3K-mediated recruitment of these proteins can be counteracted by the phosphatase and tensin homolog (PTEN), a PIP_3 phosphatase that reduces its availability in the membrane[823].

The most important PH domain-containing protein in the PI3K/AKT pathway is its namesake, AKT. AKT is the general term applied to a set of three serine/threonine kinase isoforms (AKT1, 2 and 3 also called PKBα, β and γ) that can act upon a large number of substrates involved in several different cellular dynamics, as mentioned before[803]. AKT isoform recruitment seems to always be dependent on PI3K, but different cell types show differential RTK-mediated activation of each isoform, apparently in a RAS-dependent manner[824,825]. Furthermore, expression of each isoform seems to be distinct, with AKT1 being ubiquitous, AKT2 being enriched in insulin-responsive tissues and AKT3 seeming dedicated to the brain. Perhaps because of this the majority of their targets are shared, but exceptions exist.

AKT1's activation after translocation to the plasma membrane occurs through phosphorylation by PDK1, at the T308 residue, and by mTORC2, at the S473 residue[826–829]. Equivalent phosphorylations of AKT2 and AKT3 by these mediators also occur, in the T309 and S474, and T305 and S472, respectively. PDK1 is also important for the activating phosphorylations of other AGC family protein kinases, like all isoforms of PKC, S6K, SGK and RSK[830].

The T308 phosphorylation, in the activation or T-loop of the catalytic protein kinase core, is necessary and sufficient for AKT activation, but full activation is only achieved by phosphorylation at S473 as well, in the C-terminal hydrophobic motif, which also stabilizes the previous phosphorylation[802,827]. mTORC2 activation of AKT is particularly important for its regulation of some of its downstream targets, like the FOXO transcription factors[831], which are a family of tumor suppressor transcription factors[832,33].

While the T308 and S473 phosphorylations are viewed as being obligatory and rate limiting for maximal AKT activity, many other post-translational modifications are used to fine tune its activity, localization and, possibly, substrate specificity. For example, phosphorylation of T450 is constitutively induced by mTORC2 and is necessary for proper folding of AKT, occurring co-translationally[834,835]. AKT can also be phosphorylated in its regulatory domain, in S477 and T479 in a cell cycle-dependent manner, by the CyclinA-CDK2 complex, and in S473 by mTORC2, increasing AKT activity[836]. AKT's activity can also be increased by CK2's phosphorylation at S129, while GSK3α phosphorylation of T312 has been shown to be repressive[837,838].

Besides phosphorylation, several other types of post-translational modifications are used to regulate AKT activity. Acetylation of K14 has been proposed to be necessary for AKT binding to PIP_3 for membrane translocation[839]. Besides acetylation, K14 can also be ubiquitinated and methylated. In another example, ubiquitylation of AKT's K48 residue is catalyzed by multiple

E3 ubiquitin-ligeases, targetting AKT for degradation[840]. However, not all ubiquitinations lead to degradation, as is the case of Lys residues in AKT's PH domain, where they are promoted by TRAF6, SKP2 and NEDD4-1, increasing membrane localization, a process that is counteracted by the deubiquitinating enzyme CYLD[841–844]. Another type of post-translational regulation of AKT is through SUMOylation of several Lys residues, like K276, by the SUMO E3 ligase PIAS, which have been linked with AKT activation[845].

Negative regulation of AKT activity is performed primarily by two protein phosphatase families, the protein phosphatase 2A (PP2A) and the PH domain leucine-rich repeat protein phosphatases (PHLPP). PP2As dephosphorylate AKT at the T308 residue, thus inactivating it, while PHLPPs dephosphorylate the S473 residue[846–848].

AKT isoforms have well over 100 substrates, and their parallel regulation of multiple substrates appears to lead to considerably different downstream effects depending on the context. AKT counts as its substrates lipid and protein kinases, transcription factors, regulators of small G proteins and vesicle trafficking mediators, metabolic enzymes, E3 ubiquitin ligases, cell cycle regulators, among others.

AKT regulates these substrates primarily through Ser and Thr residue phosphorylation, mostly leading to inhibitory effects. However, it is well established that a large majority of these substrates are not exclusively regulated by AKT, establishing context-dependent redundancies in the regulation of the PI3K/AKT signaling pathway. Nevertheless, a summary of AKT regulatory interactions can be found in Figure 1.10.

One of the most prominent substrates of AKT is the Ser and Thr protein kinase glycogen synthase kinase 3 (GSK3). GSK3 has two isoforms, GSK3α and GSK3β, which share 85% sequence homology and are, therefore, functionally redundant in some contexts[849]. Growth factor signaling, through AKT, leads to an inhibitory phosphorylation on the N-terminal region of GSK3, at S21 in GSK3α and S9 in GSK3β. This phosphorylation creates an intramolecular pseudo-substrate that blocks the phosphate-binding pocket of GSK3, impeding substrate accessibility.

GSK3 is generally viewed as being active in the absence of exogenous signals, being strongly inhibited upon growth factor stimulation. GSK3 regulates a large, functionally diverse set of direct downstream targets, most of which are inhibited or degraded as a consequence of GSK3's activity. Through the formation of complexes with other effectors, GSK3 also participates in other pathways, most notably the WNT pathway.

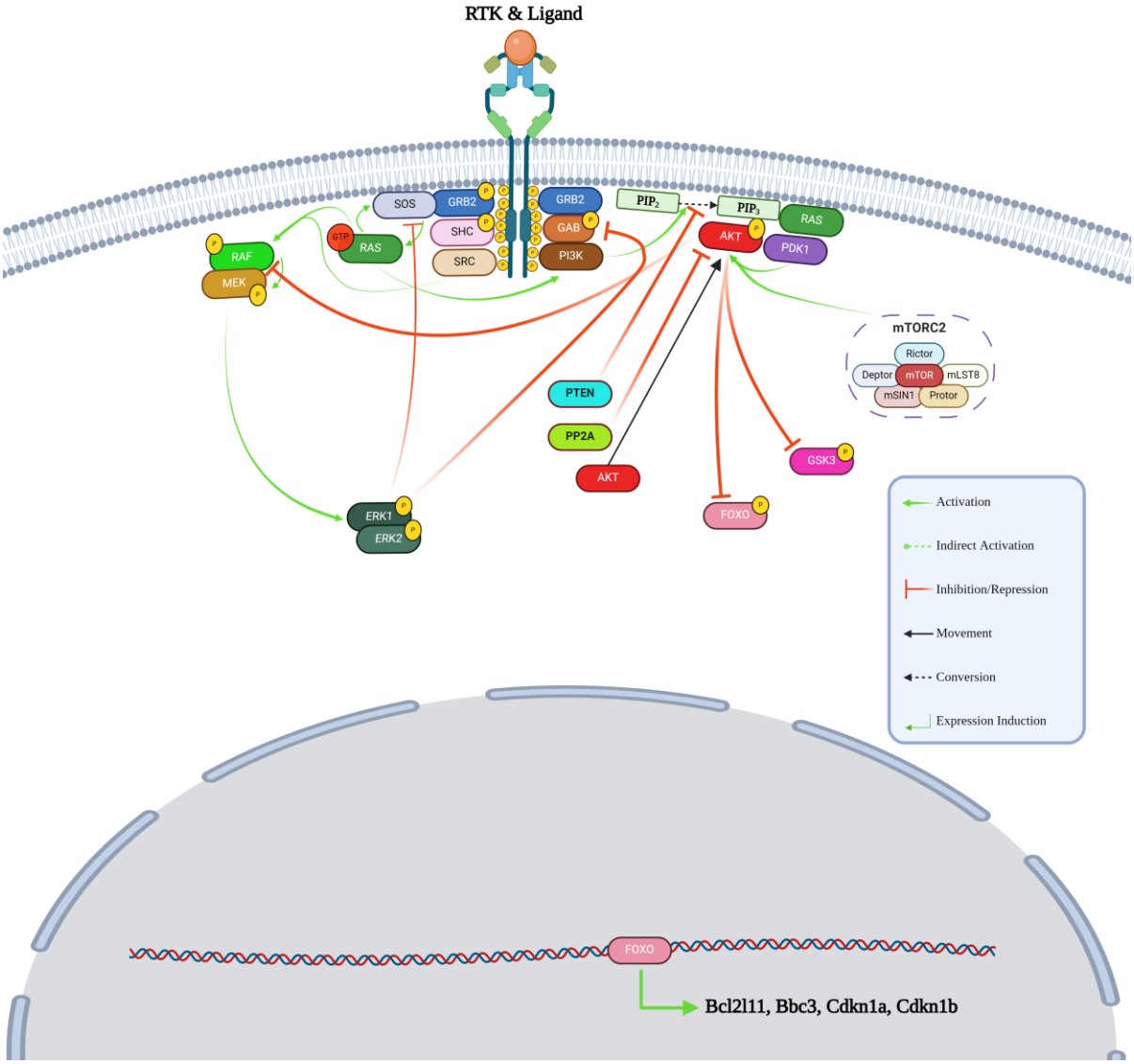

Figure 1.10 - The PI3K/AKT canonical signaling pathway. Represented in this figure are the most established factors in the PI3K/AKT pathway, as well as the relationships they establish with each other and mediators of the MAPK/ERK pathway. Image created with BioRender.com.

The phosphorylation of some of the GSK3 targets involved in cell survival and proliferation, like MCL1 and MYC, which are phosphorylated upon JNK and ERK activation respectively, creates a 'phospho-degron' that is recognized by E3 ubiquitin ligases, and degraded[850–853]. AKT's phosphorylation of GSK3 therefore prevents their degradation.

Besides cell survival and proliferation, GSK3 also regulates cellular metabolism, either directly through inhibition of metabolic enzymes (like glycogen synthase), or indirectly through the inhibitory regulation of transcription factors, like MYC, SREBP1c, HIF1α and NRF2[849,854,855].

Another very important group of AKT substrates is the Forkhead Box O (FOXO) transcription factor family. This group of proteins is composed of FoxO1, 3, 4 and 6, and controls a diverse set of genes that are involved in adaptation to fasting and low insulin, and IGF1 signaling,

among other processes[856,857]. PI3K/AKT pathway activity leads to a considerable translocation of FOXO proteins from the nucleus, minimizing their genetic regulation[858,859].

AKT's regulation of FOXO proteins occurs through direct phosphorylation of three conserved residues, especially in the amino-terminal region (T24 on FoxO1) and in the NLS (S256 in FOXO1), creating recognition motifs for the 14-3-3 family of proteins, which will facilitate the nuclear export and cytoplasmic sequestration of FOXO. This decreases the transcriptional induction of genes involved in apoptosis induction, like BIM and PUMA, cell cycle arrest, like p21 and p27, catabolism and growth inhibition, namely Sestrin3, MAP1LC3B and BNIP3, and tissue-specific metabolic changes, like PEPCK and G6PC[856,857].

PI3K/AKT evolutionarily conserved role of promoting cell, tissue and organismal growth is primarily mediated through the activation of the protein kinase complex mTORC1, responsible for stimulation of the biosynthetic processes that promote cell growth[759].

mTORC1 and mTORC2 are two complexes composed, in part, by a serine/threonine kinase called mTOR. These complexes have distinct subunits and substrates, but both are involved in anabolic metabolism, cell growth and proliferation, and in integrating mitogenic and nutritional signaling, specially mTORC1[759,860]. mTORC2, analogously to PDK1, also phosphorylates AGC kinases, with some being constitutively phosphorylated (PKCs) and others only in response to PI3K signaling (AKTs and SGKs).

Activation of mTORC2 is a poorly understood process, but a study suggested that it could involve a PH domain in the SIN1 component of mTORC2, which could bind PIP_3 and relief autoinhibitory effects of the complex over mTOR's kinase activity[861]. In this hypothesis, PIP_3 is suggested to have the dual role of relocalizing mTORC2 to the membranes, as well as relieving its autoinhibitory condition, allowing for AKT phosphorylation. Contradicting this hypothesis, another study suggested that PI3K activity is dispensable for mTORC2 activity on membranes[862].

As for mTORC1, when proliferation is induced mTORC1 is indirectly activated by AKT, ERK1/2 and RSK activity[863]. AKT activation of mTORC1 occurs through release of inhibitory activity over RHEB, which can then activate mTORC1[864]. RHEB is regulated by TSC1, TSC2 and TBC1D7s activity, which form a complex called the TSC complex, that suppresses RHEB through conversion of RHEB-GTP in RHEB-GDP[759].

TSC2 (also known as Tuberin) is phosphorylated by AKT in 5 residues, S929, 981, 1130, 1132 and T1462, and by ERK1/2 on S664, which leads to its inhibition[760,762,860,865]. Besides phosphorylating TSC2, AKT has also been suggested to directly phosphorylate mTOR on

S2448, but other studies demonstrated that this phosphorylation is mediated by S6K, downstream of mTORC1 and occurs in both mTORC1 and 2. This phosphorylation is important, but not indispensable, for mTORC complex activity[866].

mTORC1 activity promotes several anabolic processes, like protein, lipid and nucleotide synthesis, while at the same time inhibiting the catabolic process of autophagy. It also plays an important role in feedback inhibition of AKT signaling through several mechanisms. This role has been primarily associated with mTORC1-dependent degradation of the insulin receptor substrates, IRS1 and 2. These proteins serve as scaffolding to adaptors, linking IGF1 stimulation to PI3K/AKT pathway activation.

mTORC1 promotes IRS degradation through multiple Ser phosphorylations of these proteins, both directly through mTORC1, but also indirectly through S6K proteins and other as of yet unidentified downstream kinases, leading to a considerable decrease in PI3K activation[867–869]. Another PI3K/AKT signaling inhibitor adaptor protein that is a direct target of mTORC1 is the growth factor receptor bound protein 10 (GRB10). mTORC1's phosphorylation of GRB10 stabilizes it, enhancing its inhibition of IGF1 and IRS signaling, blocking PI3K/AKT activation[870,871].

Besides mTORC1 solo activity, crosstalk between both mTORC complexes also regulates full AKT activation. For example, mTORC1-activated S6K1 induces phosphorylation of mTORC2 at RICTOR's T1135, and of the aforementioned SIN1 at T86 and T398, which reduces mTORC2-mediated phosphorylation of AKT's S473 residue[872,873]. S6K1 is a direct substrate of mTORC1 that contributes to metabolic reprogramming, by increasing biosynthesis of protein, lipids and nucleotides and increasing glycolysis through its role as an activator of translation[860].

The relationship between the PI3K/AKT and MAPK/ERK is, as we have alluded to, a particularly close one, with several inhibitors of either pathway activating the other one in several effectors, like TSC, FOXO and GSK proteins[873,875]. An example of this type of interaction is the phosphorylation of RAF and BRAF on S259 and S364, respectively, inhibiting RAF activation. This promotes 14-3-3 binding, particularly when RAF is also phosphorylated in other sites by PKA and AMPK, inhibiting its activity and ERK activation[784,876,877]. Inversely, ERK can suppress RTK activation of the PI3K/AKT pathway by phosphorylating the GAB adaptors (GAB1 and 2).

A particularly important process regulated by the interaction of both these pathways is the cap-dependent translation. Regulation of this process occurs, in part, by mTORC1 activation,

through ERK and RSK-mediated multiple phosphorylation, of TSC2 and RAPTOR[760,761,878]. Activated mTORC1 mediates inhibition of the 4E-BPs, which are translation inhibitors, controlling cell proliferation and survival. Their phosphorylation at T37 and T46 by mTOR inhibits them, allowing EIF4E assembly with EIF4G and EIF4A to form an active, cap-binding translation initiation complex[860].

EIF4E activation is the result of ERK activation of MNK1/2, which then phosphorylate EIF4E at S209, promoting its ability to initiate cap-dependent translation[879,880]. The activation of this translation initiation complex results in an increased synthesis of, in particular, cell cycle-associated genes, like Cyclin D1, HIF1 and growth factors like VEGF[881–883].

The understanding of the PI3K/AKT pathway regulation has contributed to a change in perception of how cellular processes are regulated. While classically pathways have been presented as linear interactions between factors organized in hierarchical fashion, we now know that, depending on the context, interactions within the different pathways and with other pathways can change. This allows for redundancy, multiple signal integration and co-option of pathways.

For example, in the PI3K/AKT pathway, inhibitory phosphorylations of GSK3 (S21 in GSK3α and S9 in GSK3β) can be performed by either RSK or S6K, which are at distinct hierarchical levels, downstream of either ERK or mTORC1 signaling[849]. In another example, sequestration of FOXO3a in the cytoplasm can be promoted by SGK-mediated phosphorylation downstream of PI3K activity[884]. And, in a final example, mTORC1 activation by growth factors can occur independently of AKT activity, namely through ERK-RSK signaling, likely involving RSK-mediated phosphorylation of at least two AKT sites on TSC2, S939 and T1462, together with other regulatory sites[760,761].

This type of pathway regulation is of great importance to decide the appropriate cellular response to a continuously changing internal and external environment, especially for pathways that regulate several vital cellular processes. A practical example of this is a scenario of growth factor stimulation of a starved cell, resulting in enhanced survival signaling through AKT, but without the promotion of cell growth, due to attenuation of mTORC1 signaling.

Together, the MAPK/ERK and PI3K/AKT pathways synergize to regulate vertebrate cell proliferation in a multitude of contexts and in response to several internal and external cues, making them the primary regulators of proliferation in vertebrates. However, in certain contexts other pathways can regulate proliferation, either independently or in cooperation with these.

1.1.3.1.3. The WNT Pathway

The WNT pathway is a highly conserved signaling network, present in several phyla of animals, from invertebrates to vertebrates, albeit with varying numbers of known participants and some variability of interactions between effectors and outcomes[885–888].

In vertebrates, WNT signaling has been associated with cellular differentiation, migration, polarity and proliferation in events as varied as survival and propagation of stem cells (in a considerable group of tissues, i.e. intestine, stomach, skin and mammary gland), primary body axis formation, organogenesis and even in innate and adaptative immune responses[889–911].

The WNT pathway is 'classically' represented has having three distinct paths, a 'Canonical' pathway, where WNT signaling leads to stabilization and translocation of β-Catenin to the nucleus, where it activates a WNT-related transcriptional program, and two 'Non-Canonical' pathways independent of β-Catenin: the 'Planar Cell Polarity' (PCP) pathway, involved in cell polarization and migration, for instances in embryonic migration of dorsal mesodermal cells during convergent extension (CE) and neural tube closure; and the WNT/Ca^{2+} pathway, often associated with modulation of signaling for dorsal axis formation, and PCP signaling in gastrulation cell movements, as well as canonical pathway regulation[894–902].

While the 'classical' view of the WNT pathway represents each path as independent, and responsible for different cellular processes and events, the most current view likes to refer to it as a network, seeing as there is ample evidence that each 'path' can interact with the others in several contexts, thus modulating WNT response with more specificity.

Several instances of WNT pathway activation (through non-canonical paths) without receptor recognition of ligand have previously been presented. However, WNT network activation is generally associated with ligand recognition. These are the WNT proteins, a group of secreted glycoproteins that in mammals has 19 members currently identified.

WNT production in the secreting cell requires the action of two transmembrane proteins, Porcupine (PORCN) and Wntless (WLS). PORCN is a highly conserved acyltransferase, that alters WNT in the endoplasmic reticulum by adding a palmitoleic acid moiety to WNT proteins, at S209, which is essential for receptor recognition. WLS (also known as GPR177) is responsible for the trafficking of WNT proteins from the endoplasmic reticulum, where they are also glycosylated, through the Golgi network, up to the cell surface, where it contributes to WNT release along with Evenness interrupted (EVI) proteins and the retromer complex[903–913].

While this alteration of the WNT proteins is essential for receptor-mediated signaling, it renders them hydrophobic, making it impossible to distribute them significant distances in an aqueous environment. For this reason, it has been proposed that WNT signaling involves cell-cell contact through delicate cytoplasmic extensions, called cytonemes, that possibly carry WNT in vesicles. It has also been proposed that heparan sulfate proteoglycans on the cell surface, like Dally and Glypican 3, facilitate WNT movement along it once it is externalized[914–925].

The first step of WNT pathway regulation occurs here, in the extracellular space, with several WNT antagonists interfering with WNT detection and receptor activation. A few examples of this are the Dickkopf (DKK), WNT-inhibitor (WIF), soluble Frizzled-related proteins (SFRP), Cerebrus, FRZb20, and the context-dependent WNT inhibitor WISE proteins, which either sequester WNT (impeding it to reach the receptor), block WNT receptors, or remove the palmitoleic acid moiety from WNT proteins, making them unrecognizable[926–934].

WNT proteins are detected by the receiving cells through the extracellular N-terminal, cysteine-rich, domain (CRD) of a single family of transmembrane receptors, the Frizzled (FZD) family, which is composed of 10 members, in vertebrates, that have been classified as GPCRs, due to their homology (despite the lack of certain features)[935–938]. While FZD specificity towards WNT is fairly reduced, FZD receptors have been clustered in four groups on the criteria of sequence identity and WNT preference. Of these clusters, the FDZ5/FDZ8 shows the highest degree of ligand promiscuity[939–941].

To activate downstream targets, FZD receptors require a co-receptor, namely from the low-density lipoprotein receptor related protein (LRP) family, either LRP5 or LRP6, with which they form ternary complexes, or from the receptor protein tyrosine kinases family, either ROR2 or RYK. WNT stimulation of the coreceptors FZD, through the N- and C-terminal regions, and LRP, through the linker between both N- and C-terminal domains, produces several molecular changes, like phosphorylation of LRP, recruitment of Dishevelled (DVL), and its subsequent oligomerization[937,942–963].

While WNT proteins and their agonists engage both co-receptors simultaneously, antagonists, like DKK, SOST and Sclerostin, bind exclusively to FZD or LRP, blocking signaling. However, agonists like Norrin and R-Spondin2 were also shown to interact exclusively with LRPs, but to induce WNT signaling, independent of a WNT ligand.

DVL is perhaps the most important hub of WNT signaling. It is from here that, classically, the WNT pathway divides into the Canonical, PCP and WNT/Ca2+ paths. However, how DVL regulates signaling through each path is still unclear. DVL is phosphorylated by several kinases,

including Casein kinase 2, Metastasis associated kinase, Protein C kinase and Par1, and these phosphorylations likely regulate subcellular localization of DVL, which together with co-repectors and binding partners help to regulate the relative activity of each of the WNT signaling paths[946,964–968].

For example, LRP coreceptors have been associated exclusively with the canonical pathway, while NRH1, PTK7 and ROR2 selectively transduce non-canonical pathway signals[969]. Furthermore, correct subcellular localization of DVL is important for the proper activity of non-canonical pathways. It was also shown that DVL can translocate to the nucleus, although its functions there are still not evident[970–973].

DVL contains three distinct domains, the DIX, PDZ and DEP domains, with the first two being important for WNT canonical path signaling. Upon DVL activation, the DIX is responsible for binding AXIN, inhibiting β-Catenin destruction complex formation, but it has no known function in the non-canonical PCP paths. The PDZ domain, which also participates in the non-canonical paths, is responsible for the binding of mediators like Dishevelled-associated activator of morphogenesis 1 (DAAM1), Strabismus and Prickle. The DEP domain has been associated with DVL recruitment to FZD receptors[946,974–979].

In the steady state, in the absence of WNT ligands, cytoplasmic β-catenin, usually associated with adherens junctions where it interacts with E-cadherin, is continuously targeted and degraded by a destruction complex, which includes AXIN, Adenomatosis polyposis coli (APC), Protein phosphatase 2A (PP2A), GSK3 and Casein kinase 1α (CK1α), as depicted in Figure 1.11[980]. Phosphorylation of β-Catenin at S45, by CK1α, and at S33, S37 and T41 by GSK3β targets it for ubiquitination, performed by beta transducing repeat-containing protein (β-TrCP) and SKP1-Cullin-F-box (SCF) E3 ubiquitin ligases, subsequently leading to its destruction by the proteasomal machinery[981–983].

Upon receptor stimulation, the FZD/LRP complex triggers the translocation of AXIN to the membrane, which binds a phosphorylated conserved sequence in the cytoplasmic tail of LRP, likely through mediation of CK1γ and GSK3β. This seems to also lead to a dephosphorylation of AXIN and decreased cytoplasmic levels[984–988]. Sequestering of AXIN at the receptors has also been proposed to inhibit the repressive activity AXIN performs over the WNT pathway, and lead to the activation of DVL, through a process yet poorly understood[978,989,990]. In this balance of AXIN and DVL activity participates NKD1/2, a conserved antagonizer of WNT signaling that binds and destabilizes DVL in short-term WNT activation, but that can also promote WNT signaling by destabilizing AXIN during prolonged WNT stimulation[991,992].

WNT receptor stimulation also results in LRP6 phosphorylation of the intracellular Pro and Ser-rich motifs, which allows LRP6 to recruit, through DVL activation, GSK3β and directly inhibit it[993–997]. Inhibition of GSK3β prevents β-Catenin phosphorylation and subsequent ubiquitination, thus impeding its degradation and leading to its cytoplasmic accumulation[998].

Besides its action on β-Catenin, and as we have discussed previously, GSK3 has a large number of substrates, whose activity is directly inhibited by GSK3 activity, especially in the PI3K/AKT pathway. Because of this, the WNT pathway has been associated with proliferation regulation, with cells in G2 and M phases exhibiting elevated levels of WNT signaling, in a phenomenon called WNT-dependent stabilization of proteins, or WNT/STOP. This has been related with the stabilization of a series of GSK3β targets, including MYC, which are not degraded and can therefore promote cell cycle progression[999–1001].

GSK3 inhibition and stabilization of β-Catenin allows it to translocate to the nucleus, through a process poorly understood. β-Catenin has no nuclear localization sequence (NLS) and its entry in the nucleus does not seem to require Importins or Ran-mediated nuclear import[1002]. To resolve this issue, it has been proposed that β-Catenin might 'piggyback' with other factors that are translocated to the nucleus, like AXIN[1003,1004]. Alternatively, several transport proteins, including the intraflagellar transport protein IFT140, the guanine nucleotide exchange factor RAPGEF5 and the nuclear importin IPO11, have been suggested to participate in the nuclear translocation of β-Catenin[1005–1007].

As for nuclear export of β-Catenin, since it also does not possess a nuclear export sequence (NES), two alternative mechanisms have been identified, the first through the RAN-binding protein 3 (RanBP3), in cooperation with APC, which has a NES, and the second by direct interaction with proteins of the nuclear pore complex[1008].

In the nucleus, β-Catenin operates as a transcriptional co-activator to a large number of binding partners, with the best characterized being the LEF/TCF family of transcription factors[1009–1012], with which β-Catenin interacts through its Armadillo repeat domain. β-Catenin replaces Groucho family transcription repressors, and, in cooperation, these factors regulate the expression of genes like Siamois, Twin, cMyc and Ccnd1[1013–1016]. Besides transcription factors, β-Catenin's interaction with other binding partners, like BCL9, BCL9L, SOX17, MYOD, Legless and Pygopus is also very important to potentiate specific WNT-signaling transcriptional programs, since these binding partners help to retain β-Catenin in the nucleus[1017–1028].

β-Catenin is also able to regulate chromatin structure by interacting with histone acetyltransferases CBP (CREB-binding protein) and p300, and the nucleosome remodeler Brahma-related gene 1 (BRG1)[1029–1031].

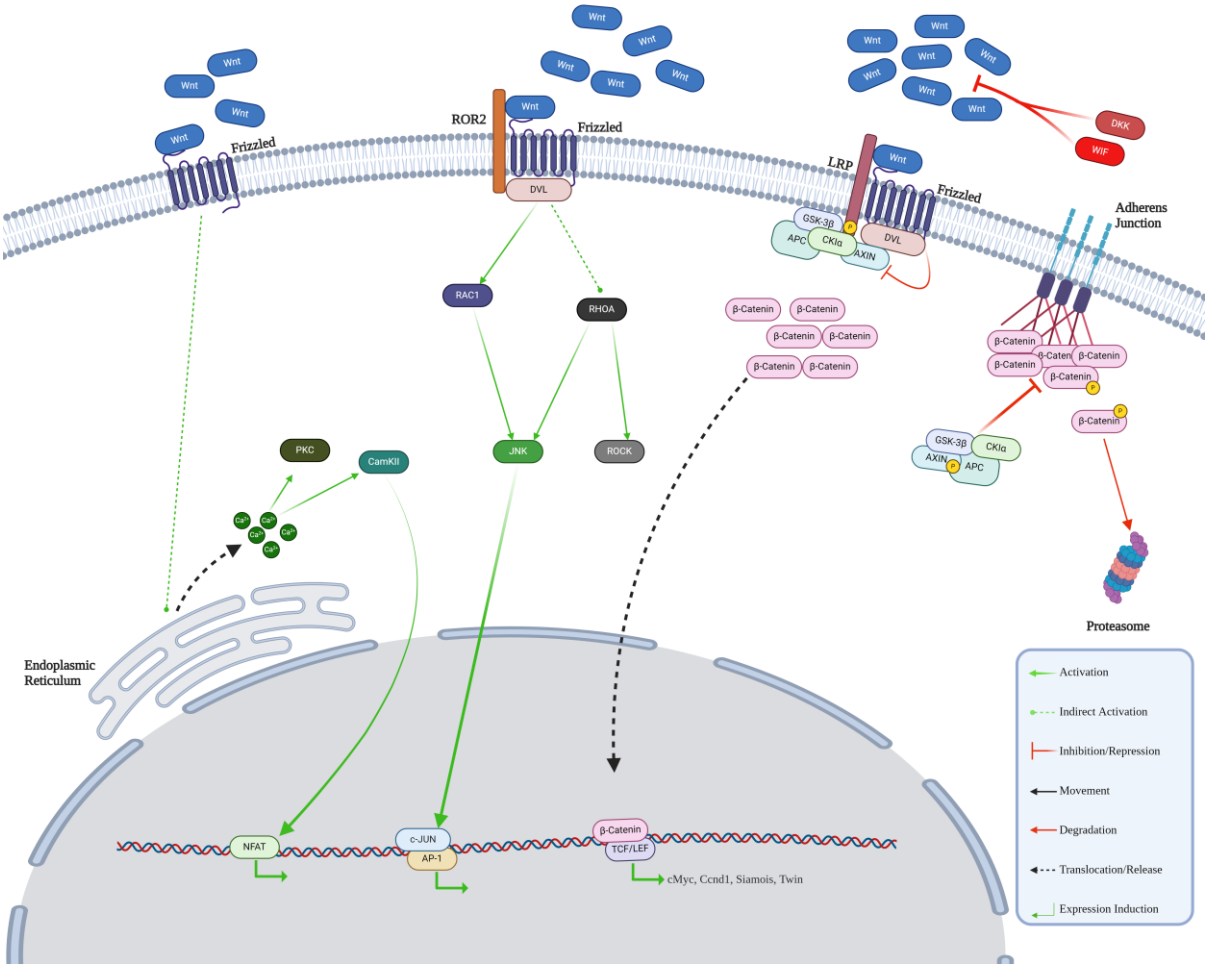

Figure 1.11 - The WNT network. Depicted are the most consensual members of the three WNT pathway. In this image are also represented some extracellular inhibitors as well as downstream transcription factors. Image created with BioRender.com

In the β-Catenin-independent PCP path of the WNT pathway, WNT signaling is thought to be mediated through FZD, particularly FZD3 and 6, without the requirement of the coreceptors LRP5/6[1032–1035]. A few WNT ligands have been specifically associated with these non-canonical paths of WNT signaling, like WNT4, WNT5a and WNT11, but some have also been shown to be able to activate the canonical path[1036]. An interesting observation, made in relation to ligand availability for the PCP path, is that what is most relevant is the establishment of an appropriate gradient of stimulants, rather than their outright presence of absence[1037–1039].

Coreceptors in the PCP path have not yet been fully defined, but candidates include NRH1, RYK, PTK779, ROR1 and ROR2[1040–1043]. In particular, ROR2 has been shown to transmit WNT5a signaling, which inhibits the WNT canonical path[1044–1046], but has also been reported to enhance canonical path depending on the FZD coreceptor. The same domain with which

WNT proteins interact with FZD was also found in RORs, and can be used by the extracellular antagonists SFRP to bind to them[1047].

RYK receptors are conserved across vertebrate and invertebrate species. In mammals, RYK is essential for axon guidance and neurite outgrowth in response to WNT stimulation, through binding of both FZD and DVL, and activation of the canonical pathway[1041,1048,1049]. RYK has been shown to also be involved in non-canonical paths through interactions with WNT5b, WNT11 and FZD7, while also having a RYK domain that allows for WIF inhibition[1041,1050–1054]. It is interesting to note that RYK can undergo cleavage, with its C-terminal fragment translocating to the nucleus, which has been shown to be essential for regulation of neuronal progenitor differentiation upon WNT3 stimulation.

Signaling through FZD receptors and these coreceptors leads to DVL recruitment and activation. Through the PDZ and DEP domains, DVL activates two parallel pathways that lead to the activation of the small GTPases RHO and RAC. Of note, GTPase activation has been associated with FZD1 and 7, and DVL1 and 2[1055–1058].

RHO activation occurs through DAAM1 activity, likely through a RHO guanine exchange factor called WGEF, and can be negatively regulated by PKA. Activation of RHO leads to activation of RHO-associated kinase (ROCK), JNK and myosin, leading to actin cytoskeleton rearrangement[1059,1060]. RAC activation is independent of DAAM1 and stimulates JNK activity, whose downstream factors in the PCP pathway are still poorly resolved[1058,1061,1062]. Coordination of RHO and RAC activities, which are thought to be opposite, is still not clear, particularly since both activate JNK[1056,30,34–39].

In the other β-Catenin-independent path, the WNT/Ca^{2+} path, which shares several components with the PCP path, WNT (WNT5a and WNT11) and FZD (FZD2) signaling stimulates intracellular Ca2+ release from the ER[40–43]. Signaling through this path is fast, and dependent on G-proteins and the activation of the phosphatidyl inositol cycle.

Intracellular accumulation of the released calcium activates several Ca2+ sensitive proteins, like Protein kinase C (PKC) and Calcium/calmodulin-dependent kinase II (CamKII). CamKII has been shown to activate NFAT, TGFβ activated kinase 1 (TAK1) and Nemo-like kinase (NLK), which phosphorylates TCFs, thereby inhibiting the canonical path[44–49]. Since NFAT is associated with the genetic regulation of cytokine production, cell cycle, differentiation and apoptosis, this suggests that all these processes can also be controlled by this WNT path[1130].

All three paths of the WNT pathway have been shown to establish several interactions, and WNT ligands and receptors have also been shown to have great promiscuity, which led to the

proposal that WNT does not establish 'pathways' per se, but rather a 'network'. In fact, WNT ligands can activate both canonical and non-canonical paths, as is the example of WNT11 and WNT3a, or activate both non-canonical paths, as is the case of WNT5a (which has, nevertheless, also been associated with the canonical pathway *in vitro*)[8,17,43,50–52].

For example, WNT5a has been shown to be able to activate the SRC kinase family member YES, which together with FYN, that has also been shown to modulate calcium signaling, have been shown to regulate CE movements[53–55]. Furthermore, WNT5a-YES signaling results in CKIα binding of NFAT, preventing its nuclear localization and accumulation, and activation of the WNT/Ca^{2+} transcription program, in a clear example of interactions between proteins associated with all three paths of WNT signaling[55–57].

Similarly, while some FZD receptors may have a preference in path activation, most seem to lead to activation of all, or more than one, path[17,51,58–62]. For example, FZD2 and FZD7 have been shown to act upstream of both the canonical and non-canonical paths[62–68]. Another clear indication that the WNT signaling operates as a network is the role DVL plays as a hub for all three paths, associating to distinct coreceptor complexes and recruiting or interacting with over 30 effectors of the signaling.

Furthermore, several coreceptors and effectors of the pathway have been shown to participate in more than one path[69–72]. While the role DVL plays in directing signaling to each path is unclear, the role of other mediators has been clarified a bit. For example, the extracellular inhibitor DKK tends to skew WNT signaling towards PCP signaling and JNK activation[73–76]. Such a rich network of interactions between mediators that, nevertheless, tend to skew the activity of the pathway to specific outcomes, has been suggested to arise from cooption of existing signaling by newly created WNT ligands[77–79].

This theory finds support in the observation that homologs of FZD, GSK3 and β-Catenin are found in life forms as basal as the soil amoeba *Dictyostelium*, while WNTs have not been identified in its genome. Furthermore, a genomic study that compared the genomes of animals, from sponges to mice, with their closest unicellular living relatives, detected seven conserved gene families associated to WNT pathway, including FZD, LRP, DVL, β-Catenin and TCFs, but WNTs themselves were not always present[80].

Supporting this hypothesis of cooption is also the observation that the WNT pathway is capable of regulating downstream targets of other pathways, like the AP-1 transcription complex, which induces a proliferative transcription program downstream of the MAPK/ERK pathway. WNT5a

stimulation through ROR2 leads to JNK activation, which interacts with AP-1 and leads to induction of its transcriptional program[34,81–84].

With such complex and context-dependent integrations of signaling from different pathways, understanding how the cell cycle machinery is influenced by each one of these pathways is essential for our comprehension of how they synergize in its regulation.

1.1.3.1.4. The Cell Cycle

As we have detailed, proliferation is regulated by several pathways in similar or different contexts. This regulation can occur synergistically or in opposition, with the evidenced interactions between the pathways contributing to a greater robustness of activation and redundancy of activating signals.

This guarantees that induction of proliferation, whose deregulation can lead to complicated pathological scenarios, occurs almost exclusively in the appropriate circumstances. Ultimately, the influence of these pathways on proliferation amounts to differential activity and/or expression of cell cycle mediators, which makes comprehension of the cell cycle dynamics paramount to understanding the mechanisms of its regulation.

The cell cycle is a highly complex process, involving DNA replication, nuclear envelope breakdown, chromosome segregation, organelle redistribution and cytokinesis, which results in the production of two daughter cells from a parental one. Deregulation of any of the many steps involved in the cell cycle can lead to pathological events, like cell death or tumorigenesis.

As a result, homeostasis is achieved, in most vertebrate adult somatic tissues, by keeping cells in a proliferation-quiescent state, also known as G0, to reduce the risk of DNA damage and cell death. For most vertebrate somatic cells, this state is never reversed, but in some tissues reservoir cells (stem/progenitor cells) regularly re-enter the cell cycle (which occurs primarily in the form of physiological regeneration, as a result of natural tissue turnover, but can also occur in the event of damage). To regulate cell cycle re-entry and stasis, cells employ a complex system of molecular strategies to direct cell cycle progression.

One of the methods cells use to accurately time cell cycle re-entry is the transcriptional repression of essential cell cycle genes, by the maintenance of the hypophosphorylated state of proteins like RB, p107 and p130, repressors of E2F transcription factors. E2F's are a family of cell cycle regulating transcription factors that is composed by inductors (E2F1, 2 and 3) and suppressors (E2F4 and 5) of key cell cycle gene expression[1268].

RB, p107 and p130 proteins are known as 'pocket proteins', due to the pocket like structure of their E2F binding domains, and in quiescent cells they are found associated with E2F4 and E2F5 on gene promoters, allowing them to recruit histone deacetylases (HDACs) and chromatin remodeling complexes (hBrm and Brg1) to genes such as cell cycle inducing E2F transcription factors (E2F1,2 and 3), among others, thus avoiding cell cycle entry[1268–1271]. Furthermore, what

little inducing E2F factors are available are also transformed into repressors by association with RB, further ensuring cell cycle arrest[1272–1279].

Another way the cell uses to regulate cell cycle progression are post-translational modifications to its effectors (Figure 1.12). CDKs (Cyclin-Dependent Kinases) are essential kinases for cell cycle progression, which are thought to be constitutively expressed. Although their Cyclin counterparts only have low expression levels outside of the cell cycle, post-translational regulation of these pairings is involved in controlling re-entry in the cell cycle[1280].

During G0, Cyclin-CDK activity is repressed by phosphorylation of CDKs at inhibitory residues, preventing their activation. These inhibitory phosphorylations occur near the N-terminal, on Y15 of CDK2 and CDK1[1281–1283], and on Y17 of CDK4 and 6[1283]. CDK2 and CDK1 can be further inhibited by a second inhibitory phosphorylation on T14[1282–1288], which possibly helps regulate the sequential activation of CDKs during the different phases of the cell cycle. These inhibitory phosphorylations are catalyzed by WEE1 and MYT1, bifunctional kinases that can phosphorylate both tyrosine and threonine residues. WEE1 is regulated by NIM1, CHEK1, 14-3-3 and CDK1, resulting in greater activity during interphase, and an inhibition and degradation towards mitosis[1289–1293]. MYT1 is regulated by RSK, Cyclin B-CDK1 complexes and MEK1[1294–1296].

A third way of inhibiting cell cycle entry/progression involves interfering with the correct Cyclin-CDK complex assembly. This interference is perpetrated by CKIs (CDK inhibitors), which can belong to two families, the INK4 family of proteins ($p15^{INK4B}$, $p16^{INK4A}$, $p18^{INK4C}$ and $p19^{ARF}$) and the CIP/KIP family ($p21^{CIP1}$, $p27^{KIP1}$ and $p57^{KIP2}$).

INK4 proteins work primarily by blocking the PSTAIRE helix domain on CDKs, thus preventing Cyclin docking and formation of complexes, as well as destabilizing pre-existing complexes[1297–1300]. CIP/KIP family members ($p21^{CIP1}$, $p27^{KIP1}$ and $p57^{KIP2}$), on the other hand, have to associate with pre-assembled Cyclin-CDK complexes, generating ternary conformations that block the entry of CAK (CDK Activating Kinase) and ATP in the catalytic site of the CDK, thus preventing its activation and complex activiy[1279,1299,1301–1304].

Curiously, phosphorylation of p27 on T27 reduces its inhibitory effect, by decreasing the stability of p27's physical interaction with the Cyclin-CDK complex, turning it into a partially inhibitory assembling factor. This is thought to help with the pre-assembly of some Cyclin – CDK complexes, which are maintained inactive by p27 association, but can be more quickly activated through p27 exclusion[1305,1306].

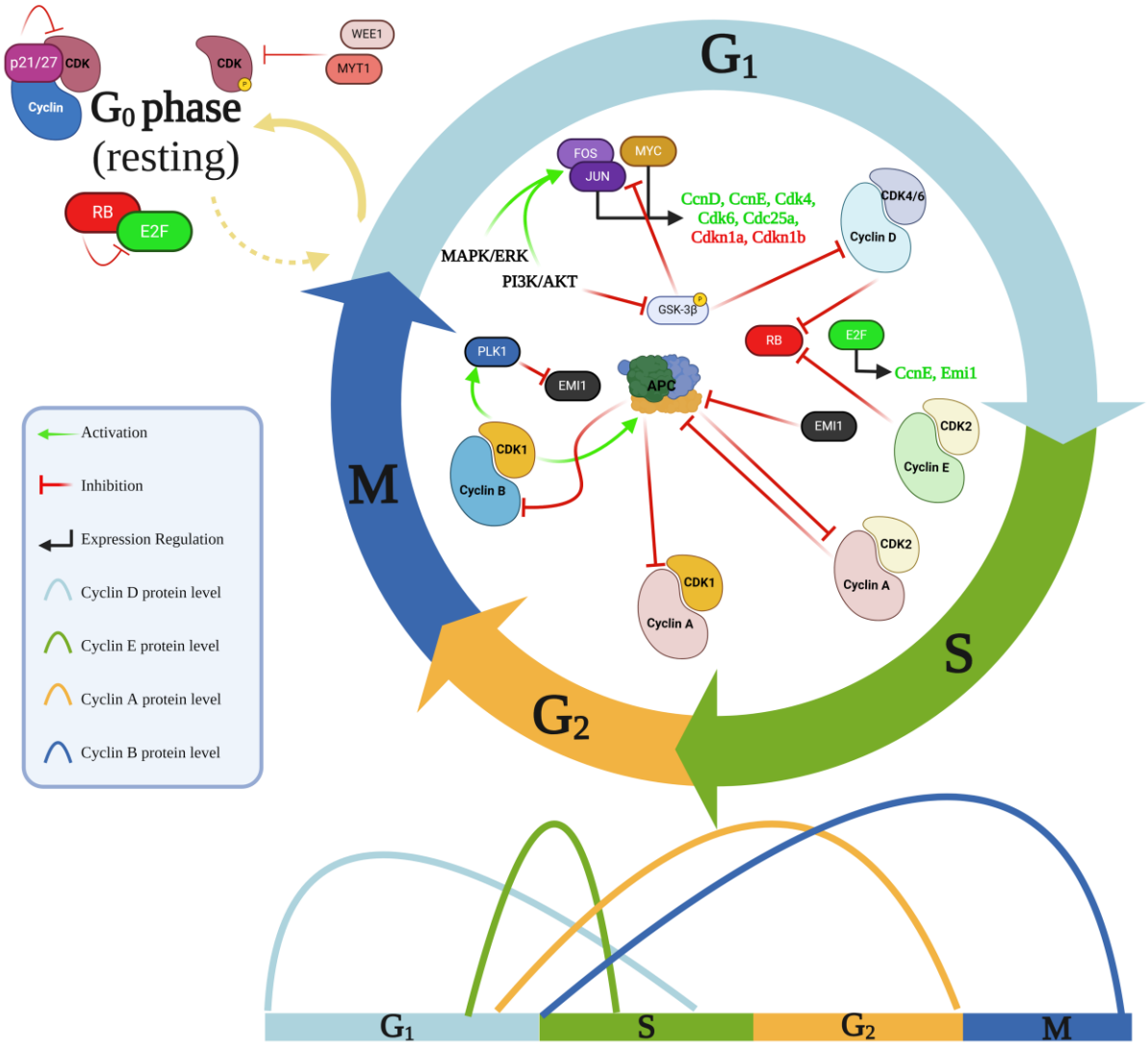

Figure 1.12 - Cell cycle phase regulation by specific Cyclin-CDK complexes. Represented are the four phases of the cell cycle, as well as the Cyclin-CDK complexes that regulate the progression through each phase, and some of the interactions of factors involved in Cyclin-CDK complex regulation and evolution. Image adapted from Yang, 2012[1397] *and created with BioRender.com.*

1.1.3.1.4.1. The G1 phase

When a need for replenishment of a cellular population occurs, a set of internal and external cues are created that inform the cell of the need to proliferate. As pointed out before, these activate intracellular pathways, such as PI3K/AKT and MAPK/ERK, that induce and activate major regulators of the cell cycle [1307–1310] like the transcription factors FOS and JUN (that compose AP-1), MYC and NF-κB. These transcription factors regulate the expression of numerous genes involved in the control of the cell cycle, such as Cyclin's D and E, CDKs 4 and 6, and CKIs p21 and p27, to name a few[1311–1323]. MYC is a particularly powerful potentiator of cell cycle re-entry that is involved in the induction of Cyclin D1 and D2, CDK4 and CDC25a, whose expression marks cell re-entry into the G1 phase of the cell cycle (Figure 1.12).

Cyclin D1 and D2 (hereafter called "Cyclin D") protein levels are dependent on transcriptional upregulation by AP-1 and MYC, and on GSK3β signaling activity. GSK3β activity leads to Cyclin D phosphorylation on T286, promoting its nuclear export and cytoplasmatic degradation[1324], while concomitantly phosphorylating and inhibiting AP-1 and MYC, reducing Cyclin D expression[1325]. Upon mitogenic stimulation and PI3K/AKT pathway activation, AKT will phosphorylate GSK3β at its S9 residue, inactivating it[1326]. This frees AP-1 and MYC from their inhibition, resulting in an induction of Cyclin D, which contributes to cell cycle re-entry. Besides affecting Cyclin D stability and expression, GSK3β has a similar effect over Cyclin E, which also contributes to an arrest of the cell cycle, as we will see further ahead[1327].

In addition to increasing levels of Cyclin D, MYC also reduces expression of CKIs by stimulating their export from the nucleus to the cytoplasm, where they are degraded[1313,1314,1316,1320,1323,1328–1330]. Furthermore, MYC induces CDC25a, a phosphatase that removes inhibitory phosphorylations from CDKs 4, 6 and 2, enabling Cyclin-CDK complexes to be activated by CAK[1318]. CKI repression and Cyclin induction leads to an increase in Cyclin-CDK complex abundance.

The association of Cyclin to CDK induces a conformational change on the CDK, exposing its T-loop to phosphorylation by CAK. CAK is a complex formed by Cyclin H and CDK7, and often associated with MAT1 which helps in the assembly of this complex[1331]. CAK is responsible for phosphorylating CDK4/6 on their T172 site, CDK2 on its T160 site and CDK1 on its T161 site, all residues found within their T-Loop's. These phosphorylations induce further changes to the CDK conformation, allowing full access of ATP to the catalytic domain, which results in full CDK activation.

CDK2 can also be activated by CAK without being bound to a Cyclin, but the lack of Cyclin association makes this activation only transient[1332]. CDK1, on the other hand, not only requires previous Cyclin binding, but also requires CAK activation to be almost simultaneous to Cyclin binding, as CAK activation is the only way of stabilizing Cyclin – CDK 1 complexes.

Another difference between CDKs and their response to CAK is the longevity of their activation. While CDK1 and 2 only require one interaction with CAK to become stably active when complexed with Cyclins, CDK4 and 6 need repeated re-activation. This is likely because there are phosphatases with the opposite function to CAK acting on CDK 4 and 6. It is proposed that mitogenic signaling also leads to an increase in CDK7 T-loop phosphorylation, increasing its activity and, therefore, phosphorylation of CDK4 and CDK6, overcoming their dephosphorylation[1332]. These differential dynamics of CDK activation might help explain different periods and durations of CDK activation throughout the cell cycle.

Fully active Cyclin D – CDK 4/6 complexes primarily target pocket proteins, possessing particularly high affinity to RB [1279,1333,1334]. Pocket proteins have multiple phosphorylation sites, and their level of activity is dependent on the overall level of phosphorylation, but Cyclin D-CDK 4/6 complexes only target a subset of these sites. This partial phosphorylation does not fully release E2F transcription factors from the influence of pocket proteins, but reduces their effects on some gene promoters, facilitating partial activation of genes like Cyclin E[1335,1336]. This partial inactivation of pocket proteins, coupled with the inductive effect of MYC and inactivation of GSK3β, leads to an increase in Cyclin E (E1 and E2) expression and protein availability.

Besides phosphorylating pocket proteins, Cyclin D - CDK4/6 complexes are crucial for cell cycle progression due to their higher affinity to p27, compared to Cyclin E – CDK2 complexes. The increase of Cyclin D-CDK4/6 in G1 helps remove part of the inhibition on Cyclin E – CDK2 complexes by sequestering p27, contributing to the progression of the cell cycle.

Towards the end of the G1 phase, upregulation of Cyclin E expression greatly increases the amount of Cyclin E – CDK2 complexes available[1335,1336]. At this time CKIs have been downregulated at the transcriptional level, and post-translational processes such as CKI nuclear export and degradation, and cytoplasmic sequestration of p27 by Cyclin D – CDK4/6 complexes, further depress CKI activity.

Concurrently, CDC25a dephosphorylates CDK2 on Y15, thus activating Cyclin-CDK2 complexes, which complete hyperphosphorylation of pocket proteins[1337,1338]. This

hyperphosphorylation releases E2F transcription factors from inhibition of pocket proteins, resulting in transcriptional activation of S-phase genes[1279,1335,1336,1339–1341].

This marks the overcoming of the G1 restriction checkpoint, and from here on the progression of the cell cycle no longer is dependent on mitogenic factors, as all the elements required to maintain the correct progression of the cycle have already been produced[1342].

1.1.3.1.4.2. The S and G2 phases

While Cyclin E – CDK2 complexes are essential to overcome the restriction checkpoint and enter S phase, they are not responsible for the progress through S phase, which is driven by Cyclin A – CDK complexes[1343,1344]. Cyclin A (A1 and A2, the latter widely expressed in adult somatic cells) begins to be expressed in late G1 when the E2F transcription factors responsible for its induction start to be released from inhibition, but Cyclin A – CDK2 complexes are maintained inactive and in low numbers until the S phase, primarily due to APC^{Cdh1}-mediated Cyclin A degradation. S phase progression requires an increase of CDK2 availability, removal of CKI inhibition of assembled complexes, and APC inactivation. The first two steps are simultaneously achieved by Cyclin E – CDK2 activity.

The activity of Cyclin E – CDK2 complexes phosphorylates both p27 and Cyclin E, targeting them for degradation by SCF^{Skp2} and SCF^{Cdc4}, respectively[1345]. This removes the inhibitory effect of p27 on Cyclin A – CDK2 complexes and raises the amount of free CDK2, resulting in an increase of active Cyclin A – CDK2 complexes[1328,1346–1350]. Because Cyclin A – CDK2 complexes also phosphorylate p27, they regulate their own activity by assuring they are not re-inhibited, even when the availability of Cyclin E – CDK2 complexes decreases.

As for the APC-mediated degradation of Cyclin A, at late G1 the activation of E2F transcription factors leads to EMI1 production and activation, which will bind and inhibit the APC cofactor CDH1, as well as CDC20, another APC cofactor. Inhibition of CDH1 and CDC20 reduces the level of Cyclin A recognition by the APC, allowing it to evade degradation, therefore becoming available to form Cyclin A – CDK2 complexes. Furthermore, Cyclin A - CDK2 complexes can also phosphorylate CDH1, targeting it for degradation, further increasing Cyclin A's evasion of degradation[1351].

Cyclin A – CDK complexes are responsible for the activation of several factors required for DNA replication initiation, like the ORC (Origin Recognition Complex) and the MCM (Mini Chromosome Maintenance), that regulate firing of the replication origins and beginning of DNA synthesis[1352,1353]. Cyclin A – CDK complexes also phosphorylate CDC6, which will then promote ORC disassembly, ensuring that replication origins only fire once per cell cycle.

The combined degradation of Cyclin E, and Cyclin A's avoidance of it, lead to Cyclin A existing in excess of CDK2 by mid-S phase (Figure 1.12). At this point, Cyclin A starts to also complex with CDK1, with which it has less affinity. Cyclin A - CDK1 association and activity is also only increased at this point because CDK2 can be activated by CAK, without being

bound to a Cyclin, while CDK1 seems to require simultaneous Cyclin binding and CAK activation, to be able to both stably bind a Cyclin and be activated[1354].

How the functions of Cyclin A - CDK complexes are distributed between Cyclin A – CDK2 complexes and Cyclin A – CDK1 complexes is still poorly understood. It is hypothesized that Cyclin A – CDK complexes also participate in early nuclear events of mitosis, like chromosome condensation, because these complexes are nuclear and activated in early prophase, before Cyclin B – CDK activity. Furthermore, there are indications that Cyclin A – CDK complexes are important for the expression of Cyclin B, CDK1 and CDC proteins, and activation of Cyclin B – CDK1 complexes, although not indispensable[1355,1356].

1.1.3.1.4.3. The M-phase

While Cyclin A – CDK complexes do play a role in M-phase, Cyclin B – CDK1 complexes, also known as MPF (M phase-promoting factor), are the main drivers of progression through this phase.

Cyclin B (B1, B2 and B3) begins to be expressed during late S phase, and early G2 phase, shortly after Cyclin A expression induction, but Cyclin B - CDK1 complexes only become active during M-phase, more specifically during prophase[1357,1358]. The activation of these complexes requires CDC25c activity, because in its absence Cyclin B association with CDK1 facilitates its phosphorylation, on residues T14 and Y15, by WEE1, MIK1 and MYT1, which inhibit CDK1. CDC25c translocation to the nucleus in early prophase allows it to counteract WEE1 activity. This results in CDK1 activation, which will fully activate PLK1. PLK1 phosphorylates CDC25c and Cyclin B on their NES (Nuclear Export Sequence), retaining them in the nucleus, as well as phosphorylates and further inhibits WEE1[1359–1362].

With the retention of Cyclin B in the nucleus and the removal of CDK1's inhibition by WEE1, active Cyclin B – CDK1 complexes increase in the nucleus towards late prophase. This leads to the induction of important cell cycle genes, and promotes nuclear envelope breakdown, resulting in activated Cyclin B – CDK1 complexes being again distributed throughout the cell. These will phosphorylate several targets involved in numerous events, like centrosome separation, chromosome condensation, Golgi reorganization, among others[1363–1367]. At the same time, Cyclin A is quickly degraded, and disappears, because CDK1 will phosphorylate APC in core subunits, enhancing CDC20 binding and increasing Cyclin A recognition by the APC[1368–1370].

As mentioned, the timing of Cyclin B – CDK1 complex activation is regulated by CDC25c, whose activity is in turn regulated by CHK1/2-mediated phosphorylation of its S216 residue, which creates a 14-3-3 binding site that masks CDC25c's NLS and prevents its entry in the nucleus. This phosphorylation likely also inhibits CDC25c's phosphatase activity. Only when these phosphorylations are removed can CDC25c enter the nucleus and antagonize WEE1, thus regulating the timing of Cyclin B-CDK1 complex activation[1359,1371].

The APC^{Cdc20} complex has two main roles in the Metaphase-to-Anaphase transition. First, it must degrade Cyclin A and Cyclin B, interrupting Cyclin – CDK activity and reducing the expression of certain cell cycle genes. Second, it must degrade Securin, releasing Separase, which will destroy the cohesion between sister chromatids, allowing their correct

segregation[1372,1373]. For this reason, the spindle checkpoint system will target CDC20 activity if it detects misaligned chromosomes, preventing chromatid separation[1374].

The timing of APC^{Cdc20} activity is determined by PLK1, through its phosphorylation of EMI1. As mentioned before, EMI1 inhibits APC activity through binding of CDH1 and CDC20 starting at late G1. However, in late prophase the activity of CDK1 leads to PLK1 activation, which phosphorylates EMI1 and labels it for degradation, activating the APC machinery[1375]. APC^{Cdc20} activity also promotes its own inactivation, since the disappearance of Cyclin – CDK complexes from the cell results in APC no longer being able to bind CDC20, since CDC20's binding sites are created by CDK1 phosphorylation of APC[1372,1373].

The absence of Cyclin – CDK activity will not only result in the removal of CDC20 from the APC, but also in a release of CDH1 from inhibition, allowing it to re-integrate the APC. Therefore, in late M-phase the APC will substitute CDC20 with CDH1, allowing the APC to continue targeting Cyclins and maintain their protein levels low, and also ubiquitinate other regulatory proteins that CDC20 does not target, like PLK1 and Aurora A, thus contributing to the end of mitosis.

1.1.3.1.4.4. Deciding Between Cell Cycle Re-Entry or Quiescence

Due to APC activity, after cytokinesis the cell will find itself without any of the S or M-phase Cyclins. At this point, two things can happen. If the correct mitogenic signals are still present during the mitogen-independent phases of the cell cycle, the cell will have been producing Cyclin D and, probably, E throughout the whole of the previous cycle. Because Cyclins D and E are not targeted by either APC^{Cdc20} or APC^{Cdh1} they will have evaded degradation and accumulated, thus inducing a reentry in G1, since the necessary machinery is available. With the presence of mitogenic signals the cell is capable of progressing through the G1/S checkpoint, and the progression through the cell cycle becomes irreversible[1280,1376].

However, if adequate levels of mitogenic signaling are not present, G1 and S-phase Cyclins will not be at the required levels when the cell completes cytokinesis and the two new daughter cells are formed, resulting in low Cyclin – CDK activity. APC/C^{Cdh1} activity further insures low levels of Cyclin – CDK activity by degrading both Cyclins and SKP2, which releases allows the increase of CKI levels. This scenario then allows for the buildup of all the previously described cell cycle "breaks", prolonging G1 until adequate mitogenic signaling levels appear or, eventually, leading to an exit from the cell cycle towards a quiescent, G0, state.

This page was intentionally left blank

1.1.3.2. Proliferation in Regeneration

Our analysis of the bibliography made it clear that, during wound healing, proliferation is regulated by a myriad of external and internal signals that coalesce into the activation or suppression of a few conserved intracellular pathways, which would be expected to produce the same results if the activating signals were the same, or equivalent.

As is fairly obvious, fibrotic and regenerative wound healing are two very distinct events, with greatly differing results. It stands to reason, therefore, that different activity of the signaling pathways that control wound healing, particularly cellular proliferation, occurs, likely due to differences in the type and magnitude of stimulating factors. Understanding these differences would help us understand how a reparative wound healing event might be transformed into a regenerative one[49,54,638].

Scarless fetal wounds show a faster deposition of collagen III (Col III), FN and TN, and a higher ratio of Col III to Col I, as well as a faster deposition and higher content of hyaluronic acid (HA)[90–95], which persisted for longer in scarless fetal wounds[49]. Higher levels of Decorin, a proteoglycan that modulates collagen extracellular matrix production and organization, was found upregulated in adult, scarring wounds, while in fetal wounds levels of Fibromodulin, another modulator of collagen matrix, are higher[96,97]. Fibromodulin was shown to have an anti-scarring effect, likely due to its capacity to inactivate TGFβ. Furthermore, scarless fetal wounds have also been associated with lower levels of pro-inflammatory cytokines, like IL-1 and TNFα[98].

In fetal wounds a differential ratio between MMPs and TIMPs has also been observed, with scarless fetal wounds favoring MMPs, leading to a more significant remodeling of the ECM[99]. This, combined with an increased and faster upregulation of ECM proteins, like tenascin and fibronectin, creates a more permissive environment for cell migration[100,101]. This is helped by the fact that migrating cells, like fibroblasts, also show differences in terms of the ECM proteins they produce.

Fetal fibroblasts, which are $En1^-$, have been shown to, *in vitro*, produce more Col III and IV than their adult counterparts[102,103], which was also accompanied by an increase in prolyl hydrolase activity, the rate-limiting enzyme in collagen synthesis[104]. Another way in which fetal fibroblasts in scarless wounds differ from scarring wounds is in their propensity to differentiate into myofibroblasts, which are nearly absent from scarless wounds[105]. Inhibition of β-catenin signaling was shown to reduce myofibroblast differentiation and Col I production *in vitro*, as well as lead to less fibrotic structures in skin repair[106,107].

However, care should be taken when labeling WNT signaling as either pro-fibrotic or pro-regenerative, since different isoforms lead to opposite results. In fact, WNT3a increases proliferation of adult mice fibroblasts, as well as Col I deposition, while also increasing TGFβ1 expression and decreasing TGFβ3 expression in fetal and postnatal fibroblasts[108]. Contrarily, WNT6 was shown to reduce EMT in response to TGFβ stimulation, suggesting a less pro-fibrotic effect[109].

In scarless fetal wound healing, lower levels of VEGF, PDGF, TGFβ, BMP2 and Il-8 were also observed, leading to less vascularity than in scarring fetal wounds[1377]. The pro-fibrotic role of these factors was confirmed by their addition to scarless wounds, converting them into scarring wounds, while in adult wounds reduction of VEGF levels decreased vascularity and scar formation[110–113]. Scarless fetal wounds have also been shown to have a faster upregulation of genes involved in cell growth and proliferation, but by 24 hours after injury, the transcriptome of scarring wounds is more enlarged than in the scarless wound[114].

Scarless wounding can also be studied in adults, since certain parts of the oral cavity mucosa can repair itself without the formation of a scar. Fibroblasts of the oral cavity are derived from the neural crest, a different origin from dorsal skin fibroblast lineages, making them intrinsically different[102]. Oral cavity fibroblasts are $Wnt1^{+}$, and transplantation experiments showed that their regenerative inclination is somewhat context-independent, with oral cavity fibroblasts being able to ameliorate back-skin wound scarring. Oral cavity wounds are also characterized by lower numbers of neutrophils and macrophages, with increased fibronectin and its splice variant ED – A[115,116].

In lower vertebrates, the ECM of the granulation tissue has also been shown to be richer in TN, FN and HA[117–120]. Furthermore, several MMPs found overexpressed during mammalian fetal wound healing are also overexpressed in lower vertebrate limb regeneration, like MMP3, MMP9, MMP10 and MMP13[121–126].

It has been proposed[7] that the primary difference between regenerative and non-regenerative wound closures is the timing of re-epithelialization. In *Ambystoma*, complete coverage of the limb stump occurs within the first day, while in mammals this can take up to three days, and this seems to be the result of an extension of the initial lag phase, as keratinocytes prepare to migrate[127].

After re-epithelialization, the epidermis of lower vertebrates undergoes a round of proliferation that thickens the epidermal layer, which begins to transform into a secretory epithelium[128,129]. This epithelium lacks a basement membrane in amphibians, while in lizards the basement

membrane is discontinuous[130], allowing it to be in direct contact with the underlying mesenchyme, where the progenitor-rich blastema will form.

A positive feedback loop between the epidermal-derived FGF8 and the mesenchymal-produced FGF10 is established in salamander limb regeneration, recapitulating the phenomenon observed during development[131–134]. Besides FGF ligands, WNT and IGF signaling have also been associated with this reciprocal instruction between wound epithelium and underlying mesenchyme in lower vertebrates[135,136].

Besides the reciprocity of instructive cues, between mesenchyme and epithelium, regeneration in vertebrates has also been regularly associated with nerve-derived signals, such as FGF2, KGF, BMPs and the newt Anterior Gradient protein (nAG)[126,137–142]. KGF is a particularly interesting factor, seeing as in the scarring wounds of mammals it is secreted by fibroblasts[143], rather than nerves, while in lower vertebrates it also has the capacity to induce upregulation of SP9 on the wound epithelium, a marker of embryonic epidermis[138].

More interesting than KGF, nAG has been proposed as the main candidate for nerve-derived signals. nAG is produced initially by Schwann cells and later by glands in the wound epidermis, in newt limbs[139], and Leydig cells in salamanders[144], and is detected by the PROD1 cell surface receptor present in blastemal cells. EGFR-ERK1/2 signaling has been shown to be strongly induced in PROD1-overexpressing newt blastema cells, which led to a great upregulation of MMP9[145]. Denervation of *A. mexicanum* limbs accounts for approximately 100 differentially expressed genes during limb regeneration, half related to cell proliferation[146].

Dependence of nerve derived signals has also been shown in lizards and fishes[147,148], where it was also shown that the effect of nerve signaling is threshold-dependent. In lizards, in particular, this dependence on nerve signals has been associated with the ependymal tube[149]. Furthermore, in *D. rerio* regenerating pectoral fin, nerve presence was shown to be essential for epidermal thickening and AEC formation[148].

The secretory epithelium, conventionally called Apical Epidermal Cap (AEC) in amphibians and Apical Epidermal Peg (AEP)[130] in lizards[7,15,655], is essential for the maintenance of the mesenchymal progenitor pool of the blastema, as well as their proliferation[150]. This has been associated with the informative role the AEC has towards the mesenchyme, through the production of WNT5, FGF2, FGF4 and the aforementioned FGF8[132,133,135,150–152], some of which have been found to be essential for regeneration[135,153,154]. Curiously, some of these factors are the same that are upregulated to preserve hair follicle stem cells during mammalian wound healing[155–157].

The importance of equivalent signals (FGFs and WNTs) was also demonstrated in the regeneration of *D. rerio*[158–160], where they cooperate with retinoic acid (RA) to sustain blastema proliferation and survival, while being antagonized by WNT5b stimulation of the PCP non-canonical WNT path. FGFs and WNT signaling were shown to be of particular importance in the regeneration of Retinal pigmented epithelium cells (RPE) of newt and *Xenopus*, and Müller glia cells in teleost fish and *Xenopus*, as well.

RPE regeneration in adult newt was shown to require an activation of ERK signaling within the first 30 minutes after injury. This causes β-catenin to translocate to the nucleus at around 3 days after injury. Extracellular factors, like FGF2, reinforce ERK signaling activation which, together with WNT signaling, promotes transdifferentiation and cell cycle re-entry of RPEs[161–165]. Fast ERK activation has been associated with an immediate activation of Ca^{2+} signaling in response to wounding[166], which seems to be a common trend among lower vertebrates[167–169], and possibly indispensable[170].

A similar phenomenon was shown in *D. rerio* Müller glia cell regeneration, where growth factors like HB-EGF, FGF2, IGF1 and Insulin activate ERK signaling. Together with WNT and JAK/STAT signaling, both through cytoplasmic and nuclear activity, transdifferentiation and proliferation is induced[171,172]. The importance of sustained ERK activation was also demonstrated in salamander and fish myotube dedifferentiation and proliferation, although the ERK-activating signals may differ[173,174].

Furthermore, in cardiac regeneration of *D. rerio*, elevated ERK signaling activation is seen in the epicardium, endothelium and injury border zone. Through H_2O_2 release, DUSP6 is destabilized and inhibited, which releases ERK to promote angiogenesis and cardiomyocyte proliferation[175,176].

Also interesting, the comparison of wound healing between the regenerating tail and scarring limb of lizards showed that several WNT ligands, namely WNT2b, WNT5a, WNT5b and WNT6, are upregulated in the tail blastema, but absent in the scarring limb, where WNT pathway inhibitors, like DKK2, were detected[177].

Another interesting commonality between the regenerating limbs of amphibians and scarring mammalian wounds is the expression of TGFβ. But while TGFβ's presence has been associated with scarring in mammalian wounds, it appears to be essential for regeneration in amphibian limb regeneration[178,179].

This has been proposed to be due to differential temporal dynamics, with the expression of TGFβ being more transient in amphibian wounds. In *Xenopus*, this TGFβ signaling was shown

to occur downstream of ERK activation, and leads to ROS production[180]. The TGFβ superfamily has further been associated, through BMP signaling, to participate in the dedifferentiation of muscle cells in the salamander limb blastema[181], and in fish cardiomyocyte dedifferentiation and proliferation[182].

Quickly after epidermal thickening, the underlying mesenchyme undergoes degeneration and histolysis, as a result of the activity of MMPs, likely also contributing to impede the basal membrane's re-assembly[183,184]. This results in the liberation of progenitor cells, primarily from bone and muscle, that contribute to the mesenchymal pool of the blastema[185–187].

In amphibian limb regeneration, the mesenchymal fibroblast population is partially dermis-derived, and re-expresses genes present during limb development of vertebrates, like Prrx1[126,188]. The expression of Prrx1 in dermal fibroblasts of the salamander limb seems to be induced through stimulation of the FGFR1 receptor by FGF ligands secreted by the dorsal root ganglia (DRG)[126,132,133,189].

Perhaps due to the re-expression of these more embryonic factors, lower vertebrate fibroblasts do not display a myofibroblast phenotype, and produce less collagen than adult mammalian fibroblasts[126,178]. Further indication of the amphibian fibroblast's more embryonic phenotype is the observation that these cells can not only regenerate the dermis, but also contribute to skeletal elements, suggesting a higher differentiation potential, akin to mesenchymal stem cells[190,191].

Another particularity of regenerating wounds of salamanders, not yet observed in mammalian wounds, is the inductive capacity of Myristoylated alanine-rich C-kinase substrate (MARCKS)-like protein (MLP), an intracellular substrate of PKC, on tail and limb regeneration, through induction of cell cycle re-entry of many cell types[192,193].

In adult mammals, comprehension of which signals control proliferation in regenerative events is not very complete, owing to the fact that mammalian regenerative models do not abound. However, it is known that mammalian digit tip regeneration seems to depend on Msx1[194,195] expression, which likely is regulated by BMP signaling[15]. It is also known, although without a very clear understanding of the mechanism, that digit tip regeneration also depends on innervation, with Schwann cell-derived precursors, from intact peripheral nerves, secreting factors like Oncostatin M and PDGFA, which have been shown to rescue regeneration after denervation[196].

On another model of mammalian regeneration, cardiac regeneration through cardiomyocyte dedifferentiation in postnatal mice was associated with ERK/YAP signaling[197,198]. This has been associated with ERBB2's capacity to activate ERK signaling, which not only contributes

to CM dedifferentiation and proliferation, but also to subsequent redifferentiation[197,199]. Activated ERK then induces YAP activation, which leads to myoskeleton and nuclear envelope component alteration, sarcomere disassembly, EMT and proliferation. In adult mice, this activation of ERK and YAP has been shown to be inducible by Agrin, through the binding of the DAG1 receptor, and lead to cardiomyocyte dedifferentiation, proliferation and maturation[198].

The nerve dependence of regenerative processes does not seem to be as common in mammals as in lower vertebrates. In fact, it seems antler regeneration is nerve independent. Denervation of antlerogenic regions did not affect pedicles or first antlers formation and growth, and was also not essential for subsequent antler regeneration after regrowth. Nevertheless, denervation did affect antler size and shape, which suggests that nerves still play a part in this process[200–202].

Proteomic analysis showed that ERK activation is seen in pedicle periosteum and antlerogenic periosteum cells of deer antlers[203]. ERK signaling appears to be activated through pilose antler peptide (PAP)-induced Insulin Signaling, which then stimulates MAPK/ERK and PI3K/AKT pathway signaling to promote osteoblast proliferation, differentiation and mineralization.

Continuing to expand our understanding of mammalian regeneration, the previously mentioned Sinha et al., 2022 work identified two sets of conserved regulatory networks in reindeer fibroblasts response to wounding, one specifically associated with the velvet fibroblasts in scarless healing, and another associated with back skin fibroblasts in scarring wound healing.

Velvet fibroblasts regulatory network appeared to be associated with the re-engagement of developmental programs, as well as restrictive leukocyte communications, while dorsal skin fibroblasts appeared to sustain myofibroblast differentiation programming and potentiate leukocyte dialogue. The authors also proposed that the transition from a scarless regulatory network to a scarring network was associated with the activation of the mechanotransduction-related signaling, namely through YAP-TEAD signaling, as CSF1 expression suggested.

A comparison of expression profiles of the identified cell types in velvet and back skin suggested that Schawann cells and fibroblasts have a higher degree of distinction. In fibroblasts, for example, several genes associated with regenerative competence were identified, like Crabp1, Mdk, Runx1, Prss35 and Ptn, while in back skin fibroblasts the unique expression of ‘pro-inflammatory’ genes, like Ptgds, Scara5, Cxcl1, Cxcl3 and Ccl2, was detected. The expression of these genes was proposed, by the authors, to be associated with NF-κB signaling

in back skin, while velvet fibroblasts activated networks associated with cell plasticity, hair follicle induction and reduction of inflammation.

To determine whether these expression behaviors were characteristic of regenerative and fibrotic wounds in mammals, the authors compared the expression profiles of reindeer velvet and back skin fibroblasts with those collected from *A. cahirinus* and *M. musculus*, as well as with human fetal and adult skin-derived fibroblasts. The authors observed considerable overlap of expression in fibrosis-primed fibroblasts, mainly through the expression of cytokines and chemokines, driven by NF-κB. Furthermore, distinctions between regenerative and fibrotic programs were also preserved among species.

Interestingly, transcriptomic analysis indicated some convergence of profiles of velvet and back skin fibroblasts of reindeer at 7 days post wounding, while the other time points analyzed showed distinct transcriptional programs, which the authors suggested as being the timepoint at which fibroblast "terminal fates were imprinted". At 7 days, both regenerative and fibrotic fibroblasts showed a significant epigenetic remodeling of regeneration-associates regions of the genome, which suggested an attempt of fibrotic fibroblasts to initiate a pro-regenerative response. However, expression of immunostimulatory genes, like Il-1α, Il-6 and Ccl5, ate day 14 post wounding, likely contributed to redirect back skin fibroblasts to a fibrotic fate.

Analysis of the regulatory networks underlying fate commitment showed an association of back skin fibroblasts with upregulation of complement and coagulation cascades, through expression of C1R, C3 and Plau, as well as with immunomodulatory cytokines, like Ccl2 and Cxcl12, and activation and sustainment of TGFβ-driven myofibroblast differentiation, as suggested by the expression of TGFβR3, CD44 and Cryab.

Velvet fibroblasts, in turn, associated with the expression of development-related genes, like Crabp1, Mdk and Lgals1, and extracellular matrix factors, like Col11a1, Col12a1 and Col27a1, as well as negative regulators of TGFβ signaling, like Lmo7 and Pmepa1. At baseline, velvet fibroblasts secrete pro-regenerative signals, like MDK, PTN, BMP3 and RSPO3, while back skin fibroblasts produce more immunostimulatory factors, like GAS6, CSF1, CXCL12 and PLAU, and this is further accentuated at day 3 post injury, with the additional expression of Il-1α, Il-1β and Il6 in back skin fibroblasts.

In another mammalian regenerative model, *Acomys spp.*, Seifert et al observed that re-epithelialization of dorsal skin wounds occurred faster than in its scarring counterpart, *M. musculus*[710]. These authors also observed that collagen fibers were less densely packed in the regenerative *Acomys*, with a more porous structure, and there was a lower abundance of Col I,

and higher of Col III, in the granulation tissue, when compared to the fibrotic wounds of Mus. After re-epithelialization, *Acomys* distal epidermis was found to be thicker, with disorganized basal keratinocytes and lack of a mature basement membrane, akin to the AEC of lower vertebrates, which was not observed in *Mus*, where a wound epidermis was only transiently observable.

Proliferation was found widespread throughout the regenerating ear pinna tissue of *Acomys* and *Mus*, except in the distal epidermis of *Acomys*, but not of *Mus*, surprisingly. However, while proliferation was sustained in *Acomys*, late-stage healing *Mus* ears had almost no proliferating cells.

Histological comparison of healing tissue at day 12 post wounding indicated high levels of FN, some TN and very low levels of Col I in *Acomys* granulation tissue, where Col III was more abundant. In *Mus*, initially the wound displayed high levels of FN and low levels of TN, similar to *Acomys*, but with higher levels of Col I, which was accumulated faster and exhibited a higher proportion to Col III. Furthermore, a higher abundance of myofibroblasts was found in *Mus* granulation tissue, while they were almost absent in *Acomys*.

Focusing instead on the healing of the dorsal skin, Brant et al., observed that in uninjured epidermis of *Acomys* and *Mus* there are similarly low levels of proliferation, that were significantly increased by day 4 after wounding, and were kept high for up to 12 days after wounding, adjacent to the cut's edge[713]. However, like in the ear pinna, around day 14 after wounding the proliferation in *Mus* wound epidermis fell significantly, while in *Acomys* it was maintained.

In the mesoderm, as in the epidermis, proliferation initially occurred at similar levels between *Acomys* and *Mus*, up to day 4 post wounding, where it diverged. From then on, proliferation levels increased similarly between species until 14 days after wounding, where they peaked. But from here on proliferation in *Mus* mesoderm decreased to basal levels, while it remained higher in *Acomys*.

As fibroblasts from the connective tissue, below the panniculus carnosus invaded the tissue, they remodeled the extracellular matrix of the wounded tissue. While in *Mus* the newly deposited collagenous ECM gave rise to a dense granulation tissue, that exhibited randomly orientated cells, in *Acomys* it appeared that there was no collagen deposition, and the granulation tissue was looser and cells appeared oriented along horizontal strands of ECM.

Analysis of collagen gene expression identified 18 isoforms significantly altered during wound healing, between *Mus* and *Acomys*. Specifically, *Mus* exhibited upregulation of Col 5, 6, 8, 14,

24 and, most noticeably, Col 12a1, which had a 22-fold increase in relation to *Acomys*, at 14 days post wounding.

In 2016, Gawriluk et al. expanded our understanding of the regenerative processes that occur in the ear pinna of *Acomys*[13]. The authors compared several models of mammalian fibrotic and regenerative healing and confirmed that in the regenerative processes of mammals the granulation tissue is usually characterized by a collagen deposition similar to the unwounded pattern. However, unlike in dorsal skin, re-epithelialization of the ear pinna wound seemed to occur more slowly in *Acomys* than in *Mus*.

Comparison of the expression patterns of wounded tissue within the first 20 days of wound healing, between the regenerating *A. cahirinus* ear pinna and the reparative *M. musculus*, showed a clear indication of fibrotic gene expression in *M. musculus*, while *A. cahirinus* revealed a unique transcriptional program associated with regeneration. For example, *Mus* overexpressed Fbn1, Col1a1, Col3a1 and Lum, which are usually associated with a scarring result. Contrarily, in *Acomys* the authors detected the increased and sustained expression of Lgi2, Lgi3, Cthrc1, Lama1, Nell1, Tnc and Fn1, usually associated with peripheral nerve stimulation and cell proliferation.

These authors also reinforced the observation that there is a clear distinction between the epidermal morphology of *A. cahirinus* and *M. musculus*, with the neo-epidermis of *M. musculus* exhibiting a fully stratified squamous epithelium by day 5 post wounding, while keratinocytes in *Acomys* still lacked apical-basal polarity and maintained contact with the underlying mesenchyme, and these differences were further confirmed by pathway analysis of the RNA-seq data.

Furthermore, the authors observed that in the early stages of wound healing there are similar levels of proliferation and cell cycle completion. However, as both processes progress, the percentage of cells that complete the cell cycle in *Mus* decreases, with several never progressing to, or through, S phase. This was demonstrated to occur by an increase of p21 and p27 nuclear levels in *M. musculus*, while in *A. cahirinus* these levels were kept low throughout the assessed period of the regenerative process, with p21 and p27 being excluded from the nucleus.

Recently, Tomasso et al. showed that ERK1/2 pathway activity is induced in *Acomys* and *Mus* shortly after wounding, within the first 10 minutes, but is more broadly activated in the tissues of *Acomys*, where it is also sustained for longer[1378]. This activity is observed both in epithelial (where it sustains the wound epithelium phenotype) and in mesenchymal tissues, but as the events progress, and the granulation tissue is formed, this activity persists only in the proximal

epithelium and underlying mesenchyme of the regenerative process, particularly associated to nerves and proliferating cells, with the fibrotic process almost completely abolishing ERK1/2 activity. Similar patterns of ERK activation in regenerative and fibrotic tissues were observed in dorsal skin healing and myocardial infarction recuperation in *Acomys* and *Mus*.

Tomasso et al. also showed that inhibition of ERK signaling in the ear pinna of *Acomys*, especially during the initial phases of wound healing, significantly delayed the process and impaired regeneration. Late inhibition of ERK signaling, after re-epithelialization, does not greatly affect the process of wound healing, yet still prevents adequate regeneration, due to the loss of AP-1-mediated gene expression, considerably influencing the expression of genes associated with blastema formation and expansion, like those involved in cell proliferation, immature wound epidermis formation, pro-regenerative ECM deposition, immunomodulation and nerve growth.

E2F target genes were found to be the top downregulated gene set in a transcriptomic analysis of the healing tissue. Furthermore, RNA-seq data analysis indicated a strong association of differentially expressed genes with AP-1, NFAT and SRF binding sites, and EGR^+ and FOS^+ cells in the blastema were found to be $pERK^+$. ERK signaling has, therefore, a clear impact on proliferation regulation, which was confirmed through the observation that the regions of tissue surrounding the wounded area exhibited fewer EdU^+ and $pHH3^+$ positive cells in ERK-inhibited tissues.

Late ERK inhibition also resulted in the downregulation of genes associated with canonical WNT signaling, like MMP9, and genes associated with a regenerative extracellular environment, like Fgf12, Timp3, Wisp1 and Tnc, while genes associated with a fibrotic result, like Cd209d, Tgfbr2, Tgrbr3 and Ccl8, were upregulated and Col I deposition was increased.

Inhibition of ERK activity after re-epithelialization also led to the sustainment of the inflammatory response in *Acomys*, particularly associated with TNFα signaling, through the NF-κB pathway, and Il-6, through the JAK/STAT pathway, as evidenced by the upregulation of Cebpd, Stat3, Socs3, Nfkbia, Irf7 and Ifitm1, and an increased number of infiltrating leukocytes.

The authors wondered whether nerve-derived signaling could be responsible for ERK activation. To test this, they inhibited upstream activators of ERK signaling, the FGFR and ERBB2 receptors, which are known to be stimulated by, among others, FGF2 and NRG1. Inhibition of these receptors strongly impaired both regeneration and ERK activation, as well as cell proliferation and EGR and FOS expression.

Subsequently, exposing *M. musculus* healing ear pinna tissue to FGF2 and NRG1 led to the induction of several hallmarks of regeneration in the otherwise fibrotic process of *M. musculus* ear pinna wound healing, like increased levels of proliferating cells, hair follicle neogenesis, increased tissue regrowth, as well as a partial recreation of the transcriptional profile of *Acomys* blastema, particularly through the modification of fibroblast expression of some genes. The authors also found increased production of Keratin 17, Fibronectin and MMP9, and reduced levels of αSMA^{+} cells, coupled with increased levels of $PDGFR\alpha^{+}$ cells, suggesting an alteration of the fibrotic program to a more regenerative one.

Despite these astonishing and conclusive results about the involvement of ERK signaling in regenerative processes in vertebrates, they suggest that ERK sustained activation might not be sufficient for full regeneration of all tissues. Perhaps this can be explained by the lack of appropriate immunostimulatory signals, or of an incorrect integration of other internal or external cues. Better understanding of the signaling controlling vertebrate regeneration is, therefore, still required.

This page was intentionally left blank

1.1.4. Remodeling

The last phase of the wound healing process is the remodeling of the tissue. In this phase, granulation tissue is gradually diminished and the innate immune cells that invaded the tissue in the early phases leave the wound or undergo apoptosis. At the same time, proteoglycan and glycosaminoglycan levels, that provided structural and regulatory roles to the tissue, are decreased.

Macrophages and myofibroblasts continue to perform the tasks they started performing during the proliferation phase, namely releasing collagen metalloproteinases and metalloproteinase inhibitors, whose combinatorial effects degrade Col III, but not as much Col I, resulting in a substitution of one for the other, and an increase in ECM organization and density, which forms a scar scarce in cells (Figure 1.13)[204–206]. This behavior can last for months.

However, this is not the end point of wound healing, and after a while, macrophages reacquire a phagocytic phenotype and a 'fibrolytic' profile[20]. These macrophages are called M2c, or Mreg-like macrophages, and they release proteases and phagocyte excessive cells and matrix, no longer required for wound closure, which results in a remodeling of the tissue, that can continue for a few more months, or even years[207,208].

Their interaction with fibroblasts is very important for the best remodeling of the granulation tissue possible. For instances, elevated expression of CD47 in murine fibroblasts prevents macrophage phagocytosis, ultimately leading to excessive matrix deposition and scar formation[209]. At this time, myofibroblasts are also stimulated to perform apoptosis. Failure to induce this behavior, and myofibroblast permanence on the repaired tissue, will lead to fibrotic situations, like hypertrophic scars[210].

Fibrotic results, which are common in the wound healing events of most non-regenerative vertebrates, can be the consequence of several deregulations of the different phases of wound healing and their participants. For example, fibrotic scarring can be the result of permanence of inflammatory macrophages, which can be explained by altered signaling between macrophages, fibroblasts, epithelial and endothelial cells, resulting in a permanent inflammatory response by the tissue. This can also lead to altered FGF, hepatocyte growth factor (HGF), EGF and TGFβ signaling, resulting in persistent phenomena of EMT[211].

Fibrosis can also be the result, as just mentioned, of an irregular maintenance of activated myofibroblasts in the wound after re-epithelialization, which leads to an excessive deposition of collagen type I in the wound. Alterations of the ECM composition, due to myofibroblast

permanence or other, also result in altered availability of growth factors, mechanotransduction and cellular migration through the ECM, all of which can equally have an impact on the outcome of the wound healing event[212–214].

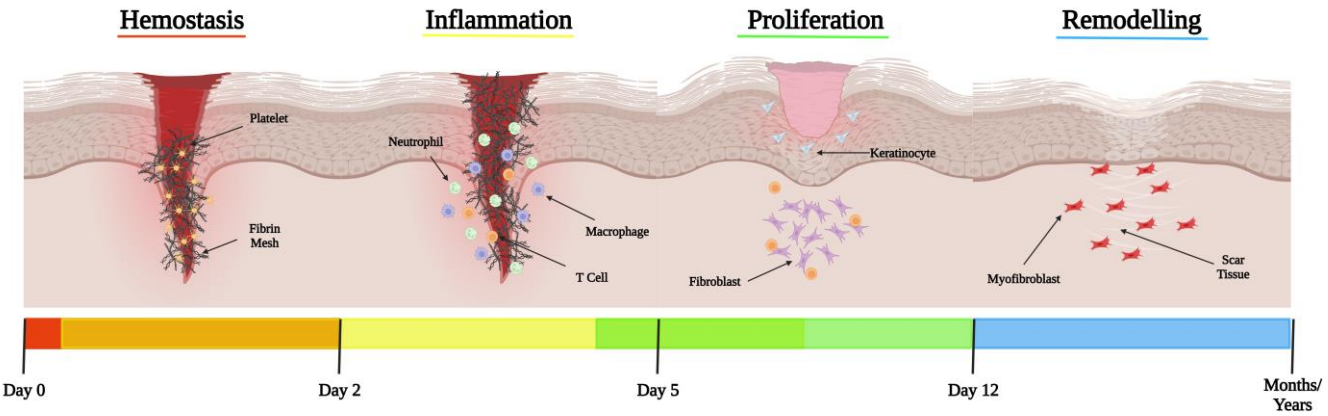

Figure 1.13 - Overview of the phases of wound healing. Schematic representation of transversal cuts of a healing tissue, with all phases and major participants represented, as well as their average durations. Image adapted from Knoedler et al., 2023[635] and created with BioRender.com.

1.1.4.1. Regeneration is Remodeling

While regenerative events are not usually described as occurring through the same phases of wound healing[655], there are sufficient communalities between the events that the same progression of phases can be used to describe both.

Perhaps the least similar, and harder to compare, is the 'Remodeling' phase. In fibrotic events, this phase is characterized by just a handful of processes, primarily ECM remodeling and blood vessel pruning, while in regeneration the scenario is very different. Instead of simply modifying the wound tissue to stabilize it, in regenerative events this is the phase where missing tissues are recreated, and this depends on considerable proliferation. For this reason, several processes occurring during regeneration could be considered a part of the proliferative, or 'growth', phase of wound healing.

However, we interpret the 'remodeling' phase of regenerative events as the group of processes that occur after blastema establishment, that encompasses blastema growth, differentiation and reshaping, to recreate the lost structures.

In that sense, fetal wounds are characterized by 'fetal (myo)fibroblasts'[215–218] that express less αSMA and secrete more Col III, whose organization is similar to uninjured ECM[54]. In lower vertebrates, progenitor cell origins were shown to be tissue-specific, with, for example, muscle cells not contributing to cartilage or epidermis regeneration, and dermis cells contributing to cartilage and connective tissue[219,220], but not muscle regeneration[8]. However, some exceptions have been found, like the contribution that dermis cells have to patterned bone regeneration during salamander limb regeneration[190,191].

Furthermore, while regeneration in vertebrates is usually associated with the expansion of stem cells, several studies have identified the capacity for some cell types to dedifferentiate and participate in regeneration, namely skeletal and cardiac muscle cells, and osteoblasts[221–227].

Two tissues have been shown to bare quite an effect on the patterning of the regenerating salamander limb. Wound epidermis has been associated with patterning through the secretion of retinoic acid (RA), which contributes to proximal identity during limb bud development[228–230]. Also contributing for the patterning of the proximal-distal axis is the nerve-derived factor nAG. nAG stimulates the PROD1 receptor, which is expressed in a gradient along the limb's proximal-distal axis, with a higher gradient in the proximal region[231].

Tissue patterning and morphogenesis has also been associated with BMP signaling, as exemplified by the role BMP2 and 6 have in regulating proximal cartilage proliferation and

hypertrophy during the lizard *A. carolinesis*'s tail regeneration, and BMP's role in dedifferentiation of muscle cells of the salamander limb[181,232].

BMP signaling was also associated with cell condensation and apoptosis, seeing as overexpression of Noggin, a BMP inhibitor, inhibits both processes[233]. This was suggested to occur through activation of DKK proteins, to counter WNT pathway signaling, also promoting osteoblast differentiation[234]. Furthermore, the Msx homeobox genes, which are immediate early BMP response transcription factors, have been suggested to play a role in development and regeneration[235–241].

Finally, Hedgehog signaling has been proposed as the key player of the last phase of regeneration, with Shh being expressed in the regions surrounding the ependymal tube in the regenerating lizard tail, where it establishes proximal organization centers and induces chondrogenesis[232]. Shh signaling was also shown to be sufficient to sustain limb regeneration when stimulated in anterior innervated limb tissue, while posterior cells did not respond to Shh stimulation, in a process reminiscent of the developmental process of limb bud[242].

BMP and Shh signaling have also been shown to cooperate in the patterning of regenerated fins[243–245], as ectopic expression of either Shh or Bmp2 led to ectopic bone deposition and mispatterning of fin rays. Exposure to cyclopamin, a Shh inhibitor, reduces proliferation and differentiation of bone-secreting cells.

Shh has also been shown to be important for mammalian remodeling of wounds, since its activation in the dermis is both necessary, and sufficient, for 'wound-induced hair neogenesis'[246], but only in some models[247]. Shh converts WNT-activated fibroblasts into dermal papilla, redirecting the fibrotic program to a regenerative one. However, this is not sufficient for a fully regenerative process, as the new hairs are restricted to wound centers, not pigmented, imbedded in fibrotic scar tissue with extensive collagen deposition, and the melanocyte niche is not re-established[155,248].

Studies of *Acomys* regenerating ear pinna have also associated WNT signaling with hair follicle regeneration in mammals. Nuclear LEF1 was found accumulated in regenerating epidermal placodes, condensing dermal fibroblasts beneath the hair germ, and in dermal papilla and matrix cells[710]. Furthermore, ERK inhibition resulted in a disappearance of $LEF1^{+}$ cells from the epidermis and dermis of the blastema, suggesting an interplay between MAPK/ERK and WNT signaling also observed in lower vertebrates[1378].

BMP signaling was also associated with differentiation of newly formed tissue in *Acomys* ear pinna, seeing has it was found activated in cells giving rise to new auricular cartilage[710].

pSMAD 1, 5 and 8, which are a good readout of canonical BMP signaling, were also detected at low levels during follicle induction, but at later stages, during dermal papilla and matrix cell differentiation, they were detected at higher levels in these cells.

This page was intentionally left blank

1.2. Acomys cahirinus: The ideal mammalian regenerative model

As we have mentioned, mammalian models of epimorphic regeneration do not abound, and some examples, like the regenerative capacity of deer antlers, have been interpreted as not belonging to this group of processes. This lack of models, in particular of easily tractable ones, has led to much of the research in mammalian regenerative abilities focusing on fairly simplistic models, like the digit tip of murids, on models whose actual capabilities have been suggested not to fit the description of "epimorphic regeneration", like the MRL strain of *M. musculus* or scarless fetal wounds, or to the usage of models that are hard to keep in most labs, like rabbits.

However, in 2012 a particularly interesting model was found. Two species of the genus *Acomys*, a fairly speciated genus that inhabits most of the African continent, as well as the Middle East and southeast parts of Europe, were described as being capable of regenerating both the dorsal skin as well as their ear pinas. While species of this genus had already been introduced to labs previously, work on them had focused on other fields, and observations of their regenerative potential were anecdotical.

Since the description of their regenerative capabilities, a lot of attention was given to this genus, in particular to one species, *Acomys cahirinus*. With their size being only slightly larger than the typical *Mus musculus*, most labs are equipped to house these animals, with only a few adjustments to feeding. Furthermore, due to their evolutionary proximity to *Mus*, many molecular tools used for this model can be adapted for *Acomys*.

While still not as tractable as *Mus*, mainly due to the lack of genetic tools, the *Acomys* genus already counts within it a few species with sequenced and annotated genomes, with *A. cahirinus* being one of them. This has already contributed to the understanding, for example, of the transcriptomic profile of cells involved in the regeneration of epidermal tissues and spinal cord.

Since the description of its regenerative potential of epidermal tissues, the *Acomys* model has been associated with the capacity, or at least the potential, to regenerate several other tissues, like skeletal muscle, spinal cord, kidneys, and even possibly heart and brain. This enormous potential has been correlated with a particular immune response, which

With this in mind, we set out to understand whether other pathways involved in the regulation of proliferation, like the PI3K/AKT and WNT pathways, also played a part in regulating the

regenerative response of *Acomys* ear pinna, and whether pathways involved in immune signaling, like JAK/STAT and NFκB, might also contribute to the regulation of wound healing in this regenerative model.

2. Materials and Methods

This page was intentionally left blank

2.1. **Animal Handling**

In our study we used two species: *Acomys cahirinus* and *Mus musculus*, which are bred in separate rooms at the University of Algarve's bioterium. During experimentation, both species are kept at 24°C, and on a 10:14 L:D light cycle. *M. musculus* husbandry is performed in accordance with EU guidelines, and *A. cahirinus* husbandry is in accordance with was previously described in Pinheiro et al., 2018[1379].

To perform this set of experiments we used young adult animals of both sexes, with *A. cahirinus* individuals ranging from 3 to 12 months of age and *M. musculus* ranging from 2 to 6 months of age. In all experimental groups we used an average distribution of sexes of 50%.

To induce wound healing event, *A. cahirinus* and *M. musculus* were anesthetized using 3,5% of Isofluorane in 1L/min of O_2, and their ear pinnas were punched with either Ø4mm biopsy punches, for *A. cahirinus*, or Ø2mm biopsy punches, for *M. musculus*, to create full thickness wounds whose volume was proportional to the ear size.

This page was intentionally left blank

2.2. **Analysis of Proliferative Cell Expression**

2.2.1. Proliferating Cell Labelling and Tissue Collection

Isolation of proliferating cells from healing tissue was performed with groups of six individuals of each species, wounded as previously described and left to heal for 3, 5, 7 and 14 days. To establish a baseline (uninjured tissue, or day 0), the circle of tissue removed with the initial biopsy punched was also used to isolate proliferating cells. Of these six individuals, two of each species were used as non-labeled controls (no exposure to EdU), while the other four (experimental group) were subsequently injected with a solution of EdU near the time of collection.

At 12, 4 and 2 hours prior to tissue collection, the experimental groups of *A. cahirinus* and *M. musculus* were anesthetized and injected with 75 mg/Kg of EdU (in 1x Phosphate-Buffered Saline (PBS) – **137mM NaCl,** VWR Chemicals 27810.364; **2,7mM KCl,** MERCK 1.04936; **10mM Na_2HPO_4,** MERCK 1.06580; **1,8mM KH_2PO_4,** MERCK 1.04873 in ddH_2O, **pH 7,4**). To collect the healing tissue, both control and experimental groups of *A. cahirinus* and *M. musculus* were again anesthetized, and their ear pinnas were re-punched over the previous whole with either a Ø5mm biopsy punch, for *A. cahirinus*, or a Ø3mm biopsy punch, for *M. musculus.* A schematic representation of the process can be seen in Figure 2.14.

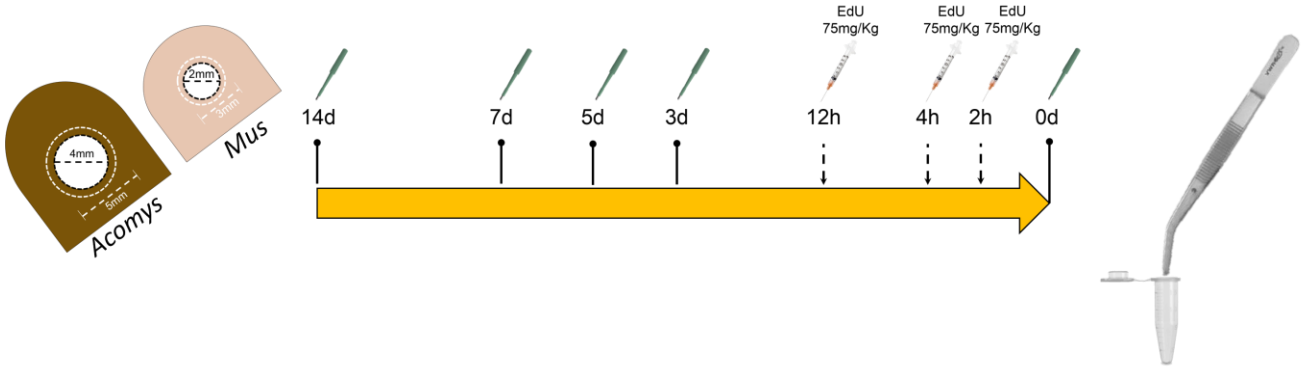

Figure 2.14 - Collection of wound healing samples at different timepoints.
Schematic representation of the preparation of animals and collection of samples for the isolation of proliferating cells from the healing ear pinna tissue of A. cahirinus and M. musculus.

The resulting ring of tissue from the punch was collected, and then rinsed, once with chilled 70% DEPC-treated EtOH, once with 1x PBS, and placed in cold 1x HBSS (Hank's Balanced Salt Solution - **140mM NaCl,** VWR Chemicals 27810.364; **5mM KCl,** MERCK 1.04936; **1mM $CaCl_2$,** Sigma-Aldrich C3881; **0,4mM $MgSO_4$–$7H_2O$**, MERCK M2773, **0,5mM $MgCl_2$–$6H_2O$,** Fluka 63069; **0,3mM Na_2HPO_4–$2H_2O$,** MERCK 1.06580; **0,4mM KH_2PO_4,** MERCK 1.04873; **6mM D-Glucose,** MERCK 1.08342; **4mM $NaHCO_3$**, MERCK S6014, in

ddH_2O), supplemented with 1x RNAProtect RNAse Inhibitor (Sigma-Aldrich R7397), and kept on ice until the next step.

2.2.2. Tissue Digestion and Single Cell Suspension Preparation

To produce a single cell suspension for FACS, tissue samples were first placed in a petri dish and washed with 1x HBSS to remove RNAProtect RNAse Inhibitor. Tissue samples were then submerged in 2mL of a solution of 0,1% Trypsin (Gibco 25-200-056) and 100U/mL of Collagenase IV (Gibco 17104019), in 1x HBSS, and minced using two #24 scalpel blades, until the tissue was almost a paste.

The tissue and digestion solution were then transferred to a 15mL centrifuge tube and incubated on a water bath at 37ºC, with 200rpm agitation, for 30min. After the incubation, the majority of the large pieces of tissue had deposited, so the supernatant was pipetted out and filtered through a 70µm nylon mesh cell strainer [VWR, 734-2761] into a new 15mL centrifuge tube, and placed at 4°C. To the previous tube, with the remaining undigested tissue, 2mL of the digestion solution were added, and re-incubated a further 30 min.

After the second incubation the re-digested tissue, and the supernatant, were filtered through the previously used filter for the same sample, now placed inside a petri dish. The leftover pieces of undigested tissue trapped in the filter were further broken down by using a 20mL syringe plunger as a pestle, to macerate the tissue. Cold Complete DMEM (DMEM, Gibco 21969-035; 10% Fetal Bovine Serum, FBS – Gibco A5670701, Glutamax, Gibco 35050-038; Pen/ Strep, Gibco 15-140-122) was used to stop digestion and wash the filter, and the filtered solution was transferred to the respective 15mL centrifuge tube, already containing the previously filtered digestion supernatant. At this point, to create a control for the labeling reaction, the control cell suspension was divided into two separate samples.

2.3. **Proliferating Cell Sorting**

Once single-cell suspensions were obtained from each group of samples, the inactivated digestion mix was removed through centrifugation, and the cells were washed with 1x PBS. EdU^+ cells were then labelled using a Click-It Reaction (969µL of 1x PBS, 200µL of 1X Click-iT reaction buffer, 7µL of $CuSO_4$, 3µL of Copper protectant and 1µL of Alexa Fluor picolyl azide), which attaches a fluorescent moiety to the EdU integrated in the DNA, through a copper-catalyzed chemical reaction. For this step we used the Thermo Fischer Scientific 'Click-iT™ Plus EdU Cell Proliferation Kit for Imaging, Alexa Fluor™ 488 dye', reference C10637.

The experimental group cell suspension, and one of the control group cell suspensions (labeling control), were exposed to 200µL of the reaction mixture for 30 min, at room temperature and in darkness, with regular agitation. The other control group cell suspension (non-labeled control) was kept in the same conditions, but in 200µL of 1x PBS. After the reaction period, β-Mercaptoethanol was added to all tubes, to stop the Click-It reaction and maintain similar conditions between samples.

The reaction solution was removed through centrifugation, and all the pelleted samples were resuspended in CSB (Cell Sorting Buffer – 1mM EDTA, MERCK E5134, 25mM HEPES, MERCK H4034, 1% FBS, FBS – Gibco A5670701, in 1x PBS) to increase the cell survival in the single cell suspensions during the sorting process. To obtain purified cell populations of EdU^- and EdU^+ cells, without contamination from other fractions, the control population not exposed to Click-It was first used to establish a baseline sign for unlabeled cells (P2), and to discriminate doublets and cell debris (Figure 2.15).

After that, the control cell suspension exposed to Click-It reaction was used to determine the levels of non-specific signaling, since they were also exposed to the fluorescent marker, but not to EdU. With this control we were able to rule out any signal that was not due to specific EdU labelling, but due to non-specific signal like, for instances, coating of the cell membranes with fluorescent moieties (P3, Figure 2.16).

After establishing these baselines, we were then able to divide the experimental population into cells without EdU labelling (EdU^-) and cells clearly labelled with EdU (EdU^+, P6, Figure 2.*17*). Non-specifically labelled cells in the experimental population were also identified and excluded from the sorted populations (P3). Both negative and positive populations were then collected into two 1,5mL tubes, containing 1mL of Nzyol (NZYTech MB18501), and kept at -80°C until further use.

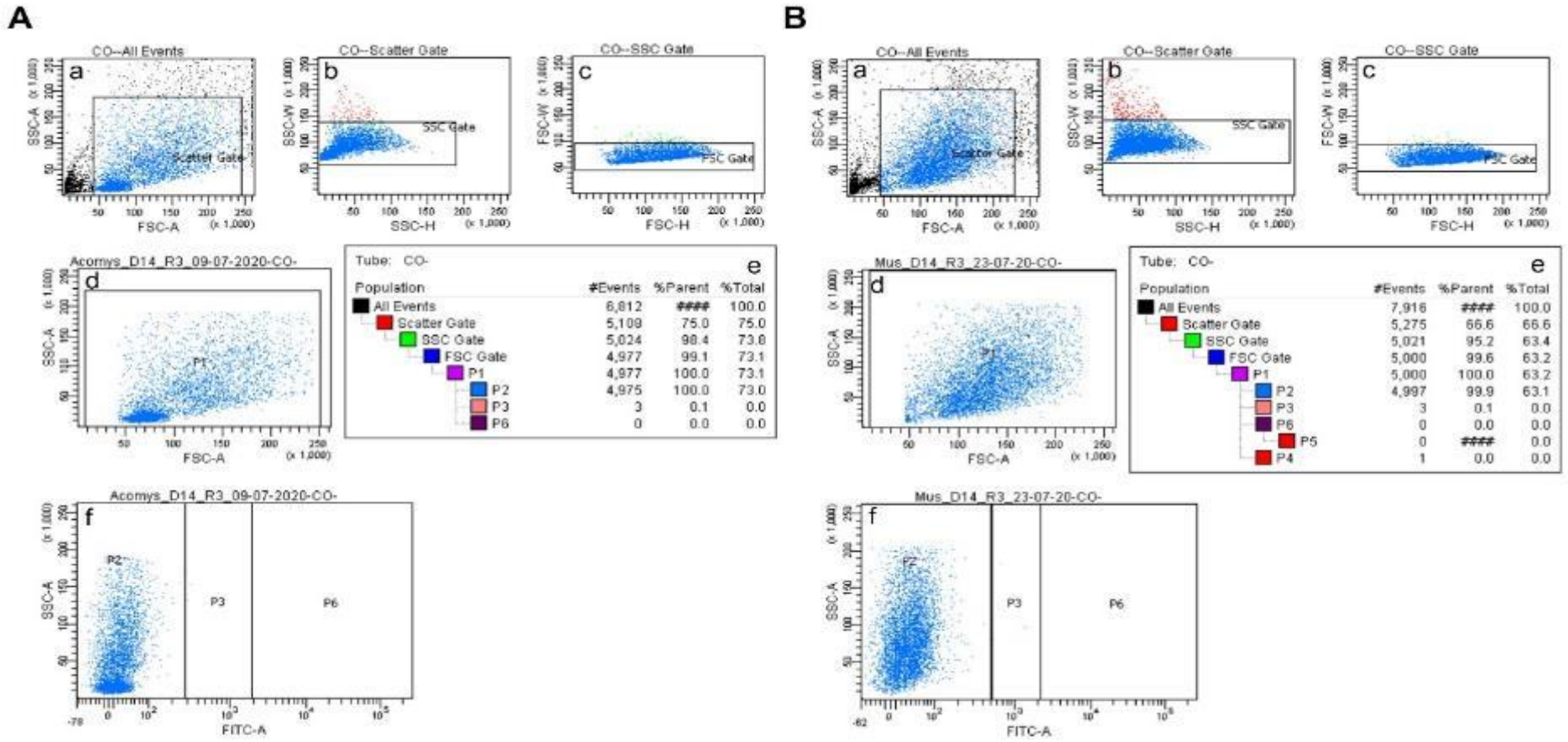

Figure 2.15 – Establishment of the P2 (Non-labelled) gate for FACS. The figure depicts how non-labeled control samples were used to establish the gate for clearly EdU negative cells (P2). A – A. cahirinus *sample. B –* M. musculus *sample. a), b) and c) represent the gates used to exclude doublets, aggregates, debris and abnormally shaped cells. d) represents the gate used to confirm that the gate population represents isolated cells. e) represents the percentages of cells passing through each gate. f) represents the gating for different levels of fluorescent signal intensity that identify the amount of EdU integration.*

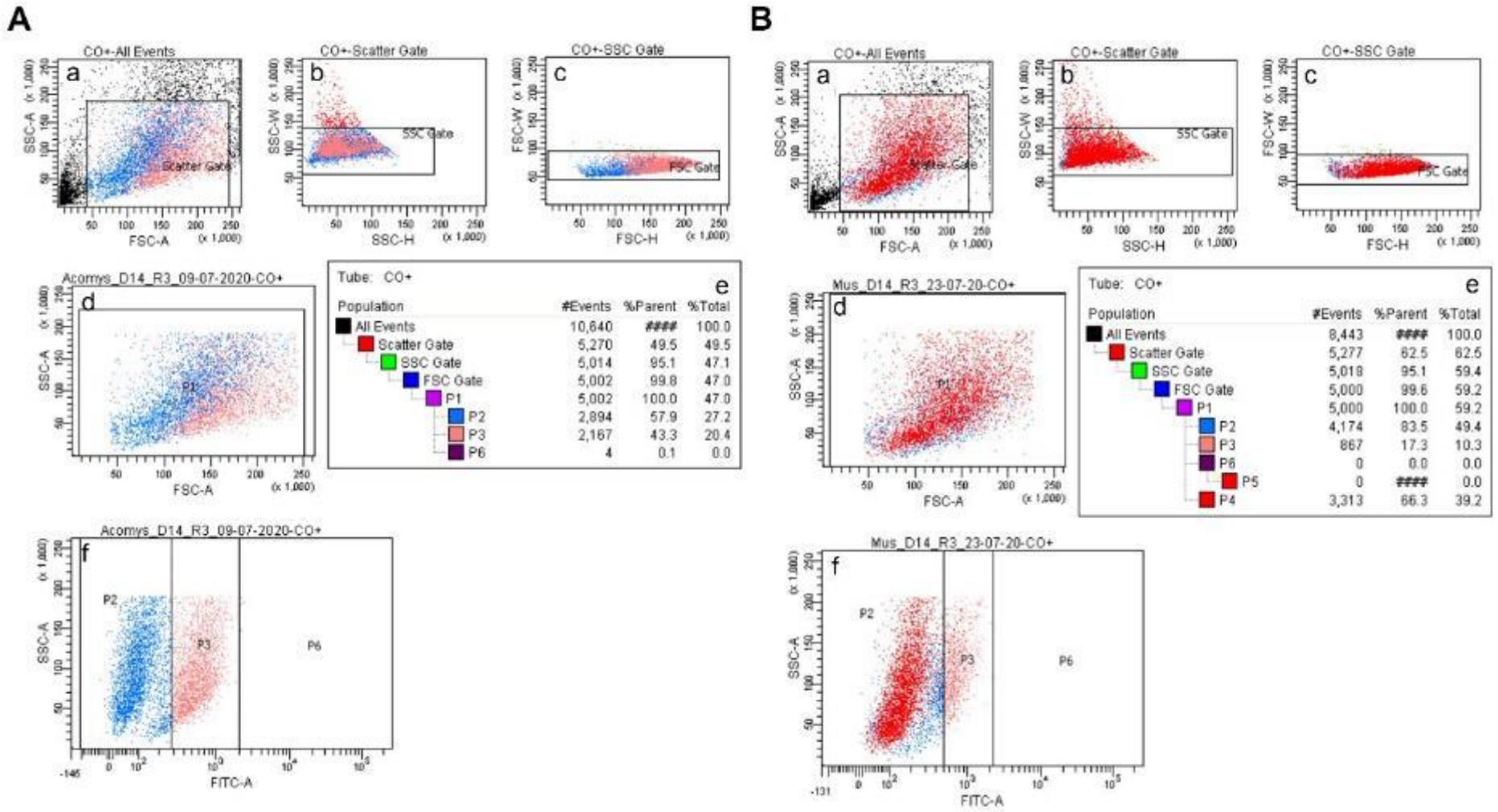

Figure 2.16 – Establishment of the P3 (Labeling Control) gate for FACS. The figure depicts how non-labeled control samples were used to establish the gate for clearly EdU negative cells (P2). A – A. cahirinus *sample. B* – M. musculus *sample. a), b) and c) represent the gates used to exclude doublets, aggregates, debris and abnormally shaped cells. d) represents the gate used to confirm that the gate population represents isolated cells. e) represents the percentages of cells passing through each gate. f) represents the gating for different levels of fluorescent signal intensity that identify the amount of EdU integration.*

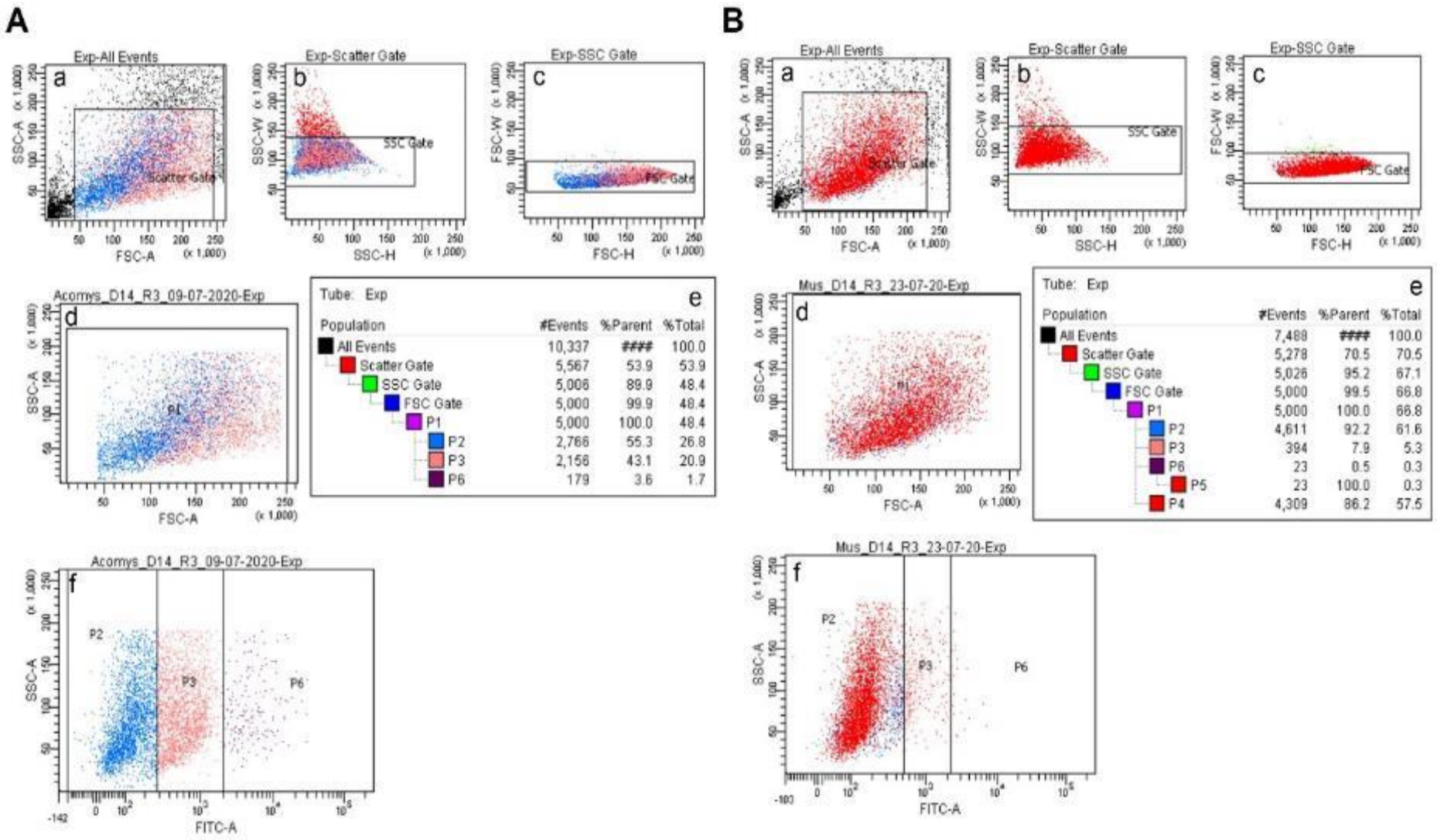

Figure 2.17 – Establishment of the P6 (Experimental Control) gate for FACS. The figure depicts how non-labeled control samples were used to establish the gate for clearly EdU negative cells (P2). A – A. cahirinus *sample. B* – M. musculus *sample. a), b) and c) represent the gates used to exclude doublets, aggregates, debris and abnormally shaped cells. d) represents the gate used to confirm that the gate population represents isolated cells. e) represents the percentages of cells passing through each gate. f) represents the gating for different levels of fluorescent signal intensity that identify the amount of EdU integration.*

2.3.1. *RNA Extraction and Quantification*

To normalize conditions of RNA extraction between samples, all cell suspension samples were kept frozen for at least 48h, at -80°C, prior to extraction. Isolation of the RNA proceeded in groups of four samples, to minimize handling errors. The samples were thawed on ice and 200µL of chilled chloroform were added, and mixed by vigorous hand shaking for 15s, to dissolve apolar substances. This shaking also contributes to the lysing of the cells and the release of their contents.

Phase separation of the Nzyol solution was achieved by centrifuging the samples at 15000g, for 15min, at 4ºC. The aqueous phase, containing the solubilized RNA, was transferred to a new 1,5mL tube, where 200µL of chilled chloroform were already placed. The solution was centrifuged again, with this process being repeated twice more to fully wash off non-soluble substances.

Fresh tubes, containing 0,9 volumes (in relation to the aqueous phase extracted) of chilled Isopropanol (Sigma-Aldrich 33539), 0,1 volumes of 3M NaAc (pH5,2 – Sigma-Aldrich S2889) and 15µg/mL of Linearized Acrylamide (Invitrogen AM9520) were prepared, and the aqueous phases obtained at the end of the washes were transferred to these tubes. The solutions were mixed by inversion, and the RNA was left to precipitate at -20ºC, overnight.

The following day, samples were centrifuged at 15000g for 10min, at 4ºC, to remove the supernatant. 1mL of chilled 75% EtOH was then added to each sample, and they were again centrifuged, this time at 7500g, for 5 min at 4ºC, to wash the RNA pellet. This EtOH wash was performed four more times.

After the last EtOH wash, as much of the supernatant as possible was removed, without perturbing the RNA pellet, and the tubes were left to dry, at room temperature, for 5min. To complete the removal of EtOH from the pellet, the tubes were placed in a dry bath, at 65ºC, for 2min. 10µL of Molecular Grade water (Nzytech MB11101) were then quickly placed in each tube, which were kept 5 more minutes in the dry bath, to resolubilize the RNA. The samples were then briefly vortexed, spined shortly, and placed on ice as quickly as possible. 2µL of each sample were removed into fresh 0,5mL tubes, and saved for later quantification, and the samples were stored at -80°C, until further use.

Evaluation of quality and concentration of RNA samples was performed using a 4200 TapeStation System (Agilent Technologies – G2991AA), using the Agilent High Sensitivity

RNA ScreenTape Assay (High Sensitivity RNA ScreenTape – 5067-5579, High Sensitivity RNA ScreenTape Sample Buffer – 5067-5580, High Sensitivity RNA ScreenTape Ladder – 5067-5581). This system was used according to the manufacturer's instructions, following the detailed protocol that can be found in:

https://www.agilent.com/cs/library/usermanuals/public/ScreenTape_HSRNA_QG.pdf

A summary of information pertaining to the sample quality and analysis of the samples that were chosen to e sequenced can be found in Table 2.4.

Table 2.4 - Summary of the relevant information of sample quality.
This table details, for each sample, the Edu Status, number of cells collected, RNA quality, sample quality analysis after sequencing and sequencing results. "Edu Labelling" pertains to the status of the sample, whether the collected pool of cells was detectably positive for EdU labelling (P6 population during FACS) or was distinctly EdU unlabeled (P2 population during FACS); RIN – RNA Integrity Number – A scale of 10 points, commonly used to represent RNA integrity, with 0 being fully degraded and 10 being intact. The FastQC test and the PCA and MDS tests evaluate sample quality through several parameters, like number of duplicated reads and replicate clustering. Total number of reads, percentage of read aligned, and percentage of uniquely aligned reads are other metrics that allow us to evaluate sample quality after sequencing. Information in red lettering represent criteria of sample exclusion from downstream analysis.

Sample	Edu Labelling	# Cells Collected	RIN	FastQC Test	PCA/MDS Test	# Total Reads	% of Aligned Reads	% of Uniquely Aligned Reads
Mus D0 R1	Negative	25000	2,3	Passed	Passed	21074421	84,55	65,4
Mus D0 R2	Negative	25000	2,9	Passed	Passed	22081763	88,05	67,9
Mus D0 R3	Negative	25000	3,1	Passed	Passed	18845994	88,66	67,88
Mus D0 R4	Negative	37000	2,3	Passed	Passed	22352641	89,22	70,01
Mus D0 R1	Positive	1280	2,3	Passed	Passed	18769482	63,25	46,64
Mus D0 R2	Positive	1211	2,3	Passed	Passed	21307594	64,52	47,75
Mus D0 R3	Positive	6230	1,7	Passed	Passed	22952159	68,8	52,19
Mus D0 R4	Positive	1874	1	Failed	Failed	NA	NA	NA
Mus D0 R5	Positive	4641	2,4	Passed	Passed	21102879	82,77	68,07
Mus D3 R1	Positive	20220	2,5	Passed	Passed	23945074	87,81	66,41
Mus D3 R2	Positive	13000	2,6	Passed	Failed	18406423	75,27	53,68
Mus D3 R3	Positive	8044	2,2	Passed	Passed	21545399	90,13	73,05
Mus D3 R4	Positive	11561	2,3	Passed	Passed	24625810	81,38	63,02
Mus D5 R1	Positive	43749	2,3	Passed	Passed	21369047	85,28	65,88
Mus D5 R2	Positive	8132	2,4	Passed	Passed	20656764	87,65	70,96
Mus D5 R3	Positive	24175	2,2	Passed	Passed	21971965	82,65	62,87
Mus D5 R4	Positive	37575	2,1	Passed	Passed	20243325	86,16	67,87
Mus D7 R1	Positive	17297	2,2	Passed	Passed	22824253	89,88	69,63
Mus D7 R2	Positive	39335	2,1	Passed	Passed	24731490	80,65	60,16
Mus D7 R3	Positive	18277	2,2	Passed	Passed	20691228	89,75	68,18
Mus D7 R4	Positive	23500	2,1	Passed	Passed	20340837	88,66	65,82
Mus D14 R1	Positive	6962	2,4	Passed	Passed	22762311	83,39	55,29
Mus D14 R2	Positive	1982	2,6	Passed	Passed	16567329	64,21	44,2
Mus D14 R3	Positive	11642	2,2	Passed	Passed	20584106	90,7	74,02
Acomys D0 R1	Negative	69156	2,2	Passed	Passed	17111374	94,01	73,68
Acomys D0 R2	Negative	50000	1,1	Passed	Passed	14992471	95,62	78,99
Acomys D0 R3	Negative	50000	5,6	Passed	Passed	14959192	97,57	76,39
Acomys D0 R4	Negative	25000	6,8	Passed	Passed	18541446	97,43	76,27
Acomys D0 R1	Positive	459	1	Passed	Passed	30566031	48,65	30,21
Acomys D0 R2	Positive	429	1	Passed	Passed	11771464	72,53	50,66
Acomys D0 R3	Positive	2515	2,3	Passed	Passed	15235203	88,44	38,59
Acomys D0 R4	Positive	2533	1	Passed	Failed	597246	34,81	31,04
Acomys D3 R1	Positive	10970	1	Failed	Failed	11460835	8,64	6,36
Acomys D3 R2	Positive	3236	2,3	Passed	Passed	19736562	94,91	53,78
Acomys D3 R3	Positive	7608	1	Failed	Failed	13498021	13,37	9,42
Acomys D3 R4	Positive	20678	2,5	Passed	Passed	20838182	95,71	59,99
Acomys D5 R1	Positive	23431	1	Passed	Passed	18097493	89,88	70,32
Acomys D5 R2	Positive	17350	1	Passed	Passed	16152826	95,97	72,63
Acomys D5 R3	Positive	5073	2,4	Passed	Passed	18555299	95,24	74,27
Acomys D5 R4	Positive	13621	2,3	Passed	Passed	10790730	96,75	69,57
Acomys D7 R1	Positive	883	1	Passed	Failed	16123677	11,65	8,18
Acomys D7 R2	Positive	12556	1	Passed	Passed	18719933	96,06	63,03
Acomys D7 R3	Positive	15310	2,4	Passed	Passed	20554948	96,54	58,21
Acomys D7 R4	Positive	38500	2,3	Passed	Passed	20040399	97,42	67,26
Acomys D14 R1	Positive	15304	2,2	Passed	Passed	20038983	97,8	63,04
Acomys D14 R2	Positive	12966	1	Passed	Passed	18268657	92,29	63,39
Acomys D14 R3	Positive	23150	2,4	Passed	Passed	14810298	98,14	67,06
Acomys D14 R4	Positive	7430	2,4	Passed	Passed	10220377	97,33	73,75

2.3.2. *Sample Preparation, Library Formation and Sequencing*

Sequencing services were outsourced to the Genomics Scientific Platform at Ipatimup, University of Porto. To perform the sequencing of our RNA samples, the colleagues at Ipatimup first reran the samples through the Agilent 2100 Bioanalyzer, using an Agilent RNA 6000 Pico Kit (Agilent 5067-1513), to confirm their quality and concentration. After analysis, a pool of 24 samples of each species (48 in total, distributed as evenly as possible between all the timepoints, with at least three replicates per timepoint, per species), of acceptable quality, were selected to be used for library construction.

To construct the libraries, the samples were processed using the SMARTer Stranded Total RNA-Seq Kit v2 – Pico Input Mammalian (TaKaRa 634411), which removes rRNA, and then amplified through 16 PCR cycles. After library construction, each library was evaluated for their quality, using a 2200 TapeStation System (Agilent Technologies – G2964AA), with the HS D1000 Screen Tapes (Agilent 5067- 5584), and the Qubit® 3.0 fluorometer (Thermo Fischer Scientific - Q33216), with the Qubit® 1x dsDNA HS Assay kit (Thermo Fisher Q33230). Libraries were composed of sequences that ranged from 353 to 461bp, and library concentration had a maximum of 133nM.

Once library quality was confirmed, samples were diluted to 4nM in nuclease-free water, and samples of the same species were pooled together in equal volumes. Final pools were prepared according to the "illumina NextSeq 500 and NextSeq 550 Sequecing Systems – Denature and Dilute Libraries Guide" (Document #15048776v16 – Protocol A; 1.5 pM + 1% PhiX), and then sequenced using an illumina NextSeq550 machine (illumina - SY-415-1002), with a High Output Kit v2.5 (illumina 20024906) and run for 75 cycles.

This page was intentionally left blank

2.4. **Transcriptomic Data Analysis**

To ascertain the quality of the sequencing data generated, all 48 individual fastq files were run (separated by species) through the FastQC tool, and analyzed in tandem with MultiQC[249], which allowed us to determine the quality of samples by analyzing several aspects of read quality, like per sequence G/C content, per sequence quality, per base sequence quality, sequence duplication levels and overrepresented sequences.

Initial quality control analysis indicated it was necessary to remove the first 8 bases of the 5' end of each read which corresponded to the adapter used to identify samples after sequencing (Index). We removed (trimmed) them by using the Cutadapt tool[250]. One base at the 3' end of each sequence was also removed, as it corresponds to a random base introduced at the end of transcription.

After trimming reads had a uniform length of 67nt, and we again evaluated their quality through the FastQC tool, to confirm if their quality improved, or was maintained at acceptable levels. This analysis indicated that three samples (*A. cahirinus* day 3, replicate 1 and 3, and *M. musculus* day 0^{+}, replicate 4) possibly did not have enough quality to be considered, as detailed in Table 2.4, but we still kept them to confirm this in subsequent analysis.

Once sample quality was determined, raw reads were aligned to their corresponding reference genome, and transcript abundance was calculated. Read alignment and transcript abundance calculation were performed using STAR aligner v2.7.5c[251], and the *A. cahirinus* reads were aligned to the Ensembl Rapid Reslease Genome Assembly GCA_004027535.1, while the *M. musculus* reads were aligned to Ensembl Assembly GCA_000001635.9. We allowed for 33% mismatch of read sequence alignment and a maximum of multiple alignment to sequences of 20 different loci. Sequences that didn't have a minimal total count of 10 reads across all timepoints were discarded.

An important aspect to consider when analyzing transcriptomic data is whether the replicates used are similar enough to return significance in further analysis. Principal Component Analysis (PCA) and Multidimension Scaling (MDS) are two methods that allow us to evaluate sample similarities. These methods compare major trends among samples and help us determine the similarity between timepoint replicates. Clustering of replicates suggests that these have similar behaviors/ expression trends, while replicates that do not cluster near their respective experimental condition are know as outliers. These outliers might indicate that a sample has

poor RNA quality or that technical issues occurred during library preparation or during sequencing. If these outliers are not removed, posterior statistical analysis of the data might be affected.

As shown in Figure 2.18 (and Table 2.4), this analysis detected four samples in *Acomys* (Day 0⁺, replicate 4, day 3, replicate 1 and 3, and day 7, replicate 1) and two in *Mus* (Day 0⁺, replicate 4, and day 3, replicate 2) that constitute outliers, when compared to other replicates of the same timepoints, and were therefore removed from further analysis.

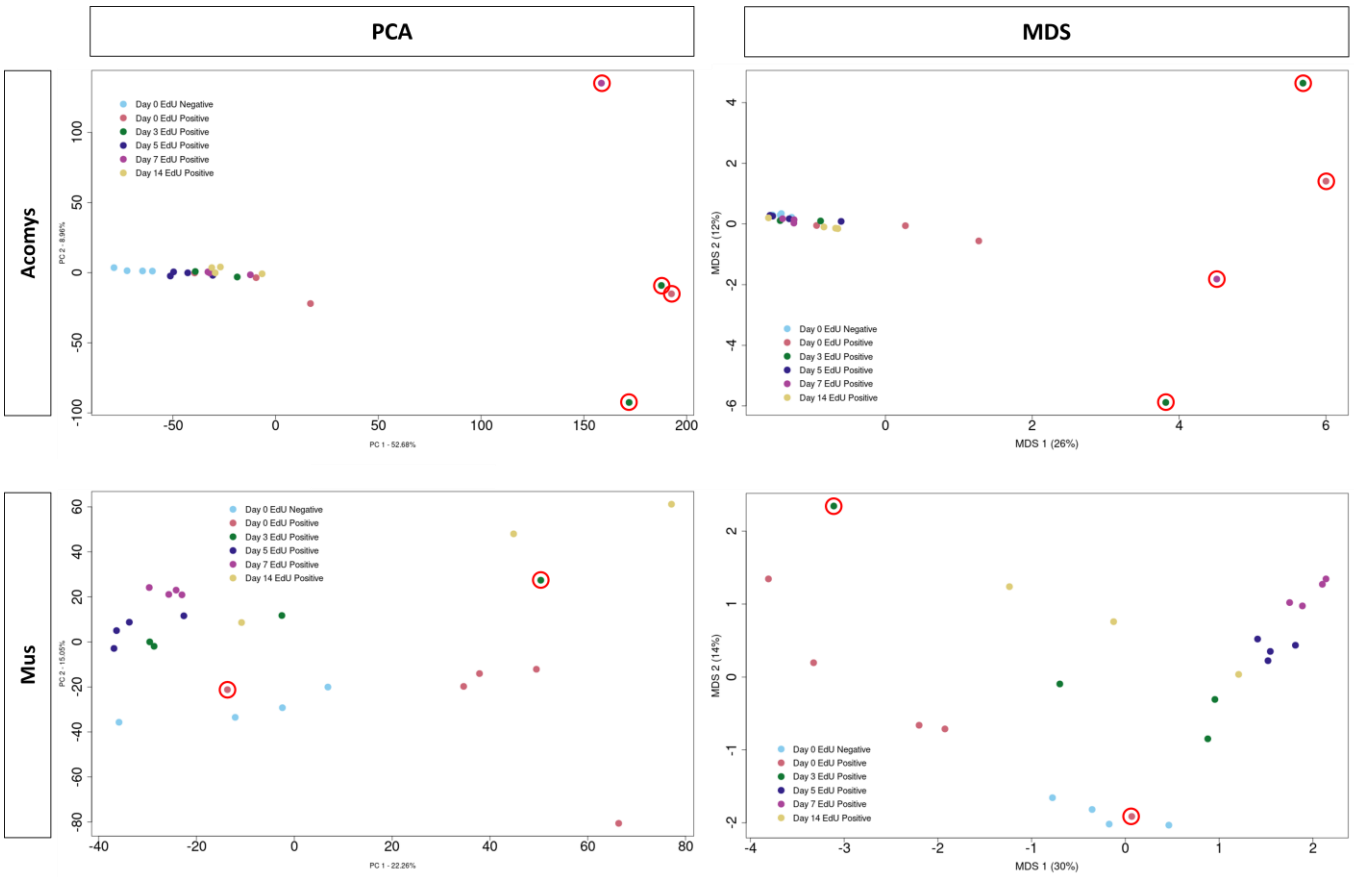

Figure 2.18 - PCA and MDS analysis of A. cahirinus and M. musculus samples after alignment. Principal Component Analysis and Multidimensional Scaling analysis of samples of A. cahirinus and M. musculus after alignment to the corresponding genomes. The red circles identify the outlier samples that were removed from further analysis.

The distinct behavior of these outliers is particularly clear in *A. cahirinus*, where the highlighted samples are outliers not only to other replicates of their own timepoints, but to the other samples as well. As Table 2.4 suggests, this is likely the result of sample quality, since the percentage of reads from these samples that aligned to the genome is particularly low.

The samples that passed quality control and pre-filtering were used to analyze the differential expression. Contrasts between timepoints day 3, 5, 7 and 14 and timepoint day 0 EdU Positive were performed. To perform this analysis, we used the DESeq2 R-package[252], v1.30.1, and

filtered the results for genes that yielded an adjust p-value lower than 0,05 and a $\log_2$ fold change higher than 1 or lower than -1. We used the BH (Benjamini & Hochberg) p-value adjusted method, which controls for false discovery rate (FDR).

2.4.1. Gene Ontology: Biological Processes and Pathways

After producing the lists of differentially expressed genes, we decided to evaluate how these changes in expression correlate with processes occurring in the healing tissues, and how these might be different between both species.

To obtain a list of biological processes (BP) related with the detected differentially expressed genes (DEGs), we built an in-house R script, that uses hyperGTest from GOstats[253], to perform gene ontology enrichment analysis (GOEA). We separated our data for each species in positive and negative differentially expressed genes prior to this analysis and set as a lower threshold of the analysis a minimum of 10 genes per category, to filter processes that, due to low amount of variation, might not be biologically relevant. We also restricted our analysis to processes with a false discovery rate (FDR) of less than 0,01 (i.e., we only considered processes that had a likelihood of 99,9% of being associated to a determined set of differentially expressed genes).

Since this filtering still yielded an enormous number of results, we decided to further restrict them by focusing exclusively on the top 20 processes associated with positive, or negative, differentially expressed genes at each timepoint, for each species.

To identify the signaling pathways that could be responsible for the processes previously obtained, we again used an in-house built R script designed to utilize the *pathfindR* package[254]. We chose this tool because it uses a two-step process of identifying active pathways. In the first step, the tool utilizes the user input (the file containing information on the differentially expressed genes) to design "subnetworks" of known gene interactions, which it establishes by searching a user pre-chosen database. We chose for this the IntAct database. After establishing the "subnetworks", *pathfindR* performs an enrichment analysis against another database, in our case Reactome since we were interested in retrieving signaling pathways. A visual representation of the process can be found in Figure 2.19.

Importantly, *pathfindR* performs several iterations of this process, pre-determined by the user (100, in our case), and counts the number of times a particular pathway is enriched by the "subnetworks" generated with the user's data. This metric, "occurrence", is an interesting additional evaluation of how likely it is that genes in the user's data set are establishing interactions found in a given pathway, thus helping to determine whether that pathway might, or might not, be of biological significance, beyond statistical significance. We decided to only consider pathways with over 20 occurrences. All other parameters were kept as suggested by

the developers of the package. A more detailed description of the tool, and its functions, can be found here:

https://cran.r-project.org/web/packages/pathfindR/vignettes/intro_vignette.html

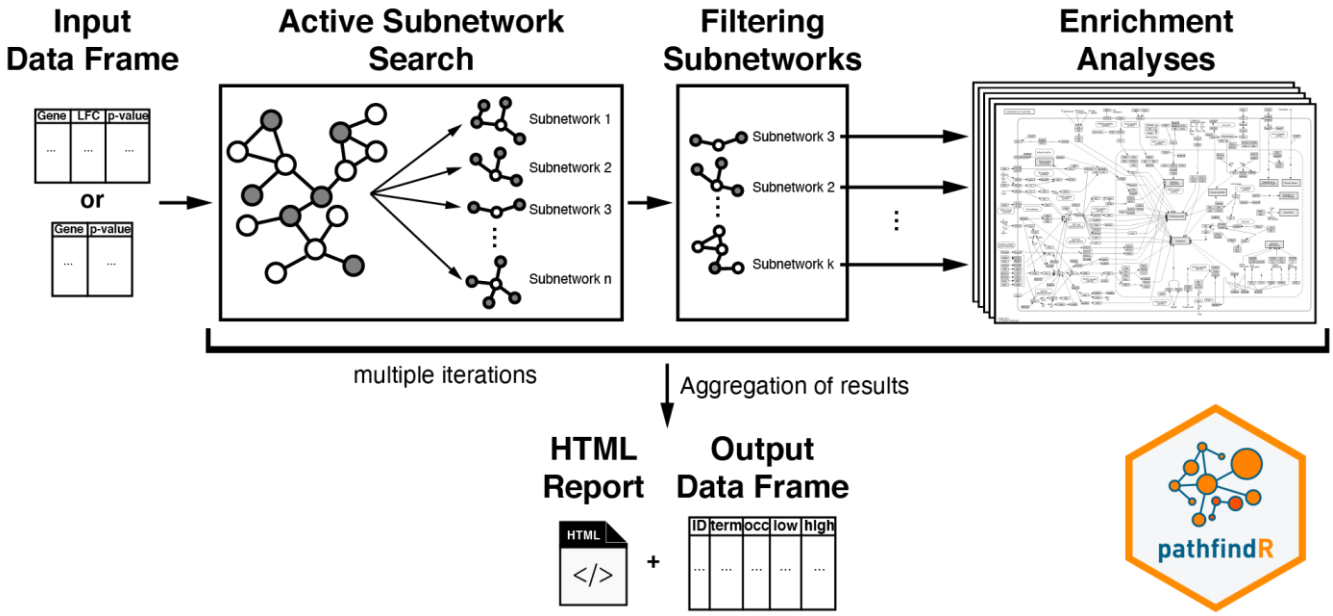

Figure 2.19 - Visual representation of the analysis process of pathfindeR.

This page was intentionally left blank

2.5. **Analysis of Signaling Pathway Activity**

2.5.1. Protein Extraction and Quantification

To extract protein from the healing tissues of the ear pinnas of *M. musculus* and *A. cahirinus*, tissue collection was perfomed at 0, 6, 12 and 24 hours, and 3, 5, 7 and 14 days after injury. To collect the healing tissue, two specimen of *A. cahirinus* or *M. musculus* were re-punched over the previously created circular wounds, on both ears, with either a Ø8mm biopsy punch, for *A. cahirinus*, or Ø4mm biopsy punch, for *M. musculus*.

Immediately after collection, tissue samples were placed inside Bullet Blender-compatible 1,5mL tubes, previously prepared with two 3,2mm stainless steel beads (Next Advance, SSB32), approximately 100µL of 0.9 - 2.0mm stainless steel beads (Next Advance, SSB14B) and 200µL of chilled Cell Extraction Buffer (10mM Tris pH7,4, Fischer Bioreagents BP152; 100mM NacL, VWR 27810.364; 1mM EDTA, Sigma ED2P; 1mM EGTA, PanReac A0878; 20 mM Sodium Pyrophosphate, Santa Cruz Biotechnology sc-203404; 2mM Sodium Orthovanadate, Sigma 450243; 1% Triton X, MERCK 1.08603; 10% Glycerol, Nzytech MB16101; 0,1% SDS, BioRad #161-0302; 0,5% Deoxycholate, Sigma D6750), and kept on ice until mechanical digestion.

To extract protein, the tissues were broken down mechanically, by running the samples on a Bullet Blender (Next Advance, Bullet Blender Storm 24) for 3 minutes, on setting #12. After thorough homogenization (two repetitions of the mechanical digestion), the samples were centrifuged at 24000g, for 20min, at 4ºC, and the supernatant containing the soluble protein was quantified and aliquoted. Aliquots were then stored at -80ºC, if not readily used. If samples were not immediately used after extraction, prior to usage they were thawed on ice and re-quantified.

To guarantee uniform loading of samples, quantification of protein concentration was performed using the BSA standard curve method, using a standardized BSA solution (Thermo Scientific, 23209) and Bradford Reagent (BioRad #500-0205).

To prepare samples to be used, we diluted them in 4x Laemmli (200mM Tris-HCL pH 6,5, Sigma T3253; 400mM DTT, Nzytech MB03101; 8% SDS, BioRad #161-0302; 6mM Bromophenol Blue, Fisher Bioreagents BP115; 32% Glycerol, Nzytech MB16101), to a final concentration of 2 or 4µg/µL (depending on initial concentration), and denaturated them at 95ºC for 5min, on a dry bath.

2.5.2. SDS-Page Electrophoresis and Protein Transfer

To detect specific proteins, we performed Western Blot analysis. Depending on the size of the target, proteins samples were run either in an 8% or 10% Acrylamide Gel (for detection of proteins over 90kDa samples were ran on a 8% gel, between 90kDa and 30kDa 10% gels were used). Gels were run at 100V during the loading phase of the gel, and at 120V during the resolving phase, for around 1h30 in total. Electrophoresis was performed in Tris-Glycine Running Buffer (250 mM Tris pH8,3, Fischer Bioreagents BP152; 1,92M Glycine, Nzytech MB01401; 1% SDS, BioRad #161-0302). A quantity of 40 µg of each sample was loaded, taking care to load equal volumes as much as possible. Four gels were run each time, in two pairs of equal loading configurations, to minimize variability between species samples and samples used for total or activated protein levels.

After the electrophoretic run, each gel was equilibrated for 15min in Towbin's Transfer Buffer (25 mM Tris pH8,3, Fischer Bioreagents BP152; 192mM Glycine, Nzytech MB01401; 0,01% SDS, BioRad #161-0302) or 10 min in homemade 1-Step Transfer Buffer (300 mM Tris pH8,3, Fischer Bioreagents BP152; 300mM Glycine, Nzytech MB01401; 20% EtOH, Sigma-Aldrich 51976, 0,01% SDS, BioRad #161-0302) at room temperature, with side-to-side agitation. Proteins were transferred to 40µm-pore PVDF membranes, activated for 60s in 100% methanol and equilibrated for 15min in either Transfer Buffer. Wet Transfer was performed at 4ºC, overnight (exactly 16h), at 30V constant current, with mild agitation, to guarantee smooth and complete transfer of protein, for thorough analysis and best visualization possible. Semi-Dry Transfer was performed using the Power Blotter System (Thermo Fischer PB0012) at 1.3A for 10min, for fast generation of technical replicates. Correct transfer was confirmed on the next day by staining the gel with BlueSafe (NZYtech MB15201) and the membrane with No-Stain Protein Labeling Reagent (Thermo Scientific A44449), which also permits Total Protein Normalization (TPN) quantification through labeling of all protein in the membrane with a fluorescent dye.

2.6. **Immunolabelling**

To immunolabel specific proteins for detection, membranes were first blocked for 1h, at room temperature, with 5% NFDM (Non-Fat Dry Milk, Nestlé Molico) in 1x TBST (200 mM Tris pH7,6, Fischer Bioreagents BP152; 1,5M NaCl, VWR 470302).

Membranes were then incubated with protein-specific unlabeled primary antibodies, against the desired proteins, in 5% NFDM in 1x TBST, overnight, at 4ºC. After primary antibody labelling, membranes were incubated with HRP (Horseradish Peroxidase)-labeled secondary antibodies, for 1h at room temperature. The relevant information about primary and secondary antibodies is summarized in **Error! Reference source not found.**.

Table 2.5 - Immunolabeling specifications for Western Blot detection of target proteins.

Target Protein	Blocking	Dilution	Reference
Total ERK1/2	5% NFDM	1:500	Cell Signaling #9102
pERK1/2 (T202/Y204)	5% NFDM	1:500	Cell Signaling #9101
Total Akt1	5% NFDM	1:500	Cell Signaling #4691
pAkt1 (S473)	5% NFDM	1:500	Cell Signaling #4060
pc-RAF (S259)	5% NFDM	1:500	Cell Signaling #9421
pPTEN (S380)	5% NFDM	1:500	Cell Signaling #9551
Jak2	5% BSA	1:300	Abcam #108596
pJak2	5% BSA	1:300	Abcam #32101
Stat3	5% NFDM	1:500	Cell Sginaling #9139
pStat3 (Y705)	5% BSA	1:500	Cell Signaling #9145
Anti-Mouse Secondary	5% NFDM	1:2000	Santa Cruz Biotechnology sc-516102
Anti-Rabbit Secondary	5% NFDM	1:2000	Santa Cruz Biotechnology sc-2357

2.6.1. Imaging and Analysis

After immunolabelling, detection of signal is achieved by incubating the membranes with a chemiluminescent HRP-substrate. We used the SuperSignal™ West Atto Ultimate Sensitivity Chemiluminescent Substrate (Thermo Scientific A38555), which has enough sensitivity to produce detectable signal even from very low levels of HRP activity.

Membranes were incubated in this substrate between 30s and 3min, depending on expected signal intensity, and then visualized in an iBright Imaging System (Thermo Scientific iBright FL1500). Camera exposure to signal ranged from 10s to 10min, depending on signal intensity, which was ascertained by the autoexposure function of the equipment. To analyze the data and perform relative quantification of each protein band we used the software associated with the imaging system (iBright Analysis Software). The relative quantification of each band was calculated by diving the intensity of the given band by the intensity of the "control" band, which we established as the 0 hours timepoint for intraspecies comparisons, and *A. cahirinus* 0 hours or 3 days timepoints for interspecies comparisons of early, or late, timepoints, respectively.

We also calculated the relative activation of some of the detected proteins, by dividing the value of the relative quantification obtained for its activated form, at a given timepoint, by the value of relative quantification obtained in the blot for the total detection of the specific protein.

3. Results

Our overview of the bibliography highlighted several commonalities between regenerative events in vertebrates, perhaps none so obviously important as the requirement of ERK signaling, and the involvement of nerve-derived factors in its activation. It also demonstrated several similarities between regenerative and reparative wound healing events, as exemplified by the early activation of ERK signaling in reparative wounds (which also occurs in the presence of damage nerve cells, although a correlation has not been established).

Seeing has several commonalities exist between vertebrate regenerative models that are not essentially exclusive to regenerative wounds, we wondered what could explain differential sustainment of proliferative responses in one type of response, but not in the other.

One such difference, shown in mammalian models in 2016 by Gawriluk et al., involves differential regulation of known tumor suppressors and cell cycle regulators, p21 and p27. These were shown to suffer a sustained nuclear exclusion in *A. cahirinus*, but not in *M. musculus*, which allows sustained cell cycle progression. In turn, in the reparative process of *M. musculus* the nucleus is progressively enriched with these factors, and cell cycle progression is inhibited.

To understand how two relatively close species could have such a distinct regulation of proliferation during their wound healing responses, when several instances indicate signaling commonalities, particularly in the initial responses to wound healing, we started by evaluating the composition of candidate pathways for regulation of proliferation, highlighting their differences between species.

To do this we resorted to the bibliography, and cross-referenced pathways known to be involved in the regulation of proliferation (like MAPK/ERK, WNT, JAK/STAT, etc.) with the transcriptomic data published in Gawriluk's 2016 article.

Second, we performed a transcriptomic profiling of *A. cahirinus* and *M. musculus* ear pinna proliferative cell populations during wound healing, to determine what are the differences in the expression profiles of these cells, and whether these differences could indicate a particularly distinctive expression profile associated with proliferative cells in either wound response processes.

Finally, after identifying potential cell cycle regulating pathways that could be responsible for the differential regulation of proliferation, we selected a few mediators of the candidate

pathways and compared the relative levels of their activity between wound responses, along several timepoints of the first two weeks of their response to injury.

This page was intentionally left blank

3.1. *A. cahirinus* vs *M. musculus* Bulk Transcriptomic Analysis

As we have previously mentioned, nuclear exclusion of p21 and p27 is achieved through either a decrease in the expression levels of these two genes, by their sequestering by Cyclin-CDK complexes in the cytoplasm, or a combination of both. Generally, regulation of both of these processes is performed by the PI3K/AKT and MAPK/ERK pathways, whose activity is the primary regulator of cell cycle induction and maintenance in most scenarios, and which has even been shown to be essential for proliferation in the *Acomys* ear pinna regeneration, as is the case of the MAPK/ERK pathway.

Our analysis of Gawriluk's data is quite unorthodox. Because these are highly conserved, essential pathways, setup during embryonic development and responsible for the regulation of several, intertwined, processes during development and in adult tissue homeostasis, our expectation was that the majority of genes expressing members of these pathways would not suffer great and significant fold changes of their expression levels. Nevertheless, this does not mean that differences in their expression levels are not relevant, especially when we compare them between the species.

Generally, transcriptomic analysis focuses on genes that are most differentially expressed between two conditions, attributing great importance to the fold change and its significance, and very little thought to the expression levels of the gene in question. This often leads to genes, whose expression is relatively low, but suffers a significant change (usually more than a duplication or halving of their relative abundance), being included in the analysis of the transcriptomic data, while genes with great transcript abundance, but whose change in expression do not reach such sizeable fold changes, being discarded. The biological relevance of this is, in our opinion, debatable.

With this in mind, rather than exclusively focus on the fold changes of genes, we performed our analysis with the added consideration of their relative abundance levels, which in Gawriluk's data are represented by the metric of 'Base Mean', a measurement of transcript abundance normalized for library depth.

As such, our analysis focused on differential expression within the species, and differences in transcript abundance between species, and followed specific criteria of gene inclusion: On the basis of fold change, only genes with $\log_2$ fold changes of 1 or higher, or -1 or lower, were

considered as formally ‘differentially expressed’ (DEG). On the basis of ‘Base Mean’ values, genes were only found to have ‘considerably’ distinct relative transcript abundances (RTA) if their normalized transcript count was: at least double the opposing species, for genes with 200 to 1000 transcripts per million; had a 50% or greater difference, for genes above 1000 transcripts per million. Genes where both species had fewer than 200 transcripts per million detected were considered as equally expressed, regardless of their disparity in transcripts count. The values of base mean and fold change for all the genes analyzed can be found in Annex I.

Because, as previously mentioned, the proliferative phase of wound healing is established within the first few days of the process, and this dataset consists of the timepoints day 5, 10, 15 and 20, we decided to use only the information associated with earliest timepoint (D5) to perform our analysis, which would more closely represent the composition of each proliferation-regulating pathway in the early response to wounding.

Since the goal of this analysis was to get a perspective on overall differences in pathway composition of several pathways, between both species considered, we created a set of figures we called “pathway-heatmaps”, designed to represent changes in composition and stoichiometry in each pathway, and whose interpretation will be dissected below. Regardless, the ‘take-home message’ of this analysis is that, overall, the pathways are distinctly setup between the species, with different composition and/or stoichiometry, which likely results in different outcomes even in the presence of the same stimulants.

3.1.1. PI3K/AKT Signaling

We started our evaluation of candidate pathways with the PI3K/AKT pathway, a pathway known to regulate not just proliferation, but several other processes of cell fate, like apoptosis, differentiation, migration, etc., which are also known to differ between regenerative and reparative events, making this a good candidate pathway.

We observed that at various levels of this pathway there are several genes with different RTA and/or differential expression. In *Acomys*, ligands like Col9a2, Col9a3, Lama2, Lamb1, Lamb2, Lamc3, Thbs1 and Vwf have a higher RTA in relation to *Mus*, while *Mus* has higher RTA for the ligands Chad, Col1a1, Col1a2, Col6a1, Efna5, Fgf2, Igf1, Igf2, Tgfa, Tnn. *Acomys* exhibited higher RTA for the receptors Csf1r, Csf3r, Fgfr1, Itga5, Itga7, Itgb4, Pdgfra and Pdgfrb, while *Mus* had higher RTA for the receptors F2r, Fgfr3, Igf1r, Itga6, and Il6ra.

Mediators and second messengers of this pathway are the largest group of genes with considerable different RTAs between both species. Genes like Akt1, Hsp90aa1, Jak1, Jak2, Map2k1, Mdm2, Ppp2cb, Ptk2, Sos2, Raf1 and Ywhaq have higher RTAs in *Acomys*, while Bcl2, Ccnd1, Ccnd2, Cdk6, Cdkn1a, Gng2, Gng12, Gsk3b, Kras, Magi1, Mapk1, Mcl1, Mtcp1, Nras, Pdpk1, Ppp2ra, Pten, Syk, Rac1, Ywhab, Ywhag and Ywhaz have higher RTAs in *Mus*.

Finally, differences in transcript abundance of transcription factors downstream of this pathway were also observed between both species. In *Acomys*, the transcription factors Rps6 and Trp53 have considerably higher base means than in *Mus*, while in *Mus* the base means of Creb1, Creb3l2, Eif4b, Foxo3, Nfkb1 and Rxra are higher than their counterparts in *Acomys*.

As for DEGs, in general the genes identified in this transcriptomic data as being associated with the PI3K/AKT pathway do not exhibit greatly differing fold changes. Moreover, despite some genes having a difference in fold change level of up to 2, these are never higher or lower than 2,5 and -2,5 $\log_2$ fold change, and their base means are approximately the same, despite the differential expression.

However, it is worth highlighting genes like Akt1, Atf4, Csf3r, Hsp90aa1, Itga5, Il6, Jak2, Map2k1, Pik3cd, Thbs1, Tlr4 and Trp53, since these are both overexpressed and have higher RTAs in *Acomys*, wile Bcl2, Chad, Col4a6, Fgf1, Fgf2, Fgfr2, Igf2 and Prkaa2 have a lower RTA than *Mus*, and are downregulated in *Acomys*.

In *Mus*, genes like Igf1, Col1a1, Col1a2, Col6a1, F2r, Gnb2, Ifnar1, Lamc2, Tnc and Tnn are both overexpressed and have a higher RTA than in *Acomys*, but Col6a6, Col9a2, Gys1 and

Lamc3 have a lower RTA and are downregulated. A summary of these observations, as well as other differences in base mean levels and differentially expressed genes in this pathway, are represented in Figure 3.*20*.

Our analysis of this pathway generated some interesting observations. First, while FGF2 has been shown to be essential for blastema formation and regeneration in *Acomys*, and capable of inducing regenerative characteristics to the reparative wound healing of *Mus*, it appears to have a higher RTA in *Mus* (73 TPM in *Acomys*, 443 in *Mus*), despite being downregulated (-1,5 $\log_2$ fold change), which would suggest that, by itself, FGF2 might not be sufficient to induce regeneration. Alternatively, and since Fgfr1 has a higher RTA in *Acomys* than in *Mus* (3153 TPM vs 1298 TPM), and the opposite is true for Fgfr3 (994 TPM vs 2296 TPM), perhaps it is the receptor most stimulated by FGF ligands that determines the outcome of the wound healing process.

Second, IGF signaling has been linked with the instructive communication between epidermis and underlying mesenchyme in order to form an informative wound epithelium, which is an essential part of the vertebrate blastema, but is only transiently established in reparative wounds. We observed higher RTA of Igf1 (427 TPM vs 1370) and 2 (175 TPM vs 481 TPM), and Igf1r (967 TPM vs 1667 TPM), with Igf1 even being overexpressed at day 5 post wounding, which could suggest that *Mus*, initially, also tries to establish the required crosstalk to sustain wound epithelium, but for some reason fails.

Third, and following this trend of *Mus* apparently expressing everything required for regeneration, we found higher RTAs of Ccnd1 (483 TPM vs 991 TPM), Ccnd2 (818 TPM vs 3024 TPM) and Cdk6 (200 TPM vs 1351 TPM). However, we did also observe higher RTA of Cdkn1a (364 TPM vs 820 TPM), perhaps meaning that cell cycle regulation occurs trough the expression of inhibitors, and not of the actual effectors of the cell cycle.

Supporting differential regulation of processes through inhibitor expression, we found a higher RTA of Pten (999 TPM vs 3296 TPM) and Gsk3b (832 TPM vs 2407 TPM) in *Mus*, two inhibitors of the PI3K/AKT pathway. Regardless, several mediators of this pathway were also found to have distinct RTAs between both species, with Akt1 (2103 TPM vs 1217 TPM), Map2k1 (1133 TPM vs 535 TPM), Ptk2 (1251 TPM vs 768 TPM), Raf1 (2031 TPM vs 984 TPM) and Sos2 (1238 TPM vs 708) possibly being more expressed in *Acomys*, while Kras (188 TPM vs 648 TPM), Mapk1 (958 TPM vs 1666 TPM), Nras (481 TPM vs 1333 TPM), Rac1 (606 TPM vs 1918 TPM) and Syk (280 TPM vs 708 TPM) have higher RTAs in *Mus*,

suggesting that the whole pathway, downstream of receptors, might be differentially setup between regenerative and fibrotic events.

On a final note, we found higher RTAs of Csf1r (2935 TPM vs 1375 TPM) and Csf3r (637 TPM vs 192 TPM) in *Acomys*, which are both upregulated (2 fold change and 5 fold change, respectively). These receptors have been associated, in vertebrates, to macrophages and neutrophils involved in fibrotic processes, respectively. However, we also found higher RTAs of Jak1 (3928 TPM vs 2793 TPM) and Jak2 (4224 TPM vs 997 TPM), two mediators of interleukin signaling. Perhaps the differential abundance of these factors is sufficient to induce distinct immune responses in response to stimulation of the same receptors.

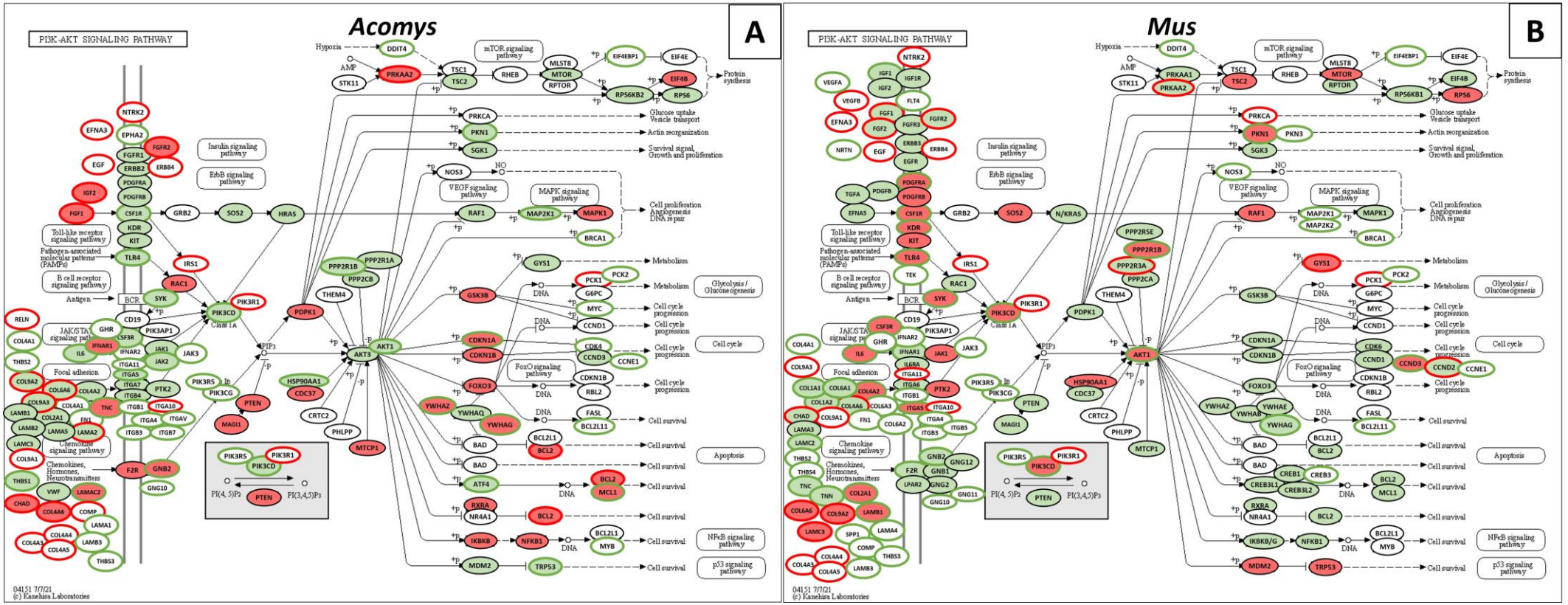

Figure 3.20 – Differential expression, in the PI3K/AKT pathway, between A. cahirinus and M. musculus. Visual representation of differentially expressed genes and genes with considerably different base means in the PI3K/AKT KEGG pathway, according to timepoint day 5 of the transcriptomic data of Gawriluk et al., 2016 paper. Overexpressed genes are represented with a green outline, while downregulated genes are represented with a red outline. A black outline represents genes that are not differentially expressed according to the dataset. A green background represents genes that have a higher base mean level in that particular species, and a red background represents a lower base mean, in relation to the opposing species' base mean levels. A white background represents genes that have similar base mean levels. This image was adapted from the KEGG Pathway Database: PI3K-Akt signaling pathway - Mus musculus.

3.1.2. MAPK/ERK Signaling

The MAPK/ERK pathways has conclusively been associated with the regenerative capacity of vertebrates, including in mammals, where it has been shown to induce regenerative characteristics in fibrotic wound healing events. However, ERK activation is not sufficient for full regeneration, even when possibly co-activated with other pathways (NRG1 can stimulate some ERBB receptors, which active other pathways besides the MAPK/ERK, like PI3K/AKT and JAK/STAT).

Because, as far as we know, ERK isoforms respond to the same upstream signals, activated levels of ERK isoforms reflect their relative abundance, but ERK isoforms are known to have some different roles in certain contexts (although this has been contested)[1380], we wondered whether different composition of the pathways could help explain why this signaling is sustained in regenerative wound healing events, and not in fibrotic.

Since the PI3K/AKT and MAPK/ERK pathways share, and interact through, several elements, some of the differences already observed in the previous comparison were also detected here. That was the case for the genes Akt1, Csf1r, Efna5, Fgf1, Fgf2, Fgfr1, Fgfr3, Gng12, Igf1, Igf2, Igf1r, Kras, Map2k1, Nfkb1, Nras, Rac1, Raf1, Sos2, Tgfa and Trp53.

Besides these, the ligand Il1b has a higher RTA in *Acomys* than in *Mus* (2686 TPM in *Acomys* vs 273 TPM in *Mus*), and the receptor Tgfbr1 has a higher RTA in *Mus* than in *Acomys* (376 TPM vs 798). As in the PI3K/AKT pathway, the mediators of the MAPK/ERK signaling pathway are the most enriched group of genes with RTA disparities between species.

In *Acomys*, the genes Dusp6, Flnc, Hspa8, Mapk8ip1, Pla2g4d, Rps6ka4 and Stmn1 exhibit a considerably higher RTA than their counterparts in *Mus*. On the other hand, in *Mus* the genes Araf, Cdc42, Crk, Dusp3, Mapk1, Map3k2, Mknk2, Rps6ka3, Taok1 and Traf6 have a higher RTA. As for transcription factors, Fos has a higher RTA in *Acomys* than in *Mus*, while Jund, Elk4 and Max have considerably higher RTAs in *Mus* than in *Acomys*.

Besides genes shared with the PI3K/AKT pathway, that were already previously highlighted, in this pathway we also identified Il1b, Dusp6, Dusp7, Flna, Flnb, Myd88, Pla2g4e, Pla2g4f, Rps6ka1 and Rps6ka4 as genes that both have a higher RTA in *Acomys* and are overexpressed, while Rasgrp1 and Hspb1 both have a lower RTA, compared to *Mus*, and are downregulated.

In *Mus*, the genes Tgfbr1, Map3k9, Mknk2 and Mapkapk2 are overexpressed and have a higher RTA than their counterparts in *Acomys*, with Cacna1s and Mapk8ip1 being downregulated and

having a lower RTA than in *Acomys*. A summary of these observations, as well as other differences in RTAs and differentially expressed genes are represented in Figure 3.*21*.

Through our analysis, we found a higher RTA of the overexpressed gene Dusp6 in *Acomys* (1088 TPM vs 321 TPM), while *Mus* has a higher RTA of Dusp3 (139 TPM vs 593 TPM). Since Dusp6 has been associated with retainment of ERK in the cytoplasm, this could constitute a way for *Acomys* to redirect some of the ERK activity to cytoplasmic targets.

Curiously, we noted a higher RTA of Mapk1 (coding for ERK2; 958 TPM vs 1666 TPM), of the IEG inducer Elk4 (532 TPM vs 1926 TPM), of the IEG JunD (297 TPM vs 773 TPM), and of the IEG helper Max (231 TPM vs 622 TPM), which potentiates cMyc's transcriptional induction. In turn, we found a higher RTA of the IEG Fos in *Acomys* (1668 TPM vs 479 TPM). Differential activation of IEGs might be due to different proportion of RSK proteins, as Rps6ka4 has a higher RTA in *Acomys* (1251 TPM vs 616 TPM), while in *Mus* we see a higher RTA of Rps6ka3 (799 TPM vs 1670 TPM). Nevertheless, these observations seem to indicate a higher proportion of MAPK/ERK signaling response elements in *Mus*, which contrasts with what would be expected.

Perhaps this can be due to an attempt of *Mus* to compensate for the incorrect activation of the MAPK/ERK pathway, either through alternative ligands or activation of different intracellular mediators, nevertheless leading to differences in the levels of IEGs and components of the AP-1 transcription factor complex. For example, Fos is known to also regulate NF-κB activity. Perhaps distinct proportions of AP-1 compositions enhance, or decrease, the capacity of the tissue to integrate information from other pathways, thus leading to a regenerative or fibrotic result.

Interleukin 1 is a stimulant of the pro-inflammatory canonical NF-κB pathway, associated with fibrotic results to the wound healing process. It was, therefore, interesting to find it overexpressed, and with a higher RTA, in *Acomys* at day 5 post wounding, while *Mus* had both a higher RTA of, and overexpressed, Tgfbr1. Downstream of Il-1 and Tgfbr1 signaling, on the canonical NF-κB pathway, are Myd88 (610 TPM vs 355 TPM) and Traf6 (518 TPM vs 1064 TPM), responsible for IKK activation, which were found to have differential RTAs between *Acomys* and *Mus*, with Myd88 being overexpressed and having a higher RTA in *Acomys*, and Traf6 having a higher RTA in *Mus*. Furthermore, we also observed a higher RTA of Nfkb1 in *Mus* (52 TPM vs 1281 TPM), which together suggest alternative strategies of canonical NF-κB signaling and integration in the MAPK/ERK pathway. Overall, our analysis points to different

arrangements of the MAPK/ERK pathway, which could lead to differential cross-communications with other pathways and result in differential gene expression.

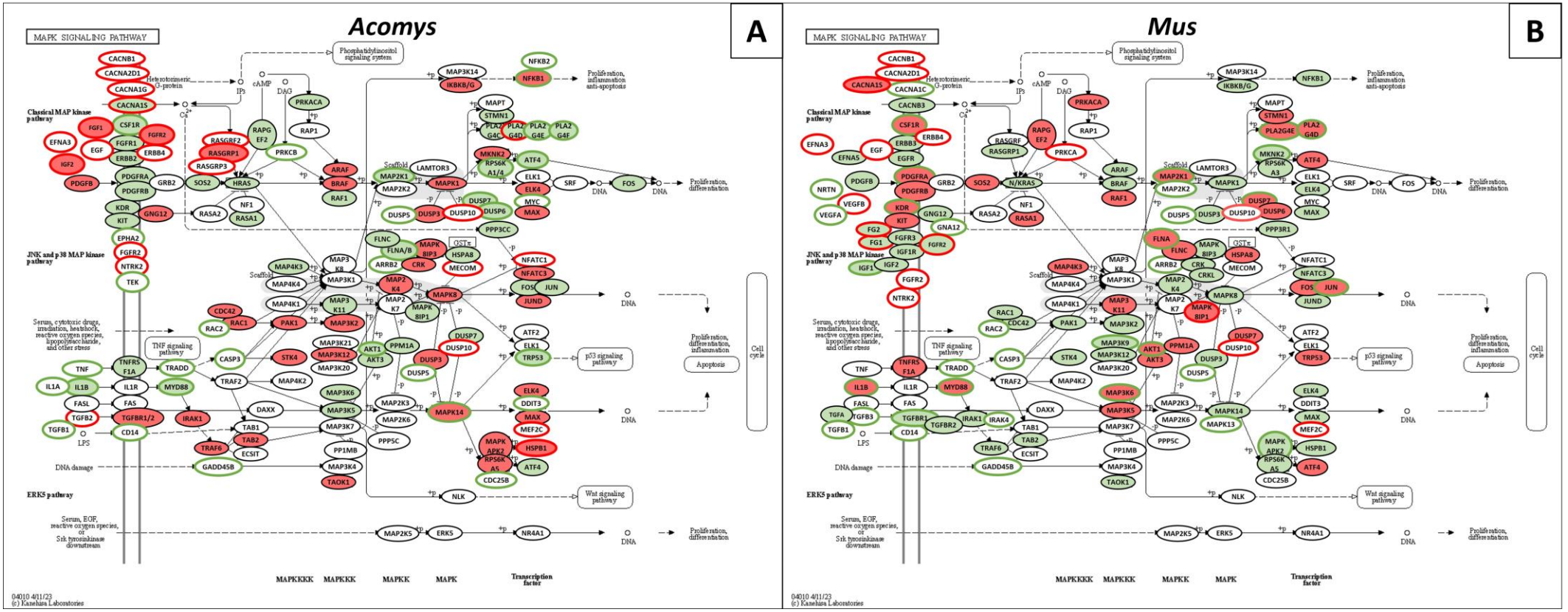

Figure 3.21 - Differential expression, in the MAPK/ERK pathway, between A. cahirinus and M. musculus.
Visual representation of differentially expressed genes and genes with considerably different base means in the MAPK/ERK KEGG pathway, according to timepoint day 5 of the transcriptomic data of Gawriluk et al., 2016 paper. Overexpressed genes are represented with a green outline, while downregulated genes are represented with a red outline. A black outline represents genes that are not differentially expressed according to the dataset. A green background represents genes that have a higher base mean level in that particular species, and a red background represents a lower base mean, in relation to the opposing species' base mean levels. A white background represents genes that have similar base mean levels. This image was adapted from the KEGG Pathway Database: MAPK signaling pathway - Mus musculus (house mouse).

3.1.3. ERBB Signaling

As we have referenced, he PI3K/AKT and MAPK/ERK pathways can be activated by some of the same receptors, but one particular group that has been shown to signal through both and is strongly associated with proliferation is the ERBB family of receptors.

To evaluate the possibility that these pathways could be interacting downstream of ERBB receptor signaling, and/or that differential composition of these pathways could be leading to different responses downstream of receptor stimulation, we next analyzed the ERBB signaling pathway. A representation of our analysis can be found in Figure 3.*22*.

The majority of genes associated with this pathway, since it has considerable similarities with the previous pathways analyzed, have already been touched upon. These are Akt1, Araf, Crk, Gsk3b, Kras, Mapk1, Map2k1, Nras, Ptk2, Raf1, Sos2 and Tgfa. Besides these, the genes Cbl, Cblb and Pak3 were also detected has having considerably higher RTAs in Mus than in Acomys.

While this is a fairly simplistic pathway analysis, with limited representation of the downstream effectors and their interactions, it still suggests a differential abundance of receptors and the core downstream effectors. This could explain why, despite both species activating the same intracellular signaling pathways, possibly even through mostly common upstream signaling, one is capable of sustaining these activations in most cell types, while the other is not.

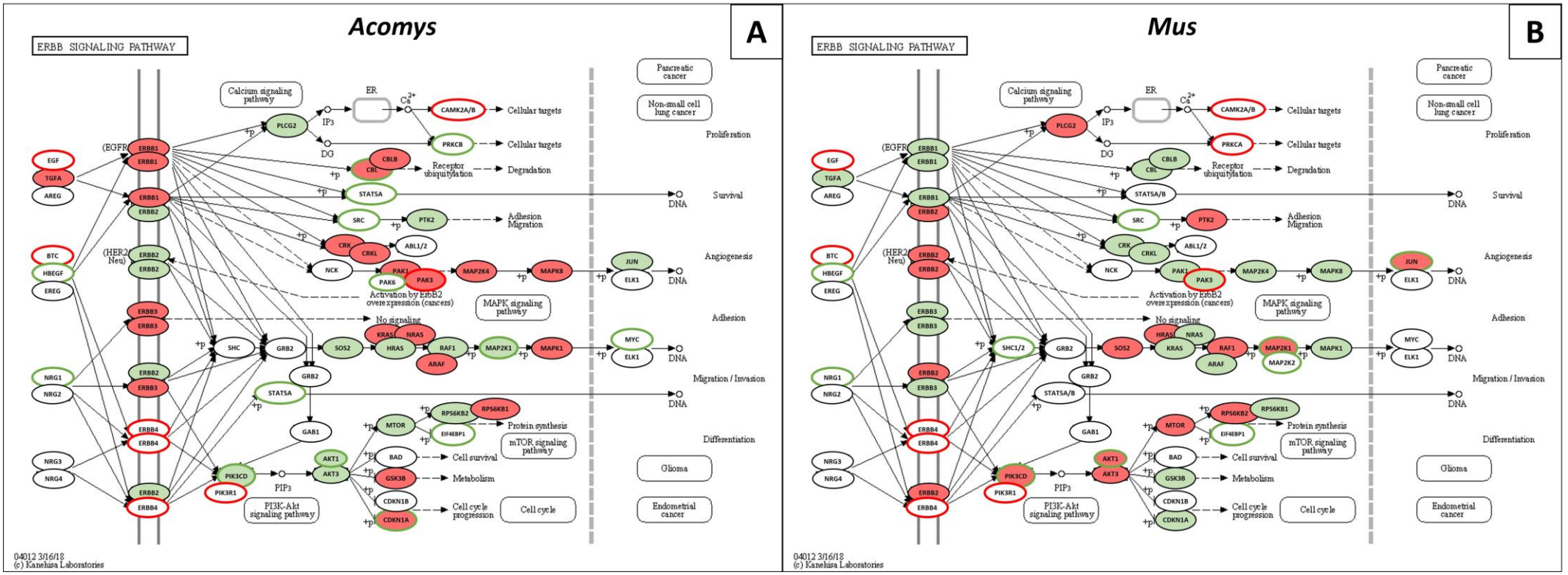

Figure 3.22 - Differential expression, in the ERBB pathway, between A. cahirinus and M. musculus.

Visual representation of differentially expressed genes and genes with considerably different base means in the ERBB KEGG pathway, according to timepoint day 5 of the transcriptomic data of Gawriluk et al., 2016 paper. Overexpressed genes are represented with a green outline, while downregulated genes are represented with a red outline. A black outline represents genes that are not differentially expressed according to the dataset. A green background represents genes that have a higher base mean level in that particular species, and a red background represents a lower base mean, in relation to the opposing species' base mean levels. A white background represents genes that have similar base mean levels. This image was adapted from the KEGG Pathway Database: ErbB signaling pathway - Mus musculus (house mouse).

3.1.4. JAK/STAT Signaling

The regulation of proliferation does not occur exclusively through the pathways already analyzed, as we have detailed. Furthermore, the immune system plays an important role in the regulation of wound healing processes, and immune signals, like cytokines and chemokines, probably regulate proliferation beyond just immune cell types. We therefore decided to also survey pathways involved in the regulation of proliferation associated with the immune system, like the JAK/STAT pathway and the NFκβ pathway, which also interact and share mediators with the PI3K/AKT and MAPK/ERK pathways.

Starting with the JAK/STAT pathway, several of the genes with more relevant differences have already been commented on previously, namely Akt1, Bcl2, Ccnd1, Ccnd2, Cdkn1a, Csf3r, Ifnar1, Il6ra, Jak1, Jak2, Mcl1, Pdgfra, Pdgfrb, Raf1 and Sos2. Additionally, we identified the receptors Csf2ra and Il22ra1 has having higher RTAs in *Acomys*, while the receptor Il15ra, the mediators Cish, Socs4 and Socs7, and the transcription factor Irf9 have higher RTAs in *Mus*.

Furthermore, because this KEGG pathway list includes some of the known downstream targets of this pathway, we were also able to observe that Aox3 and Aox4 have higher base means in *Acomys*, while Pim1 has a higher transcript abundance in *Mus*, as depicted in Figure 3.*23*.

The genes Akt1, Csf3r, Jak2 and Pik3cd, Csf2ra, Ifngr1 and Ptpn6 were also identified as being both overexpressed and having a higher RTA in *Acomys*, while the previously mentioned Bcl2, but also Aox1, Lifr and Il15ra, are both downregulated and have a lower RTA than their counterparts in *Mus*. In turn, accompanying the already mentioned Ifnar1, we should also highlight the genes Irf9 and Stat1, which are both overexpressed and have a higher RTA in *Mus*.

In general, our analysis of this transcriptomic data did not detect many differences in ligand availability, and ligand variability, likely due to it having been generated without the usage of an annotated genome, which might have impaired transcript identification. However, as we have detailed, there are known differences in ligand availability between both species.

Nevertheless, some clear distinctions are observable in receptor availability and their respective transcript abundances. For example, Csf2ra (453 TPM in *Acomys* vs 165 TPM in *Mus*) and Csf3r (637 TPM vs 192 TPM) RTAs are higher in *Acomys*, where they are also overexpressed, and Il22ra1 was also detected has having higher RTAs (1173 TPM vs 559 TPM). This could indicate an attempt of *Acomys* to mount a controlled pro-inflammatory response, with Il-22

regulating Th activity[255]. *Mus*, in turn, has higher RTAs of Il15ra (36 TPM vs 434 TPM), which has been associated with increased NK cytotoxicity, possibly contributing to the increased inflammatory response[256].

Likely, the most significant differences in pathway composition are the ones detected for the JAK family of proteins. In particular, Jak2 was found upregulated and with a higher RTA in *Acomys* (4224 TPM vs 997 TPM), which could indicate a preference for pathway mediators. Contributing to differential results of JAK/STAT pathway activation between species are the higher RTAs of Ptpn6 in *Acomys* (638 TPM vs 408 TPM) and of Socs4 (168 TPM vs 651 TPM), Socs 7 (160 TPM vs 466 TPM) and Stat1 (563 TPM vs 808 TPM) in *Mus*, which could indicate differential regulation of the pathway through different mediators, as well as alternative downstream effectors.

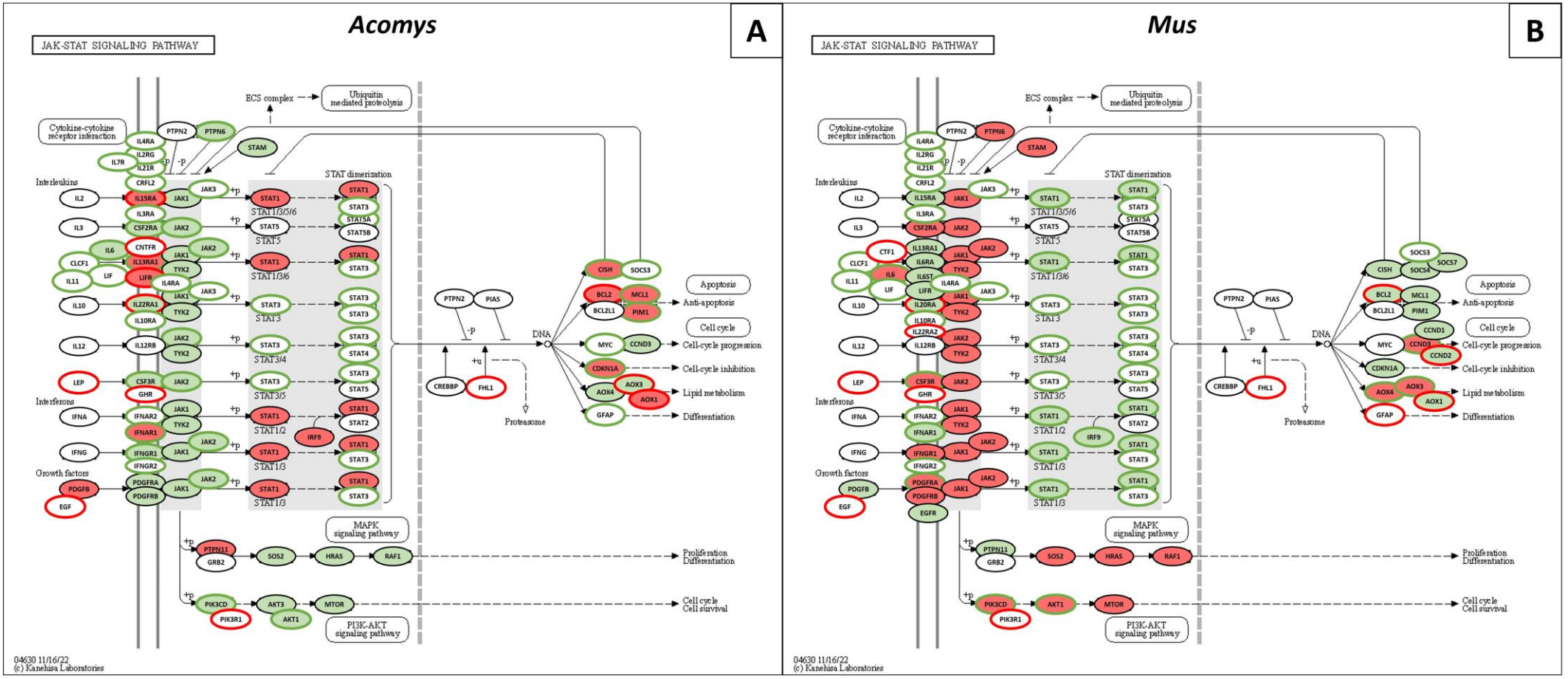

Figure 3.23 – Differential expression, in the JAK/STAT pathway, between A. cahirinus and M. musculus.

Visual representation of differentially expressed genes and genes with considerably different base means in the JAK/STAT KEGG pathway, according to timepoint day 5 of the transcriptomic data of Gawriluk et al., 2016 paper. Overexpressed genes are represented with a green outline, while downregulated genes are represented with a red outline. A black outline represents genes that are not differentially expressed according to the dataset. A green background represents genes that have a higher base mean level in that particular species, and a red background represents a lower base mean, in relation to the opposing species' base mean levels. A white background represents genes that have similar base mean levels. This image was adapted from the KEGG Pathway Database: JAK-STAT signaling pathway - Mus musculus (house mouse).

3.1.5. NF-κβ Signaling

Another pathway involved in immune response and proliferation regulation, which also shares elements with the previous pathways, is the NF-κβ pathway. As we have seen for the MAPK/ERK pathway, genes involved in this pathway have differential abundance between both species, so we wanted to evaluate whether this was a trend within the pathway, or just applicable to a few genes.

The previously detailed genes Bcl2, Il1b and Nfkb1 are also associated with this pathway. Besides these, the receptors Ltbr and Tlr4, the mediators Atm and Lyn, and the downstream target Tnfaip3 were identified as having higher base means in *Acomys*, while the ligand Cxcl12, the mediators Csnk2a2, Edaradd, Malt1 and Traf6, and the downstream target Xiap have higher transcript abundance in *Mus.*

As for genes whose differential expression and RTAs follow the same trend, Birc3, Btk, Il1b, Lyn, Myd88, Nfkb2, Tlr4 and Tnfaip3 are both overexpressed in *Acomys* and have higher base mean values in this species than in *Mus*, while, as previously reported, Bcl2 is downregulated and has a lower base mean value. Overexpressed and with a higher base mean in *Mus* are the genes Cxcl12, Syk, Trim25 and Vcam1. A visual summary of these observations can be found in Figure 3.*24*.

Of interest, Lyn, which is overexpressed and has higher RTA in *Acomys* (879 TPM in *Acomys* vs 406 TPM in *Mus*), is known to have important functions in hematopoietic cells[257,258]. Together with Btk, another gene overexpressed and with higher RTA in *Acomys* (187 TPM vs 61 TPM), it might contribute to a modulation of B cell activation and responses to injury. *Acomys* also overexpresses and has higher RTA of Tlr4 (552 TPM vs 252 TPM), a receptor that signals through Myd88 and is associated with M1-polarization, and can activate PI3K/AKT signaling, leading to FOXO inhibition and, consequently, its own transcriptional repression.

Also interesting, and possibly contradicting what was reported for TA regeneration in *Acomys*[714], we identified an overexpression and higher RTA of Cxcl12 in *Mus* (262 TPM vs 1408 TPM), which was associated with macrophage recruitment by pro-fibrotic fibroblasts in mammals[4].

Finally, higher RTA of the overexpressed Nfkb2 in *Acomys* (541 TPM vs 387 TPM), and of Edaradd (184 TPM vs 401 TPM), Malt1 (449 TPM vs 872 TPM) and Syk (280 TPM vs 518 TPM) in *Mus,* could suggest distinct cascades of NF-κB signal activation, supporting our

hypothesis that distinct configurations of conserved pathways could underline the differences in response seen in regenerative and fibrotic wound healing processes.

Overall, the analysis of this pathway did not identify many distinctly expressed genes between these two species in response to wounding. Nevertheless, some differences were observed, and these possibly suggest distinct capacities of signaling integration in other pathways, as well as distinct responses in a few immune cell types, which could be explanation for the known differences.

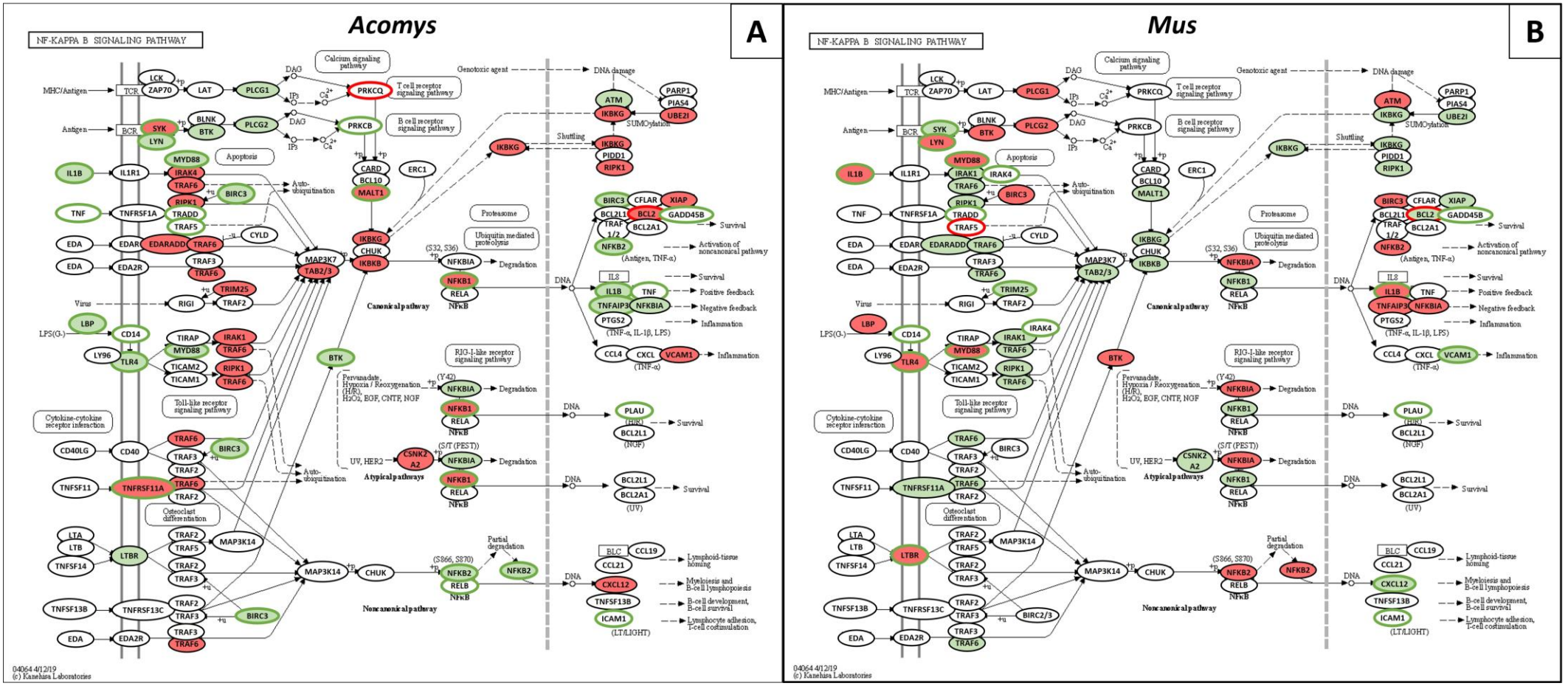

Figure 3.24 - Differential expression, in the NFKB pathway, between A. cahirinus and M. musculus.

Visual representation of differentially expressed genes and genes with considerably different base means in the NFKB KEGG pathway, according to timepoint day 5 of the transcriptomic data of Gawriluk et al., 2016 paper. Overexpressed genes are represented with a green outline, while downregulated genes are represented with a red outline. A black outline represents genes that are not differentially expressed according to the dataset. A green background represents genes that have a higher base mean level in that particular species, and a red background represents a lower base mean, in relation to the opposing species' base mean levels. A white background represents genes that have similar base mean levels. This image was adapted from the KEGG Pathway Database: NF-kappa B signaling pathway - Mus musculus (house mouse).

3.1.6. WNT Signaling

While the previously described pathways are considered in the bibliography as being the primary regulators of proliferation in most contexts, the WNT pathway also regulates proliferation in some contexts, as well as cell migration, death and differentiation. In several contexts this pathways inhibits proliferation by promoting migration, apoptosis or differentiation, but proliferation is promoted in some embryonic contexts and in stem cell niche maintenance and replenishment.

The genes Ccnd1, Ccnd2, Csnk2a2, Gsk3b, Rac1 and Trp53 are shared with other, previously described, pathways, but besides these, the receptor Apcdd1 and the mediator Ctnnb1 have higher RTAs in *Acomys*, while the ligands Wnt4 and Wnt7b, the receptor Vangle2, the mediators Csnk1a1, Ctnnbip1, Mcc, Tbl1x and Tbl1xr1, and the transcription factors Nfatc2 and Smad3 have higher RTAs in *Mus*.

Additionally, the gene Fosl1 was identified as being both overexpressed and having higher RTAs in *Acomys*, while the Nfatc2 and Nfatc4 are downregulated and have a lower RTA than in *Mus*. In fact, in *Mus* Nfatc4, as well as Wnt4, is both overexpressed and have a higher RTA. In the opposite sense, Apcdd1 is downregulated and has lower RTAs than in *Acomys*. These observations are summarized in Figure 3.*25*.

Identification of Fosl1 gene overexpressed and with higher RTA in *Acomys* (169 TPM in *Acomys* vs 14 TPM in *Mus*) supports our previous suggestion that AP-1 complex composition might differ between both species. Related with differential control of gene expression, the higher RTA of Ctnnb1 (encoding β-Catenin) might also contribute to a higher inductive capacity of WNT canonical pathway in *Acomys*, while Apcdd1, a known WNT ligand antagonist[259], might help select sources of WNT pathway activation.

Higher RTA of Ctnnbip1 (402 TPM vs 1237 TPM), a Wnt inhibitor[260], Wnt7b (134 TPM vs 459 TPM) and of Wnt4 (286 TPM vs 853 TPM), which is also overexpressed, further contribute to the suspicion that differential activation of the WNT pathway might occur between species. Furthermore, we observed a higher RTA of Smad3 in *Mus* (165 TPM vs 572 TPM), which could contribute to TGFβ signaling integration into the regulation of proliferation[261].

It is also noteworthy that several receptors and ligands of this pathway are overexpressed in *Mus*, while in *Acomys* most ligands have no differential expression, with a few downregulated, and several of the known receptors of this pathway are downregulated.

Altogether, our analysis of Gawriluk's transcriptomic data suggests that, in all likelihood, several conserved pathways involved in proliferation regulation in various contexts are distinctively composed in *A. cahirinus* and *M. musculus*. This difference in composition and mediator stoichiometry likely leads to distinct results of the wound healing processes, even in the presence of similar stimulants, further enhancing these differences in the presence of distinct ligands.

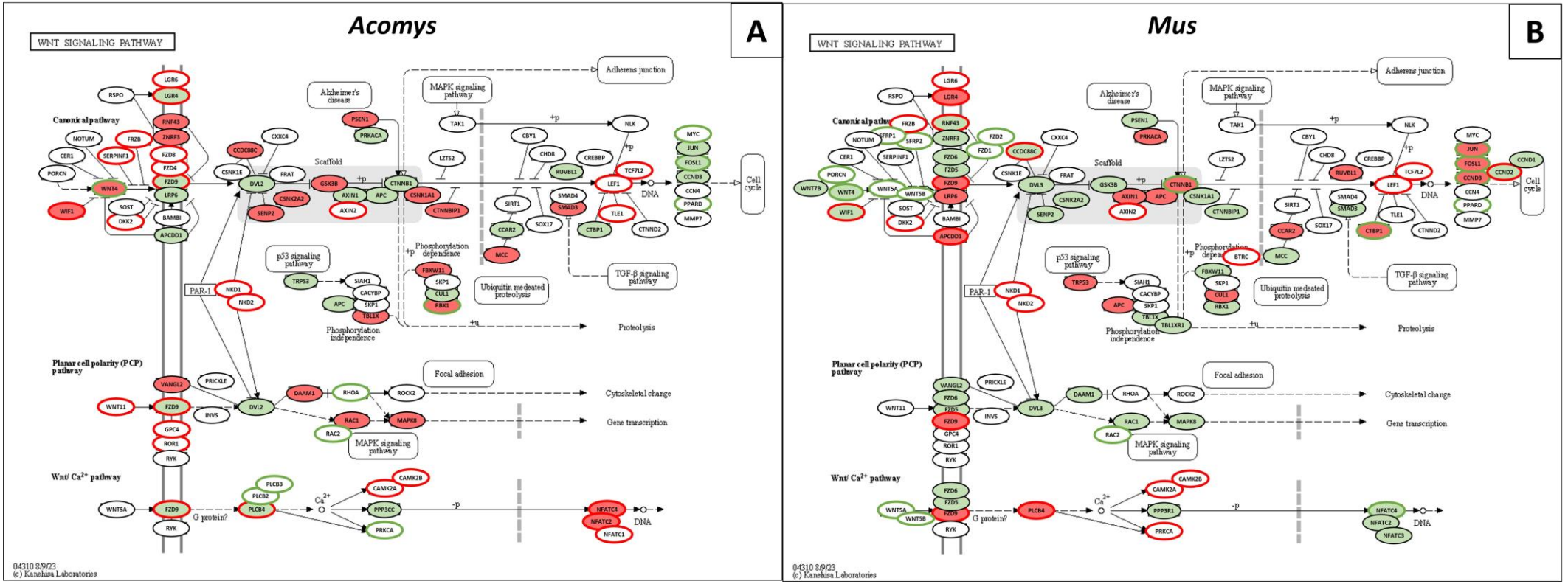

Figure 3.25 - Differential expression, in the WNT pathway, between A. cahirinus and M. musculus.
Visual representation of differentially expressed genes and genes with considerably different base means in the WNT KEGG pathway, according to timepoint day 5 of the transcriptomic data of Gawriluk et al., 2016 paper. Overexpressed genes are represented with a green outline, while downregulated genes are represented with a red outline. A black outline represents genes that are not differentially expressed according to the dataset. A green background represents genes that have a higher base mean level in that particular species, and a red background represents a lower base mean, in relation to the opposing species' base mean levels. A white background represents genes that have similar base mean levels. This image was adapted from the KEGG Pathway Database: Wnt signaling pathway - Mus musculus (house mouse).

This page was intentionally left blank

3.2. **Proliferative Cell Expression Profile**

While our analysis of Gawriluk's 2016 data suggested that several pathways, in particular the PI3K/AKT and MAPK/ERK pathways, are composed of different mediators, and might therefore contribute differently to the wound healing processes of *A. cahirinus* and *M. musculus*, it is limited in establishing a relationship between these pathways and actual proliferation regulation, since the data pertains to the response of the whole tissue, and not just of the proliferating cells. Furthermore, changes in expression of some genes associated with proliferation might be minimized or obscured due to the inclusion of non-proliferative cells in the sampling.

To ascertain whether concrete differences in pathway response and composition exist in proliferative cells, between *A. cahirinus* and *M. musculus*, we decided to generate our own transcriptomic data, focusing on the proliferative populations of the healing ear pinna tissues of these two species.

Because our primary interest is uncovering the signals that induce and regulate proliferation, and the bibliography suggests these are likely established very soon after injury, we designed a time course experiment with samples collected at timepoints day 0 (uninjured tissue), day 3, day 5, day 7 and day 14 post injury.

We collected both proliferative and non-proliferative populations at day 0h, to establish benchmarks of non-proliferative cell and proliferative cell populations from uninjured tissue, and proliferative populations at days 3, 5, 7 and 14, to identify expression changes that are specific of the proliferative processes occurring during wound healing in both species.

This page was intentionally left blank

3.2.1. Differential Expression

To analyze the data we obtained from our samples, we started by performing a PCA and MDS analysis, which allows us to reduce the various dimensions of large datasets into only two, that best represent the variability of behaviors of our samples. This does not only allow us to determine the quality of our replicates, but might also give us a clue to the degree of changes proliferative cells present in each species, throughout the wound healing processes.

Since we designed our time course hoping to detect the onset of the differential regulation of proliferation, our expectation was that the populations that sustain proliferation (*A. cahirinus* proliferative cells) would remain more similar amongst themselves than the proliferative populations that progressively exit the cell cycle, and accumulate in a common state, i.e. G0 (*M. musculus* proliferative cells).

The first thing that captured our attention in this analysis was that, curiously, in both species there is a greater similarity between samples of non-proliferative cell populations of the uninjured tissue and samples of proliferative cell populations of healing tissue, in all timepoints, than there is between the proliferative cell populations of the uninjured tissue and the proliferative cell populations of healing tissue (Figure 3.26).

This might be explained by the higher heterogeneity of the non-proliferative cell populations, which represent the several types of cells found in uninjured somatic adult tissue, including non, or slow, proliferating stem cells, and would therefore have a wider range of expressed genes with which to overlap the transcriptomic profile of proliferative cells in the wounded tissues.

Furthermore, proliferation in homeostasis is likely associated with stem cell niche preservation, or expansion of very lineage-restricted cells for physiological regeneration, which likely consist of a very particular group of transcriptomes, representing a small subset of the processes occurring during wound healing, or possibly even being abrogated in that scenario.

Regardless of cause, it is interesting to note that proliferation in response to wounding, be it with a regenerative or fibrotic outcome, seems to be its own program, sufficiently dissimilar to the proliferative programs found in uninjured tissue to suggest different purposes.

Moving to the comparison of the behaviors of proliferative cell populations in injured tissues, our analysis yielded the results we expected, were we to have captured the timeframe in which the regulation of proliferation begins to differ. The PCA and MDS analysis suggests that

proliferative populations in the regenerative process are more homogeneous among timepoints than in the fibrotic process (Figure 3.26). It is also worth pointing out that in both regenerative (*Acomys*) and fibrotic (*Mus*) wound healing events the timepoint corresponding to 14 days after wounding is the least like the other timepoints, suggesting greater commonalities of processes within the first week of healing.

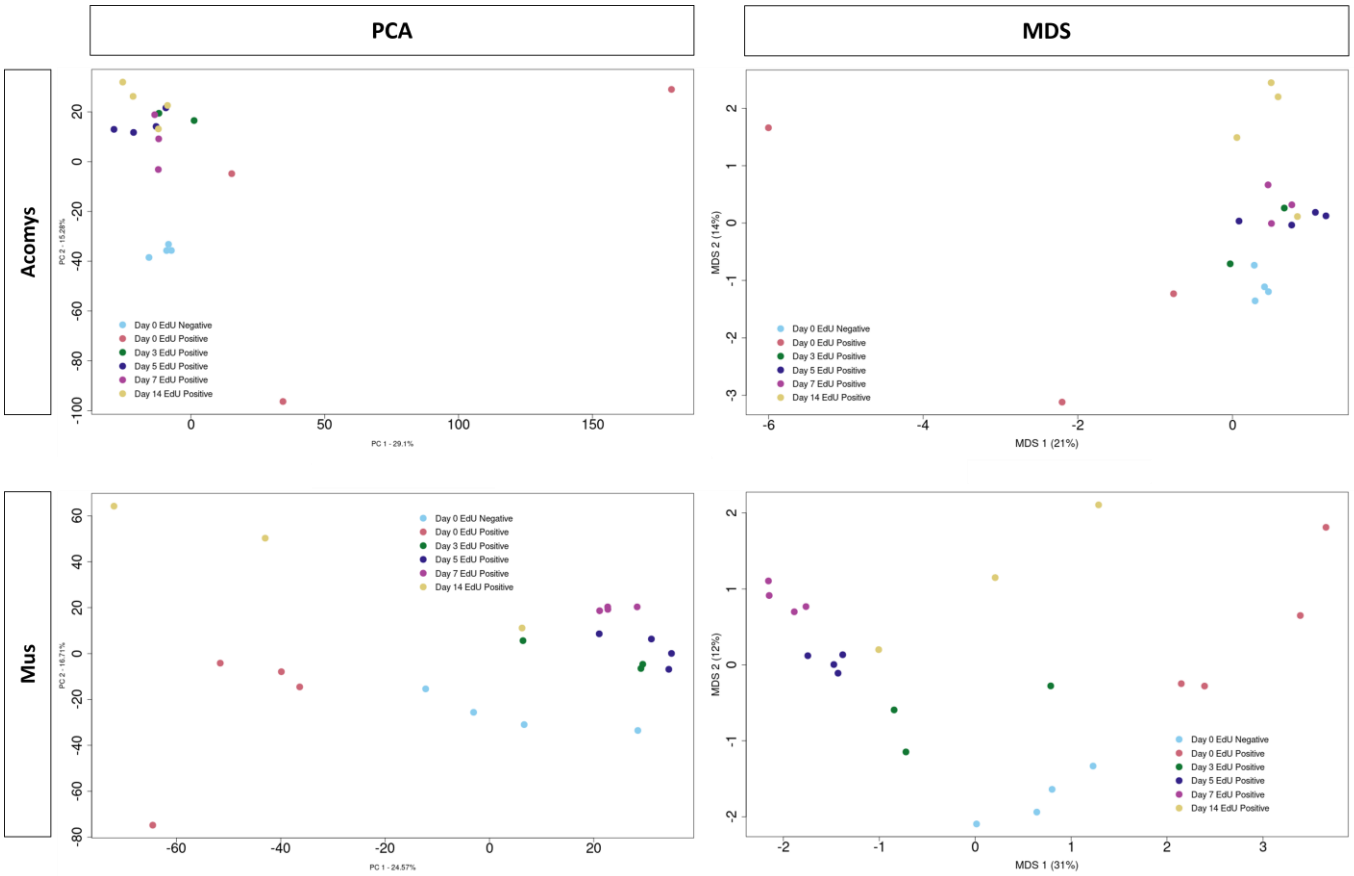

Figure 3.26 - PCA and MDS analysis of A. cahirinus and M. musculus samples selected for analysis.
PCA, or Principal Component Analysis, evaluates the similarities among samples along the two major, unidentified, components of those samples. MDS, or Multidimensional Scaling, evaluates the similarity between samples by creating two groups of components that, together, explain the majority of differences between the samples. The percentage values associated with each axis represent the fraction of sample variability that is explained by the factor represented on the axis (PC1, PC2, MDS1 or MDS2).

To rule out that these observations were the result of inferior sample quality, which could put in question the fidelity of the transcriptional analysis by causing artificial differences among samples, we looked at the number of aligned reads, percentage of alignment and number of sequences identified per sample (Table 2.4, in Materials and Methods).

Despite the variability of number of reads and proportion of reads aligned in each sample being considerable (even amongst replicates), the number of identified sequences, after a very restrictive filtering, was the same among samples of the same species, with 15766 transcripts

identified in all samples of *A. cahirinus* and 21557 in all samples of *M. musculus*. This suggested to us that the differences and similarities, observed in the PCA and MDS analysis, are likely to be due to actual differential expression of genes, rather than due to differential representation of the transcriptomes.

Having ruled out sample quality as the source of behavior variability, we wondered whether the differences in behavior along the time course, between species, could be explained by a less steep increase in differentially expressed genes (DEGs) in *Mus* samples, while *Acomys* might more quickly adapt its genetic regulation, and then sustain it throughout the wound healing process.

With that in mind, we compared the numbers of DEGs (in relation to proliferative cells of each species at D0) in all timepoints between species. In *Acomys*, we identified 161 DEGs on day 3 (123 Overexpressed, Oe., 38 Downregulated, Dr.), 650 DEGs at day 5 (473 Oe., 177 Dr.), 261 DEGs at day 7 (234 Oe., 27 Dr.) and 504 DEGs at day 14 (460 Oe., 44 Dr.). In *Mus*, the same comparison yielded 117 DEGs at day 3 (55 Oe., 62 Dr.), 207 at day 5 (129 Oe., 78 Dr.), 274 DEGs at day 7 (199 Oe., 75 Dr.) and 102 DEGs at day 14 (97 Oe., 5 Dr.). These results are curious, since there seems to be higher variability of DEGs in *Acomys* than in *Mus*, so it would not explain the behavior of samples.

We next wondered whether this was perhaps due to a greater variability of which genes are differentially expressed, from time point to time point, in *Mus*. Since *Acomys* sustains proliferation throughout the time course, but *Mus* does note, we expected to find more DEGs shared among multiple timepoints in *Acomys*, while *Mus* samples likely exhibit different DEGs, as the proliferative program gets increasingly abrogated.

Indeed, looking at DEGs that are shared by more than one timepoint, we observed that *Acomys* has 375 DEGs shared between two or more timepoints, with 87 being identified at all four timepoints (81 Oe., 6 Dr.), while *Mus* has 221 DEGs shared among two or more timepoints, with only 10 being common to all timepoints (9 Oe., 1 Dr.).

These results might explain why samples of different timepoints of the *Acomys* wound healing process tend to cluster more closely together in our PCA and MDS analysis than *Mus*. Reversely, DEGs that were found associated to only one particular timepoint were also more abundant in *Acomys*, with 542 genes (383 Oe., 159 Dr.) identified: day 3 having 17 uniquely differentially expressed genes (4 Oe., 13 Dr.), day 5 having 319 (190 Oe., 129 Dr.), day 7 having 19 (13 Oe., 6 Dr.) and day 14 having 187 (176 Oe., 11 Dr.), as depicted in Figure 3.27. As for

Mus, we identified a total of 247 DEGs (145 Oe., 102 Dr.) exclusive of a particular timepoint: 60 identified on day 3 (20 Oe., 40 Dr.), 43 on day 5 (13 Oe., 30 Dr.), 105 on day 7 (75 Oe., 30 Dr.) and 39 on day 14 (37 Oe., 2 Dr., Figure 3.27).

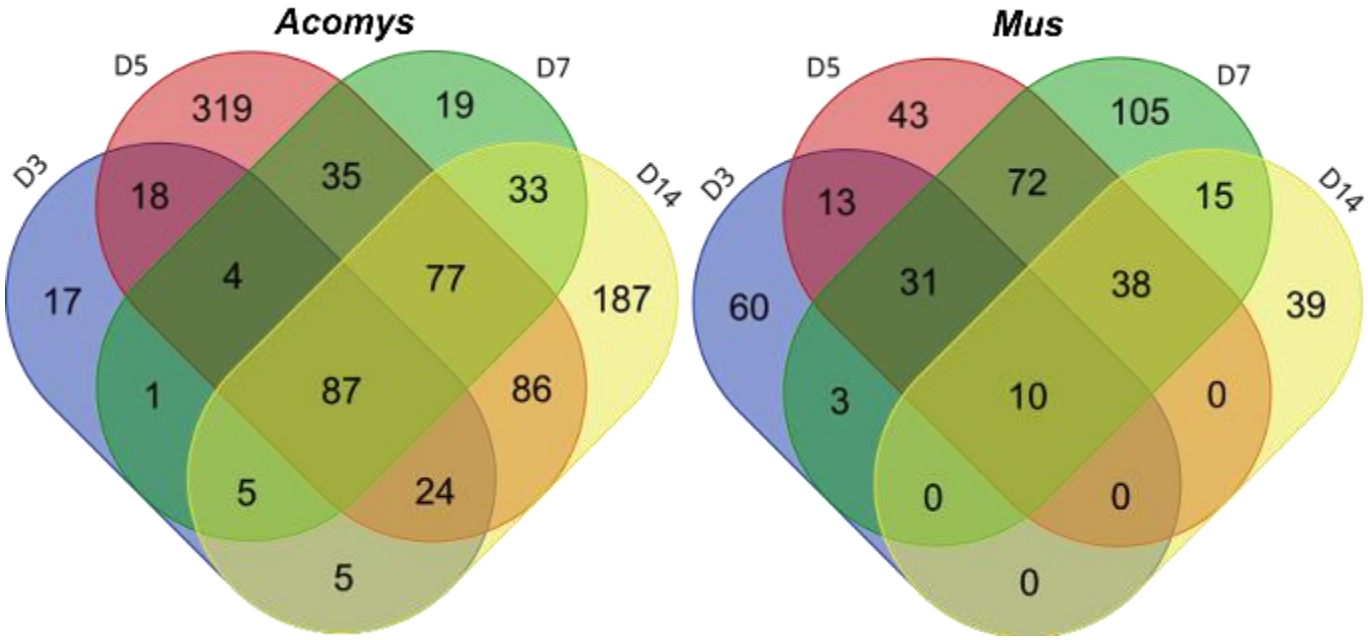

Figure 3.27 – Distribution of DEGs throughout the analyzed timeframe, in each species.
In this image is represented, through a Venn diagram, the distribution of DEGs, within each species, throughout the time course. Numbers in the overlaps of ovals represent the number of DEGs shared by the timepoints represented by those ovals. Blue oval represents day 3, red oval represents day 5, green oval represents day 7 and yellow oval represents day 14.

Regardless of a greater number of shared DEGs in *Acomys*, both species have a very considerable number of DEGs uniquely identified at a specific timepoint. Nevertheless, DEGs associated exclusively to one timepoint represent a higher percentage in *Mus* (an average of 41% of DEGs at each timepoint, versus only 26% in *Acomys*). In both species we identified a higher proportion of downregulated genes being associated exclusively to one timepoint, with *Acomys* having an average of 39% of its downregulated genes being exclusively associated with one timepoint, versus 22% of overexpressed genes, and *Mus* having 46% of timepoint-specific downregulated genes, versus 32% of overexpressed.

In short, differential expression of genes between timepoints likely explains the different behavior of samples across timepoints, in each species, and negative regulation of expression appears to be the biggest contributing factor for intraspecies variability. Although we identified fewer DEGs in *M. musculus*, and their evolution throughout the wound healing process is different to that of those detected in *A. cahirinus*, it is still possible that several of these DEGs

are common between species, and it is their distinct expression dynamics that underline the different results of the wound healing processes.

To test the possibility that perhaps the regulation of proliferation in the *M. musculus* wound healing event could represent only a subset of the processes that occur in the wound healing process of *A. cahirinus*, with different temporal dynamics, we compared the lists of genes positively (overexpressed) and negatively (downregulated) differentially expressed detected in each species. As depicted in Figure 3.28, the majority of DEGs are exclusive to either species, with only 98 DEGs being shared among both species (80 are overexpressed in both species and 16 are downregulated).

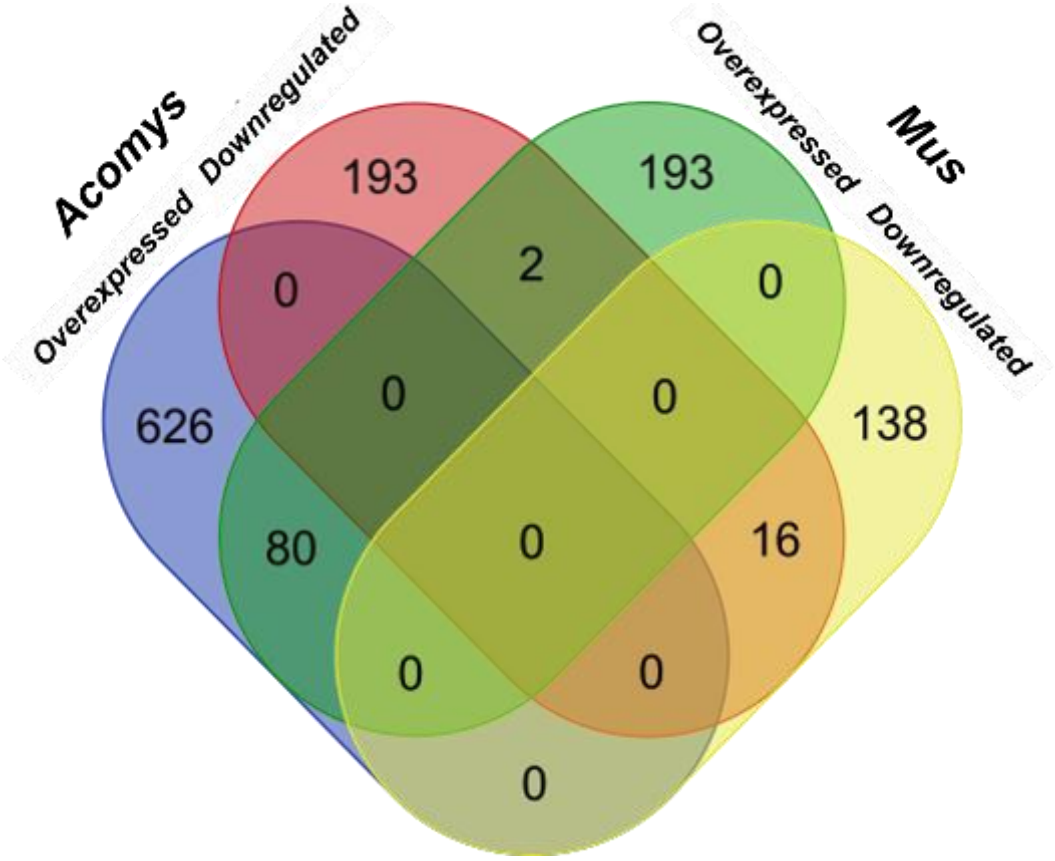

Figure 3.28 - Representation of DEGs common to both species and/or that change signal.
This image is a representation, in the form of a Venn diagram, of DEGs that are shared between species, according to their signal. Numbers in the overlaps of ovals represent either the number of DEGs shared between species, or DEGs that at were found to change signal within each species. The blue oval represents positive DEGs in A. cahirinus, the red oval represents negative DEGs in A. cahirinus, the green oval represents positive DEGs in M. musculus and the yellow oval represents negative DEGs in M. musculus.

Curiously, only two genes, Tmem125 and Zfp334, have opposite differential expression, and they constitute a cell adhesion molecule, enriched in oligodendrocytes[262], of unknown function, and a zinc finger protein that could be associated with transcriptional regulation and tumor suppression[263], and they are both overexpressed in *M. musculus* and downregulated in *A.*

cahirinus. Furthermore, it is also interesting to note that, for both *A. cahirinus* and *M. musculus*, none of the DEGs identified as positively differentially expressed were found as negatively differentially expressed (or vice-versa) at another timepoint, within the same species, which suggests a unidirectional development of processes.

This suggests that the regulation of proliferation in *Mus* is not just an "incomplete" regenerative event, nor that it is simply an opposite regulation of the same processes or pathways, but rather two clearly distinct sets regulatory profiles, with largely distinct participants, that probably begin to be defined and separate very early after injury, if not even prior.

Besides suggesting that the regulation of the two wound healing events is quite distinct, our analysis also suggested that in each event there might be a considerable evolution of processes, or their regulation, within this timeframe, particularly in *Mus*. To expand our understanding of how differential gene expression evolution might reflect alterations in processes throughout the wound healing events, we decided to look at the evolution of the top DEGs at each timepoint, in both species, and whether any most DEG is shared between them.

In this comparison we considered the top 10 most differentially expressed genes at each timepoint, in each species. Our analysis yielded only a few genes that share this relevance between timepoints, within each species, and even fewer between the species. Starting with common top DEGs between species, only Fn1, Col6a2 and Col6a3, coding for constituents of the extracellular matrix, were found.

As for top DEGs common to more than one timepoint within each species, we only found three genes in *A. cahirinus*, with the gene Egflam, coding for an extracellular matrix component associated with proliferation, the PI3K/AKT pathway and orientation of dendrites, being identified at three timepoints (day 5, 7 and 14)[264].

In *M. musculus* we in turn identified 10 genes shared between timepoints, with the genes Fn1 and Bgn, the first coding for an extracellular matrix protein mostly associated with incipient and immature matrix, and the latter coding a proteoglycan involved in several processes, from cell growth and migration to differentiation, and which can also be a proinflammatory factor, being shared by three timepoints (day 5, 7 and 14)[265,266].

The behavior of the most differentially expressed genes indeed suggests an evolution throughout both wound healing events, and few commonalities among them. However, it seems there are more commonalities among timepoints in *Mus*, than in *Acomys*. This hints at the

possibility that, in this timeframe, and contrarily to what PCA and MDS analysis suggested, gene regulatory programs are less variable in *Mus*, at least for the genes with greater expression changes. To add support to this observation, we reexamined the data, but focusing on genes whose differential expression was found to be most significant.

The majority of *Acomys* genes identified in this re-analysis match with the previously identified, but the same is not true for *Mus*, with less than half of the topmost differentially expressed genes corresponding to the top 10 most significative. This actually resulted in a few more identified DEGs being shared between timepoints in *M. musculus*. As we can see in Figure 3.29 (F, G, H, I), most labelled genes in *M. musculus* samples of day 5, 7 and 14 are the same.

In *Acomys*, we found that the top significant DEGs are associated with cell-ECM and cell-cell contact (9 genes, Col1a1, Col5a2, Col6a3, Col25a1, Smoc2, Tnc, Arvcf and Cdhr1), cell differentiation status (5 genes, Cbx7, Ivl, Krt23, Prox1 and Wnt2b), cell cycle regulation (4 genes, Prune2, Sept3, Stradb and Zmat1) and immune response (3 genes, Fcho1, Nox4 and Tnf), among others.

Interestingly, while most other DEGs are negatively regulated in relation to proliferative cells in unwounded tissue, DEGs related with cell-ECM contact become increasingly more expressed throughout the regenerative event (Figure 3.29, E). But, overall, the most significant DEGs suggest a fairly stable transcriptomic profile of proliferative cells during *A. cahirinus* ear pinna regeneration, as well as a fair degree of separation from the transcriptomic profile of proliferating cells in unwounded tissues.

In *Mus*, the topmost significant DEGs identified were mostly associated with cell-ECM and cell-cell contact (15 genes, Ablim3, Adamts14, Col5a1, Col5a2, Col6a1, Col6a2, Col6a3, Col11a1, Eln, Fbln2, Fbn1, Fn1, Ltbp1 and Sparc) and cell differentiation status (7 genes, Cald1, Cstdc5, Frem2, Fstl1, Krt6a, Krt15 and Vim), which appear to relate with the evolution of the epithelial phenotype (Ablim3, Cstdc5, Frem2, Krt6a and Krt15) and mesenchymal dynamics (Adamts14, Cald1, Col5a1, Col5a2, Col6a1, Col6a2, Col6a3, Col11a1, Eln, Fnln2, Fbn1, Fn1, Fstl1, Ltbp1, Sparc and Vim) of the healing tissue (*Figure 1.1*Figure 3.29, J). Furthermore, these genes suggest a greater evolution of the transcriptional profile of proliferative cells in *Mus*.

Interestingly, while both species show an increased expression of ECM-related genes throughout the respective wound healing processes, the relevance of this seems to be anticipated

in *Mus* by a week. Associated with an early alteration of the expression of epithelial-related genes, his might indicate an early differentiation of proliferative cells in *Mus*.

Altogether, our analysis of differential expression suggests a few things. First, it is possible that, overall, proliferation in response to wounding in *Acomys* elicits similar trends among a majority of induced DEGs, many of which are similarly differentially overexpressed throughout the analyzed time course. Nevertheless, it appears that *Mus* has a higher conservation of differential expression of certain genes, perhaps more relevant to the processes it elicits during wound healing.

Second, they suggest that the transcriptomic profiles of proliferative cells during wound healing are largely distinct between these two species, with only 12% of DEGs identified in *A. cahirinus*, and 30% of DEGs identified in *M. musculus*, being shared between species. This might reflect differential cell type involvement, differential signaling pathway activation or distinct sources of activation of those pathways, resulting in differential regulation of expression.

Third, and final, suggestion, the dynamics of expression of ECM-associated genes suggest an anticipation of some processes, which might also be terminated earlier, in *Mus*. This could be related with an earlier differentiation of certain cell types, particularly mesenchymal, in response to the alterations of epithelial profile identified at earlier timepoints, and explain why proliferation is sustained more transiently in *M. musculus*.

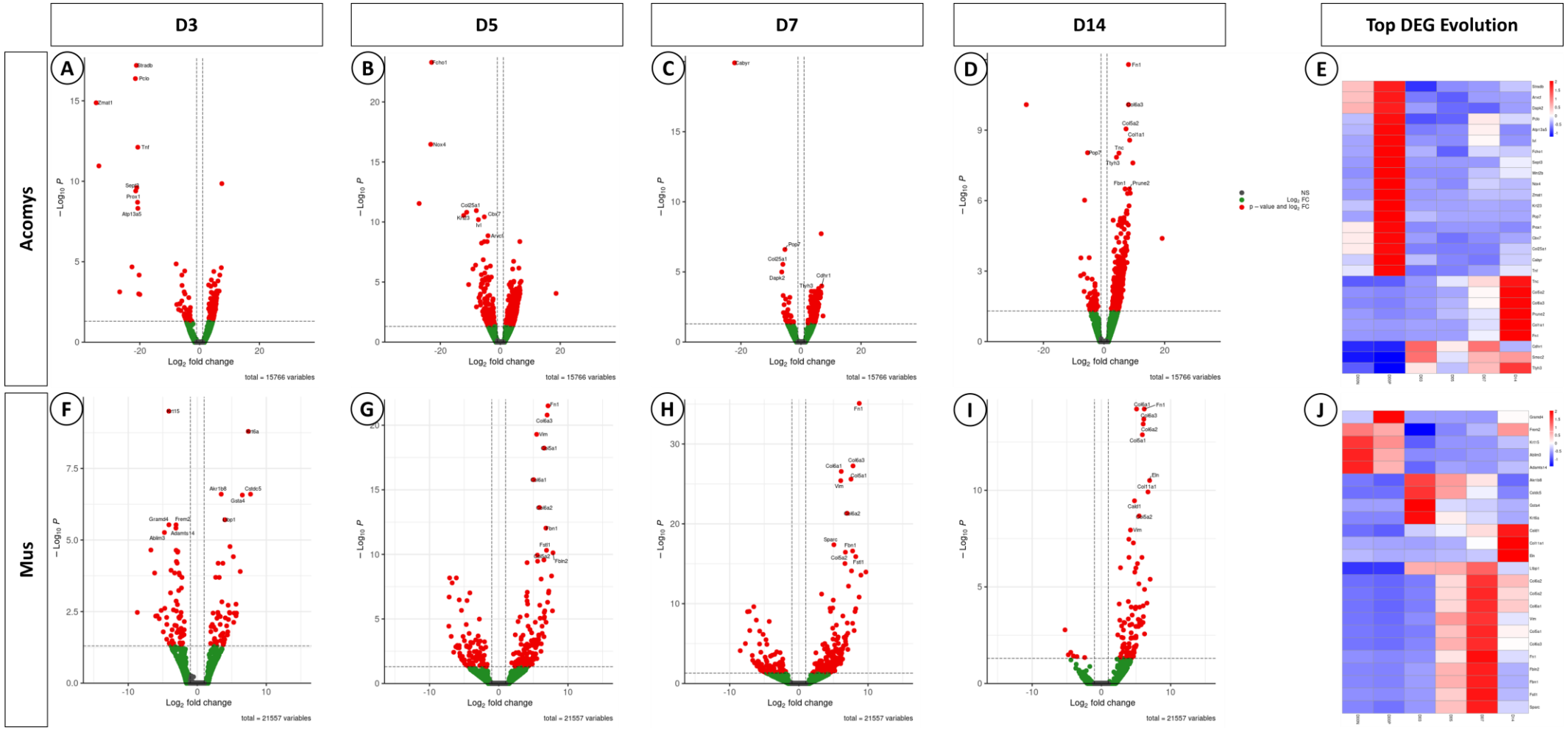

Figure 3.29 - Top 10 significative DEGs at each timepoint, for both species.

The volcano plots depicted in this figure represent the distribution of all identified sequences at each timepoint, and species, in relation to their fold change and significance. Each dot represents an aligned sequence, and their fold changes are represented in the horizontal axis (log2 scale), while their significance is represented in the vertical axis (-Log10 scale). Non-differentially expressed sequences are represented by grey dots. Non-significant, differentially expressed sequences are represented by green dots. Significant, differentially expressed sequences are represented by red dots. The top 10 most significantly differentially expressed genes at each timepoint are identified. Absence of 10 identified dots in a plot means that some of the topmost significant differentially expressed sequences at that timepoint, in that species, were not identified as any particular gene. A, B, C, D – Distribution of identified sequences in A. cahirinus, *according to fold change and significance, for timepoints day 3, 5, 7 and 14, respectively. F, G, H, I - Distribution of identified sequences in* M. musculus, *according to fold change and significance, for timepoints day 3, 5, 7 and 14, respectively. E, J – Comparison of normalized read counts for the Top 10 most significant DEGs identified in* A. cahirinus *and* M. musculus, *respectively. Warmer color (red) represents a higher z-score, while colder (blue) represents a lower. White represents the average z-score for that DEG.*

3.2.2. Biological Processes

Our analysis of DEGs produced some hypothesis about how proliferation regulation might differ, and evolve in different manners, through the initial phases of regenerative and fibrotic wound healing. To test our hypothesis, we performed a gene ontology (G.O.) analysis focused on Biological Processes (B.P.). This type of approach identifies the processes to which our DEGs might be associated to, and paints a clearer picture of how the processes change in time.

To perform this analysis, we decided to separate the positive DEGs and negative DEGs, as we wanted to determine whether positive and negative regulation of genes could be associated with distinct processes, or not. Represented on Figure 3.30 are the top 20 results (for each timepoint, in both species) of the most significant biological processes associated with positive DEGs.

Immediately observable is that, in both species, the processes associated with day 3 post wounding are fairly distinct from the other timepoints, with fewer DEGs associated and lower significance. This is possibly due to proliferative cell populations, in both species, being in a process of adaptation, transitioning from a homeostatic profile to a healing profile.

We can also see that only approximately 20% of the processes identified are shared between species (17% in *Acomys*, 22% in *Mus*). Seven of these processes share similar relevance at some of the timepoints, but only two are relevant at exactly the same timepoints ("Positive Regulation of Cellular Processes" and "Response to Chemical", both significant at day 3).

Of the 11, 64% become relevant in *M. musculus* earlier than in *A. cahirinus* ("Biological Regulation", "Cell Adhesion", "Cellular Response to Endogenous Stimulus", "Circulatory System Development", "Collagen Fibril Organization", "Regulation of Anatomical Structure Morphogenesis" and "Tube Development"), with only two having the opposite trend ("Extracellular Matrix Organization" and "Regulation of Biological Process"). This supports our previous interpretations that the wound healing processes in *Acomys* and *Mus* are inherently, and in *Mus* there is an anticipation of some, which might correlate with earlier differentiation.

Contrarily to what our DEG analysis had suggested, in *A. cahirinus* there are fewer common processes across multiple timepoints, with the ratio of processes significant at just one timepoint being higher than in *Mus* (81% in *Acomys*, versus 62% in *Mus*), as we can see in Figure 3.31.

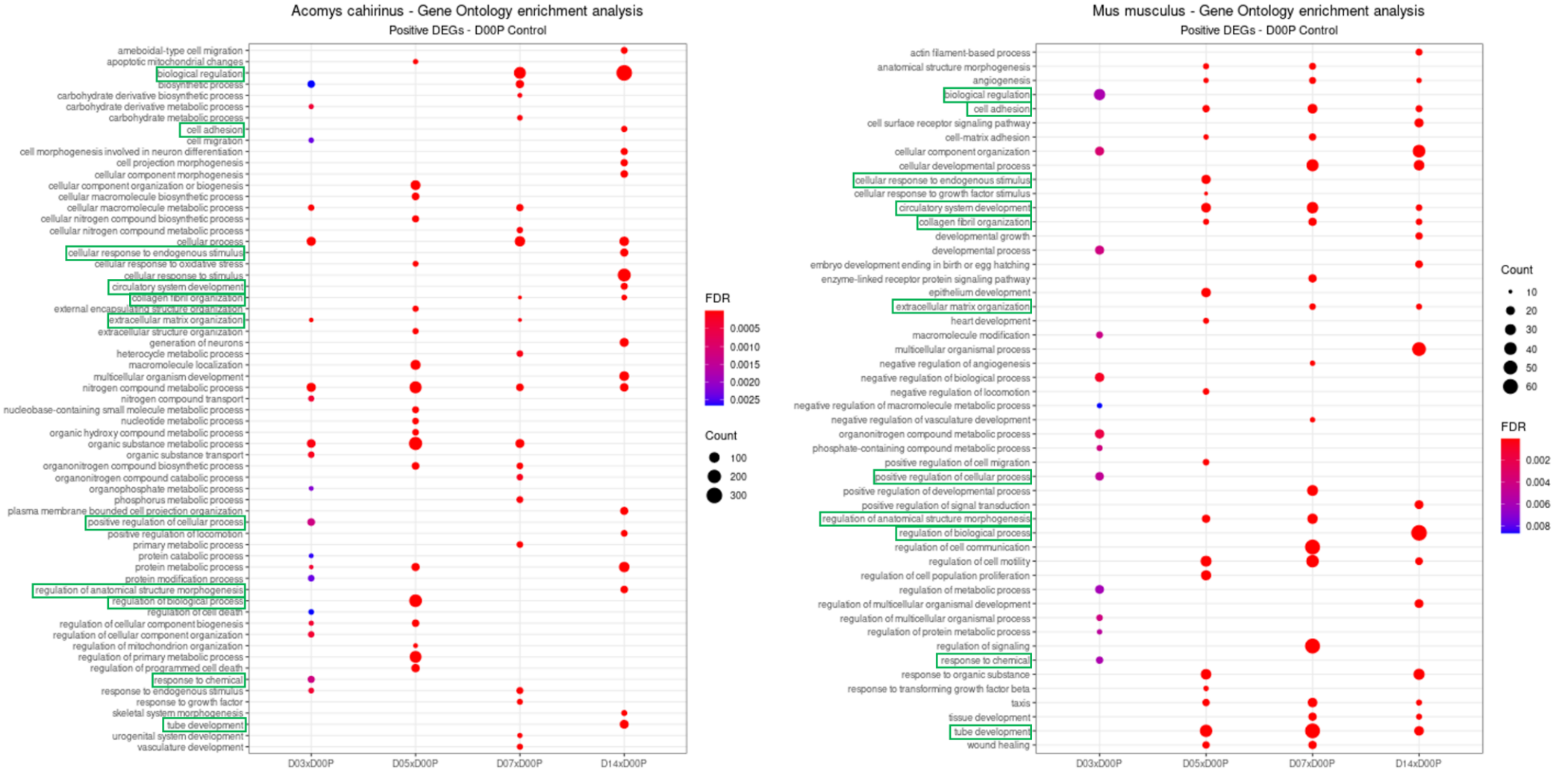

Figure 3.30 – Gene Ontology analysis of Biological Processes associated to positive DEGs.
This figure represents the Top 20 biological processes identified at each timepoint, for both species, associated with positive DEGs, and their significance at other timepoints. Dot size represents an approximate amount of DEGs associated with that process, at that timepoint, in that species. Processes with less than 10 genes associated to them were not considered, despite significance. Dot color indicates the significance of the process, with hotter (redder) colors representing higher significance, and cooler colors (bluer) representing lower significance. Process names framed by a green frame are processes identified in both species. FDR – False Discovery Rate (a measure of significance).

In *Acomys*, 12 processes are relevant in more than one day, but only four are significant at three timepoints or more ("Cellular Process", "Nitrogen Compound Metabolic Process", "Organic Substance Metabolic Process" and "Protein Metabolic Process"), while in *Mus* 16 processes are relevant at two or more timepoints, with 7 being significant at three or more timepoints ("Angiogenesis", "Cell Adhesion", "Circulatory System Development", "Collagen Fibril Organization", "Regulation of Cell Motility", "Taxis" and "Tube Development"

As we had suggested in our interpretation of the DEG analysis, we interpret these results, in association with the observations made in the PCA and MDS analysis, to mean that while the response to wounding in *A. cahirinus* is characterized by a more similar behavior of DEGs (i.e, being overexpressed, perhaps with more similar fold changes), and elicits differential expression of more genes important at several points of the wound healing process, in *Mus* the key genes and processes have more sustained behaviors, suggesting that the transcriptomic regulation that underlies the processes of wound healing in *Mus* are established sooner and more stably than in *Acomys*.

Alternatively, the proliferative cell populations might be composed of distinct cell types in each species, and more heterogeneous in *A. cahirinus*, resulting in more variability in gene regulation than in *M. musculus*.

To better understand how each species responds to wounds, we next focused on processes that are unique to each species, and identified a few that symbolize the distinct strategies employed. In *A. cahirinus,* we identified processes like "Apoptotic mitochondrial changes", "Cell morphogenesis involved in neuron differentiation", "Cellular nitrogen compound biosynthetic process", "Cellular response to oxidative stress", "Generation of neurons", "Nitrogen compound metabolic process", "Regulation of cell death", "Response to growth factor" and "Regulation of programmed cell death".

In *M. musculus,* we identified the processes "Negative regulation of angiogenesis", "Negative regulation of locomotion", "Negative regulation of macromolecule metabolic process", "Negative regulation of vasculature development" and "Response to transforming growth factor beta". These again suggest quite distinct strategies to wound healing, with *Acomys* DEGs uniquely associating with processes linked with more regenerative outcomes, while *Mus* 's unique processes were particularly associated with inhibitory regulation, has had already been suggested by the higher proportion of negative DEGs found in this species.

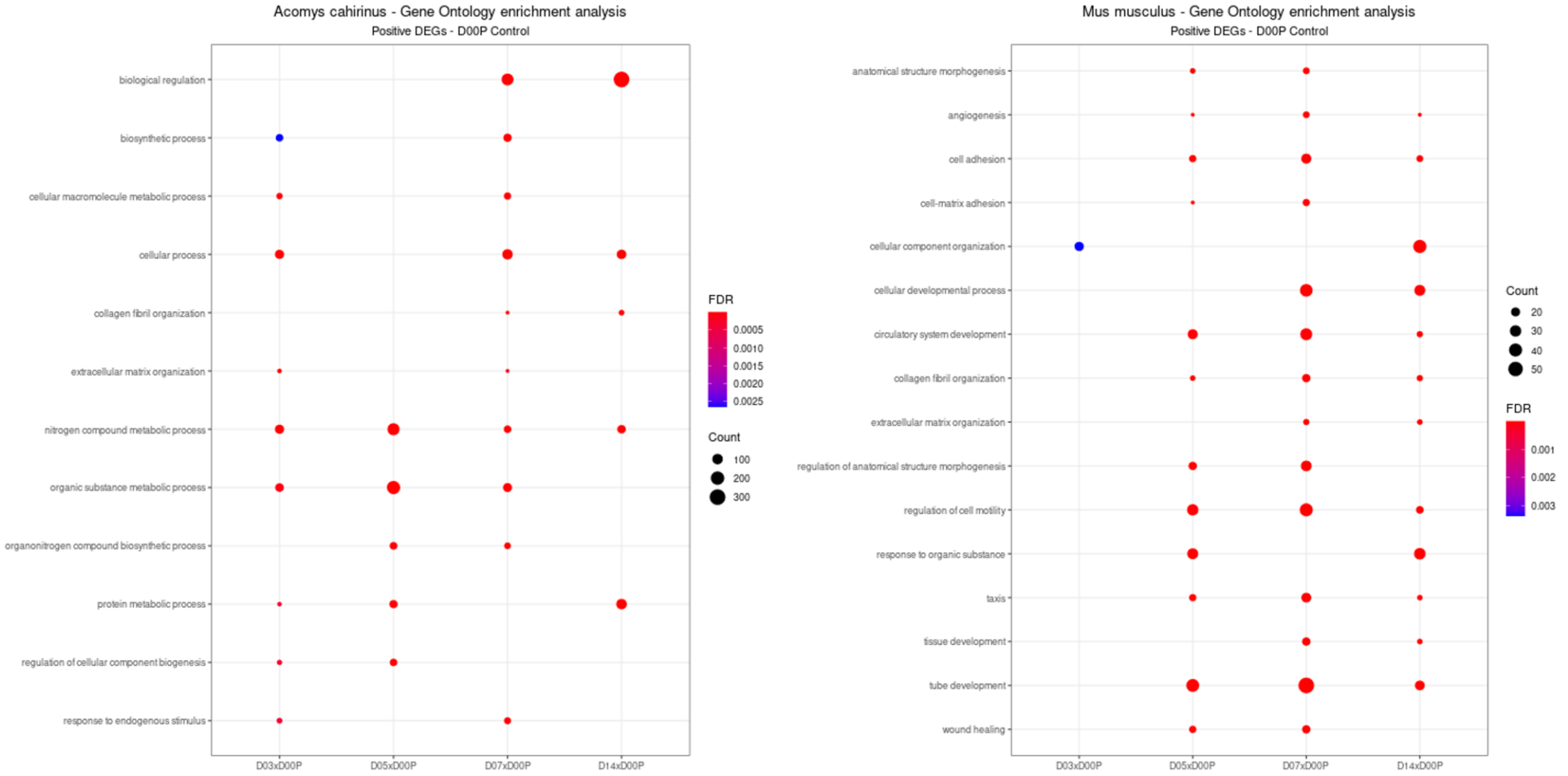

Figure 3.31 - Biological Processes (positive DEGs) shared by two or more timepoints.
This figure represents biological processes that, within each species, were identified as significant in more than one timepoint. Dot size represents an approximate amount of DEGs associated with that process, at that timepoint, in that species. Processes with less than 10 genes associated to them were not considered, despite significance. Dot color indicates the significance of the process, with hotter (redder) colors representing higher significance, and cooler colors (bluer) representing lower significance. FDR – False Discovery Rate (a measure of significance).

Seeing as there seems to be a distinct weight of negatively regulated genes between species, we decided to analyze the relevance of these DEGs separately. Despite having detected a higher number of negative DEGs in *A. cahirinus*, and one timepoint of *M. musculus* being excluded from the analysis (due to the small number of negative DEGs identified in it), we identified a higher number of significant processes associated with *M. musculus* negative DEGs (43) than with *A. cahirinus* negative DEGs (29, Figure 3.32).

Of these, 9 were identified in both species ("Cellular component organization", "Cellular component organization or biogenesis", "Cellular developmental process", "Cellular localization", "Cytoskeleton organization", "Developmental process", "Negative regulation of cellular process", "Positive regulation of cellular process" and "Regulation of biological process"), with three having also been identified with the positive DEGs ("Cellular component organization", "Positive regulation of cellular process" and "Regulation of biological process").

Associated with *A. cahirinus* negative DEGs, we found two processes also associated with the positive DEGs ("Cellular component organization or biogenesis" and "Protein metabolic process") and, more interestingly, 6 processes that were identified exclusively with *M. musculus* positive DEGs.

As for *M. musculus*, we found associated with the negative DEGs two processes equally identified with the positive DEGs ("Cellular developmental process" and "Developmental process") and 7 processes in common with the processes identified associated with positive DEGs in *A. cahirinus.* This, contrarily to what we had inferred from the DEG analysis, suggests that some of the processes occurring in *A. cahirinus*, during its wound healing event, are shut down in *M. musculus*, and vice-versa, indicating that at least a subset of processes is shared between wound healing strategies, with opposite regulation.

Interestingly, the considerable association of negative DEGs with processes at timepoint day 5 in *A. cahirinus* could represent a period of significant decisions, with several processes being interrupted, or altered. This hypothesis is also supported by the DEG analysis, due to the shear increase in negative DEGs at this timepoint.

This association of negative DEGs is also seen, although with less contrast, in *M. musculus*. Since the inflammatory phase of wound healing peaks around day 3 – 4, and then begins to be resolved around day 5, we hypothesize that this negative regulation of processes might relate to the transition from pro-inflammatory to immunomodulatory signals. Furthermore, *M. musculus* has a similar association of negative DEGs with processes at day 7. We interpret this

observation as these being processes involved in, or resulting from, the sustainment of proliferation, which begin to be switched off in *M. musuculus*.

Overall, our analysis of biological processes gives support to some of our previous interpretations. First, it confirms that while *A. cahirinus* and *M. musculus* proliferative cell populations have some commonalities, in general they respond in different ways to wounding, through different processes. While they primarily respond through different processes, some shared processes were identified, but these species seem to mostly regulate them oppositely. So, it is possible that at least part of their responses occur through the same signaling pathways, but with different outcomes.

Second, as we had proposed, it appears that the response to wounding of proliferative cells in *Mus* is stabilized sooner, with more processes being shared by multiple timepoints in *M. musculus,* particularly from day 5 post wounding onwards. This stability in profile is associated with processes related with cell adhesion and development, suggesting an earlier differentiation of these cells.

Another aspect coming through this analysis is that most biological processes common to both species become relevant in *Acomys* later than in Mus (Figure 3.30). This again points to the idea that differences in the onset of some processes, especially those that could be associated with differentiation, might be a contributor to why *A. cahirinus* is able to sustain proliferation for longer than *M. musculus*.

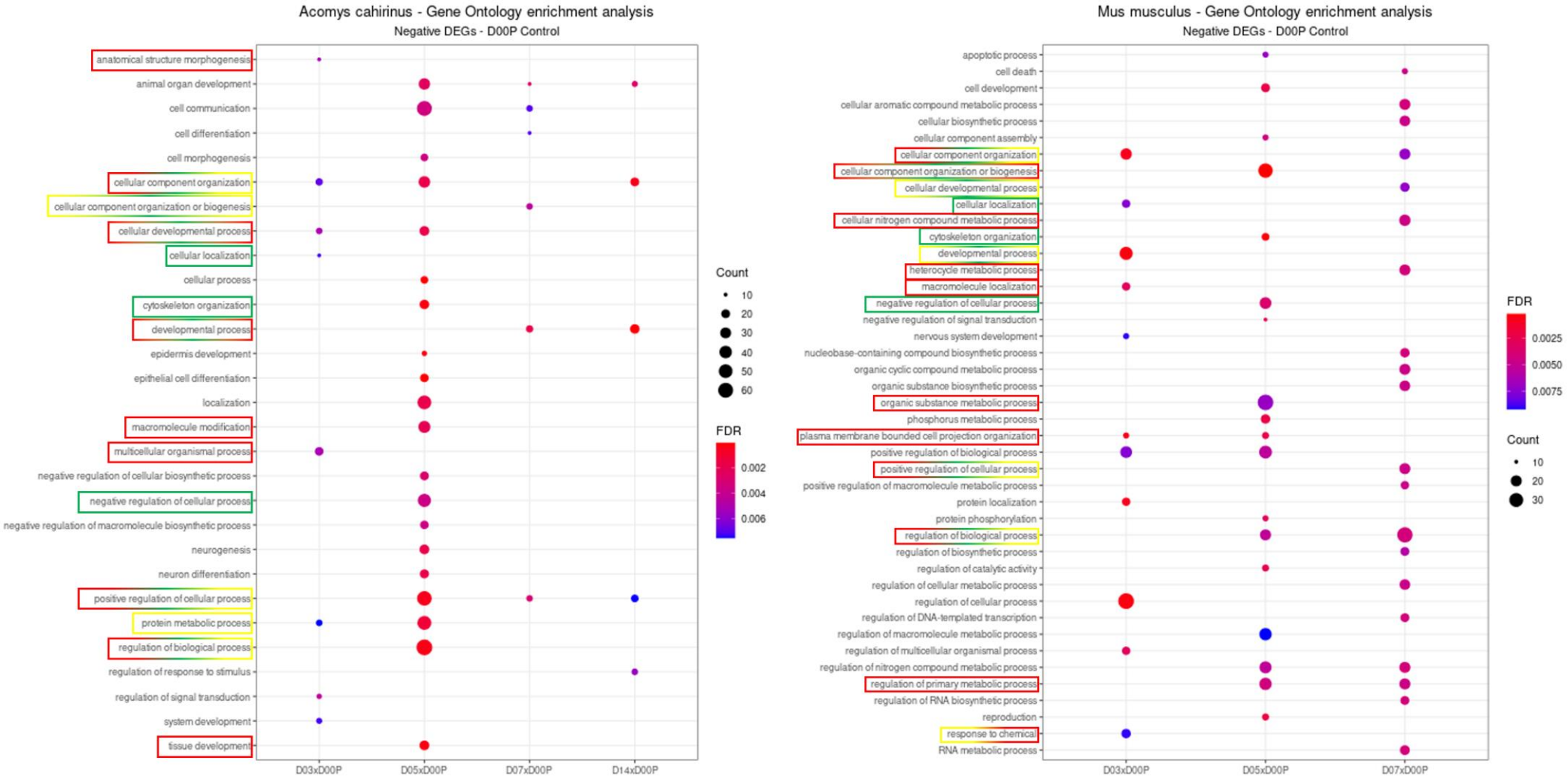

Figure 3.32 - Gene Ontology analysis of Biological Processes associated to negative DEGs.

This figure represents the Top 20 biological processes identified at each timepoint, for both species, associated with negative DEGs, and their significance at other timepoints. Dot size represents an approximate amount of DEGs associated with that process, at that timepoint, in that species. Processes with less than 10 genes associated to them were not considered, despite significance. Dot color indicates the significance of the process, with hotter (redder) colors representing higher significance, and cooler colors (bluer) representing lower significance. Process names framed by green frames are processes identified in both species. Process names framed by yellow frames were identified associated with positive DEGs on the same species. Process names framed by red frames were identified associated with positive DEGs of the opposite species. Multicolored frames identify processes that combine the characteristics previously described, according to the colors represented on the frame. FDR – False Discovery Rate (a measure of significance).

3.2.3. Pathways

Our analysis of Gene Ontology: Biological Processes identified some common processes between *A. cahirinus* and *M. musculus* proliferative cells, but also demonstrated that in general these populations execute distinct processes, and in general the common processes have opposing regulations, which could indicate distinct signaling pathway involvement or regulation.

To investigate whether the similarities and differences observed are the result of differential regulation of the same signaling pathways, or whether different pathways are engaged in either species, we decided to perform another DEG enrichment analysis, this time focusing on signaling pathways.

To perform this analysis we used the pathfindeR tool, which was shown to be able to detect with more accuracy the significance of biologically relevant pathways[254]. This tool performs a pre-determine number of iterations of pathway association with the provided data (as was explained in Materials and Methods), and counts how many times, or "occurrences", a specific pathway is associated with the input. Because we consider this another metric of significance, we performed 100 iterations and decided to only consider pathways with more than 20 occurrences.

Through our analysis, we identified 217 significant terms associated with the DEGs of day 3 of *A. cahirinus*, 307 with day 5, 272 with day 7 and 323 with day 14, while in *M. musculus* we found no term significantly associated with day 3, 67 associated with day 5, 28 associated with day 7 and only two associated with day 14.

Because a large number of these terms are associated exclusively to one DEG, and therefore might have little biological significance, we decided to further restrict our analysis to terms associated to three or more DEGs. Following this filtering, 45 terms associated with *A. cahirinus* day 3 remained, 233 with day 5, 94 with day 7 and 135 with day 14, while in *M. musculus* only 20 terms passed the filter at day 5, 13 at day 7 and the two remained at day 14. This suggests that very few described pathways are active in the wound healing response of *Mus*, with few DEGs clearly associating with a specific pathway.

We began our study of these results by looking at the top 20 most significant terms at each timepoint (or all, where fewer were available), in each species. Looking at *A. cahirinus*, at day 3 we found four terms associated with mitochondrial metabolism, 5 with proliferation or DNA

replication, 6 to cytoplasmic protein production or modification, two with intracellular dynamics and three with immune response (Table 3.6).

At day 5 we identified 5 terms associated to mitochondrial metabolism, 8 to proliferation or DNA replication, 3 to protein production or modification and 4 with intracellular dynamics. At day 7, we again found 4 terms associated with mitochondrial metabolism, 13 with proliferation or DNA replication and three with protein production or modification (Table 3.6).

Finally, at day 14 we found 5 terms associated with mitochondrial metabolism, 5 with proliferation or DNA replication, 3 to protein production or modification, 5 with intracellular dynamics and two with immune response, as depicted in Table 3.6. It is noteworthy that 4 of the 5 terms associated with mitochondrial metabolism were detected at all timepoints, and were always in the top 5 most significant terms.

Looking at *M. musculus*, as we mentioned before, no significant terms were identified at day 3, and only two at day 14, which are associated with protein modification and downstream receptor signaling. However, at day 5 the top 20 most significant terms pertain to cell cycle regulation (1), protein production or modification (2), hemostasis (3), transcription regulation (3), downstream receptor signaling (4) and intracellular dynamics (7). As for day 7, two of the identified terms pertain to protein production or modification, 3 to transcription regulation, 4 to intracellular dynamics and 4 to downstream receptor signaling, as depicted in Table 3.7.

Of the terms identified at each timepoint for *A. cahirinus*, 5 (11% of terms identified in *A. cahirinus*) are shared by all timepoints and 15 (33%) are shared among two or three timepoints. Most of these terms (9, 20%) are shared between day 5 and day 14. As for *Mus*, the timepoints day 5 and day 7 share 12 terms (55% of terms identified in *M. musculus*), and two of these are also shared with day 14 (9%).

Acomys top 20 terms at day 3 share three terms (5% of all terms) with *Mus* at day 5 ("Cell cycle", "Membrane trafficking" and "Vesicle-mediated transport"). *Acomys* day 5 shares two terms with *Mus* day 5 (3%) "Rac1 GTPase cycle" and "RHO GTPase cycle"), with the latter also being shared with *Mus* day 7. *Acomys* day 7 shares a single term (2%) with *Mus* day 5 ("Cell Cycle"), while *Acomys* day 14 shares 5 terms (8%) with *Mus* day 5 ("Cell cycle", "Membrane trafficking", "RHO GTPase cycle", "Signaling by RHO GTPases" and "Signaling by RHO GTPases, Miro GTPases and RHOBTB3"), with the last three also being shared with *Mus* day 7.

Table 3.6 - A. cahirinus *Top 20 Most Significant Pathways.*
This table depicts the top 20 most significant pathway associations to A. cahirinus *DEGs, at each timepoint of the surveyed time course.*

Day 3

Term	Fold Enrichment	occurrence	lowest p value
Mitochondrial translation elongation	6,33	100	6,2007E-09
Mitochondrial translation initiation	6,33	100	6,2007E-09
Mitochondrial translation termination	6,33	100	6,2007E-09
Mitochondrial translation	5,93	100	6,94332E-09
Translation	2,40	100	4,77297E-07
Cell Cycle	0,87	100	6,72583E-06
Membrane Trafficking	0,70	100	2,23514E-05
Vesicle-mediated transport	0,63	100	2,31604E-05
M Phase	1,12	100	5,14461E-05
Metabolism of polyamines	7,29	100	5,15071E-05
Mitotic Anaphase	1,81	100	5,15071E-05
Mitotic Metaphase and Anaphase	1,81	100	5,15071E-05
Ub-specific processing proteases	2,28	100	6,67994E-05
Cell Cycle, Mitotic	0,81	100	7,00238E-05
Deubiquitination	1,63	100	7,68512E-05
Metabolism of amino acids and derivatives	1,98	45	0,00011156
TNFR2 non-canonical NF-kB pathway	4,27	100	0,00019348
Metabolism of proteins	1,91	100	0,00028504
Signaling by Interleukins	2,17	100	0,00041797I
Adaptive Immune System	0,55	100	0,00053677I

Day 5

Term	Fold Enrichment	occurrence	lowest p value
Mitochondrial translation elongation	3,83	100	6,2007E-09
Mitochondrial translation initiation	3,83	100	6,2007E-09
Mitochondrial translation termination	3,83	100	6,2007E-09
Mitochondrial translation	3,58	100	6,94332E-09
The citric acid (TCA) cycle and respiratory electron transport	2,59	100	1,06409E-07
Cell Cycle Checkpoints	1,72	100	3,61521E-07
Translation	1,81	100	4,77297E-07
RHO GTPase cycle	1,28	100	1,3874E-06
RAC1 GTPase cycle	1,65	100	1,3874E-06
RHOJ GTPase cycle	4,20	100	1,3874E-06
RHOQ GTPase cycle	3,85	100	1,49648E-06
SUMO E3 ligases SUMOylate target proteins	2,03	100	1,62757E-06
SUMOylation	1,96	100	1,62757E-06
HDR through Homologous Recombination (HRR) or Single Strand Annealing (SSA)	2,50	100	1,74422E-06
Homology Directed Repair	2,36	100	1,74422E-06
Nonhomologous End-Joining (NHEJ)	2,58	100	2,89245E-06
DNA Double-Strand Break Repair	2,40	100	2,89245E-06
Cdc20:Phospho-APC/C mediated degradation of Cyclin A	3,11	55	4,36345E-06
APC:Cdc20 mediated degradation of cell cycle proteins prior to satisfation of the cell cycle checkpoint	3,07	55	4,36345E-06
APC/C:Cdc20 mediated degradation of mitotic proteins	2,99	55	4,36345E-06

Day 7

Term	Fold Enrichment	occurrence	lowest p value
Mitochondrial translation elongation	5,97	100	6,2007E-09
Mitochondrial translation initiation	5,97	100	6,2007E-09
Mitochondrial translation termination	5,97	100	6,2007E-09
Mitochondrial translation	5,60	100	6,94332E-09
Cell Cycle Checkpoints	1,34	100	3,61521E-07
Translation	2,72	100	4,77297E-07
HDR through Homologous Recombination (HRR) or Single Strand Annealing (SSA)	2,51	100	5,84317E-07
Homology Directed Repair	2,37	100	5,84317E-07
DNA Double-Strand Break Repair	3,12	100	1,45551E-06
Neddylation	1,50	100	3,74996E-06
Cdc20:Phospho-APC/C mediated degradation of Cyclin A	3,64	59	4,36345E-06
APC:Cdc20 mediated degradation of cell cycle proteins prior to satisfation of the cell cycle checkpoint	3,59	59	4,36345E-06
APC/C:Cdc20 mediated degradation of mitotic proteins	3,50	59	4,36345E-06
Activation of APC/C and APC/C:Cdc20 mediated degradation of mitotic proteins	3,45	100	4,36345E-06
Regulation of APC/C activators between G1/S and early anaphase	3,28	100	4,36345E-06
APC/C-mediated degradation of cell cycle proteins	3,02	100	4,36431E-06
Regulation of mitotic cell cycle	3,02	100	4,36431E-06
Nonhomologous End-Joining (NHEJ)	4,03	100	5,33836E-06
Antigen processing: Ubiquitination & Proteasome degradation	1,47	100	6,33793E-06
Cell Cycle	1,37	100	6,72583E-06

Day 14

Term	Fold Enrichment	occurrence	lowest p value
Mitochondrial translation elongation	2,72	100	6,2007E-09
Mitochondrial translation initiation	2,72	100	6,2007E-09
Mitochondrial translation termination	2,72	100	6,2007E-09
Mitochondrial translation	2,55	100	6,94332E-09
The citric acid (TCA) cycle and respiratory electron transport	1,66	100	1,06409E-07
Cell Cycle Checkpoints	0,55	100	3,61521E-07
Translation	1,16	100	4,77297E-07
HDR through Homologous Recombination (HRR) or Single Strand Annealing (SSA)	2,74	100	5,84317E-07
Homology Directed Repair	2,59	100	5,84317E-07
DNA Double-Strand Break Repair	3,07	100	1,45551E-06
SUMO E3 ligases SUMOylate target proteins	1,15	100	1,62757E-06
SUMOylation	1,11	100	1,62757E-06
RHO GTPase cycle	0,65	100	2,98561E-06
RHOJ GTPase cycle	2,69	100	2,98561E-06
Cell Cycle	1,27	100	6,72583E-06
Interleukin-1 signaling	1,71	100	1,52111E-05
Signaling by Rho GTPases, Miro GTPases and RHOBTB3	0,66	100	1,7277BE-05
Signaling by Rho GTPases	0,60	100	1,7277BE-05
TCR signaling	1,20	100	1,83709E-05
Membrane Trafficking	1,53	100	2,23514E-05

Table 3.7 – M. musculus *Top 20 Most Significant Pathways.*
This table depicts the top 20 (or all, where not sufficient were identified) most significant pathway associations to M. musculus *DEGs, at each timepoint of the surveyed time course.*

Day 5

Term	Fold Enrichment	occurrence	lowest p value
Cell Cycle	0,54	100	3,44118E-16
RHO GTPase Effectors	1,32	100	4,35924E-06
Signaling by Rho GTPases	1,09	100	4,39239E-06
Signaling by Rho GTPases, Miro GTPases and RHOBTB3	1,06	100	4,9876E-06
Membrane Trafficking	1,75	100	0,001622352
Hemostasis	2,50	100	0,001690598
Generic Transcription Pathway	0,50	100	0,002319143
Vesicle-mediated transport	2,45	100	0,002978075
RNA Polymerase II Transcription	0,45	100	0,003275652
Gene expression (Transcription)	0,41	100	0,004216089
Post-translational protein phosphorylation	9,93	94	0,004685912
Regulation of Insulin-like Growth Factor (IGF) transport and uptake by Insulin-like Growth Factor Binding Proteins (IGFBPs)	8,77	94	0,004685912
RAC1 GTPase cycle	1,92	69	0,005696133
RHO GTPase cycle	1,31	100	0,006138433
Signal Transduction	1,76	93	0,00908423
Platelet degranulation	6,45	91	0,014323431
Response to elevated platelet cytosolic Ca2+	6,20	91	0,014323431
Post-translational protein modification	1,57	29	0,02614649
MAPK1/MAPK3 signaling	2,15	99	0,027020662
MAPK family signaling cascades	1,87	99	0,037120041

Day 7

Term	Fold Enrichment	occurrence	lowest p value
Generic Transcription Pathway	0,71	100	0,002319143
RNA Polymerase II Transcription	0,65	100	0,003275652
Gene expression (Transcription)	0,59	100	0,004216089
Post-translational protein phosphorylation	9,72	32	0,004685912
Regulation of Insulin-like Growth Factor (IGF) transport and uptake by Insulin-like Growth Factor Binding Proteins (IGFBPs)	8,59	32	0,004685912
RHO GTPase cycle	1,26	100	0,006138433
RHO GTPase Effectors	1,06	98	0,008695256
Signaling by Rho GTPases, Miro GTPases and RHOBTB3	1,14	96	0,009838691
Signaling by Rho GTPases	1,17	97	0,009838691
Signal Transduction	1,88	75	0,014174418
RHOA GTPase cycle	1,93	57	0,025914733
MAPK1/MAPK3 signaling	2,07	99	0,027020662
MAPK family signaling cascades	1,80	99	0,037120041

Day 14

Term	Fold Enrichment	occurrence	lowest p value
Post-translational protein phosphorylation	13,15	32	0,004685912
Regulation of Insulin-like Growth Factor (IGF) transport and uptake by Insulin-like Growth Factor Binding Proteins (IGFBPs)	11,62	32	0,004685912

These results point to what we had previously suggested, which is that despite some similarities, *A. cahirinus* and *M. musculus* wound healing events are inherently different. While the terms identified in *Acomys* associate primarily with proliferation and energy production (likely to sustain the energetically demanding process of proliferation), in *Mus*, despite these being proliferative populations, very few terms identified relate to proliferation.

Furthermore, as we had already suggested with our analysis of biological processes, *Mus* timepoints share a higher proportion of significant terms than those of *Acomys*. This, again, suggests a greater evolution of processes in *Acomys* that in *Mus*. This observation links with another interesting one, which is that the signaling in proliferating cells at day 3 and day 14 of the *M. musculus* wound healing event does not significantly associate with any particular signaling pathway. This is a curious observation, seeing as a reasonable amount of DEGs were identified at both timepoints.

As we have previously detailed, proliferation is mostly regulated by external stimuli that activate a few intracellular signaling cascades. In our analysis, we identified several terms related with the signaling pathways of MAPK/ERK, PI3K/AKT and WNT, which we decided to further explore.

We therefore filtered our results to just pathways pertaining to RTK signaling and proliferation, namely associated with terms like 'RAS', 'RAF', 'MAPK', 'AKT', 'PI3K', 'PTEN', 'WNT', 'Beta-Catenin', 'AXIN' and 'Receptor Tyrosine Kinase'. We also included pathways associated with terms like 'RHO' and 'RAC', which are related to cytoskeletal dynamics, like ECM deposition and migration, downstream of RTK singaling, and 'TRAF6', which could act as an integrator of Toll receptor signaling into the other pathways, particularly MAPK/ERK and PI3K/AKT.

As we can see in Figure 3.33, the differences between *A. cahirinus* and *M. musculus* are striking. Following our finding of barely any pathway associated with day 3 and 14 post wounding in *Mus*, and the low number of pathways associated to the other timepoints, it is not surprising that, generally, fewer pathways related with these terms were associated with *Mus*'s DEGs.

Nevertheless, while we found several terms pertaining to MAPK, AKT, WNT and NF-κB signaling in *Acomys*, throughout the timepoints, we only found terms associated with MAPK signaling in *Mus*, and only 30% (3 terms in 10) associated with both timepoints. Furthermore, the terms associated with this pathway in *Mus* are less enriched (were found in fewer iterations of the pathfinder analysis), and have a lower significance, generally speaking.

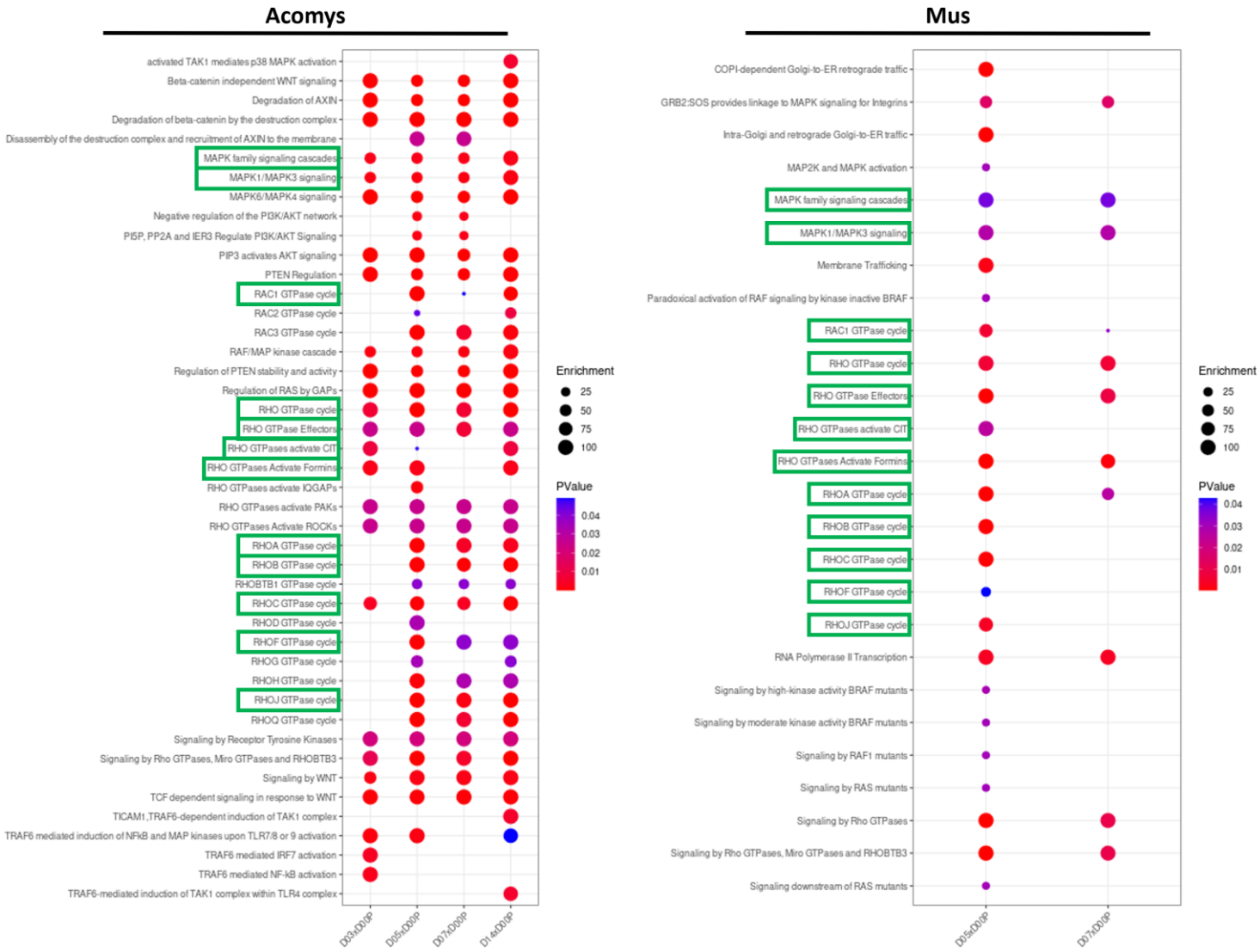

Figure 3.33 - RTK signaling-related pathways in A. cahirinus *and* M. musculus.
This image depicts the signaling pathways, associated with A. cahirinus *and* M. musculus *DEGs, that contain or associate with the terms 'RAS', 'RAF', 'MAPK', 'AKT', 'PI3K', 'PTEN', 'WNT', 'Beta-Catenin', 'AXIN' 'RHO', 'RAC', 'TRAF6' and 'Receptor Tyrosine Kinase'. Depicted is also the 'Enrichment' (approx. average number of DEGs) of each term, at each timepoint, and the approx. adj. p value of their association with the DEGs (the hotter (redder) the color of the dot, the higher its significance). DEGs highlighted by a green frame are the ones common to both species.*

Focusing our analysis on *A. cahirinus*, of the 44 pathways identified, close to half (51%, 23 terms) could be related with proliferation regulation, while the remaining 49% are associated with cytoskeletal dynamics. Furthermore, the association of these terms throughout the timepoints is quite homogeneous and significant, with each pathway being considerably enriched. Only terms associated with Traf6, and a few related to PI3K and AKT regulation, seem to be slightly more time restricted.

In *Mus*, of the 26 pathways identified only 31% (8 terms) could be related with proliferation regulation, while 46% (12 terms) pertain to cytoskeletal dynamics, while the remaining 23% (6 terms) are associated with protein production and trafficking. As expected, most pathways shared with *Acomys* (83%,) relate to cytoskeletal dynamics, likely to do with ECM deposition and migration. To further explore how pathway regulation compares between both species, we decided to analyze the expression dynamics of the genes associated with the previously identified terms.

As shown in Figure 3.34, fewer DEGs are associated with these terms in *Mus* (33 DEGs) than in *Acomys* (79 DEGs), and only 7 were detected in both species. However, and interestingly, both species exhibit three groups of DEGs that have similar behaviors between themselves: A group of DEGs that have a higher expression in proliferative cells in unwounded tissue, where two DEGs in common were identified; a group that has an early peak of expression, likely related with early response to wounding, which is much smaller in *Mus*; and a group of genes with a later peak of expression, which contains most of the common DEGs to both species, but whose peak expression is anticipated one week in *Mus*.

To understand how each of these groups of DEGs associates with particular pathways, we used the online tool Enrichr[267–269] to perform GSEA against the Reactome 2022 library. We also performed GSEA against the 'TF Perturbations Followed by Expression' database, to understand if the regulation of these DEGs could be associated to any particular set of transcription factors.

Starting with DEGs with higher expression in proliferative cells in the unwounded tissue, this group in *Acomys* primarily associated with PI3K/AKT and MAPK/ERK signaling downstream of RTK stimulation, and regulation by HSF1, a transcription factor associated with IEG inhibition but capable of inducing proliferation by other paths[270,271], was associated with the most DEGs in this group. In *Mus*, this group of DEGs did not associate to any signaling pathway, nor to any particular transcription factor.

Moving on to genes whose expression peaks early, this group of DEGs in *Acomys* associated with interleukin signaling pathways, and with regulation by the transcription factors MYC, JUN, NF-κB1 and MAF, which is involved in the differentiation of T cells[272273]. As for *Mus*, the small number of DEGs associated with this group makes it difficult to generate significance in any result. However, two DEGs strongly associate with ERBB signaling, and all four DEGs associate with the transcription factor MECOM, involved proliferation and stem cell maintenance through TGFβ-signaling antagonism[274].

Finally, genes with a later peak of expression in *Acomys* were associated more significantly with RTK signaling, in particular through PDGF, and regulation by transcription factors like ATF6, FOXO1, GATA6, OVOL2 and STAT3, which are involved in the development and homeostasis of several tissues[275,276], glucose metabolism[277], cell differentiation[278] or have a wide pleiotropic involvement in several aspects of organism function and development. As for *Mus,* the DEGs with this behavior associated most significantly to MAPK signaling, which constitutes but one of the several intracellular pathways through which RTK receptors can signal[279], and FOXO1 and GATA6 transcription factor regulation, but also with SOX2 and PAX3, involved in stem cell maintenance[280] and tissue development and homeostasis[281].

During our broader analysis of signaling pathways, we also detected several terms associated with apoptosis and cell death. Because proliferation and apoptosis have regularly been associated with one another, even depicted as going 'hand-in-hand' in many scenarios[282], and there are also evidences that induction of apoptosis might be important for induction of proliferation and regeneration[283], we decided to also analyze DEG association with apoptotic pathways in both species.

To do this, we filtered our results to yield pathways associated with the terms 'Apoptosis', 'Apoptotic', 'Cell Death' and 'BAD'. Because NF-κB is involved in many aspects of the cellular response to external cues, particularly to inflammatory signals, and involved in cell death regulation, we included the term 'NF-κB' in our filtering, as we wanted to know whether any association between the inflammatory environment and programmed cell death existed.

Our results were quite interesting, particularly seeing as we identified several of these terms associated with pathways detected in our analysis of *Acomys* DEGs, but analysis of *Mus* DEGs did not yield any result associated with these terms.

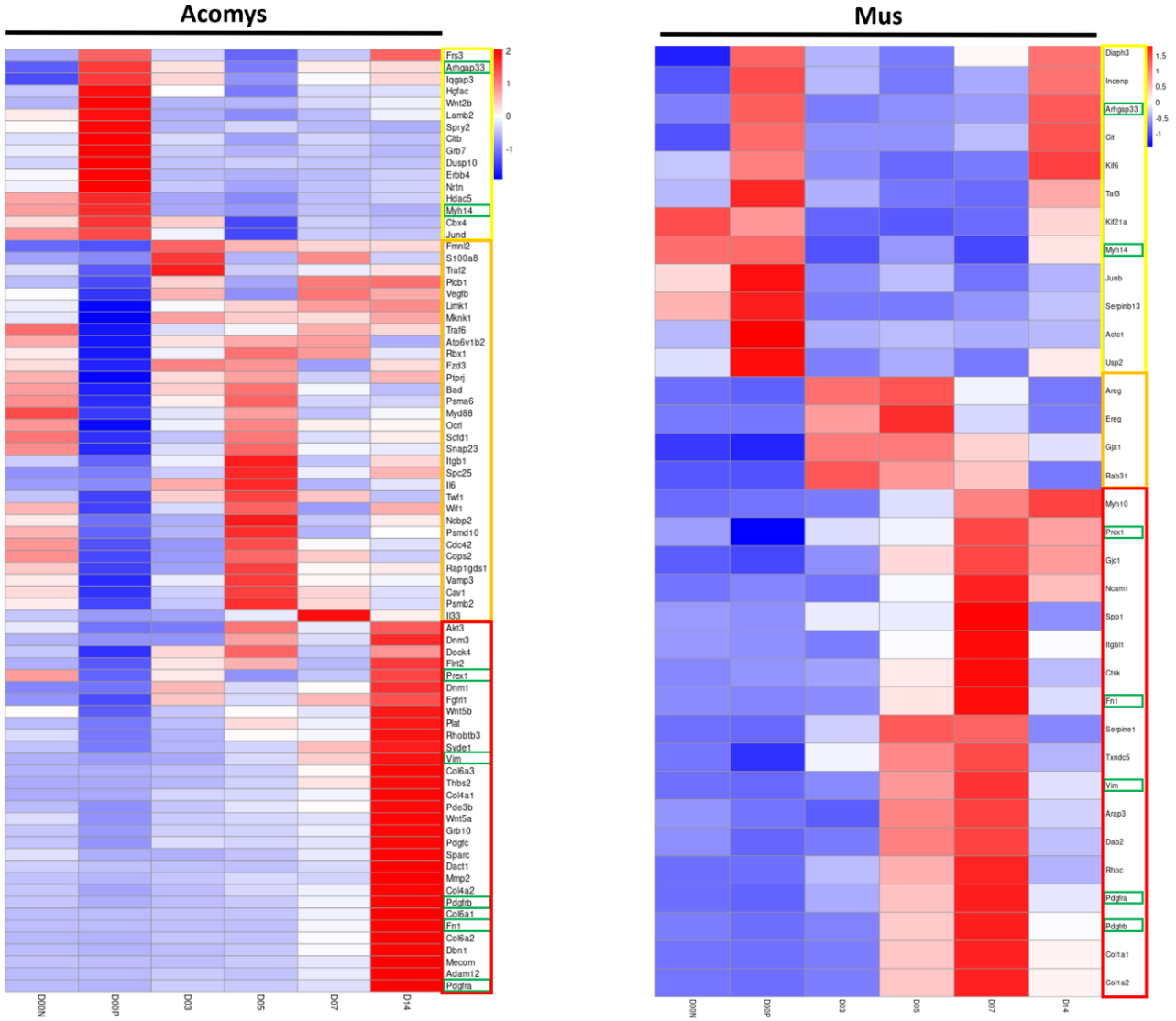

Figure 3.34 - RTK signaling-related DEGs in A. cahirinus *and* M. musculus.
This image depicts the DEGs associated with the previously referenced pathways, that contain or associate with the terms 'RAS', 'RAF', 'MAPK', 'AKT', 'PI3K', 'PTEN', 'WNT', 'Beta-Catenin', 'AXIN' 'RHO', 'RAC', 'TRAF6' and 'Receptor Tyrosine Kinase', as well as their z-score at each timepoint, in both species. Hotter (redder) color represents a higher average expression of a particular DEG at a given timepoint, while colder (bluer) color repressents a lower expression. White represents the average expression level of the DEG in the analyzed time course. DEGs highlighted by a green frame are the ones common to both species. DEGs highlighted by yellow, orange and red frames represent three sets with distinct behaviors whithin, and between, species. DEGs in the yellow frame have higher expression in proliferating cells in unwounded tissue. DEGs in orange frame have an early peak of expression. DEGs in red have a later peak in expression.

As shown in Figure 3.35, while most pathways associated with the 'NF-κB' term are identified at all timepoints of the time course, the majority of terms associated with cell death and apoptosis are excluded from day 3. Nevertheless, some terms associated with apoptotic pathways were also identified at day 3 post wounding, possibly representing an initiation of apoptotic processes in proliferative cells, which might also represent a response to cytokine signaling.

Looking specifically at what DEGs were identified associated with the pathways containing these terms, we again detected the same patterns of DEG expression we had previously detailed, plus and additional group of genes whose expression variation is slightly more homogeneous, but which we nevertheless included in one of the previously determined groups for subsequent analysis.

Starting with the group of genes whose expression is highest in proliferative cells of unwounded tissue, and again resorting to Enrichr, we found a clear association of these DEGs with pathways pertaining to extrinsic apoptotic signaling, but not to any particular transcription factor. The group of early peak expression DEGs associated in particular to the intrinsic apoptotic pathway, which is triggered in response to cellular damage and stress[284], and the transcription factors SOX2, NANOG and SRF, the last two also involved in stem cell maintenance[285] and differentiation[286], respectively. Finally, the group of later peak expression also associated with the intrinsic apoptotic pathway, but not as strongly, and did not associate specifically with any given transcription factor.

Overall, our analysis of signaling pathways yielded several interesting observations, and put forth a few hypothesis worth exploring. First, it gave further credence to our previous interpretation that regulation of proliferation in *A. cahirinus* and *M. musculus* are quite distinct, but share some common themes. While most pathways associated with *M. musculus* DEGs are distinct from those associated with *A. cahirinus* DEGs, some common pathways were identified.

This is expanded in a second observation, which suggests that while proliferation regulation during regeneration in *Acomys* is associated with several intracellular signaling pathways, namely MAPK/ERK, PI3K/AKT, WNT and NF-κB, differential proliferation regulation during wound healing is solely associated with MAPK/ERK signaling in *Mus*.

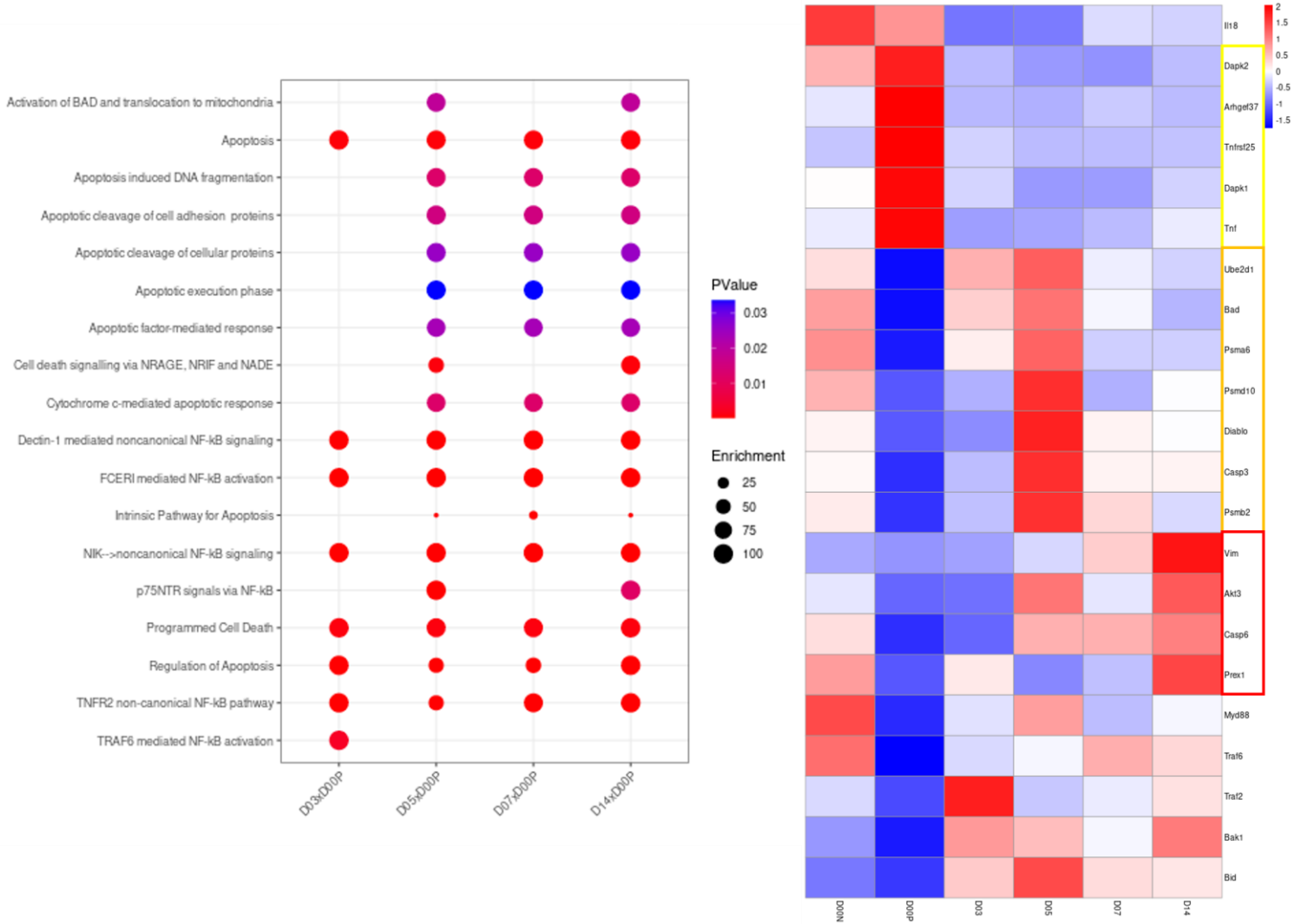

Figure 3.35 - Apoptosis-related pathways and DEGs in A. cahirinus.

This image depicts the pathways and DEGs associated with the terms 'Apoptosis', 'Apoptotic', 'Cell Death', 'BAD' and 'NF-κB'. Pathway information also includes their 'enrichment' and adjusted p value of association with DEGs. DEG information also includes the z-score at each timepoint. Hotter (redder) color represents a higher average expression of a particular DEG at a given timepoint, while colder (bluer) color repressents a lower expression. White represents the average expression level of the DEG in the analyzed time course. DEGs highlighted by yellow, orange and red frames represent three sets with distinct behaviors whithin species, also previously identified for other DEGs pertaining to other pathways. DEGs in the yellow frame have higher expression in proliferating cells in unwounded tissue. DEGs in orange frame have an early peak of expression. DEGs in red have a later peak in expression.

Furthermore, while *DEGs* in *Acomys* associated with several intracellular signaling pathways associated with proliferation throughout all timepoints surveyed, *Mus's* DEGs almost exclusively associated with MAPK/ERK signaling at day 5 post wounding. This is, naturally, also a reflex of the number of DEGs identified at each timepoint in each species, and suggests that *Mus*'s failure to sustain proliferation during the response to wounding is related to an inability to distance its regulation from the one in place during homeostasis.

Third, analysis of DEGs associated with the aforementioned pathways revealed a curious set of expression dynamics, equivalent in both species. These DEGs could be grouped in three distinct sets of expression profiles. One had their highest expressions in proliferative cells in homeostasis, the other early during wound healing, within the first 5 days, and the last had their peak expression later during the wound healing events, either at 14 days post wounding in *Acomys* or 7 days in *Mus*. Also interesting, while most DEGs associated with the first profile in *Mus* kept their expression lower throughout the surveyed time course, a large proportion of DEGs from this group in *Mus* had their expression higher again by day 14, further suggesting a reduced distancing of proliferative cells in wound healing in *Mus* from their baseline in homeostasis, leading to a quicker return.

Linked with this third observation, we detected differential associations of each of these groups to signaling pathways, between species. In *Acomys*, the expression profile of proliferative cells in unwounded tissue related with MAPK/ERK and PI3K/AKT signaling downstream of RTKs, possibly through an IEG-independent path. In *Mus* no pathways were detected associated to the DEGs.

As for the DEGs belonging to the group with the second expression profile identified, in *Acomys* these associated with cytokine signaling and IEG regulation, while in *Mus* the DEGs associated with ERBB signaling and the MECOM transcription factor. While capable of eliciting activation of some of the same downstream signaling pathways, stimulation by these two distinct sets of factors likely leads to considerable variability in gene expression alterations, as suggested by the differential association to transcription factors.

Finally, DEGs associated with the last expression profile, boasting a peak of expression later in the wound healing event, in *Acomys* related strongly with PDGF signaling through RTKs, which can elicit the activation of several intracellular signaling pathways, while in *Mus* the DEGs also associated to RTK downstream signaling, but only through MAPK/ERK. Furthermore, while the regulation of DEGs was associated with some common transcription

factors, namely FOX1 and GATA6, it also associated with other, distinct transcription factors. Additionally, the peak expression of DEGs belonging to this group in *Mus* is anticipated one week, in relation to *Acomys*, in our time course, returning close to basal in *Mus* by the time their expression peaks in *Acomys*.

All in all, it seems that the regulation of proliferation in *Mus* during wound healing distances itself less from that occurring in homeostasis than in *Acomys*, likely because it is the result of the activation of only a subset of the pathways activated in *Acomys*, which also control different subsets of genes.

This page was intentionally left blank

3.3. **Signaling Pathway Activity**

Having identified several signaling pathways which could be responsible for proliferation regulation associated with the DEGs in *Acomys* and *Mus*, we decided to further investigate whether these pathways could indeed explain the differences in proliferation regulation between these two species, by looking at the activation of their signaling cascades.

Signaling cascades are post-translationally regulated through several types of chemical alterations to their effectors, which interfere in their ability to interact with each other, and the most studied and understood type of post-translational alteration involved in signaling pathway regulation are phosphorylations. We therefore used the presence, or absence, of specific phosphorylations in known regulatory residues of downstream effectors of each pathway to evaluate their level of activation.

We began by analyzing the MAPK/ERK pathway, whose activity has already been shown to be related with a regenerative outcome in mammals[287]. In the MAPK/ERK pathway, the two major effectors are ERK1 and ERK2, which are generally co-expressed and thought of as having redundant regulatory functions. To evaluate their activity in both species, we decided to measure the relative quantity of ERK1 and ERK2 protein, as well as their post-translationally modified forms, phosphorylated at residues T202 and Y204, which have been linked with the activation of both proteins.

As we can see in Figure 3.36 (A, B), the relative abundance of ERK1 and ERK2 skews in favor of the first in *M. musculus*, while in *Acomys*, in homeostasis the ERK2 isoform has a slightly higher prevalence, but during the first five days of wound healing the relative abundance of each isoform is approximately the same, starting to skew in favor of ERK1 by day 7 post wounding.

Comparing the relative abundance of each protein between species, the results seem to indicate that ERK1 is more abundant in *Mus* in homeostasis, but tends to a similar abundance within the first 24h of wound healing, returning to a relative higher abundance in *Mus* from then on (Figure 3.36F). ERK2, on the other hand, appears to exist in similar amounts both during homeostasis and wound healing, with the exception of the period compromised between 12h and 24h post wounding, where A. cahirinus appears to have a higher relative abundance of ERK2 (Figure 3.36F).

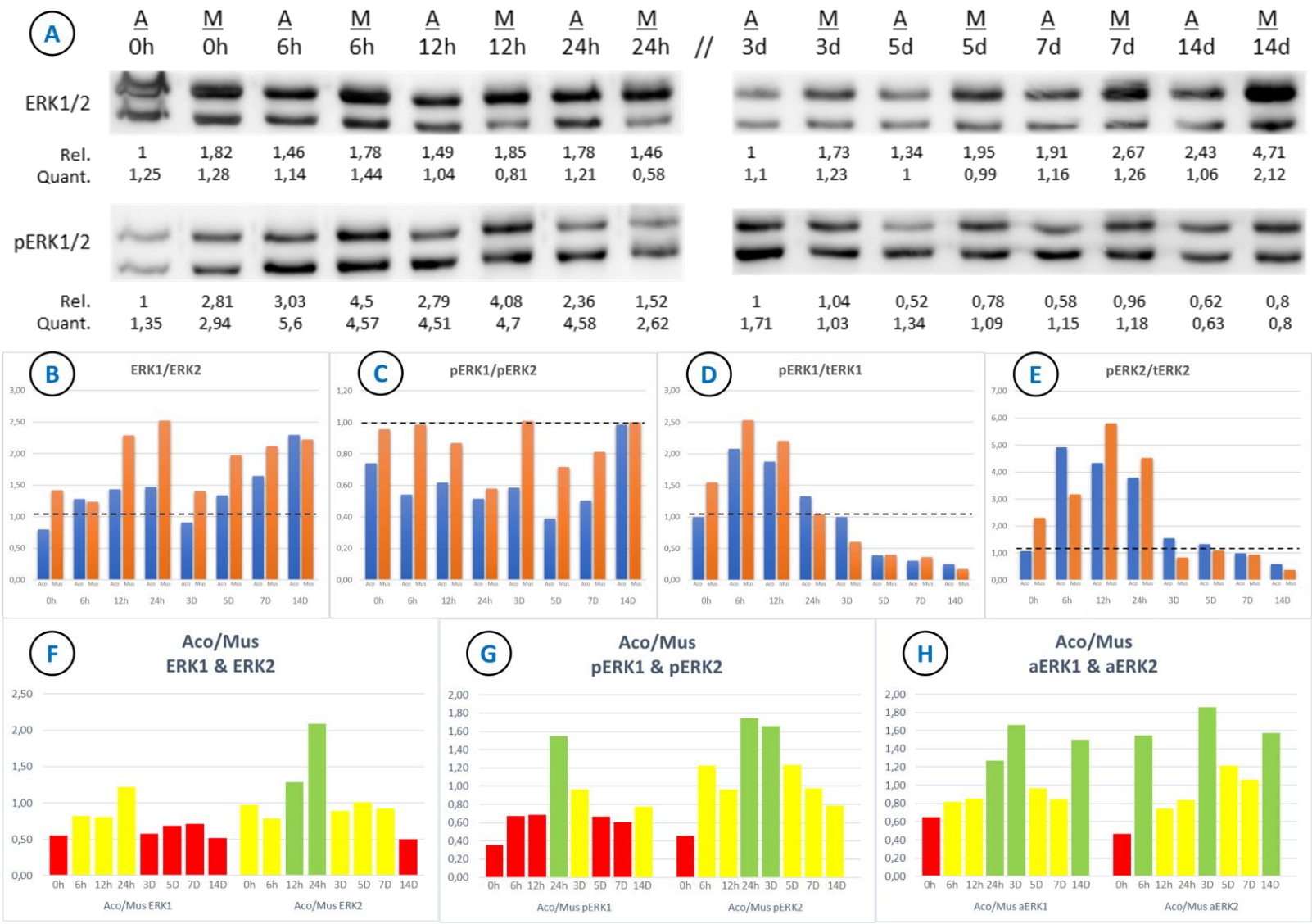

Figure 3.36 - Evaluation of MAPK/ERK signaling pathway activity through detection of post-translational modifications.
This figure represents the relative abundance of ERK1 and ERK2, and their respective phosphorylated versions, as detected through the Western Blot technique. Relative quantification (Rel. Quant). of protein abundance was performed by comparing signal intensity of each detected band with the signal of the most leftward band in each membrane (Aco 0h or Aco 3d), and to the top band on the leftmost lane, where applicable. A) Depiction of membrane signal detection for each isoform, at each timepoint, in A. cahirinus *and* M. musculus. *Also depicted are the values of relative quantification for each isoform of detected proteins. B, C) Evolution of the ratio between relative quantifications of each isoform, within each species, of B) total ERK and C) pERK. D, E) Evolution of the proportion of activated isoform (ratio between relative quantifications of phosphorylated and total protein), within each species, for D) ERK1 and E) ERK2. F, G) Evolution of the ratio between relative quantification of each isoform in each species for F) total ERK1 and ERK2, and G) pERK1 and pERK2. H) Evolution of the ratio between proportions of activated isoforms (aERK,), between species, for both isoforms, ERK1 and ERK2. In figures F, G and H, red bars represent timepoints were the ratio between* A. cahirinus *and* M. musculus *values favor* M. musculus. *Yellow bars represent a ratio of approximately 1 (between 0,75 and 1,25) indicating similarity between species, and green bars represent a ratio that favors* A. cahirinus. *A, Aco* – Acomys cahirinus. *M, Mus* – Mus musculus. *pERK1/2 – phosphorylated ERK1/2. tERK1/2 – Total ERK1/2. aERK1/2 – Ratio between pERK1/2 and tERK1/2.*

Looking at the phosphorylated forms, ERK1 (pERK1) appears to be less abundant than ERK2 (pERK2) in *Acomys*, while in *Mus* the proportion of both forms indicate similar abundance (Figure 3.36 A, C). These results suggest a higher relative abundance of pERK1 in *Mus*, as depicted in Figure 3.36G, which relates with equally higher levels of tERK1 in *Mus*. However, at day 14 post wounding, both species tend to a higher abundance of ERK1, but an approximately equal abundance of both activated isoforms.

As for ERK2, while the phosphorylated version seems to have a similar relative abundance throughout wound healing in both species, it is clear that between 12h and 24h, and in accordance with the relative abundance of the total protein, the relative abundance of pERK2 is higher in *Acomys* than in *Mus*.

To determine whether the different abundance of each phosphorylated isoform could reflect preferential activation of the pathway through a specific isoform, in either species, we decided to look at the proportion of phosphorylated (pERK1/2) to total (tERK1/2) protein for both isoforms (which we will call aERK1/2, for activated), and compare them.

As we can see in Figure 3.36 (A, D, E), in homeostasis there is a tendency for *Mus* to have a higher proportion of each isoform activated than *Acomys*. During wound healing, while there is, in the first day, an increase in aERK1 in both species, this seems to be inverted around day 3 post injury, with aERK1 returning to base levels, or even lower. aERK2 also follows a similar trend, with a considerable increase of activity in both species in the first 24h, but with a slight decrease below baseline at 14 days.

However, while aERK1 dynamics are concomitant with aERK2 in *A. cahirinus*, they seem to be slightly delayed (6h) in *M*us (Figure 3.36D, E). This suggests that perhaps both isoforms are not activated by the same stimuli, or there is differential regulation of their activation. If that is the case, then it would also suggest that the MAPK/ERK pathway-activating signals are not the same in both species.

Finally, when we compared the proportion of activation of each isoform between species (Figure 3.36H) we observed distinct patterns. While the overall activation of both isoforms is higher in unwounded tissue of *M. musculus*, quickly after wounding (6h) proportion of aERK2 becomes higher in *Acomys*. During the first 12h post wounding the relative activation of both isoforms equalizes between species, but at 24h post wounding aERK1 is already higher in *Acomys* than in *Mus*, and remains so until 3 days post wounding, where aERK2 also shows the

same proportion. From there, both aERK1 and aERK2 levels become similar between species, until day 14 post wounding, where aERK1 and aERK2 become higher in *Acomys* again.

These results suggest a differential abundance of each isoform between species, as well as differential activation dynamics of the pathway through each isoform, which could underline the differences already observed in the capacity of MAPK/ERK signaling to sustain proliferation and induce regenerative characteristics in both species.

Moving on to the analysis of the PI3K/AKT pathway activity, we evaluated its activation level by measuring the relative abundance of AKT1, its most abundant and ubiquitously expressed effector, and of its activated form, which is phosphorylated at residue S473.

To evaluated how activation of AKT1 is translated in downstream activity of the pathway, we also looked at the relative abundance of pc-RAF. c-RAF is a mediator of the MAPK/ERK pathway, which acts upstream of ERK, and whose activity can be regulated by AKT1, through phosphorylation of its residue S259, creating an anchoring motif that leads to its inhibition[288].

As the analysis depicted in Figure 3.37 (A, E) indicates, the overall abundance of AKT1 seems to be approximately the same in unwounded tissue. Upon wounding, and for the first 12h, the proportion of ATK1 between the species favors *A. cahirinus*, but becomes similar again at 24h. From then on, for timepoints day 3 and 5, the ratio between relative abundances favors *M. musculus*, but return to similar levels again by day 7 post wounding, through day 14. The activated form of AKT1 (pAKT1, Figure 3.37A, E), however, appears to be consistently more abundant in *Mus* than in *Acomys*, throughout all of the assessed timeframe.

Looking at the proportion of activated AKT1 (aAKT1) within, and between, both species (Figure 3.37B, G), we observe that in the uninjured tissue, and for the first 24h post wounding, there seems to be a much greater activation of AKT1 in *Mus*, peaking at around 12h. At day 3 post wounding, however, the relative level of aAKT1 seems to be similar between species, but by day 5 the previous trend resumes, with *Mus* exhibiting a higher proportion of aAKT1 which, nevertheless, appears to fall below or near the baseline comparison.

To understand whether this difference in aAKT1 levels could actually represent an increase in pathway activity, we decided to look at the relative abundance of pc-RAF, since this post-translational alteration is directly produced by activated AKT1, and therefore works as a readout of its activity.

As we can see in Figure 3.37F, the relative abundance of pc-RAF is superior in *Acomys* in homeostasis, and remains so during the first 6h after wounding. At 12h and 24h hours post wounding the relative abundance of this form of c-RAF becomes similar between species, but at day 3 the ratio favors *Acomys* again. From then on, however, the ratio of relative abundances clearly favors *Mus*.

When we look at the proportion of pAKT1 to pc-RAF (Figure 3.37C), we see that in *Acomys* this is relatively direct throughout the timeframe, with the ratio of relative protein abundance remaining approximately 1. In *Mus*, on the other hand, this ratio seems to indicate a much higher proportion of pAKT1 than pc-RAF in unwounded tissue, and during the first 24h post wounding (Figure 3.37C, G), with a clear peak in *Mus* at 6h post wounding. At day 5, however, and from then on, the ratio of this proportion between species approaches 1 (with the exception of timepoint day 7).

From these results, we conclude that despite a much higher relative abundance of pAKT1, and a higher proportion of aAKT1, during the first 24h post wounding, and in unwounded tissue, in *Mus*, this did not translate to a higher modification of c-RAF. This could suggest that there is a different regulation of AKT1 downstream targets, between *A. cahirinus* and *M. musculus*, at least in unwounded tissue and within the first 24h of wound healing, but which might become more similar by day 5 post wounding.

Besides looking at downstream regulation of the pathway, we also evaluated upstream activation. The major inhibitor in the PI3K/AKT pathway is PTEN, a dual phosphatase that dephosphorylates PIP_3, leading to a decrease in AKT recruitment to the cell membrane, and its activation. Phosphorylation of PTEN on its S380 residue increases the stability of PTEN, but also inhibits its activity, contributing to an increase in the activation levels of AKT1. To evaluate whether differential levels of pAKT1 between species could result from PTEN's activity, we decided to look at the relative abundance of its phosphorylated form (pPTEN).

As shown in Figure 3.37 (A, F), in uninjured tissue pPTEN is more abundant in *Mus* than in *Acomys*, but in the first 12 hours post wounding the relative abundance proportion between species is altered, with *Acomys* exhibiting higher levels of pPTEN. At 24h, however, this is reverted, and the relative abundance of pPTEN again becomes higher in *Mus*, for the remainder of the timeframe analyzed.

Comparing the ratio of pAKT1 to pPTEN within and between species (Figure 3.37D, G), we observed that this ratio is higher in *Mus* in unwounded tissue, as well as during the first 12h of

wound healing, with *Mus* exhibiting a particularly considerable peak in this ratio at 6h post wounding. From 24h post wounding up to 5 days, the ratio between species indicate similar proportions of pAKT1 to pPTEN, which return to values similar to those observed in *Acomys* unwounded tissues. At day 7, because pPTEN relative abundance increases but pAKT1 levels decrease, the ratio of this proportion again favors *Mus*, but by day 14 post wounding it is in clear favor of *Acomys*.

These results suggest that, at least during early wound response (within the first 12h), PTEN might not be the major regulator of AKT1 activation. While pPTEN levels should be directly proportional to pAKT1 levels, if this were the case, this proportionality is not always observed, in particular during the early response, which suggests that there could be two distinct phases of PI3K/AKT signaling regulation during wound healing, but also between species, as *Mus* seems to escape this proportionality more.

We have previously detailed how the MAPK/ERK and PI3K/AKT pathways are shared by several families of RTKs, with the one of the most prominent being the ERBB family, which can also interact with the JAK/STAT, and could therefore constitute a way for the cell to integrate the context of immune response into the regulation of proliferation[289].

Because this pathway showed considerable differences in effector and downstream target expression levels in our analysis of Gawriluk's data, we decided to also evaluate its activity during wound healing in these two species, focusing on JAK2 and STAT3 (which exists in two isoforms, α and β), two mediators which exhibited considerable differences between species in Gawriluk's data.

JAK2 is activated by phosphorylation at residues Y1007 and Y1008, and activated JAK2 can activate both isoforms of STAT3, phosphorylating them on residue Y705, so we decided to use antibodies against these altered forms of these mediators, besides antibodies capable of identifying all versions of each protein, to evaluate relative activation of each one.

Figure 3.38 (A, B) depicts the relative abundance of JAK2 and its activated form (pJAK2), and of STAT3 and its activated form (pSTAT3) (D). As observable, the relative abundance of JAK2 seems to be close between both species, but generally higher in *Acomys*. On the other hand, pJAK2 is consistently more abundant in *Acomys* than in *Mus*, including in uninjured tissue, where abundance of JAK2 is similar.

Figure 3.37 - Evaluation of PI3K/AKT signaling pathway activity through detection of post-translational modifications.
This figure represents the relative abundance of AKT1, pAKT1, pc-RAF and pPTEN, as detected through the Western Blot technique. Relative quantification (Rel. Quant). of protein abundance was performed by comparing signal intensity of each detected band with the signal of the most leftward band in each membrane (Aco 0h or Aco 3d). The two bands of c-RAF, as well as the smear in between, were considered as a single band in the relative quantification. A) Depiction of membrane signal detection for each isoform, at each timepoint, in A. cahirinus *and* M. musculus. *Also depicted are the values of relative quantification for each isoform of detected proteins. B) Evolution of the ratio between relative quantifications of pAKT1 and tAKT1 for each species. C, D) Evolution of the proportion between pAKT1 and C) pc-RAF and D) pPTEN for each species. E, F) Evolution of the ratio between species of E) AKT1 and pAKT1, and F) pc-RAF and pPTEN for all timepoints. G) Evolution of the ratio, between species, of the proportion of activated AKT1 (aAKT1), of the proportion of pAKT1 to pc-RAF, and of the proportion of pAKT1 to pPTEN. In figures E, F and G, red bars represent timepoints were the ratio between* A. cahirinus *and* M. musculus *values favor* M. musculus. *Yellow bars represent a ratio of approximately 1 (between 0,75 and 1,25) indicating similarity between species, and green bars represent a ratio that favors* A. cahirinus. *A, Aco* – Acomys cahirinus. *M, Mus* – Mus musculus. *pAKT1 – phosphorylated AKT1. tAKT1 – Total AKT1. pcRAF – phosphorylated c-RAF. pPTEN – phosphorylated PTEN. aAKT1 – pAKT1/tAKT1*

Looking at the ratio of activation of JAK2 (Figure 3.38C), while in unwounded tissue there is a considerably higher proportion of activated JAK2 in *Acomys* than in *Mus*, within the first 24h post wounding the levels of this proportion fall, in *Acomys*, well below the baseline, to levels almost similar to *Mus*. This trend is inverted by day 3 post wounding, where levels of aJAK2 raise, again to baseline levels in *Acomys* but not as greatly in *Mus*, and continue to raise in *Acomys* until day 5 post wounding. At day 7 they are again decreased in both species, with *Acomys* dipping below the baseline level and *Mus* returning to its, and by day 14 both have returned to baseline levels.

Looking at the ratio of aJAK2 between both species, despite variations in its levels within species, we observed that these are consistently higher in *Acomys* than in *Mus* (Figure 3.38F). To understand if this differential activation of JAK2 translated to differential activation of downstream effectors, we looked at the relative abundance of STAT3 and its activated version, pSTAT3.

The relative abundance of STAT3 in *Mus* and *Acomys* appears to be very similar between them in wounded tissue, except for the period around timepoints day 5 and 7 post wounding where it is higher in *Mus*, while in unwounded tissue and at day 14 post wounding the abundance of STAT3 appears to be higher in *Acomys* (Figure 3.38A, D).

Abundance of pSTAT3 appears to follow this trend in unwounded tissue and between 24h and 14 days post wounding (Figure 3.38A, D). However, during the first 12h after wounding we observed a decrease in the ratio of pSTAT3 abundance between the two species, suggesting a relative higher abundance in *Mus*.

Comparison of the proportion of activated STAT3 (aSTAT3, Figure 3.38E, F) between species confirmed the notion that there is higher activation of STAT3 in *Mus* at 6h and 12h post wounding, but overall, in unwounded and the remaining time course of wound healing, the proportion of activated STAT3 seems to be similar between species, with the exception of day 14, where it becomes higher in *Acomys*.

Since STAT3 can be directly activated by JAK2, we wondered whether the levels of aJAK2 had a direct proportion with aSTAT3 in both species. As we can see in Figure 3.38C, E and G, this is not the case. This ratio is much higher in *Acomys* unwounded tissue than it is *Mus*, reflecting the higher levels of aJAK2, but soon after wounding, and for the first 24h, the levels of aJAK2 decrease, or are kept low, in both species, while aSTAT3 levels increase.

Figure 3.38 - Evaluation of JAK/STAT signaling pathway activity through detection of post-translational modifications. This figure represents the relative abundance of JAK2, pJAK2, STAT3 and pSTAT3, as detected through the Western Blot technique. Relative quantification (Rel. Quant). of protein abundance was performed by comparing signal intensity of each detected band with the signal of the most leftward band in each membrane (Aco 0h or Aco 3d). For pSTAT3, where two bands were observed in each lane, they were treated as a single band, for the purposes of relative quantification. A) Depiction of membrane signal detection for each isoform, at each timepoint, in A. cahirinus *and* M. musculus. *Also depicted are the values of relative quantification for each isoform of detected proteins. B, D) Evolution of the ratio between species of B) pJAK2 and tJAK2, and D) pSTAT3 and tSTAT3. C, E) Evolution of the proportion of activated C) JAK2 and E) STAT3 in each species. F) Evolution of the ratio between species of aJAK2, aSTAT3 and of the ratio between aJAK2 and aSTAT3 G) Evolution of the ratio, within each species, of aJAK2 to aSTAT3. In figures B, D and F, red bars represent timepoints were the ratio between* A. cahirinus *and* M. musculus *values favor* M. musculus. *Yellow bars represent a ratio of approximately 1 (between 0,75 and 1,25) indicating similarity between species, and green bars represent a ratio that favors* A. cahirinus. *A, Aco* – Acomys cahirinus. *M, Mus* – Mus musculus. *pJAK2 – phosphorylated JAK2. tJAK2 – Total JAK2. pSTAT3 – phosphorylated STAT3. tSTAT3 – Total STAT3. aJAK – pJAK2/tJAK2. aSTAT3 –pSTAT3/tSTAT3.*

By day 3 post wounding this ratio is again increased, matching baseline levels in *Acomys* and increasing beyond that in *Mus*, but on day 5 they again decrease in both species, matching the values observed during the first 24h hours after wounding by day 7. Finally, at day 14 the levels increase again in both species, to near basal levels in *Mus* but not in *Acomys*. Despite these temporal dynamics, the ration between aJAK2 and aSTAT3 between both species is consistently higher in *Acomys* in unwounded and wounded tissue, except at day 7 post wounding where it becomes similar.

Together, these observations suggest that while regulation of STAT3 activity is similar between *A. cahirinus* and *M. musculus*, with the exception of the first 12h where it is slightly more activated in *Mus*, this activity does not directly relate with JAK2 activity levels. While JAK2 activation is consistently higher in *Acomys*, this does not translate to STAT3 activation. Furthermore, the proportion of activated JAK2 to activated STAT3 is consistently higher in *Acomys*, which suggests that JAK2 might play a role in other pathways.

As a brief summary, our observations on signaling pathway activity suggest that, not only are the levels of activity of each pathway distinct between species, but it is very plausible, specially following our observations on Gawriluk's data, that each of the pathways analyzed have distinct regulations between species, seeing as the relations between the same effectors are not necessarily preserved.

4. Discussion

In mammals, the most common response to wounding involves a strong inflammatory environment that leads to the formation of a fibrotic tissue that is incapable of fully functionally replacing the lost ones. However, a few examples of regeneration, epimorphic or otherwise, do exist in mammals[10], and these constitute great models to understand what transforms a wound healing response into a regenerative or fibrotic one.

Through our study of these models, and comparison with the known mechanisms that have been described in other vertebrates, we now have an idea of what contributes to the distinction between a regenerative and a fibrotic response to wounding in mammals. Processes like ECM assembly[13,710,713,1381], inflammatory response[709,711,712,1382] and activation of specific cell types[4] are now becoming established as the major contributors to the type of outcome to wound healing.

However, this last point in particular, and especially the mechanisms that contribute to a selective cell type activation, are still poorly understood. While recently it was shown that MAPK/ERK signaling is indispensable for mammalian regeneration, and increasing its activation can potentiate certain regenerative characteristics in an otherwise fibrotic wound healing response[4,1378], it appears that this by itself is not sufficient to fully divert a fibrotic wound healing process into a regenerative result. This means that a better understanding of the signaling pathways involved in these processes, and how they differ, is still required.

Because the capacity to proliferate underlines the regenerative potential of almost all vertebrate tissues[6–8,15,655], we decided to look for differences in the composition, regulation and activation, between two mammalian species, one associated with heightened regenerative potential (*Acomys cahirinus*), the other with fibrotic wound healing (*Mus musculus*), of other signaling pathways known to participate in regulation of proliferation in vertebrates.

We started our search by re-analyzing bulk transcriptomic data already published[13], in a seminal work that compared the wound healing responses of these two species in the same wound healing model, the full thickness circular punch to the ear pinna. Our analysis suggested that all the signaling pathways surveyed could be differentially setup between both species, in types of effectors and/or their stoichiometry, but the MAPK/ERK and PI3K/AKT, possibly because of their higher complexity, exhibited the highest degree of variation between both species.

These pathways are both intimately connected[812], so it makes sense that where a particular regulatory state of one has to be established for a particular result, the other must follow[1383]. To understand if the differential regulation, between species, of these, and other, pathways is really involved in regulating proliferation we performed our own transcriptomic analysis of these two wound healing models, but this time focusing on the transcriptomic profiles of their proliferative populations.

Our analysis of these transcriptomic profiles suggests several things, some of which confirm other observations already published, while other expand on them. It indicated that, for both species, there is a clear distinction between proliferation regulation during homeostasis and in response to wound healing, and this is particularly evident in *A. cahirinus*, where the number of DEGs detected was considerably higher than in *M. musculus*.

Furthermore, while these regulatory changes in *A. cahirinus* were mostly associated with positive regulation of gene expression, in *M. musculus* this was less evident, with the levels of positively and negatively regulated genes being more similar between them in the majority of surveyed timepoints. The differences we found in the DEGs, related to the MAPK/ERK and PI3K/AKT pathways, clearly indicate that the pathways that regulate proliferation in response to wound healing operate differently in each species.

Our analysis also suggested that there is less evolution of this differential regulation in *Mus* than in *Acomys*, with *Mus* taking longer to distinguish its wound-responsive transcriptional profile from its profile in homeostasis, and less to return to the proliferative profile observed in unwounded tissue. This was to be expected, seeing as *M. musculus* is incapable of sustaining cell cycle progression like *A. cahirinus* does. Furthermore, processes involved in response to wounding are more preserved in *M. musculus* than in *A. cahirinus*, which likely correlates with the inferior regenerative capacity of *M. musculus*.

These expression dynamics are likely associated with an earlier differentiation of proliferative cells in *M. musculus*. Indeed, a more 'fetal' profile of some cell types has been associated with a higher regenerative potential in mammals[4]. This is also reflected in the processes most significantly associated with the expression profiles of proliferative cells of each species, during wound healing, with *A. cahirinus*'s exhibiting a considerable association with processes pertaining with metabolic regulation, likely required to support the more sustained proliferative behavior of these cells, while *Mus*'s associated with more terms pertaining to development of several tissues.

To understand how these different processes are setup, in response to what are, mostly, similar stimuli, we looked at which signaling pathways associated with the transcription profiles of proliferative cells in each species, during the surveyed period of wound healing. In *A. cahirinus* we found a clear association, throughout the whole time course, with mitochondrial metabolism pathways, with high significance, which was not found in *M. musculus*.

We also found that, as expected, a great proportion of the most significant pathway associations in *A. cahirinus* involved pathways pertaining to proliferation and cell cycle. In *M. musculus*, however, these associations were more heterogeneous, with less prevalence of cell cycle-related pathways and more pertaining with intracellular dynamics, possibly linked to migration. Furthermore, two timepoints in *M. musculus* (day 3 and 14 post wounding) did not have significant associations with any specific group of pathways, further supporting our observation that the departure from the regulatory profile of proliferation during homeostasis is less extensive, and much more transient, in *M. musculus* than in *A. cahirinus*.

We then decided to focus our analysis of pathway association on pathways that are known to participate in proliferation regulation, particularly downstream of RTK signaling. While we found associations with a few distinct signaling pathways for *A. cahirinus*, namely MAPK/ERK, PI3K/AKT, WNT and NF-κB, we only found association with MAPK/ERK signaling in *M. musculus*, and then just at day 5 post wounding, suggesting a very transient differential regulation of genes associated with this signaling pathway, and with proliferation regulation in general.

Despite the different associations to signaling pathways, when we looked at expression dynamics of the DEGs associated with these pathways, we observed that, common to both species, these could be organized in three distinct patterns of behavior. One group of genes had higher expression in proliferative cell populations of unwounded tissue, and consistently lower during response to wounding, indicating that these genes are specific of proliferation regulation during homeostasis, but might be contradictory to proliferation in response to wounding. Associated with this expression profile in *A. cahirinus*, we found genes that associated with the MAPK/ERK signaling, possibly influencing expression regulation through an alternative mechanism to IEGs, while the genes that exhibited this behavior in *M. musculus* did not significantly associate with any signaling pathway or transcription factor regulation.

A second group of DEGs was detected has having a higher expression in the earlier timepoints after wounding, around day 3 and 5, which coincides with the inflammatory phase of wound

healing[7,20,43,632]. While this group of genes associated, very interestingly, in *A. cahirinus*, with cytokine signaling and expression regulation by IEGs, which suggests that in *A. cahirinus* early proliferation induction in response to wounding might be controlled by a crosstalk with the immune system, in *M. musculus* the DEGs with this behavior associated with signaling through ERBB, which could indicate a higher proportion of epithelial cells in the proliferative population, thus having less representation of mesenchymal cell types, which would make sense with the absence of a blastema formation in *M. musculus*.

The final group of genes exhibited an expression profile with a later peak of expression during our time course, in day 14 post wounding in *A. cahirinus* and day 7 post wounding in *M. musculus*. The DEGs with this profile associated, in *A. cahirinus*, with RTK signaling, possibly in response to PDGF stimulation, which might signal through several intracellular signaling pathways[1384], while in *M. musculus* it also associated with RTK downstream signaling, but only through MAPK/ERK. These DEGs also associated with regulation by some of the same transcription factors, namely FOXO1 and GATA6, but also with regulation by distinct transcription factors, possibly explaining why proliferation, despite involving similar signaling pathways, is differentially regulated.

The fact that these "late response" genes have an anticipated peak of expression in *M. musculus*, in association with the fact that several of the DEGs belonging to the first group recover to baseline levels of expression by day 14 in this species, further supports our interpretation that proliferative cells in wounded tissue of *M. musculus* return to a homeostatic regulatory profile sooner than in *A. cahirinus*, likely because of an early differentiation. This links with the recent observation that there is a convergence of epigenetic regulation of regeneration-associated genes around day 7, between fibrosis-associated and regeneration-associated fibroblasts in a mammalian model[4], but this convergence is dissipated by day 14 post wounding.

To understand how processes associated with some of the same signaling pathways could lead to such distinctive results to wound healing events, we analyzed how pathway activity differed between both species, for some of the pathways previously analyzed and associated with proliferation regulation in these models.

Our analysis of the activity of MAPK/ERK signaling, which has already been shown to participate in the decision between regenerative and fibrotic results to mammalian wound healing[4,1378], showed that the proportion of ERK isoforms (ERK1 and ERK2) is not identical in both species, with *M. musculus* exhibiting a preference for ERK1 during homeostasis, which

tends to increase during wounding, while *A. cahirinus* appears to have a more stable proportion of isoforms.

Curiously, while *M. musculus* tends to maintain a proportion between activated isoforms, suggesting that MAPK/ERK activation in this species, in this context, equally stimulates both isoforms, both in unwounded and wounded tissue, this is not the case for *A. cahirinus*, which seems to have a preference for ERK2 phosphorylation.

However, when we look at the temporal dynamics of isoform activation, while the proportion of activated protein of both isoforms seems to follow the same activation profile in *A. cahirinus*, with a peak of activation at 6h that returns to baseline between 24h and 3 days post wounding, this only occurs for ERK1 in *M. musculus*, with ERK2 exhibiting a 6h delay its dynamics.

This results in higher aERK2 at 6h in *A. cahirinus*, perhaps anticipating important regulatory changes for the setup of a proliferative population. This higher proportion of activated isoforms in *A. cahirinus* was also observed at 24h and 3 days post wound for ERK1, and at 3 days post wounding for ERK2, suggesting that it is around the day 3 mark, around the peak of the inflammatory phase, that a greater distinction in MAPK/ERK signaling activation is established, thus leading to subsequent differential regulation of proliferation. This higher proportion of activation of both isoforms in *A. cahirinus* was also observed at 14 days post wounding, which correlates nicely with the observation that at this time *M. musculus* already has fewer proliferative cells completing the cell cycle[13].

Our work leads us to propose that the MAPK/ERK signaling pathway is not equally setup between both species, as we suggested with the re-analysis of Gawriluk's transcriptomic data[13] and observed in the relative quantification of protein isoform abundance, nor does it have the same activity dynamics in response to wounding, or preference for isoform activation. All of these differences could explain why, despite both species activating this pathway in response to wounding, only in *A. cahirinus* is this performed in an appropriate fashion for a regenerative response.

Moving on to the PI3K/AKT pathway, despite knowledge of its involvement in the regeneration of some tissues, in vertebrates and invertebrates[1385–1388], its contribution to epimorphic regeneration in mammals has not yet been clearly established. The PI3K/AKT pathway is known to operate downstream of many of the same receptor families as the MAPK/ERK pathway, and to establish several regulatory interactions with it[812,1383,1384].

We therefore decided to look at how the activity of this pathway compared between species, and whether it could have a synergistic effect on proliferation. Curiously, that might not be the case, at least in both species. While we saw a clear activation of this pathway in *M. musculus* in the early response to wounding (in the first 24h), this was not the case for *A. cahirinus*, which even exhibited a lower proportion of activated AKT1 through most of the surveyed timeframe.

M. musculus also exhibited higher AKT1 activation in unwounded tissue, despite the relative levels of this protein being similar between both species, which could indicate a pre-established alternative regulation and function of this pathway. Curiously, when we looked at how activation of AKT1 in both species resulted in modifications to downstream targets, we found a slightly higher proportion of pc-RAF in *A. cahirinus* unwounded tissue than in *M. musculus*. This was more or less sustained for the first 3 days after wounding, period in which we see a sharp increase in aAKT1 in *M. musculus*.

This suggests that AKT1 in *M. musculus* might have different functions during the early response to wounding, or be regulated differently, but from day 3 onwards the relations AKT1 establishes with other mediators of PI3K/AKT signaling seem to be similar between both species. This differential role could be involved with the prevention of apoptosis in *M. musculus*, which can be controlled by the PI3K/AKT pathway[1389], and has been shown to be important for regeneration and cell proliferation in some contexts[1390]. Indeed, our GSEA for terms related with apoptosis identified several in *A. cahirinus*, but none in *M. musculus*, suggesting that regulation of apoptosis in response to wounding differs between these two species. We tried to further confirm if differences in apoptotic processes existed between the two species through western blot and immunofluorescence detection, but were unsuccessful.

Finally, because it has been associated with regeneration, proliferation and stem cell maintenance in several contexts[395,1386,1391–1393], and has been shown to be activated by some of the same receptors, namely RTKs, as the two previous pathways[827,1386,1394], with which it might even establish some interactions, we decided to also look at the activity of the JAK/STAT pathway, since it could constitute an integrator of immune signaling in the regulation of proliferation in this context.

What we found was that, despite similar levels of JAK2 in unwounded tissue, its activation is already higher in *A. cahirinus*. This contrast of activity is kept throughout the whole response to wounding, despite initially, within the first 24h, there being a sharp decrease in the proportion of activated JAK2 in *A. cahirinus*, which increases again by day 3 and day 5 post wounding,

during the peak of the inflammatory phase. A slight increase in aJAK2 in *M. musculus* was also observed around day 3, while by day 7, towards the end of the inflammatory phase, both species showed again a decrease in aJAK2 levels. By day 14, these levels had returned to baseline in *A. cahirinus*, but not in *M. musculus*.

These observations suggest that JAK2 activity might not be solely controlled by immune signals in unwounded tissue of *A. cahirinus* and by day 14 post wounding, but otherwise seem to relate with the inflammatory phase of wound healing. Furthermore, activation levels of JAK2 were consistently higher in *A. cahirinus*.

To determine whether this translated to downstream activation of the JAK/STAT pathway, we analyzed the levels of activated STAT3, and found that while the levels of pSTAT3 are higher in unwounded tissue in *A. cahirinus*, this is not the case for most timepoints during the wound healing responses, particularly during the first 12 hours, where the proportion of activated STAT3 is higher in *M. musculus*.

However, during this initial response, the proportion of aJAK2 does not follow this trend of aSTAT3, in either species, suggesting that STAT3 activity might not be, at least fully, regulated by JAK2. Furthermore, when we looked at the ratio between aJAK2 and aSTAT3, we observed that this was consistently higher in *A. cahirinus*, and was the highest in unwounded tissue, and then again by day 3 post wounding, with another, smaller increase by day 14. This could indicate that JAK2 has two distinct modes of activation, one relating with inflammatory cues and the other not, but that its activity is not primarily directed at STAT activation.

Indeed, JAK2 is known to be able to activate ERBB receptors[826,827], mimicking ligand stimulation or synergizing with it, leading to the activation of other signaling pathways that operate downstream of RTK receptors. It would, therefore, be interesting to know if inhibition of JAK2 activity interferes with the activity of the other analyzed pathways, and whether it has an impact on the overall result of wound healing.

Equally interesting would be to have an overview of the activity of the other signaling pathways we detected in our GSEA, namely the WNT and NF-κB pathways. Unfortunately, we were unable to detect GSK3β through Western Blot, and our immunofluorescent attempts at detecting β-Catenin subcellular localization also did not yield clear results. We were, however, able to detect the NF-κB component RELA through Western Blot (data not shown), but in *A. cahirinus* this took the form of a very small sized peptide which has not been previously described, so we could not conclude anything from these results. It would also be interesting to

correlate the activation dynamics we saw with the proliferative state of cells in each tissue, which we also attempted to do through immunofluorescence, but were unable to obtain clear results from.

In conclusion, our results indicate that the differential ability, observed between *A. cahirinus* and *M. musculus*, to sustain proliferation is connected to their capacity to distance their regulation of proliferation from that established in homeostasis. This distancing involves the activity of several pathways, namely the previously described MAPK/ERK, but also PI3K/AKT, JAK/STAT, and likely WNT and NF-κB, which our results suggest to be differentially setup between these two species, with altered proportions of several mediators. These differences would explain the different activation in response to similar stimuli, and would result in the differential regulation of proliferation already described. Further understanding of the activity of these pathways during wound healing, and their influence in regulation of proliferation in mammals, is required.

This page was intentioally left blank

5. References

1. Morgan, T. H. *Regeneration, by Thomas Hunt Morgan ...* (The Macmillan Company;, New York, 1901). doi:10.5962/bhl.title.1114.

2. Seifert, A. W. *et al.* The influence of fundamental traits on mechanisms controlling appendage regeneration. *Biological Reviews* **87**, 330–345 (2012).

3. Kierdorf, U., Kierdorf, H. & Szuwart, T. Deer antler regeneration: Cells, concepts, and controversies. *J Morphol* **268**, 726–738 (2007).

4. Sinha, S. *et al.* Fibroblast inflammatory priming determines regenerative versus fibrotic skin repair in reindeer. *Cell* **185**, 4717-4736.e25 (2022).

5. Seifert, A. W. & Muneoka, K. The blastema and epimorphic regeneration in mammals. *Dev Biol* **433**, (2018).

6. Brockes, J. P. & Kumar, A. Comparative Aspects of Animal Regeneration. (2008) doi:10.1146/annurev.cellbio.24.110707.175336.

7. Murawala, P., Tanaka, E. M. & Currie, J. D. Regeneration: The ultimate example of wound healing. *Seminars in Cell and Developmental Biology* vol. 23 954–962 Preprint at https://doi.org/10.1016/j.semcdb.2012.09.013 (2012).

8. Tanaka, E. M. & Reddien, P. W. The Cellular Basis for Animal Regeneration. *Developmental Cell* vol. 21 172–185 Preprint at https://doi.org/10.1016/j.devcel.2011.06.016 (2011).

9. Agata, K., Saito, Y. & Nakajima, E. Unifying principles of regeneration I: Epimorphosis versus morphallaxis. *Development Growth and Differentiation* vol. 49 73–78 Preprint at https://doi.org/10.1111/j.1440-169X.2007.00919.x (2007).

10. Seifert, A. W. & Muneoka, K. The blastema and epimorphic regeneration in mammals. *Developmental Biology* vol. 433 190–199 Preprint at https://doi.org/10.1016/j.ydbio.2017.08.007 (2018).

11. Tsonis, P. A., Madhavan, M., Tancous, E. E. & Del Rio-Tsonis, K. A newt's eye view of lens regeneration. *International Journal of Developmental Biology* vol. 48 975–980 Preprint at https://doi.org/10.1387/ijdb.041867pt (2004).

12. Lepilina, A. *et al.* A Dynamic Epicardial Injury Response Supports Progenitor Cell Activity during Zebrafish Heart Regeneration. *Cell* **127**, 607–619 (2006).

13. Gawriluk, T. R. *et al.* Comparative analysis of ear-hole closure identifies epimorphic regeneration as a discrete trait in mammals. *Nat Commun* **7**, (2016).

14. Seifert, A. W. & Maden, M. New insights into vertebrate skin regeneration. in *International Review of Cell and Molecular Biology* vol. 310 129–169 (Elsevier Inc., 2014).

15. Khyeam, S., Lee, S. & Huang, G. N. Genetic, epigenetic, and post-transcriptional basis of divergent tissue regenerative capacities among vertebrates. *Advanced Genetics* **2**, (2021).

16. Bely, A. E. & Nyberg, K. G. Evolution of animal regeneration: re-emergence of a field. *Trends Ecol Evol* **25**, 161–170 (2010).

17. Daponte, V., Tylzanowski, P. & Forlino, A. Appendage Regeneration in Vertebrates: What Makes This Possible? *Cells* **10**, 242 (2021).

18. Joven, A., Elewa, A. & Simon, A. Model systems for regeneration: salamanders. *Development* **146**, (2019).

19. Gemberling, M., Bailey, T. J., Hyde, D. R. & Poss, K. D. The zebrafish as a model for complex tissue regeneration. *Trends in Genetics* **29**, 611–620 (2013).

20. Rodrigues, M., Kosaric, N., Bonham, C. A. & Gurtner, G. C. Wound Healing: A Cellular Perspective. *Physiol Rev* **99**, 665–706 (2019).

21. Nurden, A. T., Nurden, P., Sanchez, M., Andia, I. & Anitua, E. *Platelets and Wound Healing*. *Frontiers in Bioscience* vol. 13 (2008).

22. Sang, Y., Roest, M., de Laat, B., de Groot, P. G. & Huskens, D. Interplay between platelets and coagulation. *Blood Reviews* vol. 46 Preprint at https://doi.org/10.1016/j.blre.2020.100733 (2021).

23. Margraf, A. & Zarbock, A. Platelets in Inflammation and Resolution. *The Journal of Immunology* **203**, 2357–2367 (2019).

24. Sarratt, K. L. *et al.* GPVI and α2β1 play independent critical roles during platelet adhesion and aggregate formation to collagen under flow. *Blood* **106**, 1268–1277 (2005).

25. Savage, B., Saldívar, E. & Ruggeri, Z. M. Initiation of Platelet Adhesion by Arrest onto Fibrinogen or Translocation on von Willebrand Factor. *Cell* **84**, 289–297 (1996).

26. Jackson, S. P., Nesbitt, W. S. & Kulkarni, S. Signaling events underlying thrombus formation. *Journal of Thrombosis and Haemostasis* **1**, 1602–1612 (2003).

27. Obergfell, A. *et al.* Coordinate interactions of Csk, Src, and Syk kinases with αIIbβ3 initiate integrin signaling to the cytoskeleton. *J Cell Biol* **157**, 265–275 (2002).

28. Golebiewska, E. M. & Poole, A. W. Platelet secretion: From haemostasis to wound healing and beyond. *Blood Rev* **29**, 153–162 (2015).

29. Pryzdial, E. L. G. *et al.* Blood coagulation dissected. *Transfusion and Apheresis Science* **57**, 449–457 (2018).

30. Starke, K. & Br, F. I. *The Vascular Endothelium II*. vol. 176/II (Springer Berlin Heidelberg, Berlin, Heidelberg, 2006).

31. Sims, P. J. & Wiedmer, T. Unraveling the mysteries of phospholipid scrambling. *Thromb Haemost* **86**, 266–75 (2001).

32. Rapaport, S. I. & Rao, L. V. The tissue factor pathway: how it has become a 'prima ballerina'. *Thromb Haemost* **74**, 7–17 (1995).

33. Butenas, S. Tissue Factor Structure and Function. *Scientifica (Cairo)* **2012**, 1–15 (2012).

34. Zarbock, A., Polanowska-Grabowska, R. K. & Ley, K. Platelet-neutrophil-interactions: Linking hemostasis and inflammation. *Blood Rev* **21**, 99–111 (2007).

35. Arenas Gómez, C. M., Sabin, K. Z. & Echeverri, K. Wound healing across the animal kingdom: Crosstalk between the immune system and the extracellular matrix. *Developmental Dynamics* **249**, 834–846 (2020).

36. Szpaderska, A. M., Egozi, E. I., Gamelli, R. L. & DiPietro, L. A. The Effect of Thrombocytopenia on Dermal Wound Healing. *Journal of Investigative Dermatology* **120**, 1130–1137 (2003).

37. Etulain, J. Platelets in wound healing and regenerative medicine. *Platelets* **29**, 556–568 (2018).

38. Nurden, A. Platelets, inflammation and tissue regeneration. *Thromb Haemost* **105**, S13–S33 (2011).

39. Gawaz, M. & Vogel, S. Blood Spotlight Platelets in tissue repair: control of apoptosis and interactions with regenerative cells. (2013) doi:10.1182/blood-2013-05.

40. Moore, A. L. *et al.* Scarless wound healing: Transitioning from fetal research to regenerative healing. *Wiley Interdisciplinary Reviews: Developmental Biology* vol. 7 Preprint at https://doi.org/10.1002/wdev.309 (2018).

41. Larson, B. J., Longaker, M. T. & Lorenz, H. P. Scarless Fetal Wound Healing: A Basic Science Review. *Plast Reconstr Surg* **126**, 1172–1180 (2010).

42. Olutoye, O. O., Yager, D. R., Cohen, I. K. & Diegelmann, R. F. Lower cytokine release by fetal porcine platelets: A possible explanation for reduced inflammation after fetal wounding. *J Pediatr Surg* **31**, 91–95 (1996).

43. Olutoye, O. O., Barone, E. J., Yager, D. R., Cohen, I. K. & Diegelmann, R. F. Collagen induces cytokine release by fetal platelets: Implications in scarless healing. *J Pediatr Surg* **32**, 827–830 (1997).

44. Haynes, J. H. *et al.* Platelet-derived growth factor induces fetal wound fibrosis. *J Pediatr Surg* **29**, 1405–1408 (1994).

45. Krummel, T. M. *et al.* Transforming growth factor beta (TGF-β) induces fibrosis in a fetal wound model. *J Pediatr Surg* **23**, 647–652 (1988).

46. Moretti, L., Stalfort, J., Barker, T. H. & Abebayehu, D. The interplay of fibroblasts, the extracellular matrix, and inflammation in scar formation. *Journal of Biological Chemistry* vol. 298 Preprint at https://doi.org/10.1016/j.jbc.2021.101530 (2022).

47. Brown, A. C. *et al.* Fibrin Network Changes in Neonates after Cardiopulmonary Bypass. *Anesthesiology* **124**, 1021–1031 (2016).

48. Charlemagne, J. Aspects morphologiques de la différenciation des éléments sanguins chez l'Axolotl,Ambystoma mexicanum Shaw. *Zeitschrift für Zellforschung und Mikroskopische Anatomie* **123**, 224–239 (1971).

49. Chiu, I. M., von Hehn, C. A. & Woolf, C. J. Neurogenic inflammation and the peripheral nervous system in host defense and immunopathology. *Nat Neurosci* **15**, 1063–1067 (2012).

50. Aubdool, A. A. & Brain, S. D. Neurovascular Aspects of Skin Neurogenic Inflammation. *Journal of Investigative Dermatology Symposium Proceedings* **15**, 33–39 (2011).

51. Granstein, R. D., Wagner, J. A., Stohl, L. L. & Ding, W. Calcitonin gene-related peptide: key regulator of cutaneous immunity. *Acta Physiologica* **213**, 586–594 (2015).

52. Rosa, A. C. & Fantozzi, R. The role of histamine in neurogenic inflammation. *Br J Pharmacol* **170**, 38–45 (2013).

53. Golebiewska, E. M. & Poole, A. W. Platelet secretion: From haemostasis to wound healing and beyond. *Blood Rev* **29**, 153–162 (2015).

54. Anitua, E., Andia, I., Ardanza, B., Nurden, P. & Nurden, A. Autologous platelets as a source of proteins for healing and tissue regeneration. *Thromb Haemost* **91**, 4–15 (2004).

55. von Hundelshausen, P. *et al.* Heterophilic interactions of platelet factor 4 and RANTES promote monocyte arrest on endothelium. *Blood* **105**, 924–930 (2005).

56. Kasper, B., Brandt, E., Ernst, M. & Petersen, F. Neutrophil adhesion to endothelial cells induced by platelet factor 4 requires sequential activation of Ras, Syk, and JNK MAP kinases. *Blood* **107**, 1768–1775 (2006).

57. Weyrich, A. S., McIntyre, T. M., McEver, R. P., Prescott, S. M. & Zimmerman, G. A. Monocyte tethering by P-selectin regulates monocyte chemotactic protein-1 and tumor necrosis factor-alpha secretion. Signal integration and NF-kappa B translocation. *Journal of Clinical Investigation* **95**, 2297–2303 (1995).

58. Blanks, J. E., Moll, T., Eytner, R. & Vestweber, D. Stimulation of P-selectin glycoprotein ligand-1 on mouse neutrophils activates β2 -integrin mediated cell attachment to ICAM-1. *Eur J Immunol* **28**, 433–443 (1998).

59. Carvalho-Tavares, J. *et al.* A Role for Platelets and Endothelial Selectins in Tumor Necrosis Factor-α–Induced Leukocyte Recruitment in the Brain Microvasculature. *Circ Res* **87**, 1141–1148 (2000).

60. Gear, A. R. L. & Camerini, D. Platelet Chemokines and Chemokine Receptors: Linking Hemostasis, Inflammation, and Host Defense. *Microcirculation* **10**, 335–350 (2003).

61. Tamagawa-Mineoka, R. Important roles of platelets as immune cells in the skin. *J Dermatol Sci* **77**, 93–101 (2015).

62. Nami, N. *et al.* Crosstalk between platelets and PBMC: New evidence in wound healing. *Platelets* 1–6 (2015) doi:10.3109/09537104.2015.1048216.

63. Kolaczkowska, E. & Kubes, P. Neutrophil recruitment and function in health and inflammation. *Nature Reviews Immunology* vol. 13 159–175 Preprint at https://doi.org/10.1038/nri3399 (2013).

64. Mantovani, A., Cassatella, M. A., Costantini, C. & Jaillon, S. Neutrophils in the activation and regulation of innate and adaptive immunity. *Nature Reviews Immunology* vol. 11 519–531 Preprint at https://doi.org/10.1038/nri3024 (2011).

65. Fournier, B. M. & Parkos, C. A. The role of neutrophils during intestinal inflammation. *Mucosal Immunol* **5**, 354–366 (2012).

66. Su, Y. & Richmond, A. Chemokine Regulation of Neutrophil Infiltration of Skin Wounds. *Adv Wound Care (New Rochelle)* **4**, 631–640 (2015).

67. Ridiandries, A., Tan, J. & Bursill, C. The Role of Chemokines in Wound Healing. *Int J Mol Sci* **19**, 3217 (2018).

68. Summers, C. *et al.* Neutrophil kinetics in health and disease. *Trends Immunol* **31**, 318–324 (2010).

69. Kim, M.-H. *et al.* Dynamics of Neutrophil Infiltration during Cutaneous Wound Healing and Infection Using Fluorescence Imaging. *Journal of Investigative Dermatology* **128**, 1812–1820 (2008).

70. Su, Y. & Richmond, A. Chemokine Regulation of Neutrophil Infiltration of Skin Wounds. *Adv Wound Care (New Rochelle)* **4**, 631–640 (2015).

71. Cua, D. J. & Tato, C. M. Innate IL-17-producing cells: the sentinels of the immune system. *Nat Rev Immunol* **10**, 479–489 (2010).

72. Ng, L. G. *et al.* Visualizing the Neutrophil Response to Sterile Tissue Injury in Mouse Dermis Reveals a Three-Phase Cascade of Events. *Journal of Investigative Dermatology* **131**, 2058–2068 (2011).

73. Christoffersson, G. *et al.* VEGF-A recruits a proangiogenic MMP-9–delivering neutrophil subset that induces angiogenesis in transplanted hypoxic tissue. *Blood* **120**, 4653–4662 (2012).

74. Kubes, P. The enigmatic neutrophil: what we do not know. *Cell and Tissue Research* vol. 371 399–406 Preprint at https://doi.org/10.1007/s00441-018-2790-5 (2018).

75. Fridlender, Z. G. *et al.* Polarization of Tumor-Associated Neutrophil Phenotype by TGF-β: "N1" versus "N2" TAN. *Cancer Cell* **16**, 183–194 (2009).

76. Denny, M. F. *et al.* A Distinct Subset of Proinflammatory Neutrophils Isolated from Patients with Systemic Lupus Erythematosus Induces Vascular Damage and Synthesizes Type I IFNs. *The Journal of Immunology* **184**, 3284–3297 (2010).

77. Shaul, M. E. *et al.* Tumor-associated neutrophils display a distinct N1 profile following TGFβ modulation: A transcriptomics analysis of pro- vs. antitumor TANs. *Oncoimmunology* **5**, e1232221 (2016).

78. Soehnlein, O. & Lindbom, L. Neutrophil-derived azurocidin alarms the immune system. *J Leukoc Biol* **85**, 344–351 (2009).

79. Soehnlein, O. *et al.* Neutrophil secretion products pave the way for inflammatory monocytes. *Blood* **112**, 1461–1471 (2008).

80. Hurst, S. M. *et al.* IL-6 and Its Soluble Receptor Orchestrate a Temporal Switch in the Pattern of Leukocyte Recruitment Seen during Acute Inflammation. *Immunity* **14**, 705–714 (2001).

81. Cantürk, N. Z. *et al.* The Relationship between Neutrophils and Incisional Wound Healing. *Skin Pharmacol Physiol* **14**, 108–116 (2001).

82. Puga, I. *et al.* B cell–helper neutrophils stimulate the diversification and production of immunoglobulin in the marginal zone of the spleen. *Nat Immunol* **13**, 170–180 (2012).

83. Pelletier, M. *et al.* Evidence for a cross-talk between human neutrophils and Th17 cells. *Blood* **115**, 335–343 (2010).

84. Abi Abdallah, D. S., Egan, C. E., Butcher, B. A. & Denkers, E. Y. Mouse neutrophils are professional antigen-presenting cells programmed to instruct Th1 and Th17 T-cell differentiation. *Int Immunol* **23**, 317–326 (2011).

85. Duffy, D. *et al.* Neutrophils Transport Antigen from the Dermis to the Bone Marrow, Initiating a Source of Memory CD8+ T Cells. *Immunity* **37**, 917–929 (2012).

86. Tillack, K., Breiden, P., Martin, R. & Sospedra, M. T Lymphocyte Priming by Neutrophil Extracellular Traps Links Innate and Adaptive Immune Responses. *The Journal of Immunology* **188**, 3150–3159 (2012).

87. Ellis, T. N. & Beaman, B. L. Murine polymorphonuclear neutrophils produce interferon-gamma in response to pulmonary infection with Nocardia asteroides. *J Leukoc Biol* **72**, 373–81 (2002).

88. Yin, J. & Ferguson, T. A. Identification of an IFN-γ-Producing Neutrophil Early in the Response to *Listeria monocytogenes*. *The Journal of Immunology* **182**, 7069–7073 (2009).

89. Wilgus, T. A., Roy, S. & McDaniel, J. C. Neutrophils and Wound Repair: Positive Actions and Negative Reactions. *Adv Wound Care (New Rochelle)* **2**, 379–388 (2013).

90. Cauwe, B., Martens, E., Proost, P. & Opdenakker, G. Multidimensional degradomics identifies systemic autoantigens and intracellular matrix proteins as novel gelatinase B/MMP-9 substrates. *Integrative Biology* **1**, 404 (2009).

91. Segel, G. B., Halterman, M. W. & Lichtman, M. A. The paradox of the neutrophil's role in tissue injury. *J Leukoc Biol* **89**, 359–372 (2011).

92. Serhan, C. N. Novel Lipid Mediators and Resolution Mechanisms in Acute Inflammation. *Am J Pathol* **177**, 1576–1591 (2010).

93. Serhan, C. N., Chiang, N. & Van Dyke, T. E. Resolving inflammation: dual anti-inflammatory and pro-resolution lipid mediators. *Nat Rev Immunol* **8**, 349–361 (2008).

94. Schwab, J. M., Chiang, N., Arita, M. & Serhan, C. N. Resolvin E1 and protectin D1 activate inflammation-resolution programmes. *Nature* **447**, 869–874 (2007).

95. Spite, M. *et al.* Resolvin D2 is a potent regulator of leukocytes and controls microbial sepsis. *Nature* **461**, 1287–1291 (2009).

96. Serhan, C. N. *et al.* Maresins: novel macrophage mediators with potent antiinflammatory and proresolving actions. *Journal of Experimental Medicine* **206**, 15–23 (2009).

97. Arita, M. *et al.* Resolvin E1 Selectively Interacts with Leukotriene B4 Receptor BLT1 and ChemR23 to Regulate Inflammation. *The Journal of Immunology* **178**, 3912–3917 (2007).

98. Ariel, A. *et al.* Apoptotic neutrophils and T cells sequester chemokines during immune response resolution through modulation of CCR5 expression. *Nat Immunol* **7**, 1209–1216 (2006).

99. McKimmie, C. S. *et al.* Hemopoietic Cell Expression of the Chemokine Decoy Receptor D6 Is Dynamic and Regulated by GATA1. *The Journal of Immunology* **181**, 3353–3363 (2008).

100. Bourke, E. *et al.* IL-1β Scavenging by the Type II IL-1 Decoy Receptor in Human Neutrophils. *The Journal of Immunology* **170**, 5999–6005 (2003).

101. Bazzoni, F., Tamassia, N., Rossato, M. & Cassatella, M. A. Understanding the molecular mechanisms of the multifaceted IL-10-mediated anti-inflammatory response: Lessons from neutrophils. *Eur J Immunol* **40**, 2360–2368 (2010).

102. Fox, S., Leitch, A. E., Duffin, R., Haslett, C. & Rossi, A. G. Neutrophil Apoptosis: Relevance to the Innate Immune Response and Inflammatory Disease. *J Innate Immun* **2**, 216–227 (2010).

103. Soehnlein, O. & Lindbom, L. Phagocyte partnership during the onset and resolution of inflammation. *Nat Rev Immunol* **10**, 427–439 (2010).

104. Willenborg, S. & Eming, S. A. Macrophages – sensors and effectors coordinating skin damage and repair. *JDDG: Journal der Deutschen Dermatologischen Gesellschaft* **12**, 214–221 (2014).

105. Silva, M. T. When two is better than one: macrophages and neutrophils work in concert in innate immunity as complementary and cooperative partners of a myeloid phagocyte system. *J Leukoc Biol* **87**, 93–106 (2009).

106. Shapouri-Moghaddam, A. *et al.* Macrophage plasticity, polarization, and function in health and disease. *Journal of Cellular Physiology* vol. 233 6425–6440 Preprint at https://doi.org/10.1002/jcp.26429 (2018).

107. Sica, A. & Mantovani, A. Macrophage plasticity and polarization: in vivo veritas. *Journal of Clinical Investigation* **122**, 787–795 (2012).

108. Murray, P. J. Macrophage Polarization. *Annu Rev Physiol* **79**, 541–566 (2017).

109. Biswas, S. K., Chittezhath, M., Shalova, I. N. & Lim, J.-Y. Macrophage polarization and plasticity in health and disease. *Immunol Res* **53**, 11–24 (2012).

110. Locati, M., Mantovani, A. & Sica, A. Macrophage Activation and Polarization as an Adaptive Component of Innate Immunity. in 163–184 (2013). doi:10.1016/B978-0-12-417028-5.00006-5.

111. Murray, P. J. & Wynn, T. A. Protective and pathogenic functions of macrophage subsets. *Nat Rev Immunol* **11**, 723–737 (2011).

112. Wang, N., Liang, H. & Zen, K. Molecular Mechanisms That Influence the Macrophage M1â€“M2 Polarization Balance. *Front Immunol* **5**, (2014).

113. Mantovani, A. *et al.* The chemokine system in diverse forms of macrophage activation and polarization. *Trends Immunol* **25**, 677–686 (2004).

114. Das, A. *et al.* Monocyte and Macrophage Plasticity in Tissue Repair and Regeneration. *Am J Pathol* **185**, 2596–2606 (2015).

115. Porta, C., Riboldi, E., Ippolito, A. & Sica, A. Molecular and epigenetic basis of macrophage polarized activation. *Semin Immunol* **27**, 237–248 (2015).

116. Kurowska-Stolarska, M. *et al.* IL-33 Amplifies the Polarization of Alternatively Activated Macrophages That Contribute to Airway Inflammation. *The Journal of Immunology* **183**, 6469–6477 (2009).

117. Schultze, J. L. & Schmidt, S. V. Molecular features of macrophage activation. *Semin Immunol* **27**, 416–423 (2015).

118. Biswas, S. K. & Mantovani, A. Orchestration of Metabolism by Macrophages. *Cell Metab* **15**, 432–437 (2012).

119. Orihuela, R., McPherson, C. A. & Harry, G. J. Microglial <scp>M1/M2</scp> polarization and metabolic states. *Br J Pharmacol* **173**, 649–665 (2016).

120. Ferrante, C. J. *et al.* The Adenosine-Dependent Angiogenic Switch of Macrophages to an M2-Like Phenotype is Independent of Interleukin-4 Receptor Alpha (IL-4Rα) Signaling. *Inflammation* **36**, 921–931 (2013).

121. Haskó, G., Pacher, P., Deitch, E. A. & Vizi, E. S. Shaping of monocyte and macrophage function by adenosine receptors. *Pharmacol Ther* **113**, 264–275 (2007).

122. Martinez, F. O., Sica, A., Mantovani, A. & Locati, M. Macrophage activation and polarization. *Frontiers in Bioscience* **13**, 453 (2008).

123. Zizzo, G., Hilliard, B. A., Monestier, M. & Cohen, P. L. Efficient Clearance of Early Apoptotic Cells by Human Macrophages Requires M2c Polarization and MerTK Induction. *The Journal of Immunology* **189**, 3508–3520 (2012).

124. Fadok, V. A., McDonald, P. P., Bratton, D. L. & Henson, P. M. Regulation of macrophage cytokine production by phagocytosis of apoptotic and post-apoptotic cells. *Biochem Soc Trans* **26**, 653–656 (1998).

125. Mantovani, A., Biswas, S. K., Galdiero, M. R., Sica, A. & Locati, M. Macrophage plasticity and polarization in tissue repair and remodelling. *J Pathol* **229**, 176–185 (2013).

126. Schultze, J. L., Freeman, T., Hume, D. A. & Latz, E. A transcriptional perspective on human macrophage biology. *Semin Immunol* **27**, 44–50 (2015).

127. Jeannin, P., Jaillon, S. & Delneste, Y. Pattern recognition receptors in the immune response against dying cells. *Curr Opin Immunol* **20**, 530–537 (2008).

128. Das, A., Ganesh, K., Khanna, S., Sen, C. K. & Roy, S. Engulfment of Apoptotic Cells by Macrophages: A Role of MicroRNA-21 in the Resolution of Wound Inflammation. *The Journal of Immunology* **192**, 1120–1129 (2014).

129. Khanna, S. *et al.* Macrophage Dysfunction Impairs Resolution of Inflammation in the Wounds of Diabetic Mice. *PLoS One* **5**, e9539 (2010).

130. Wetzler, C., Kämpfer, H., Stallmeyer, B., Pfeilschifter, J. & Frank, S. Large and Sustained Induction of Chemokines during Impaired Wound Healing in the Genetically Diabetic Mouse: Prolonged Persistence of Neutrophils and Macrophages during the Late Phase of Repair. *Journal of Investigative Dermatology* **115**, 245–253 (2000).

131. Cheng, C.-I., Chen, P.-H., Lin, Y.-C. & Kao, Y.-H. High glucose activates Raw264.7 macrophages through RhoA kinase-mediated signaling pathway. *Cell Signal* **27**, 283–292 (2015).

132. Suzuki, H. *et al.* Glycolytic pathway affects differentiation of human monocytes to regulatory macrophages. *Immunol Lett* **176**, 18–27 (2016).

133. Torres-Castro, I. *et al.* Human monocytes and macrophages undergo M1-type inflammatory polarization in response to high levels of glucose. *Immunol Lett* **176**, 81–89 (2016).

134. Englander, H. R. Fluoridation protects occlusal areas. *The Journal of the American Dental Association* **98**, 11 (1979).

135. Sorokin, L. The impact of the extracellular matrix on inflammation. *Nat Rev Immunol* **10**, 712–723 (2010).

136. Takeuchi, O. & Akira, S. Pattern Recognition Receptors and Inflammation. *Cell* **140**, 805–820 (2010).

137. Yanez, D. A., Lacher, R. K., Vidyarthi, A. & Colegio, O. R. The role of macrophages in skin homeostasis. *Pflugers Arch* **469**, 455–463 (2017).

138. DiPietro, L. A., Polverini, P. J., Rahbe, S. M. & Kovacs, E. J. Modulation of JE/MCP-1 expression in dermal wound repair. *Am J Pathol* **146**, 868–75 (1995).

139. Melgarejo, E., Medina, M. Á., Sánchez-Jiménez, F. & Urdiales, J. L. Monocyte chemoattractant protein-1: A key mediator in inflammatory processes. *Int J Biochem Cell Biol* **41**, 998–1001 (2009).

140. Leibovich, S. J. *et al.* Macrophage-induced angiogenesis is mediated by tumour necrosis factor-α. *Nature* **329**, 630–632 (1987).

141. Corliss, B. A., Azimi, M. S., Munson, J. M., Peirce, S. M. & Murfee, W. L. Macrophages: An Inflammatory Link Between Angiogenesis and Lymphangiogenesis. *Microcirculation* **23**, 95–121 (2016).

142. Okuno, Y., Nakamura-Ishizu, A., Kishi, K., Suda, T. & Kubota, Y. Bone marrow-derived cells serve as proangiogenic macrophages but not endothelial cells in wound healing. *Blood* **117**, 5264–5272 (2011).

143. Fantin, A. *et al.* Tissue macrophages act as cellular chaperones for vascular anastomosis downstream of VEGF-mediated endothelial tip cell induction. *Blood* **116**, 829–840 (2010).

144. Willenborg, S. *et al.* CCR2 recruits an inflammatory macrophage subpopulation critical for angiogenesis in tissue repair. *Blood* **120**, 613–625 (2012).

145. Tamoutounour, S. *et al.* Origins and Functional Specialization of Macrophages and of Conventional and Monocyte-Derived Dendritic Cells in Mouse Skin. *Immunity* **39**, 925–938 (2013).

146. Bursch, L. S. *et al.* Identification of a novel population of Langerin+ dendritic cells. *J Exp Med* **204**, 3147–3156 (2007).

147. Ahrens, S. *et al.* F-Actin Is an Evolutionarily Conserved Damage-Associated Molecular Pattern Recognized by DNGR-1, a Receptor for Dead Cells. *Immunity* **36**, 635–645 (2012).

148. Heath, W. R. & Carbone, F. R. The skin-resident and migratory immune system in steady state and memory: innate lymphocytes, dendritic cells and T cells. *Nat Immunol* **14**, 978–985 (2013).

149. Zhang, J.-G. *et al.* The Dendritic Cell Receptor Clec9A Binds Damaged Cells via Exposed Actin Filaments. *Immunity* **36**, 646–657 (2012).

150. McLachlan, J. B., Catron, D. M., Moon, J. J. & Jenkins, M. K. Dendritic Cell Antigen Presentation Drives Simultaneous Cytokine Production by Effector and Regulatory T Cells in Inflamed Skin. *Immunity* **30**, 277–288 (2009).

151. Bedoui, S. *et al.* Cross-presentation of viral and self antigens by skin-derived CD103+ dendritic cells. *Nat Immunol* **10**, 488–495 (2009).

152. Merad, M. *et al.* Langerhans cells renew in the skin throughout life under steady-state conditions. *Nat Immunol* **3**, 1135–1141 (2002).

153. Merad, M., Ginhoux, F. & Collin, M. Origin, homeostasis and function of Langerhans cells and other langerin-expressing dendritic cells. *Nat Rev Immunol* **8**, 935–947 (2008).

154. Tang, A., Amagai, M., Granger, L. G., Stanley, J. R. & Uddy, M. C. Adhesion of epidermal Langerhans cells to keratinocytes mediated by E-cadherin. *Nature* **361**, 82–85 (1993).

155. Kissenpfennig, A. *et al.* Dynamics and Function of Langerhans Cells In Vivo. *Immunity* **22**, 643–654 (2005).

156. Castagnoli, C. *et al.* Characterization of T-cell subsets infiltrating post-burn hypertrophic scar tissues. *Burns* **23**, 565–572 (1997).

157. Kaech, S. M. & Wherry, E. J. Heterogeneity and Cell-Fate Decisions in Effector and Memory CD8+ T Cell Differentiation during Viral Infection. *Immunity* **27**, 393–405 (2007).

158. Chen, Y., Zander, R., Khatun, A., Schauder, D. M. & Cui, W. Transcriptional and Epigenetic Regulation of Effector and Memory CD8 T Cell Differentiation. *Front Immunol* **9**, (2018).

159. Xin, A. *et al.* A molecular threshold for effector CD8+ T cell differentiation controlled by transcription factors Blimp-1 and T-bet. *Nat Immunol* **17**, 422–432 (2016).

160. Curtsinger, J. M., Agarwal, P., Lins, D. C. & Mescher, M. F. Autocrine IFN-γ Promotes Naive CD8 T Cell Differentiation and Synergizes with IFN-α To Stimulate Strong Function. *The Journal of Immunology* **189**, 659–668 (2012).

161. Kaech, S. M. & Cui, W. Transcriptional control of effector and memory CD8+ T cell differentiation. *Nat Rev Immunol* **12**, 749–761 (2012).

162. Crotty, S., Johnston, R. J. & Schoenberger, S. P. Effectors and memories: Bcl-6 and Blimp-1 in T and B lymphocyte differentiation. *Nat Immunol* **11**, 114–120 (2010).

163. Zhao, X., Shan, Q. & Xue, H.-H. TCF1 in T cell immunity: a broadened frontier. *Nat Rev Immunol* **22**, 147–157 (2022).

164. Dan, H. C. *et al.* Akt-dependent Activation of mTORC1 Complex Involves Phosphorylation of mTOR (Mammalian Target of Rapamycin) by IκB Kinase α (IKKα). *Journal of Biological Chemistry* **289**, 25227–25240 (2014).

165. Pearce, E. L. *et al.* Enhancing CD8 T-cell memory by modulating fatty acid metabolism. *Nature* **460**, 103–107 (2009).

166. O'Sullivan, D. *et al.* Memory CD8+ T Cells Use Cell-Intrinsic Lipolysis to Support the Metabolic Programming Necessary for Development. *Immunity* **41**, 75–88 (2014).

167. Gupta, S. S. *et al.* NIX-Mediated Mitophagy Promotes Effector Memory Formation in Antigen-Specific CD8+ T Cells. *Cell Rep* **29**, 1862-1877.e7 (2019).

168. van der Windt, G. J. W. *et al.* Mitochondrial Respiratory Capacity Is a Critical Regulator of CD8+ T Cell Memory Development. *Immunity* **36**, 68–78 (2012).

169. Shan, Q. *et al.* Tcf1 preprograms the mobilization of glycolysis in central memory CD8+ T cells during recall responses. *Nat Immunol* **23**, 386–398 (2022).

170. Chung, H. K., McDonald, B. & Kaech, S. M. The architectural design of CD8+ T cell responses in acute and chronic infection: Parallel structures with divergent fates. *Journal of Experimental Medicine* **218**, (2021).

171. Mackay, L. K. *et al.* Long-lived epithelial immunity by tissue-resident memory T (T_{RM}) cells in the absence of persisting local antigen presentation. *Proceedings of the National Academy of Sciences* **109**, 7037–7042 (2012).

172. Shedlock, D. J. & Shen, H. Requirement for CD4 T Cell Help in Generating Functional CD8 T Cell Memory. *Science (1979)* **300**, 337–339 (2003).

173. Janssen, E. M. *et al.* CD4+ T cells are required for secondary expansion and memory in CD8+ T lymphocytes. *Nature* **421**, 852–856 (2003).

174. Bourgeois, C., Rocha, B. & Tanchot, C. A Role for CD40 Expression on $CD8^+$ T Cells in the Generation of $CD8^+$ T Cell Memory. *Science (1979)* **297**, 2060–2063 (2002).

175. Williams, M. A., Tyznik, A. J. & Bevan, M. J. Interleukin-2 signals during priming are required for secondary expansion of CD8+ memory T cells. *Nature* **441**, 890–893 (2006).

176. Barker, B. R., Gladstone, M. N., Gillard, G. O., Panas, M. W. & Letvin, N. L. Critical role for IL-21 in both primary and memory anti-viral $CD8^+$ T-cell responses. *Eur J Immunol* **40**, 3085–3096 (2010).

177. Sokke Umeshappa, C. *et al.* CD154 and IL-2 Signaling of CD4+ T Cells Play a Critical Role in Multiple Phases of CD8+ CTL Responses Following Adenovirus Vaccination. *PLoS One* **7**, e47004 (2012).

178. Luckheeram, R. V., Zhou, R., Verma, A. D. & Xia, B. $CD4^+$ T Cells: Differentiation and Functions. *Clin Dev Immunol* **2012**, 1–12 (2012).

179. Cenerenti, M., Saillard, M., Romero, P. & Jandus, C. The Era of Cytotoxic CD4 T Cells. *Front Immunol* **13**, (2022).

180. Meitei, H. T. & Lal, G. T cell receptor signaling in the differentiation and plasticity of CD4+ T cells. *Cytokine Growth Factor Rev* **69**, 14–27 (2023).

181. Dobrzanski, M. J. Expanding Roles for CD4 T Cells and Their Subpopulations in Tumor Immunity and Therapy. *Front Oncol* **3**, (2013).

182. Saravia, J., Chapman, N. M. & Chi, H. Helper T cell differentiation. *Cell Mol Immunol* **16**, 634–643 (2019).

183. Afkarian, M. *et al.* T-bet is a STAT1-induced regulator of IL-12R expression in naïve CD4+ T cells. *Nat Immunol* **3**, 549–557 (2002).

184. Ylikoski, E. *et al.* IL-12 up-regulates T-bet independently of IFN-γ in human CD4+ T cells. *Eur J Immunol* **35**, 3297–3306 (2005).

185. Mann, G. J. *et al.* BRAF Mutation, NRAS Mutation, and the Absence of an Immune-Related Expressed Gene Profile Predict Poor Outcome in Patients with Stage III Melanoma. *Journal of Investigative Dermatology* **133**, 509–517 (2013).

186. Curtis, C. *et al.* The genomic and transcriptomic architecture of 2,000 breast tumours reveals novel subgroups. *Nature* **486**, 346–352 (2012).

187. Ascierto, M. L. *et al.* A signature of immune function genes associated with recurrence-free survival in breast cancer patients. *Breast Cancer Res Treat* **131**, 871–880 (2012).

188. Leffers, N. *et al.* Identification of genes and pathways associated with cytotoxic T lymphocyte infiltration of serous ovarian cancer. *Br J Cancer* **103**, 685–692 (2010).

189. Tosolini, M. *et al.* Clinical Impact of Different Classes of Infiltrating T Cytotoxic and Helper Cells (Th1, Th2, Treg, Th17) in Patients with Colorectal Cancer. *Cancer Res* **71**, 1263–1271 (2011).

190. Xu, X. *et al.* Expression of Th1- Th2- and Th17-associated cytokines in laryngeal carcinoma. *Oncol Lett* **12**, 1941–1948 (2016).

191. Konjević, G. M., Vuletić, A. M., Mirjačić Martinović, K. M., Larsen, A. K. & Jurišić, V. B. The role of cytokines in the regulation of NK cells in the tumor environment. *Cytokine* **117**, 30–40 (2019).

192. Jabrane-Ferrat, N. *et al.* Effect of gamma interferon on HLA class-I and -II transcription and protein expression in human breast adenocarcinoma cell lines. *Int J Cancer* **45**, 1169–1176 (1990).

193. Shankaran, V. *et al.* IFNγ and lymphocytes prevent primary tumour development and shape tumour immunogenicity. *Nature* **410**, 1107–1111 (2001).

194. Walker, J. A. & McKenzie, A. N. J. TH2 cell development and function. *Nat Rev Immunol* **18**, 121–133 (2018).

195. Aleebrahim-Dehkordi, E. *et al.* T helper type (Th1/Th2) responses to SARS-CoV-2 and influenza A (H1N1) virus: From cytokines produced to immune responses. *Transpl Immunol* **70**, 101495 (2022).

196. Noben-Trauth, N., Hu-Li, J. & Paul, W. E. IL-4 secreted from individual naive CD4+ T cells acts in an autocrine manner to induce Th2 differentiation. *Eur J Immunol* **32**, 1428 (2002).

197. Spinner, C. A. & Lazarevic, V. Transcriptional regulation of adaptive and innate lymphoid lineage specification. *Immunol Rev* **300**, 65–81 (2021).

198. Liao, W. *et al.* Priming for T helper type 2 differentiation by interleukin 2–mediated induction of interleukin 4 receptor α-chain expression. *Nat Immunol* **9**, 1288–1296 (2008).

199. Tepper, R. I., Coffman, R. L. & Leder, P. An Eosinophil-Dependent Mechanism for the Antitumor Effect of Interleukin-4. *Science (1979)* **257**, 548–551 (1992).

200. Hung, K. *et al.* The Central Role of CD4+ T Cells in the Antitumor Immune Response. *J Exp Med* **188**, 2357–2368 (1998).

201. Lorvik, K. B. *et al.* Adoptive Transfer of Tumor-Specific Th2 Cells Eradicates Tumors by Triggering an *In Situ* Inflammatory Immune Response. *Cancer Res* **76**, 6864–6876 (2016).

202. Kitajima, M. *et al.* Memory Type 2 Helper T Cells Induce Long-Lasting Antitumor Immunity by Activating Natural Killer Cells. *Cancer Res* **71**, 4790–4798 (2011).

203. Boieri, M. *et al.* CD4+ T helper 2 cells suppress breast cancer by inducing terminal differentiation. *Journal of Experimental Medicine* **219**, (2022).

204. Rodriguez-Tirado, C. *et al.* Interleukin 4 Controls the Pro-Tumoral Role of Macrophages in Mammary Cancer Pulmonary Metastasis in Mice. *Cancers (Basel)* **14**, 4336 (2022).

205. Lee, H. L. *et al.* Inflammatory cytokines and change of Th1/Th2 balance as prognostic indicators for hepatocellular carcinoma in patients treated with transarterial chemoembolization. *Sci Rep* **9**, 3260 (2019).

206. Johansson, M., DeNardo, D. G. & Coussens, L. M. Polarized immune responses differentially regulate cancer development. *Immunol Rev* **222**, 145–154 (2008).

207. Veldhoen, M. *et al.* Transforming growth factor-β 'reprograms' the differentiation of T helper 2 cells and promotes an interleukin 9–producing subset. *Nat Immunol* **9**, 1341–1346 (2008).

208. Plitas, G. & Rudensky, A. Y. Regulatory T Cells: Differentiation and Function. *Cancer Immunol Res* **4**, 721–725 (2016).

209. Hori, S. FOXP3 as a master regulator of Treg cells. *Nat Rev Immunol* **21**, 618–619 (2021).

210. Hori, S., Nomura, T. & Sakaguchi, S. Control of Regulatory T Cell Development by the Transcription Factor *Foxp3*. *Science (1979)* **299**, 1057–1061 (2003).

211. Fontenot, J. D., Gavin, M. A. & Rudensky, A. Y. Foxp3 programs the development and function of CD4+CD25+ regulatory T cells. *Nat Immunol* **4**, 330–336 (2003).

212. Ohkura, N. *et al.* T Cell Receptor Stimulation-Induced Epigenetic Changes and Foxp3 Expression Are Independent and Complementary Events Required for Treg Cell Development. *Immunity* **37**, 785–799 (2012).

213. Morikawa, H. & Sakaguchi, S. Genetic and epigenetic basis of Treg cell development and function: from a FoxP3-centered view to an epigenome-defined view of natural Treg cells. *Immunol Rev* **259**, 192–205 (2014).

214. Long, M., Park, S.-G., Strickland, I., Hayden, M. S. & Ghosh, S. Nuclear Factor-κB Modulates Regulatory T Cell Development by Directly Regulating Expression of Foxp3 Transcription Factor. *Immunity* **31**, 921–931 (2009).

215. Isomura, I. *et al.* c-Rel is required for the development of thymic Foxp3+ CD4 regulatory T cells. *Journal of Experimental Medicine* **206**, 3001–3014 (2009).

216. Barbi, J., Pardoll, D. & Pan, F. Treg functional stability and its responsiveness to the microenvironment. *Immunol Rev* **259**, 115–139 (2014).

217. Maruyama, T., Konkel, J. E., Zamarron, B. F. & Chen, W. The molecular mechanisms of Foxp3 gene regulation. *Semin Immunol* **23**, 418–423 (2011).

218. Chinen, T. *et al.* An essential role for the IL-2 receptor in Treg cell function. *Nat Immunol* **17**, 1322–1333 (2016).

219. Josefowicz, S. Z., Lu, L.-F. & Rudensky, A. Y. Regulatory T Cells: Mechanisms of Differentiation and Function. *Annu Rev Immunol* **30**, 531–564 (2012).

220. Kanamori, M., Nakatsukasa, H., Okada, M., Lu, Q. & Yoshimura, A. Induced Regulatory T Cells: Their Development, Stability, and Applications. *Trends Immunol* **37**, 803–811 (2016).

221. Cao, X. *et al.* Granzyme B and Perforin Are Important for Regulatory T Cell-Mediated Suppression of Tumor Clearance. *Immunity* **27**, 635–646 (2007).

222. Volpe, E., Sambucci, M., Battistini, L. & Borsellino, G. Fas–Fas Ligand: Checkpoint of T Cell Functions in Multiple Sclerosis. *Front Immunol* **7**, (2016).

223. Wei, X. *et al.* Reciprocal Expression of IL-35 and IL-10 Defines Two Distinct Effector Treg Subsets that Are Required for Maintenance of Immune Tolerance. *Cell Rep* **21**, 1853–1869 (2017).

224. Sarhan, D. *et al.* Adaptive NK Cells Resist Regulatory T-cell Suppression Driven by IL37. *Cancer Immunol Res* **6**, 766–775 (2018).

225. Hatzioannou, A. *et al.* An intrinsic role of IL-33 in Treg cell–mediated tumor immunoevasion. *Nat Immunol* **21**, 75–85 (2020).

226. Zappasodi, R. *et al.* CTLA-4 blockade drives loss of Treg stability in glycolysis-low tumours. *Nature* **591**, 652–658 (2021).

227. Aksoylar, H.-I. & Boussiotis, V. A. PD-1+ Treg cells: a foe in cancer immunotherapy? *Nat Immunol* **21**, 1311–1312 (2020).

228. Kurtulus, S. *et al.* TIGIT predominantly regulates the immune response via regulatory T cells. *Journal of Clinical Investigation* **125**, 4053–4062 (2015).

229. Wing, K. *et al.* CTLA-4 Control over Foxp3 $^{+}$ Regulatory T Cell Function. *Science (1979)* **322**, 271–275 (2008).

230. Qureshi, O. S. *et al.* Trans-Endocytosis of CD80 and CD86: A Molecular Basis for the Cell-Extrinsic Function of CTLA-4. *Science (1979)* **332**, 600–603 (2011).

231. Gu, P. *et al.* Trogocytosis of CD80 and CD86 by induced regulatory T cells. *Cell Mol Immunol* **9**, 136–146 (2012).

232. Tekguc, M., Wing, J. B., Osaki, M., Long, J. & Sakaguchi, S. Treg-expressed CTLA-4 depletes CD80/CD86 by trogocytosis, releasing free PD-L1 on antigen-presenting cells. *Proceedings of the National Academy of Sciences* **118**, (2021).

233. Kalia, V., Penny, L. A., Yuzefpolskiy, Y., Baumann, F. M. & Sarkar, S. Quiescence of Memory CD8+ T Cells Is Mediated by Regulatory T Cells through Inhibitory Receptor CTLA-4. *Immunity* **42**, 1116–1129 (2015).

234. Cinier, J. *et al.* Recruitment and Expansion of Tregs Cells in the Tumor Environment—How to Target Them? *Cancers (Basel)* **13**, 1850 (2021).

235. Zhang, Y. *et al.* Deep single-cell RNA sequencing data of individual T cells from treatment-naïve colorectal cancer patients. *Sci Data* **6**, 131 (2019).

236. O'Shea, J. J. *et al.* The JAK-STAT Pathway: Impact on Human Disease and Therapeutic Intervention. *Annu Rev Med* **66**, 311–328 (2015).

237. Darnell, J. E. STATs and Gene Regulation. *Science (1979)* **277**, 1630–1635 (1997).

238. Kim, S.-K. *et al.* Melittin enhances apoptosis through suppression of IL-6/sIL-6R complex-induced NF-κB and STAT3 activation and Bcl-2 expression for human fibroblast-like synoviocytes in rheumatoid arthritis. *Joint Bone Spine* **78**, 471–477 (2011).

239. Cai, B., Cai, J., Luo, Y., Chen, C. & Zhang, S. The Specific Roles of JAK/STAT Signaling Pathway in Sepsis. *Inflammation* **38**, 1599–1608 (2015).

240. O'Shea, J. J., Pesu, M., Borie, D. C. & Changelian, P. S. A new modality for immunosuppression: targeting the JAK/STAT pathway. *Nat Rev Drug Discov* **3**, 555–564 (2004).

241. Jaime-Figueroa, S. *et al.* Discovery of a series of novel 5H-pyrrolo[2,3-b]pyrazine-2-phenyl ethers, as potent JAK3 kinase inhibitors. *Bioorg Med Chem Lett* **23**, 2522–2526 (2013).

242. Marrero, M. B. Introduction to JAK/STAT signaling and the vasculature. *Vascul Pharmacol* **43**, 307–309 (2005).

243. Greenlund, A. C., Farrar, M. A., Viviano, B. L. & Schreiber, R. D. Ligand-induced IFN gamma receptor tyrosine phosphorylation couples the receptor to its signal transduction system (p91). *EMBO J* **13**, 1591–1600 (1994).

244. Yu, H., Pardoll, D. & Jove, R. STATs in cancer inflammation and immunity: a leading role for STAT3. *Nat Rev Cancer* **9**, 798–809 (2009).

245. Boengler, K., Hilfikerkleiner, D., Drexler, H., Heusch, G. & Schulz, R. The myocardial JAK/STAT pathway: From protection to failure. *Pharmacol Ther* **120**, 172–185 (2008).

246. Gao, Q. *et al.* JAK/STAT Signal Transduction: Promising Attractive Targets for Immune, Inflammatory and Hematopoietic Diseases. *Curr Drug Targets* **19**, 487–500 (2018).

247. Philips, R. L. *et al.* The JAK-STAT pathway at 30: Much learned, much more to do. *Cell* vol. 185 3857–3876 Preprint at https://doi.org/10.1016/j.cell.2022.09.023 (2022).

248. Rawlings, J. S., Rosler, K. M. & Harrison, D. A. The JAK/STAT signaling pathway. *J Cell Sci* **117**, 1281–1283 (2004).

249. Darnell, J. E., Kerr, Ian M. & Stark, G. R. Jak-STAT Pathways and Transcriptional Activation in Response to IFNs and Other Extracellular Signaling Proteins. *Science (1979)* **264**, 1415–1421 (1994).

250. Gao, B. Cytokines, STATs and liver disease. *Cell Mol Immunol* **2**, 92–100 (2005).

251. Begitt, A. *et al.* STAT1-cooperative DNA binding distinguishes type 1 from type 2 interferon signaling. *Nat Immunol* **15**, 168–176 (2014).

252. Lin, J.-X. *et al.* Critical Role of STAT5 Transcription Factor Tetramerization for Cytokine Responses and Normal Immune Function. *Immunity* **36**, 586–599 (2012).

253. Vinkemeier, U., Moarefi, I., Darnell, J. E. & Kuriyan, J. Structure of the Amino-Terminal Protein Interaction Domain of STAT-4. *Science (1979)* **279**, 1048–1052 (1998).

254. Mandal, M. *et al.* Epigenetic repression of the Igk locus by STAT5-mediated recruitment of the histone methyltransferase Ezh2. *Nat Immunol* **12**, 1212–1220 (2011).

255. Zhang, X. & Darnell, J. E. Functional Importance of Stat3 Tetramerization in Activation of the α2-Macroglobulin Gene. *Journal of Biological Chemistry* **276**, 33576–33581 (2001).

256. Platanitis, E. *et al.* A molecular switch from STAT2-IRF9 to ISGF3 underlies interferon-induced gene transcription. *Nat Commun* **10**, 2921 (2019).

257. Rengachari, S. *et al.* Structural basis of STAT2 recognition by IRF9 reveals molecular insights into ISGF3 function. *Proceedings of the National Academy of Sciences* **115**, (2018).

258. O'Shea, J. J. & Plenge, R. JAK and STAT Signaling Molecules in Immunoregulation and Immune-Mediated Disease. *Immunity* **36**, 542–550 (2012).

259. van Boxel-Dezaire, A. H. H., Rani, M. R. S. & Stark, G. R. Complex Modulation of Cell Type-Specific Signaling in Response to Type I Interferons. *Immunity* **25**, 361–372 (2006).

260. Berenson, L. S., Gavrieli, M., Farrar, J. D., Murphy, T. L. & Murphy, K. M. Distinct Characteristics of Murine STAT4 Activation in Response to IL-12 and IFN-α. *The Journal of Immunology* **177**, 5195–5203 (2006).

261. Nguyen, K. B. *et al.* Interferon α/β-mediated inhibition and promotion of interferon γ: STAT1 resolves a paradox. *Nat Immunol* **1**, 70–76 (2000).

262. Nguyen, K. B. *et al.* Critical Role for STAT4 Activation by Type 1 Interferons in the Interferon-γ Response to Viral Infection. *Science (1979)* **297**, 2063–2066 (2002).

263. Murray, P. Understanding and exploiting the endogenous interleukin-10/STAT3-mediated anti-inflammatory response. *Curr Opin Pharmacol* **6**, 379–386 (2006).

264. Murray, P. J. The primary mechanism of the IL-10-regulated antiinflammatory response is to selectively inhibit transcription. *Proceedings of the National Academy of Sciences* **102**, 8686–8691 (2005).

265. Williams, L. M., Ricchetti, G., Sarma, U., Smallie, T. & Foxwell, B. M. J. Interleukin-10 suppression of myeloid cell activation — a continuing puzzle. *Immunology* **113**, 281–292 (2004).

266. Williams, L. M. *et al.* Expression of Constitutively Active STAT3 Can Replicate the Cytokine-suppressive Activity of Interleukin-10 in Human Primary Macrophages. *Journal of Biological Chemistry* **282**, 6965–6975 (2007).

267. El Kasmi, K. C. *et al.* General Nature of the STAT3-Activated Anti-Inflammatory Response. *The Journal of Immunology* **177**, 7880–7888 (2006).

268. Chen, Z. *et al.* Identification of Novel IL-4/Stat6-Regulated Genes in T Lymphocytes. *The Journal of Immunology* **171**, 3627–3635 (2003).

269. Chtanova, T., Kemp, R. A., Sutherland, A. P. R., Ronchese, F. & Mackay, C. R. Gene Microarrays Reveal Extensive Differential Gene Expression in Both CD4+ and CD8+ Type 1 and Type 2 T Cells. *The Journal of Immunology* **167**, 3057–3063 (2001).

270. Lund, R., Aittokallio, T., Nevalainen, O. & Lahesmaa, R. Identification of Novel Genes Regulated by IL-12, IL-4, or TGF-β during the Early Polarization of CD4+ Lymphocytes. *The Journal of Immunology* **171**, 5328–5336 (2003).

271. Lund, R. *et al.* Identification of genes involved in the initiation of human Th1 or Th2 cell commitment. *Eur J Immunol* **35**, 3307–3319 (2005).

272. Edwards, J. P., Zhang, X., Frauwirth, K. A. & Mosser, D. M. Biochemical and functional characterization of three activated macrophage populations. *J Leukoc Biol* **80**, 1298–1307 (2006).

273. Loke, P. *et al.* IL-4 dependent alternatively-activated macrophages have a distinctive in vivo gene expression phenotype. *BMC Immunol* **3**, 7 (2002).

274. Welch, J. S. *et al.* TH2 Cytokines and Allergic Challenge Induce Ym1 Expression in Macrophages by a STAT6-dependent Mechanism. *Journal of Biological Chemistry* **277**, 42821–42829 (2002).

275. Zimmermann, N. *et al.* Dissection of experimental asthma with DNA microarray analysis identifies arginase in asthma pathogenesis. *Journal of Clinical Investigation* **111**, 1863–1874 (2003).

276. Qing, Y. & Stark, G. R. Alternative Activation of STAT1 and STAT3 in Response to Interferon-γ. *Journal of Biological Chemistry* **279**, 41679–41685 (2004).

277. Costa-Pereira, A. P. *et al.* Mutational switch of an IL-6 response to an interferon-γ-like response. *Proceedings of the National Academy of Sciences* **99**, 8043–8047 (2002).

278. Park, J.-H. *et al.* Signaling by intrathymic cytokines, not T cell antigen receptors, specifies CD8 lineage choice and promotes the differentiation of cytotoxic-lineage T cells. *Nat Immunol* **11**, 257–264 (2010).

279. Jacobson, N. G. *et al.* Interleukin 12 signaling in T helper type 1 (Th1) cells involves tyrosine phosphorylation of signal transducer and activator of transcription (Stat)3 and Stat4. *J Exp Med* **181**, 1755–1762 (1995).

280. Lischke, A. *et al.* The Interleukin-4 Receptor Activates STAT5 by a Mechanism That Relies upon Common γ-Chain. *Journal of Biological Chemistry* **273**, 31222–31229 (1998).

281. Villarino, A. *et al.* The IL-27R (WSX-1) Is Required to Suppress T Cell Hyperactivity during Infection. *Immunity* **19**, 645–655 (2003).

282. Hirahara, K. *et al.* Asymmetric Action of STAT Transcription Factors Drives Transcriptional Outputs and Cytokine Specificity. *Immunity* **42**, 877–889 (2015).

283. Wan, C.-K. *et al.* Opposing roles of STAT1 and STAT3 in IL-21 function in CD4 $^{+}$ T cells. *Proceedings of the National Academy of Sciences* **112**, 9394–9399 (2015).

284. Miyagi, T. *et al.* High basal STAT4 balanced by STAT1 induction to control type 1 interferon effects in natural killer cells. *J Exp Med* **204**, 2383–2396 (2007).

285. Gil, M. P. *et al.* Regulating type 1 IFN effects in CD8 T cells during viral infections: changing STAT4 and STAT1 expression for function. *Blood* **120**, 3718–3728 (2012).

286. Villarino, A. *et al.* Signal transducer and activator of transcription 5 (STAT5) paralog dose governs T cell effector and regulatory functions. *Elife* **5**, (2016).

287. Usui, T., Nishikomori, R., Kitani, A. & Strober, W. GATA-3 Suppresses Th1 Development by Downregulation of Stat4 and Not through Effects on IL-12Rβ2 Chain or T-bet. *Immunity* **18**, 415–428 (2003).

288. Gollob, J. A., Schnipper, C. P., Murphy, E. A., Ritz, J. & Frank, D. A. The functional synergy between IL-12 and IL-2 involves p38 mitogen-activated protein kinase and is associated with the augmentation of STAT serine phosphorylation. *J Immunol* **162**, 4472–81 (1999).

289. Break, T. J. *et al.* Aberrant type 1 immunity drives susceptibility to mucosal fungal infections. *Science (1979)* **371**, (2021).

290. Liu, L. *et al.* Gain-of-function human *STAT1* mutations impair IL-17 immunity and underlie chronic mucocutaneous candidiasis. *Journal of Experimental Medicine* **208**, 1635–1648 (2011).

291. Wiedemann, G. M. *et al.* Deconvoluting global cytokine signaling networks in natural killer cells. *Nat Immunol* **22**, 627–638 (2021).

292. Seif, F. *et al.* The role of JAK-STAT signaling pathway and its regulators in the fate of T helper cells. *Cell Communication and Signaling* **15**, 23 (2017).

293. Pfeifer, A. C., Timmer, J. & Klingmüller, U. Systems biology of JAK/STAT signalling. *Essays Biochem* **45**, 109–120 (2008).

294. Alexander, W. S. & Hilton, D. J. T <scp>he</scp> R <scp>ole of</scp> S <scp>uppressors of</scp> C <scp>ytokine</scp> S <scp>ignaling</scp> (SOCS) P <scp>roteins in</scp> R <scp>egulation of the</scp> I <scp>mmune</scp> R <scp>esponse</scp>. *Annu Rev Immunol* **22**, 503–529 (2004).

295. Dickensheets, H. *et al.* Suppressor of cytokine signaling-1 is an IL-4-inducible gene in macrophages and feedback inhibits IL-4 signaling. *Genes Immun* **8**, 21–27 (2007).

296. Cornish, A. L. *et al.* Suppressor of Cytokine Signaling-1 Regulates Signaling in Response to Interleukin-2 and Other γc-dependent Cytokines in Peripheral T Cells. *Journal of Biological Chemistry* **278**, 22755–22761 (2003).

297. Yoshimura, A., Naka, T. & Kubo, M. SOCS proteins, cytokine signalling and immune regulation. *Nat Rev Immunol* **7**, 454–465 (2007).

298. Boyle, K. *et al.* Deletion of the SOCS box of suppressor of cytokine signaling 3 (SOCS3) in embryonic stem cells reveals SOCS box-dependent regulation of JAK but not STAT phosphorylation. *Cell Signal* **21**, 394–404 (2009).

299. Yan, Z., Gibson, S. A., Buckley, J. A., Qin, H. & Benveniste, E. N. Role of the JAK/STAT signaling pathway in regulation of innate immunity in neuroinflammatory diseases. *Clinical Immunology* **189**, 4–13 (2018).

300. Mahony, R., Ahmed, S., Diskin, C. & Stevenson, N. J. SOCS3 revisited: a broad regulator of disease, now ready for therapeutic use? *Cellular and Molecular Life Sciences* **73**, 3323–3336 (2016).

301. Chikuma, S., Kanamori, M., Mise-Omata, S. & Yoshimura, A. Suppressors of cytokine signaling: Potential immune checkpoint molecules for cancer immunotherapy. *Cancer Sci* **108**, 574–580 (2017).

302. Giordanetto, F. & Kroemer, R. T. A three-dimensional model of Suppressor Of Cytokine Signalling 1 (SOCS-1). *Protein Engineering, Design and Selection* **16**, 115–124 (2003).

303. Kershaw, N. J. *et al.* SOCS3 binds specific receptor–JAK complexes to control cytokine signaling by direct kinase inhibition. *Nat Struct Mol Biol* **20**, 469–476 (2013).

304. Malemud, C. & Pearlman, E. Targeting JAK/STAT Signaling Pathway in Inflammatory Diseases. *Curr Signal Transduct Ther* **4**, 201–221 (2009).

305. Ivashkiv, L. B. & Hu, X. Signaling by STATs. *Arthritis Res Ther* **6**, 159 (2004).

306. Stark, G. R. & Darnell, J. E. The JAK-STAT Pathway at Twenty. *Immunity* **36**, 503–514 (2012).

307. Heppler, L. N. & Frank, D. A. Targeting Oncogenic Transcription Factors: Therapeutic Implications of Endogenous STAT Inhibitors. *Trends Cancer* **3**, 816–827 (2017).

308. Kotaja, N., Karvonen, U., Jänne, O. A. & Palvimo, J. J. PIAS Proteins Modulate Transcription Factors by Functioning as SUMO-1 Ligases. *Mol Cell Biol* **22**, 5222–5234 (2002).

309. Yuan, J., Zhang, F. & Niu, R. Multiple regulation pathways and pivotal biological functions of STAT3 in cancer. *Sci Rep* **5**, 17663 (2015).

310. Ungureanu, D. *et al.* PIAS proteins promote SUMO-1 conjugation to STAT1. *Blood* **102**, 3311–3313 (2003).

311. Shuai, K. Regulation of cytokine signaling pathways by PIAS proteins. *Cell Res* **16**, 196–202 (2006).

312. Dagvadorj, A. *et al.* N-terminal truncation of Stat5a/b circumvents PIAS3-mediated transcriptional inhibition of Stat5 in prostate cancer cells. *Int J Biochem Cell Biol* **42**, 2037–2046 (2010).

313. Huang, Y., Zhang, Y., Ge, L., Lin, Y. & Kwok, H. The Roles of Protein Tyrosine Phosphatases in Hepatocellular Carcinoma. *Cancers (Basel)* **10**, 82 (2018).

314. Zhang, Z.-Y. Chemical and Mechanistic Approaches to the Study of Protein Tyrosine Phosphatases. *Acc Chem Res* **36**, 385–392 (2003).

315. Alonso, A. *et al.* Protein Tyrosine Phosphatases in the Human Genome. *Cell* **117**, 699–711 (2004).

316. Takeda, K. *et al.* Defective NK Cell Activity and Th1 Response in IL-18–Deficient Mice. *Immunity* **8**, 383–390 (1998).

317. Foster, F. M., Traer, C. J., Abraham, S. M. & Fry, M. J. The phosphoinositide (PI) 3-kinase family. *J Cell Sci* **116**, 3037–3040 (2003).

318. Silvennoinen, O., Schindler, C., Schlessinger, J. & Levy, D. E. Ras-Independent Growth Factor Signaling by Transcription Factor Tyrosine Phosphorylation. *Science (1979)* **261**, 1736–1739 (1993).

319. Ross, S. H. *et al.* Phosphoproteomic Analyses of Interleukin 2 Signaling Reveal Integrated JAK Kinase-Dependent and -Independent Networks in CD8 + T Cells. *Immunity* **45**, 685–700 (2016).

320. Moustakas, A. Smad signalling network. *J Cell Sci* **115**, 3355–3356 (2002).

321. Gilmore, T. D. & Wolenski, F. S. *NF-JB: Where Did It Come from and Why? Immunological Reviews* vol. 246 www.immunologicalreviews.com (2012).

322. Sun, S. C. The non-canonical NF-κB pathway in immunity and inflammation. *Nature Reviews Immunology* vol. 17 545–558 Preprint at https://doi.org/10.1038/nri.2017.52 (2017).

323. Zhang, T., Ma, C., Zhang, Z., Zhang, H. & Hu, H. NF-κB signaling in inflammation and cancer. *MedComm* vol. 2 618–653 Preprint at https://doi.org/10.1002/mco2.104 (2021).

324. Lawrence, T. The nuclear factor NF-kappaB pathway in inflammation. *Cold Spring Harbor perspectives in biology* vol. 1 Preprint at https://doi.org/10.1101/cshperspect.a001651 (2009).

325. Moynagh, P. N. The NF-κB pathway. *J Cell Sci* **118**, 4589–4592 (2005).

326. Perkins, N. D. The Rel/NF-κB family: friend and foe. *Trends Biochem Sci* **25**, 434–440 (2000).

327. Bottex-Gauthier, C., Pollet, S., Favier, A. & Vidal, D. R. Les facteurs de transcription Rel/NF-B : rôle complexe dans les régulations cellulaires. *Pathologie Biologie* **50**, 204–211 (2002).

328. Yu, H., Lin, L., Zhang, Z., Zhang, H. & Hu, H. Targeting NF-κB pathway for the therapy of diseases: mechanism and clinical study. *Signal Transduct Target Ther* **5**, 209 (2020).

329. Alcamo, E. *et al.* Targeted Mutation of TNF Receptor I Rescues the RelA-Deficient Mouse and Reveals a Critical Role for NF-κB in Leukocyte Recruitment. *The Journal of Immunology* **167**, 1592–1600 (2001).

330. Lawrence, T., Gilroy, D. W., Colville-Nash, P. R. & Willoughby, D. A. Possible new role for NF-κB in the resolution of inflammation. *Nat Med* **7**, 1291–1297 (2001).

331. Greten, F. R. *et al.* NF-κB Is a Negative Regulator of IL-1β Secretion as Revealed by Genetic and Pharmacological Inhibition of IKKβ. *Cell* **130**, 918–931 (2007).

332. Lawrence, T. & Gilroy, D. W. Chronic inflammation: a failure of resolution? *Int J Exp Pathol* **88**, 85–94 (2007).

333. Ju, S.-T. *et al.* Fas(CD95)/FasL interactions required for programmed cell death after T-cell activation. *Nature* **373**, 444–448 (1995).

334. Teixeiro, E., García-Sahuquillo, A., Alarcón, B. & Bragado, R. Apoptosis-resistant T cells have a deficiency in NF-κB-mediated induction of Fas ligand transcription. *Eur J Immunol* **29**, 745–754 (1999).

335. Hettmann, T., DiDonato, J., Karin, M. & Leiden, J. M. An Essential Role for Nuclear Factor κB in Promoting Double Positive Thymocyte Apoptosis. *J Exp Med* **189**, 145–158 (1999).

336. Lin, B. *et al.* NF-κB functions as both a proapoptotic and antiapoptotic regulatory factor within a single cell type. *Cell Death Differ* **6**, 570–582 (1999).

337. Sun, S.-C., Chang, J.-H. & Jin, J. Regulation of nuclear factor-κB in autoimmunity. *Trends Immunol* **34**, 282–289 (2013).

338. Gilmore, T. D. NF-κB and Human Cancer: What Have We Learned over the Past 35 Years? *Biomedicines* **9**, 889 (2021).

339. Yamamoto, Y. & Gaynor, R. B. IκB kinases: key regulators of the NF-κB pathway. *Trends Biochem Sci* **29**, 72–79 (2004).

340. Beinke, S. & Ley, S. C. Functions of NF-κB1 and NF-κB2 in immune cell biology. *Biochemical Journal* **382**, 393–409 (2004).

341. Neumann, M. & Naumann, M. Beyond IκBs: alternative regulation of NF-KB activity. *The FASEB Journal* **21**, 2642–2654 (2007).

342. Mulero, M. C., Wang, V. Y.-F., Huxford, T. & Ghosh, G. Genome reading by the NF-κB transcription factors. *Nucleic Acids Res* **47**, 9967–9989 (2019).

343. Ji, Z., He, L., Regev, A. & Struhl, K. Inflammatory regulatory network mediated by the joint action of NF-kB, STAT3, and AP-1 factors is involved in many human cancers. *Proceedings of the National Academy of Sciences* **116**, 9453–9462 (2019).

344. Bohuslav, J. *et al.* Regulation of an essential innate immune response by the p50 subunit of NF-kappaB. *Journal of Clinical Investigation* **102**, 1645–1652 (1998).

345. Bours, V. *et al.* The oncoprotein Bcl-3 directly transactivates through κB motifs via association with DNA-binding p50B homodimers. *Cell* **72**, 729–739 (1993).

346. Dechend, R. *et al.* The Bcl-3 oncoprotein acts as a bridging factor between NF-κB/Rel and nuclear co-regulators. *Oncogene* **18**, 3316–3323 (1999).

347. Richard, M., Louahed, J., Demoulin, J. B. & Renauld, J. C. Interleukin-9 regulates NF-kappaB activity through BCL3 gene induction. *Blood* **93**, 4318–27 (1999).

348. Wessells, J. *et al.* BCL-3 and NF-κB p50 Attenuate Lipopolysaccharide-induced Inflammatory Responses in Macrophages. *Journal of Biological Chemistry* **279**, 49995–50003 (2004).

349. Napetschnig, J. & Wu, H. Molecular Basis of NF-κB Signaling. *Annu Rev Biophys* **42**, 443–468 (2013).

350. Karin, M. & Greten, F. R. NF-κB: linking inflammation and immunity to cancer development and progression. *Nat Rev Immunol* **5**, 749–759 (2005).

351. Vallabhapurapu, S. & Karin, M. Regulation and Function of NF-κB Transcription Factors in the Immune System. *Annu Rev Immunol* **27**, 693–733 (2009).

352. Mogensen, T. H. Pathogen Recognition and Inflammatory Signaling in Innate Immune Defenses. *Clin Microbiol Rev* **22**, 240–273 (2009).

353. Hayden, M. S. & Ghosh, S. NF-κB in immunobiology. *Cell Res* **21**, 223–244 (2011).

354. Ebner, K., Bandion, A., Binder, B. R., de Martin, R. & Schmid, J. A. GMCSF activates NF-κB via direct interaction of the GMCSF receptor with IκB kinase β. *Blood* **102**, 192–199 (2003).

355. Gerondakis, S., Grossmann, M., Nakamura, Y., Pohl, T. & Grumont, R. Genetic approaches in mice to understand Rel/NF-κB and IκB function: transgenics and knockouts. *Oncogene* **18**, 6888–6895 (1999).

356. Karin, M., Cao, Y., Greten, F. R. & Li, Z.-W. NF-κB in cancer: from innocent bystander to major culprit. *Nat Rev Cancer* **2**, 301–310 (2002).

357. Li, Q. & Verma, I. M. NF-κB regulation in the immune system. *Nat Rev Immunol* **2**, 725–734 (2002).

358. Gordon, S. & Taylor, P. R. Monocyte and macrophage heterogeneity. *Nat Rev Immunol* **5**, 953–964 (2005).

359. Gordon, S. Alternative activation of macrophages. *Nat Rev Immunol* **3**, 23–35 (2003).

360. Senftleben, U. *et al.* Activation by IKKα of a Second, Evolutionary Conserved, NF-κB Signaling Pathway. *Science (1979)* **293**, 1495–1499 (2001).

361. Bonizzi, G. *et al.* Activation of IKKα target genes depends on recognition of specific κB binding sites by RelB:p52 dimers. *EMBO J* **23**, 4202–4210 (2004).

362. Caamaño, J. H. *et al.* Nuclear Factor (NF)-κB2 (p100/p52) Is Required for Normal Splenic Microarchitecture and B Cell–mediated Immune Responses. *J Exp Med* **187**, 185–196 (1998).

363. Franzoso, G. *et al.* Mice Deficient in Nuclear Factor (NF)-κB/p52 Present with Defects in Humoral Responses, Germinal Center Reactions, and Splenic Microarchitecture. *J Exp Med* **187**, 147–159 (1998).

364. Wu, L. *et al.* RelB Is Essential for the Development of Myeloid-Related CD8α− Dendritic Cells but Not of Lymphoid-Related CD8α+ Dendritic Cells. *Immunity* **9**, 839–847 (1998).

365. Weih, D. S., Yilmaz, Z. B. & Weih, F. Essential Role of RelB in Germinal Center and Marginal Zone Formation and Proper Expression of Homing Chemokines. *The Journal of Immunology* **167**, 1909–1919 (2001).

366. Speirs, K., Lieberman, L., Caamano, J., Hunter, C. A. & Scott, P. Cutting Edge: NF-κB2 Is a Negative Regulator of Dendritic Cell Function. *The Journal of Immunology* **172**, 752–756 (2004).

367. Cao, X. Self-regulation and cross-regulation of pattern-recognition receptor signalling in health and disease. *Nat Rev Immunol* **16**, 35–50 (2016).

368. Kumar, H., Kawai, T. & Akira, S. Pathogen Recognition by the Innate Immune System. *Int Rev Immunol* **30**, 16–34 (2011).

369. Akira, S., Uematsu, S. & Takeuchi, O. Pathogen Recognition and Innate Immunity. *Cell* **124**, 783–801 (2006).

370. Kawai, T. & Akira, S. The role of pattern-recognition receptors in innate immunity: update on Toll-like receptors. *Nat Immunol* **11**, 373–384 (2010).

371. Taniguchi, K. & Karin, M. NF-κB, inflammation, immunity and cancer: coming of age. *Nat Rev Immunol* **18**, 309–324 (2018).

372. Karin, M. & Ben-Neriah, Y. Phosphorylation Meets Ubiquitination: The Control of NF-κB Activity. *Annu Rev Immunol* **18**, 621–663 (2000).

373. O'Neill, L. A. J., Fitzgerald, K. A. & Bowie, A. G. The Toll–IL-1 receptor adaptor family grows to five members. *Trends Immunol* **24**, 286–289 (2003).

374. Martin, M. U. & Wesche, H. Summary and comparison of the signaling mechanisms of the Toll/interleukin-1 receptor family. *Biochimica et Biophysica Acta (BBA) - Molecular Cell Research* **1592**, 265–280 (2002).

375. Ninomiya-Tsuji, J. *et al.* The kinase TAK1 can activate the NIK-IκB as well as the MAP kinase cascade in the IL-1 signalling pathway. *Nature* **398**, 252–256 (1999).

376. Deng, L. *et al.* Activation of the IκB Kinase Complex by TRAF6 Requires a Dimeric Ubiquitin-Conjugating Enzyme Complex and a Unique Polyubiquitin Chain. *Cell* **103**, 351–361 (2000).

378. Wang, C. *et al.* TAK1 is a ubiquitin-dependent kinase of MKK and IKK. *Nature* **412**, 346–351 (2001).

379. Xia, Z.-P. *et al.* Direct activation of protein kinases by unanchored polyubiquitin chains. *Nature* **461**, 114–119 (2009).

380. Kopp, E. *et al.* ECSIT is an evolutionarily conserved intermediate in the Toll/IL-1 signal transduction pathway. *Genes Dev* **13**, 2059–2071 (1999).

381. Huang, Q. *et al.* Differential regulation of interleukin 1 receptor and Toll-like receptor signaling by MEKK3. *Nat Immunol* **5**, 98–103 (2004).

382. Sun, S.-C. & Ley, S. C. New insights into NF-κB regulation and function. *Trends Immunol* **29**, 469–478 (2008).

383. Israel, A. The IKK Complex, a Central Regulator of NF- B Activation. *Cold Spring Harb Perspect Biol* **2**, a000158–a000158 (2010).

384. Rao, P. *et al.* IκBβ acts to inhibit and activate gene expression during the inflammatory response. *Nature* **466**, 1115–1119 (2010).

385. Karin, M. Nuclear factor-κB in cancer development and progression. *Nature* **441**, 431–436 (2006).

386. Hayden, M. S. & Ghosh, S. Shared Principles in NF-κB Signaling. *Cell* **132**, 344–362 (2008).

387. Schuster, M., Annemann, M., Plaza-Sirvent, C. & Schmitz, I. Atypical IκB proteins – nuclear modulators of NF-κB signaling. *Cell Communication and Signaling* **11**, 23 (2013).

388. Sun, S.-C. Non-canonical NF-κB signaling pathway. *Cell Res* **21**, 71–85 (2011).

389. Mussbacher, M. *et al.* Cell Type-Specific Roles of NF-κB Linking Inflammation and Thrombosis. *Front Immunol* **10**, (2019).

390. Sun, S.-C., Ganchi, P. A., Ballard, D. W. & Greene, W. C. NF-κB Controls Expression of Inhibitor IκBα: Evidence for an Inducible Autoregulatory Pathway. *Science (1979)* **259**, 1912–1915 (1993).

391. Tam, W. F. & Sen, R. IκB Family Members Function by Different Mechanisms. *Journal of Biological Chemistry* **276**, 7701–7704 (2001).

392. Whiteside, S. T. I kappa B epsilon, a novel member of the Ikappa B family, controls RelA and cRel NF-kappa B activity. *EMBO J* **16**, 1413–1426 (1997).

393. Kearns, J. D., Basak, S., Werner, S. L., Huang, C. S. & Hoffmann, A. IκBε provides negative feedback to control NF-κB oscillations, signaling dynamics, and inflammatory gene expression. *J Cell Biol* **173**, 659–664 (2006).

394. Ghosh, S., May, M. J. & Kopp, E. B. NF-κB AND REL PROTEINS: Evolutionarily Conserved Mediators of Immune Responses. *Annu Rev Immunol* **16**, 225–260 (1998).

395. Scheibel, M. *et al.* IκBβ is an essential co-activator for LPS-induced IL-1β transcription in vivo. *Journal of Experimental Medicine* **207**, 2621–2630 (2010).

396. Dempsey, P. W., Doyle, S. E., He, J. Q. & Cheng, G. The signaling adaptors and pathways activated by TNF superfamily. *Cytokine Growth Factor Rev* **14**, 193–209 (2003).

397. Gaur, U. & Aggarwal, B. B. Regulation of proliferation, survival and apoptosis by members of the TNF superfamily. *Biochem Pharmacol* **66**, 1403–1408 (2003).

398. Yang, J. *et al.* The essential role of MEKK3 in TNF-induced NF-κB activation. *Nat Immunol* **2**, 620–624 (2001).

399. Dejardin, E. *et al.* The Lymphotoxin-β Receptor Induces Different Patterns of Gene Expression via Two NF-κB Pathways. *Immunity* **17**, 525–535 (2002).

400. Novack, D. V. *et al.* The IκB Function of NF-κB2 p100 Controls Stimulated Osteoclastogenesis. *J Exp Med* **198**, 771–781 (2003).

401. Nishikori, M., Ohno, H., Haga, H. & Uchiyama, T. Stimulation of CD30 in anaplastic large cell lymphoma leads to production of nuclear factor-κB p52, which is associated with hyperphosphorylated Bcl-3. *Cancer Sci* **96**, 487–497 (2005).

402. Nonaka, M. *et al.* Aberrant NF-κB2/p52 expression in Hodgkin/Reed–Sternberg cells and CD30-transformed rat fibroblasts. *Oncogene* **24**, 3976–3986 (2005).

403. Murray, S. E. *et al.* NF-κB–inducing kinase plays an essential T cell–intrinsic role in graft-versus-host disease and lethal autoimmunity in mice. *Journal of Clinical Investigation* **121**, 4775–4786 (2011).

404. McPherson, A. J., Snell, L. M., Mak, T. W. & Watts, T. H. Opposing Roles for TRAF1 in the Alternative versus Classical NF-κB Pathway in T Cells. *Journal of Biological Chemistry* **287**, 23010–23019 (2012).

405. Saitoh, T. *et al.* TWEAK Induces NF-κB2 p100 Processing and Long Lasting NF-κB Activation. *Journal of Biological Chemistry* **278**, 36005–36012 (2003).

406. Ramakrishnan, P., Wang, W. & Wallach, D. Receptor-Specific Signaling for Both the Alternative and the Canonical NF-κB Activation Pathways by NF-κB-Inducing Kinase. *Immunity* **21**, 477–489 (2004).

407. Jin, J. *et al.* Noncanonical NF-κB Pathway Controls the Production of Type I Interferons in Antiviral Innate Immunity. *Immunity* **40**, 342–354 (2014).

408. Zarnegar, B. J. *et al.* Noncanonical NF-κB activation requires coordinated assembly of a regulatory complex of the adaptors cIAP1, cIAP2, TRAF2 and TRAF3 and the kinase NIK. *Nat Immunol* **9**, 1371–1378 (2008).

409. Vallabhapurapu, S. *et al.* Nonredundant and complementary functions of TRAF2 and TRAF3 in a ubiquitination cascade that activates NIK-dependent alternative NF-κB signaling. *Nat Immunol* **9**, 1364–1370 (2008).

410. Liao, G., Zhang, M., Harhaj, E. W. & Sun, S.-C. Regulation of the NF-κB-inducing Kinase by Tumor Necrosis Factor Receptor-associated Factor 3-induced Degradation. *Journal of Biological Chemistry* **279**, 26243–26250 (2004).

411. Sanjo, H., Zajonc, D. M., Braden, R., Norris, P. S. & Ware, C. F. Allosteric Regulation of the Ubiquitin:NIK and Ubiquitin:TRAF3 E3 Ligases by the Lymphotoxin-β Receptor. *Journal of Biological Chemistry* **285**, 17148–17155 (2010).

412. Ganeff, C. *et al.* Induction of the Alternative NF-κB Pathway by Lymphotoxin αβ (LTαβ) Relies on Internalization of LTβ Receptor. *Mol Cell Biol* **31**, 4319–4334 (2011).

413. Ge, J. *et al.* A *Legionella* type IV effector activates the NF-κB pathway by phosphorylating the IκB family of inhibitors. *Proceedings of the National Academy of Sciences* **106**, 13725–13730 (2009).

414. Bram, R. J. TBK1 suppression of IgA in the NIK of time. *Nat Immunol* **13**, 1027–1029 (2012).

415. Jin, J. *et al.* The kinase TBK1 controls IgA class switching by negatively regulating noncanonical NF-κB signaling. *Nat Immunol* **13**, 1101–1109 (2012).

416. Razani, B. *et al.* Negative Feedback in Noncanonical NF-κB Signaling Modulates NIK Stability Through IKKα-Mediated Phosphorylation. *Sci Signal* **3**, (2010).

417. Xiao, G., Harhaj, E. W. & Sun, S.-C. NF-κB-Inducing Kinase Regulates the Processing of NF-κB2 p100. *Mol Cell* **7**, 401–409 (2001).

418. Liang, C., Zhang, M. & Sun, S.-C. β-TrCP binding and processing of NF-κB2/p100 involve its phosphorylation at serines 866 and 870. *Cell Signal* **18**, 1309–1317 (2006).

419. Cildir, G., Low, K. C. & Tergaonkar, V. Noncanonical NF-κB Signaling in Health and Disease. *Trends Mol Med* **22**, 414–429 (2016).

420. Betts, J. C. & Nabel, G. J. Differential Regulation of NF-κB2(p100) Processing and Control by Amino-Terminal Sequences. *Mol Cell Biol* **16**, 6363–6371 (1996).

421. Sun, S. C., Ganchi, P. A., Béraud, C., Ballard, D. W. & Greene, W. C. Autoregulation of the NF-kappa B transactivator RelA(p65) by multiple cytoplasmic inhibitors containing ankyrinmotifs. *Proceedings of the National Academy of Sciences* **91**, 1346–1350 (1994).

422. Tucker, E. *et al.* A Novel Mutation in the *Nfkb2* Gene Generates an NF-κB2 "Super Repressor". *The Journal of Immunology* **179**, 7514–7522 (2007).

423. Zarnegar, B., Yamazaki, S., He, J. Q. & Cheng, G. Control of canonical NF-κB activation through the NIK–IKK complex pathway. *Proceedings of the National Academy of Sciences* **105**, 3503–3508 (2008).

424. Grivennikov, S. I. & Karin, M. Dangerous liaisons: STAT3 and NF-κB collaboration and crosstalk in cancer. *Cytokine Growth Factor Rev* **21**, 11–19 (2010).

425. Oeckinghaus, A., Hayden, M. S. & Ghosh, S. Crosstalk in NF-κB signaling pathways. *Nat Immunol* **12**, 695–708 (2011).

426. Zhong, B., Tien, P. & Shu, H.-B. Innate immune responses: Crosstalk of signaling and regulation of gene transcription. *Virology* **352**, 14–21 (2006).

427. Xia, Y. *et al.* RelB Modulation of IκBα Stability as a Mechanism of Transcription Suppression of Interleukin-1α (IL-1α), IL-1β, and Tumor Necrosis Factor Alpha in Fibroblasts. *Mol Cell Biol* **19**, 7688–7696 (1999).

428. Jacque, E., Tchenio, T., Piton, G., Romeo, P.-H. & Baud, V. RelA repression of RelB activity induces selective gene activation downstream of TNF receptors. *Proceedings of the National Academy of Sciences* **102**, 14635–14640 (2005).

429. Saccani, S., Pantano, S. & Natoli, G. Modulation of NF-κB Activity by Exchange of Dimers. *Mol Cell* **11**, 1563–1574 (2003).

430. Lawrence, T., Bebien, M., Liu, G. Y., Nizet, V. & Karin, M. IKKα limits macrophage NF-κB activation and contributes to the resolution of inflammation. *Nature* **434**, 1138–1143 (2005).

431. deLuca, L. S. & Gommerman, J. L. Fine-tuning of dendritic cell biology by the TNF superfamily. *Nat Rev Immunol* **12**, 339–351 (2012).

432. Gerondakis, S. *et al.* Unravelling the complexities of the NF-κB signalling pathway using mouse knockout and transgenic models. *Oncogene* **25**, 6781–6799 (2006).

433. Seki, T. *et al.* Visualization of RelB expression and activation at the single-cell level during dendritic cell maturation in *Relb-Venus* knock-in mice. *J Biochem* mvv064 (2015) doi:10.1093/jb/mvv064.

434. Lind, E. F. *et al.* Dendritic Cells Require the NF-κB2 Pathway for Cross-Presentation of Soluble Antigens. *The Journal of Immunology* **181**, 354–363 (2008).

435. Katakam, A. K. *et al.* Dendritic cells require NIK for CD40-dependent cross-priming of CD8 + T cells. *Proceedings of the National Academy of Sciences* **112**, 14664–14669 (2015).

436. Croft, M. The role of TNF superfamily members in T-cell function and diseases. *Nat Rev Immunol* **9**, 271–285 (2009).

437. Elewaut, D. *et al.* NIK-dependent RelB Activation Defines a Unique Signaling Pathway for the Development of Vα14 *i* NKT Cells. *J Exp Med* **197**, 1623–1633 (2003).

438. Sivakumar, V., Hammond, K. J. L., Howells, N., Pfeffer, K. & Weih, F. Differential Requirement for Rel/Nuclear Factor κB Family Members in Natural Killer T Cell Development. *J Exp Med* **197**, 1613–1621 (2003).

439. Mair, F. *et al.* The NFκB-inducing kinase is essential for the developmental programming of skin-resident and IL-17-producing γδ T cells. *Elife* **4**, (2015).

440. Aronica, M. A. *et al.* Preferential role for NF-kappa B/Rel signaling in the type 1 but not type 2 T cell-dependent immune response in vivo. *J Immunol* **163**, 5116–24 (1999).

441. Balasubramani, A., Mukasa, R., Hatton, R. D. & Weaver, C. T. Regulation of the *Ifng* locus in the context of T-lineage specification and plasticity. *Immunol Rev* **238**, 216–232 (2010).

442. Weil, R. & Israël, A. T-cell-receptor- and B-cell-receptor-mediated activation of NF-κB in lymphocytes. *Curr Opin Immunol* **16**, 374–381 (2004).

443. Lee, K.-Y., D'Acquisto, F., Hayden, M. S., Shim, J.-H. & Ghosh, S. PDK1 Nucleates T Cell Receptor-Induced Signaling Complex for NF-κB Activation. *Science (1979)* **308**, 114–118 (2005).

444. Jane-wit, D. *et al.* Complement membrane attack complexes activate noncanonical NF-κB by forming an Akt + NIK + signalosome on Rab5 + endosomes. *Proceedings of the National Academy of Sciences* **112**, 9686–9691 (2015).

445. Kamura, T. *et al.* The Elongin BC complex interacts with the conserved SOCS-box motif present in members of the SOCS, ras, WD-40 repeat, and ankyrin repeat families. *Genes Dev* **12**, 3872–3881 (1998).

446. Nakagawa, R. *et al.* SOCS-1 Participates in Negative Regulation of LPS Responses. *Immunity* **17**, 677–687 (2002).

447. Kinjyo, I. *et al.* SOCS1/JAB Is a Negative Regulator of LPS-Induced Macrophage Activation. *Immunity* **17**, 583–591 (2002).

448. Liu, B. *et al.* PIAS1 selectively inhibits interferon-inducible genes and is important in innate immunity. *Nat Immunol* **5**, 891–898 (2004).

449. Liu, B. *et al.* Proinflammatory Stimuli Induce IKKα-Mediated Phosphorylation of PIAS1 to Restrict Inflammation and Immunity. *Cell* **129**, 903–914 (2007).

450. Liu, B. *et al.* Negative Regulation of NF-κB Signaling by PIAS1. *Mol Cell Biol* **25**, 1113–1123 (2005).

451. Hallam, S., Escorcio-Correia, M., Soper, R., Schultheiss, A. & Hagemann, T. Activated macrophages in the tumour microenvironment—dancing to the tune of TLR and NF-κB. *J Pathol* **219**, 143–152 (2009).

452. Li-Weber, M., Giaisi, M., Baumann, S., Pálfi, K. & Krammer, P. H. NF-κB synergizes with NF-AT and NF-IL6 in activation of the IL-4 gene in T cells. *Eur J Immunol* **34**, 1111–1118 (2004).

453. Goenka, S. & Kaplan, M. H. Transcriptional regulation by STAT6. *Immunol Res* **50**, 87–96 (2011).

454. Mescher, A. L., Neff, A. W. & King, M. W. Inflammation and immunity in organ regeneration. *Dev Comp Immunol* **66**, 98–110 (2017).

455. Cañedo-Dorantes, L. & Cañedo-Ayala, M. Skin acute wound healing: A comprehensive review. *International Journal of Inflammation* vol. 2019 Preprint at https://doi.org/10.1155/2019/3706315 (2019).

456. Kloc, M. *et al.* Macrophage functions in wound healing. *Journal of Tissue Engineering and Regenerative Medicine* vol. 13 99–109 Preprint at https://doi.org/10.1002/term.2772 (2019).

457. Takeo, M., Lee, W. & Ito, M. Wound healing and skin regeneration. *Cold Spring Harb Perspect Med* **5**, (2015).

458. Knoedler, S. *et al.* Regulatory T cells in skin regeneration and wound healing. *Military Medical Research* vol. 10 Preprint at https://doi.org/10.1186/s40779-023-00484-6 (2023).

459. Lichtman, M. K., Otero-Vinas, M. & Falanga, V. Transforming growth factor beta (TGF-β) isoforms in wound healing and fibrosis. *Wound Repair and Regeneration* **24**, 215–222 (2016).

460. Nath, R. K., LaRegina, M., Markham, H., Ksander, G. A. & Weeks, P. M. The expression of transforming growth factor type beta in fetal and adult rabbit skin wounds. *J Pediatr Surg* **29**, 416–421 (1994).

461. Jiang, D. & Rinkevich, Y. Scars or regeneration?—dermal fibroblasts as drivers of diverse skin wound responses. *International Journal of Molecular Sciences* vol. 21 Preprint at https://doi.org/10.3390/ijms21020617 (2020).

462. Jennings, R. W. *et al.* Ontogeny of fetal sheep polymorphonuclear leukocyte phagocytosis. *J Pediatr Surg* **26**, 853–855 (1991).

463. Liechty, K. W., Adzick, N. S. & Crombleholme, T. M. DIMINISHED INTERLEUKIN 6 (IL-6) PRODUCTION DURING SCARLESS HUMAN FETAL WOUND REPAIR. *Cytokine* **12**, 671–676 (2000).

464. Liechty, K. W., Crombleholme, T. M., Cass, D. L., Martin, B. & Adzick, N. S. Diminished interleukin-8 (IL-8) production in the fetal wound healing response. *J Surg Res* **77**, 80–4 (1998).

465. Eming, S. A., Wynn, T. A. & Martin, P. Inflammation and metabolism in tissue repair and regeneration. *Science (1979)* **356**, 1026–1030 (2017).

466. McGovern, N. *et al.* Human fetal dendritic cells promote prenatal T-cell immune suppression through arginase-2. *Nature* **546**, 662–666 (2017).

467. Ashcroft, G. S. *et al.* Mice lacking Smad3 show accelerated wound healing and an impaired local inflammatory response. *Nat Cell Biol* **1**, 260–6 (1999).

468. Shah, M., Foreman, D. M. & Ferguson, M. W. Neutralisation of TGF-beta 1 and TGF-beta 2 or exogenous addition of TGF-beta 3 to cutaneous rat wounds reduces scarring. *J Cell Sci* **108 (Pt 3)**, 985–1002 (1995).

469. Hsu, M., Peled, Z. M., Chin, G. S., Liu, W. & Longaker, M. T. Ontogeny of expression of transforming growth factor-beta 1 (TGF-beta 1), TGF-beta 3, and TGF-beta receptors I and II in fetal rat fibroblasts and skin. *Plast Reconstr Surg* **107**, 1787–94; discussion 1795-6 (2001).

470. Occleston, N. L. *et al.* Discovery and development of avotermin (recombinant human transforming growth factor beta 3): A new class of prophylactic therapeutic for the improvement of scarring. *Wound Repair and Regeneration* **19**, (2011).

471. Ferguson, M. W. J. & O'Kane, S. Scar–free healing: from embryonic mechanisms to adult therapeutic intervention. *Philos Trans R Soc Lond B Biol Sci* **359**, 839–850 (2004).

472. Finnson, K. W., McLean, S., Di Guglielmo, G. M. & Philip, A. Dynamics of Transforming Growth Factor Beta Signaling in Wound Healing and Scarring. *Adv Wound Care (New Rochelle)* **2**, 195–214 (2013).

473. Martin, P., Dickson, M. C., Millan, F. A. & Akhurst, R. J. Rapid induction and clearance of TGFβ1 is an early response to wounding in the mouse embryo. *Dev Genet* **14**, 225–238 (1993).

474. Gordon, A. *et al.* Permissive environment in postnatal wounds induced by adenoviral-mediated overexpression of the anti-inflammatory cytokine interleukin-10 prevents scar formation. *Wound Repair and Regeneration* **16**, 70–79 (2008).

475. Liechty, K. W., Kim, H. B., Adzick, N. S. & Crombleholme, T. M. Fetal wound repair results in scar formation in interleukin-10–deficient mice in a syngeneic murine model of scarless fetal wound repair. *J Pediatr Surg* **35**, 866–873 (2000).

476. Balaji, S. *et al.* Interleukin-10–mediated regenerative postnatal tissue repair is dependent on regulation of hyaluronan metabolism *via* fibroblast-specific STAT3 signaling. *The FASEB Journal* **31**, 868–881 (2017).

477. Xue, M. & Jackson, C. J. Extracellular Matrix Reorganization During Wound Healing and Its Impact on Abnormal Scarring. *Adv Wound Care (New Rochelle)* **4**, 119–136 (2015).

478. Daponte, V., Tylzanowski, P. & Forlino, A. Appendage regeneration in vertebrates: What makes this possible? *Cells* vol. 10 1–28 Preprint at https://doi.org/10.3390/cells10020242 (2021).

479. Bolaños-Castro, L. A., Walters, H. E., García Vázquez, R. O. & Yun, M. H. Immunity in salamander regeneration: Where are we standing and where are we headed? *Developmental Dynamics* **250**, 753–767 (2021).

480. Lopez, D. *et al.* Mapping hematopoiesis in a fully regenerative vertebrate: the axolotl. *Blood* **124**, 1232–1241 (2014).

481. Durand, C., Charlemagne, J. & Fellah, J. S. RAG expression is restricted to the first year of life in the Mexican axolotl. *Immunogenetics* **51**, 681–687 (2000).

482. André, S., Kerfourn, F. & Fellah, J. S. Molecular and biochemical characterization of the Mexican axolotl CD3 (CD3ε and CD3γ/δ). *Immunogenetics* **63**, 847–853 (2011).

483. Fellah, J. S., Vaulot, D., Tournefier, A. & Charlemagne, J. Ontogeny of immunoglobulin expression in the Mexican axolotl. *Development* **107**, 253–263 (1989).

484. Fellah, J. S., Kerfourn, F., Dumay, A.-M., Aubet, G. & Charlemagne, J. Structure and diversity of the T-cell receptor α chain in the Mexican axolotl. *Immunogenetics* **45**, 235–241 (1997).

485. Fellah, J. S. *et al.* Structure, diversity and expression of the TCRδ chains in the Mexican axolotl. *Eur J Immunol* **32**, 1349 (2002).

486. Schaerlinger, B., Bascove, M. & Frippiat, J.-P. A new isotype of immunoglobulin heavy chain in the urodele amphibian Pleurodeles waltl predominantly expressed in larvae. *Mol Immunol* **45**, 776–786 (2008).

487. Frippiat, J.-P., Frippiat, C., Kremarik, P., Ropars, A. & Dournon, C. The recombination-activating gene 1 of Pleurodeles waltl (urodele amphibian) is transcribed in lymphoid tissues and in the central nervous system. *Immunogenetics* **52**, 264–275 (2001).

488. Ropars, A., Bautz, A.-M. & Dournon, C. Sequencing and expression of the CD3 γ/δ mRNA in Pleurodeles waltl (urodele amphibian). *Immunogenetics* **54**, 130–138 (2002).

489. Godwin, J. W., Debuque, R., Salimova, E. & Rosenthal, N. A. Heart regeneration in the salamander relies on macrophage-mediated control of fibroblast activation and the extracellular landscape. *NPJ Regen Med* **2**, 22 (2017).

490. Morales, R. A. & Allende, M. L. Peripheral Macrophages Promote Tissue Regeneration in Zebrafish by Fine-Tuning the Inflammatory Response. *Front Immunol* **10**, (2019).

491. Reyer, R. W. Macrophage invasion and phagocytic activity during lens regeneration from the iris epithelium in newts. *American Journal of Anatomy* **188**, 329–344 (1990).

492. Nguyen-Chi, M. *et al.* TNF signaling and macrophages govern fin regeneration in zebrafish larvae. *Cell Death Dis* **8**, e2979–e2979 (2017).

493. Pei, W. *et al.* Extracellular HSP60 triggers tissue regeneration and wound healing by regulating inflammation and cell proliferation. *NPJ Regen Med* **1**, 16013 (2016).

494. Alibardi, L. Immunolocalization of 5BrdU long retaining labeled cells and macrophage infiltration in the scarring limb of lizard after limb amputation. *Tissue Cell* **48**, 197–207 (2016).

495. Alibardi, L. Autoradiography and inmmunolabeling suggests that lizard blastema contains arginase-positive M2-like macrophages that may support tail regeneration. *Annals of Anatomy - Anatomischer Anzeiger* **231**, 151549 (2020).

496. Kanao, T. & Miyachi, Y. Lymphangiogenesis promotes lens destruction and subsequent lens regeneration in the newt eyeball, and both processes can be accelerated by transplantation of dendritic cells. *Dev Biol* **290**, 118–124 (2006).

497. Godwin, J. W., Pinto, A. R. & Rosenthal, N. A. Macrophages are required for adult salamander limb regeneration. *Proceedings of the National Academy of Sciences* **110**, 9415–9420 (2013).

498. Londono, R. *et al.* Single cell sequencing analysis of lizard phagocytic cell populations and their role in tail regeneration. *J Immunol Regen Med* **8**, 100029 (2020).

499. Tsai, S. L., Baselga-Garriga, C. & Melton, D. A. Blastemal progenitors modulate immune signaling during early limb regeneration. *Development* **146**, (2019).

500. Gerber, T. *et al.* Single-cell analysis uncovers convergence of cell identities during axolotl limb regeneration. *Science (1979)* **362**, (2018).

501. Tournefier, A. *et al.* Structure of MHC class I and class II cDNAs and possible immunodeficiency linked to class II expression in the Mexican axolotl. *Immunol Rev* **166**, 259–277 (1998).

502. Rodgers, A. K., Smith, J. J. & Voss, S. R. Identification of immune and non-immune cells in regenerating axolotl limbs by single-cell sequencing. *Exp Cell Res* **394**, 112149 (2020).

503. Leigh, N. D. *et al.* Transcriptomic landscape of the blastema niche in regenerating adult axolotl limbs at single-cell resolution. *Nat Commun* **9**, (2018).

504. Grow, M., Neff, A. W., Mescher, A. L. & King, M. W. Global analysis of gene expression in *Xenopus* hindlimbs during stage-dependent complete and incomplete regeneration. *Developmental Dynamics* **235**, 2667–2685 (2006).

505. Zimmerman, L. M., Vogel, L. A. & Bowden, R. M. Understanding the vertebrate immune system: insights from the reptilian perspective. *Journal of Experimental Biology* **213**, 661–671 (2010).

506. Fahmy, G. H. & Sicard, R. E. A role for effectors of cellular immunity in epimorphic regeneration of amphibian limbs. *In Vivo* **16**, 179–84 (2002).

507. Franchini, A. & Bertolotti, E. The thymus and tail regenerative capacity in Xenopus laevis tadpoles. *Acta Histochem* **114**, 334–341 (2012).

508. Hui, S. P. *et al.* Zebrafish Regulatory T Cells Mediate Organ-Specific Regenerative Programs. *Dev Cell* **43**, 659-672.e5 (2017).

509. Mescher, A. L. *et al.* Cells of cutaneous immunity in Xenopus: Studies during larval development and limb regeneration. *Dev Comp Immunol* **31**, 383–393 (2007).

510. Mescher, A. L. Macrophages and fibroblasts during inflammation and tissue repair in models of organ regeneration. *Regeneration* **4**, 39–53 (2017).

511. Zhang, S. & Cui, P. Complement system in zebrafish. *Dev Comp Immunol* **46**, 3–10 (2014).

512. Natarajan, N. *et al.* Complement Receptor C5aR1 Plays an Evolutionarily Conserved Role in Successful Cardiac Regeneration. *Circulation* **137**, 2152–2165 (2018).

513. Del Rio-Tsonis, K., Tsonis, P. A., Zarkadis, I. K., Tsagas, A. G. & Lambris, J. D. Expression of the third component of complement, C3, in regenerating limb blastema cells of urodeles. *J Immunol* **161**, 6819–24 (1998).

514. Kimura, Y. *et al.* Expression of Complement 3 and Complement 5 in Newt Limb and Lens Regeneration. *The Journal of Immunology* **170**, 2331–2339 (2003).

515. Sibai, M. *et al.* Comparison of protein expression profile of limb regeneration between neotenic and metamorphic axolotl. *Biochem Biophys Res Commun* **522**, 428–434 (2020).

516. Delavary, B. M., van der Veer, W. M., van Egmond, M., Niessen, F. B. & Beelen, R. H. J. Macrophages in skin injury and repair. *Immunobiology* **216**, 753–762 (2011).

517. Rabiller, L. *et al.* Driving regeneration, instead of healing, in adult mammals: the decisive role of resident macrophages through efferocytosis. *NPJ Regen Med* **6**, (2021).

518. Wu, J. *et al.* Macrophage phenotypic switch orchestrates the inflammation and repair/regeneration following acute pancreatitis injury. *EBioMedicine* **58**, (2020).

519. Arnold, L. *et al.* Inflammatory monocytes recruited after skeletal muscle injury switch into antiinflammatory macrophages to support myogenesis. *J Exp Med* **204**, 1057–1069 (2007).

520. Nahrendorf, M. *et al.* The healing myocardium sequentially mobilizes two monocyte subsets with divergent and complementary functions. *J Exp Med* **204**, 3037–3047 (2007).

521. Perdiguero, E. *et al.* p38/MKP-1–regulated AKT coordinates macrophage transitions and resolution of inflammation during tissue repair. *Journal of Cell Biology* **195**, 307–322 (2011).

522. Lu, H. *et al.* Macrophages recruited *via* CCR2 produce insulin-like growth factor-1 to repair acute skeletal muscle injury. *The FASEB Journal* **25**, 358–369 (2011).

523. Saclier, M. *et al.* Differentially Activated Macrophages Orchestrate Myogenic Precursor Cell Fate During Human Skeletal Muscle Regeneration. *Stem Cells* **31**, 384–396 (2013).

524. Lin, S.-L. *et al.* Macrophage Wnt7b is critical for kidney repair and regeneration. *Proceedings of the National Academy of Sciences* **107**, 4194–4199 (2010).

525. Boulter, L. *et al.* Macrophage-derived Wnt opposes Notch signaling to specify hepatic progenitor cell fate in chronic liver disease. *Nat Med* **18**, 572–579 (2012).

526. Burzyn, D. *et al.* A Special Population of Regulatory T Cells Potentiates Muscle Repair. *Cell* **155**, 1282–1295 (2013).

527. Heredia, J. E. *et al.* Type 2 Innate Signals Stimulate Fibro/Adipogenic Progenitors to Facilitate Muscle Regeneration. *Cell* **153**, 376–388 (2013).

528. Yang, W. *et al.* Neutrophils promote the development of reparative macrophages mediated by ROS to orchestrate liver repair. *Nat Commun* **10**, 1076 (2019).

529. Martin, P. *et al.* Wound Healing in the PU.1 Null Mouse—Tissue Repair Is Not Dependent on Inflammatory Cells. *Current Biology* **13**, 1122–1128 (2003).

530. Zhang, C. *et al.* Complement C3a signaling facilitates skeletal muscle regeneration by regulating monocyte function and trafficking. *Nat Commun* **8**, 2078 (2017).

531. Simkin, J., Gawriluk, T. R., Gensel, J. C. & Seifert, A. W. Macrophages are necessary for epimorphic regeneration in African spiny mice. (2017) doi:10.7554/eLife.24623.001.

532. Seifert, A. W. *et al.* Skin shedding and tissue regeneration in African spiny mice (Acomys). *Nature* **489**, 561–565 (2012).

533. Cyr, J. L. *et al.* Regeneration-Competent and -Incompetent Murids Differ in Neutrophil Quantity and Function. *Integr Comp Biol* **59**, (2019).

534. Gawriluk, T. R. *et al.* Complex Tissue Regeneration in Mammals Is Associated With Reduced Inflammatory Cytokines and an Influx of T Cells. *Front Immunol* **11**, (2020).

535. Brant, J. O., Yoon, J. H., Polvadore, T., Barbazuk, W. B. & Maden, M. Cellular events during scar-free skin regeneration in the spiny mouse, Acomys. *Wound Repair and Regeneration* **24**, 75–88 (2016).

536. Maden, M. *et al.* Perfect chronic skeletal muscle regeneration in adult spiny mice, Acomys cahirinus. *Sci Rep* **8**, (2018).

537. Rousselle, P., Braye, F. & Dayan, G. Re-epithelialization of adult skin wounds: Cellular mechanisms and therapeutic strategies. *Adv Drug Deliv Rev* **146**, 344–365 (2019).

538. Rousselle, P., Montmasson, M. & Garnier, C. Extracellular matrix contribution to skin wound re-epithelialization. *Matrix Biology* **75–76**, 12–26 (2019).

539. Pastar, I. *et al.* Epithelialization in Wound Healing: A Comprehensive Review. *Adv Wound Care (New Rochelle)* **3**, 445–464 (2014).

540. Nyström, A. & Bruckner-Tuderman, L. Matrix molecules and skin biology. *Semin Cell Dev Biol* **89**, 136–146 (2019).

541. Wynn, T. & Barron, L. Macrophages: Master Regulators of Inflammation and Fibrosis. *Semin Liver Dis* **30**, 245–257 (2010).

542. Santoro, M. & Gaudino, G. Cellular and molecular facets of keratinocyte reepithelization during wound healing. *Exp Cell Res* **304**, 274–286 (2005).

543. Werner, S., Krieg, T. & Smola, H. Keratinocyte–Fibroblast Interactions in Wound Healing. *Journal of Investigative Dermatology* **127**, 998–1008 (2007).

544. Hobbs, R. M., Silva-Vargas, V., Groves, R. & Watt, F. M. Expression of Activated MEK1 in Differentiating Epidermal Cells Is Sufficient to Generate Hyperproliferative and Inflammatory Skin Lesions. *Journal of Investigative Dermatology* **123**, 503–515 (2004).

545. Werner, S. *et al.* The Function of KGF in Morphogenesis of Epithelium and Reepithelialization of Wounds. *Science (1979)* **266**, 819–822 (1994).

546. Freedberg, I. M., Tomic-Canic, M., Komine, M. & Blumenberg, M. Keratins and the Keratinocyte Activation Cycle. *Journal of Investigative Dermatology* **116**, 633–640 (2001).

547. Yan, C. *et al.* Epithelial to Mesenchymal Transition in Human Skin Wound Healing Is Induced by Tumor Necrosis Factor-α through Bone Morphogenic Protein-2. *Am J Pathol* **176**, 2247–2258 (2010).

548. Barrientos, S., Stojadinovic, O., Golinko, M. S., Brem, H. & Tomic-Canic, M. PERSPECTIVE ARTICLE: Growth factors and cytokines in wound healing. *Wound Repair and Regeneration* **16**, 585–601 (2008).

549. Krampert, M. *et al.* Activities of the Matrix Metalloproteinase Stromelysin-2 (MMP-10) in Matrix Degradation and Keratinocyte Organization in Wounded Skin. *Mol Biol Cell* **15**, 5242–5254 (2004).

550. Salonurmi, T. *et al.* Overexpression of TIMP-1 under the MMP-9 promoter interferes with wound healing in transgenic mice. *Cell Tissue Res* **315**, 27–37 (2004).

551. Nakamura, K., Williams, I. R. & Kupper, T. S. Keratinocyte-Derived Monocyte Chemoattractant Protein 1 (MCP-1): Analysis in a Transgenic Model Demonstrates MCP-1 Can Recruit Dendritic and Langerhans Cells to Skin. *Journal of Investigative Dermatology* **105**, 635–643 (1995).

552. Fries, K. M. *et al.* Evidence of Fibroblast Heterogeneity and the Role of Fibroblast Subpopulations in Fibrosis. *Clin Immunol Immunopathol* **72**, 283–292 (1994).

553. Tracy, L. E., Minasian, R. A. & Caterson, E. J. Extracellular Matrix and Dermal Fibroblast Function in the Healing Wound. *Adv Wound Care (New Rochelle)* **5**, 119–136 (2016).

554. Singhal, P. K. *et al.* Mouse embryonic fibroblasts exhibit extensive developmental and phenotypic diversity. *Proceedings of the National Academy of Sciences* **113**, 122–127 (2016).

555. Chrissouli, S., Pratsinis, H., Velissariou, V., Anastasiou, A. & Kletsas, D. Human amniotic fluid stimulates the proliferation of human fetal and adult skin fibroblasts: The roles of bFGF and PDGF and of the ERK and Akt signaling pathways. *Wound Repair and Regeneration* **18**, 643–654 (2010).

556. Giannouli, C. & Kletsas, D. TGF-β regulates differentially the proliferation of fetal and adult human skin fibroblasts via the activation of PKA and the autocrine action of FGF-2. *Cell Signal* **18**, 1417–1429 (2006).

557. Xu, J. & Clark, R. A. Extracellular matrix alters PDGF regulation of fibroblast integrins. *J Cell Biol* **132**, 239–249 (1996).

558. Gray, A. J., Bishop, J. E., Reeves, J. T. & Laurent, G. J. Aα and Bβ chains of fibrinogen stimulate proliferation of human fibroblasts. *J Cell Sci* **104**, 409–413 (1993).

559. Koskela, A., Engström, K., Hakelius, M., Nowinski, D. & Ivarsson, M. Regulation of fibroblast gene expression by keratinocytes in organotypic skin culture provides possible mechanisms for the antifibrotic effect of reepithelialization. *Wound Repair and Regeneration* **18**, 452–459 (2010).

560. Gurtner, G. C., Werner, S., Barrandon, Y. & Longaker, M. T. Wound repair and regeneration. *Nature* **453**, 314–321 (2008).

561. Driskell, R. R. *et al.* Distinct fibroblast lineages determine dermal architecture in skin development and repair. *Nature* **504**, 277–281 (2013).

562. Tomasek, J. J., Gabbiani, G., Hinz, B., Chaponnier, C. & Brown, R. A. Myofibroblasts and mechano-regulation of connective tissue remodelling. *Nat Rev Mol Cell Biol* **3**, 349–363 (2002).

563. García-de-Alba, C. *et al.* Expression of Matrix Metalloproteases by Fibrocytes. *Am J Respir Crit Care Med* **182**, 1144–1152 (2010).

564. Hartlapp, I. *et al.* Fibrocytes induce an angiogenic phenotype in cultured endothelial cells and promote angiogenesis in vivo. *The FASEB Journal* **15**, 2215–2224 (2001).

565. Hinz, B., Celetta, G., Tomasek, J. J., Gabbiani, G. & Chaponnier, C. Alpha-Smooth Muscle Actin Expression Upregulates Fibroblast Contractile Activity. *Mol Biol Cell* **12**, 2730–2741 (2001).

566. Chambers, R. C., Leoni, P., Kaminski, N., Laurent, G. J. & Heller, R. A. Global Expression Profiling of Fibroblast Responses to Transforming Growth Factor-β1 Reveals the Induction of Inhibitor of Differentiation-1 and Provides Evidence of Smooth Muscle Cell Phenotypic Switching. *Am J Pathol* **162**, 533–546 (2003).

567. Crider, B. J., Risinger, G. M., Haaksma, C. J., Howard, E. W. & Tomasek, J. J. Myocardin-Related Transcription Factors A and B Are Key Regulators of TGF-β1-Induced Fibroblast to Myofibroblast Differentiation. *Journal of Investigative Dermatology* **131**, 2378–2385 (2011).

568. Abe, R., Donnelly, S. C., Peng, T., Bucala, R. & Metz, C. N. Peripheral Blood Fibrocytes: Differentiation Pathway and Migration to Wound Sites. *The Journal of Immunology* **166**, 7556–7562 (2001).

569. Pilling, D., Buckley, C. D., Salmon, M. & Gomer, R. H. Inhibition of Fibrocyte Differentiation by Serum Amyloid P. *The Journal of Immunology* **171**, 5537–5546 (2003).

570. Pilling, D., Tucker, N. M. & Gomer, R. H. Aggregated IgG inhibits the differentiation of human fibrocytes. *J Leukoc Biol* **79**, 1242–1251 (2006).

571. Greaves, N. S., Ashcroft, K. J., Baguneid, M. & Bayat, A. Current understanding of molecular and cellular mechanisms in fibroplasia and angiogenesis during acute wound healing. *J Dermatol Sci* **72**, 206–217 (2013).

572. Gabbiani, G., Ryan, G. B. & Majno, G. Presence of modified fibroblasts in granulation tissue and their possible role in wound contraction. *Experientia* **27**, 549–550 (1971).

573. Goffin, J. M. *et al.* Focal adhesion size controls tension-dependent recruitment of α-smooth muscle actin to stress fibers. *J Cell Biol* **172**, 259–268 (2006).

574. Macri, L. & Clark, R. A. F. Tissue Engineering for Cutaneous Wounds: Selecting the Proper Time and Space for Growth Factors, Cells and the Extracellular Matrix. *Skin Pharmacol Physiol* **22**, 83–93 (2009).

575. Goldberg, M. T., Han, Y.-P., Yan, C., Shaw, M. C. & Garner, W. L. TNF-α Suppresses α-Smooth Muscle Actin Expression in Human Dermal Fibroblasts: An Implication for Abnormal Wound Healing. *Journal of Investigative Dermatology* **127**, 2645–2655 (2007).

576. Hinz, B. The role of myofibroblasts in wound healing. *Curr Res Transl Med* **64**, 171–177 (2016).

577. Chiquet, M., Gelman, L., Lutz, R. & Maier, S. From mechanotransduction to extracellular matrix gene expression in fibroblasts. *Biochimica et Biophysica Acta (BBA) - Molecular Cell Research* **1793**, 911–920 (2009).

578. Eckes, B. *et al.* Mechanical Tension and Integrin α2β1 Regulate Fibroblast Functions. *Journal of Investigative Dermatology Symposium Proceedings* **11**, 66–72 (2006).

579. Cheng, F. *et al.* Vimentin coordinates fibroblast proliferation and keratinocyte differentiation in wound healing via TGF-β–Slug signaling. *Proceedings of the National Academy of Sciences* **113**, (2016).

580. Schultz, G. S., Davidson, J. M., Kirsner, R. S., Bornstein, P. & Herman, I. M. Dynamic reciprocity in the wound microenvironment. *Wound Repair and Regeneration* **19**, 134–148 (2011).

581. Sappino, A. P., Schürch, W. & Gabbiani, G. Differentiation repertoire of fibroblastic cells: expression of cytoskeletal proteins as marker of phenotypic modulations. *Lab Invest* **63**, 144–61 (1990).

582. Gabbiani, G. The myofibroblast in wound healing and fibrocontractive diseases. *J Pathol* **200**, 500–503 (2003).

583. Serini, G. *et al.* The Fibronectin Domain ED-A Is Crucial for Myofibroblastic Phenotype Induction by Transforming Growth Factor-β1. *J Cell Biol* **142**, 873–881 (1998).

584. Hinz, B. The extracellular matrix and transforming growth factor-β1: Tale of a strained relationship. *Matrix Biology* **47**, 54–65 (2015).

585. Duscher, D. *et al.* Mechanotransduction and fibrosis. *J Biomech* **47**, 1997–2005 (2014).

586. Desmoulière, A., Redard, M., Darby, I. & Gabbiani, G. Apoptosis mediates the decrease in cellularity during the transition between granulation tissue and scar. *Am J Pathol* **146**, 56–66 (1995).

587. Cañedo-Dorantes, L. & Cañedo-Ayala, M. Skin acute wound healing: A comprehensive review. *International Journal of Inflammation* vol. 2019 Preprint at https://doi.org/10.1155/2019/3706315 (2019).

588. Murdoch, C., Muthana, M. & Lewis, C. E. Hypoxia Regulates Macrophage Functions in Inflammation. *The Journal of Immunology* **175**, 6257–6263 (2005).

589. Duscher, D. *et al.* Fibroblast-Specific Deletion of Hypoxia Inducible Factor-1 Critically Impairs Murine Cutaneous Neovascularization and Wound Healing. *Plast Reconstr Surg* **136**, 1004–1013 (2015).

590. Skuli, N. *et al.* Endothelial HIF-2α regulates murine pathological angiogenesis and revascularization processes. *Journal of Clinical Investigation* **122**, 1427–1443 (2012).

591. Rezvani, H. R. *et al.* Loss of epidermal hypoxia-inducible factor-1α accelerates epidermal aging and affects re-epithelialization in human and mouse. *J Cell Sci* **124**, 4172–4183 (2011).

592. Eelen, G., de Zeeuw, P., Simons, M. & Carmeliet, P. Endothelial Cell Metabolism in Normal and Diseased Vasculature. *Circ Res* **116**, 1231–1244 (2015).

593. Folkman, J. & D'Amore, P. A. Blood Vessel Formation: What Is Its Molecular Basis? *Cell* **87**, 1153–1155 (1996).

594. Iruela-Arispe, M. L. & Dvorak, H. F. Angiogenesis: a dynamic balance of stimulators and inhibitors. *Thromb Haemost* **78**, 672–7 (1997).

595. Risau, W. Mechanisms of angiogenesis. *Nature* **386**, 671–674 (1997).

596. Sahni, A. & Francis, C. W. Vascular endothelial growth factor binds to fibrinogen and fibrin and stimulates endothelial cell proliferation. *Blood* **96**, 3772–8 (2000).

597. Senger, D. R. *et al.* Stimulation of endothelial cell migration by vascular permeability factor/vascular endothelial growth factor through cooperative mechanisms involving the alphavbeta3 integrin, osteopontin, and thrombin. *Am J Pathol* **149**, 293–305 (1996).

598. Senger, D. R. *et al.* Angiogenesis promoted by vascular endothelial growth factor: Regulation through $\alpha_1\beta_1$ and $\alpha_2\beta_1$ integrins. *Proceedings of the National Academy of Sciences* **94**, 13612–13617 (1997).

599. Eilken, H. M. & Adams, R. H. Dynamics of endothelial cell behavior in sprouting angiogenesis. *Curr Opin Cell Biol* **22**, 617–625 (2010).

600. Mace, K. A., Yu, D. H., Paydar, K. Z., Boudreau, N. & Young, D. M. Sustained expression of *Hif-1α* in the diabetic environment promotes angiogenesis and cutaneous wound repair. *Wound Repair and Regeneration* **15**, 636–645 (2007).

601. Kimura, H. & Esumi, H. Reciprocal regulation between nitric oxide and vascular endothelial growth factor in angiogenesis. *Acta Biochim Pol* **50**, 49–59 (2003).

602. Knighton, D. R., Silver, I. A. & Hunt, T. K. Regulation of wound-healing angiogenesis-effect of oxygen gradients and inspired oxygen concentration. *Surgery* **90**, 262–70 (1981).

603. Potente, M., Gerhardt, H. & Carmeliet, P. Basic and Therapeutic Aspects of Angiogenesis. *Cell* **146**, 873–887 (2011).

604. Wong, B. W., Marsch, E., Treps, L., Baes, M. & Carmeliet, P. Endothelial cell metabolism in health and disease: impact of hypoxia. *EMBO J* **36**, 2187–2203 (2017).

605. Tonnesen, M. G., Feng, X. & Clark, R. A. F. Angiogenesis in Wound Healing. *Journal of Investigative Dermatology Symposium Proceedings* **5**, 40–46 (2000).

606. Partanen, J. *et al.* A Novel Endothelial Cell Surface Receptor Tyrosine Kinase with Extracellular Epidermal Growth Factor Homology Domains. *Mol Cell Biol* **12**, 1698–1707 (1992).

607. Staton, C. A., Valluru, M., Hoh, L., Reed, M. W. R. & Brown, N. J. Angiopoietin-1, angiopoietin-2 and Tie-2 receptor expression in human dermal wound repair and scarring. *British Journal of Dermatology* **163**, 920–927 (2010).

608. Papapetropoulos, A. *et al.* Angiopoietin-1 Inhibits Endothelial Cell Apoptosis via the Akt/Survivin Pathway. *Journal of Biological Chemistry* **275**, 9102–9105 (2000).

609. Sottile, J. Regulation of angiogenesis by extracellular matrix. *Biochimica et Biophysica Acta (BBA) - Reviews on Cancer* **1654**, 13–22 (2004).

610. Wijelath, E. S. *et al.* Novel Vascular Endothelial Growth Factor Binding Domains of Fibronectin Enhance Vascular Endothelial Growth Factor Biological Activity. *Circ Res* **91**, 25–31 (2002).

611. Gerhardt, H. *et al.* VEGF guides angiogenic sprouting utilizing endothelial tip cell filopodia. *J Cell Biol* **161**, 1163–1177 (2003).

612. Ruhrberg, C. *et al.* Spatially restricted patterning cues provided by heparin-binding VEGF-A control blood vessel branching morphogenesis. *Genes Dev* **16**, 2684–2698 (2002).

613. Petitclerc, E. *et al.* New Functions for Non-collagenous Domains of Human Collagen Type IV. *Journal of Biological Chemistry* **275**, 8051–8061 (2000).

614. Armstrong, L. C. *et al.* Thrombospondin 2 Inhibits Microvascular Endothelial Cell Proliferation by a Caspase-independent Mechanism. *Mol Biol Cell* **13**, 1893–1905 (2002).

615. Davies, C. de L. *et al.* Decorin Inhibits Endothelial Migration and Tube-like Structure Formation: Role of Thrombospondin-1. *Microvasc Res* **62**, 26–42 (2001).

616. Tolsma, S. *et al.* Peptides derived from two separate domains of the matrix protein thrombospondin-1 have anti-angiogenic activity. *J Cell Biol* **122**, 497–511 (1993).

617. Guo, N., Krutzsch, H. C., Inman, J. K. & Roberts, D. D. Thrombospondin 1 and type I repeat peptides of thrombospondin 1 specifically induce apoptosis of endothelial cells. *Cancer Res* **57**, 1735–42 (1997).

618. Gaengel, K., Genové, G., Armulik, A. & Betsholtz, C. Endothelial-Mural Cell Signaling in Vascular Development and Angiogenesis. *Arterioscler Thromb Vasc Biol* **29**, 630–638 (2009).

619. Senger, D. R. & Davis, G. E. Angiogenesis. *Cold Spring Harb Perspect Biol* **3**, a005090–a005090 (2011).

620. Neve, A., Cantatore, F. P., Maruotti, N., Corrado, A. & Ribatti, D. Extracellular Matrix Modulates Angiogenesis in Physiological and Pathological Conditions. *Biomed Res Int* **2014**, 1–10 (2014).

621. Carmeliet, P. Angiogenesis in health and disease. *Nat Med* **9**, 653–660 (2003).

622. Nagaoka, T. *et al.* Delayed Wound Healing in the Absence of Intercellular Adhesion Molecule-1 or L-Selectin Expression. *Am J Pathol* **157**, 237–247 (2000).

623. Subramaniam, M. *et al.* Role of endothelial selectins in wound repair. *Am J Pathol* **150**, 1701–9 (1997).

624. Dimmeler, S. & Zeiher, A. M. Endothelial Cell Apoptosis in Angiogenesis and Vessel Regression. *Circ Res* **87**, 434–439 (2000).

625. Korn, C. & Augustin, H. G. Mechanisms of Vessel Pruning and Regression. *Dev Cell* **34**, 5–17 (2015).

626. Rotshenker, S. Wallerian degeneration: the innate-immune response to traumatic nerve injury. *J Neuroinflammation* **8**, 109 (2011).

627. Chen, P., Piao, X. & Bonaldo, P. Role of macrophages in Wallerian degeneration and axonal regeneration after peripheral nerve injury. *Acta Neuropathol* **130**, 605–618 (2015).

628. Cattin, A.-L. *et al.* Macrophage-Induced Blood Vessels Guide Schwann Cell-Mediated Regeneration of Peripheral Nerves. *Cell* **162**, 1127–1139 (2015).

629. Kruger, G. M. *et al.* Neural Crest Stem Cells Persist in the Adult Gut but Undergo Changes in Self-Renewal, Neuronal Subtype Potential, and Factor Responsiveness. *Neuron* **35**, 657–669 (2002).

630. Namikawa, K., Okamoto, T., Suzuki, A., Konishi, H. & Kiyama, H. Pancreatitis-Associated Protein-III Is a Novel Macrophage Chemoattractant Implicated in Nerve Regeneration. *The Journal of Neuroscience* **26**, 7460–7467 (2006).

631. Parrinello, S. *et al.* EphB Signaling Directs Peripheral Nerve Regeneration through Sox2-Dependent Schwann Cell Sorting. *Cell* **143**, 145–155 (2010).

632. Fujiwara, T. *et al.* Direct contact of fibroblasts with neuronal processes promotes differentiation to myofibroblasts and induces contraction of collagen matrix in vitro. *Wound Repair and Regeneration* **21**, 588–594 (2013).

633. Downward, J. *et al.* Close similarity of epidermal growth factor receptor and v-erb-B oncogene protein sequences. *Nature 1984 307:5951* **307**, 521–527 (1984).

634. Wee, P. & Wang, Z. Epidermal growth factor receptor cell proliferation signaling pathways. *Cancers* vol. 9 Preprint at https://doi.org/10.3390/cancers9050052 (2017).

635. Nicholson, R. I., Gee, J. M. W. & Harper, M. E. EGFR and cancer prognosis. *Eur J Cancer* **37**, 9 (2001).

636. Normanno, N. *et al.* Epidermal growth factor receptor (EGFR) signaling in cancer. *Gene* **366**, 2–16 (2006).

637. Edwin, F. *et al.* A historical perspective of the EGF receptor and related systems. *Methods Mol Biol* **327**, 1–24 (2006).

638. Normanno, N. *et al.* Epidermal growth factor receptor (EGFR) signaling in cancer. *Gene* vol. 366 2–16 Preprint at https://doi.org/10.1016/j.gene.2005.10.018 (2006).

639. Lemmon, M. A. & Schlessinger, J. Cell signaling by receptor tyrosine kinases. *Cell* **141**, 1117–1134 (2010).

640. Citri, A., Skaria, K. B. & Yarden, Y. The deaf and the dumb: The biology of ErbB-2 and ErbB-3. *The EGF Receptor Family: Biologic Mechanisms and Role in Cancer* 57–68 (2003) doi:10.1016/B978-012160281-9/50005-0.

641. Singh, A. B. & Harris, R. C. Autocrine, paracrine and juxtacrine signaling by EGFR ligands. *Cell Signal* **17**, 1183–1193 (2005).

642. Elenius, K. *et al.* Characterization of a naturally occurring ErbB4 isoform that does not bind or activate phosphatidyl inositol 3-kinase. *Oncogene* **18**, 2607–2615 (1999).

643. Fedi, P., Pierce, J. H., Paolo, P., Fiore, D. I. & Kraus, M. H. Efficient coupling with phosphatidylinositol 3-kinase, but not phospholipase C gamma or GTPase-activating protein, distinguishes ErbB-3 signaling from that of other ErbB/EGFR family members. *Mol Cell Biol* **14**, 492–500 (1994).

644. Burgess, A. W. *et al.* An Open-and-Shut Case? Recent Insights into the Activation of EGF/ErbB Receptors. *Mol Cell* **12**, 541–552 (2003).

645. Jura, N. *et al.* Mechanism for Activation of the EGF Receptor Catalytic Domain by the Juxtamembrane Segment. *Cell* **137**, 1293–1307 (2009).

646. Zhang, X., Gureasko, J., Shen, K., Cole, P. A. & Kuriyan, J. An Allosteric Mechanism for Activation of the Kinase Domain of Epidermal Growth Factor Receptor. *Cell* **125**, 1137–1149 (2006).

647. Cho, H. S. *et al.* Structure of the extracellular region of HER2 alone and in complex with the Herceptin Fab. *Nature 2003 421:6924* **421**, 756–760 (2003).

648. Yamauchi, T. *et al.* Constitutive tyrosine phosphorylation of ErbB-2 via Jak2 by autocrine secretion of prolactin in human breast cancer. *Journal of Biological Chemistry* **275**, 33937–33944 (2000).

649. Yamauchi, T. *et al.* Tyrosine phosphorylation of the EGF receptor by the kinase Jak2 is induced by growth hormone. *Nature 1997 390:6655* **390**, 91–96 (1997).

650. Sato, K. ichi. Cellular Functions Regulated by Phosphorylation of EGFR on Tyr845. *International Journal of Molecular Sciences 2013, Vol. 14, Pages 10761-10790* **14**, 10761–10790 (2013).

651. Hunter, T., Ling, N. & Cooper, J. A. Protein kinase C phosphorylation of the EGF receptor at a threonine residue close to the cytoplasmic face of the plasma membrane. *Nature 1984 311:5985* **311**, 480–483 (1984).

652. Lavoie, H., Gagnon, J. & Therrien, M. ERK signalling: a master regulator of cell behaviour, life and fate. *Nature Reviews Molecular Cell Biology* vol. 21 607–632 Preprint at https://doi.org/10.1038/s41580-020-0255-7 (2020).

653. Guo, Y. *et al.* ERK/MAPK signalling pathway and tumorigenesis (Review). *Exp Ther Med* (2020) doi:10.3892/etm.2020.8454.

654. Barbosa, R., Acevedo, L. A. & Marmorstein, R. The MEK/ERK Network as a Therapeutic Target in Human Cancer. *Molecular cancer research : MCR* vol. 19 361–374 Preprint at https://doi.org/10.1158/1541-7786.MCR-20-0687 (2021).

655. Pearson, G. *et al.* Mitogen-Activated Protein (MAP) Kinase Pathways: Regulation and Physiological Functions. *Endocr Rev* **22**, 153–183 (2001).

656. Chen, Z. *et al.* MAP kinases. *Chem Rev* **101**, 2449–2476 (2001).

657. Coulombe, P. & Meloche, S. Atypical mitogen-activated protein kinases: Structure, regulation and functions. *Biochimica et Biophysica Acta (BBA) - Molecular Cell Research* **1773**, 1376–1387 (2007).

658. Lawrence, M. C. *et al.* The roles of MAPKs in disease. *Cell Res* **18**, 436–442 (2008).

659. Lowenstein, E. J. *et al.* The SH2 and SH3 domain-containing protein GRB2 links receptor tyrosine kinases to ras signaling. *Cell* **70**, 431–442 (1992).

660. Buday, L. & Downward, J. Epidermal growth factor regulates p21ras through the formation of a complex of receptor, Grb2 adapter protein, and Sos nucleotide exchange factor. *Cell* **73**, 611–620 (1993).

661. van der Geer, P. *et al.* A conserved amino-terminal Shc domain binds to phosphotyrosine motifs in activated receptors and phosphopeptides. *Current Biology* **5**, 404–412 (1995).

662. Rozakis-Adcock, M., Fernley, R., Wade, J., Pawson, T. & Bowtell, D. The SH2 and SH3 domains of mammalian Grb2 couple the EGF receptor to the Ras activator mSos1. *Nature 1993 363:6424* **363**, 83–85 (1993).

663. Lee, C. S. *et al.* The phox homology domain of phospholipase D activates dynamin GTPase activity and accelerates EGFR endocytosis. *Nature Cell Biology 2006 8:5* **8**, 477–484 (2006).

664. Zhao, C., Du, G., Skowronek, K., Frohman, M. A. & Bar-Sagi, D. Phospholipase D2-generated phosphatidic acid couples EGFR stimulation to Ras activation by Sos. *Nature Cell Biology 2007 9:6* **9**, 707–712 (2007).

665. Boriack-Sjodin, P. A., Margarit, S. M., Bar-Sagi, D. & Kuriyan, J. The structural basis of the activation of Ras by Sos. *Nature 1998 394:6691* **394**, 337–343 (1998).

666. Muñoz-Maldonado, C., Zimmer, Y. & Medová, M. A Comparative Analysis of Individual RAS Mutations in Cancer Biology. *Front Oncol* **9**, (2019).

667. Bandaru, P., Kondo, Y. & Kuriyan, J. The Interdependent Activation of Son-of-Sevenless and Ras. *Cold Spring Harb Perspect Med* **9**, a031534 (2019).

668. Simanshu, D. K., Nissley, D. V. & McCormick, F. RAS Proteins and Their Regulators in Human Disease. *Cell* **170**, 17–33 (2017).

669. Gureasko, J. *et al.* Membrane-dependent signal integration by the Ras activator Son of sevenless. *Nature Structural & Molecular Biology 2008 15:5* **15**, 452–461 (2008).

670. Bunda, S. *et al.* Src promotes GTPase activity of Ras via tyrosine 32 phosphorylation. *Proc Natl Acad Sci U S A* **111**, E3785–E3794 (2014).

671. Bunda, S. *et al.* Inhibition of SHP2-mediated dephosphorylation of Ras suppresses oncogenesis. *Nature Communications 2015 6:1* **6**, 1–12 (2015).

672. Rodriguez-Viciana, P. *et al.* Phosphatidylinositol-3-OH kinase direct target of Ras. *Nature 1994 370:6490* **370**, 527–532 (1994).

673. Hofer, F., Fields, S., Schneider, C. & Martin, G. S. Activated Ras interacts with the Ral guanine nucleotide dissociation stimulator. *Proceedings of the National Academy of Sciences* **91**, 11089–11093 (1994).

674. Fabian, J. R., Daar, I. 0 & Morrison", D. K. Critical tyrosine residues regulate the enzymatic and biological activity of Raf-1 kinase. *Mol Cell Biol* **13**, 7170–7179 (1993).

675. Diaz, B. *et al.* Phosphorylation of Raf-1 serine 338-serine 339 is an essential regulatory event for Ras-dependent activation and biological signaling. *Mol Cell Biol* **17**, 4509–4516 (1997).

676. Zang, M. *et al.* Characterization of Ser338 phosphorylation for Raf-1 activation. *Journal of Biological Chemistry* **283**, 31429–31437 (2008).

677. Xiang, X., Zang, M., Waelde, C. A., Wen, R. & Luo, Z. Phosphorylation of 338SSYY341 regulates specific interaction between Raf-1 and MEK1. *Journal of Biological Chemistry* **277**, 44996–45003 (2002).

678. Brtva, T. R. *et al.* Two distinct Raf domains mediate interaction with Ras. *Journal of Biological Chemistry* **270**, 9809–9812 (1995).

679. Nan, X. *et al.* Ras-GTP dimers activate the Mitogen-Activated Protein Kinase (MAPK) pathway. *Proceedings of the National Academy of Sciences* **112**, 7996–8001 (2015).

680. Yuan, J. *et al.* The dimer-dependent catalytic activity of RAF family kinases is revealed through characterizing their oncogenic mutants. *Oncogene* **37**, 5719–5734 (2018).

681. Hu, J. *et al.* Allosteric Activation of Functionally Asymmetric RAF Kinase Dimers. *Cell* **154**, 1036–1046 (2013).

682. Mason, C. S. *et al.* Serine and tyrosine phosphorylations cooperate in Raf-1, but not B-Raf activation. *EMBO J* **18**, 2137–2148 (1999).

683. Zimmermann, S. & Moelling, K. Phosphorylation and Regulation of Raf by Akt (Protein Kinase B). *Science (1979)* **286**, 1741–1744 (1999).

684. Dougherty, M. K. *et al.* Regulation of Raf-1 by Direct Feedback Phosphorylation. *Mol Cell* **17**, 215–224 (2005).

685. Ding, Q., Wang, Q. & Evers, B. M. Alterations of MAPK Activities Associated with Intestinal Cell Differentiation. *Biochem Biophys Res Commun* **284**, 282–288 (2001).

686. Tohgo, A., Pierce, K. L., Choy, E. W., Lefkowitz, R. J. & Luttrell, L. M. β-Arrestin Scaffolding of the ERK Cascade Enhances Cytosolic ERK Activity but Inhibits ERK-mediated Transcription following Angiotensin AT1a Receptor Stimulation. *Journal of Biological Chemistry* **277**, 9429–9436 (2002).

687. Yoon, S. & Seger, R. The extracellular signal-regulated kinase: Multiple substrates regulate diverse cellular functions. *Growth Factors* **24**, 21–44 (2006).

688. Maik-Rachline, G., Hacohen-Lev-Ran, A. & Seger, R. Nuclear ERK: Mechanism of Translocation, Substrates, and Role in Cancer. *Int J Mol Sci* **20**, 1194 (2019).

689. Yeung, K. *et al.* Mechanism of Suppression of the Raf/MEK/Extracellular Signal-Regulated Kinase Pathway by the Raf Kinase Inhibitor Protein. *Mol Cell Biol* **20**, 3079–3085 (2000).

690. Shin, S.-Y. *et al.* Positive- and negative-feedback regulations coordinate the dynamic behavior of the Ras-Raf-MEK-ERK signal transduction pathway. *J Cell Sci* **122**, 425–435 (2009).

691. Wellbrock, C., Karasarides, M. & Marais, R. The RAF proteins take centre stage. *Nature Reviews Molecular Cell Biology 2004 5:11* **5**, 875–885 (2004).

692. Roberts, P. J. & Der, C. J. Targeting the Raf-MEK-ERK mitogen-activated protein kinase cascade for the treatment of cancer. *Oncogene 2007 26:22* **26**, 3291–3310 (2007).

693. Bondzi, C., Grant, S. & Krystal, G. W. A novel assay for the measurement of Raf-1 kinase activity. *Oncogene 2000 19:43* **19**, 5030–5033 (2000).

694. Muta, Y., Matsuda, M. & Imajo, M. Divergent Dynamics and Functions of ERK MAP Kinase Signaling in Development, Homeostasis and Cancer: Lessons from Fluorescent Bioimaging. *Cancers (Basel)* **11**, 513 (2019).

695. Zhou, B. & Zhang, Z.-Y. The Activity of the Extracellular Signal-regulated Kinase 2 Is Regulated by Differential Phosphorylation in the Activation Loop. *Journal of Biological Chemistry* **277**, 13889–13899 (2002).

696. Zhou, L. *et al.* MEK1 and MEK2 isoforms regulate distinct functions in pancreatic cancer cells. *Oncol Rep* **24**, (2010).

697. Haystead, T. A. J., Dent, P., Wu, J., Haystead, C. M. M. & Sturgill, T. W. Ordered phosphorylation of p42 ^{mapk} by MAP kinase kinase. *FEBS Lett* **306**, 17–22 (1992).

698. Burack, W. R. & Shaw, A. S. Live Cell Imaging of ERK and MEK. *Journal of Biological Chemistry* **280**, 3832–3837 (2005).

699. Catalanotti, F. *et al.* A Mek1–Mek2 heterodimer determines the strength and duration of the Erk signal. *Nat Struct Mol Biol* **16**, 294–303 (2009).

700. Lefloch, R., Pouysségur, J. & Lenormand, P. Total ERK1/2 activity regulates cell proliferation. *Cell Cycle* **8**, 705–711 (2009).

701. Yoon, S. & Seger, R. The extracellular signal-regulated kinase: Multiple substrates regulate diverse cellular functions. *Growth Factors* **24**, 21–44 (2006).

702. Khokhlatchev, A. V *et al.* Phosphorylation of the MAP Kinase ERK2 Promotes Its Homodimerization and Nuclear Translocation. *Cell* **93**, 605–615 (1998).

703. Yuan, J. *et al.* Activating mutations in MEK1 enhance homodimerization and promote tumorigenesis. *Sci Signal* **11**, (2018).

704. Cargnello, M. & Roux, P. P. Activation and Function of the MAPKs and Their Substrates, the MAPK-Activated Protein Kinases. *Microbiology and Molecular Biology Reviews* **75**, 50–83 (2011).

705. Karlsson, M., Mathers, J., Dickinson, R. J., Mandl, M. & Keyse, S. M. Both Nuclear-Cytoplasmic Shuttling of the Dual Specificity Phosphatase MKP-3 and Its Ability to Anchor MAP Kinase in the Cytoplasm Are Mediated by a Conserved Nuclear Export Signal. *Journal of Biological Chemistry* **279**, 41882–41891 (2004).

706. Formstecher, E. *et al.* PEA-15 Mediates Cytoplasmic Sequestration of ERK MAP Kinase. *Dev Cell* **1**, 239–250 (2001).

707. Dalby, K. N., Morrice, N., Caudwell, F. B., Avruch, J. & Cohen, P. Identification of regulatory phosphorylation sites in mitogen-activated protein kinase (MAPK)-activated protein kinase-1a/p90(rsk) that are inducible by MAPK. *Journal of Biological Chemistry* **273**, 1496–1505 (1998).

708. Smith, J. A., Poteet-Smith, C. E., Malarkey, K. & Sturgill, T. W. Identification of an extracellular signal-regulated kinase (ERK) docking site in ribosomal S6 kinase, a sequence critical for activation by ERK in vivo. *Journal of Biological Chemistry* **274**, 2893–2898 (1999).

709. SUTHERLAND, C., CAMPBELL, D. G. & COHEN, P. Identification of insulin-stimulated protein kinase-1 as the rabbit equivalent of rskmo-2. Identification of two threonines phosphorylated during activation by mitogen-activated protein kinase. *Eur J Biochem* **212**, 581–588 (1993).

710. Vik, T. A. & Ryder, J. W. Identification of Serine 380 as the Major Site of Autophosphorylation of Xenopus pp90rsk. *Biochem Biophys Res Commun* **235**, 398–402 (1997).

711. Richards, S. A., Fu, J., Romanelli, A., Shimamura, A. & Blenis, J. Ribosomal S6 kinase 1 (RSK1) activation requires signals dependent on and independent of the MAP kinase ERK. *Current Biology* **9**, 810-S1 (1999).

712. Schouten, G. J. *et al.* IκBα is a target for the mitogen-activated 90 kDa ribosomal S6 kinase. *EMBO J* **16**, 3133–3144 (1997).

713. Xu, S., Bayat, H., Hou, X. & Jiang, B. Ribosomal S6 kinase-1 modulates interleukin-1+-induced persistent activation of NF-κB through phosphorylation of IκBβ. *Am J Physiol Cell Physiol* **291**, 1336–1345 (2006).

714. Wingate, A. D., Campbell, D. G., Peggie, M. & Arthur, J. S. C. Nur77 is phosphorylated in cells by RSK in response to mitogenic stimulation. *Biochemical Journal* **393**, 715–724 (2006).

715. Rivera, V. M. *et al.* A growth factor-induced kinase phosphorylates the serum response factor at a site that regulates its DNA-binding activity. *Mol Cell Biol* **13**, 6260–6273 (1993).

716. Davis, I. J., Hazel, T. G., Chen, R.-H., Blenis, J. & Lau, L. F. Functional Domains and Phosphorylation of the Orphan Receptor Nur77. *Molecular Endocrinology* **7**, 953–964 (1993).

717. Chen, R. H., Abate, C. & Blenis, J. Phosphorylation of the c-Fos transrepression domain by mitogen-activated protein kinase and 90-kDa ribosomal S6 kinase. *Proceedings of the National Academy of Sciences* **90**, 10952–10956 (1993).

718. Fujita, N., Sato, S. & Tsuruo, T. Phosphorylation of p27Kip1 at threonine 198 by p90 ribosomal protein S6 kinases promotes its binding to 14-3-3 and cytoplasmic localization. *J Biol Chem* **278**, 49254–49260 (2003).

719. Larrea, M. D. *et al.* RSK1 drives p27Kip1 phosphorylation at T198 to promote RhoA inhibition and increase cell motility. *Proc Natl Acad Sci U S A* **106**, 9268–9273 (2009).

720. Zhu, J., Blenis, J. & Yuan, J. Activation of PI3K/Akt and MAPK pathways regulates Myc-mediated transcription by phosphorylating and promoting the degradation of Mad1. *Proc Natl Acad Sci U S A* **105**, 6584–6589 (2008).

721. Casar, B., Pinto, A. & Crespo, P. Essential Role of ERK Dimers in the Activation of Cytoplasmic but Not Nuclear Substrates by ERK-Scaffold Complexes. *Mol Cell* **31**, 708–721 (2008).

722. Herrero, A. *et al.* Small Molecule Inhibition of ERK Dimerization Prevents Tumorigenesis by RAS-ERK Pathway Oncogenes. *Cancer Cell* **28**, 170–182 (2015).

723. Zehorai, E., Yao, Z., Plotnikov, A. & Seger, R. The subcellular localization of MEK and ERK—A novel nuclear translocation signal (NTS) paves a way to the nucleus. *Mol Cell Endocrinol* **314**, 213–220 (2010).

724. Zehorai, E. & Seger, R. Beta-Like Importins Mediate the Nuclear Translocation of MAPKs. *Cellular Physiology and Biochemistry* **52**, 802–821 (2019).

725. Lenormand, P., Brondello, J.-M., Brunet, A. & Pouysségur, J. Growth Factor–induced p42/p44 MAPK Nuclear Translocation and Retention Requires Both MAPK Activation and Neosynthesis of Nuclear Anchoring Proteins. *J Cell Biol* **142**, 625–633 (1998).

726. Lopez-Bergami, P., Lau, E. & Ronai, Z. Emerging roles of ATF2 and the dynamic AP1 network in cancer. *Nat Rev Cancer* **10**, 65–76 (2010).

727. Morton, S., Davis, R. J., McLaren, A. & Cohen, P. A reinvestigation of the multisite phosphorylation of the transcription factor c-Jun. *EMBO J* **22**, 3876–3886 (2003).

728. Okazaki, K. & Sagata, N. The Mos/MAP kinase pathway stabilizes c-Fos by phosphorylation and augments its transforming activity in NIH 3T3 cells. *EMBO J* **14**, 5048–5059 (1995).

729. Sears, R. *et al.* Multiple Ras-dependent phosphorylation pathways regulate Myc protein stability. *Genes Dev* **14**, 2501–2514 (2000).

730. Yeh, E. *et al.* A signalling pathway controlling c-Myc degradation that impacts oncogenic transformation of human cells. *Nat Cell Biol* **6**, 308–318 (2004).

731. Maekawa, M., Nishida, E. & Tanoue, T. Identification of the Anti-proliferative Protein Tob as a MAPK Substrate. *Journal of Biological Chemistry* **277**, 37783–37787 (2002).

732. Yang, J.-Y. *et al.* ERK promotes tumorigenesis by inhibiting FOXO3a via MDM2-mediated degradation. *Nat Cell Biol* **10**, 138–148 (2008).

733. Ritt, D. A., Monson, D. M., Specht, S. I. & Morrison, D. K. Impact of Feedback Phosphorylation and Raf Heterodimerization on Normal and Mutant B-Raf Signaling. *Mol Cell Biol* **30**, 806–819 (2010).

734. Langlois, W. J., Sasaoka, T., Saltiel, A. R. & Olefsky, J. M. Negative Feedback Regulation and Desensitization of Insulin- and Epidermal Growth Factor-stimulated p21ras Activation. *Journal of Biological Chemistry* **270**, 25320–25323 (1995).

735. Douville, E. & Downward, J. EGF induced SOS phosphorylation in PC12 cells involves P90 RSK-2. *Oncogene* **15**, 373–383 (1997).

736. Kawasaki, Y. *et al.* Feedback control of ErbB2 via ERK-mediated phosphorylation of a conserved threonine in the juxtamembrane domain. *Sci Rep* **6**, 31502 (2016).

737. McKay, M. M., Ritt, D. A. & Morrison, D. K. Signaling dynamics of the KSR1 scaffold complex. *Proceedings of the National Academy of Sciences* **106**, 11022–11027 (2009).

738. Lavoie, H. *et al.* MEK drives BRAF activation through allosteric control of KSR proteins. *Nature* **554**, 549–553 (2018).

739. Corbit, K. C. *et al.* Activation of Raf-1 Signaling by Protein Kinase C through a Mechanism Involving Raf Kinase Inhibitory Protein. *Journal of Biological Chemistry* **278**, 13061–13068 (2003).

740. Ekerot, M. *et al.* Negative-feedback regulation of FGF signalling by DUSP6/MKP-3 is driven by ERK1/2 and mediated by Ets factor binding to a conserved site within the *DUSP6* / *MKP - 3* gene promoter. *Biochemical Journal* **412**, 287–298 (2008).

741. Caunt, C. J. & Keyse, S. M. Dual-specificity MAP kinase phosphatases (MKPs). *FEBS J* **280**, 489–504 (2013).

742. Ozaki, K. *et al.* ERK Pathway Positively Regulates the Expression of Sprouty Genes. *Biochem Biophys Res Commun* **285**, 1084–1088 (2001).

743. Kucharska, A., Rushworth, L. K., Staples, C., Morrice, N. A. & Keyse, S. M. Regulation of the inducible nuclear dual-specificity phosphatase DUSP5 by ERK MAPK. *Cell Signal* **21**, 1794–1805 (2009).

744. Caunt, C. J., Rivers, C. A., Conway-Campbell, B. L., Norman, M. R. & McArdle, C. A. Epidermal Growth Factor Receptor and Protein Kinase C Signaling to ERK2. *Journal of Biological Chemistry* **283**, 6241–6252 (2008).

745. Brondello, J.-M., Pouysségur, J. & McKenzie, F. R. Reduced MAP Kinase Phosphatase-1 Degradation After p42/p44 ^{MAPK} -Dependent Phosphorylation. *Science (1979)* **286**, 2514–2517 (1999).

746. Cagnol, S. & Rivard, N. Oncogenic KRAS and BRAF activation of the MEK/ERK signaling pathway promotes expression of dual-specificity phosphatase 4 (DUSP4/MKP2) resulting in nuclear ERK1/2 inhibition. *Oncogene* **32**, 564–576 (2013).

747. Yusoff, P. *et al.* Sprouty2 Inhibits the Ras/MAP Kinase Pathway by Inhibiting the Activation of Raf. *Journal of Biological Chemistry* **277**, 3195–3201 (2002).

748. Gross, I., Bassit, B., Benezra, M. & Licht, J. D. Mammalian Sprouty Proteins Inhibit Cell Growth and Differentiation by Preventing Ras Activation. *Journal of Biological Chemistry* **276**, 46460–46468 (2001).

749. Sasaki, A. *et al.* Mammalian Sprouty4 suppresses Ras-independent ERK activation by binding to Raf1. *Nat Cell Biol* **5**, 427–432 (2003).

750. Hanafusa, H., Torii, S., Yasunaga, T. & Nishida, E. Sprouty1 and Sprouty2 provide a control mechanism for the Ras/MAPK signalling pathway. *Nat Cell Biol* **4**, 850–858 (2002).

751. Brady, S. C. *et al.* Sprouty2 Association with B-Raf Is Regulated by Phosphorylation and Kinase Conformation. *Cancer Res* **69**, 6773–6781 (2009).

752. Baek, J. H. *et al.* Hypoxia-induced VEGF enhances tumor survivability via suppression of serum deprivation-induced apoptosis. *Oncogene* **19**, 4621–4631 (2000).

753. Lu, Z. & Xu, S. ERK1/2 MAP kinases in cell survival and apoptosis. *IUBMB Life* **58**, 621–631 (2006).

754. Biswas, S. C. & Greene, L. A. Nerve Growth Factor (NGF) Down-regulates the Bcl-2 Homology 3 (BH3) Domain-only Protein Bim and Suppresses Its Proapoptotic Activity by Phosphorylation. *Journal of Biological Chemistry* **277**, 49511–49516 (2002).

755. Domina, A. M., Vrana, J. A., Gregory, M. A., Hann, S. R. & Craig, R. W. MCL1 is phosphorylated in the PEST region and stabilized upon ERK activation in viable cells, and at additional sites with cytotoxic okadaic acid or taxol. *Oncogene* **23**, 5301–5315 (2004).

756. Edlich, F. BCL-2 proteins and apoptosis: Recent insights and unknowns. *Biochem Biophys Res Commun* **500**, 26–34 (2018).

757. Kale, J., Osterlund, E. J. & Andrews, D. W. BCL-2 family proteins: changing partners in the dance towards death. *Cell Death Differ* **25**, 65–80 (2018).

758. Chen, L. *et al.* Differential Targeting of Prosurvival Bcl-2 Proteins by Their BH3-Only Ligands Allows Complementary Apoptotic Function. *Mol Cell* **17**, 393–403 (2005).

759. Hübner, A., Barrett, T., Flavell, R. A. & Davis, R. J. Multisite Phosphorylation Regulates Bim Stability and Apoptotic Activity. *Mol Cell* **30**, 415–425 (2008).

760. Ewings, K. E. *et al.* ERK1/2-dependent phosphorylation of BimEL promotes its rapid dissociation from Mcl-1 and Bcl-xL. *EMBO J* **26**, 2856–2867 (2007).

761. Lopez, J. *et al.* Src tyrosine kinase inhibits apoptosis through the Erk1/2- dependent degradation of the death accelerator Bik. *Cell Death Differ* **19**, 1459–1469 (2012).

762. Shao, Y. & Aplin, A. E. ERK2 phosphorylation of serine 77 regulates Bmf pro-apoptotic activity. *Cell Death Dis* **3**, e253–e253 (2012).

763. Bonni, A. *et al.* Cell Survival Promoted by the Ras-MAPK Signaling Pathway by Transcription-Dependent and -Independent Mechanisms. *Science (1979)* **286**, 1358–1362 (1999).

764. Shimamura, A., Ballif, B. A., Richards, S. A. & Blenis, J. Rsk1 mediates a MEK–MAP kinase cell survival signal. *Current Biology* **10**, 127–135 (2000).

765. Allan, L. A. *et al.* Inhibition of caspase-9 through phosphorylation at Thr 125 by ERK MAPK. *Nat Cell Biol* **5**, 647–654 (2003).

766. Boucher, M. J. *et al.* MEK/ERK signaling pathway regulates the expression of Bcl-2, Bcl-X(L), and Mcl-1 and promotes survival of human pancreatic cancer cells. *J Cell Biochem* **79**, 355–69 (2000).

767. Ye, Q., Cai, W., Zheng, Y., Evers, B. M. & She, Q.-B. ERK and AKT signaling cooperate to translationally regulate survivin expression for metastatic progression of colorectal cancer. *Oncogene* **33**, 1828–1839 (2014).

768. Ito, K. & Suda, T. Metabolic requirements for the maintenance of self-renewing stem cells. *Nat Rev Mol Cell Biol* **15**, 243–256 (2014).

769 Falck Miniotis, M. *et al.* MEK1/2 Inhibition Decreases Lactate in BRAF-Driven Human Cancer Cells. *Cancer Res* **73**, 4039–4049 (2013).

770. Parmenter, T. J. *et al.* Response of *BRAF* -Mutant Melanoma to BRAF Inhibition Is Mediated by a Network of Transcriptional Regulators of Glycolysis. *Cancer Discov* **4**, 423–433 (2014).

771. Kim, J., Gao, P., Liu, Y.-C., Semenza, G. L. & Dang, C. V. Hypoxia-Inducible Factor 1 and Dysregulated c-Myc Cooperatively Induce Vascular Endothelial Growth Factor and Metabolic Switches Hexokinase 2 and Pyruvate Dehydrogenase Kinase 1. *Mol Cell Biol* **27**, 7381–7393 (2007).

772. Richard, D. E., Berra, E., Gothié, E., Roux, D. & Pouysségur, J. p42/p44 Mitogen-activated Protein Kinases Phosphorylate Hypoxia-inducible Factor 1α (HIF-1α) and Enhance the Transcriptional Activity of HIF-1. *Journal of Biological Chemistry* **274**, 32631–32637 (1999).

773. Mylonis, I. *et al.* Identification of MAPK Phosphorylation Sites and Their Role in the Localization and Activity of Hypoxia-inducible Factor-1α. *Journal of Biological Chemistry* **281**, 33095–33106 (2006).

774. Ying, H. *et al.* Oncogenic Kras Maintains Pancreatic Tumors through Regulation of Anabolic Glucose Metabolism. *Cell* **149**, 656–670 (2012).

775. Schödel, J. *et al.* High-resolution genome-wide mapping of HIF-binding sites by ChIP-seq. *Blood* **117**, e207–e217 (2011).

776. Osthus, R. C. *et al.* Deregulation of Glucose Transporter 1 and Glycolytic Gene Expression by c-Myc. *Journal of Biological Chemistry* **275**, 21797–21800 (2000).

777. Papandreou, I., Cairns, R. A., Fontana, L., Lim, A. L. & Denko, N. C. HIF-1 mediates adaptation to hypoxia by actively downregulating mitochondrial oxygen consumption. *Cell Metab* **3**, 187–197 (2006).

778. Kim, J., Tchernyshyov, I., Semenza, G. L. & Dang, C. V. HIF-1-mediated expression of pyruvate dehydrogenase kinase: A metabolic switch required for cellular adaptation to hypoxia. *Cell Metab* **3**, 177–185 (2006).

779. Dayton, T. L., Jacks, T. & Vander Heiden, M. G. <scp>PKM</scp> 2, cancer metabolism, and the road ahead. *EMBO Rep* **17**, 1721–1730 (2016).

780. Yang, W. *et al.* ERK1/2-dependent phosphorylation and nuclear translocation of PKM2 promotes the Warburg effect. *Nat Cell Biol* **14**, 1295–1304 (2012).

781. Houles, T. *et al.* RSK Regulates PFK-2 Activity to Promote Metabolic Rewiring in Melanoma. *Cancer Res* **78**, 2191–2204 (2018).

782. Tanimura, S. & Takeda, K. ERK signalling as a regulator of cell motility. *The Journal of Biochemistry* **162**, 145–154 (2017).

783. te Boekhorst, V., Preziosi, L. & Friedl, P. Plasticity of Cell Migration In Vivo and In Silico. *Annu Rev Cell Dev Biol* **32**, 491–526 (2016).

784. Lawson, C. D. & Ridley, A. J. Rho GTPase signaling complexes in cell migration and invasion. *Journal of Cell Biology* **217**, 447–457 (2018).

785. Miki, H., Fukuda, M., Nishida, E. & Takenawa, T. Phosphorylation of WAVE Downstream of Mitogen-activated Protein Kinase Signaling. *Journal of Biological Chemistry* **274**, 27605–27609 (1999).

786. Mendoza, M. C. *et al.* ERK-MAPK Drives Lamellipodia Protrusion by Activating the WAVE2 Regulatory Complex. *Mol Cell* **41**, 661–671 (2011).

787. Danson, C. M., Pocha, S. M., Bloomberg, G. B. & Cory, G. O. Phosphorylation of WAVE2 by MAP kinases regulates persistent cell migration and polarity. *J Cell Sci* **120**, 4144–4154 (2007).

788. Mendoza, M. C., Vilela, M., Juarez, J. E., Blenis, J. & Danuser, G. ERK reinforces actin polymerization to power persistent edge protrusion during motility. *Sci Signal* **8**, (2015).

789. Woo, M. S., Ohta, Y., Rabinovitz, I., Stossel, T. P. & Blenis, J. Ribosomal S6 Kinase (RSK) Regulates Phosphorylation of Filamin A on an Important Regulatory Site. *Mol Cell Biol* **24**, 3025–3035 (2004).

790. Klein, R. M., Spofford, L. S., Abel, E. V., Ortiz, A. & Aplin, A. E. B-RAF Regulation of Rnd3 Participates in Actin Cytoskeletal and Focal Adhesion Organization. *Mol Biol Cell* **19**, 498–508 (2008).

791. Choi, C. & Helfman, D. M. The Ras-ERK pathway modulates cytoskeleton organization, cell motility and lung metastasis signature genes in MDA-MB-231 LM2. *Oncogene* **33**, 3668–3676 (2014).

792. Fincham, V. J. Active ERK/MAP kinase is targeted to newly forming cell-matrix adhesions by integrin engagement and v-Src. *EMBO J* **19**, 2911–2923 (2000).

793. Ishibe, S., Joly, D., Zhu, X. & Cantley, L. G. Phosphorylation-Dependent Paxillin-ERK Association Mediates Hepatocyte Growth Factor-Stimulated Epithelial Morphogenesis. *Mol Cell* **12**, 1275–1285 (2003).

794. Slack-Davis, J. K. *et al.* PAK1 phosphorylation of MEK1 regulates fibronectin-stimulated MAPK activation. *J Cell Biol* **162**, 281–291 (2003).

795. Ishibe, S., Joly, D., Liu, Z.-X. & Cantley, L. G. Paxillin Serves as an ERK-Regulated Scaffold for Coordinating FAK and Rac Activation in Epithelial Morphogenesis. *Mol Cell* **16**, 257–267 (2004).

796. Woodrow, M. Ras-induced serine phosphorylation of the focal adhesion protein paxillin is mediated by the Raf→MEK→ERK pathway. *Exp Cell Res* **287**, 325–338 (2003).

797. Zheng, Y. *et al.* FAK Phosphorylation by ERK Primes Ras-Induced Tyrosine Dephosphorylation of FAK Mediated by PIN1 and PTP-PEST. *Mol Cell* **35**, 11–25 (2009).

798. Kubiniok, P., Lavoie, H., Therrien, M. & Thibault, P. Time-resolved Phosphoproteome Analysis of Paradoxical RAF Activation Reveals Novel Targets of ERK. *Molecular & Cellular Proteomics* **16**, 663–679 (2017).

799. Salvany, L., Muller, J., Guccione, E. & Rørth, P. The core and conserved role of MAL is homeostatic regulation of actin levels. *Genes Dev* **28**, 1048–1053 (2014).

800. Esnault, C. *et al.* Rho-actin signaling to the MRTF coactivators dominates the immediate transcriptional response to serum in fibroblasts. *Genes Dev* **28**, 943–958 (2014).

801. Hemmings, B. A. & Restuccia, D. F. PI3K-PKB/Akt pathway. *Cold Spring Harb Perspect Biol* **4**, (2012).

802. Manning, B. D. & Toker, A. AKT/PKB Signaling: Navigating the Network. *Cell* **169**, 381–405 (2017).

803. Fruman, D. A. *et al.* The PI3K Pathway in Human Disease. *Cell* vol. 170 605–635 Preprint at https://doi.org/10.1016/j.cell.2017.07.029 (2017).

804. Thorpe, L. M., Yuzugullu, H. & Zhao, J. J. PI3K in cancer: divergent roles of isoforms, modes of activation and therapeutic targeting. *Nature Reviews Cancer 2015 15:1* **15**, 7–24 (2014).

805. Vanhaesebroeck, B., Guillermet-Guibert, J., Graupera, M. & Bilanges, B. The emerging mechanisms of isoform-specific PI3K signalling. *Nat Rev Mol Cell Biol* **11**, 329–341 (2010).

806. Fruman, D. A. & Cantley, L. C. Phosphoinositide 3-kinase in immunological systems. *Semin Immunol* **14**, 7–18 (2002).

807. Hirsch, E. *et al.* Central role for G protein-coupled phosphoinositide 3-kinase γ in inflammation. *Science (1979)* **287**, 1049–1052 (2000).

808. Clayton, E. *et al.* A Crucial Role for the p110δ Subunit of Phosphatidylinositol 3-Kinase in B Cell Development and Activation. *Journal of Experimental Medicine* **196**, 753–763 (2002).

809. Bi, L., Okabe, I., Bernard, D. J. & Nussbaum, R. L. Early embryonic lethality in mice deficient in the p110β catalytic subunit of PI 3-kinase. *Mammalian Genome 2002 13:3* **13**, 169–172 (2002).

810. Bi, L., Okabe, I., Bernard, D. J., Wynshaw-Boris, A. & Nussbaum, R. L. Proliferative defect and embryonic lethality in mice homozygous for a deletion in the p110α subunit of phosphoinositide 3-kinase. *Journal of Biological Chemistry* **274**, 10963–10968 (1999).

811. Whitman, M., Downes, C. P., Keeler, M., Keller, T. & Cantley, L. Type I phosphatidylinositol kinase makes a novel inositol phospholipid, phosphatidylinositol-3-phosphate. *Nature* **332**, 644–646 (1988).

812. Soltoff, S. P. & Cantley, L. C. p120cbl Is a Cytosolic Adapter Protein That Associates with Phosphoinositide 3-Kinase in Response to Epidermal Growth Factor in PC12 and Other Cells. *Journal of Biological Chemistry* **271**, 563–567 (1996).

813. Kim, H. H., Sierke, S. L. & Koland, J. G. Epidermal growth factor-dependent association of phosphatidylinositol 3-kinase with the erbB3 gene product. *Journal of Biological Chemistry* **269**, 24747–24755 (1994).

814. Soltoff, S. P., Carraway Iii, K. L., Prigent, S. A., Gullick, W. G. & Cantley', L. C. ErbB3 is involved in activation of phosphatidylinositol 3-kinase by epidermal growth factor. *Mol Cell Biol* **14**, 3550–3558 (1994).

815. Maroun, C. R. *et al.* The Gab1 PH Domain Is Required for Localization of Gab1 at Sites of Cell-Cell Contact and Epithelial Morphogenesis Downstream from the Met Receptor Tyrosine Kinase. *Mol Cell Biol* **19**, 1784–1799 (1999).

816. Liu, Y. & Rohrschneider, L. R. The gift of Gab. *FEBS Lett* **515**, 1–7 (2002).

817. Lock, L. S., Royal, I., Naujokas, M. A. & Park, M. Identification of an atypical Grb2 carboxyl-terminal SH3 domain binding site in Gab docking proteins reveals Grb2-dependent and -independent recruitment of Gab1 to receptor tyorosine kinases. *Journal of Biological Chemistry* **275**, 31536–31545 (2000).

818. Mattoon, D. R., Lamothe, B., Lax, I. & Schlessinger, J. The docking protein Gab1 is the primary mediator of EGF-stimulated activation of the PI-3K/Akt cell survival pathway. *BMC Biol* **2**, 1–12 (2004).

819. Rodriguez-Viciana, P., Warne, P. H., Vanhaesebroeck, B., Waterfield, M. D. & Downward, J. Activation of phosphoinositide 3-kinase by interaction with Ras and by point mutation. *EMBO J* **15**, 2442–2451 (1996).

820. Sjolander, A., Yamamoto, K., Huber, B. E. & Lapetina, E. G. Association of p21ras with phosphatidylinositol 3-kinase. *Proceedings of the National Academy of Sciences* **88**, 7908–7912 (1991).

821. Vogt, P. K. *et al.* Phosphatidylinositol 3-Kinase: The Oncoprotein. in 79–104 (2010). doi:10.1007/82_2010_80.

822. Vanhaesebroeck, B., Stephens, L. & Hawkins, P. PI3K signalling: the path to discovery and understanding. *Nature Reviews Molecular Cell Biology 2012 13:3* **13**, 195–203 (2012).

823. Maehama, T. & Dixon, J. E. The Tumor Suppressor, PTEN/MMAC1, Dephosphorylates the Lipid Second Messenger, Phosphatidylinositol 3,4,5-Trisphosphate. *Journal of Biological Chemistry* **273**, 13375–13378 (1998).

824. Zhou, B. P. *et al.* HER-2/neu blocks tumor necrosis factor-induced apoptosis via the Akt/NF- κB pathway. *Journal of Biological Chemistry* **275**, 8027–8031 (2000).

825. Okano, J. I., Gaslightwala, I., Birnbaum, M. J., Rustgi, A. K. & Nakagawa, H. Akt/protein kinase B isoforms are differentially regulated by epidermal growth factor stimulation. *Journal of Biological Chemistry* **275**, 30934–30942 (2000).

826. Stephens, L. *et al.* Protein kinase B kinases that mediate phosphatidylinositol 3,4,5-trisphosphate-dependent activation of protein kinase B. *Science* **279**, 710–714 (1998).

827. Sarbassov, D. D., Guertin, D. A., Ali, S. M. & Sabatini, D. M. Phosphorylation and regulation of Akt/PKB by the rictor-mTOR complex. *Science* **307**, 1098–1101 (2005).

828. Pearce, L. R., Komander, D. & Alessi, D. R. The nuts and bolts of AGC protein kinases. *Nature Reviews Molecular Cell Biology 2010 11:1* **11**, 9–22 (2010).

829. Toker, A. & Newton, A. C. Akt/protein kinase B is regulated by autophosphorylation at the hypothetical PDK-2 site. *Journal of Biological Chemistry* **275**, 8271–8274 (2000).

830. Mora, A., Komander, D., van Aalten, D. M. F. & Alessi, D. R. PDK1, the master regulator of AGC kinase signal transduction. *Semin Cell Dev Biol* **15**, 161–170 (2004).

831. Jacinto, E. *et al.* SIN1/MIP1 Maintains rictor-mTOR Complex Integrity and Regulates Akt Phosphorylation and Substrate Specificity. *Cell* **127**, 125–137 (2006).

832. Schmidt, M. *et al.* Cell Cycle Inhibition by FoxO Forkhead Transcription Factors Involves Downregulation of Cyclin D. *Mol Cell Biol* **22**, 7842–7852 (2002).

833. Calnan, D. R. & Brunet, A. The FoxO code. *Oncogene 2008 27:16* **27**, 2276–2288 (2008).

834. Facchinetti, V. *et al.* The mammalian target of rapamycin complex 2 controls folding and stability of Akt and protein kinase C. *EMBO J* **27**, 1932–1943 (2008).

835. Ikenoue, T., Inoki, K., Yang, Q., Zhou, X. & Guan, K.-L. Essential function of TORC2 in PKC and Akt turn motif phosphorylation, maturation and signalling. *EMBO J* **27**, 1919–1931 (2008).

836. Liu, P. *et al.* Cell-cycle-regulated activation of Akt kinase by phosphorylation at its carboxyl terminus. *Nature* **508**, 541–545 (2014).

837. Di Maira, G. *et al.* Protein kinase CK2 phosphorylates and upregulates Akt/PKB. *Cell Death Differ* **12**, 668–677 (2005).

838. Gulen, M. F. *et al.* Inactivation of the Enzyme GSK3α by the Kinase IKKi Promotes AKT-mTOR Signaling Pathway that Mediates Interleukin-1-Induced Th17 Cell Maintenance. *Immunity* **37**, 800–812 (2012).

839. Sundaresan, N. R. *et al.* The Deacetylase SIRT1 Promotes Membrane Localization and Activation of Akt and PDK1 During Tumorigenesis and Cardiac Hypertrophy. *Sci Signal* **4**, (2011).

840. Chan, C.-H. *et al.* Posttranslational regulation of Akt in human cancer. *Cell Biosci* **4**, 59 (2014).

841. Yang, W.-L. *et al.* The E3 Ligase TRAF6 Regulates Akt Ubiquitination and Activation. *Science (1979)* **325**, 1134–1138 (2009).

842. Fan, C.-D., Lum, M. A., Xu, C., Black, J. D. & Wang, X. Ubiquitin-dependent Regulation of Phospho-AKT Dynamics by the Ubiquitin E3 Ligase, NEDD4-1, in the Insulin-like Growth Factor-1 Response. *Journal of Biological Chemistry* **288**, 1674–1684 (2013).

843. Chan, C.-H. *et al.* The Skp2-SCF E3 Ligase Regulates Akt Ubiquitination, Glycolysis, Herceptin Sensitivity, and Tumorigenesis. *Cell* **149**, 1098–1111 (2012).

844. Lim, J. H. *et al.* CYLD negatively regulates transforming growth factor-β-signalling via deubiquitinating Akt. *Nat Commun* **3**, 771 (2012).

845. Li, R. *et al.* Akt SUMOylation Regulates Cell Proliferation and Tumorigenesis. *Cancer Res* **73**, 5742–5753 (2013).

846. Andjelković, M. *et al.* Activation and phosphorylation of a pleckstrin homology domain containing protein kinase (RAC-PK/PKB) promoted by serum and protein phosphatase inhibitors. *Proceedings of the National Academy of Sciences* **93**, 5699–5704 (1996).

847. Brognard, J., Sierecki, E., Gao, T. & Newton, A. C. PHLPP and a Second Isoform, PHLPP2, Differentially Attenuate the Amplitude of Akt Signaling by Regulating Distinct Akt Isoforms. *Mol Cell* **25**, 917–931 (2007).

848. Gao, T., Furnari, F. & Newton, A. C. PHLPP: A Phosphatase that Directly Dephosphorylates Akt, Promotes Apoptosis, and Suppresses Tumor Growth. *Mol Cell* **18**, 13–24 (2005).

849. Kaidanovich-Beilin, O. & Woodgett, J. R. GSK-3: Functional Insights from Cell Biology and Animal Models. *Front Mol Neurosci* **4**, (2011).

850. Maurer, U., Charvet, C., Wagman, A. S., Dejardin, E. & Green, D. R. Glycogen Synthase Kinase-3 Regulates Mitochondrial Outer Membrane Permeabilization and Apoptosis by Destabilization of MCL-1. *Mol Cell* **21**, 749–760 (2006).

851. Morel, C., Carlson, S. M., White, F. M. & Davis, R. J. Mcl-1 Integrates the Opposing Actions of Signaling Pathways That Mediate Survival and Apoptosis. *Mol Cell Biol* **29**, 3845–3852 (2009).

852. Sears, R. *et al.* Multiple Ras-dependent phosphorylation pathways regulate Myc protein stability. *Genes Dev* **14**, 2501–2514 (2000).

853. Welcker, M. *et al.* The Fbw7 tumor suppressor regulates glycogen synthase kinase 3 phosphorylation-dependent c-Myc protein degradation. *Proceedings of the National Academy of Sciences* **101**, 9085–9090 (2004).

854. Rylatt, D. B. *et al.* Glycogen synthase from rabbit skeletal muscle. Amino acid sequence at the sites phosphorylated by glycogen synthase kinase-3, and extension of the N-terminal sequence containing the site phosphorylated by phosphorylase kinase. *Eur J Biochem* **107**, 529–37 (1980).

855. Parker, P. J., Caudwell, F. B. & Cohen, P. Glycogen Synthase from Rabbit Skeletal Muscle; Effect of Insulin on the State of phosphorylation of the Seven Phosphoserine Residues *in vivo*. *Eur J Biochem* **130**, 227–234 (1983).

856. van der Vos, K. E. & Coffer, P. J. The Extending Network of FOXO Transcriptional Target Genes. *Antioxid Redox Signal* **14**, 579–592 (2011).

857. Webb, A. E. & Brunet, A. FOXO transcription factors: key regulators of cellular quality control. *Trends Biochem Sci* **39**, 159–169 (2014).

858. Kops, G. J. P. L. *et al.* Direct control of the Forkhead transcription factor AFX by protein kinase B. *Nature* **398**, 630–634 (1999).

859. Brunet, A. *et al.* Akt Promotes Cell Survival by Phosphorylating and Inhibiting a Forkhead Transcription Factor. *Cell* **96**, 857–868 (1999).

860. Dibble, C. C. & Cantley, L. C. Regulation of mTORC1 by PI3K signaling. *Trends Cell Biol* **25**, 545–555 (2015).

861. Liu, P. *et al.* PtdIns(3,4,5) *P* 3-Dependent Activation of the mTORC2 Kinase Complex. *Cancer Discov* **5**, 1194–1209 (2015).

862. Ebner, M., Sinkovics, B., Szczygieł, M., Ribeiro, D. W. & Yudushkin, I. Localization of mTORC2 activity inside cells. *Journal of Cell Biology* **216**, 343–353 (2017).

863. Shaw, R. J. & Cantley, L. C. Ras, PI(3)K and mTOR signalling controls tumour cell growth. *Nature 2006 441:7092* **441**, 424–430 (2006).

864. Huang, J. & Manning, B. D. The TSC1–TSC2 complex: a molecular switchboard controlling cell growth. *Biochemical Journal* **412**, 179–190 (2008).

865. Manning, B. D., Tee, A. R., Logsdon, M. N., Blenis, J. & Cantley, L. C. Identification of the Tuberous Sclerosis Complex-2 Tumor Suppressor Gene Product Tuberin as a Target of the Phosphoinositide 3-Kinase/Akt Pathway. *Mol Cell* **10**, 151–162 (2002).

866. Scott, P. H., Brunn, G. J., Kohn, A. D., Roth, R. A. & Lawrence, J. C. Evidence of insulin-stimulated phosphorylation and activation of the mammalian target of rapamycin mediated by a protein kinase B signaling pathway. *Proceedings of the National Academy of Sciences* **95**, 7772–7777 (1998).

867. Tzatsos, A. & Kandror, K. V. Nutrients Suppress Phosphatidylinositol 3-Kinase/Akt Signaling via Raptor-Dependent mTOR-Mediated Insulin Receptor Substrate 1 Phosphorylation. *Mol Cell Biol* **26**, 63–76 (2006).

868. Shah, O. J. & Hunter, T. Turnover of the Active Fraction of IRS1 Involves Raptor-mTOR- and S6K1-Dependent Serine Phosphorylation in Cell Culture Models of Tuberous Sclerosis. *Mol Cell Biol* **26**, 6425–6434 (2006).

869. Harrington, L. S. *et al.* The TSC1-2 tumor suppressor controls insulin–PI3K signaling via regulation of IRS proteins. *J Cell Biol* **166**, 213–223 (2004).

870. Hsu, P. P. *et al.* The mTOR-Regulated Phosphoproteome Reveals a Mechanism of mTORC1-Mediated Inhibition of Growth Factor Signaling. *Science (1979)* **332**, 1317–1322 (2011).

871. Yu, Y. *et al.* Phosphoproteomic Analysis Identifies Grb10 as an mTORC1 Substrate That Negatively Regulates Insulin Signaling. *Science (1979)* **332**, 1322–1326 (2011).

872. Liu, P. *et al.* Sin1 phosphorylation impairs mTORC2 complex integrity and inhibits downstream Akt signalling to suppress tumorigenesis. *Nat Cell Biol* **15**, 1340–1350 (2013).

873. Julien, L.-A., Carriere, A., Moreau, J. & Roux, P. P. mTORC1-Activated S6K1 Phosphorylates Rictor on Threonine 1135 and Regulates mTORC2 Signaling. *Mol Cell Biol* **30**, 908–921 (2010).

874. Mendoza, M. C., Er, E. E. & Blenis, J. The Ras-ERK and PI3K-mTOR pathways: cross-talk and compensation. *Trends Biochem Sci* **36**, 320–328 (2011).

875. Lu, Y. *et al.* Kinome siRNA-phosphoproteomic screen identifies networks regulating AKT signaling. *Oncogene* **30**, 4567–4577 (2011).

876. Dumaz, N. & Marais, R. Protein Kinase A Blocks Raf-1 Activity by Stimulating 14-3-3 Binding and Blocking Raf-1 Interaction with Ras. *Journal of Biological Chemistry* **278**, 29819–29823 (2003).

877. Guan, K.-L. *et al.* Negative regulation of the serine/threonine kinase B-Raf by Akt. *Journal of Biological Chemistry* (2000) doi:10.1074/jbc.M004371200.

878. Romeo, Y., Zhang, X. & Roux, P. P. Regulation and function of the RSK family of protein kinases. *Biochemical Journal* **441**, 553–569 (2012).

879. Waskiewicz, A. J., Flynn, A., Proud, C. G. & Cooper, J. A. Mitogen-activated protein kinases activate the serine/threonine kinases Mnk1 and Mnk2. *EMBO J* **16**, 1909–1920 (1997).

880. Wang, X. *et al.* The phosphorylation of eukaryotic initiation factor eIF4E in response to phorbol esters, cell stresses, and cytokines is mediated by distinct MAP kinase pathways. *Journal of Biological Chemistry* **273**, 9373–9377 (1998).

881. Averous, J., Fonseca, B. D. & Proud, C. G. Regulation of cyclin D1 expression by mTORC1 signaling requires eukaryotic initiation factor 4E-binding protein 1. *Oncogene 2008 27:8* **27**, 1106–1113 (2007).

882. Grewe, M., Gansauge, F., Schmid, R. M., Adler, G. & Seufferlein, T. Regulation of cell growth and cyclin D1 expression by the constitutively active FRAP-p70s6K pathway in human pancreatic cancer cells. *Cancer Res* **59**, 3581–7 (1999).

883. Abraham, R. T. mTOR as a Positive Regulator of Tumor Cell Responses to Hypoxia. in *Current Topics in Microbiology and Immunology* vol. 279 299–319 (Springer, Berlin, Heidelberg, 2004).

884. Brunet, A. *et al.* Protein Kinase SGK Mediates Survival Signals by Phosphorylating the Forkhead Transcription Factor FKHRL1 (FOXO3a). *Mol Cell Biol* **21**, 952–965 (2001).

885. Adamska, M. *et al.* Structure and expression of conserved Wnt pathway components in the demosponge *Amphimedon queenslandica*. *Evol Dev* **12**, 494–518 (2010).

886. Hobmayer, B. *et al.* WNT signalling molecules act in axis formation in the diploblastic metazoan Hydra. *Nature* **407**, 186–189 (2000).

887. Holstein, T. W. The Evolution of the Wnt Pathway. *Cold Spring Harb Perspect Biol* **4**, a007922–a007922 (2012).

888. Srivastava, M. *et al.* The Trichoplax genome and the nature of placozoans. *Nature* **454**, 955–960 (2008).

889. Komiya, Y. & Habas, R. Wnt signal transduction pathways. *Organogenesis* **4**, 68–75 (2008).

890. Kestler, H. A. & Kühl, M. From individual Wnt pathways towards a Wnt signalling network. *Philosophical Transactions of the Royal Society B: Biological Sciences* vol. 363 1333–1347 Preprint at https://doi.org/10.1098/rstb.2007.2251 (2008).

891. George, S. J. Wnt pathway: A new role in regulation of inflammation. *Arteriosclerosis, Thrombosis, and Vascular Biology* vol. 28 400–402 Preprint at https://doi.org/10.1161/ATVBAHA.107.160952 (2008).

892. Rim, E. Y., Clevers, H. & Nusse, R. The Wnt Pathway: From Signaling Mechanisms to Synthetic Modulators. (2022) doi:10.1146/annurev-biochem-040320.

893. van Amerongen, R. Alternative Wnt pathways and receptors. *Cold Spring Harb Perspect Biol* **4**, (2012).

894. Habas, R. & Dawid, I. B. Dishevelled and Wnt signaling: is the nucleus the final frontier? *J Biol* **4**, 2 (2005).

895. Veeman, M. T., Axelrod, J. D. & Moon, R. T. A Second Canon. *Dev Cell* **5**, 367–377 (2003).

896. De Calisto, J., Araya, C., Marchant, L., Riaz, C. F. & Mayor, R. Essential role of non-canonical Wnt signalling in neural crest migration. *Development* **132**, 2587–2597 (2005).

897. Matsui, T. *et al.* Noncanonical Wnt signaling regulates midline convergence of organ primordia during zebrafish development. *Genes Dev* **19**, 164–175 (2005).

898. Westfall, T. A. *et al.* Wnt-5/ *pipetail* functions in vertebrate axis formation as a negative regulator of Wnt/β-catenin activity. *J Cell Biol* **162**, 889–898 (2003).

899. Saneyoshi, T., Kume, S., Amasaki, Y. & Mikoshiba, K. The Wnt/calcium pathway activates NF-AT and promotes ventral cell fate in Xenopus embryos. *Nature* **417**, 295–299 (2002).

900. Kühl, M., Sheldahl, L. C., Malbon, C. C. & Moon, R. T. Ca2+/Calmodulin-dependent Protein Kinase II Is Stimulated by Wnt and Frizzled Homologs and Promotes Ventral Cell Fates in Xenopus. *Journal of Biological Chemistry* **275**, 12701–12711 (2000).

901. Ishitani, T. *et al.* The TAK1-NLK Mitogen-Activated Protein Kinase Cascade Functions in the Wnt-5a/Ca $^{2+}$ Pathway To Antagonize Wnt/β-Catenin Signaling. *Mol Cell Biol* **23**, 131–139 (2003).

902. Garriock, R. J. & Krieg, P. A. Wnt11-R signaling regulates a calcium sensitive EMT event essential for dorsal fin development of Xenopus. *Dev Biol* **304**, 127–140 (2007).

903. Barrott, J. J., Cash, G. M., Smith, A. P., Barrow, J. R. & Murtaugh, L. C. Deletion of mouse *Porcn* blocks Wnt ligand secretion and reveals an ectodermal etiology of human focal dermal hypoplasia/Goltz syndrome. *Proceedings of the National Academy of Sciences* **108**, 12752–12757 (2011).

904. Biechele, S., Cox, B. J. & Rossant, J. Porcupine homolog is required for canonical Wnt signaling and gastrulation in mouse embryos. *Dev Biol* **355**, 275–285 (2011).

905. Coombs, G. S. *et al.* WLS-dependent secretion of WNT3A requires Ser209 acylation and vacuolar acidification. *J Cell Sci* **123**, 3357–3367 (2010).

906. Kadowaki, T., Wilder, E., Klingensmith, J., Zachary, K. & Perrimon, N. The segment polarity gene porcupine encodes a putative multitransmembrane protein involved in Wingless processing. *Genes Dev* **10**, 3116–3128 (1996).

907. Takada, R. *et al.* Monounsaturated Fatty Acid Modification of Wnt Protein: Its Role in Wnt Secretion. *Dev Cell* **11**, 791–801 (2006).

908. Willert, K. *et al.* Wnt proteins are lipid-modified and can act as stem cell growth factors. *Nature* **423**, 448–452 (2003).

909. Bänziger, C. *et al.* Wntless, a Conserved Membrane Protein Dedicated to the Secretion of Wnt Proteins from Signaling Cells. *Cell* **125**, 509–522 (2006).

910. Bartscherer, K., Pelte, N., Ingelfinger, D. & Boutros, M. Secretion of Wnt Ligands Requires Evi, a Conserved Transmembrane Protein. *Cell* **125**, 523–533 (2006).

911. Gao, X. & Hannoush, R. N. Single-cell imaging of Wnt palmitoylation by the acyltransferase porcupine. *Nat Chem Biol* **10**, 61–68 (2014).

912. Hausmann, G., Bänziger, C. & Basler, K. Helping Wingless take flight: how WNT proteins are secreted. *Nat Rev Mol Cell Biol* **8**, 331–336 (2007).

913. Hofmann, K. A superfamily of membrane-bound O -acyltransferases with implications for Wnt signaling. *Trends Biochem Sci* **25**, 111–112 (2000).

914. Capurro, M. I., Xiang, Y.-Y., Lobe, C. & Filmus, J. Glypican-3 Promotes the Growth of Hepatocellular Carcinoma by Stimulating Canonical Wnt Signaling. *Cancer Res* **65**, 6245–6254 (2005).

915. Franch-Marro, X. *et al.* Glypicans shunt the Wingless signal between local signalling and further transport. *Development* **132**, 659–666 (2005).

916. Hufnagel, L., Kreuger, J., Cohen, S. M. & Shraiman, B. I. On the role of glypicans in the process of morphogen gradient formation. *Dev Biol* **300**, 512–522 (2006).

917. Li, N. *et al.* A Frizzled-Like Cysteine-Rich Domain in Glypican-3 Mediates Wnt Binding and Regulates Hepatocellular Carcinoma Tumor Growth in Mice. *Hepatology* **70**, 1231–1245 (2019).

918. Lin, X. & Perrimon, N. Dally cooperates with Drosophila Frizzled 2 to transduce Wingless signalling. *Nature* **400**, 281–284 (1999).

919. Tsuda, M. *et al.* The cell-surface proteoglycan Dally regulates Wingless signalling in Drosophila. *Nature* **400**, 276–280 (1999).

920. Yan, D., Wu, Y., Feng, Y., Lin, S.-C. & Lin, X. The Core Protein of Glypican Dally-Like Determines Its Biphasic Activity in Wingless Morphogen Signaling. *Dev Cell* **17**, 470–481 (2009).

921. Mattes, B. *et al.* Wnt/PCP controls spreading of Wnt/β-catenin signals by cytonemes in vertebrates. *Elife* **7**, (2018).

922. Moti, N., Yu, J., Boncompain, G., Perez, F. & Virshup, D. M. Wnt traffic from endoplasmic reticulum to filopodia. *PLoS One* **14**, e0212711 (2019).

923. Stanganello, E. *et al.* Filopodia-based Wnt transport during vertebrate tissue patterning. *Nat Commun* **6**, 5846 (2015).

924. Brunt, L. *et al.* Vangl2 promotes the formation of long cytonemes to enable distant Wnt/β-catenin signaling. *Nat Commun* **12**, 2058 (2021).

925. Lin, X. Functions of heparan sulfate proteoglycans in cell signaling during development. *Development* **131**, 6009–6021 (2004).

926. Glinka, A. *et al.* Dickkopf-1 is a member of a new family of secreted proteins and functions in head induction. *Nature* **391**, 357–362 (1998).

927. Hsieh, J.-C. *et al.* A new secreted protein that binds to Wnt proteins and inhibits their activites. *Nature* **398**, 431–436 (1999).

928. Hoang, B. H. *et al.* Expression pattern of twoFrizzled-related genes,Frzb-1 andSfrp-1, during mouse embryogenesis suggests a role for modulating action ofWnt family members. *Developmental Dynamics* **212**, 364–372 (1998).

929. Bouwmeester, T., Kim, S.-H., Sasai, Y., Lu, B. & Robertis, E. M. De. Cerberus is a head-inducing secreted factor expressed in the anterior endoderm of Spemann's organizer. *Nature* **382**, 595–601 (1996).

930. Wang, S., Krinks, M., Lin, K., Luyten, F. P. & Moos, M. Frzb, a Secreted Protein Expressed in the Spemann Organizer, Binds and Inhibits Wnt-8. *Cell* **88**, 757–766 (1997).

931. Itasaki, N. *et al.* Wise, a context-dependent activator and inhibitor of Wnt signalling. *Development* **130**, 4295–4305 (2003).

932. Kawano, Y. & Kypta, R. Secreted antagonists of the Wnt signalling pathway. *J Cell Sci* **116**, 2627–2634 (2003).

933. Kakugawa, S. *et al.* Notum deacylates Wnt proteins to suppress signalling activity. *Nature* **519**, 187–192 (2015).

934. Zhang, X. *et al.* Notum Is Required for Neural and Head Induction via Wnt Deacylation, Oxidation, and Inactivation. *Dev Cell* **32**, 719–730 (2015).

935. Wodarz, A. & Nusse, R. MECHANISMS OF WNT SIGNALING IN DEVELOPMENT. *Annu Rev Cell Dev Biol* **14**, 59–88 (1998).

936. Schulte, G. & Bryja, V. The Frizzled family of unconventional G-protein-coupled receptors. *Trends Pharmacol Sci* **28**, 518–525 (2007).

937. He, X., Semenov, M., Tamai, K. & Zeng, X. LDL receptor-related proteins 5 and 6 in Wnt/β-catenin signaling:Arrows point the way. *Development* **131**, 1663–1677 (2004).

938. Schulte, G. International Union of Basic and Clinical Pharmacology. LXXX. The Class Frizzled Receptors. *Pharmacol Rev* **62**, 632–667 (2010).

939. Voloshanenko, O., Gmach, P., Winter, J., Kranz, D. & Boutros, M. Mapping of Wnt-Frizzled interactions by multiplex CRISPR targeting of receptor gene families. *The FASEB Journal* **31**, 4832–4844 (2017).

940. Alok, A. *et al.* Wnts synergize to activate β-catenin signaling. *J Cell Sci* (2017) doi:10.1242/jcs.198093.

941. Steinhart, Z. *et al.* Genome-wide CRISPR screens reveal a Wnt–FZD5 signaling circuit as a druggable vulnerability of RNF43-mutant pancreatic tumors. *Nat Med* **23**, 60–68 (2017).

942. Bhanot, P. *et al.* A new member of the frizzled family from Drosophila functions as a Wingless receptor. *Nature* **382**, 225–230 (1996).

943. Cong, F., Schweizer, L. & Varmus, H. Wnt signals across the plasma membrane to activate the β-catenin pathway by forming oligomers containing its receptors, Frizzled and LRP. *Development* **131**, 5103–5115 (2004).

944. Pinson, K. I., Brennan, J., Monkley, S., Avery, B. J. & Skarnes, W. C. An LDL-receptor-related protein mediates Wnt signalling in mice. *Nature* **407**, 535–538 (2000).

945. Tamai, K. *et al.* LDL-receptor-related proteins in Wnt signal transduction. *Nature* **407**, 530–535 (2000).

946. Wallingford, J. B. & Habas, R. The developmental biology of Dishevelled: an enigmatic protein governing cell fate and cell polarity. *Development* **132**, 4421–4436 (2005).

947. Hirai, H., Matoba, K., Mihara, E., Arimori, T. & Takagi, J. Crystal structure of a mammalian Wnt–frizzled complex. *Nat Struct Mol Biol* **26**, 372–379 (2019).

948. Bourhis, E. *et al.* Reconstitution of a Frizzled8·Wnt3a·LRP6 Signaling Complex Reveals Multiple Wnt and Dkk1 Binding Sites on LRP6. *Journal of Biological Chemistry* **285**, 9172–9179 (2010).

949. Bafico, A., Liu, G., Yaniv, A., Gazit, A. & Aaronson, S. A. Novel mechanism of Wnt signalling inhibition mediated by Dickkopf-1 interaction with LRP6/Arrow. *Nat Cell Biol* **3**, 683–686 (2001).

950. Li, X. *et al.* Sclerostin Binds to LRP5/6 and Antagonizes Canonical Wnt Signaling. *Journal of Biological Chemistry* **280**, 19883–19887 (2005).

951. Mao, B. *et al.* LDL-receptor-related protein 6 is a receptor for Dickkopf proteins. *Nature* **411**, 321–325 (2001).

952. Semënov, M., Tamai, K. & He, X. SOST Is a Ligand for LRP5/LRP6 and a Wnt Signaling Inhibitor. *Journal of Biological Chemistry* **280**, 26770–26775 (2005).

953. Semënov, M., Tamai, K. & He, X. SOST Is a Ligand for LRP5/LRP6 and a Wnt Signaling Inhibitor. *Journal of Biological Chemistry* **280**, 26770–26775 (2005).

954. Xu, Q. *et al.* Vascular Development in the Retina and Inner Ear. *Cell* **116**, 883–895 (2004).

955. Kazanskaya, O. *et al.* R-Spondin2 Is a Secreted Activator of Wnt/β-Catenin Signaling and Is Required for Xenopus Myogenesis. *Dev Cell* **7**, 525–534 (2004).

956. Pinson, K. I., Brennan, J., Monkley, S., Avery, B. J. & Skarnes, W. C. An LDL-receptor-related protein mediates Wnt signalling in mice. *Nature* **407**, 535–538 (2000).

957. Wehrli, M. *et al.* arrow encodes an LDL-receptor-related protein essential for Wingless signalling. *Nature* **407**, 527–530 (2000).

958. Mikels, A. J. & Nusse, R. Purified Wnt5a Protein Activates or Inhibits β-Catenin–TCF Signaling Depending on Receptor Context. *PLoS Biol* **4**, e115 (2006).

959. Hikasa, H., Shibata, M., Hiratani, I. & Taira, M. The *Xenopus* receptor tyrosine kinase Xror2 modulates morphogenetic movements of the axial mesoderm and neuroectoderm via Wnt signaling. *Development* **129**, 5227–5239 (2002).

960. Inoue, T. *et al.* C. elegans LIN-18 Is a Ryk Ortholog and Functions in Parallel to LIN-17/Frizzled in Wnt Signaling. *Cell* **118**, 795–806 (2004).

961. Lu, W., Yamamoto, V., Ortega, B. & Baltimore, D. Mammalian Ryk Is a Wnt Coreceptor Required for Stimulation of Neurite Outgrowth. *Cell* **119**, 97–108 (2004).

962. Cadigan, K. M. & Liu, Y. I. Wnt signaling: complexity at the surface. *J Cell Sci* **119**, 395–402 (2006).

963. Semënov, M. V *et al.* Head inducer Dickkopf-1 is a ligand for Wnt coreceptor LRP6. *Current Biology* **11**, 951–961 (2001).

964. Willert, K., Brink, M., Wodarz, A., Varmus, H. & Nusse, R. Casein kinase 2 associates with and phosphorylates dishevelled. *EMBO J* **16**, 3089–96 (1997).

965. Kibardin, A., Ossipova, O. & Sokol, S. Y. Metastasis-associated kinase modulates Wnt signaling to regulate brain patterning and morphogenesis. *Development* **133**, 2845–2854 (2006).

966. Chen, W. *et al.* Dishevelled 2 Recruits ß-Arrestin 2 to Mediate Wnt5A-Stimulated Endocytosis of Frizzled 4. *Science (1979)* **301**, 1391–1394 (2003).

967. Ossipova, O., Dhawan, S., Sokol, S. & Green, J. B. A. Distinct PAR-1 Proteins Function in Different Branches of Wnt Signaling during Vertebrate Development. *Dev Cell* **8**, 829–841 (2005).

968. Axelrod, J. D., Miller, J. R., Shulman, J. M., Moon, R. T. & Perrimon, N. Differential recruitment of Dishevelled provides signaling specificity in the planar cell polarity and Wingless signaling pathways. *Genes Dev* **12**, 2610–2622 (1998).

969. Endo, Y. & Rubin, J. S. Wnt signaling and neurite outgrowth: Insights and questions. *Cancer Sci* **98**, 1311–1317 (2007).

970. Boutros, M., Paricio, N., Strutt, D. I. & Mlodzik, M. Dishevelled Activates JNK and Discriminates between JNK Pathways in Planar Polarity and wingless Signaling. *Cell* **94**, 109–118 (1998).

971. Rosin-Arbesfeld, R., Townsley, F. & Bienz, M. The APC tumour suppressor has a nuclear export function. *Nature* **406**, 1009–1012 (2000).

972. Wallingford, J. B. *et al.* Dishevelled controls cell polarity during Xenopus gastrulation. *Nature* **405**, 81–85 (2000).

973. Itoh, K., Brott, B. K., Bae, G.-U., Ratcliffe, M. J. & Sokol, S. Y. Nuclear localization is required for Dishevelled function in Wnt/beta-catenin signaling. *J Biol* **4**, 3 (2005).

974. Gammons, M. V., Rutherford, T. J., Steinhart, Z., Angers, S. & Bienz, M. Essential role of the Dishevelled DEP domain in a Wnt-dependent human-cell-based complementation assay. *J Cell Sci* **129**, 3892–3902 (2016).

975. Gammons, M. V., Renko, M., Johnson, C. M., Rutherford, T. J. & Bienz, M. Wnt Signalosome Assembly by DEP Domain Swapping of Dishevelled. *Mol Cell* **64**, 92–104 (2016).

976. Pan, W. J. *et al.* Characterization of function of three domains in dishevelled-1: DEP domain is responsible for membrane translocation of dishevelled-1. *Cell Res* **14**, 324–30 (2004).

977. Tauriello, D. V. F. *et al.* Wnt/β-catenin signaling requires interaction of the Dishevelled DEP domain and C terminus with a discontinuous motif in Frizzled. *Proceedings of the National Academy of Sciences* **109**, (2012).

978. Wharton, K. A. Runnin' with the Dvl: Proteins That Associate with Dsh/Dvl and Their Significance to Wnt Signal Transduction. *Dev Biol* **253**, 1–17 (2003).

979. Rothbächer, U. *et al.* Dishevelled phosphorylation, subcellular localization and multimerization regulate its role in early embryogenesis. *EMBO J* **19**, 1010–1022 (2000).

980. Gordon, M. D. & Nusse, R. Wnt Signaling: Multiple Pathways, Multiple Receptors, and Multiple Transcription Factors. *Journal of Biological Chemistry* **281**, 22429–22433 (2006).

981. Liu, C. *et al.* Control of β-Catenin Phosphorylation/Degradation by a Dual-Kinase Mechanism. *Cell* **108**, 837–847 (2002).

982. van Noort, M., Meeldijk, J., van der Zee, R., Destree, O. & Clevers, H. Wnt Signaling Controls the Phosphorylation Status of β-Catenin. *Journal of Biological Chemistry* **277**, 17901–17905 (2002).

983. Jiang, J. & Struhl, G. Regulation of the Hedgehog and Wingless signalling pathways by the F-box/WD40-repeat protein Slimb. *Nature* **391**, 493–496 (1998).

984. Mao, J. *et al.* Low-Density Lipoprotein Receptor-Related Protein-5 Binds to Axin and Regulates the Canonical Wnt Signaling Pathway. *Mol Cell* **7**, 801–809 (2001).

985. Zeng, X. *et al.* Initiation of Wnt signaling: control of Wnt coreceptor Lrp6 phosphorylation/activation via frizzled, dishevelled and axin functions. *Development* **135**, 367–375 (2008).

986. Tolwinski, N. S. *et al.* Wg/Wnt Signal Can Be Transmitted through Arrow/LRP5,6 and Axin Independently of Zw3/Gsk3β Activity. *Dev Cell* **4**, 407–418 (2003).

987. Willert, K., Logan, C. Y., Arora, A., Fish, M. & Nusse, R. A *Drosophila Axin* homolog, *Daxin* , inhibits Wnt signaling. *Development* **126**, 4165–4173 (1999).

988. Yamamoto, H. *et al.* Phosphorylation of Axin, a Wnt Signal Negative Regulator, by Glycogen Synthase Kinase-3β Regulates Its Stability. *Journal of Biological Chemistry* **274**, 10681–10684 (1999).

989. Kishida, S. *et al.* DIX Domains of Dvl and Axin Are Necessary for Protein Interactions and Their Ability To Regulate β-Catenin Stability. *Mol Cell Biol* **19**, 4414–4422 (1999).

990. Wong, H.-C. *et al.* Direct Binding of the PDZ Domain of Dishevelled to a Conserved Internal Sequence in the C-Terminal Region of Frizzled. *Mol Cell* **12**, 1251–1260 (2003).

991. Zeng, W. *et al.* naked cuticle encodes an inducible antagonist of Wnt signalling. *Nature* **403**, 789–795 (2000).

992. Gammons, M. V, Renko, M., Flack, J. E., Mieszczanek, J. & Bienz, M. Feedback control of Wnt signaling based on ultrastable histidine cluster co-aggregation between Naked/NKD and Axin. *Elife* **9**, (2020).

993. Davidson, G. *et al.* Casein kinase 1 γ couples Wnt receptor activation to cytoplasmic signal transduction. *Nature* **438**, 867–872 (2005).

994. Piao, S. *et al.* Direct Inhibition of GSK3β by the Phosphorylated Cytoplasmic Domain of LRP6 in Wnt/β-Catenin Signaling. *PLoS One* **3**, e4046 (2008).

995. Zeng, X. *et al.* A dual-kinase mechanism for Wnt co-receptor phosphorylation and activation. *Nature* **438**, 873–877 (2005).

996. Stamos, J. L., Chu, M. L.-H., Enos, M. D., Shah, N. & Weis, W. I. Structural basis of GSK-3 inhibition by N-terminal phosphorylation and by the Wnt receptor LRP6. *Elife* **3**, (2014).

997. Wu, G., Huang, H., Abreu, J. G. & He, X. Inhibition of GSK3 Phosphorylation of β-Catenin via Phosphorylated PPPSPXS Motifs of Wnt Coreceptor LRP6. *PLoS One* **4**, e4926 (2009).

998. McManus, E. J. *et al.* Role that phosphorylation of GSK3 plays in insulin and Wnt signalling defined by knockin analysis. *EMBO J* **24**, 1571–1583 (2005).

999. Acebron, S. P., Karaulanov, E., Berger, B. S., Huang, Y.-L. & Niehrs, C. Mitotic Wnt Signaling Promotes Protein Stabilization and Regulates Cell Size. *Mol Cell* **54**, 663–674 (2014).

1000. Madan, B. *et al.* Temporal dynamics of Wnt-dependent transcriptome reveal an oncogenic Wnt/MYC/ribosome axis. *Journal of Clinical Investigation* **128**, 5620–5633 (2018).

1001. Taelman, V. F. *et al.* Wnt Signaling Requires Sequestration of Glycogen Synthase Kinase 3 inside Multivesicular Endosomes. *Cell* **143**, 1136–1148 (2010).

1002. Fagotto, F., Glück, U. & Gumbiner, B. M. Nuclear localization signal-independent and importin/karyopherin-independent nuclear import of β-catenin. *Current Biology* **8**, 181–190 (1998).

1003. Cong, F. & Varmus, H. Nuclear-cytoplasmic shuttling of Axin regulates subcellular localization of β-catenin. *Proceedings of the National Academy of Sciences* **101**, 2882–2887 (2004).

1004. Schwarz-Romond, T., Metcalfe, C. & Bienz, M. Dynamic recruitment of axin by Dishevelled protein assemblies. *J Cell Sci* **120**, 2402–2412 (2007).

1005. Mis, M. *et al.* IPO11 mediates βcatenin nuclear import in a subset of colorectal cancers. *Journal of Cell Biology* **219**, (2020).

1006. Vuong, L. T. *et al.* Kinesin-2 and IFT-A act as a complex promoting nuclear localization of β-catenin during Wnt signalling. *Nat Commun* **9**, 5304 (2018).

1007. Griffin, J. N. *et al.* RAPGEF5 Regulates Nuclear Translocation of β-Catenin. *Dev Cell* **44**, 248-260.e4 (2018).

1008. Hendriksen, J. *et al.* RanBP3 enhances nuclear export of active β-catenin independently of CRM1. *J Cell Biol* **171**, 785–797 (2005).

1009. Clevers, H. Wnt/β-Catenin Signaling in Development and Disease. *Cell* **127**, 469–480 (2006).

1010. Cadigan, K. M. & Waterman, M. L. TCF/LEFs and Wnt Signaling in the Nucleus. *Cold Spring Harb Perspect Biol* **4**, a007906–a007906 (2012).

1011. Molenaar, M. *et al.* XTcf-3 Transcription Factor Mediates β-Catenin-Induced Axis Formation in Xenopus Embryos. *Cell* **86**, 391–399 (1996).

1012. Valenta, T., Hausmann, G. & Basler, K. The many faces and functions of β-catenin. *EMBO J* **31**, 2714–2736 (2012).

1013. Reya, T. & Clevers, H. Wnt signalling in stem cells and cancer. *Nature* **434**, 843–850 (2005).

1014. Brantjes, H. All Tcf HMG box transcription factors interact with Groucho-related co-repressors. *Nucleic Acids Res* **29**, 1410–1419 (2001).

1015. Cavallo, R. A. *et al.* Drosophila Tcf and Groucho interact to repress Wingless signalling activity. *Nature* **395**, 604–608 (1998).

1016. Roose, J. *et al.* The Xenopus Wnt effector XTcf-3 interacts with Groucho-related transcriptional repressors. *Nature* **395**, 608–612 (1998).

1017. Kramps, T. *et al.* Wnt/Wingless Signaling Requires BCL9/Legless-Mediated Recruitment of Pygopus to the Nuclear β-Catenin-TCF Complex. *Cell* **109**, 47–60 (2002).

1018. Parker, D. S., Jemison, J. & Cadigan, K. M. Pygopus, a nuclear PHD-finger protein required for Wingless signaling in *Drosophila*. *Development* **129**, 2565–2576 (2002).

1019. Thompson, B., Townsley, F., Rosin-Arbesfeld, R., Musisi, H. & Bienz, M. A new nuclear component of the Wnt signalling pathway. *Nat Cell Biol* **4**, 367–373 (2002).

1020. Townsley, F. M., Cliffe, A. & Bienz, M. Pygopus and Legless target Armadillo/β-catenin to the nucleus to enable its transcriptional co-activator function. *Nat Cell Biol* **6**, 626–633 (2004).

1021. Söderholm, S. & Cantù, C. The WNT/β-catenin dependent transcription: A tissue-specific business. *WIREs Mechanisms of Disease* **13**, (2021).

1022. Ramakrishnan, A.-B., Chen, L., Burby, P. E. & Cadigan, K. M. Wnt target enhancer regulation by a CDX/TCF transcription factor collective and a novel DNA motif. *Nucleic Acids Res* **49**, 8625–8641 (2021).

1023. van Tienen, L. M., Mieszczanek, J., Fiedler, M., Rutherford, T. J. & Bienz, M. Constitutive scaffolding of multiple Wnt enhanceosome components by Legless/BCL9. *Elife* **6**, (2017).

1024. Cantù, C. *et al.* Mutations in *Bcl9* and *Pygo* genes cause congenital heart defects by tissue-specific perturbation of Wnt/β-catenin signaling. *Genes Dev* **32**, 1443–1458 (2018).

1025. Parker, D. S., Jemison, J. & Cadigan, K. M. Pygopus, a nuclear PHD-finger protein required for Wingless signaling in *Drosophila*. *Development* **129**, 2565–2576 (2002).

1026. Zimmerli, D. *et al.* TBX3 acts as tissue-specific component of the Wnt/β-catenin transcriptional complex. *Elife* **9**, (2020).

1027. Kim, C.-H., Neiswender, H., Baik, E. J., Xiong, W. C. & Mei, L. Beta-catenin interacts with MyoD and regulates its transcription activity. *Mol Cell Biol* **28**, 2941–51 (2008).

1028. Mukherjee, S. *et al.* Sox17 and β-catenin co-occupy Wnt-responsive enhancers to govern the endoderm gene regulatory network. *Elife* **9**, (2020).

1029. Barker N. The chromatin remodelling factor Brg-1 interacts with beta-catenin to promote target gene activation. EMBO J. 2001;20(17):4935-4943. doi:10.1093/emboj/20.17.4935

1030. Hecht A. The p300/CBP acetyltransferases function as transcriptional coactivators of beta-catenin in vertebrates. EMBO J. 2000;19(8):1839-1850. doi:10.1093/emboj/19.8.1839

1031. Takemaru KI, Moon RT. The Transcriptional Coactivator Cbp Interacts with β-Catenin to Activate Gene Expression. J Cell Biol. 2000;149(2):249-254. doi:10.1083/jcb.149.2.249

1032. He X, Semenov M, Tamai K, Zeng X. LDL receptor-related proteins 5 and 6 in Wnt/β-catenin signaling:Arrows point the way. Development. 2004;131(8):1663-1677. doi:10.1242/dev.01117

1033. Guo N, Hawkins C, Nathans J. Frizzled6 controls hair patterning in mice. Proc Natl Acad Sci. 2004;101(25):9277-9281. doi:10.1073/pnas.0402802101

1034. Montcouquiol M, Rachel RA, Lanford PJ, Copeland NG, Jenkins NA, Kelley MW. Identification of Vangl2 and Scrb1 as planar polarity genes in mammals. Nature. 2003;423(6936):173-177. doi:10.1038/nature01618

1035. Wang Y, Guo N, Nathans J. The Role of Frizzled3 and Frizzled6 in Neural Tube Closure and in the Planar Polarity of Inner-Ear Sensory Hair Cells. J Neurosci. 2006;26(8):2147-2156. doi:10.1523/JNEUROSCI.4698-05.2005

1036. Tao Q, Yokota C, Puck H, et al. Maternal Wnt11 Activates the Canonical Wnt Signaling Pathway Required for Axis Formation in Xenopus Embryos. Cell. 2005;120(6):857-871. doi:10.1016/j.cell.2005.01.013

1037. Djiane A, Riou JF, Umbhauer M, Boucaut JC, Shi DL. Role of frizzled 7 in the regulation of convergent extension movements during gastrulation in Xenopus laevis. Development. 2000;127(14):3091-3100. doi:10.1242/dev.127.14.3091

1038. Darken RS. The planar polarity gene strabismus regulates convergent extension movements in Xenopus. EMBO J. 2002;21(5):976-985. doi:10.1093/emboj/21.5.976

1039. Krasnow RE, Adler PN. A single frizzled protein has a dual function in tissue polarity. Development. 1994;120(7):1883-1893. doi:10.1242/dev.120.7.1883

1040. Sasai N, Nakazawa Y, Haraguchi T, Sasai Y. The neurotrophin-receptor-related protein NRH1 is essential for convergent extension movements. Nat Cell Biol. 2004;6(8):741-748. doi:10.1038/ncb1158

1041. Lu W, Yamamoto V, Ortega B, Baltimore D. Mammalian Ryk Is a Wnt Coreceptor Required for Stimulation of Neurite Outgrowth. Cell. 2004;119(1):97-108. doi:10.1016/j.cell.2004.09.019

1042. Lu X, Borchers AGM, Jolicoeur C, Rayburn H, Baker JC, Tessier-Lavigne M. PTK7/CCK-4 is a novel regulator of planar cell polarity in vertebrates. Nature. 2004;430(6995):93-98. doi:10.1038/nature02677

1043. Nishita M, Yoo SK, Nomachi A, et al. Filopodia formation mediated by receptor tyrosine kinase Ror2 is required for Wnt5a-induced cell migration. J Cell Biol. 2006;175(4):555-562. doi:10.1083/jcb.200607127

1044. Mikels A, Minami Y, Nusse R. Ror2 Receptor Requires Tyrosine Kinase Activity to Mediate Wnt5A Signaling. J Biol Chem. 2009;284(44):30167-30176. doi:10.1074/jbc.M109.041715

1045. Mikels AJ, Nusse R. Purified Wnt5a Protein Activates or Inhibits β-Catenin–TCF Signaling Depending on Receptor Context. PLoS Biol. 2006;4(4):e115. doi:10.1371/journal.pbio.0040115

1046. Li C, Chen H, Hu L, et al. Ror2 modulates the canonical Wnt signaling in lung epithelial cells through cooperation with Fzd2. BMC Mol Biol. 2008;9(1):11. doi:10.1186/1471-2199-9-11

1047. Saldanha J, Singh J, Mahadevan D. Identification of a frizzled-like cysteine rich domain in the extracellular region of developmental receptor tyrosine kinases. Protein Sci. 1998;7(7):1632-1635. doi:10.1002/pro.5560070718

1048. Keeble TR, Halford MM, Seaman C, et al. The Wnt Receptor Ryk Is Required for Wnt5a-Mediated Axon Guidance on the Contralateral Side of the Corpus Callosum. J Neurosci. 2006;26(21):5840-5848. doi:10.1523/JNEUROSCI.1175-06.2006

1049. Berndt JD, Aoyagi A, Yang P, Anastas JN, Tang L, Moon RT. Mindbomb 1, an E3 ubiquitin ligase, forms a complex with RYK to activate Wnt/β-catenin signaling. J Cell Biol. 2011;194(5):737-750. doi:10.1083/jcb.201107021

1050. Yoshikawa S, McKinnon RD, Kokel M, Thomas JB. Wnt-mediated axon guidance via the Drosophila Derailed receptor. Nature. 2003;422(6932):583-588. doi:10.1038/nature01522

1051. Inoue T, Oz HS, Wiland D, et al. C. elegans LIN-18 Is a Ryk Ortholog and Functions in Parallel to LIN-17/Frizzled in Wnt Signaling. Cell. 2004;118(6):795-806. doi:10.1016/j.cell.2004.09.001

1052. Lin S, Baye LM, Westfall TA, Slusarski DC. Wnt5b–Ryk pathway provides directional signals to regulate gastrulation movement. J Cell Biol. 2010;190(2):263-278. doi:10.1083/jcb.200912128

1053. Lyu J, Wesselschmidt RL, Lu W. Cdc37 Regulates Ryk Signaling by Stabilizing the Cleaved Ryk Intracellular Domain. J Biol Chem. 2009;284(19):12940-12948. doi:10.1074/jbc.M900207200

1054. Lyu J, Yamamoto V, Lu W. Cleavage of the Wnt Receptor Ryk Regulates Neuronal Differentiation during Cortical Neurogenesis. Dev Cell. 2008;15(5):773-780. doi:10.1016/j.devcel.2008.10.004

1055. Tanegashima K, Zhao H, Dawid IB. WGEF activates Rho in the Wnt–PCP pathway and controls convergent extension in Xenopus gastrulation. EMBO J. 2008;27(4):606-617. doi:10.1038/emboj.2008.9

1056. Habas R, Kato Y, He X. Wnt/Frizzled Activation of Rho Regulates Vertebrate Gastrulation and Requires a Novel Formin Homology Protein Daam1. Cell. 2001;107(7):843-854. doi:10.1016/S0092-8674(01)00614-6

1057. Park E, Kim GH, Choi SC, Han JK. Role of PKA as a negative regulator of PCP signaling pathway during Xenopus gastrulation movements. Dev Biol. 2006;292(2):344-357. doi:10.1016/j.ydbio.2006.01.011

1058. Habas R, Dawid IB, He X. Coactivation of Rac and Rho by Wnt/Frizzled signaling is required for vertebrate gastrulation. Genes Dev. 2003;17(2):295-309. doi:10.1101/gad.1022203

1059. Marlow F, Topczewski J, Sepich D, Solnica-Krezel L. Zebrafish Rho Kinase 2 Acts Downstream of Wnt11 to Mediate Cell Polarity and Effective Convergence and Extension Movements. Curr Biol. 2002;12(11):876-884. doi:10.1016/S0960-9822(02)00864-3

1060. Weiser DC, Pyati UJ, Kimelman D. Gravin regulates mesodermal cell behavior changes required for axis elongation during zebrafish gastrulation. Genes Dev. 2007;21(12):1559-1571. doi:10.1101/gad.1535007

1061. Keller R, Davidson LA, Shook DR. How we are shaped: The biomechanics of gastrulation. Differentiation. 2003;71(3):171-205. doi:10.1046/j.1432-0436.2003.710301.x

1062. Li L, Yuan H, Xie W, et al. Dishevelled Proteins Lead to Two Signaling Pathways. J Biol Chem. 1999;274(1):129-134. doi:10.1074/jbc.274.1.129

1063. Kim G, Han J. JNK and ROKα function in the noncanonical Wnt/RhoA signaling pathway to regulate Xenopus convergent extension movements. Dev Dyn. 2005;232(4):958-968. doi:10.1002/dvdy.20262

1064. Marinissen MJ, Chiariello M, Tanos T, Bernard O, Narumiya S, Gutkind JS. The Small GTP-Binding Protein RhoA Regulates c-Jun by a ROCK-JNK Signaling Axis. Mol Cell. 2004;14(1):29-41. doi:10.1016/S1097-2765(04)00153-4

1065. Matthews HK, Marchant L, Carmona-Fontaine C, et al. Directional migration of neural crest cells in vivo is regulated by Syndecan-4/Rac1 and non-canonical Wnt signaling/RhoA. Development. 2008;135(10):1771-1780. doi:10.1242/dev.017350

1066. Moriguchi T, Kawachi K, Kamakura S, et al. Distinct Domains of Mouse Dishevelled Are Responsible for the c-Jun N-terminal Kinase/Stress-activated Protein Kinase Activation and the Axis Formation in Vertebrates. J Biol Chem. 1999;274(43):30957-30962. doi:10.1074/jbc.274.43.30957

1067. Rosso SB, Sussman D, Wynshaw-Boris A, Salinas PC. Wnt signaling through Dishevelled, Rac and JNK regulates dendritic development. Nat Neurosci. 2005;8(1):34-42. doi:10.1038/nn1374

1068. Ma L, Wang H yu. Suppression of Cyclic GMP-dependent Protein Kinase Is Essential to the Wnt/cGMP/Ca2+ Pathway. J Biol Chem. 2006;281(41):30990-31001. doi:10.1074/jbc.M603603200

1069. Slusarski DC, Corces VG, Moon RT. Interaction of Wnt and a Frizzled homologue triggers G-protein-linked phosphatidylinositol signalling. Nature. 1997;390(6658):410-413. doi:10.1038/37138

1070. Kohn AD, Moon RT. Wnt and calcium signaling: β-Catenin-independent pathways. Cell Calcium. 2005;38(3-4):439-446. doi:10.1016/j.ceca.2005.06.022

1071. Slusarski DC, Pelegri F. Calcium signaling in vertebrate embryonic patterning and morphogenesis. Dev Biol. 2007;307(1):1-13. doi:10.1016/j.ydbio.2007.04.043

1072. Meneghini MD, Ishitani T, Carter JC, et al. MAP kinase and Wnt pathways converge to downregulate an HMG-domain repressor in Caenorhabditis elegans. Nature. 1999;399(6738):793-797. doi:10.1038/21666

1073. Ishitani T, Kishida S, Hyodo-Miura J, et al. The TAK1-NLK Mitogen-Activated Protein Kinase Cascade Functions in the Wnt-5a/Ca 2+ Pathway To Antagonize Wnt/β-Catenin Signaling. Mol Cell Biol. 2003;23(1):131-139. doi:10.1128/MCB.23.1.131-139.2003

1074. Ishitani T, Ninomiya-Tsuji J, Nagai S ichi, et al. The TAK1–NLK–MAPK-related pathway antagonizes signalling between β-catenin and transcription factor TCF. Nature. 1999;399(6738):798-802. doi:10.1038/21674

1075. Sheldahl LC, Slusarski DC, Pandur P, Miller JR, Kühl M, Moon RT. Dishevelled activates Ca2+ flux, PKC, and CamKII in vertebrate embryos. J Cell Biol. 2003;161(4):769-777. doi:10.1083/jcb.200211094

1076. Kühl M, Sheldahl LC, Malbon CC, Moon RT. Ca2+/Calmodulin-dependent Protein Kinase II Is Stimulated by Wnt and Frizzled Homologs and Promotes Ventral Cell Fates in Xenopus. J Biol Chem. 2000;275(17):12701-12711. doi:10.1074/jbc.275.17.12701

1077. Saneyoshi T, Kume S, Amasaki Y, Mikoshiba K. The Wnt/calcium pathway activates NF-AT and promotes ventral cell fate in Xenopus embryos. Nature. 2002;417(6886):295-299. doi:10.1038/417295a

1078. Pandur P, Maurus D, Kühl M. Increasingly complex: New players enter the Wnt signaling network. BioEssays. 2002;24(10):881-884. doi:10.1002/bies.10164

1079. He X, Saint-Jeannet JP, Wang Y, Nathans J, Dawid I, Varmus H. A Member of the Frizzled Protein Family Mediating Axis Induction by Wnt-5A. Science (80-). 1997;275(5306):1652-1654. doi:10.1126/science.275.5306.1652

1080. Tu X, Joeng KS, Nakayama KI, et al. Noncanonical Wnt Signaling through G Protein-Linked PKCδ Activation Promotes Bone Formation. Dev Cell. 2007;12(1):113-127. doi:10.1016/j.devcel.2006.11.003

1081. Sharma D, Holets L, Zhang X, Kinsey WH. Role of Fyn kinase in signaling associated with epiboly during zebrafish development. Dev Biol. 2005;285(2):462-476. doi:10.1016/j.ydbio.2005.07.018

1082. Jopling C, den Hertog J. Fyn/Yes and non-canonical Wnt signalling converge on RhoA in vertebrate gastrulation cell movements. EMBO Rep. 2005;6(5):426-431. doi:10.1038/sj.embor.7400386

1083. Dejmek J, Säfholm A, Kamp Nielsen C, Andersson T, Leandersson K. Wnt-5a/Ca 2+ -Induced NFAT Activity Is Counteracted by Wnt-5a/Yes-Cdc42-Casein Kinase 1α Signaling in Human Mammary Epithelial Cells. Mol Cell Biol. 2006;26(16):6024-6036. doi:10.1128/MCB.02354-05

1084. Okamura H, Garcia-Rodriguez C, Martinson H, Qin J, Virshup DM, Rao A. A Conserved Docking Motif for CK1 Binding Controls the Nuclear Localization of NFAT1. Mol Cell Biol. 2004;24(10):4184-4195. doi:10.1128/MCB.24.10.4184-4195.2004

1085. Zhu J, Shibasaki F, Price R, et al. Intramolecular Masking of Nuclear Import Signal on NF-AT4 by Casein Kinase I and MEKK1. Cell. 1998;93(5):851-861. doi:10.1016/S0092-8674(00)81445-2

1086. Huang HC, Klein PS. The Frizzled family: receptors for multiple signal transduction pathways. Genome Biol. 2004;5(7):234. doi:10.1186/gb-2004-5-7-234

1087. Cadigan KM, Liu YI. Wnt signaling: complexity at the surface. J Cell Sci. 2006;119(3):395-402. doi:10.1242/jcs.02826

1088. Weeraratna AT, Jiang Y, Hostetter G, et al. Wnt5a signaling directly affects cell motility and invasion of metastatic melanoma. Cancer Cell. 2002;1(3):279-288. doi:10.1016/S1535-6108(02)00045-4

1089. Robitaille J, MacDonald MLE, Kaykas A, et al. Mutant frizzled-4 disrupts retinal angiogenesis in familial exudative vitreoretinopathy. Nat Genet. 2002;32(2):326-330. doi:10.1038/ng957

1090. Medina A, Reintsch W, Steinbeisser H. Xenopus frizzled 7 can act in canonical and non-canonical Wnt signaling pathways: implications on early patterning and morphogenesis. Mech Dev. 2000;92(2):227-237. doi:10.1016/S0925-4773(00)00240-9

1091. VERKAAR F, VANROSMALEN J, SMITS J, BLANKESTEIJN W, ZAMAN G. Stably overexpressed human Frizzled-2 signals through the β-catenin pathway and does not activate Ca2+-mobilization in Human Embryonic Kidney 293 cells. Cell Signal. 2009;21(1):22-33. doi:10.1016/j.cellsig.2008.09.008

1092. Sumanas S, Strege P, Heasman J, Ekker SC. The putative Wnt receptor Xenopus frizzled-7 functions upstream of β-catenin in vertebrate dorsoventral mesoderm patterning. Development. 2000;127(9):1981-1990. doi:10.1242/dev.127.9.1981

1093. Sato A, Yamamoto H, Sakane H, Koyama H, Kikuchi A. Wnt5a regulates distinct signalling pathways by binding to Frizzled2. EMBO J. 2010;29(1):41-54. doi:10.1038/emboj.2009.322

1094. Ma L, Wang H yu. Mitogen-activated Protein Kinase p38 Regulates the Wnt/Cyclic GMP/Ca2+ Non-canonical Pathway. J Biol Chem. 2007;282(39):28980-28990. doi:10.1074/jbc.M702840200

1095. Liu X, Liu T, Slusarski DC, et al. Activation of a Frizzled-2/β-adrenergic receptor chimera promotes Wnt signaling and differentiation of mouse F9 teratocarcinoma cells via Gαo and Gαt. Proc Natl Acad Sci. 1999;96(25):14383-14388. doi:10.1073/pnas.96.25.14383

1096. Abu-Elmagd M, Garcia-Morales C, Wheeler GN. Frizzled7 mediates canonical Wnt signaling in neural crest induction. Dev Biol. 2006;298(1):285-298. doi:10.1016/j.ydbio.2006.06.037

1097. Cong F, Schweizer L, Varmus H. Wnt signals across the plasma membrane to activate the β-catenin pathway by forming oligomers containing its receptors, Frizzled and LRP. Development. 2004;131(20):5103-5115. doi:10.1242/dev.01318

1098. Klein TJ, Jenny A, Djiane A, Mlodzik M. CKIε/discs overgrown Promotes Both Wnt-Fz/β-Catenin and Fz/PCP Signaling in Drosophila. Curr Biol. 2006;16(13):1337-1343. doi:10.1016/j.cub.2006.06.030

1099. Liao G, Tao Q, Kofron M, et al. Jun NH 2 -terminal kinase (JNK) prevents nuclear β-catenin accumulation and regulates axis formation in Xenopus embryos. Proc Natl Acad Sci. 2006;103(44):16313-16318. doi:10.1073/pnas.0602557103

1100. Schwarz-Romond T, Asbrand C, Bakkers J, et al. The ankyrin repeat protein Diversin recruits Casein kinase Iε to the β-catenin degradation complex and acts in both canonical Wnt and Wnt/JNK signaling. Genes Dev. 2002;16(16):2073-2084. doi:10.1101/gad.230402

1101. Glinka A, Wu W, Delius H, Monaghan AP, Blumenstock C, Niehrs C. Dickkopf-1 is a member of a new family of secreted proteins and functions in head induction. Nature. 1998;391(6665):357-362. doi:10.1038/34848

1102. Caneparo L, Huang YL, Staudt N, et al. Dickkopf-1 regulates gastrulation movements by coordinated modulation of Wnt/βcatenin and Wnt/PCP activities, through interaction with the Dally-like homolog Knypek. Genes Dev. 2007;21(4):465-480. doi:10.1101/gad.406007

1103. Lee AY, He B, You L, et al. Dickkopf-1 antagonizes Wnt signaling independent of β-catenin in human mesothelioma. Biochem Biophys Res Commun. 2004;323(4):1246-1250. doi:10.1016/j.bbrc.2004.09.001

1104. Pandur P, Läsche M, Eisenberg LM, Kühl M. Wnt-11 activation of a non-canonical Wnt signalling pathway is required for cardiogenesis. Nature. 2002;418(6898):636-641. doi:10.1038/nature00921

1105. Grimson MJ, Coates JC, Reynolds JP, Shipman M, Blanton RL, Harwood AJ. Adherens junctions and β-catenin-mediated cell signalling in a non-metazoan organism. Nature. 2000;408(6813):727-731. doi:10.1038/35047099

1106. Plyte SE, O'Donovan E, Woodgett JR, Harwood AJ. Glycogen synthase kinase-3 (GSK-3) is regulated during Dictyostelium development via the serpentine receptor cAR3. Development. 1999;126(2):325-333. doi:10.1242/dev.126.2.325

1107. Prabhu Y, Eichinger L. The Dictyostelium repertoire of seven transmembrane domain receptors. Eur J Cell Biol. 2006;85(9-10):937-946. doi:10.1016/j.ejcb.2006.04.003

1108. Richter DJ, Fozouni P, Eisen MB, King N. Gene family innovation, conservation and loss on the animal stem lineage. Elife. 2018;7. doi:10.7554/eLife.34226

1109. Weber U, Paricio N, Mlodzik M. Jun mediates Frizzled-induced R3/R4 cell fate distinction and planar polarity determination in the Drosophila eye. Development. 2000;127(16):3619-3629. doi:10.1242/dev.127.16.3619

1110. Yamanaka H, Moriguchi T, Masuyama N, et al. JNK functions in the non-canonical Wnt pathway to regulate convergent extension movements in vertebrates. EMBO Rep. 2002;3(1):69-75. doi:10.1093/embo-reports/kvf008

1111. Oishi I, Suzuki H, Onishi N, et al. The receptor tyrosine kinase Ror2 is involved in non-canonical Wnt5a/JNK signalling pathway. Genes to Cells. 2003;8(7):645-654. doi:10.1046/j.1365-2443.2003.00662.x

1112. Karner CM, Chirumamilla R, Aoki S, Igarashi P, Wallingford JB, Carroll TJ. Wnt9b signaling regulates planar cell polarity and kidney tubule morphogenesis. Nat Genet. 2009;41(7):793-799. doi:10.1038/ng.400

1113. Attwooll, C., Denchi, E. L. & Helin, K. The E2F family: specific functions and overlapping interests. *EMBO J* **23**, 4709–4716 (2004).

1114. Takahashi, Y., Rayman, J. B. & Dynlacht, B. D. Analysis of promoter binding by the E2F and pRB families in vivo: distinct E2F proteins mediate activation and repression. *Genes Dev* **14**, 804–816 (2000).

1115. Rubin, S. M., Gall, A. L., Zheng, N. & Pavletich, N. P. Structure of the Rb C-Terminal Domain Bound to E2F1-DP1: A Mechanism for Phosphorylation-Induced E2F Release. *Cell* **123**, 1093–1106 (2005).

1116. Rayman, J. B. *et al.* E2F mediates cell cycle-dependent transcriptional repression in vivo by recruitment of an HDAC1/mSin3B corepressor complex. *Genes Dev* **16**, 933–947 (2002).

1117. Ikeda, M. A., Jakoi, L. & Nevins, J. R. A unique role for the Rb protein in controlling E2F accumulation during cell growth and differentiation. *Proceedings of the National Academy of Sciences* **93**, 3215–3220 (1996).

1118. Sellers, W. R., Rodgers, J. W. & Kaelin, W. G. A potent transrepression domain in the retinoblastoma protein induces a cell cycle arrest when bound to E2F sites. *Proceedings of the National Academy of Sciences* **92**, 11544–11548 (1995).

1119. Weintraub, S. J. *et al.* Mechanism of active transcriptional repression by the retinoblastoma protein. *Nature* **375**, 812–816 (1995).

1120. Brehm, A. *et al.* Retinoblastoma protein recruits histone deacetylase to repress transcription. *Nature* **391**, 597–601 (1998).

1121. Ohtani, K. Implication of transcription factor E2F in regulation of DNA replication. *Frontiers in Bioscience* **4**, d793 (1999).

1122. Dyson, N. The regulation of E2F by pRB-family proteins. *Genes Dev* **12**, 2245–2262 (1998).

1123. Thalmeier, K., Synovzik, H., Mertz, R., Winnacker, E. L. & Lipp, M. Nuclear factor E2F mediates basic transcription and trans-activation by E1a of the human MYC promoter. *Genes Dev* **3**, 527–536 (1989).

1124. Obaya, A. J. & Sedivy, J. M. Regulation of cyclin-Cdk activity in mammalian cells. *Cell Mol Life Sci* **59**, 126–142 (2002).

1125. Sherr, C. J. Mammalian G1 cyclins. *Cell* **73**, 1059–1065 (1993).

1126. Honda, R., Ohba, Y., Nagata, A., Okayama, H. & Yasuda, H. Dephosphorylation of human p34 ^{cdc2} kinase on both Thr-14 and Tyr-15 by human cdc25B phosphatase. *FEBS Lett* **318**, 331–334 (1993).

1127. Sebastian, B., Kakizuka, A. & Hunter, T. Cdc25M2 activation of cyclin-dependent kinases by dephosphorylation of threonine-14 and tyrosine-15. *Proceedings of the National Academy of Sciences* **90**, 3521–3524 (1993).

1128. Nilsson, I. & Hoffmann, I. Cell cycle regulation by the Cdc25 phosphatase family. in *Progress in Cell Cycle Research* 107–114 (Springer US, Boston, MA, 2000). doi:10.1007/978-1-4615-4253-7_10.

1129. Mueller, P. R., Coleman, T. R., Kumagai, A. & Dunphy, W. G. Myt1: A Membrane-Associated Inhibitory Kinase That Phosphorylates Cdc2 on Both Threonine-14 and Tyrosine-15. *Science (1979)* **270**, 86–90 (1995).

1130. McGowan, C. H. & Russell, P. Human Wee1 kinase inhibits cell division by phosphorylating p34cdc2 exclusively on Tyr15. *EMBO J* **12**, 75–85 (1993).

1131. Parker, L. & Piwnica-Worms, H. Inactivation of the p34cdc2-cyclin B complex by the human WEE1 tyrosine kinase. *Science (1979)* **257**, 1955–1957 (1992).

1132. Morgan, D. O. CYCLIN-DEPENDENT KINASES: Engines, Clocks, and Microprocessors. *Annu Rev Cell Dev Biol* **13**, 261–291 (1997).

1133. Morgan, D. O. Principles of CDK regulation. *Nature* **374**, 131–134 (1995).

1134. Harvey, S. L., Charlet, A., Haas, W., Gygi, S. P. & Kellogg, D. R. Cdk1-Dependent Regulation of the Mitotic Inhibitor Wee1. *Cell* **122**, 407–420 (2005).

1135. Lee, J., Kumagai, A. & Dunphy, W. G. Positive Regulation of Wee1 by Chk1 and 14-3-3 Proteins. *Mol Biol Cell* **12**, 551–563 (2001).

1136. O'Connell, M. J. Chk1 is a wee1 kinase in the G2 DNA damage checkpoint inhibiting cdc2 by Y15 phosphorylation. *EMBO J* **16**, 545–554 (1997).

1137. Wu, L. & Russell, P. Nim1 kinase promotes mitosis by inactivating Wee1 tyrosine kinase. *Nature* **363**, 738–741 (1993).

1138. Parker, L. L., Walter, S. A., Young, P. G. & Piwnica-Worms, H. Phosphorylation and inactivation of the mitotic inhibitor Weel by the nim1/cdr1 kinase. *Nature* **363**, 736–738 (1993).

1139. Villeneuve, J., Scarpa, M., Ortega-Bellido, M. & Malhotra, V. MEK1 inactivates Myt1 to regulate Golgi membrane fragmentation and mitotic entry in mammalian cells. *EMBO J* **32**, 72–85 (2012).

1140. Ruiz, E. J., Vilar, M. & Nebreda, A. R. A Two-Step Inactivation Mechanism of Myt1 Ensures CDK1/Cyclin B Activation and Meiosis I Entry. *Current Biology* **20**, 717–723 (2010).

1141. Palmer, A., Gavin, A.-C. & Nebreda, A. R. A link between MAP kinase and p34cdc2/cyclin B during oocyte maturation: p90rsk phosphorylates and inactivates the p34cdc2 inhibitory kinase Myt1. *EMBO J* **17**, 5037–5047 (1998).

1142. Coleman, K. G. *et al.* Identification of CDK4 Sequences Involved in Cyclin D1 and p16 Binding. *Journal of Biological Chemistry* **272**, 18869–18874 (1997).

1143. Adachi, M., Roussel, M. F., Havenith, K. & Sherr, C. J. Features of macrophage differentiation induced by p19INK4d, a specific inhibitor of cyclin D-dependent kinases. *Blood* **90**, 126–37 (1997).

1144. Reynisdóttir, I. & Massagué, J. The subcellular locations of p15(Ink4b) and p27(Kip1) coordinate their inhibitory interactions with cdk4 and cdk2. *Genes Dev* **11**, 492–503 (1997).

1145. Jeffrey, P. D., Tong, L. & Pavletich, N. P. Structural basis of inhibition of CDK–cyclin complexes by INK4 inhibitors. *Genes Dev* **14**, 3115–3125 (2000).

1146. Wade Harper, J., Adami, G. R., Wei, N., Keyomarsi, K. & Elledge, S. J. The p21 Cdk-interacting protein Cip1 is a potent inhibitor of G1 cyclin-dependent kinases. *Cell* **75**, 805–816 (1993).

1147. Toyoshima, H. & Hunter, T. p27, a novel inhibitor of G1 cyclin-Cdk protein kinase activity, is related to p21. *Cell* **78**, 67–74 (1994).

1148. Lee, M. H., Reynisdóttir, I. & Massagué, J. Cloning of p57KIP2, a cyclin-dependent kinase inhibitor with unique domain structure and tissue distribution. *Genes Dev* **9**, 639–649 (1995).

1149. Xiong, Y. *et al.* p21 is a universal inhibitor of cyclin kinases. *Nature* **366**, 701–704 (1993).

1150. Soos, T. J. *et al.* Formation of p27-CDK complexes during the human mitotic cell cycle. *Cell Growth Differ* **7**, 135–46 (1996).

1151. Cheng, M. *et al.* The p21Cip1 and p27Kip1 CDK `inhibitors' are essential activators of cyclin D-dependent kinases in murine fibroblasts. *EMBO J* **18**, 1571–1583 (1999).

1152. Zörnig, M. & Evan, G. I. Cell cycle: On target with Myc. *Current Biology* **6**, (1996).

1153. García-Gutiérrez, L., Delgado, M. D. & León, J. MYC Oncogene Contributions to Release of Cell Cycle Brakes. *Genes (Basel)* **10**, 244 (2019).

1154. Bretones, G., Delgado, M. D. & León, J. Myc and cell cycle control. *Biochimica et Biophysica Acta - Gene Regulatory Mechanisms* vol. 1849 506–516 Preprint at https://doi.org/10.1016/j.bbagrm.2014.03.013 (2015).

1155. Ledoux, A. C. & Perkins, N. D. NF-κB and the cell cycle. *Biochem Soc Trans* **42**, 76–81 (2014).

1156. Obaya, A. J., Mateyak, M. K. & Sedivy, J. M. Mysterious liaisons: the relationship between c-Myc and the cell cycle. *Oncogene* **18**, 2934–2941 (1999).

1157. Jansen-Durr, P. *et al.* Differential modulation of cyclin gene expression by MYC. *Proceedings of the National Academy of Sciences* **90**, 3685–3689 (1993).

1158. Bretones, G., Delgado, M. D. & León, J. Myc and cell cycle control. *Biochimica et Biophysica Acta - Gene Regulatory Mechanisms* vol. 1849 506–516 Preprint at https://doi.org/10.1016/j.bbagrm.2014.03.013 (2015).

1159. Zörnig, M. & Evan, G. I. Cell cycle: On target with Myc. *Current Biology* **6**, (1996).

1160. Dang, C. V. *C-Myc Target Genes Involved in Cell Growth*. *MOLECULAR AND CELLULAR BIOLOGY* vol. 19 (1999).

1161. García-Gutiérrez, L., Delgado, M. D. & León, J. MYC Oncogene Contributions to Release of Cell Cycle Brakes. *Genes (Basel)* **10**, 244 (2019).

1162. Hermeking, H. *et al. Identification of CDK4 as a Target of C-MYC*. www.pnas.orgcgidoi10.1073pnas.050586197 (1999).

1163. Galaktionov, K., Chen, X. & Beach, D. Cdc25 cell-cycle phosphatase as a target of c-myc. *Nature* **382**, 511–517 (1996).

1164. Leone, G., DeGregori, J., Sears, R., Jakoi, L. & Nevins, J. R. Myc and Ras collaborate in inducing accumulation of active cyclin E/Cdk2 and E2F. *Nature* **387**, 422–426 (1997).

1165. García-Gutiérrez, L. *et al.* Myc stimulates cell cycle progression through the activation of Cdk1 and phosphorylation of p27. *Sci Rep* **9**, 18693 (2019).

1166. Bouchard, C. *et al. Direct Induction of Cyclin D2 by Myc Contributes to Cell Cycle Progression and Sequestration of P27*. *The EMBO Journal* vol. 18 (1999).

1167. Coller, H. A. *et al.* Expression analysis with oligonucleotide microarrays reveals that MYC regulates genes involved in growth, cell cycle, signaling, and adhesion. *Proceedings of the National Academy of Sciences* **97**, 3260–3265 (2000).

1168. Wu, S. *et al.* Myc represses differentiation-induced p21CIP1 expression via Miz-1-dependent interaction with the p21 core promoter. *Oncogene* **22**, 351–360 (2003).

1169. Diehl, J. A., Cheng, M., Roussel, M. F. & Sherr, C. J. Glycogen synthase kinase-3beta regulates cyclin D1 proteolysis and subcellular localization. *Genes Dev* **12**, 3499–3511 (1998).

1170. Tullai, J. W., Graham, J. R. & Cooper, G. M. A GSK-3-mediated transcriptional network maintains repression of immediate early genes in quiescent cells. *Cell Cycle* **10**, 3072–3077 (2011).

1171. Stambolic, V. & Woodgett, J. R. Mitogen inactivation of glycogen synthase kinase-3 beta in intact cells via serine 9 phosphorylation. *Biochem J* **303 (Pt 3)**, 701–704 (1994).

1172. Welcker, M. *et al.* Multisite phosphorylation by Cdk2 and GSK3 controls cyclin E degradation. *Mol Cell* **12**, 381–392 (2003).

1173. Muè Ller, D. *et al. Cdk2-Dependent Phosphorylation of P27 Facilitates Its Myc-Induced Release from Cyclin E/Cdk2 Complexes*. (1997).

1174. Xu. Suppression of p21 by c-Myc through members of miR-17 family at the post-transcriptional level. *Int J Oncol* **37**, (2010).

1175. Peâ Rez-Roger, I., Solomon, D. L., Sewing, A. & Land, H. *Myc Activation of Cyclin E/Cdk2 Kinase Involves Induction of Cyclin E Gene Transcription and Inhibition of P27 Kip1 Binding to Newly Formed Complexes*. (1997).

1176. Kaldis, P. *The Cdk-Activating Kinase (CAK): From Yeast to Mammals*. *CMLS, Cell. Mol. Life Sci* vol. 55 (1999).

1177. Schachter, M. M. *et al.* A Cdk7-Cdk4 T-Loop Phosphorylation Cascade Promotes G1 Progression. *Mol Cell* **50**, 250–260 (2013).

1178. Kato, J., Matsushime, H., Hiebert, S. W., Ewen, M. E. & Sherr, C. J. Direct binding of cyclin D to the retinoblastoma gene product (pRb) and pRb phosphorylation by the cyclin D-dependent kinase CDK4. *Genes Dev* **7**, 331–342 (1993).

1179. Beijersbergen, R. L., Carlée, L., Kerkhoven, R. M. & Bernards, R. Regulation of the retinoblastoma protein-related p107 by G1 cyclin complexes. *Genes Dev* **9**, 1340–1353 (1995).

1180. Botz, J. *et al.* Cell cycle regulation of the murine cyclin E gene depends on an E2F binding site in the promoter. *Mol Cell Biol* **16**, 3401–3409 (1996).

1181. Geng, Y. *et al.* Regulation of cyclin E transcription by E2Fs and retinoblastoma protein. *Oncogene* **12**, 1173–80 (1996).

1182. Lundberg, A. S. & Weinberg, R. A. Functional Inactivation of the Retinoblastoma Protein Requires Sequential Modification by at Least Two Distinct Cyclin-cdk Complexes. *Mol Cell Biol* **18**, 753–761 (1998).

1183. Zarkowska, T. & Mittnacht, S. Differential Phosphorylation of the Retinoblastoma Protein by G1/S Cyclin-dependent Kinases. *Journal of Biological Chemistry* **272**, 12738–12746 (1997).

1184. Zhao, J., Dynlacht, B., Imai, T., Hori, T. -a. & Harlow, E. Expression of NPAT, a novel substrate of cyclin E-CDK2, promotes S-phase entry. *Genes Dev* **12**, 456–461 (1998).

1185. Zhao, J. *et al.* NPAT links cyclin E–Cdk2 to the regulation of replication-dependent histone gene transcription. *Genes Dev* **14**, 2283–2297 (2000).

1186. Ohtani, K. Implication of transcription factor E2F in regulation of DNA replication. *Frontiers in Bioscience* **4**, d793 (1999).

1187. Pardee, A. B. A Restriction Point for Control of Normal Animal Cell Proliferation. *Proceedings of the National Academy of Sciences* **71**, 1286–1290 (1974).

1188. Cardoso, M. C., Leonhardt, H. & Nadal-Ginard, B. Reversal of terminal differentiation and control of DNA replication: Cyclin A and cdk2 specifically localize at subnuclear sites of DNA replication. *Cell* **74**, 979–992 (1993).

1189. Coverley, D., Laman, H. & Laskey, R. A. Distinct roles for cyclins E and A during DNA replication complex assembly and activation. *Nat Cell Biol* **4**, 523–528 (2002).

1190. Hao, B. *et al.* Structural Basis of the Cks1-Dependent Recognition of p27Kip1 by the SCFSkp2 Ubiquitin Ligase. *Mol Cell* **20**, 9–19 (2005).

1191. Hoffmann, I., Draetta, G. & Karsenti, E. Activation of the phosphatase activity of human cdc25A by a cdk2-cyclin E dependent phosphorylation at the G1/S transition. *EMBO J* **13**, 4302–4310 (1994).

1192. Vlach, J., Hennecke, S. & Amati, B. Phosphorylation-dependent degradation of the cyclin-dependent kinase inhibitor p27Kip1. *EMBO J* **16**, 5334–5344 (1997).

1193. Sheaff, R. J., Groudine, M., Gordon, M., Roberts, J. M. & Clurman, B. E. Cyclin E-CDK2 is a regulator of p27Kip1. *Genes Dev* **11**, 1464–1478 (1997).

1194. Clurman, B. E., Sheaff, R. J., Thress, K., Groudine, M. & Roberts, J. M. Turnover of cyclin E by the ubiquitin-proteasome pathway is regulated by cdk2 binding and cyclin phosphorylation. *Genes Dev* **10**, 1979–1990 (1996).

1195. Won, K. A. & Reed, S. I. Activation of cyclin E/CDK2 is coupled to site-specific autophosphorylation and ubiquitin-dependent degradation of cyclin E. *EMBO J* **15**, 4182–4193 (1996).

1196. Lukas, C. *et al.* Accumulation of cyclin B1 requires E2F and cyclin-A-dependent rearrangement of the anaphase-promoting complex. *Nature 1999 401:6755* **401**, 815–818 (1999).

1197. Petersen, B. O., Lukas, J., Sørensen, C. S., Bartek, J. & Helin, K. Phosphorylation of mammalian CDC6 by Cyclin A/CDK2 regulates its subcellular localization. *EMBO J* **18**, 396–410 (1999).

1198. Lei, M. & Tye, B. K. Initiating DNA synthesis: from recruiting to activating the MCM complex. *J Cell Sci* **114**, 1447–1454 (2001).

1199. Larochelle, S. *et al.* Requirements for Cdk7 in the Assembly of Cdk1/Cyclin B and Activation of Cdk2 Revealed by Chemical Genetics in Human Cells. *Mol Cell* **25**, 839–850 (2007).

1200. Fung, T. K., Ma, H. T. & Poon, R. Y. C. Specialized Roles of the Two Mitotic Cyclins in Somatic Cells: Cyclin A as an Activator of M Phase-promoting Factor □ D. *Mol Biol Cell* **18**, 1861–1873 (2007).

1201. Chae, H. D., Kim, J. & Shin, D. Y. NF-Y binds to both G1- and G2-specific cyclin promoters; a possible role in linking CDK2/cyclin a to CDK1/cyclin B. *BMB Rep* **44**, 553–557 (2011).

1202. Murray, A. W. & Kirschner, M. W. Cyclin synthesis drives the early embryonic cell cycle. *Nature* **339**, 275–280 (1989).

1203. Minshull, J., Blow, J. J. & Hunt, T. Translation of cyclin mRNA is necessary for extracts of activated xenopus eggs to enter mitosis. *Cell* **56**, 947–956 (1989).

1204. Toyoshima-Morimoto, F., Taniguchi, E. & Nishida, E. Plk1 promotes nuclear translocation of human Cdc25C during prophase. *EMBO Rep* **3**, 341–348 (2002).

1205. Yang, J., Song, H., Walsh, S., Bardes, E. S. G. & Kornbluth, S. Combinatorial control of cyclin B1 nuclear trafficking through phosphorylation at multiple sites. *J Biol Chem* **276**, 3604–3609 (2001).

1206. Li, J., Meyer, A. N. & Donoghue, D. J. Nuclear localization of cyclin B1 mediates its biological activity and is regulated by phosphorylation. *Proc Natl Acad Sci U S A* **94**, 502–507 (1997).

1207. Hagting, A., Jackman, M., Simpson, K. & Pines, J. Translocation of cyclin B1 to the nucleus at prophase requires a phosphorylation-dependent nuclear import signal. *Curr Biol* **9**, 680–689 (1999).

1208. Draviam, V. M., Orrechia, S., Lowe, M., Pardi, R. & Pines, J. The localization of human cyclins B1 and B2 determines CDK1 substrate specificity and neither enzyme requires MEK to disassemble the Golgi apparatus. *J Cell Biol* **152**, 945–958 (2001).

1209. Gavet, O. & Pines, J. Activation of cyclin B1-Cdk1 synchronizes events in the nucleus and the cytoplasm at mitosis. *J Cell Biol* **189**, 247–259 (2010).

1210. Meyer, H., Drozdowska, A. & Dobrynin, G. A role for Cdc48/p97 and Aurora B in controlling chromatin condensation during exit from mitosis. *Biochem Cell Biol* **88**, 23–28 (2010).

1211. McHugh, B. & Heck, M. M. S. Regulation of chromosome condensation and segregation. *Curr Opin Genet Dev* **13**, 185–190 (2003).

1212. Crasta, K., Lim, H. H., Giddings, T. H., Winey, M. & Surana, U. Inactivation of Cdh1 by synergistic action of Cdk1 and polo kinase is necessary for proper assembly of the mitotic spindle. *Nature Cell Biology 2008 10:6* **10**, 665–675 (2008).

1213. Jackman, M., Lindon, C., Niggt, E. A. & Pines, J. Active cyclin B1-Cdk1 first appears on centrosomes in prophase. *Nat Cell Biol* **5**, 143–148 (2003).

1214. Takizawa, C. G. & Morgan, D. O. Control of mitosis by changes in the subcellular location of cyclin-B1-Cdk1 and Cdc25C. *Curr Opin Cell Biol* **12**, 658–665 (2000).

1215. Peters, J. M. The anaphase-promoting complex: proteolysis in mitosis and beyond. *Mol Cell* **9**, 931–943 (2002).

1216. Takizawa, C. G. & Morgan, D. O. Control of mitosis by changes in the subcellular location of cyclin-B1–Cdk1 and Cdc25C. *Curr Opin Cell Biol* **12**, 658–665 (2000).

1217. Peters, J. M. The anaphase-promoting complex: proteolysis in mitosis and beyond. *Mol Cell* **9**, 931–943 (2002).

1218. Wade Harper, J., Burton, J. L. & Solomon, M. J. The anaphase-promoting complex: it's not just for mitosis any more. *Genes Dev* **16**, 2179–2206 (2002).

1219. Hagting, A. *et al.* Human securin proteolysis is controlled by the spindle checkpoint and reveals when the APC/C switches from activation by Cdc20 to Cdh1. *J Cell Biol* **157**, 1125–1137 (2002).

1220. Hansen, D. V., Loktev, A. V., Ban, K. H. & Jackson, P. K. Plk1 regulates activation of the anaphase promoting complex by phosphorylating and triggering SCFbetaTrCP-dependent destruction of the APC Inhibitor Emi1. *Mol Biol Cell* **15**, 5623–5634 (2004).

1221. Won, K. A., Xiong, Y., Beach, D. & Gilman, M. Z. Growth-regulated expression of D-type cyclin genes in human diploid fibroblasts. *Proceedings of the National Academy of Sciences* **89**, 9910–9914 (1992).

1222. Greaves, N. S., Ashcroft, K. J., Baguneid, M. & Bayat, A. Current understanding of molecular and cellular mechanisms in fibroplasia and angiogenesis during acute wound healing. *Journal of Dermatological Science* vol. 72 206–217 Preprint at https://doi.org/10.1016/j.jdermsci.2013.07.008 (2013).

1223. Tomasso, A., Koopmans, T., Lijnzaad, P., Bartscherer, K. & Seifert, A. W. An ERK-dependent molecular switch antagonizes fibrosis and promotes regeneration in spiny mice (*Acomys*). *Sci Adv* **9**, 2022.06.27.497314 (2023).

1224. Pinheiro, G., Prata, D. F., Araújo, I. M. & Tiscornia, G. The African spiny mouse (Acomys spp.) as an emerging model for development and regeneration. *Lab Anim* **52**, 565–576 (2018).

1225. Buscà, R., Pouysségur, J. & Lenormand, P. ERK1 and ERK2 map kinases: Specific roles or functional redundancy? *Frontiers in Cell and Developmental Biology* vol. 4 Preprint at https://doi.org/10.3389/fcell.2016.00053 (2016).

1226. Stewart, D. C. *et al.* Unique behavior of dermal cells from regenerative mammal, the African Spiny Mouse, in response to substrate stiffness. *J Biomech* **81**, 149–154 (2018).

1227. Aloysius, A., Saxena, S. & Seifert, A. W. Metabolic regulation of innate immune cell phenotypes during wound repair and regeneration. *Current Opinion in Immunology* vol. 68 72–82 Preprint at https://doi.org/10.1016/j.coi.2020.10.012 (2021).

1228. Adlung, L. *et al.* Protein abundance of AKT and ERK pathway components governs cell type-specific regulation of proliferation. *Mol Syst Biol* **13**, (2017).

1229. Ying, H. Z. *et al.* PDGF signaling pathway in hepatic fibrosis pathogenesis and therapeutics (Review). *Molecular Medicine Reports* vol. 16 7879–7889 Preprint at https://doi.org/10.3892/mmr.2017.7641 (2017).

1230. Chen, Y. *et al.* PI3K/Akt signaling pathway is essential for de novo hair follicle regeneration. *Stem Cell Res Ther* **11**, 144 (2020).

1231. Kretz, A., Happold, C. J., Marticke, J. K. & Isenmann, S. Erythropoietin promotes regeneration of adult CNS neurons via Jak2/Stat3 and PI3K/AKT pathway activation. *Molecular and Cellular Neuroscience* **29**, 569–579 (2005).

1232. Song, Y. *et al.* Regeneration of *Drosophila* sensory neuron axons and dendrites is regulated by the Akt pathway involving *Pten* and microRNA *bantam*. *Genes Dev* **26**, 1612–1625 (2012).

1233. Peiris, T. H., Ramirez, D., Barghouth, P. G. & Oviedo, N. J. The Akt signaling pathway is required for tissue maintenance and regeneration in planarians. *BMC Dev Biol* **16**, 7 (2016).

1234. Zhang, X., Tang, N., Hadden, T. J. & Rishi, A. K. Akt, FoxO and regulation of apoptosis. *Biochimica et Biophysica Acta (BBA) - Molecular Cell Research* **1813**, 1978–1986 (2011).

1235. Ryoo, H. D. & Bergmann, A. The role of apoptosis-induced proliferation for regeneration and cancer. *Cold Spring Harbor Perspectives in Biology* vol. 4 Preprint at https://doi.org/10.1101/cshperspect.a008797 (2012).

1236. Stine, R. R. & Matunis, E. L. JAK-STAT Signaling in Stem Cells. in 247–267 (2013). doi:10.1007/978-94-007-6621-1_14.

1237. Herrera, S. C. & Bach, E. A. JAK/STAT signaling in stem cells and regeneration: From drosophila to vertebrates. *Development (Cambridge)* **146**, (2019).

1238. Elsaeidi, F., Bemben, M. A., Zhao, X. F. & Goldman, D. Jak/Stat signaling stimulates zebrafish optic nerve regeneration and overcomes the inhibitory actions of Socs3 and Sfpq. *Journal of Neuroscience* **34**, 2632–2644 (2014).

1239. Colomiere, M. *et al.* Cross talk of signals between EGFR and IL-6R through JAK2/STAT3 mediate epithelial-mesenchymal transition in ovarian carcinomas. *Br J Cancer* **100**, 134–144 (2009).

1240. Pérez, S. & Rius-Pérez, S. Macrophage Polarization and Reprogramming in Acute Inflammation: A Redox Perspective. *Antioxidants* vol. 11 Preprint at https://doi.org/10.3390/antiox11071394 (2022).

1241. Sun, L., Su, Y., Jiao, A., Wang, X. & Zhang, B. T cells in health and disease. *Signal Transduction and Targeted Therapy* vol. 8 Preprint at https://doi.org/10.1038/s41392-023-01471-y (2023).

1242. Yang, V. W. The Cell Cycle. in *Physiology of the Gastrointestinal Tract, Two Volume Set* 451–471 (Elsevier, 2012). doi:10.1016/B978-0-12-382026-6.00015-4.

1243. Kimata, Y. APC/C Ubiquitin Ligase: Coupling Cellular Differentiation to G1/G0 Phase in Multicellular Systems. *Trends in Cell Biology* vol. 29 591–603 Preprint at https://doi.org/10.1016/j.tcb.2019.03.001 (2019).

1244. Whitby DJ, Ferguson MWJ. The extracellular matrix of lip wounds in fetal, neonatal and adult mice. Development. 1991;112(2):651-668. doi:10.1242/dev.112.2.651

1245. Beanes SR, Hu FY, Soo C, et al. Confocal microscopic analysis of scarless repair in the fetal rat: defining the transition. Plast Reconstr Surg. 2002;109(1):160-170. doi:10.1097/00006534-200201000-00026

1246. Merkel JR, DiPaolo BR, Hallock GG, Rice DC. Type I and type III collagen content of healing wounds in fetal and adult rats. Proc Soc Exp Biol Med. 1988;187(4):493-497. doi:10.3181/00379727-187-42694

1247. Alaish SM, Yager D, Diegelmann RF, Cohen IK. Biology of fetal wound healing: hyaluronate receptor expression in fetal fibroblasts. J Pediatr Surg. 1994;29(8):1040-1043. doi:10.1016/0022-3468(94)90275-5

1248. Longaker MT, Chiu ES, Harrison MR, et al. Studies in fetal wound healing. IV. Hyaluronic acid-stimulating activity distinguishes fetal wound fluid from adult wound fluid. Ann Surg. 1989;210(5):667-672. doi:10.1097/00000658-198911000-00016

1249. Longaker MT, Chiu ES, Adzick NS, Stern M, Harrison MR, Stern R. Studies in fetal wound healing. V. A prolonged presence of hyaluronic acid characterizes fetal wound fluid. Ann Surg. 1991;213(4):292-296. doi:10.1097/00000658-199104000-00003

1250. Beanes SR, Dang C, Soo C, et al. Down-regulation of decorin, a transforming growth factor-beta modulator, is associated with scarless fetal wound healing. J Pediatr Surg. 2001;36(11):1666-1671. doi:10.1053/jpsu.2001.27946

1251. Soo C, Hu FY, Zhang X, et al. Differential expression of fibromodulin, a transforming growth factor-beta modulator, in fetal skin development and scarless repair. Am J Pathol. 2000;157(2):423-433. doi:10.1016/s0002-9440(10)64555-5

1252. Kennedy CI, Diegelmann RF, Haynes JH, Yager DR. Proinflammatory cytokines differentially regulate hyaluronan synthase isoforms in fetal and adult fibroblasts. J Pediatr Surg. 2000;35(6):874-879. doi:10.1053/jpsu.2000.6869

1253. Dang CM, Beanes SR, Lee H, Zhang X, Soo C, Ting K. Scarless fetal wounds are associated with an increased matrix metalloproteinase-to-tissue-derived inhibitor of metalloproteinase ratio. Plast Reconstr Surg. 2003;111(7):2273-2285. doi:10.1097/01.PRS.0000060102.57809.DA

1254. Whitby DJ, Longaker MT, Harrison MR, Adzick NS, Ferguson MW. Rapid epithelialisation of fetal wounds is associated with the early deposition of tenascin. J Cell Sci. 1991;99 (Pt 3):583-586. doi:10.1242/jcs.99.3.583

1255. Longaker MT, Whitby DJ, Jennings RW, et al. Fetal diaphragmatic wounds heal with scar formation. J Surg Res. 1991;50(4):375-385. doi:10.1016/0022-4804(91)90206-2

1256. Rinkevich Y, Walmsley GG, Hu MS, et al. Identification and isolation of a dermal lineage with intrinsic fibrogenic potential. Science (80-). 2015;348(6232). doi:10.1126/science.aaa2151

1257. Jiang D, Correa-Gallegos D, Christ S, et al. Two succeeding fibroblastic lineages drive dermal development and the transition from regeneration to scarring. Nat Cell Biol. 2018;20(4):422-431. doi:10.1038/s41556-018-0073-8

1258. Lorenz HP, Adzick NS. Scarless skin wound repair in the fetus. West J Med. 1993;159(3):350-355.

1259. Estes JM, Vande Berg JS, Adzick NS, MacGillivray TE, Desmoulière A, Gabbiani G. Phenotypic and functional features of myofibroblasts in sheep fetal wounds. Differentiation. 1994;56(3):173-181. doi:10.1046/j.1432-0436.1994.5630173.x

1259. Lee SH, Kim MY, Kim HY, et al. The Dishevelled-binding protein CXXC5 negatively regulates cutaneous wound healing. J Exp Med. 2015;212(7):1061-1080. doi:10.1084/jem.20141601

1260. Bastakoty D, Saraswati S, Cates J, Lee E, Nanney LB, Young PP. Inhibition of Wnt/β-catenin pathway promotes regenerative repair of cutaneous and cartilage injury. FASEB J. 2015;29(12):4881-4892. doi:10.1096/fj.15-275941

1261. Carre AL, James AW, MacLeod L, et al. Interaction of Wingless Protein (Wnt), Transforming Growth Factor-β1, and Hyaluronan Production in Fetal and Postnatal Fibroblasts. Plast Reconstr Surg. 2010;125(1):74-88. doi:10.1097/PRS.0b013e3181c495d1

1262. Beaton H, Andrews D, Parsons M, et al. Wnt6 regulates epithelial cell differentiation and is dysregulated in renal fibrosis. Am J Physiol Renal Physiol. 2016;311(1):F35-45. doi:10.1152/ajprenal.00136.2016

1263. Haynes JH, Johnson DE, Mast BA, et al. Platelet-derived growth factor induces fetal wound fibrosis. J Pediatr Surg. 1994;29(11):1405-1408. doi:10.1016/0022-3468(94)90130-9

1264. Liu W, Wang DR, Cao YL. TGF-beta: a fibrotic factor in wound scarring and a potential target for anti-scarring gene therapy. Curr Gene Ther. 2004;4(1):123-136. doi:10.2174/1566523044578004

1265. Liechty KW, Crombleholme TM, Cass DL, Martin B, Adzick NS. Diminished interleukin-8 (IL-8) production in the fetal wound healing response. J Surg Res. 1998;77(1):80-84. doi:10.1006/jsre.1998.5345

1266. Stelnicki EJ, Longaker MT, Holmes D, et al. Bone morphogenetic protein-2 induces scar formation and skin maturation in the second trimester fetus. Plast Reconstr Surg. 1998;101(1):12-19. doi:10.1097/00006534-199801000-00003

1267. Colwell AS, Longaker MT, Peter Lorenz H. Identification of differentially regulated genes in fetal wounds during regenerative repair. Wound Repair Regen. 2008;16(3):450-459. doi:10.1111/j.1524-475X.2008.00383.x

1268. Glim JE, Everts V, Niessen FB, Ulrich MM, Beelen RHJ. Extracellular matrix components of oral mucosa differ from skin and resemble that of foetal skin. Arch Oral Biol. 2014;59(10):1048-1055. doi:10.1016/j.archoralbio.2014.05.019

1269. Glim JE, Beelen RHJ, Niessen FB, Everts V, Ulrich MMW. The number of immune cells is lower in healthy oral mucosa compared to skin and does not increase after scarring. Arch Oral Biol. 2015;60(2):272-281. doi:10.1016/j.archoralbio.2014.10.008

1270. Tassava RA, Nace JD, Wei Y. Extracellular matrix protein turnover during salamander limb regeneration. Wound Repair Regen. 1996;4(1):75-81. doi:10.1046/j.1524-475X.1996.40113.x

1271. Nace JD, Tassava RA. Examination of fibronectin distribution and its sources in the regenerating newt limb by immunocytochemistry and in situ hybridization. Dev Dyn. 1995;202(2):153-164. doi:10.1002/aja.1002020207

1272. Onda H, Poulin ML, Tassava RA, Chiu IM. Characterization of a newt tenascin cDNA and localization of tenascin mRNA during newt limb regeneration by in situ hybridization. Dev Biol. 1991;148(1):219-232. doi:10.1016/0012-1606(91)90331-V

1273. Calve S, Odelberg SJ, Simon HG. A transitional extracellular matrix instructs cell behavior during muscle regeneration. Dev Biol. 2010;344(1):259-271. doi:10.1016/j.ydbio.2010.05.007

1274. Namazi MR, Fallahzadeh MK, Schwartz RA. Strategies for prevention of scars: what can we learn from fetal skin? Int J Dermatol. 2011;50(1):85-93. doi:10.1111/j.1365-4632.2010.04678.x

1275. Miyazaki K, Uchiyama K, Imokawa Y, Yoshizato K. Cloning and characterization of cDNAs for matrix metalloproteinases of regenerating newt limbs. Proc Natl Acad Sci. 1996;93(13):6819-6824. doi:10.1073/pnas.93.13.6819

1276. Vinarsky V, Atkinson DL, Stevenson TJ, Keating MT, Odelberg SJ. Normal newt limb regeneration requires matrix metalloproteinase function. Dev Biol. 2005;279(1):86-98. doi:10.1016/j.ydbio.2004.12.003

1277. Yang E V, Gardiner DM, Carlson MR, Nugas CA, Bryant S V. Expression of Mmp-9 and related matrix metalloproteinase genes during axolotl limb regeneration. Dev Dyn. 1999;216(1):2-9. doi:10.1002/(SICI)1097-0177(199909)216:1<2::AID-DVDY2>3.0.CO;2-P

1278. Sawai T, Usui N, Sando K, et al. Hyaluronic acid of wound fluid in adult and fetal rabbits. J Pediatr Surg. 1997;32(1):41-43. doi:10.1016/S0022-3468(97)90089-0

1279. Satoh A, makanae A, Hirata A, Satou Y. Blastema induction in aneurogenic state and Prrx-1 regulation by MMPs and FGFs in Ambystoma mexicanum limb regeneration. Dev Biol. 2011;355(2):263-274. doi:10.1016/j.ydbio.2011.04.017

1280. Ferris DR, Satoh A, Mandefro B, Cummings GM, Gardiner DM, Rugg EL. Ex vivo generation of a functional and regenerative wound epithelium from axolotl (Ambystoma mexicanum) skin. Dev Growth Differ. 2010;52(8):715-724. doi:10.1111/j.1440-169X.2010.01208.x

1281. Maden M, Turner RN. Supernumerary limbs in the axolotl. Nature. 1978;273(5659):232-235. doi:10.1038/273232a0

1282. Iten LE, Bryant S V. The interaction between the blastema and stump in the establishment of the anterior-posterior and proximal-distal organization of the limb regenerate. Dev Biol. 1975;44(1):119-147. doi:10.1016/0012-1606(75)90381-4

1283. Alibardi L. Review: Biological and Molecular Differences between Tail Regeneration and Limb Scarring in Lizard: An Inspiring Model Addressing Limb Regeneration in Amniotes. J Exp Zool Part B Mol Dev Evol. 2017;328(6):493-514. doi:10.1002/jez.b.22754

1284. Martin GR. The roles of FGFs in the early development of vertebrate limbs. Genes Dev. 1998;12(11):1571-1586. doi:10.1101/gad.12.11.1571

1285. Han MJ, An JY, Kim WS. Expression patterns of Fgf-8 during development and limb regeneration of the axolotl. Dev Dyn. 2001;220(1):40-48. doi:10.1002/1097-0177(2000)9999:9999<::AID-DVDY1085>3.0.CO;2-8

1286. Christensen RN, Weinstein M, Tassava RA. Expression of fibroblast growth factors 4, 8, and 10 in limbs, flanks, and blastemas of Ambystoma. Dev Dyn. 2002;223(2):193-203. doi:10.1002/dvdy.10049

1287. Yokoyama H, Ide H, Tamura K. FGF-10 Stimulates Limb Regeneration Ability in Xenopus laevis. Dev Biol. 2001;233(1):72-79. doi:10.1006/dbio.2001.0180

1288. Kawakami Y, Rodriguez Esteban C, Raya M, et al. Wnt/beta-catenin signaling regulates vertebrate limb regeneration. Genes Dev. 2006;20(23):3232-3237. doi:10.1101/gad.1475106

1289. Chablais F, Jaźwińska A. IGF signaling between blastema and wound epidermis is required for fin regeneration. Development. 2010;137(6):871-879. doi:10.1242/dev.043885

1290. Mullen LM, Bryant S V, Torok MA, Blumberg B, Gardiner DM. Nerve dependency of regeneration: the role of Distal-less and FGF signaling in amphibian limb regeneration. Development. 1996;122(11):3487-3497. doi:10.1242/dev.122.11.3487

1291. Satoh A, Graham GMC, Bryant SV, Gardiner DM. Neurotrophic regulation of epidermal dedifferentiation during wound healing and limb regeneration in the axolotl (Ambystoma mexicanum). Dev Biol. 2008;319(2):321-335. doi:10.1016/j.ydbio.2008.04.030

1292. Kumar A, Godwin JW, Gates PB, Garza-Garcia AA, Brockes JP. Molecular basis for the nerve dependence of limb regeneration in an adult vertebrate. Science. 2007;318(5851):772-777. doi:10.1126/science.1147710

1293. Werner S, Smola H, Liao X, et al. The Function of KGF in Morphogenesis of Epithelium and Reepithelialization of Wounds. Science (80-). 1994;266(5186):819-822. doi:10.1126/science.7973639

1294. TRAMPUSCH HA. NERVES AS MORPHOGENETIC MEDIATORS IN REGENERATION. Prog Brain Res. 1964;13:214-227. doi:10.1016/s0079-6123(08)60145-4

1295. Farkas JE, Monaghan JR. A brief history of the study of nerve dependent regeneration. Neurogenes (Austin, Tex). 2017;4(1):e1302216. doi:10.1080/23262133.2017.1302216

1296. Werner S, Krieg T, Smola H. Keratinocyte–Fibroblast Interactions in Wound Healing. J Invest Dermatol. 2007;127(5):998-1008. doi:10.1038/sj.jid.5700786

1297. Kumar A, Nevill G, Brockes JP, Forge A. A comparative study of gland cells implicated in the nerve dependence of salamander limb regeneration. J Anat. 2010;217(1):16-25. doi:10.1111/j.1469-7580.2010.01239.x

1298. Blassberg RA, Garza-Garcia A, Janmohamed A, Gates PB, Brockes JP. Functional convergence of signalling by GPI-anchored and anchorless forms of a salamander protein implicated in limb regeneration. J Cell Sci. 2011;124(Pt 1):47-56. doi:10.1242/jcs.076331

1299. Monaghan JR, Athippozhy A, Seifert AW, et al. Gene expression patterns specific to the regenerating limb of the Mexican axolotl. Biol Open. 2012;1(10):937-948. doi:10.1242/bio.20121594

1300. Kamrin RP, Singer M. The influence of the spinal cord in regeneration of the tail of the lizard, Anolis carolinensis. J Exp Zool. 1955;128(3):611-627. doi:10.1002/jez.1401280314

1301. Simões MG, Bensimon-Brito A, Fonseca M, et al. Denervation impairs regeneration of amputated zebrafish fins. BMC Dev Biol. 2014;14:49. doi:10.1186/s12861-014-0049-2

1302. SIMPSON SB. ANALYSIS OF TAIL REGENERATION IN THE LIZARD LYGOSOMA LATERALE. I. INITIATION OF REGENERATION AND CARTILAGE DIFFERENTIATION: THE ROLE OF EPENDYMA. J Morphol. 1964;114:425-435. doi:10.1002/jmor.1051140305

1303. Mescher AL. Effects on adult newt limb regeneration of partial and complete skin flaps over the amputation surface. J Exp Zool. 1976;195(1):117-127. doi:10.1002/jez.1401950111

1304. Ghosh S, Roy S, Séguin C, Bryant S V., Gardiner DM. Analysis of the expression and function of Wnt-5a and Wnt-5b in developing and regenerating axolotl (Ambystoma mexicanum) limbs. Dev Growth Differ. 2008;50(4):289-297. doi:10.1111/j.1440-169X.2008.01000.x

1305. Yokoyama H, Maruoka T, Ochi H, et al. Different Requirement for Wnt/β-Catenin Signaling in Limb Regeneration of Larval and Adult Xenopus. PLoS One. 2011;6(7):e21721. doi:10.1371/journal.pone.0021721

1306. Alibardi L. FGFs Treatment on Amputated Lizard Limbs Stimulate the Regeneration of Long Bones, Opening New Avenues for Limb Regeneration in Amniotes: A Morphological Study. J Funct Morphol Kinesiol. 2017;2(3):25. doi:10.3390/jfmk2030025

1307. Christensen RN, Weinstein M, Tassava RA. Fibroblast growth factors in regenerating limbs of Ambystoma: cloning and semi-quantitative RT-PCR expression studies. J Exp Zool. 2001;290(5):529-540. doi:10.1002/jez.1097

1308. Ito M, Yang Z, Andl T, et al. Wnt-dependent de novo hair follicle regeneration in adult mouse skin after wounding. Nature. 2007;447(7142):316-320. doi:10.1038/nature05766

1309. Ortega S, Ittmann M, Tsang SH, Ehrlich M, Basilico C. Neuronal defects and delayed wound healing in mice lacking fibroblast growth factor 2. Proc Natl Acad Sci U S A. 1998;95(10):5672-5677. doi:10.1073/pnas.95.10.5672

1310. Tsuboi R, Shi CM, Sato C, Cox GN, Ogawa H. Co-administration of insulin-like growth factor (IGF)-I and IGF-binding protein-1 stimulates wound healing in animal models. J Invest Dermatol. 1995;104(2):199-203. doi:10.1111/1523-1747.ep12612755

1311. Poss KD, Shen J, Nechiporuk A, et al. Roles for Fgf signaling during zebrafish fin regeneration. Dev Biol. 2000;222(2):347-358. doi:10.1006/dbio.2000.9722

1312. Whitehead GG, Makino S, Lien CL, Keating MT. fgf20 Is Essential for Initiating Zebrafish Fin Regeneration. Science (80-). 2005;310(5756):1957-1960. doi:10.1126/science.1117637

1313. Stoick-Cooper CL, Weidinger G, Riehle KJ, et al. Distinct Wnt signaling pathways have opposing roles in appendage regeneration. Development. 2007;134(3):479-489. doi:10.1242/dev.001123

1314. Yasumuro H, Sakurai K, Toyama F, Maruo F, Chiba C. Implications of a Multi-Step Trigger of Retinal Regeneration in the Adult Newt. Biomedicines. 2017;5(4):25. doi:10.3390/biomedicines5020025

1315. Yoshikawa T, Mizuno A, Yasumuro H, et al. MEK–ERK and heparin-susceptible signaling pathways are involved in cell-cycle entry of the wound edge retinal pigment epithelium cells in the adult newt. Pigment Cell Melanoma Res. 2012;25(1):66-82. doi:10.1111/j.1755-148X.2011.00935.x

1316. Mizuno A, Yasumuro H, Yoshikawa T, Inami W, Chiba C. MEK–ERK signaling in adult newt retinal pigment epithelium cells is strengthened immediately after surgical induction of retinal regeneration. Neurosci Lett. 2012;523(1):39-44. doi:10.1016/j.neulet.2012.06.037

1317. Susaki K, Chiba C. MEK mediates in vitro neural transdifferentiation of the adult newt retinal pigment epithelium cells: Is FGF2 an induction factor? Pigment Cell Res. 2007;20(5):364-379. doi:10.1111/j.1600-0749.2007.00407.x

1318. Vergara MN, Del Rio-Tsonis K. Retinal regeneration in the Xenopus laevis tadpole: a new model system. Mol Vis. 2009;15:1000-1013.

1319. Okuda KS, Keyser MS, Gurevich DB, et al. Live-imaging of endothelial Erk activity reveals dynamic and sequential signalling events during regenerative angiogenesis. Elife. 2021;10. doi:10.7554/eLife.62196

1320. Tu MK, Borodinsky LN. Spontaneous calcium transients manifest in the regenerating muscle and are necessary for skeletal muscle replenishment. Cell Calcium. 2014;56(1):34-41. doi:10.1016/j.ceca.2014.04.004

1321. Kujawski S, Lin W, Kitte F, et al. Calcineurin Regulates Coordinated Outgrowth of Zebrafish Regenerating Fins. Dev Cell. 2014;28(5):573-587. doi:10.1016/j.devcel.2014.01.019

1322. Özkucur N, Epperlein H, Funk RHW. Ion imaging during axolotl tail regeneration in vivo. Dev Dyn. 2010;239(7):2048-2057. doi:10.1002/dvdy.22323

1323. Franklin BM, Voss SR, Osborn JL. Ion channel signaling influences cellular proliferation and phagocyte activity during axolotl tail regeneration. Mech Dev. 2017;146:42-54. doi:10.1016/j.mod.2017.06.001

1324. Wan J, Ramachandran R, Goldman D. HB-EGF Is Necessary and Sufficient for Müller Glia Dedifferentiation and Retina Regeneration. Dev Cell. 2012;22(2):334-347. doi:10.1016/j.devcel.2011.11.020

1325. Wan J, Zhao XF, Vojtek A, Goldman D. Retinal Injury, Growth Factors, and Cytokines Converge on β-Catenin and pStat3 Signaling to Stimulate Retina Regeneration. Cell Rep. 2014;9(1):285-297. doi:10.1016/j.celrep.2014.08.048

1326. Yun MH, Gates PB, Brockes JP. Sustained ERK Activation Underlies Reprogramming in Regeneration-Competent Salamander Cells and Distinguishes Them from Their Mammalian Counterparts. Stem Cell Reports. 2014;3(1):15-23. doi:10.1016/j.stemcr.2014.05.009

1327. Saera-Vila A, Kish PE, Kahana A. Fgf regulates dedifferentiation during skeletal muscle regeneration in adult zebrafish. Cell Signal. 2016;28(9):1196-1204. doi:10.1016/j.cellsig.2016.06.001

1328. Han P, Zhou XH, Chang N, et al. Hydrogen peroxide primes heart regeneration with a derepression mechanism. Cell Res. 2014;24(9):1091-1107. doi:10.1038/cr.2014.108

1329. Missinato MA, Saydmohammed M, Zuppo DA, et al. Dusp6 attenuates Ras/MAPK signaling to limit zebrafish heart regeneration. Development. Published online January 1, 2018. doi:10.1242/dev.157206

1330. Vitulo N, Dalla Valle L, Skobo T, Valle G, Alibardi L. Transcriptome analysis of the regenerating tail vs. the scarring limb in lizard reveals pathways leading to successful vs. unsuccessful organ regeneration in amniotes. Dev Dyn. 2017;246(2):116-134. doi:10.1002/dvdy.24474

1331. Lévesque M, Villiard É, Roy S. Skin wound healing in axolotls: a scarless process. J Exp Zool Part B Mol Dev Evol. 2010;314B(8):684-697. doi:10.1002/jez.b.21371

1332. Lévesque M, Gatien S, Finnson K, et al. Transforming Growth Factor: β Signaling Is Essential for Limb Regeneration in Axolotls. PLoS One. 2007;2(11):e1227. doi:10.1371/journal.pone.0001227

1333. Sato K, Umesono Y, Mochii M. A transgenic reporter under control of an es1 promoter/enhancer marks wound epidermis and apical epithelial cap during tail regeneration in Xenopus laevis tadpole. Dev Biol. 2018;433(2):404-415. doi:10.1016/j.ydbio.2017.08.012

1334. Wagner I, Wang H, Weissert PM, et al. Serum Proteases Potentiate BMP-Induced Cell Cycle Re-entry of Dedifferentiating Muscle Cells during Newt Limb Regeneration. Dev Cell. 2017;40(6):608-617.e6. doi:10.1016/j.devcel.2017.03.002

1335. Wu CC, Kruse F, Vasudevarao MD, et al. Spatially Resolved Genome-wide Transcriptional Profiling Identifies BMP Signaling as Essential Regulator of Zebrafish Cardiomyocyte Regeneration. Dev Cell. 2016;36(1):36-49. doi:10.1016/j.devcel.2015.12.010

1336. BAI S, THUMMEL R, GODWIN A, et al. Matrix metalloproteinase expression and function during fin regeneration in zebrafish: Analysis of MT1-MMP, MMP2 and TIMP2. Matrix Biol. 2005;24(4):247-260. doi:10.1016/j.matbio.2005.03.007

1337. Delorme SL, Lungu IM, Vickaryous MK. Scar-Free Wound Healing and Regeneration Following Tail Loss in the Leopard Gecko, Eublepharis macularius. Anat Rec. 2012;295(10):1575-1595. doi:10.1002/ar.22490

1338. Thornton CS. The histogenesis of the regenerating fore limb of larval Amblystoma after exarticulation of the humerus. J Morphol. 1938;62(2):219-241. doi:10.1002/jmor.1050620204

1339. Campbell LJ, Crews CM. Molecular and Cellular Basis of Regeneration and Tissue Repair. Cell Mol Life Sci. 2008;65(1):73-79. doi:10.1007/s00018-007-7433-z

1340. Chassot B, Pury D, Jaźwińska A. Zebrafish fin regeneration after cryoinjury-induced tissue damage. Biol Open. 2016;5(6):819-828. doi:10.1242/bio.016865

1341. Yokoyama H, Maruoka T, Aruga A, et al. Prx-1 Expression in Xenopus laevis Scarless Skin-Wound Healing and Its Resemblance to Epimorphic Regeneration. J Invest Dermatol. 2011;131(12):2477-2485. doi:10.1038/jid.2011.223

1342. Poulin ML, Patrie KM, Botelho MJ, Tassava RA, Chiu IM. Heterogeneity in the expression of fibroblast growth factor receptors during limb regeneration in newts (Notophthalmus viridescens). Development. 1993;119(2):353-361. doi:10.1242/dev.119.2.353

1343. Kragl M, Knapp D, Nacu E, et al. Cells keep a memory of their tissue origin during axolotl limb regeneration. Nature. 2009;460(7251):60-65. doi:10.1038/nature08152

1344. Dunis DA, Namenwirth M. The role of grafted skin in the regeneration of X-irradiated axolotl limbs. Dev Biol. 1977;56(1):97-109. doi:10.1016/0012-1606(77)90157-9

1345. Sugiura T, Wang H, Barsacchi R, Simon A, Tanaka EM. MARCKS-like protein is an initiating molecule in axolotl appendage regeneration. Nature. 2016;531(7593):237-240. doi:10.1038/nature16974

1346. Aderem A. The Marcks brothers: A family of protein kinase C substrates. Cell. 1992;71(5):713-716. doi:10.1016/0092-8674(92)90546-O

1347. Reginelli AD, Wang YQ, Sassoon D, Muneoka K. Digit tip regeneration correlates with regions of Msx1 (Hox 7) expression in fetal and newborn mice. Development. 1995;121(4):1065-1076. doi:10.1242/dev.121.4.1065

1348. Han M, Yang X, Farrington JE, Muneoka K. Digit regeneration is regulated by Msx1 and BMP4 in fetal mice. Development. 2003;130(21):5123-5132. doi:10.1242/dev.00710

1349. Johnston APW, Yuzwa SA, Carr MJ, et al. Dedifferentiated Schwann Cell Precursors Secreting Paracrine Factors Are Required for Regeneration of the Mammalian Digit Tip. Cell Stem Cell. 2016;19(4):433-448. doi:10.1016/j.stem.2016.06.002

1350. D'Uva G, Aharonov A, Lauriola M, et al. ERBB2 triggers mammalian heart regeneration by promoting cardiomyocyte dedifferentiation and proliferation. Nat Cell Biol. 2015;17(5):627-638. doi:10.1038/ncb3149

1351. Bassat E, Mutlak YE, Genzelinakh A, et al. The extracellular matrix protein agrin promotes heart regeneration in mice. Nature. 2017;547(7662):179-184. doi:10.1038/nature22978

1352. Strash N, DeLuca S, Janer Carattini GL, Heo SC, Gorsuch R, Bursac N. Human Erbb2-induced Erk activity robustly stimulates cycling and functional remodeling of rat and human cardiomyocytes. Elife. 2021;10. doi:10.7554/eLife.65512

1353. Li C, Sheard PW, Corson ID, Suttie JM. Pedicle and antler development following sectioning of the sensory nerves to the antlerogenic region of red deer (Cervus elaphus). J Exp Zool. 1993;267(2):188-197. doi:10.1002/jez.1402670212

1354. Suttie JM, Fennessy PF. Regrowth of amputated velvet antlers with and without innervation. J Exp Zool. 1985;234(3):359-366. doi:10.1002/jez.1402340305

1355. Wislocki GB, Singer M. The occurrence and function of nerves in the growing antlers of deer. J Comp Neurol. 1946;85(1):1-19. doi:10.1002/cne.900850102

1356. Yun C, Qian W, Wu J, Yuan C, Jiang S, Lv J. Pilose antler peptide promotes osteoblast proliferation, differentiation and mineralization via the insulin signaling pathway. Exp Ther Med. Published online December 5, 2019. doi:10.3892/etm.2019.8286

1357. Novak ML, Koh TJ. Phenotypic Transitions of Macrophages Orchestrate Tissue Repair. Am J Pathol. 2013;183(5):1352-1363. doi:10.1016/j.ajpath.2013.06.034

1358. Caley MP, Martins VLC, O'Toole EA. Metalloproteinases and Wound Healing. Adv Wound Care. 2015;4(4):225-234. doi:10.1089/wound.2014.0581

1359. Desmouliere A, Darby IA, Laverdet B, Bonté F. Fibroblasts and myofibroblasts in wound healing. Clin Cosmet Investig Dermatol. Published online November 2014:301. doi:10.2147/CCID.S50046

1360. Lech M, Anders HJ. Macrophages and fibrosis: How resident and infiltrating mononuclear phagocytes orchestrate all phases of tissue injury and repair. Biochim Biophys Acta - Mol Basis Dis. 2013;1832(7):989-997. doi:10.1016/j.bbadis.2012.12.001

1361. Sindrilaru A, Scharffetter-Kochanek K. Disclosure of the Culprits: Macrophages—Versatile Regulators of Wound Healing. Adv Wound Care. 2013;2(7):357-368. doi:10.1089/wound.2012.0407

1362. Wernig G, Chen SY, Cui L, et al. Unifying mechanism for different fibrotic diseases. Proc Natl Acad Sci. 2017;114(18):4757-4762. doi:10.1073/pnas.1621375114

1363. Desmoulière A, Redard M, Darby I, Gabbiani G. Apoptosis mediates the decrease in cellularity during the transition between granulation tissue and scar. Am J Pathol. 1995;146(1):56-66.

1364. Wynn TA, Ramalingam TR. Mechanisms of fibrosis: therapeutic translation for fibrotic disease. Nat Med. 2012;18(7):1028-1040. doi:10.1038/nm.2807

1365. Volk SW, Iqbal SA, Bayat A. Interactions of the Extracellular Matrix and Progenitor Cells in Cutaneous Wound Healing. Adv Wound Care. 2013;2(6):261-272. doi:10.1089/wound.2012.0417

1366. Klingberg F, Hinz B, White ES. The myofibroblast matrix: implications for tissue repair and fibrosis. J Pathol. 2013;229(2):298-309. doi:10.1002/path.4104

1367. Eming SA, Wynn TA, Martin P. Inflammation and metabolism in tissue repair and regeneration. Science (80-). 2017;356(6342):1026-1030. doi:10.1126/science.aam7928

1368. Moulin V, Tam BYY, Castilloux G, et al. Fetal and adult human skin fibroblasts display intrinsic differences in contractile capacity. J Cell Physiol. 2001;188(2):211-222. doi:10.1002/jcp.1110

1369. Julia MV, Albert A, Morales L, Miro D, Sancho MA, Garcia X. Wound healing in the fetal period: The resistance of the scar to rupture. J Pediatr Surg. 1993;28(11):1458-1462. doi:10.1016/0022-3468(93)90430-S

1370. Lovvorn HN, Cheung DT, Nimni ME, Perelman N, Estes JM, Adzick NS. Relative distribution and crosslinking of collagen distinguish fetal from adult sheep wound repair. J Pediatr Surg. 1999;34(1):218-223. doi:10.1016/S0022-3468(99)90261-0

1371. Aarabi S, Bhatt KA, Shi Y, et al. Mechanical load initiates hypertrophic scar formation through decreased cellular apoptosis. FASEB J. 2007;21(12):3250-3261. doi:10.1096/fj.07-8218com

1372. Gargioli C, Slack JMW. Cell lineage tracing during Xenopus tail regeneration. Development. 2004;131(11):2669-2679. doi:10.1242/dev.01155

1373. Tu S, Johnson SL. Fate Restriction in the Growing and Regenerating Zebrafish Fin. Dev Cell. 2011;20(5):725-732. doi:10.1016/j.devcel.2011.04.013

1374. Echeverri K, Clarke JDW, Tanaka EM. In Vivo Imaging Indicates Muscle Fiber Dedifferentiation Is a Major Contributor to the Regenerating Tail Blastema. Dev Biol. 2001;236(1):151-164. doi:10.1006/dbio.2001.0312

1375. Kumar A, Velloso CP, Imokawa Y, Brockes JP. Plasticity of Retrovirus-Labelled Myotubes in the Newt Limb Regeneration Blastema. Dev Biol. 2000;218(2):125-136. doi:10.1006/dbio.1999.9569

1376. Laube F, Heister M, Scholz C, Borchardt T, Braun T. Re-programming of newt cardiomyocytes is induced by tissue regeneration. J Cell Sci. 2006;119(22):4719-4729. doi:10.1242/jcs.03252

1377. Lo DC, Allen F, Brockes JP. Reversal of muscle differentiation during urodele limb regeneration. Proc Natl Acad Sci. 1993;90(15):7230-7234. doi:10.1073/pnas.90.15.7230

1378. Jopling C, Boue S, Belmonte JCI. Dedifferentiation, transdifferentiation and reprogramming: three routes to regeneration. Nat Rev Mol Cell Biol. 2011;12(2):79-89. doi:10.1038/nrm3043

1379. Kikuchi K, Holdway JE, Werdich AA, et al. Primary contribution to zebrafish heart regeneration by gata4+ cardiomyocytes. Nature. 2010;464(7288):601-605. doi:10.1038/nature08804

1380. Knopf F, Hammond C, Chekuru A, et al. Bone Regenerates via Dedifferentiation of Osteoblasts in the Zebrafish Fin. Dev Cell. 2011;20(5):713-724. doi:10.1016/j.devcel.2011.04.014

1381. Viviano CM, Brockes JP. Is retinoic acid an endogenous ligand during urodele limb regeneration? Int J Dev Biol. 1996;40(4):817-822.

1382. Viviano CM, Horton CE, Maden M, Brockes JP. Synthesis and release of 9- cis retinoic acid by the urodele wound epidermis. Development. 1995;121(11):3753-3762. doi:10.1242/dev.121.11.3753

1383. Scadding SR, Maden M. The effects of local application of retinoic acid on limb development and regeneration in tadpoles of Xenopus laevis. J Embryol Exp Morphol. 1986;91:55-63.

1384. da Silva SM, Gates PB, Brockes JP. The Newt Ortholog of CD59 Is Implicated in Proximodistal Identity during Amphibian Limb Regeneration. Dev Cell. 2002;3(4):547-555. doi:10.1016/S1534-5807(02)00288-5

1385. Lozito TP, Tuan RS. Lizard tail skeletal regeneration combines aspects of fracture healing and blastema-based regeneration. Development. Published online January 1, 2016. doi:10.1242/dev.129585

1386. Guimond JC, Lévesque M, Michaud PL, et al. BMP-2 functions independently of SHH signaling and triggers cell condensation and apoptosis in regenerating axolotl limbs. BMC Dev Biol. 2010;10(1):15. doi:10.1186/1471-213X-10-15

1387. Stewart S, Gomez AW, Armstrong BE, Henner A, Stankunas K. Sequential and Opposing Activities of Wnt and BMP Coordinate Zebrafish Bone Regeneration. Cell Rep. 2014;6(3):482-498. doi:10.1016/j.celrep.2014.01.010

1388. Yokoyama H. Initiation of limb regeneration: The critical steps for regenerative capacity. Dev Growth Differ. 2008;50(1):13-22. doi:10.1111/j.1440-169X.2007.00973.x

1389. Alibardi L. <scp>Msx</scp> 1-2 immunolocalization in the regenerating tail of a lizard but not in the scarring limb suggests its involvement in the process of regeneration. Acta Zool. 2018;99(2):143-150. doi:10.1111/azo.12198

1390. Kumar A, Velloso CP, Imokawa Y, Brockes JP. The Regenerative Plasticity of Isolated Urodele Myofibers and Its Dependence on Msx1. PLoS Biol. 2004;2(8):e218. doi:10.1371/journal.pbio.0020218

1391. Koshiba K, Kuroiwa A, Yamamoto H, Tamura K, Ide H. Expression ofMsx genes in regenerating and developing limbs of axolotl. J Exp Zool. 1998;282(6):703-714. doi:10.1002/(SICI)1097-010X(19981215)282:6<703::AID-JEZ6>3.0.CO;2-P

1392. Akimenko MA, Johnson SL, Westerfield M, Ekker M. Differential induction of four msx homeobox genes during fin development and regeneration in zebrafish. Development. 1995;121(2):347-357. doi:10.1242/dev.121.2.347

1393. Nechiporuk A, Keating MT. A proliferation gradient between proximal and msxb -expressing distal blastema directs zebrafish fin regeneration. Development. 2002;129(11):2607-2617. doi:10.1242/dev.129.11.2607

1394. Thummel R, Bai S, Sarras MP, et al. Inhibition of zebrafish fin regeneration using in vivo electroporation of morpholinos against fgfr1 and msxb. Dev Dyn. 2006;235(2):336-346. doi:10.1002/dvdy.20630

1395. Nacu E, Gromberg E, Oliveira CR, Drechsel D, Tanaka EM. FGF8 and SHH substitute for anterior–posterior tissue interactions to induce limb regeneration. Nature. 2016;533(7603):407-410. doi:10.1038/nature17972

1396. Quint E, Smith A, Avaron F, et al. Bone patterning is altered in the regenerating zebrafish caudal fin after ectopic expression of sonic hedgehog and bmp2b or exposure to cyclopamine. Proc Natl Acad Sci. 2002;99(13):8713-8718. doi:10.1073/pnas.122571799

1397. Zhang J, Jeradi S, Strähle U, Akimenko MA. Laser ablation of the sonic hedgehog-a-expressing cells during fin regeneration affects ray branching morphogenesis. Dev Biol. 2012;365(2):424-433. doi:10.1016/j.ydbio.2012.03.008

1398. Armstrong BE, Henner A, Stewart S, Stankunas K. Shh promotes direct interactions between epidermal cells and osteoblast progenitors to shape regenerated zebrafish bone. Development. 2017;144(7):1165-1176. doi:10.1242/dev.143792

1399. Lim CH, Sun Q, Ratti K, et al. Hedgehog stimulates hair follicle neogenesis by creating inductive dermis during murine skin wound healing. Nat Commun. 2018;9(1):4903. doi:10.1038/s41467-018-07142-9

1400. Guerrero-Juarez CF, Astrowski AA, Murad R, et al. Wound Regeneration Deficit in Rats Correlates with Low Morphogenetic Potential and Distinct Transcriptome Profile of Epidermis. J Invest Dermatol. 2018;138(6):1409-1419. doi:10.1016/j.jid.2017.12.030

1401. Lee HL, Jang JW, Lee SW, et al. Inflammatory cytokines and change of Th1/Th2 balance as prognostic indicators for hepatocellular carcinoma in patients treated with transarterial chemoembolization. Sci Rep. 2019;9(1):3260. doi:10.1038/s41598-019-40078-8

1402. Ewels P, Magnusson M, Lundin S, Käller M. MultiQC: summarize analysis results for multiple tools and samples in a single report. Bioinformatics. 2016;32(19):3047-3048. doi:10.1093/bioinformatics/btw354

1403. Martin M. Cutadapt removes adapter sequences from high-throughput sequencing reads. EMBnet.journal. 2011;17(1):10. doi:10.14806/ej.17.1.200

1404. Dobin A, Davis CA, Schlesinger F, et al. STAR: ultrafast universal RNA-seq aligner. Bioinformatics. 2013;29(1):15-21. doi:10.1093/bioinformatics/bts635

1405. Love MI, Huber W, Anders S. Moderated estimation of fold change and dispersion for RNA-seq data with DESeq2. Genome Biol. 2014;15(12):550. doi:10.1186/s13059-014-0550-8

1406. Falcon S, Gentleman R. Using GOstats to test gene lists for GO term association. Bioinformatics. 2007;23(2):257-258. doi:10.1093/bioinformatics/btl567

1407. Ulgen E, Ozisik O, Sezerman OU. pathfindR: An R Package for Comprehensive Identification of Enriched Pathways in Omics Data Through Active Subnetworks. Front Genet. 2019;10. doi:10.3389/fgene.2019.00858

1408. Xie MH, Aggarwal S, Ho WH, et al. Interleukin (IL)-22, a Novel Human Cytokine That Signals through the Interferon Receptor-related Proteins CRF2–4 and IL-22R. J Biol Chem. 2000;275(40):31335-31339. doi:10.1074/jbc.M005304200

1409. Finch DK, Stolberg VR, Ferguson J, et al. Lung Dendritic Cells Drive Natural Killer Cytotoxicity in Chronic Obstructive Pulmonary Disease via IL-15Rα. Am J Respir Crit Care Med. 2018;198(9):1140-1150. doi:10.1164/rccm.201712-2513OC

1410. Ingley E. Functions of the Lyn tyrosine kinase in health and disease. Cell Commun Signal. 2012;10(1):21. doi:10.1186/1478-811X-10-21

1411. Scapini P, Pereira S, Zhang H, Lowell CA. Multiple roles of Lyn kinase in myeloid cell signaling and function. Immunol Rev. 2009;228(1):23-40. doi:10.1111/j.1600-065X.2008.00758.x

1412. Shimomura Y, Agalliu D, Vonica A, et al. APCDD1 is a novel Wnt inhibitor mutated in hereditary hypotrichosis simplex. Nature. 2010;464(7291):1043-1047. doi:10.1038/nature08875

1413. Satoh K, Kasai M, Ishidao T, et al. Anteriorization of neural fate by inhibitor of β-catenin and T cell factor (ICAT), a negative regulator of Wnt signaling. Proc Natl Acad Sci. 2004;101(21):8017-8021. doi:10.1073/pnas.0401733101

1414. Kobayashi T, Liu X, Wen FQ, et al. Smad3 mediates TGF-β1 induction of VEGF production in lung fibroblasts. Biochem Biophys Res Commun. 2005;327(2):393-398. doi:10.1016/j.bbrc.2004.12.032

1415. Golan N, Adamsky K, Kartvelishvily E, et al. Identification of Tmem10/Opalin as an oligodendrocyte enriched gene using expression profiling combined with genetic cell ablation. Glia. 2008;56(11):1176-1186. doi:10.1002/glia.20688

1416. Yang B, Tang H, Wang N, Gu J, Wang Q. Targeted DNA demethylation of the ZNF334 promoter inhibits colorectal cancer growth. Cell Death Dis. 2023;14(3):210. doi:10.1038/s41419-023-05743-x

1417. Chen J, Zhang J, Hong L, Zhou Y. EGFLAM correlates with cell proliferation, migration, invasion and poor prognosis in glioblastoma. Cancer Biomarkers. 2019;24(3):343-350. doi:10.3233/CBM-181740

1418. Miguez PA. Evidence of biglycan structure-function in bone homeostasis and aging. Connect Tissue Res. 2020;61(1):19-33. doi:10.1080/03008207.2019.1669577

1419. Frey H, Schroeder N, Manon-Jensen T, Iozzo R V., Schaefer L. Biological interplay between proteoglycans and their innate immune receptors in inflammation. FEBS J. 2013;280(10):2165-2179. doi:10.1111/febs.12145

1420. Chen EY, Tan CM, Kou Y, et al. Enrichr: interactive and collaborative HTML5 gene list enrichment analysis tool. BMC Bioinformatics. 2013;14(1):128. doi:10.1186/1471-2105-14-128

1421. Kuleshov M V., Jones MR, Rouillard AD, et al. Enrichr: a comprehensive gene set enrichment analysis web server 2016 update. Nucleic Acids Res. 2016;44(W1):W90-W97. doi:10.1093/nar/gkw377

1422. Xie Z, Bailey A, Kuleshov M V., et al. Gene Set Knowledge Discovery with Enrichr. Curr Protoc. 2021;1(3). doi:10.1002/cpz1.90

1423. Chen C, Xie Y, Stevenson MA, Auron PE, Calderwood SK. Heat Shock Factor 1 Represses Ras-induced Transcriptional Activation of the c-fos Gene. J Biol Chem. 1997;272(43):26803-26806. doi:10.1074/jbc.272.43.26803

1424. Asano Y, Kawase T, Okabe A, et al. IER5 generates a novel hypo-phosphorylated active form of HSF1 and contributes to tumorigenesis. Sci Rep. 2016;6(1):19174. doi:10.1038/srep19174

1425. Kroenke MA, Eto D, Locci M, et al. Bcl6 and Maf Cooperate To Instruct Human Follicular Helper CD4 T Cell Differentiation. J Immunol. 2012;188(8):3734-3744. doi:10.4049/jimmunol.1103246

1426. Apetoh L, Quintana FJ, Pot C, et al. The aryl hydrocarbon receptor interacts with c-Maf to promote the differentiation of type 1 regulatory T cells induced by IL-27. Nat Immunol. 2010;11(9):854-861. doi:10.1038/ni.1912

1427. Chen P, Zuo N, Wu C, et al. MECOM promotes supporting cell proliferation and differentiation in cochlea. J Otol. 2022;17(2):59-66. doi:10.1016/j.joto.2021.11.002

1428. Hillary RF, FitzGerald U. A lifetime of stress: ATF6 in development and homeostasis. J Biomed Sci. 2018;25(1):48. doi:10.1186/s12929-018-0453-1

1429. Maeda M, Ohashi K, Ohashi-Kobayashi A. Further extension of mammalian GATA-6. Dev Growth Differ. 2005;47(9):591-600. doi:10.1111/j.1440-169X.2005.00837.x

1430. Kousteni S. FoxO1, the transcriptional chief of staff of energy metabolism. Bone. 2012;50(2):437-443. doi:10.1016/j.bone.2011.06.034

1431. Jiang Y, Zhang Z. OVOL2: an epithelial lineage determiner with emerging roles in energy homeostasis. Trends Cell Biol. 2023;33(10):824-833. doi:10.1016/j.tcb.2023.05.008

1432. Ying HZ, Chen Q, Zhang WY, et al. PDGF signaling pathway in hepatic fibrosis pathogenesis and therapeutics (Review). Mol Med Rep. 2017;16(6):7879-7889. doi:10.3892/mmr.2017.7641

1433. Liu K, Lin B, Zhao M, et al. The multiple roles for Sox2 in stem cell maintenance and tumorigenesis. Cell Signal. 2013;25(5):1264-1271. doi:10.1016/j.cellsig.2013.02.013

1434. Boudjadi S, Chatterjee B, Sun W, Vemu P, Barr FG. The expression and function of PAX3 in development and disease. Gene. 2018;666:145-157. doi:10.1016/j.gene.2018.04.087

1435. Alenzi FQB. Links between apoptosis, proliferation and the cell cycle. Br J Biomed Sci. 2004;61(2):99-102. doi:10.1080/09674845.2004.11732652

1436. Ryoo HD, Bergmann A. The role of apoptosis-induced proliferation for regeneration and cancer. Cold Spring Harb Perspect Biol. 2012;4(8). doi:10.1101/cshperspect.a008797

1437. Elmore S. Apoptosis: A Review of Programmed Cell Death. Toxicol Pathol. 2007;35:495-516. doi:10.1080/01926230701320337

1438. Chambers I, Silva J, Colby D, et al. Nanog safeguards pluripotency and mediates germline development. Nature. 2007;450(7173):1230-1234. doi:10.1038/nature06403

1439. Miano J. Serum response factor: toggling between disparate programs of gene expression. J Mol Cell Cardiol. 2003;35(6):577-593. doi:10.1016/S0022-2828(03)00110-X

1440. Tomasso A, Koopmans T, Lijnzaad P, Bartscherer K, Seifert AW. An ERK-dependent molecular switch antagonizes fibrosis and promotes regeneration in spiny mice (Acomys). Sci Adv. 2023;9(17). doi:10.1126/sciadv.adf2331

1441. Zimmermann S, Moelling K. Phosphorylation and Regulation of Raf by Akt (Protein Kinase B). Science (80-). 1999;286(5445):1741-1744. doi:10.1126/SCIENCE.286.5445.1741

1442. Hu X, li J, Fu M, Zhao X, Wang W. The JAK/STAT signaling pathway: from bench to clinic. Signal Transduct Target Ther. 2021;6(1):402. doi:10.1038/s41392-021-00791-1

6. Annexes

Annex I

Contained in this annex are the Base Mean values and Fold Changes for the genes involved in the named pathways, as produced by Shishir Biswas, using Gawriluk et al., 2016's data.

PI3K/AKT

	Acomys			Mus		
Gene	**Base Mean**	**Fold Change**	**Significance**	**Base Mean**	**Fold Change**	**Significance**
Akt1	2103	1	Yes	1217	1	Yes
Akt2	1144	No	No	981	No	No
Akt3	522	-0,5	Yes	365	No	No
Angpt1	94	-1	Yes	104	No	No
Angpt2	68	No	No	139	No	No
Angpt4	14	No	No	24	No	No
Artn	11	No	No	7	No	No
Atf2	422	No	No	570	No	No
Atf4	1464	1	Yes	1084	0,5	Yes
Atf6b	462	0,5	Yes	329	0,5	Yes
Bad	162	No	No	175	No	No
Bcl2	17	-1,5	Yes	251	-1	Yes
Bcl2l11	80	1	Yes	252	1	Yes
Bdnf	19	-1,5	Yes	23	No	No
Brca1	259	1	Yes	156	1	Yes
Casp9	79	No	No	207	No	No
Ccnd1	483	No	No	991	0,5	Yes
Ccnd2	818	-0,5	Yes	3024	-1,5	Yes
Ccnd3	696	0,5	Yes	433	1	Yes
Ccne1	103	3	Yes	60	2	Yes
Ccne2	139	No	No	168	No	No
Cd19	10	No	No	5	-1	No
Cdc37	726	No	No	1041	0,5	Yes
Cdk2	210	0,5	Yes	338	No	No
Cdk4	596	1	Yes	694	0,5	Yes
Cdk6	200	1	Yes	1351	No	No
Cdkn1a	364	1	Yes	820	No	No
Cdkn1b	636	-0,5	Yes	911	-0,5	Yes
Chad	268	-2	Yes	861	-2	Yes
Chrm1	6	No	No	12	No	No
Chrm2	29	No	No	11	No	No
Chuk	525	No	No	517	No	No
	Acomys			Mus		

Gene	Base Mean	Fold Change	Significance	Base Mean	Fold Change	Significance
	Acomys			Mus		
Col4a1	4300	1	Yes	4327	2,5	Yes
Col4a2	3642	0,5	Yes	2772	2	Yes
Col4a3	183	-2	Yes	51	-2	Yes
Col4a4	200	-2	Yes	87	-1,5	Yes
Col4a5	326	-1,5	Yes	357	-1,5	Yes
Col4a6	105	-2	Yes	375	-2	Yes
Col6a1	4035	No	No	7346	1,5	Yes
Col6a2	6366	No	No	6955	1,5	Yes
Col6a3	16717	No	No	14683	2,5	Yes
Col6a5	21	-1	No	127	-1,5	No
Col6a6	396	-2,5	Yes	143	-1	No
Col9a1	62	-1,5	Yes	201	-1	Yes
Col9a2	476	-1	Yes	147	-1	Yes
Col9a3	792	-2	Yes	361	-1	Yes
Comp	780	-1	Yes	708	1	Yes
Creb1	394	No	No	802	No	No
Creb3	377	No	No	349	1	Yes
Creb3l1	198	No	No	326	0,5	Yes
Creb3l2	227	No	No	678	No	No
Creb3l3	23	No	No	43	2	Yes
Creb3l4	17	No	No	12	No	No
Crtc2	269	No	No	234	No	No
Csf1	490	No	No	634	No	No
Csf1r	2935	2	Yes	1375	1	Yes
Csf3	20	No	No	2	4	No
Csf3r	637	5	Yes	192	5	Yes
Ddit4	317	1	Yes	240	1	Yes
Efna1	407	No	No	343	No	No
Efna2	16	1	No	18	No	No
Efna3	622	-1	Yes	570	-1	Yes
Efna4	64	No	No	96	No	No
Efna5	88	No	No	607	No	No
Egf	251	-1,5	Yes	74	-1	Yes
Egfr	1701	-0,5	Yes	2368	No	No
Eif4b	2569	No	No	4143	No	No
Eif4e	902	0,5	Yes	805	0,5	Yes
Eif4e2	446	0,5	Yes	656	0,5	Yes
Eif4ebp1	216	2	Yes	210	1,5	Yes
Epha2	613	1	Yes	498	0,5	Yes
Epor	25	1,5	Yes	9	No	No
Erbb2	2087	No	No	1419	No	No
Erbb3	1479	No	No	2179	No	No
Erbb4	43	-2	Yes	69	-4	Yes

Gene	Base Mean	Fold Change	Significance	Base Mean	Fold Change	Significance
		Acomys			Mus	
Fgf10	26	No	No	25	No	No
Fgf17	3	No	No	0	-2,5	No
Fgf18	27	-2	Yes	35	No	No
Fgf2	73	No	No	443	-1,5	Yes
Fgf22	87	No	No	105	1	Yes
Fgf23	12	5	Yes	6	5	Yes
Fgf5	4	No	No	4	No	No
Fgf6	1	No	No	9	No	No
Fgf7	222	No	No	186	No	No
Fgf9	6	-5	Yes	18	No	No
Fgfr1	3153	No	No	1298	No	No
Fgfr2	1922	-1	Yes	2562	-1	Yes
Fgfr3	994	-0,5	Yes	2296	-0,5	Yes
Fgfr4	45	No	No	31	No	No
Flt1	372	0,5	Yes	332	No	No
Flt3	78	2	Yes	72	No	No
Flt3l	54	No	No	111	-1	Yes
Flt4	324	No	No	284	1	Yes
Fn1	16906	1,5	Yes	17394	1	Yes
Foxo3	615	No	No	1521	0,5	Yes
G6pc3	91	No	No	98	No	No
Gdnf	6	No	No	51	No	No
Ghr	984	-1	Yes	1042	-1	Yes
Gnb1	1194	0,5	Yes	1640	0,5	Yes
Gnb2	972	1	Yes	1591	1	Yes
Gnb3	1	-3	No	8	-1	No
Gnb5	73	No	No	108	1	Yes
Gng10	103	1	Yes	208	1	Yes
Gng11	298	-0,5	Yes	113	1,5	Yes
Gng12	125	-0,5	Yes	1768	-0,5	Yes
Gng13	0	-2	No	6	-2	No
Gng2	31	No	No	255	No	No
Gng3	10	2	No	16	No	No
Gng4	12	1	No	27	No	No
Gng8	0	2	No	10	No	No
Gngt2	29	1	Yes	47	No	No
Grb2	442	0,5	Yes	508	No	No
Gsk3b	832	No	No	2407	No	No
Gys1	812	-0,5	Yes	468	-1	Yes
Gys2	51	-2,5	Yes	1	-3,5	No
Hgf	183	No	No	102	No	No
Hras	911	No	No	674	No	No
Hsp90aa1	2823	1	Yes	1003	0,5	Yes

Gene	Base Mean	Fold Change	Significance	Base Mean	Fold Change	Significance
Igf1	427	No	No	1370	1	Yes
Igf1r	967	No	No	1667	No	No
Igf2	175	-2	Yes	481	No	No
Ikbkb	647	0,5	Yes	1017	No	No
Ikbkg	269	No	No	558	No	No
Il2ra	8	3	No	37	2	Yes
Il2rb	31	No	No	67	No	No
Il2rg	62	3,5	Yes	116	2	Yes
Il3ra	171	1,5	Yes	56	1,5	Yes
Il4ra	1016	1,5	Yes	1253	2,5	Yes
Il6	67	4	Yes	7	5	Yes
Il6ra	478	No	No	1345	No	No
Il7	70	No	No	57	No	No
Il7r	129	1	Yes	142	No	No
Insr	1010	No	No	1122	-0,5	Yes
Irs1	1266	-2	Yes	1031	-1	Yes
Itga10	225	-1	Yes	155	-1	Yes
Itga11	152	-2,5	Yes	236	2	Yes
Itga2	377	0,5	Yes	376	No	No
Itga2b	4	No	No	82	1	Yes
Itga3	806	1,5	Yes	696	No	No
Itga4	349	1	Yes	354	1	Yes
Itga5	1111	2,5	Yes	594	2	Yes
Itga6	2833	0,5	Yes	4245	0,5	Yes
Itga7	851	No	No	354	No	No
Itga9	471	No	No	368	No	No
Itgav	1739	1	Yes	1988	0,5	Yes
Itgb1	4796	1	Yes	4208	1	Yes
Itgb3	95	1	Yes	262	2	Yes
Itgb4	5730	1	Yes	3077	No	No
Itgb5	1432	No	No	1242	1	Yes
Itgb6	292	-0,5	Yes	242	-0,5	Yes
Itgb7	208	1	Yes	126	No	No
Itgb8	251	-0,5	Yes	359	No	No
Jak1	3928	0,5	Yes	2793	No	No
Jak2	4224	1,5	Yes	997	0,5	Yes
Jak3	161	2	Yes	147	1,5	Yes
Kdr	821	-0,5	Yes	509	1	Yes
Kit	400	No	No	202	No	No
Kitl	649	No	No	501	No	No
Kras	188	No	No	648	No	No
Lama1	141	5	Yes	38	No	No
Lama2	3500	-1,5	Yes	1531	-0,5	Yes
		Acomys			**Mus**	

Gene	Base Mean	Fold Change	Significance	Base Mean	Fold Change	Significance
Lamb1	2394	No	No	1343	2	Yes
Lamb2	3314	-0,5	Yes	1441	No	No
Lamb3	1579	1	Yes	1574	1	Yes
Lamc2	1736	3	Yes	2630	3	Yes
Lamc3	1296	No	No	137	-1,5	Yes
Lpar1	279	0,5	Yes	389	No	No
Lpar2	18	No	No	154	No	No
Lpar3	64	-2	Yes	72	-1	Yes
Lpar4	96	-1	Yes	69	No	No
Lpar5	72	1	Yes	70	No	No
Lpar6	320	-0,5	Yes	319	No	No
Magi1	182	-0,5	Yes	471	No	No
Magi2	95	-2	Yes	86	-1	Yes
Map2k1	1133	1	Yes	535	1	Yes
Map2k2	692	No	No	677	1	Yes
Mapk1	958	No	No	1666	No	No
Mapk3	738	No	No	769	No	No
Mcl1	943	1	Yes	2103	0,5	Yes
Mdm2	1301	0,5	Yes	758	No	No
Met	730	No	No	717	No	No
Mlst8	115	No	No	198	No	No
Mtcp1	26	No	No	192	-0,5	Yes
Mtor	1644	No	No	1115	No	No
Myb	32	1,5	Yes	39	No	No
Myc	344	1	Yes	332	No	No
Nfkb1	52	1	Yes	1281	0,5	Yes
Ngf	51	2	Yes	47	1	Yes
Ngfr	74	No	No	153	No	No
Nos3	257	-0,5	Yes	114	1,5	Yes
Nr4a1	289	No	No	137	No	No
Nras	481	0,5	Yes	1333	0,5	Yes
Nrtn	43	No	No	93	2	Yes
Ntf3	46	-1	Yes	41	-1,5	Yes
Ntf5	17	No	No	24	No	No
Ntrk1	6	5	Yes	8	No	No
Ntrk2	525	-1	Yes	616	-2	Yes
Osm		5	Yes	20	3	Yes
Osmr	1020	1	Yes	906	0,5	Yes
Pck1	187	-2,5	Yes	47	-2	Yes
Pck2	173	1	Yes	171	1	Yes
Pdgfa	146	No	No	195	No	No
Pdgfb	82	No	No	285	0,5	Yes
Pdgfc	43	No	No	203	No	No
	Acomys			**Mus**		

Gene	Base Mean	Fold Change	Significance	Base Mean	Fold Change	Significance
Pdpk1	559	No	No	1505	No	No
Pgf	26	-1	Yes	12	No	No
Phlpp1	466	No	No	360	No	No
Phlpp2	351	-0,5	Yes	196	No	No
Pik3ca	1135	No	No	1048	No	No
Pik3cb	758	No	No	787	No	No
Pik3cd	467	2	Yes	274	1	Yes
Pik3cg	383	2,5	Yes	243	1	Yes
Pik3r1	1830	-1	Yes	2119	-1	Yes
Pik3r2	695	No	No	747	No	No
Pik3r5	311	2,5	Yes	159	2	Yes
Pik3r6	84	No	No	87	No	No
Pkn1	759	1	Yes	473	1	Yes
Pkn2	1110	No	No	1132	No	No
Pkn3	129	No	No	155	1	Yes
Ppp2ca	1174	No	No	1843	0,5	Yes
Ppp2cb	902	0,5	Yes	333	No	No
Ppp2r1a	1949	0,5	Yes	1429	0,5	Yes
Ppp2r1b	792	1	Yes	518	1	Yes
Ppp2r2a	892	No	No	826	No	No
Ppp2r2b	50	-3	Yes	7	-1,5	Yes
Ppp2r2c	32	1,5	Yes	105	No	No
Ppp2r2d	363	0,5	Yes	358	No	No
Ppp2r3a	714	No	No	2895	-1	Yes
Ppp2r3c	334	No	No	231	No	No
Ppp2r5b	244	-0,5	Yes	224	No	No
Ppp2r5c	991	No	No	1222	No	No
Ppp2r5d	580	No	No	432	No	No
Ppp2r5e	363	No	No	635	No	No
Prkaa1	411	No	No	682	-0,5	Yes
Prkaa2	174	-1,5	Yes	349	-2	Yes
Prkca	244	-0,5	Yes	366	-1	Yes
Pspn	5	No	No	2	No	No
Pten	999	No	No	3296	No	No
Ptk2	1251	No	No	768	No	No
Rac1	606	0,5	Yes	1918	0,5	Yes
Raf1	2031	No	No	984	No	No
Rbl2	862	-0,5	Yes	741	-0,5	Yes
Rela	552	No	No	450	No	No
Reln	710	-1,5	Yes	467	-0,5	Yes
Ret	33	No	No	69	No	No
Rheb	725	No	No	647	No	No
Rps6	8463	No	No	2976	No	No
	Acomys			**Mus**		

Gene	Base Mean	Fold Change	Significance	Base Mean	Fold Change	Significance
Rxra	990	No	No	2745	0,5	Yes
Sgk1	1501	No	No	1075	0,5	Yes
Sgk3	350	No	No	709	-0,5	Yes
Sos1	774	-0,5	Yes	811	-0,5	Yes
Sos2	1238	No	No	708	No	No
Syk	280	2	Yes	518	1,5	Yes
Tek	181	-0,5	Yes	224	1	Yes
Tgfa	100	0,5	Yes	453	0,5	Yes
Thbs1	14814	1	Yes	4959	No	No
Thbs2	2383	1,5	Yes	2211	1,5	Yes
Thbs3	609	-1,5	Yes	424	1	Yes
Thbs4	1665	No	No	1355	2	Yes
Them4	22	1	No	81	No	No
Tlr2	42	1,5	Yes	123	2	Yes
Tlr4	552	2	Yes	252	1	Yes
Tnc	8555	4	Yes	14335	4	Yes
Tnn	117	-0,5	Yes	631	5	Yes
Tnr	12	-1	Yes	10	-0,5	Yes
Trp53	1062	1	Yes	388	No	No
Tsc1	569	-0,5	Yes	574	-0,5	Yes
Tsc2	1166	-0,5	Yes	766	No	No
Vegfa	473	No	No	515	1	Yes
Vegfb	90	-0,5	Yes	81	-1	Yes
Vegfc	131	No	No	46	No	No
Vegfd	78	-1	Yes	116	No	No
Vtn	56	-1	Yes	31	-1	No
Vwf	1213	0,5	Yes	572	0,5	Yes
Ywhab	981	No	No	1812	0,5	Yes
Ywhae	1377	No	No	1838	No	No
Ywhag	673	1	Yes	1384	1	Yes
Ywhah	513	1	Yes	570	0,5	Yes
Ywhaq	1645	0,5	Yes	665	0,5	Yes
Ywhaz	2291	1	Yes	5197	0,5	Yes

MAPK/ERK

	Acomys			Mus		
Gene	**Base Mean**	**Fold Change**	**Significance**	**Base Mean**	**Fold Change**	**Significance**
AKT1	2103	1	Yes	1217	1	Yes
AKT2	1144	No	No	981	No	No
AKT3	522	-0,5	Yes	365	No	No
ANGPT1	94	-1	Yes	104	No	No
ANGPT2	68	No	No	139	No	No
ANGPT4	14	No	No	24	No	No
ARAF	469	No	No	955	No	No
ARRB2	341	1	Yes	267	1	Yes
ARTN	11	No	No	7	No	No
ATF2	422	No	No	570	No	No
ATF4	1464	1	Yes	1084	0,5	Yes
BDNF	19	-1,5	Yes	23	No	No
BRAF	711	No	No	1080	No	No
CACNA1A	69	-1	Yes	144	-1	Yes
CACNA1B	75	-2	Yes	8	No	No
CACNA1C	249	No	No	346	1	Yes
CACNA1D	82	-1,5	Yes	188	No	No
CACNA1G	596	-1	Yes	471	0,5	Yes
CACNA1H	36	No	No	18	No	No
CACNA1I	4	5	Yes	1	3	No
CACNA1S	1181	-3	No	829	-2,5	Yes
CACNA2D1	799	-2	Yes	810	-1,5	Yes
CACNA2D2	28	-1	Yes	28	-1	No
CACNA2D3	9	-4	Yes	31	No	No
CACNA2D4	24	No	No	23	No	No
CACNB1	181	-2	Yes	230	-1,5	Yes
CACNB2	166	No	No	87	No	No
CACNB3	62	No	No	267	No	No
CACNB4	54	-1	Yes	72	-1	Yes
CACNG1	113	-0,5	Yes	76	No	No
CACNG2	1	No	No	2	No	No
CACNG4	7	No	No	17	-2	Yes
CACNG6	18	-2	Yes	28	No	No
CACNG7	2	No	No	15	No	No
CASP3	337	1	Yes	184	1	Yes
CD14	264	2	Yes	184	4	Yes
CDC25B	463	2,5	Yes	401	No	No
CDC42	1582	No	No	2928	0,5	Yes
CHUK	525	No	No	517	No	No
CRK	707	No	No	1339	0,5	Yes
CRKL	337	No	No	595	No	No

Gene	Acomys			Mus		
	Base Mean	Fold Change	Significance	Base Mean	Fold Change	Significance
DAXX	356	0,5	Yes	231	No	No
DDIT3	134	1,5	Yes	142	No	No
DUSP10	174	-1,5	Yes	90	-1,5	Yes
DUSP2	37	4	Yes	20	2,5	Yes
DUSP3	139	No	No	593	No	No
DUSP4	119	0,5	Yes	42	No	No
DUSP5	287	1	Yes	199	1,5	Yes
DUSP6	1088	1	Yes	321	0,5	Yes
DUSP7	1314	1	Yes	834	1	Yes
DUSP8	83	-1	Yes	73	No	No
DUSP9	5	2	No	15	2	No
ECSIT	346	No	No	234	No	No
EFNA1	407	No	No	343	No	No
EFNA2	16	No	No	18	No	No
EFNA3	622	-1	Yes	570	-1	Yes
EFNA4	64	No	No	96	No	No
EFNA5	88	No	No	607	No	No
EGF	251	-1,5	Yes	74	-1	Yes
EGFR	1701	-0,5	Yes	2368	No	No
ELK1	227	No	No	181	No	No
ELK4	532	No	No	1926	No	No
EPHA2	613	1	Yes	498	0,5	Yes
ERBB2	2087	No	No	1419	No	No
ERBB3	1479	No	No	2179	No	No
ERBB4	43	-2	Yes	69	-4	Yes
FAS	142	No	No	96	No	No
FGF1	31	-2	Yes	196	-2	Yes
FGF10	26	No	No	25	No	No
FGF17	3	No	No	0	-2,5	No
FGF18	27	-2	Yes	35	No	No
FGF2	73	No	No	443	-1,5	Yes
FGF22	87	No	No	105	1	Yes
FGF23	12	5	Yes	6	5	Yes
FGF5	4	No	No	4	No	No
FGF6	1	No	No	9	No	No
FGF7	222	No	No	186	No	No
FGF9	6	5	Yes	18	No	No
FGFR1	3153	No	No	1298	No	No
FGFR2	1922	-1	Yes	2562	-1	Yes
FGFR3	994	-0,5	Yes	2296	-0,5	Yes
FGFR4	45	No	No	31	No	No
FLNA	12886	1,5	Yes	8644	1,5	Yes
FLNB	4134	1	Yes	3427	0,5	Yes

Gene	Acomys			Mus		
	Base Mean	Fold Change	Significance	Base Mean	Fold Change	Significance
FLT4	324	No	No	284	1	Yes
FOS	1668	No	No	479	No	No
GADD45A	213	0,5	Yes	174	No	No
GADD45B	359	1	Yes	250	1	Yes
GADD45G	90	No	No	67	1,5	Yes
GDNF	6	No	No	51	No	No
GNA12	799	0,5	Yes	614	1	Yes
GNG12	125	-0,5	Yes	1768	-0,5	Yes
GRB2	442	0,5	Yes	508	No	No
HGF	183	No	No	102	No	No
HRAS	911	No	No	674	No	No
HSPA8	13438	No	No	4002	No	No
HSPB1	667	-1	Yes	998	-0,5	Yes
IGF1	427	No	No	1370	1	Yes
IGF1R	967	No	No	1667	No	No
IGF2	175	-2	Yes	481	No	No
IKBKB	647	0,5	Yes	1017	No	No
IKBKG	269	No	No	558	No	No
IL1A	120	2,5	Yes	158	No	No
IL1B	2686	5	Yes	273	5	Yes
IL1RAP	613	0,5	Yes	658	No	No
INSR	1010	No	No	1122	-0,5	Yes
IRAK1	375	No	No	651	No	No
IRAK4	169	No	No	250	1	Yes
JUN	1159	No	No	809	1	Yes
JUND	297	-0,5	No	773	0,5	No
KDR	821	-0,5	Yes	509	1	Yes
KIT	400	No	No	202	No	No
KRAS	188	No	No	648	No	No
MAP2K1	1133	1	Yes	535	1	Yes
MAP2K2	692	No	No	677	1	Yes
MAP2K3	778	No	No	881	0,5	Yes
MAP2K4	833	No	No	1304	No	No
MAP2K5	206	No	No	204	No	No
MAP2K6	176	-0,5	Yes	137	No	No
MAP3K1	1815	-0,5	Yes	1877	-0,5	Yes
MAP3K10	111	No	No	117	No	No
MAP3K11	748	0,5	Yes	430	0,5	Yes
MAP3K12	154	No	No	378	No	No
MAP3K13	27	No	No	40	No	No
MAP3K14	190	No	No	234	No	No
MAP3K2	456	No	No	1143	No	No
MAP3K21	32	-1,5	Yes	12	No	No

Gene	Acomys			Mus		
	Base Mean	Fold Change	Significance	Base Mean	Fold Change	Significance
MAP3K6	715	0,5	Yes	370	1	Yes
MAP3K7	821	No	No	977	No	No
MAP3K8	270	0,5	Yes	351	No	No
MAP3K9	258	0,5	Yes	656	1	Yes
MAP4K2	205	No	No	357	No	No
MAP4K3	1353	0,5	Yes	1085	No	No
MAPK1	958	No	No	1666	No	No
MAPK10	31	No	No	9	No	No
MAPK11	10	No	No	51	No	No
MAPK12	57	-2,5	Yes	139	No	No
MAPK13	1194	No	No	1112	1	Yes
MAPK14	524	1	Yes	1009	0,5	Yes
MAPK3	738	No	No	769	No	No
MAPK7	148	0,5	Yes	168	No	No
MAPK8	351	No	No	599	No	No
MAPK8IP1	564	No	No	135	-1	Yes
MAPK8IP2	24	-1,5	Yes	2	-4	No
MAPK8IP3	569	No	No	845	No	No
MAPK9	416	No	No	423	No	No
MAPKAPK2	747	No	No	1097	1	Yes
MAPKAPK3	680	No	No	835	No	No
MAX	231	No	No	622	No	No
MECOM	331	-1	Yes	274	No	No
MEF2C	1543	-2	Yes	1506	-1	Yes
MET	730	No	No	717	No	No
MKNK1	323	0,5	Yes	296	No	No
MKNK2	793	0,5	Yes	1328	1	Yes
MRAS	80	No	No	180	No	No
MYC	344	1	Yes	332	No	No
MYD88	610	1	Yes	355	1	Yes
NFATC1	472	-1	Yes	668	No	No
NFATC3	894	No	No	1247	No	No
NFKB1	52	1	Yes	1281	0,5	Yes
NFKB2	541	1,5	Yes	387	0,5	Yes
NGF	51	2	Yes	47	1	Yes
NGFR	74	No	No	153	No	No
NLK	314	No	No	311	No	No
NR4A1	289	No	No	137	No	No
NRAS	481	0,5	Yes	1333	0,5	Yes
NRTN	43	No	No	93	2	Yes
NTF3	46	-1	Yes	41	-1,5	Yes
NTRK1	6	5	Yes	8	No	No
NTRK2	525	-1	Yes	616	-2	Yes

Gene	Acomys			Mus		
	Base Mean	Fold Change	Significance	Base Mean	Fold Change	Significance
PDGFB	82	No	No	285	0,5	Yes
PDGFC	43	No	No	203	No	No
PDGFD	96	-1	Yes	34	No	No
PDGFRA	2861	0,5	Yes	1741	1	Yes
PDGFRB	2062	No	No	1068	0,5	Yes
PGF	26	-1	Yes	12	No	No
PLA2G4A	471	No	No	357	No	No
PLA2G4C	121	No	No	16	No	No
PLA2G4D	617	-1	Yes	111	5	Yes
PLA2G4E	616	2	Yes	408	2,5	Yes
PLA2G4F	1305	3,5	No	937	0,5	Yes
PPM1A	1933	-0,5	Yes	1406	No	No
PPM1B	549	No	No	778	No	No
PPP3CA	1442	-0,5	Yes	1749	No	No
PPP3CB	718	No	No	814	No	No
PPP3CC	364	-0,5	Yes	136	-0,5	Yes
PPP3R1	619	No	No	946	No	No
PPP5C	448	No	No	287	No	No
PRKACA	971	No	No	571	No	No
PRKACB	782	No	No	958	No	No
PRKCA	244	-0,5	Yes	366	-1	Yes
PRKCB	377	1,5	Yes	260	No	No
PRKCG	6	No	No	27	No	No
PSPN	5	No	No	2	No	No
PTPN5	5	No	No	41	No	No
PTPN7	28	No	No	85	No	No
PTPRR	8	No	No	10	No	No
RAC1	606	0,5	Yes	1918	0,5	Yes
RAC2	183	3	Yes	113	2	Yes
RAC3	81	No	No	79	No	No
RAF1	2031	No	No	984	No	No
RAPGEF2	1236	-0,5	Yes	770	-0,5	Yes
RASA1	1574	0,5	Yes	1175	No	No
RASA2	576	No	No	631	No	No
RASGRF2	106	-1,5	Yes	110	No	No
RASGRP1	187	-1	Yes	503	-0,5	Yes
RASGRP2	53	No	No	58	No	No
RASGRP3	148	-1	Yes	140	No	No
RELA	552	No	No	450	No	No
RELB	194	1	Yes	187	No	No
RET	33	No	No	69	No	No
RPS6KA1	647	1	Yes	333	No	No
RPS6KA2	391	-0,5	Yes	164	-1	Yes

Gene	Acomys			Mus		
	Base Mean	Fold Change	Significance	Base Mean	Fold Change	Significance
RPS6KA3	799	No	No	1670	No	No
RPS6KA4	1251	1,5	Yes	616	1,5	Yes
RPS6KA5	134	-0,5	Yes	307	-0,5	Yes
RPS6KA6	542	No	No	561	No	No
RRAS	232	-0,5	Yes	128	No	No
RRAS2	93	No	No	188	No	No
SOS1	774	-0,5	Yes	811	-0,5	Yes
SOS2	1238	No	No	708	No	No
SRF	285	0,5	Yes	279	0,5	Yes
STK3	383	-0,5	Yes	272	No	No
STK4	508	No	No	946	No	No
STMN1	693	No	No	213	No	No
TAB1	150	No	No	219	No	No
TAB2	1107	No	No	1741	No	No
TAOK1	2398	No	No	5395	No	No
TAOK2	778	No	No	1104	No	No
TAOK3	451	0,5	Yes	308	No	No
TEK	181	-0,5	Yes	224	1	Yes
TGFA	100	0,5	Yes	453	0,5	Yes
TGFB1	320	2	Yes	292	1	Yes
TGFB2	262	-1,5	Yes	411	-0,5	Yes
TGFB3	689	0,5	Yes	786	1	Yes
TGFBR1	376	0,5	Yes	798	1	Yes
TGFBR2	1700	No	No	2145	No	No
TNF	28	1,5	Yes	48	No	No
TNFRSF1A	1410	0,5	Yes	1102	0,5	Yes
TRADD	144	1	Yes	118	1,5	Yes
TRAF2	239	No	No	240	No	No
TRAF6	518	No	No	1064	0,5	Yes
Trp53	1062	1	Yes	388	No	No
VEGFA	473	No	No	515	1	Yes
VEGFB	90	-0,5	Yes	81	-1	Yes
VEGFC	131	No	No	46	No	No
VEGFD	78	-1	Yes	116	No	No

ERBB

	Acomys			Mus		
Gene	**Base Mean**	**Fold Change**	**Significance**	**Base Mean**	**Fold Change**	**Significance**
Abl1	935	No	No	1104	No	No
Abl2	585	0,5	Yes	735	No	No
Akt1	2103	1	Yes	1217	1	Yes
Akt2	1144	No	No	981	No	No
Akt3	522	-0,5	Yes	365	No	No
ARAF	469	No	No	955	No	No
Bad	162	No	No	175	No	No
BRAF	711	No	No	1080	No	No
Btc	266	-1	Yes	123	-2	Yes
Camk2a	47	-2	Yes	103	-2	Yes
Camk2b	310	-1,5	Yes	203	-1,5	Yes
Camk2d	1069	No	No	1315	No	No
Camk2g	319	No	No	504	No	No
Cbl	502	1	Yes	1883	0,5	Yes
Cblb	380	0,5	Yes	859	No	No
Cdkn1a	364	1	Yes	820	No	No
Cdkn1b	636	-0,5	Yes	911	-0,5	Yes
CRK	707	No	No	1339	0,5	Yes
CRKL	337	No	No	595	No	No
Egf	251	-1,5	Yes	74	-1	Yes
Egfr	1701	-0,5	Yes	2368	No	No
Eif4ebp1	216	2	Yes	210	1,5	Yes
ELK1	227	No	No	181	No	No
Erbb2	2087	No	No	1419	No	No
Erbb3	1479	No	No	2179	No	No
ERBB4	43	-2	Yes	69	-4	Yes
Gab1	780	0,5	Yes	988	No	No
Grb2	442	0,5	Yes	508	No	No
Gsk3b	832	No	No	2407	No	No
Hbegf	184	3,5	Yes	189	2	Yes
Hras	911	No	No	674	No	No
JUN	1159	No	No	809	1	Yes
Kras	188	No	No	648	No	No
Map2k1	1133	1	Yes	535	1	Yes
Map2k2	692	No	No	677	1	Yes
MAP2K4	833	No	No	1304	No	No
Mapk1	958	No	No	1666	No	No
MAPK10	31	No	No	9	No	No
Mapk3	738	No	No	769	No	No
MAPK8	351	No	No	599	No	No
MAPK9	416	No	No	423	No	No

Gene	Acomys			Mus		
	Base Mean	Fold Change	Significance	Base Mean	Fold Change	Significance
Nck2	246	-0,5	Yes	235	0,5	Yes
Nras	481	0,5	Yes	1333	0,5	Yes
Nrg1	172	2,5	Yes	174	2,5	Yes
Nrg2	31	-1,5	Yes	36	-1,5	Yes
Nrg4	56	No	No	144	No	No
PAK1	276	0,5	Yes	580	No	No
PAK2	1438	0,5	Yes	1252	No	No
Pak3	195	-2	Yes	736	-2	Yes
Pak4	363	No	No	327	No	No
Pak6	398	1	Yes	561	0,5	Yes
Pik3ca	1135	No	No	1048	No	No
Pik3cb	758	No	No	787	No	No
Pik3cd	467	2	Yes	274	1	Yes
Pik3r1	1830	-1	Yes	2119	-1	Yes
Pik3r2	695	No	No	747	No	No
Plcg1	1653	No	No	1548	No	No
Plcg2	701	No	No	433	No	No
Prkca	244	-0,5	Yes	366	-1	Yes
PRKCB	377	1,5	Yes	260	No	No
PRKCG	6	No	No	27	No	No
Ptk2	1251	No	No	768	No	No
Raf1	2031	No	No	984	No	No
Rps6kb1	508	No	No	878	No	No
Rps6kb2	785	0,5	Yes	448	0,5	Yes
Shc1	562	0,5	Yes	731	1	Yes
Shc2	79	No	No	123	1	Yes
Shc3	5	-1	No	10	No	No
Shc4	86	-1	Yes	45	-1	Yes
Sos1	774	-0,5	Yes	811	-0,5	Yes
Sos2	1238	No	No	708	No	No
Src	541	1	Yes	376	1	Yes
Stat5a	309	1	Yes	397	No	No
Stat5b	697	0,5	Yes	582	No	No
Tgfa	100	0,5	Yes	453	0,5	Yes

JAK/STAT

	Acomys			Mus		
Gene	**Base Mean**	**Fold Change**	**Significance**	**Base Mean**	**Fold Change**	**Significance**
Akt1	2103	1	Yes	1217	1	Yes
Akt2	1144	No	No	981	No	No
Akt3	522	-0,5	Yes	365	No	No
Aox1	62	-3	No	394	-1	Yes
Aox2	40	No	No	17	No	No
Aox3	325	-2	Yes	24	1,5	No
Aox4	2679	-0,5	Yes	1278	2,5	Yes
Bcl2	17	-1,5	Yes	251	-1	Yes
Ccnd1	483	No	No	991	0,5	Yes
Ccnd2	818	-0,5	Yes	3024	-1,5	Yes
Ccnd3	696	0,5	Yes	433	1	Yes
Cdkn1a	364	1	Yes	820	No	No
Cish	60	1	Yes	313	No	No
Clcf1	153	3,5	Yes	142	1	Yes
Cntf	35	No	No	12	No	No
Cntfr	70	-3	No	42	No	No
Crebbp	3261	No	No	3362	-0,5	Yes
Crlf2	116	2	Yes	65	1,5	Yes
Csf2ra	453	3	Yes	165	No	No
Csf3	20	No	No	2	4	No
Csf3r	637	5	Yes	192	5	Yes
Ctf1	53	No	No	27	-1	No
Ctf2	2	-1	No	6	-1,5	No
Egf	251	-1,5	Yes	74	-1	Yes
Egfr	1701	-0,5	Yes	2368	No	No
Epor	25	1,5	Yes	9	No	No
Fhl1	2689	-2	Yes	2563	-2	Yes
Gfap	103	2	Yes	37	-2,5	Yes
Ghr	984	-1	Yes	1042	-1	Yes
Grb2	442	0,5	Yes	508	No	No
Hras	911	No	No	674	No	No
Ifnar1	400	1	Yes	789	1	Yes
Ifnar2	321	1	Yes	256	1	Yes
Ifne	0	No	No	0	No	No
Ifngr1	1554	1	Yes	917	0,5	Yes
Ifngr2	393	1,5	Yes	405	0,5	Yes
Ifnlr1	107	No	No	235	-0,5	Yes
Il10ra	143	2	Yes	198	2	Yes
Il10rb	281	0,5	Yes	338	0,5	Yes
Il11	25	5	Yes	23	2,5	Yes
Il12a	5	No	No	3	1	No

Gene	Acomys			Mus		
	Base Mean	Fold Change	Significance	Base Mean	Fold Change	Significance
Il15	97	No	No	69	No	No
Il15ra	36	-1	Yes	434	-0,5	Yes
Il20ra	122	No	No	319	-1	Yes
Il20rb	984	-0,5	Yes	1293	-1	Yes
Il21r	30	5	Yes	17	5	Yes
Il22ra1	1173	-1	Yes	559	No	No
Il22ra2	6	No	No	32	-1,5	Yes
Il23a	8	1	No	5	No	No
Il23r	19	-1	No	16	1,5	No
Il27ra	10	No	No	25	No	No
Il2ra	8	3	No	37	2	Yes
Il2rb	31	No	No	67	No	No
Il2rg	62	3,5	Yes	116	2	Yes
Il3ra	171	1,5	Yes	56	1,5	Yes
Il4ra	1016	1,5	Yes	1253	2,5	Yes
Il5	2	-4,5	No	4	-2	No
Il6	67	4	Yes	7	5	Yes
Il6ra	478	No	No	1345	No	No
Il6st	4079	No	No	5419	No	No
Il7	70	No	No	57	No	No
Il7r	129	1	Yes	142	No	No
Il9r	8	No	No	8	No	No
Irf9	249	0,5	Yes	459	1	Yes
Jak1	3928	0,5	Yes	2793	No	No
Jak2	4224	1,5	Yes	997	0,5	Yes
Jak3	161	2	Yes	147	1,5	Yes
Lep	37	-5	Yes	38	-1,5	Yes
Lif	38	2,5	Yes	32	1	No
Lifr	966	-1	Yes	1588	-0,5	Yes
Mcl1	943	1	Yes	2103	0,5	Yes
Mpl	4	-1	No	0	-1	No
Mtor	1644	No	No	1115	No	No
Myc	344	1	Yes	332	No	No
Osm		5	Yes	20	3	Yes
Osmr	1020	1	Yes	906	0,5	Yes
Pdgfa	146	No	No	195	No	No
Pdgfb	82	No	No	285	0,5	Yes
Pdgfra	2861	0,5	Yes	1741	1	Yes
Pdgfrb	2062	No	No	1068	0,5	Yes
Pias1	528	-0,5	Yes	586	No	No
Pias2	380	-0,5	Yes	391	-0,5	Yes
Pias3	376	No	No	472	No	No
Pias4	197	No	No	230	No	No

	Acomys			Mus		
Gene	**Base Mean**	**Fold Change**	**Significance**	**Base Mean**	**Fold Change**	**Significance**
Pik3r1	1830	-1	Yes	2119	-1	Yes
Pik3r2	695	No	No	747	No	No
Pim1	363	2	Yes	1038	0,5	Yes
Ptpn11	1012	No	No	1600	0,5	Yes
Ptpn6	638	1,5	Yes	408	No	No
Raf1	2031	No	No	984	No	No
Socs1	40	1	Yes	59	No	No
Socs3	529	4	Yes	421	1,5	Yes
Socs4	168	No	No	651	No	No
Socs5	438	0,5	Yes	390	0,5	Yes
Socs6	474	No	No	662	No	No
Socs7	160	-0,5	Yes	466	No	No
Sos1	774	-0,5	Yes	811	-0,5	Yes
Sos2	1238	No	No	708	No	No
Stam	728	0,5	Yes	466	No	No
Stam2	503	No	No	741	0,5	Yes
Stat1	563	No	No	808	1,5	Yes
Stat2	361	0,5	Yes	491	0,5	Yes
Stat3	2722	1	Yes	2468	1	Yes
Stat4	54	1,5	Yes	16	3	Yes
Stat5a	309	1	Yes	397	No	No
Stat5b	697	0,5	Yes	582	No	No
Stat6	1405	0,5	Yes	1208	0,5	Yes
Thpo	28	-1	No	4	-2	No
Tyk2	838	No	No	476	No	No

NF-κB

	Acomys			Mus		
Gene	**Base Mean**	**Fold Change**	**Significance**	**Base Mean**	**Fold Change**	**Significance**
Atm	1586	No	No	663	No	No
Bcl10	385	No	No	361	0,5	Yes
Bcl2	17	-1,5	Yes	251	-1	Yes
Bcl2l1		No	No	465	No	No
Birc3	842	1,5	Yes	514	0,5	Yes
Blnk	170	No	No	200	No	No
Btk	187	2	Yes	61	No	No
Card10	316	0,5	Yes	243	No	No
Card11	25	No	No	33	No	No
Card14	541	No	No	528	-0,5	Yes
Ccl4	99	5	Yes	8	5	Yes
CD14	264	2	Yes	184	4	Yes
Cd40	84	1	Yes	37	2	Yes
Cd40lg	5	1	No	2	No	No
Cflar	1122	0,5	Yes	1223	No	No
Chuk	525	No	No	517	No	No
Csnk2a2	557	No	No	2025	No	No
Csnk2b	569	No	No	803	No	No
Cxcl12	262	-0,5	Yes	1408	1,5	Yes
Eda	11	No	No	93	No	No
Eda2r	21	-1,5	Yes	109	No	No
Edar	19	No	No	24	-2	Yes
Edaradd	184	-0,5	Yes	401	-0,5	Yes
Erc1	611	No	No	771	No	No
GADD45A	213	0,5	Yes	174	No	No
GADD45B	359	1	Yes	250	1	Yes
GADD45G	90	No	No	67	1,5	Yes
Icam1	464	2	Yes	321	1	Yes
Ikbkb	647	0,5	Yes	1017	No	No
Ikbkg	269	No	No	558	No	No
IL1B	2686	5	Yes	273	5	Yes
IRAK1	375	No	No	651	No	No
IRAK4	169	No	No	250	1	Yes
Lat	33	No	No	33	No	No
Lbp	763	3	Yes	467	No	No
Lck	31	No	No	39	No	No
Ltb	25	2,5	Yes	37	3	Yes
Ltbr	1073	0,5	Yes	399	1	Yes
Ly96	65	2	Yes	23	1	No
Lyn	879	2,5	Yes	406	2	Yes
Malt1	449	1	Yes	872	No	No
MAP3K14	190	No	No	234	No	No

	Acomys			Mus		
Gene	**Base Mean**	**Fold Change**	**Significance**	**Base Mean**	**Fold Change**	**Significance**
NFKB2	541	1,5	Yes	387	0,5	Yes
Nfkbia	1054	0,5	No	718	No	No
Parp1	461	No	No	536	No	No
Pias4	197	No	No	230	No	No
Plau	667	1,5	Yes	684	1	Yes
Plcg1	1653	No	No	1548	No	No
Plcg2	701	No	No	433	No	No
PRKCB	377	1,5	Yes	260	No	No
Prkcq	155	-1	Yes	170	-0,5	No
Rela	552	No	No	450	No	No
RELB	194	1	Yes	187	No	No
Ripk1	416	0,5	Yes	653	No	No
Syk	280	2	Yes	518	1,5	Yes
TAB1	150	No	No	219	No	No
TAB2	1107	No	No	1741	No	No
Tab3	256	No	No	474	No	No
Ticam1	117	No	No	128	No	No
Ticam2	44	2	Yes	38	No	No
Tirap	96	1	Yes	177	1	Yes
Tlr4	552	2	Yes	252	1	Yes
TNF	28	1,5	Yes	48	No	No
Tnfaip3	657	2	Yes	287	No	No
Tnfrsf11a	211	1,5	Yes	371	No	No
Tnfrsf13c	4	2,5	No	4	-1,5	No
TNFRSF1A	1410	0,5	Yes	1102	0,5	Yes
Tnfsf11	26	1	Yes	40	4	Yes
Tnfsf13b	14	1,5	Yes	17	No	No
Tnfsf14	6	3,5	No	13	1,5	No
Tradd	144	1	Yes	118	1,5	Yes
Traf1	68	3	Yes	93	1,5	Yes
TRAF2	239	No	No	240	No	No
Traf3	526	0,5	Yes	456	0,5	Yes
Traf5	192	1	Yes	174	-1,5	Yes
TRAF6	518	No	No	1064	0,5	Yes
Trim25	414	No	No	754	1	Yes
Ube2i	890	No	No	1551	No	No
Vcam1	80	No	No	253	2	Yes
Xiap	501	-0,5	Yes	1377	No	No
Zap70	19	No	No	21	No	No

WNT

	Acomys			Mus		
Gene	**Base Mean**	**Fold Change**	**Significance**	**Base Mean**	**Fold Change**	**Significance**
4930544G11Rik	1	-1	No	1	-4	No
Apc	2287	No	No	1687	No	No
Apc2	49	No	No	56	No	No
Apcdd1	1341	-0,5	Yes	512	-1	Yes
Axin1	996	No	No	514	No	No
Axin2	663	-1	Yes	670	-1	Yes
Bambi	43	-2	Yes	70	-1	Yes
Btrc	192	-1	Yes	325	-0,5	Yes
Camk2a	47	-2	Yes	103	-2	Yes
Camk2b	310	-1,5	Yes	203	-1,5	Yes
Camk2d	1069	No	No	1315	No	No
Camk2g	319	No	No	504	No	No
Cby1	103	No	No	85	No	No
Ccar2	917	0,5	Yes	583	No	No
Ccdc88c	568	No	No	914	-1	Yes
Ccnd1	483	No	No	991	0,5	Yes
Ccnd2	818	-0,5	Yes	3024	-1,5	Yes
Ccnd3	696	0,5	Yes	433	1	Yes
Chd8	2047	No	No	1830	No	No
Crebbp	3261	No	No	3362	-0,5	Yes
Csnk1a1	3971	0,5	Yes	6108	0,5	Yes
Csnk1e	576	-0,5	Yes	626	0,5	Yes
Csnk2a2	557	No	No	2025	No	No
Csnk2b	569	No	No	803	No	No
Ctbp1	1378	0,5	Yes	923	1	Yes
Ctnnb1	7877	0,5	Yes	4614	1	Yes
Ctnnbip1	402	No	No	1237	0,5	Yes
Ctnnd2	63	No	No	133	-2	Yes
Cul1	1632	No	No	1113	No	No
Cxxc4	8	-1	No	36	-1	No
Daam1	1431	No	No	2082	No	No
Dkk2	172	-1	Yes	310	-1	Yes
Dkk4	7	No	No	3	No	No
Dvl1	749	-0,5	Yes	688	No	No
Dvl2	404	No	No	278	No	No
Dvl3	302	No	No	505	No	No
Fbxw11	541	No	No	809	0,5	Yes
Fosl1	169	3	Yes	14	1	No
Frzb	338	-2	Yes	371	-4	Yes
Fzd1	1160	No	No	919	1	Yes
Fzd10	449	No	No	484	No	No

Gene	Acomys			Mus		
	Base Mean	Fold Change	Significance	Base Mean	Fold Change	Significance
Fzd5	57	No	No	248	No	No
Fzd6	510	0,5	Yes	997	0,5	Yes
Fzd7	338	-0,5	Yes	558	No	No
Fzd8	142	-1	Yes	155	No	No
Fzd9	352	-1,5	Yes	209	-1,5	Yes
Gpc4	514	-1	Yes	385	No	No
Gsk3b	832	No	No	2407	No	No
JUN	1159	No	No	809	1	Yes
Lef1	77	-1,5	Yes	53	-1,5	Yes
Lgr4	906	-1	Yes	586	-1	Yes
Lgr5	60	No	No	148	No	No
Lgr6	253	-1	Yes	386	-2	Yes
Lrp5	1229	-0,5	Yes	1634	0,5	Yes
Lrp6	2506	-0,5	Yes	2097	-0,5	Yes
Lzts2	423	-0,5	Yes	355	No	No
MAP3K7	821	No	No	977	No	No
MAPK10	31	No	No	9	No	No
MAPK8	351	No	No	599	No	No
MAPK9	416	No	No	423	No	No
Mcc	717	-0,5	Yes	1502	-0,5	Yes
MYC	344	1	Yes	332	No	No
NFATC1	472	-1	Yes	668	No	No
Nfatc2	174	-1,5	Yes	537	No	No
NFATC3	894	No	No	1247	No	No
Nfatc4	266	-1	Yes	407	1,5	Yes
Nkd1	220	-1	Yes	84	-1	Yes
Nkd2	256	-1,5	Yes	333	-1,5	Yes
Nlk	314	No	No	311	No	No
Notum	72	-2	Yes	33	No	No
Plcb1	254	No	No	188	No	No
Plcb2	197	1,5	Yes	156	No	No
Plcb3	1170	1	Yes	1169	0,5	Yes
Plcb4	541	-1	Yes	336	-1	Yes
Porcn	296	No	No	130	1,5	Yes
Ppard	251	2	Yes	470	1,5	Yes
PPP3CA	1442	-0,5	Yes	1749	No	No
PPP3CB	718	No	No	814	No	No
PPP3CC	364	-0,5	Yes	136	-0,5	Yes
PPP3R1	619	No	No	946	No	No
Prickle1	312	No	No	249	No	No
Prickle3	190	0,5	Yes	382	No	No
PRKACA	971	No	No	571	No	No
PRKACB	782	No	No	958	No	No

Gene	Acomys			Mus		
	Base Mean	Fold Change	Significance	Base Mean	Fold Change	Significance
Psen1	768	No	No	1391	No	No
RAC1	606	0,5	Yes	1918	0,5	Yes
RAC2	183	3	Yes	113	2	Yes
RAC3	81	No	No	79	No	No
Rbx1	298	1	Yes	465	No	No
Rhoa	2028	1	Yes	2199	0,5	Yes
Rnf43	107	No	No	296	-1	Yes
Rock2	1641	No	No	2033	No	No
Ror1	75	-1	Yes	145	No	No
Ror2	171	No	No	98	1,5	Yes
Rspo1	102	No	No	41	-1,5	Yes
Rspo2	3	-1,5	No	5	No	No
Rspo3	68	-1,5	Yes	70	-2	Yes
Rspo4	19	No	No	12	1	No
Ruvbl1	426	0,5	Yes	146	0,5	Yes
Ryk	1119	No	No	955	No	No
Senp2	332	No	No	682	No	No
Serpinf1	1344	-1	Yes	1145	No	No
Sfrp1	394	0,5	Yes	657	1	Yes
Sfrp2	352	No	No	487	2,5	Yes
Sfrp4	68	1,5	Yes	54	No	No
Sfrp5	60	-2	Yes	65	-3,5	Yes
Siah1a	386	No	No	318	No	No
Sirt1	329	No	No	398	No	No
Skp1	1714	No	No	1689	No	No
Smad3	165	No	No	572	No	No
Smad4	969	No	No	785	No	No
Sost	12	-4,5	Yes	0	1,5	No
Sox17	34	-1	Yes	40	No	No
Tbl1x	696	No	No	1268	No	No
Tbl1xr1	796	No	No	1754	No	No
Tcf7	149	No	No	107	No	No
Tcf7l2	226	-1	Yes	368	-1	Yes
Tle1	258	-1	Yes	379	No	No
Tle3	1347	0,5	Yes	1704	0,5	Yes
Tle4	536	0,5	Yes	401	No	No
Trp53	1062	0,5	Yes	388	No	No
Vangl1	369	No	No	464	No	No
Vangl2	197	No	No	568	No	No
Wif1	2035	-1	Yes	2846	-3	Yes
Wnt10a	139	No	No	181	No	No
Wnt10b	34	-1,5	Yes	62	-0,5	No
Wnt11	105	-1,5	Yes	33	-0,5	No

Gene	Acomys			Mus		
	Base Mean	Fold Change	Significance	Base Mean	Fold Change	Significance
Wnt3	344	-1	Yes	263	-0,5	Yes
Wnt3a	64	No	No	75	No	No
Wnt4	286	1	Yes	853	1	Yes
Wnt5a	375	No	No	519	1,5	Yes
Wnt5b	45	No	No	31	1	No
Wnt6	17	No	No	26	-1	No
Wnt7a	7	No	No	5	-1	No
Wnt7b	134	No	No	459	No	No
Wnt9a	18	-1,5	Yes	76	1	Yes
Znrf3	246	-0,5	Yes	456	-0,5	Yes